TECTONICS AND METALLOGENY OF THE THIRTYMILE RANGE, YUKON TERRITORY, CANADA

Timothy Liverton BSc (Hons), FGS

A Thesis submitted in fulfillment of the
Requirements of the University of london
For the degree of Doctor of Philosophy

Department of Geology,
Royal Holloway and Bedford New College,
University of London

August 1992

ABSTRACT

The Thirtymile Range in the south-central Yukon Territory of Canada, is a 1.2 km thick, disrupted sequence of low grade clastic, chert and carbonate metasediments in the Dorsey terrane. This terrane is at the western edge of the Omineca plutonic-metamorphic belt at the margin of the Palaeozoic North American continent. The sequence has been disrupted by zones of low-angle shearing that contain local mylonites and which is interpreted as a east-vergent thrust belt. Fabric of the tectonites is consistent with NE transport by thrust faulting resulting from oblique (dextral) compression at the Teslin suture, immediately west of the study area. The unfossiliferous metasediments are lithologically correlated with L. Proterozoic to Devonian-Mississippian continental sequences of ancestral North America. The Dorsey terrane is considered to be essentially parautochthonous rather than an accreted terrane. The terrane has been intruded by two suites of basic-intermediate and granitic plutons that are undeformed and have been dated at Middle Jurassic and Middle Cretaceous. The age of the older suite places an upper limit to the penetrative deformation that occurred during imbrication of the continental margin upon collision of the Superterrane 1 (composed of Quesnellia, Cache Creek, Stikinia and Slide mountain terranes). The hornblende-rich NW Thirtymile and 181.5± 2.5 Ma old (Sr_i= 0.7045) SW Thirtymile stocks have trace-element compositions that indicate an origin from either oceanic crustal subduction- or crustally contaminated mantle-derived magma.

Extensional faulting preceded and accompanied emplacement of the acid Thirtymile and Ork stocks in the Thirtymile Range. Major and trace element rock and mica geochemistry and Rb/Sr geochronology indicate that the Thirtymile (101.0±2.5; 100±4 Ma Sr_i= 0.7060-0.7074) and Ork granite stocks and the larger Hake (98.3±2.9 Ma) and Seagull batholiths further to the SE are one suite of consanguineous intrusions. These one-mica granites are meta- to peraluminous with a marked trend toward enrichment in F, Li, Rb and depletion in Sr and Ba which is comparable to the highly fractionated 'tin-granites' of Europe, S.E. Asia and Alaska. These are interpreted as derived from a largely I-type continental crustal source. Timing of emplacement of these granites may

correspond to initiation of major transcurrent faulting of the continental margin.

Sn-W bearing skarns are found adjacent to the Ork stock. Extensional faulting is considered to have been instrumental in controlling skarn mineralisation. Faults closest to the Mindy prospect carry W-mineralisation in breccia and an adjacent manto skarn is developed in marble. The Mindy skarn displays complex replacement of early diopside then later fracture-controlled salite to ferrosalite or andradite-vesuvianite primary skarns by increasingly Fe-rich amphibole and chlorite, principally along fracture systems.

Tin is not present in large amounts in silicate phases, but first appears in the form of cassiterite accompanying magnetite with later hülsite and ludwigite accompanying fluorides. A phlogopite-ferrophengite greisen overprint of the skarns is accompanied by fluorite. Skarn mineralogy therefore reflects the F-rich nature of the nearby highly evolved leucogranites. Ultrafractionation, in common with Alaskan examples, is favoured for generation of the alkali-halogen enriched leucogranites of the Thirtymile Range. Late-stage magmatic processes are considered to be more important in the generation of these specialised granites than perhaps origin of the magma. Extreme variation in range of chemical parameters (Rb= >250 ppm and Sr <175 ppm; very variable Ba, decreasing by a factor ≈30x in the Seagull-Thirtymile suite and the Ba/Rb ratio consequently decreasing to 0.1 of its values in least-fractionated lithofacies) are typical of these granites. Micas from granites in this study have a range of Mg/Fe* from 0.165 to 0.001 for least to most evolved lithofacies. The low Mg content of biotite is, therefore, quite diagnostic (Mg/Fe* threshold of ≈0.15) of tin granites.

ACKNOWLEDGEMENTS

This topic for this research project was suggested by Jim Morin in 1987, when he was Chief Geologist of the Exploration and Geological Services Division, Yukon, of the Department of Indian Affairs and Northern Development (D.I.A.N.D.), Government of Canada. A large part of the cost of field work in the Yukon was funded by D.I.A.N.D. Grant Abbott, Trevor Bremner and Steve Morrison are thanked for their encouragement and assistance.

Professor K.R. McClay and Dr. D.H.M. Alderton are thanked for their supervision of this project. Much time was spent providing assistance with analytical techniques by Dr. J.N. Walsh, Dr. M.F. Thirlwall, Dr. G.C.F. Marriner and Dr. A. Hall of the Royal Holloway and Bedford New College. Miss C. Lowe, Mr. N. Holloway, Miss C. Warren, Mr I. Gill, Mr. J. Ingram, Mr. K. D'Souza, Mr. M. Longbottom, Mrs. J. Riddell and Mr. S. White are thanked for their large amounts of technical assistance.

Dr. S.O. Agrell provided very useful assistance in showing and lending me thin sections of the rare skarn minerals from the Harker Collection at Cambridge. Dr. Andrew Shaw kindly provided a selection of his chemical and isotopic analyses to be used for comparison. Dr. Luiz Del Rey Silva is thanked for much time spent in discussion. Miss S. Meredith and her staff at the Geological Society Library are thanked for their cheerful help.

CONTENTS

CONTENTS

CHAPTER 1: INTRODUCTION

CHAPTER 2: TECTONICS OF THE NORTHERN CANADIAN CORDILLERA

CHAPTER 3: GEOLOGY OF THE THIRTYMILE AND ENGLISHMANS RANGES

CHAPTER 4: PETROGRAPHY AND GEOCHEMISTRY OF THE JURASSIC AND CRETACEOUS INTRUSIONS

CHAPTER 5: SKARNS OF THE THIRTYMILE RANGE

CHAPTER 6: DISCUSSION

CHAPTER 7: CONCLUSIONS

LIST OF TABLES

CHAPTER 1

CHAPTER 2

CHAPTER 4

CHAPTER 5

CHAPTER 6

LIST OF FIGURES

CHAPTER 1

CHAPTER 2

CHAPTER 3

CHAPTER 4

CHAPTER 5

CHAPTER 6

APPENDIX

CHAPTER 1

INTRODUCTION

CHAPTER 1: INTRODUCTION

1.1 INTRODUCTION TO THE GEOLOGY OF THE THIRTYMILE RANGE

The Thirtymile Range is located in the southern Yukon Territory of Canada, 145 km east of Whitehorse (Figure 1.1). The range is a NW-SE trending prominent topographic feature composed of Palaeozoic low metamorphic grade predominantly siliciclastic sediments that are at the western edge of the Omineca Crystalline belt of the northern Canadian Cordillera (Table 1.1). The succession has been deformed during Early Jurassic low angle east-vergent thrust faulting and displaced by generally E-W striking, steeply-dipping extensional faults. The metasediments have been intruded by Middle Jurassic gabbro to granodiorite and Middle Cretaceous granite stocks, the younger of the plutonic suites being associated with the tin-tungsten mineralisation that is the focus of this study. This thrustbelt is the westernmost preserved edge of the Mesozoic North American continent in the southern Yukon.

The Thirtymile Range has previously only been geologically mapped at 1:250,000 scale during preparation of the Teslin map sheet (Mulligan, 1963). The metasediments forming the Thirtymile Range were described as simple conformable sedimentary succession. Subsequent geological work consisted of prospecting (Newmont and JC Stephen Explorations) and mineral claim evaluation which discovered scheelite tungsten and tin mineralisation (Stephen, 1981; Nebocat, 1981). This study represents the first attempt at mapping a significant part of this mountain range at 1:25,000 scale and shows that, rather than being a gently folded sequence, the Thirtymile metasediments (Englishmans Group) are part of an east verging thrust belt. A constraint on the upper limit to the age of penetrative deformation that accompanied thrust faulting of the Englishmans Group is provided by the geochronology presented in this study. The NW and SW Thirtymile stocks have been dated by Rb/Sr methods as Middle Jurassic.

The granitic stocks mapped in the Thirtymile Range, which are dated as Middle Cretaceous by Rb/Sr methods in this study, contain lithofacies displaying the widest compositional range from the one suite of consanguineous intrusions that include the Seagull batholith, Hake batholith, Thirtymile and Ork stocks. This suite is here called the Seagull-Thirtymile plutonic suite. This study documents the first topaz granites to be

Seagull-Thirtymile plutonic suite. This study documents the first topaz granites to be recognised in the Yukon. These are comparable in chemistry to the most evolved 'specialised' granites of other tinfields. The associated F-B- rich Sn skarns reflect the unusual chemistry of the plutonic lithofacies. The tin-related plutons of the Thirtymile Range are considered to have an origin separate from that of the major tungsten-related granites of the Yukon and N.W.T. The leucogranites of the Thirtymile Range are

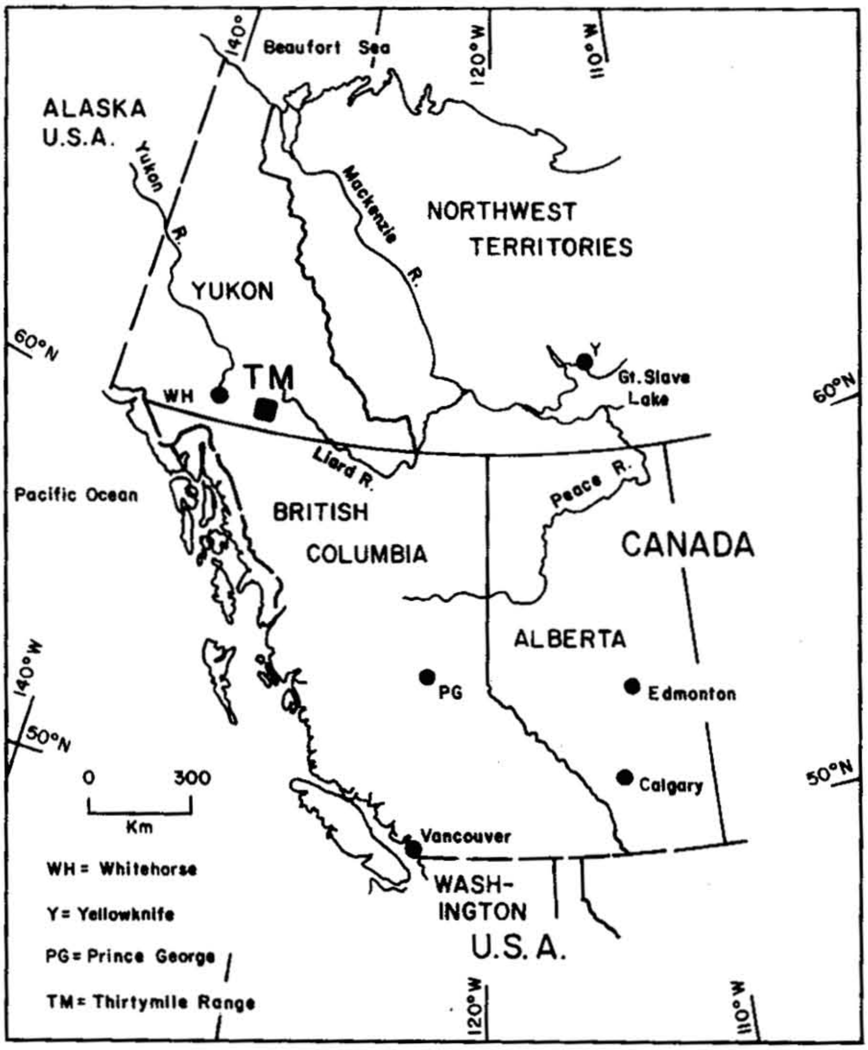

Fig. 1.1 The Thirtymile Range: location.

Figure 1.2 The Thirtymile Range. A view looking south towards the highest peak (1997) from point {427276}. The top of the marble unit (and Thirtymile Thrust) is just visible as a lighter coloured area at the left hand base of this peak. Other marble exposures may be seen as white areas in the left middle distance.

BELT	DESCRIPTION
Rocky Mountain	Northeasterly tapering wedge of Mid-Proterozoic to Upper Jurassic (1500-150 Ma) miogeoclinal and platformal carbonates and cratob-derived clastics, and overlying Upper Jurassic to Paleogene exogeoclinal, cordillera-derived clastics; horizontally compressed and displaced up to 200 km NE onto the craton in Late Jurassic to Paleogene time.
Omineca Crystalline	Mid Proterozoic to Mid Palaeozoic miogeoclinal rock, Palaeozoic and Lower Mesozoic volcanogenic and pelitic rock, local Precambrian crystalline basement, highly deformed and variably metamorphosed (up to high grade) in Mid-Mesozoic to Early Tertiary and intruded by Jurassic and Cretaceous plutons.
Intermontane	Upper Palaeozoic to Mid-Mesozoic marine volvanic and sedimentary rock, mid-Mesozoic to Upper Tertiary marine and nonmarine sediments and volcanics; granitic intrusions comagmatic with the volcanics; deformed at various times (Early Mesozoic to Neogene)
Coast Plutonic Complex	Sedimentary and volcanic strata of known Late Palaeozoic to Tertiary age and probable Early Palaeozoic and Precambrian age, variably metamorphosed up to high grades and dominant, mainly Cretaceous and Tertiary granitic rock.
Insular	Upper Cambrian to Neogene volcanic and sedimentary strata, granitic rocks in part comagmatic with the volcanics; deformed at various times from Palaeozoic to Neogene

Table 1.1 Tectonic belts of the Canadian Cordillera

interpreted to be the result of a process of 'ultrafractionation', in common with Alaskan examples.

1.2 AIMS OF THIS RESEARCH

This research aims to:

1) Present a geological map of the central and northern portions of the Thirtymile Range; to determine the structure of the Englishman's Group and to correlate these with established sequences in the northern Canadian Cordillera and to elucidate the geological history of the region in terms of tectonic evolution of the Northern Cordillera.

2) To define the setting of tin-tungsten mineralisation in the Thirtymile Range in terms of tectonics and structural controls: to determine chemical trends in formation of the skarn mineralisation and compare the unusual chemistry of the metasomatic mineralisation with that of the adjacent intrusions.

3) To investigate rock and mineral chemistry and geochronology of the Thirtymile plutons. Sampling and analysis of the Hake and Seagull batholiths is to be undertaken on a reconnaissance scale to allow comparison. This data is to be used to infer the affinity of these intrusions with one another and these nearby granitic batholiths. Timing and structural controls of igneous intrusion are to be considered relative to northern Canadian Cordilleran tectonics. The chemical evolution of the various granite lithofacies is to be

considered relative to concentration processes of the economic metals. Compositions of intrusive lithofacies and their micas are sought that are diagnostic of proximal tin mineralisation.

1.3 THE STUDY AREA

1.3.1 LOCATION OF MAPPING

The research area is a 115 km long by 25 km wide strip, that covers the Thirtymile Range, Englishmans Range and NW end of the Cassiar Mountains (Dorsey Range) in the Yukon Territory centred between latitude 60°49'N, longitude 132°44'W and latitude 60°05'N, longitude 131°08'W. The relevant topographic map sheets of the National Topographic System (N.T.S.) at 1:50,000 scale are 105C 15; 105 C 10; 105C 9; 105 B 4 and 105 B 3.

1.3.2 TOPOGRAPHY, ACCESS AND VEGETATION

The region is mountainous. Elevations vary from 900 metres to 2012 metres. Below 1350 metres elevation the hills are covered with dense spruce or pine forest. Above 1350 metres a densely tangled, stunted willow growing up to 1.8 m high known as 'buckbrush' survives to around 1470 metres elevation. Balsam pine inhabits the sheltered valleys between 1380 and 1500 metres elevation and forms dense mats of branches and sub-horizontal trunks. Above 1500m altitude only alpine tundra survives (Fig. 1.2). The mountain ranges generally follow the NW-SE fabric of the northern Canadian Cordillera. Streams run eventually southward into Teslin Lake, thence NW to the Yukon River. The extreme SE corner of the study area is at the divide of the Cordilleran watershed.

The study area is uninhabited and not traversed by any roads. Access to the field was made using either a seaplane to fly to the larger lakes or a helicopter to set out fly camps.

1.3.3 CLIMATE

The Southern Yukon has a sub-arctic climate. The normal working season in the mountains is from the end of the first week of June until late September. Minimum temperatures as low as -58°C can occur during the winter. Permafrost exists below all high north-facing slopes and may penetrate the rock for 180 metres.

1.3.4 ROCK EXPOSURE

The region studied was glaciated during the last (McConnell) Ice advance (Hughes et al., 1969) and little modification of the topography has resulted since retreat of the ice roughly 8000 years ago. Matterhorns, hanging valleys and cirques are the landforms of the higher ranges. Rock exposure is excellent along ridges and spurs that are above timber line. On the flanks of the ridges huge exposures exist as felsenmeer (frost-wedged blocks of rock from 0.5 to several metres across, that have moved little distance down slope) or scree. Below timber line the exposure is sparse, occurring as the odd knoll or in creek beds. Major river valleys have a thick veneer of reworked glacial till.

1.4 MAPPING DURING THE 1988 to 1990 SEASONS IN THE THIRTYMILE RANGE.

1.4.1 SCOPE OF THE MAPPING

The central portion of the Thirtymile Range (111 km^2) has been mapped, compiled at 1:25,000 scale and sampled in detail. The region to the west of the NW Thirtymile granodiorite stock has been traversed and a map (of 38 km^2) prepared at 1:25,000 scale. Mapping of 10 km^2 around the SW Thirtymile stock has been compiled at 1:50,000 scale. The Hake and Seagull batholiths have been sampled, where logistically possible, for geochemical studies. The Hake batholith (Mulligan, 1963; Poole et al., 1960) forms the spectacular topography of the Englishmans Range immediately SE of the Thirtymile Range and the Seagull batholith (Poole et al., 1960; Abbott, 1981) is located in the

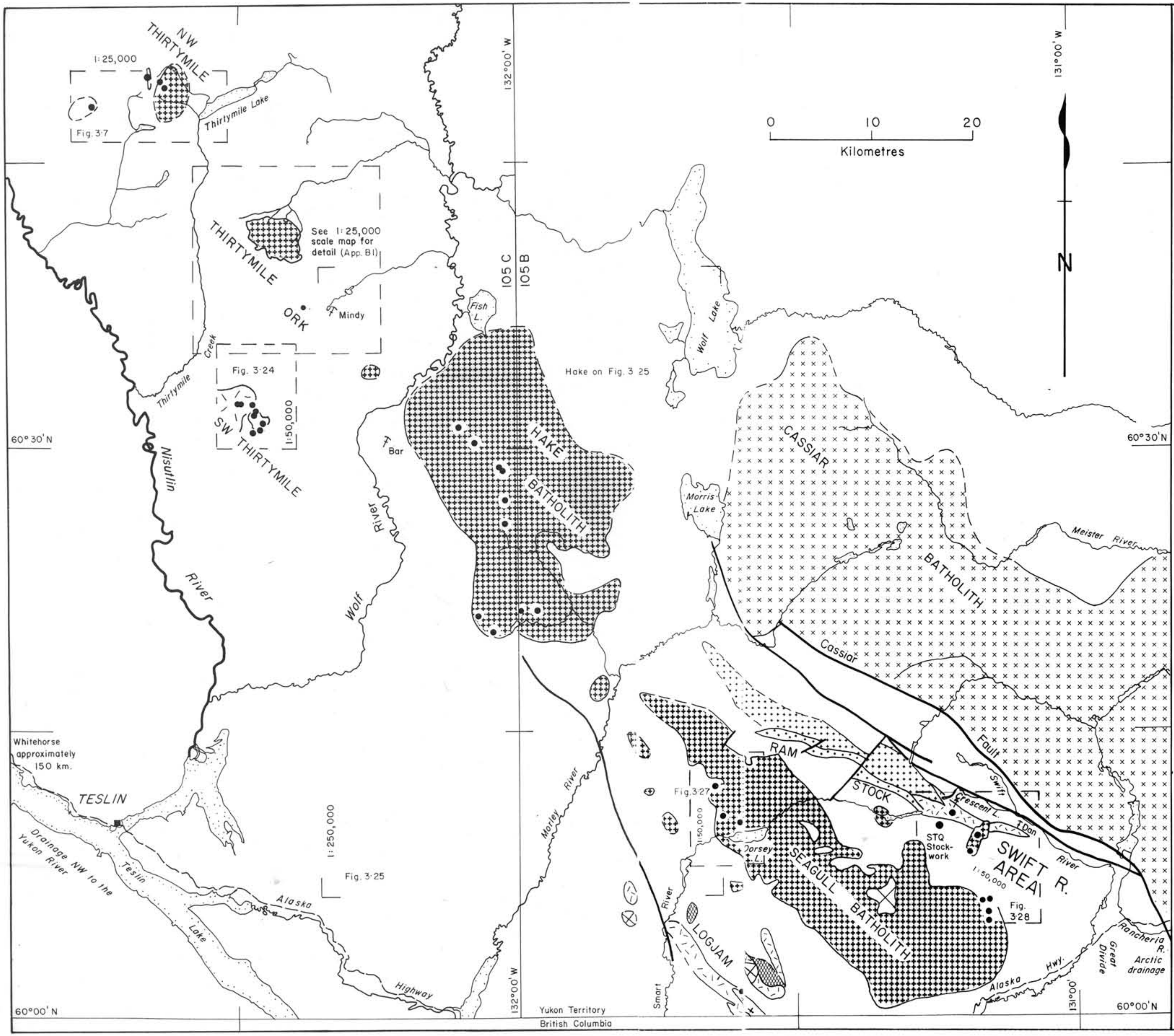

LEGEND

CRETACEOUS

- × × Quartz monzonite Cassiar Batholith
- ▦ Granite: Seagull, Hake and Thirtymile plutons. NW Thirtymile possibly older

JURASSIC

- Diorite (Logjam), Gabbro to granodiorite (SW Thirtymile)
- ▨ Quartz monzonite
- ☒ Gabbro and ultrabasics

PALAEOZOIC TO MESOZOIC

- **Foliated diorite to granodiorite**
- Quartz monzonite and granodiorite

Geology from Poole, Roddick and Green (1960), Mulligan (1963) and Abbott (1981).

Drawn: T. Liverton, September 1990

Dots indicate localities sampled (intrusions) ⚒ indicates mineral deposit mapped- Mindy, Crescent Lake and Dan. The Bar prospect is also shown.

GRANITIC PLUTONS OF THE SOUTH CENTRAL YUKON

THIRTYMILE, LOGJAM AND RAM STOCKS; SEAGULL, HAKE AND CASSIAR BATHOLITHS.

Fig. 1·3

Dorsey Range, a further 5 to 27 km SE of the Hake granite (Fig. 1.3).

1.4.2 MAPPING METHODS

The primary effort in the Thirtymile Range was made in order to map the region that contained the known tin/tungsten mineral showings (Fig. 1.3), adjacent to the Thirtymile stock. Mapping was performed by plotting localities on 1.5x enlargements of approximately 1:33,000 scale aerial photographs supplied by Energy Mines and Resources, Canada, for the central portion of the Range and directly onto contact prints for the remainder of the area. Geological details were compiled on 1:25,000 scale enlargements of the 1:50,000 scale published contour maps (sheets 105 C-15, 105 C-9 and 10). Stereo pairs of aerial photograph contact prints were used extensively in the field. Where additional aid in location was required approximate elevations were obtained using an altimeter and compass resection from nearby peaks or other landmarks helped to resolve some ambiguities. Limited traversing was carried out using compass, tape and clinometer where detail was required for the mapping of the central portion of the Thirtymile stock. Detailed mapping of the Mindy prospect was performed by theodolite tachymetry in order to provide accurate vertical control. Specimens from five localities of the various Thirtymile granite lithofacies were collected by drilling out rounds with a Cobra jackhammer and blasting. These yielded useful slabs for the study of enclaves and contact relationships.

1.5 STRUCTURE OF THIS THESIS

The following chapters in this thesis are:

CHAPTER 2 *The Northern Canadian Cordillera*:

A review of published literature concerning the tectonics and evolution of the northern Cordillera, with emphasis on the southern Yukon.

CHAPTER 3 *Geology of the Thirtymile Range* :

The geology of the Thirtymile Range is described.

CHAPTER 4 *Igneous Intrusions* :

The petrography, geochemistry and geochronology of the Seagull-Thirtymile plutonic suite are presented and evidence given to indicate that the NW and SW Thirtymile stocks are older. Chemical trends producing highly fractionated, extremely Li-Rb-F enriched leucogranites are demonstrated and comparison made with Cornubian and Alaskan examples.

CHAPTER 5 *Skarns of the Thirtymile Range* :

Contact metamorphic assemblages in the Thirtymile Range are described, with emphasis on the Mindy Sn±W skarn prospect and the controls on mineralisation.

CHAPTER 6 *Discussion* :

A model for the structural development of the Thirtymile Range and emplacement of the various plutons is postulated. Correlation of the metasediments with North American continental assemblages is proposed. The granites of the Thirtymile Range and nearby batholiths are postulated to be one plutonic suite. The possible tectonic setting for magma generation in this region and implications of geochronology are discussed. Cordilleran tin metallogeny and the 'ultrafractionation' hypothesis are discussed. Parameters for recognition of tin granites by their anomalous geochemistry are proposed. Comparison is made between the chemistry of the evolved intrusions and that of the metasomatic mineralisation. Targets for possible future mineral exploration are outlined.

CHAPTER 7 *Conclusions* :

The conclusions reached during the preceding discussions are given.

APPENDIX

(A) Description of analytical techniques

(B) Large maps, sketches and comparative tables

(C) Tables of analyses of rock and micas

(D) X-ray diffraction data

CHAPTER 2

TECTONICS OF THE NORTHERN CANADIAN CORDILLERA

CHAPTER 2: TECTONICS OF THE NORTHERN CANADIAN CORDILLERA

2.1 INTRODUCTION

This chapter reviews recent literature concerning the tectonic evolution of the northern Canadian Cordillera. The western margin of the North American continent has been the site of rifting and sedimentation throughout the Late Proterozoic and Palaeozoic eras and of repeated arc-continent collision tectonics during the Mesozoic and Cenozoic eras. Development of the Cordilleran orogen from a passive margin began with accretion of allochthonous terranes in the Late Triassic and has continued until the present.

The Cordillera is composed of five morphogeological belts from east to west (Gabrielse and Yorath, 1990), see Table 2.1.

1) The Foreland Belt: sedimentary miogeosynclinal strata.

2) The Omineca Crystalline Belt: metamorphic and granitic rocks. Culmination of plutonism is evident from 110-90 Ma (Armstrong, 1988).

3) The Intermontane Belt: unmetamorphosed or low-grade sedimentary and volcanic eugeosynclinal and epieugeosynclinal strata.

4) The Coast Belt: predominantly granitic lithologies with culminations of magmatic activity at 130-84 Ma and 64-40 Ma (Armstrong, 1988).

5) Insular Belt: Palaeozoic to Quaternary sediments and volcanics with comagmatic granites (Monger et al., 1982).

TERRANE	DESCRIPTION
Alexander (composite)	Precambrian (?), Paleozoic and Mesozoic volcanic, clastic and carbonate rocks
Cascadia (composite)	Crystalline and pelitic gneiss, in part Precambrian; Palaeozoic and Mesozoic volcanics and associated sediments; disrupted Mesozoic greenschist, blueschist and phyllite
Chugach (composite)	Deformed Upper Mesozoic flysch and melange; lower Cenozoic flysch and volcanics
Cache Creek	Mississippian to Late Triassic melange and tectonically disrupted chert, argillite, basalt, alpine-type ultramafics, extensive carbonate and local blueschist
Eastern	Upper Palaeozoic and (?) lower Palaeozoic basalt, alpine-type ultramafics, chert argillite (See Slide Mountain terrane in later work)
Olympic	Early Cenozoic volcanics and associated deep- and shallow-water sediments. Basement considered to be oceanic.
Pacific Rim	Late Jurassic and Early Cretaceous flysch and melange
Quesnellia	Upper Palaeozoic and Early Triassic volcanics, volcaniclastics and carbonates; Late Triassic to Early Jurassic volcanics, clastics and argillite; Late Triassic and Early Jurassic strata lie stratigraphically on Eastern and probably on Cache Creek. In the Yukon includes possible Upper Cambrian to lower Palaeozoic metamorphics with continental affinity.
Stikinia	Possible upper Precambrian basement, with Mississippian and Permian volcaniclastic rocks, basic to acid volcanics and carbonates. Locally deformed and intruded in middle to Late Triassic. Overlain by Late Triassic to Middle Jurassic andesitic volcanics. Late Triassic to Middle Jurassic rocks linked to Cache Creek.
Wrangellia	Palaeozoic volcanic complexes composed of flows, breccias and volcaniclastics overlain by limestone, clastic rocks and chert and Late Triassic pillowed and subaerial basalt flows. Succeded by Triassic and Jurassic limestone, cherty limestone and volcanics.

Table 2.1 Major terranes of the Canadian Cordillera (after Monger et al., 1982)

2.2 TECTONICS OF THE CANADIAN CORDILLERA

2.2.1 PASSIVE MARGIN

Sedimentation that occurred along the margin of the North American continent during four main episodes of extension and thermal subsidence is preserved in sequences from the Upper Proterozoic and throughout the Palaeozoic eras. The craton that formed the west side of the sedimentary basin was thought to have been the Siberian Platform (Struik, 1987), however Young (1992) has postulated correlation between the Upper Proterozoic glacigenic sediments of South Australia-N.S.W. and those of the Windermere Supergroup of the northern Canadian Cordillera. Each episode of rifting and thermal subsidence provided the setting for deposition of the major Palaeozoic sedimentary sequences of the miogeocline (Thompson et al., 1987). These overlap each other: the younger sedimentation axis being westward (Monger et al., 1982). The various passive-margin sequences of the Cordilleran miogeocline were deposited from: (a) 1500-800 Ma (Belt-Purcell sequence in the southern Canadian Rocky Mountains and the Wernicke, Pinguicula and Mackenzie Mountain sequence in the north); 800-600 Ma (Windermere sequence); (b) 600-370 Ma and (c) 370-180 Ma (Thompson, et al., 1987). The Upper Proterozoic and Lower Palaeozoic extensional events produced sedimentary basins, but did not result in complete separation of the western part of the craton. Horsts (i.e. topographic highs) separated individual earlier Palaeozoic basins (Struik, 1987). Devonian-Carboniferous history in the western Rocky Mountains is marked by black clastic sedimentation in half-graben basins of 8-12 km wide by 50-70 km long, overlain by Mississippian carbonates (McClay et al., 1989; Gordey et al., 1982).

After possibly Early Carboniferous time complete separation of continental crust from the North American margin was a result of initiation of a spreading ridge and the development of oceanic crust of the Cache Creek terrane. A portion of the craton margin that had been detached from the North American continent formed the basement for the Quesnellia island arc microcontinent. Palaeozoic sediments deposited on this basement are overlain by Middle Triassic to Early Jurassic subduction-generated volcanics (Struik, 1987).

Compression from Middle Jurassic to Cretaceous time resulted in inversion of Palaeozoic basins and incorporation of these into fold- and thrust-belts. Original geometry of the extensional basins had a profound control on the orientation of later thrust systems: in the Ogilvie mountains (Thompson et al., 1987) and in the Kechika Trough (McClay et al., 1989).

2.2.2 ACCRETION OF ALLOCHTHONOUS TERRANES

As a result of destruction of Upper Palaeozoic to Lower Mesozoic oceanic crust by subduction and subsequent repeated collision of island arcs with the North American craton since the Mesozoic, the western part of the northern Canadian Cordillera is now a collage of terranes derived from oceanic crust, magmatic arcs and marginal to oceanic basin sediments. These terranes are allochthonous or 'suspect' (Coney et al., 1980) with respect to the North American craton. Displacements (in latitude) of many hundreds of kilometres for many of the 200 terranes that comprise the North American Cordillera are indicated by comparison of the allochthonous fossil faunas and continental equivalents and by palaeomagnetic data (Monger, 1989).

Hansen (1990) considers that Triassic westward-directed subduction of oceanic crust beneath the island-arc terranes lead to eventual collision of the 'exotic' terranes with the North American continent (but see also Brown et al., 1986). Quesnellia formed a west-facing arc developed on oceanic or marginal basin sediments (Slide Mountain terrane) extending for the full length of the Canadian section of the Cordillera in Late Triassic time. This is considered to be the result of motion of the upper plate away from the already established subduction zone, thus creating the extensional environment for arc formation. Change in relative plate motion to a contractional mode is considered to have commenced underplating of this arc, calc-alkaline magmatism in the upper plate and eventual collision with the North American continent (Monger, 1989). This was the first of two episodes of arc-continent collision that are recognised as having caused compression and inversion of the Palaeozoic sedimentary basins and, through crustal thickening, the formation of first the Omineca, then the Coast plutonic-metamorphic belts. The two episodes of accretion are reported to be first Middle Jurassic (Monger et al., 1982; but the geochronology of Hansen, 1992 and of this study would indicate collision earlier in the Jurassic) for Terrane 1 and then Cretaceous to Tertiary time for Terrane 2 (Monger et al., 1982).Terrane 1 or the Intermontane Superterrane (Gabrielse and Yorath, 1990) is composed of the Stikine and Cache Creek terranes in the north (Yukon and adjacent British Columbia) and Stikine, Quesnel and Slide Mountain terranes in southern British Columbia Superterrane 2 is composed of the Alexander and Wrangellia terranes (Figs. 2.1, 2.2). In Alaska collision of Wrangellia with the continental margin has been dated as ≈115 Ma (Jones et al., 1986). Terrane boundaries are predominantly crustal-scale thrust faults (Monger, 1989).

The crustal structure resulting from accretion of these two superterranes is one of stacking: Jurassic accretion thrust parautochthonous high-grade metamorphics onto the craton, structurally below Palaeozoic metamorphics and sediments to form the Omineca Belt in the southern Canadian Cordillera. The crystalline basement below the Omineca was shortened by perhaps 50% by formation of east-verging thrust duplexes in Cretaceous to Paleocene time (Parrish et al., 1988). Two models have been proposed for

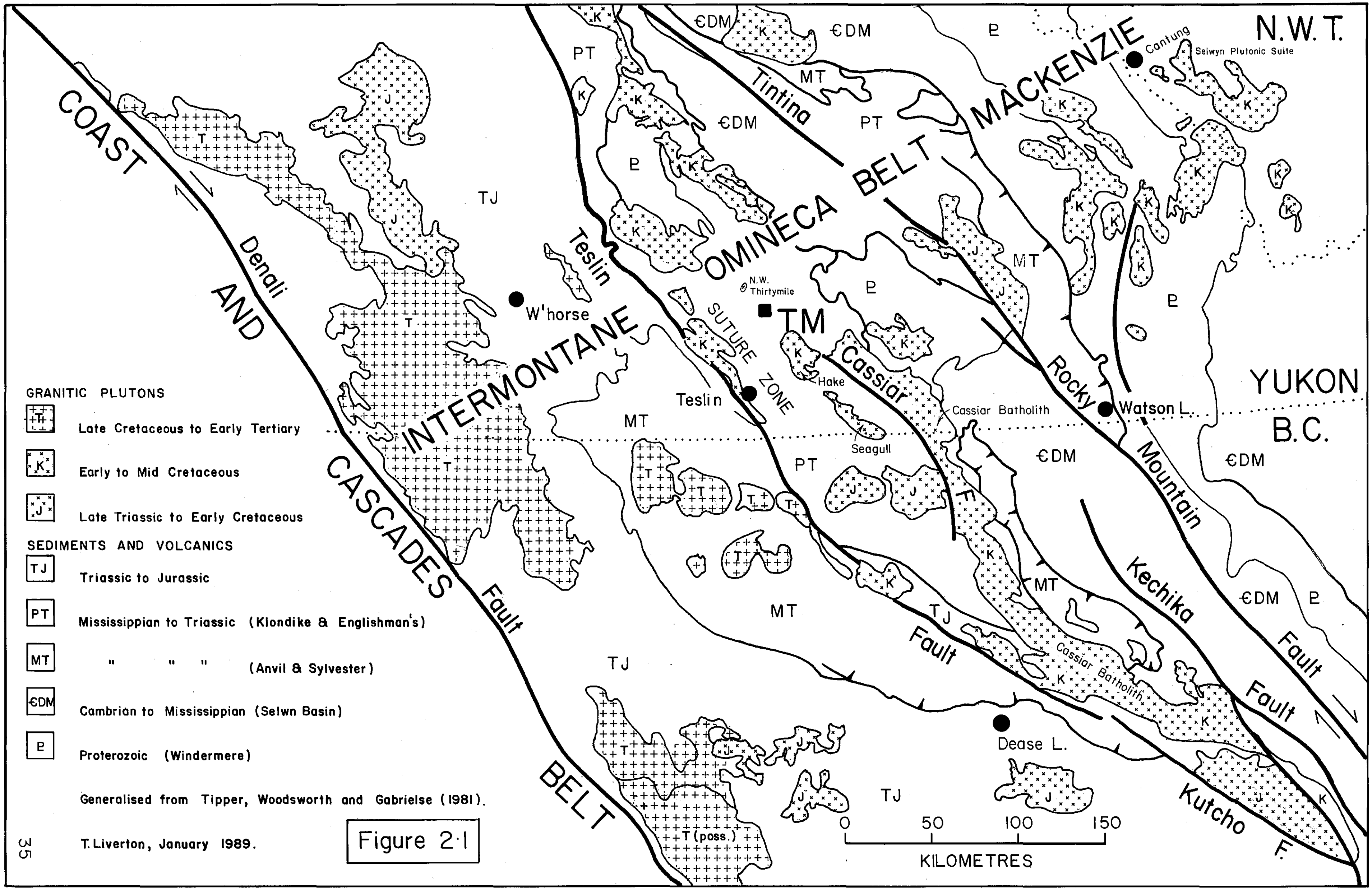

Generalised from Tipper, Woodsworth and Gabrielse (1981).

T.Liverton, January 1989.

Figure 2·1

the details of crustal structure produced by terrane 1 collision: obduction and eastward underthrusting of sialic crust as a result of eastward subduction of the Slide Mountain terrane (the oceanic crust to the east of Quesnellia microcontinent: Brown et al., 1986) and obduction with wedging of lower crustal basement (Price, 1986). Both models consider that the North American basement extended beneath the imbricated Omineca belt, which is in accordance with seismic reflection data that indicates that in southern British Columbia the North American basement extends westwards beneath the Purcell anticlinorium, but has thinned from 35 km thickness below the Rocky Mountain Trench to about 20 km further west (Cook et al., 1988). In coastal British Columbia accreted terranes structurally underlie the Coast and Insular belts as a result of Cretaceous crustal shortening by underthrusting (Monger, 1989). The Insular superterrane is bounded by east-verging thrusts to the east and a west-vergent thrust zone on its west edge against remnants of Cretaceous and Tertiary accretionary prisms (Yorath, 1985; Monger, 1989).

2.2.3 TRANSCURRENT FAULTING

A change from orthogonal to oblique convergence of the Pacific (Farallon) and continental plates occurred in late Cretaceous time (Engbretson et al., 1985) which initiated dextral transcurrent motion of the obducting terranes against the craton. This change in plate motion is considered to be the result of development of a mantle 'super-plume' in the Pacific, with a maximum in crust formation from 125-100 Ma (Larson, 1991). The distance of translation of the accreted terranes northward is large, but estimates from palaeontological, palaeomagnetic and geological correlation are at variance. Jones et al. (1986) quote palaeomagnetic data indicating that the Alaskan portion of Wrangellia may have been displaced up to 3100 km northward and rotated 90° anticlockwise. Irving and Wynne (1990) suggest approximately 2000 km northward translation of parts of the Coast belt. Palaeontological correlation suggests hundreds of kilometres displacement (see discussion in Monger, 1989) in the Canadian part of the Cordillera. Geological correlations indicate at least 750 km combined strike-slip on the Tintina-Rocky Mountain fault system (Fig. 2.3) and movement on faults to the west are >100 km (Gabrielse, 1985). Palaeomagnetic data for part of the Slide Mountain terrane, between these systems, is in agreement with this magnitude of displacement (Butler et

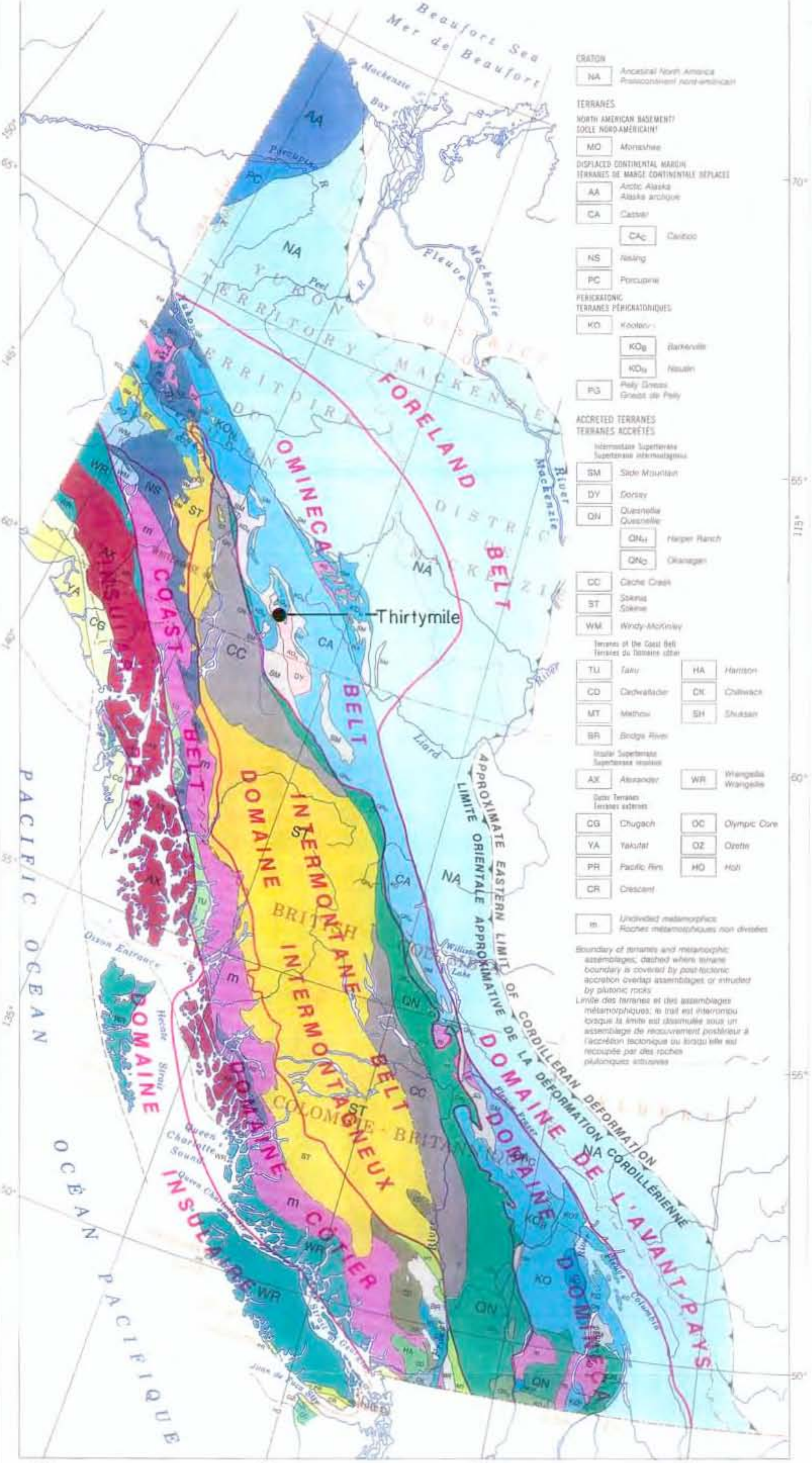

Figure 2.2 Major terranes of the Canadian Cordillera. After Wheeler & McFeely (1991).

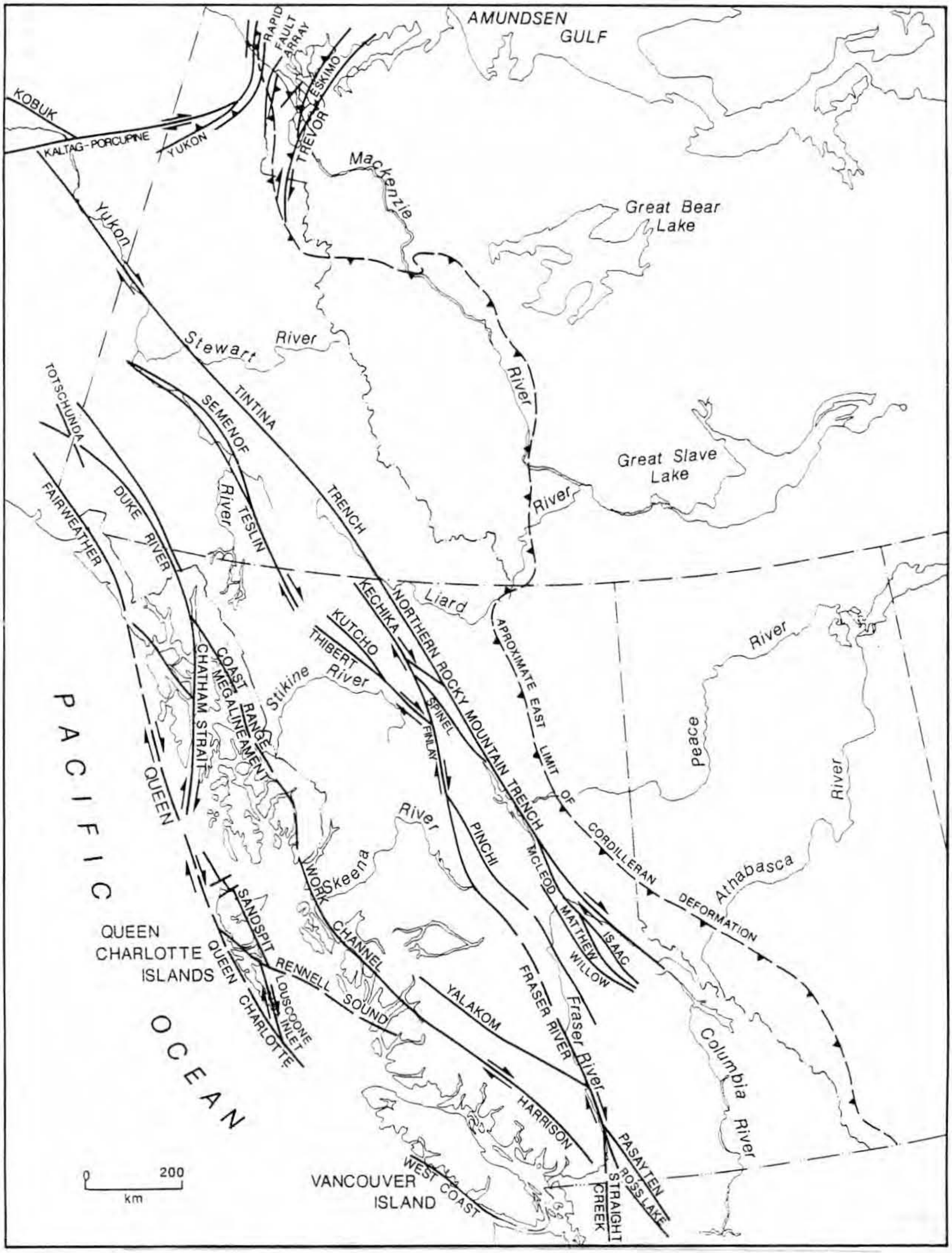

Figure 2.3 Major fault systems of the Canadian Cordillera (after Gabrielse and Yorath, 1989).

al., 1985). The paradox of estimates of the amount of terrane displacement made by stratigraphic correlation being different from some palaeomagnetic data is partially resolved once displacements on the Tintina-Rocky Mountain trench and Fraser River-Straight Creek fault zones are fitted to small-circle trajectories and a common pole of rotation (Price and Carmichael, 1986). Post Middle Cretaceous strike-slip of 450 km is estimated for the former system in southern British Columbia and estimates for the latter vary from 80 to 1100 km. Much of the displacement on these faults in southern British Columbia has occurred as right-hand oblique convergence, that is responsible for the greater amount of crustal shortening in the south of the Province, and which accounts partly for smaller geological displacement estimates (Price and Carmichael, 1986).

2.2.4 CENOZOIC EXTENSION

Local extension during the early Eocene resulted in formation of east-dipping crustal scale normal faults that cut the upper portions of major thrusts. These thrusts were then reactivated as extensional faults. This extension resulted in uplift of the Omineca and exposure of core complexes (Coney, 1980; Brown and Read, 1983; Simony et al., 1980; Plint et al., 1992) in southern British Columbia and also in the Horseranch Range, at the eastern edge of the Omineca belt 140 km SE of the study area. Local extension also along the Tintina structure at 50 Ma is indicated by extrusion of bimodal volcanic suites (Jackson, et al., 1986; Pride, 1988).

2.2.5 MAGMATISM IN THE NORTHERN CORDILLERA

The widely varying tectonic setting of magmatism, particularly the source-regions for magmas are reflected in their isotopic compositions. Initial Sr isotopic compositions of $^{87}Sr/^{86}Sr$ greater than 0.706 are considered indicative of genesis from, or assimilation of, Precambrian crust or its underlying lithospheric mantle in the U.S.A. (Miller et al., 1990; Armstrong, 1988). Ratios of 0.703 to 0.704 are indicative of an island arc setting (Armstrong, 1988).

The Sr initial ratios in the Insular, Coast and Intermontane Belts are commonly less than 0.704, but those of the Omineca and and Rocky Mountain-Mackenzie belts are invariably greater, demonstrating a difference between the miogeoclinal and eugeoclinal parts of the Cordillera (Armstrong, 1988). The southern Coast Plutonic Complex has ratios comparable to Vancouver Island (≤0.704, irrespective of age) and suggestive of an arc or ocean island setting derived from young basement. The north Coast Plutonic Complex shows a range from 0.704-0.706, correlating with a change from Wrangellia to the older Alexander Terrane basement and late Precambrian basement of the Stikine Terrane. In the Intermontane Belt Mesozoic rocks show low ratios, but those of early Cenozoic age have more radiogenic Sr, indicating the evolution of sufficiently thick radiogenic crust to be involved in magma generation (Armstrong, 1988).

The Omineca Belt, particularly the Yukon portion, shows a wide variety of initial ratios: Jurassic and early Cenozoic magmas show a range of $^{87}Sr/^{86}Sr$ from 0.704 to 0.712, indicating a variable crustal component to the magmas. Mid Cretaceous ratios range from commonly >0.710 to occasionally >0.730, over a strike length of 2000 km. Such exceptionally radiogenic magmas are considered to be a result of significantly elevated lower-crustal temperatures having existed during that time to produce much crustal contamination of magma and anatexis, which was coincident with the Rocky Mountain deformation (Armstrong, 1988).

The various episodes of magmatic activity were:

1) The interval of 200-155 Ma produced magmatism on the N. American continent only after 180 Ma. The earlier magmatism is recorded in the accreted terranes.

2) 155-140 Ma: A few plutons from the last arc magmatism intruded Wrangellia, Quesnel and Stikine terranes.

3) 135-125 Ma marked a major hiatus in magmatism.

4) 110-90 Ma: Produced widespread plutonism in all terranes, culminating in both the plutonic belts. In the study area the Cassiar and Seagull-Thirtymile suites were generated during this interval.

5) 55-45 Ma Was again a period of widespread magmatism in all terranes causing resetting of isotopic ratios in metamorphic areas of both plutonic belts (extension-related volcanism).

This periodicity of magmatism is linked to brief periods of extension in the history of the Mesozoic-Cenozoic Cordillera (Armstrong, 1990). The last two culminations in magmatism are well represented in the southern Yukon: the Albian by granitic plutonism

(Gabrielse et al., 1980; Sinclair, 1986) and the Eocene by extrusion of olivine basalt (e.g. Jackson, et al., 1986; Pride, 1988).

2.3 THE NORTHERN CANADIAN CORDILLERA

2.3.1 TERRANE BOUNDARIES

The Teslin fault system marks the Eastern boundary of the Intermontane belt in the southern Yukon (Tempelman-Kluit, 1979; Hansen, 1986) and in northern British Columbia this boundary continues its SE trend along the Kutcho fault system (Gabrielse and Yorath, 1990; Wheeler and McFeely, 1991). In the southern Yukon the Cache Creek terrane forms a 110 km wide allochthon that is terminated to the east by this fault system. Low metamorphic grade volcanics and sediments of the Quesnel terrane are present as discontinuous, narrow fault slices of the Nicola assemblage along the Teslin fault system. The Teslin suture zone consists of fault-bounded, amphibolite-grade tectonites of the pericratonic Nisutlin allochthon and parautochthonous tectonites developed at the leading edge of the craton i.e. Cassiar terrane (Wheeler and McFeely, 1991; Hansen, 1992).

2.3.2 THE TESLIN SUTURE

The tectonic model postulated for the development of the Teslin suture is: a west-dipping subduction complex formed on the distal side of the ocean (now preserved as the obducted fragments of the Cache Creek terrane) that separated the island arc of Superterrane 1 from North America and which was active during Permo-Triassic time. Continued subduction resulted in A-type subduction of the edge of the continental margin which underplated the continental rocks onto the accreted terrane at a depth beneath that of the brittle-ductile transition zone. The tectonites so formed were uplifted en-masse in Early Jurassic time due to continued continental subduction (Hansen, 1992).

Metamorphic fabrics and isotopic compositions of tectonites in the Teslin suture (Fig. 2.1) also provide data concerning the geometry of continent-arc collision and timing of deformation. The tectonites (formerly called the Yukon-Tanana terrane) show two fabrics: an early fabric developed during dip-slip deformation and a later dextral strike-slip fabric. This ductile deformation postdates orthogneiss primary crystallisation and precedes early Jurassic cooling (Hansen, 1986 a & b; Hansen et al., 1989). The Yukon-Tanana terrane has been subdivided into two separate terranes by Hansen (1990): the Nisling terrane tectonites have early Cretaceous cooling ages, are Devonian-Mississippian orthogneisses derived from an early Proterozoic source (from U-Pb inheritance and Sm/Nd model ages) i.e., they are North American continental margin crust, and represent a lower structural level than the Teslin-Taylor Mountain terrane. The Teslin-Taylor Mountain terrane is an inverted sequence of greenschist to amphibolite grade metamorphics with local blueschist yielding maximum P, T estimates of 575-750°C and which had cooled by late Jurassic time. The Teslin-Taylor Mountain terrane is interpreted to have been transported over the parautochthonous Nisling terrane at that time (Hansen, 1990; 1992). A collision zone oblique to the continental margin is postulated for Permo-Triassic time, involving subduction of the oceanic terrane toward the west. Deformation of the Teslin Suture tectonites, therefore, occurred in the hanging-wall of this subduction zone which was obducted onto the deformed continental margin (Cassiar tectonites) in the late Early Triassic (Hansen, 1992).

2.3.3 THE DORSEY TERRANE

This study is concerned with the Dorsey terrane (Fig. 2.2) which is found immediately east of the Teslin suture metamorphics. It is a fault-bounded unit that is described as: an "Upper unit of chert, quartzite, slate-clast conglomerate, grit, quartzite, ribbon chert and slate and a lower unit of quartzite, argillite and chert interbeds separated by crinoidal and chert nodule limestone; marine" (Wheeler and McFeely, 1992). It is considered to be an accreted terrane of the Intermontane Superterrane by those authors. Correlation of the Devonian-Carboniferous sediments and meta-volcanics now included in the Dorsey terrane is disputable due to deformation, the near certainty that unrelated units are juxtaposed, and sparse fossils (Abbott, 1981).

The eastern limits and stratigraphic correlation within this terrane require much more field work to be confidently defined. At the eastern edge of this study area metavolcanics have been tentatively correlated with the Anvil Allochthon (Unit CPav of Abbott, 1981), i.e. the Slide Mountain terrane (Wheeler and McFeely, 1991); foliated intrusions (Ram Stock) considered allochthonous and correlated with the Simpson

Allochthon (Abbott, 1981; see Tempelman-Kluit, 1979, for the regional context) and the clastic and the carbonate and volcanic succession (Abbott, 1981 units PMs1-6) correlated with the Nisutlin Allochthon. The whole eastern part of the Yukon Cataclastic Complex is considered to be allochthonous by Abbott (1981), and this 'complex' may include a melange of diverse terranes and not be one tectono-stratigraphic unit.

Current fieldwork (Gordey, 1992; Harms, 1992; Liverton, 1992) indicates that the clastic metasediments in the Thirtymile Range (Fig. 2.4), which form an east verging thrust stack, are more plausibly correlated with the North American Palaeozoic assemblages, rather than with the accreted Intermontane terranes. The Dorsey terrane is therefore likely parautochthonous. It has been intruded by two deformed diorite to quartz-monzonite stocks, two small undeformed batholiths (Seagull and Hake), six granitic stocks and three undeformed diorite to quartz monzonite stocks (Logjam). K-Ar dating of the Seagull batholith indicates cooling ages of 97 Ma (Gabrielse et al., 1980) and 100.3± 1.1 Ma (Sinclair, 1987).

The eastern limit of the Dorsey Terrane is probably the fault system along the upper Swift River (Fig. 2.5). Inclusion of the siliciclastic units in the Swift River-Munson area within the Dorsey terrane by Wheeler and McFeely (1991) implies correlation with the Englishmans Group. These clastic sediments are lithologically similar to those of the Thirtymile Range, contain similar sub-horizontal zones of mylonite and may well be correlable. The east-verging thrust fault system in the Swift River connects with the Cassiar fault, which is a dextral transcurrent structure that forms the west contact of the Cassiar batholith. Intrusion of this pluton places one constraint on the timing of transport of the Dorsey terrane. Ductile deformation of an already-crystallised Cassiar pluton is indicated by formation of narrow mylonite zones over a distance of several hundred metres into the batholith (Gabrielse, 1985; this study). The Cassiar batholith is otherwise undeformed and yields K-Ar cooling ages of from 98-105 Ma in the north (Gabrielse et al., 1980) and 102-105 Ma in the British Columbia portion (Souther et al., 1979). Where its intrusive contacts are preserved it has cut the Slide Mountain terrane in the north; the Upper Proterozoic Windermere equivalent assemblage and Proterozoic to Cambrian continental-margin sediments of the Cassiar terrane on the northeast. Emplacement of this batholith therefore postdates the imbrication of the craton margin and emplacement of the Slide Mountain and Dorsey allochthons, but predates transcurrent faulting that is likely to

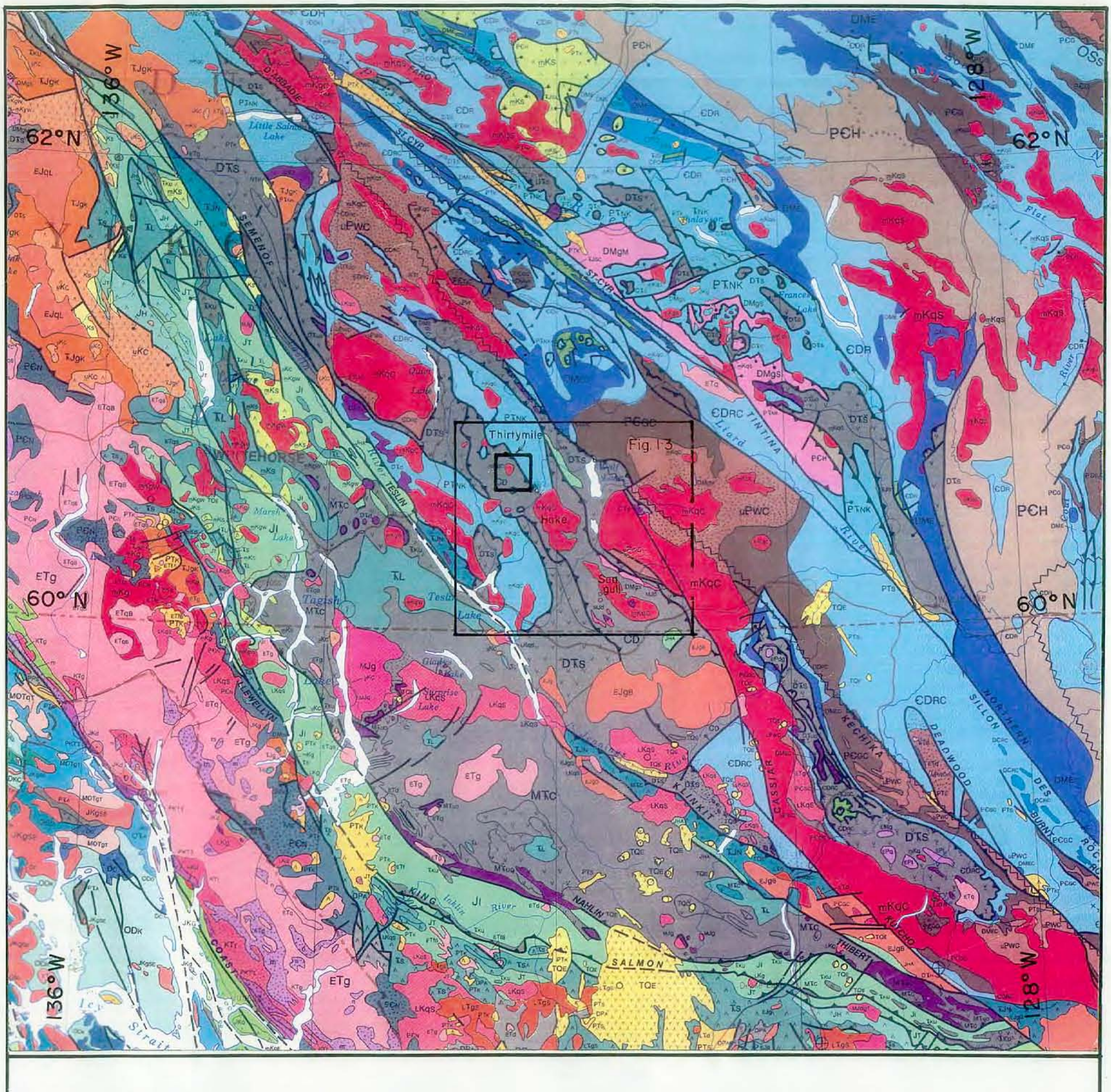

The location of the Thirtymile 1:25,000 scale map (Appendix B1) area is outlined, as well as the index map Fig. 1·3

TQE	**QUATERNARY**	Edziza transtensional rift volcanics	
PTK	**PALEOGENE**	Transtensional arc volcanics	
KTI	**CRETACEOUS TO TERTIARY**	Tonalite	(Coast Plutonic Complex)
KTg		Granodiorite	(Coast Plutonic Complex)
LKqs	**LATE CRETACEOUS**	Alaskite, granite	
mKqc	**MIDDLE CRETACEOUS**	Quartz monzonite and granodiorite	
JK	**L. JURASSIC TO E. CRET.**	Granodiorite, quartz diorite	
JKgse		Hornblende-biotite granodiorite (St. Elias)	
JKg		Gabbro	
JH	**JURASSIC**	Hazelton volcanics	*Stikinia*
JI		Inklin volcanics (above Cache Creek terrane)	
JT		Takwahoni Stikinia-derived clastics	
TRJN	**TRIASSIC TO JURASSIC**	Nicola arc volcanics	***Quesnellia***
TRL		Lewes River clastics	*Cache Creek terrane*
TRJgk		Foliated granodiorite (Klotassin batholith)	

MTRC	**MISS. TO U. TRIASSIC**	Volcanics & sediments	*Cache Creek terrane*
DTRS	**DEVONIAN TO TRIASSIC**	Oceanic basin volcanics & sediments	***Slide Mt. terrane***
DPA	**DEVONIAN TO PERMIAN**	Metasediments & greenstone	
DMEC	**DEVONIAN TO MISS.**	Clastic wedge sediments (Earn Group)	
OTRA	**ORDOVICIAN TO TRIASSIC**	Phyllite	*Alexander terrane*
OSD	**ORDOVICIAN TO SILURIAN**	Descon ocean arc volcanics	
ODK	**ORDOVICIAN TO DEVONIAN**	Kaskawulsh back-arc carbonate and pelite	
ЄDN	**CAMBRIAN TO DEVONIAN**	Nasina carbonaceous offshore sediments	
ЄDR		Passive margin sediments (includes Road River)	
ЄDRC		Passive margin sediments	
PTRNK	**U. PROT. TO TRIASSIC**	Nisutlin clastics & volcanics	*Kootenay terrane*
Cd	**U. PROT. TO MISS.**	Continental margin sediments	*Dorsey terrane*
PЄH	**U. PROT. TO CAMBRIAN**	Hyland clastic continental margin sediments	
PЄN		Nisling metamorphosed continental margin sediments	
uPWC	**U. PROTEROZOIC**	Windermere continental margin sediments	

Fig. 2.4 TECTONO-STRATIGRAPHIC UNITS OF THE YUKON-BRITISH COLUMBIA BORDER REGION
(After Wheeler & McFeely, 1991)

be linked to the Tintina fault system.

2.4 REGIONAL GEOLOGY OF THE STUDY AREA

2.4.1 THE ENGLISHMANS GROUP

In the south-central Yukon the youngest autochthonous strata are Triassic marine clastic sediments, although sequences preserved are east of the study area. Allochthons of cataclasite, ophiolite and deformed granitic intrusives are now found over 100 km NE of the Mesozoic Teslin suture zone (Tempelman-Kluit, 1979; Gordey, 1982).

The first low grade metasediments encountered to the east of the suture in the study area are units 2 and 3 of Mulligan (1963): the Englishmans Group, that forms the Thirtymile and Englishmans Ranges and is the principal component of the Dorsey terrane. The Englishmans Group is subdivided into three principal informal lithologic divisions by Mulligan:

1) Unit 2. "Intermittent bands of fossiliferous limestone".
2) Unit 3, unsubdivided: "Argillaceous quartzite, slate; phyllite, chert".
   Unit 3, where subdivided: "3a, arkosic grit; 3b, conglomerate; 3c, limestone; 3d, greenstone".
3) Unit 3A: "Quartzose and argillaceous schist and phyllite; minor limestone, mainly equivalent to 2 and 3, but in part to 1, and in part of uncertain age". This includes the phyllite-phyllonite unit mapped in this study to the NW of Thirtymile Lake (Chapter 3).

No fossils were reported by Mulligan from the limestone (marble) members within unit 3. Unit 2 carbonates are reported to contain Spiriferid brachiopods, Lithostrotion and Triplophyllum corals which were assigned to Middle Mississippian age (Mulligan, 1963, p.28). On the basis that unit 3 overlies unit 2, Mulligan also assigned it a Mississippian age. Units 3 a to d are all represented in the study area, although the greenstone has been observed only as two tiny tectonic slices in this study. More extensive exposures of basic volcanics are reported from immediately SW of the study area by Harms (1992).

The scale of deformation within the clastic metasediments of unit 3 was not described by Mulligan, who remarks only on occasional "sheared conglomerates" and flat-lying cleavage in the SW part of the Thirtymile Range and highly folded quartzite and phyllite to the NW of Thirtymile Lake.

Current mapping indicates that the stratigraphy of the Thirtymile Range is discontinuous along strike and disrupted by many flat-lying and steep normal faults (Gordey, 1992; Liverton, 1992). Tentative correlation has been made between quartz sandstone units in the Range (Gordey, 1992 loc. 3: c.f. Chapter 4 unit C) and the Proterozoic to Lower Cambrian Ingenika Group, and overlying cherts with the Ordovician to Devonian Road River Group.

Basalt and pyroclastics are reported from the upper portion of the sandstone unit, immediately south of the area mapped in this study (Harms, 1992), which may correlate with volcanics reported by Gordey (his locality 1) and which are possibly correlable with Mississippian North American strata (Gordey, 1992).

To the SE of the Thirtymile Range a succession of thin, at least partly fault-bounded, slices of from possible Proterozoic (Windermere equivalent) quartzite through Cambrian to Silurian limestone and dolomite to Devono-Mississippian greenstone, siliclastic sediments and minor carbonates is exposed to the north of the Seagull batholith. These units consist of imbricated Cassiar terrane plus a horse of Slide Mountain terrane (greenstone, Unit 7a). An extensive Devono-Mississippian sequence (i.e. Dorsey terrane) is exposed to the south of the granite. The regional attitudes of bedding suggest a very broad synformal structure (Fig. 2.5) across the Dorsey Range (Poole et al., 1960), however many of the major contacts are faulted, lithologic units show zones of shearing or mylonitisation and have little strike continuity. Superposition by thrust faulting has been suggested (Abbott, 1981). This part of the 'Yukon Cataclastic Complex' (Abbott, 1981), or Dorsey terrane, may best be interpreted as an east-verging imbricate structure (Abbott, pers. comm; Bremner and Liverton, 1991).

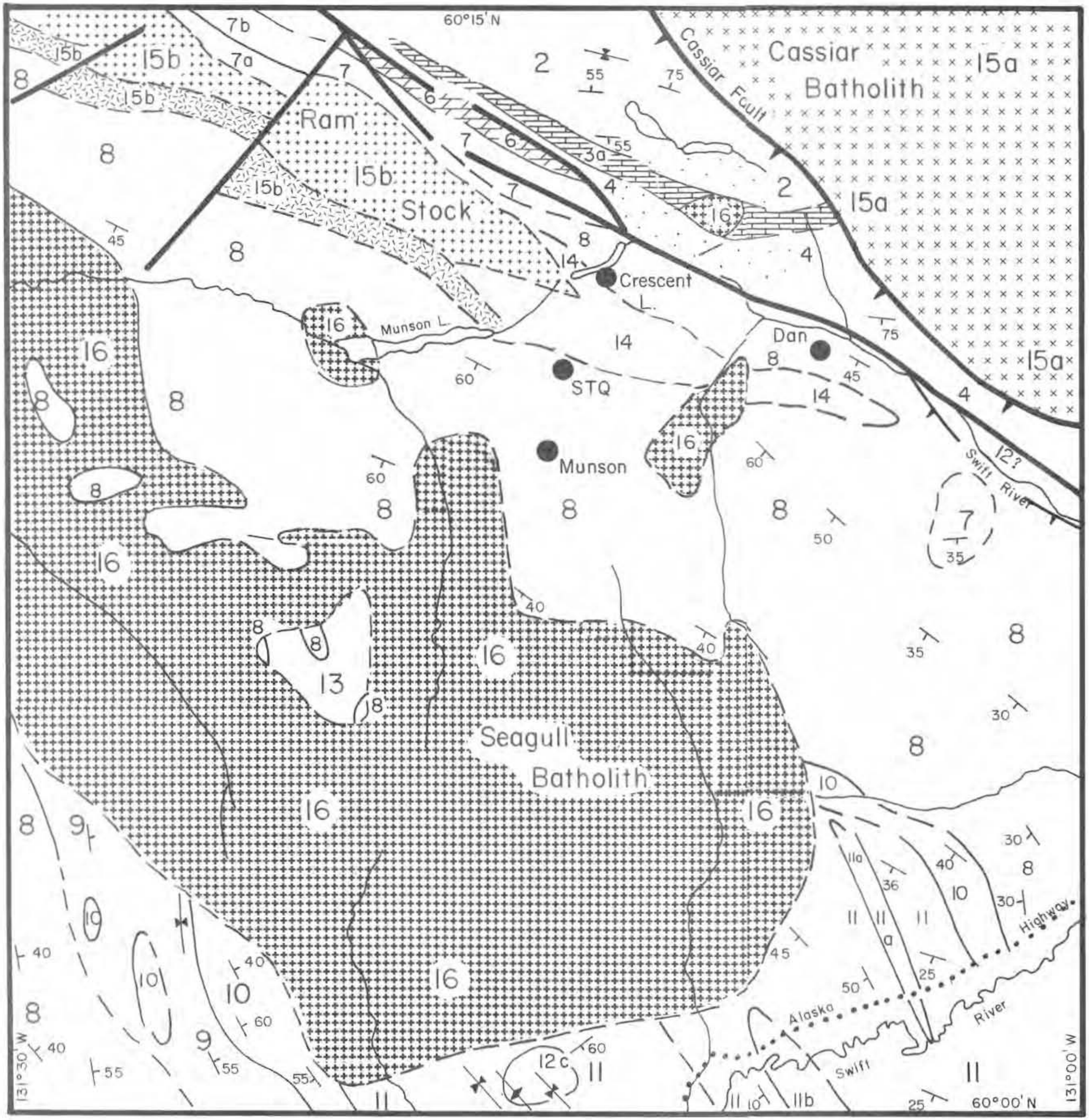

LEGEND

		INTRUSIONS
16	Cretaceous	Seagull batholith: quartz monzonite to granite.
15a	Cretaceous	Cassiar batholith: quartz monzonite.
15b	Jurassic to Cretaceous	Ram stock: quartz monzonite and diorite (dashes).
14	Jurassic to Cretaceous	Diorite stocks.
13	Jurassic to Cretaceous	Ultramafics: pyroxenite and serpentine.
		SLIDE MOUNTAIN TERRANE
12	Permian to Triassic (?)	Greenstone.
		DORSEY TERRANE
11	Lower to Mid Mississippian	Chert, slate argillite, minor greywacke; (a) limestone and dolomite (b) sandy and conglomeratic tuff.
10	Lower to Mid Mississippian	Chert, conglomerate, chert and quartzite pebble conglomerate, chert, quartzite, slate and hornfels.
9	Devonian to L. Mississippian	Limestone, dolomite (chert nodules) and skarn.
8	Devonian to L. Mississippian	Chert, hornfels, argillite, slate, phyllite, quartzite, tremolite marble, dolomite and skarn.
7	U. Dev. to L. Mississippian	Greenstone, chlorite schist, quartzite, phyllite, slate and chert.
		CASSIAR TERRANE
6	M.Silurian to M. Devonian	Foetid dolomite, quartzite and dolomitic quartzite.
4	M. Cambrian to M. Silurian	Slate, phyllite and limestone.
2	L. Cambrian ?	Quartzite, slate, phyllite, grit and conglomerate.

Fig. 2.5 Geology of Map sheet 105 B-3: the Swift River region.
After Poole, Roddick and Greene (1960) and Abbott (1981). Mineral prospects shown are (1) Skarns: Dan, Crescent L., Munson and (2) Tin stockwork: STQ.

5 km

Figure 2·5

NTS MAP SHEET 105B-3

2.4.2 IGNEOUS INTRUSIONS

The various igneous intrusions in the Thirtymile-Englishmans-Seagull area are (Fig. 1.3):

1) Four undeformed stocks of mappable scale in the Thirtymile Range (undifferentiated granite to gabbro in Mulligan (1963). Three have been included in this study, the small SE stock being inaccessible. These stocks are assumed to be Cretaceous, without isotopi data by Mulligan (1963). The sizes and location of the intrusions are:

(a) NW of Thirtymile Lake: Topographic map sheet 105C-15; outcrop 3x5 km; hornblende monzogranodiorite (NW Thirtymile stock in this study).

(b) Thirtymile: Map 105C-9; outcrop 4.5x5 km; biotite granite to Li-mica topaz leucogranite; plus Ork stock (outcrop <0.5 km across): Li-mica topaz leucogranite (this study) and dated at 101 Ma (Thirtymile stock: this study).

(c) SW Thirtymile: Map 105C-9; outcrop 2x4 km (Mulligan, 1963), gabbro to hornblende quartz diorite. Western contact extends to and truncated by hornblende granodiorite (this study) that outcrops over 6x9 km (Mulligan, 1963).

(d) SE Thirtymile: Map 105C-9; outcrop 1.5x1.5 km (Mulligan, 1963).

2) Hake batholith: Topographic map sheets 105C-8&9 and 105B-4&5; outcrop 19x28 km assumed Cretaceous (Mulligan, 1963) or Cretaceous to Tertiary and described as biotite quartz monzonite to granodiorite (Poole et al., 1960). Porphyritic to megacrystic biotite granite and granophyre (this study).

3) Seagull batholith: Map sheets 105B 3&4; outcrop 11x43 km with a NW-SE elongation; described similarly to (2) in Poole et al., (1960). Minor east to NE striking normal faults cut the batholith (Abbott, 1981). Ages: 100.27±1.11 and 101±4 Ma with a Sr_i= 0.712 (Sinclair, 1986) and K-Ar age of 97 Ma (Gabrielse et al., 1980). Porphyritic to even-grained biotite granite (this study).

4) Diorite stocks: maximum outcrop 2x5 km; 105B 3&4; assumed to be Jurassic (Poole et al., 1960). The Logtung stock has yielded ages of 109±2 and 118±2, with Sr_i= 0.708 (Sinclair, 1986).

5) Ram stock: outcrop 3x26 km; sheets 105C-3&5; saussuritised, sheared, biotite-hornblende quartz monzonite Mapped as Jurassic, without isotopic data (Poole et al., 1960).

Considered allochthonous by Abbott (1981).

6) Cassiar batholith. The NW tip of the batholith is exposed immediately to the NE of the study area (centre of 1:250,000 sheet 105B). The western margin of the batholith is bounded by a complex fault system that likely postdates deformation of the Yukon Cataclastic Complex. Evidence for both normal and dextral strike-slip movement on this structure exists (Abbott, 1981). The batholith is likely composite and a variety of ages are published for granite intrusions that have been previously mapped as part of the same batholith: Biotite K-Ar ages= 98-101 Ma, muscovite K-Ar ages= 87-105 Ma for specimens from the batholith in the Yukon (Gabrielse et al., 1980); Ash Mountain area, 80±4 Ma, Mt. Haskin intrusion, 52.6±1.6 Ma with Sr_i= 0.710 (Sinclair, 1986). The amount of erosion of the Cassiar batholith may be greater than that of the Seagull batholith, which still displays roof pendants, reflecting relative east-block-up throw on the largely transcurrent Cassiar fault (Abbott, 1981).

2.4.3 GRANITE-RELATED MINERALISATION

MAP SHEETS 104O & P, 105B & C:

Tin mineralisation is known from a few prospects around the Cassiar batholith, many localities peripheral to the Seagull batholith and from the Thirtymile Range. In contrast, scheelite prospects are widespread.

(1) Cassiar batholith: Tin-tungsten mineralisation in quartz vein stockworks close to the Cassiar batholith has been prospected since 1945 (Yukon Tungsten or Fiddler prospect: NTS sheet 105 B 1; Mulligan, 1968 p.4 loc. 36). Sn-bearing silicate minerals are known from the Blue Light (59°39'N, 130°28'W) and Ash Mountain (59° 18N, 130°31'W) prospects and in Be-bearing magnetite skarn at Needlepoint mountain (104 P 4), 20 km south of Cassiar, B.C. (Mulligan, 1968). Scheelite prospects are widespread throughout the aureole of this granite. Sn-rich garnet veins are found at the Mt. Reed scheelite prospect near Cassiar, B.C. (NTS Ref. 105P-6; U.T.M. 747739: Canadian Superior Exploration, 1981 unpublished data).

(2) Seagull batholith: tin stockwork prospects discovered adjacent to the Seagull batholith during the 1970s are the DU and STQ properties (Fig. 1.3). These are

respectively: immediately adjacent to the west contact of the batholith and above a stock intersected by diamond drilling 3 km north of the main granite (Fig. 2.6). The JC Sn-F skarn deposit is of significant size ($2x10^6$ tonnes) and is found in the aureole of a small apophysis at the NW end of the batholith (Layne and Spooner, 1986).

(3) Hake batholith: a gold-bearing skarn is reported to be associated with the Hake batholith (Mulligan, 1963) and the Bar zinc prospect (Fig. 1.3) is also likely underlain by that granite. Opinions differ as to the type of deposit (J. Moran; K. Dawson, pers. comm., 1987) it could be Devonian stratiform mineralisation rather than a skarn (Gordey, 1992).

(4) Thirtymile Range: B-F mineralisation and untested Sn-W geochemical anomalies exist adjacent to the Ork stock (Stephen and Mysyk, 1980; Campbell and Stephens, 1982). The Mindy prospect consists of magnetite-rich F-B-Sn±W skarns 3 km east, above a postulated unexposed stock (Nebocat, 1981 &1982).

2.5 SUMMARY

The study area is at the western margin of the Omineca Belt in the northern Canadian Cordillera. This metamorphic-plutonic belt is considered to have been formed by compression and crustal thickening caused by the late Jurassic to early Cretaceous 'docking' of a Triassic amalgamation of island arc terranes against the North American margin. Deformation of the immediate margin and of oceanic crustal material from the allochthon is recorded in the Teslin Suture metamorphics (Hansen, 1986, Hansen et al, 1989) and obducted ophiolitic material forms klippen displaced up to 120 km inboard of the suture (Tempelman-Kluit, 1979). Uplift of portion of the suture during the Jurassic by thrust faulting (Hansen, 1989) resulted in easterly transport of imbricated continental margin. A major contractional fault system, 120 km inland of the suture-the Tintina Fault-was active in Late Cretaceous time, when motion of the Pacific plates relative to N. America changed (Engebretson et al., 1985) and strike-slip motion became dominant. Timing of the compressional movement coincides with that estimated for the 'docking' of Wrangellia against North America and the accreted terranes (≈115 Ma in Alaska: Jones et al., 1986). Initiation of strike-slip movement on the Tintina Fault is approximately contemporaneous with the emplacement of Late Middle Cretaceous granitic intrusions. This plutonism was widespread in a narrow region between the Suture and Tintina Fault, forming the 300 km long Cassiar batholith and the smaller, slightly younger Seagull and Hake batholiths. Sn-quartz stockwork, F-B-Sn±W skarn and Zn skarn mineralisation is spatially associated with these plutons. Correlation of the siliciclastic metasediments of the study area is open to debate: they may be parautochthonous (Gordey, 1992; Harms, 1992; and this study), or allochthonous as suggested in Abbott (1981).

CHAPTER 3

GEOLOGY OF THE THIRTYMILE AND ENGLISHMANS RANGES

CHAPTER 3: GEOLOGY OF THE THIRTYMILE & ENGLISHMAN'S RANGES

3.1 INTRODUCTION

The two areas mapped and compiled at 1:25,000 scale are in the north and central parts of the Thirtymile Range and are within the Dorsey terrane the geology of which has been introduced in sections 2.3.3 to 2.4.2. Sampling at a reconnaissance scale and limited mapping has been performed over the Hake and Seagull batholiths that outcrop in the Englishmans and Dorsey Ranges (Fig. 1.3).

3.2 THE THIRTYMILE RANGE

3.2.1 ENGLISHMANS GROUP.

At a cursory examination the Englishman's Group appears to be a gently-warped sedimentary sequence of chert and siliciclastic sediments containing one major and several smaller marble beds. It has been mapped as such by Mulligan (1963) and exploration geologists (Stephen, 1981). Closer examination reveals that some lithologic units are obviously fault-bounded e.g. the marble at U.T.M. grid {443249} (Appendices B.1 & B.2), a near-horizontal slaty cleavage pervades the finer-grained pelites and a flat-lying anastomosing pressure-solution cleavage penetrates the coarser-grained lithologies. The Englishmans Group might be considered a tectonic mélange within the very broad definition of Raymond (1984). Disruption of the metasediments is such that individual lithologic units can only be traced laterally for distances of less than 5 km. Two tectonic slices of volcanics, with no local equivalent and more extensive phyllonite units are found within the thrust-faulted sequence of siliciclastic metasediments. One exposure of volcanics mapped in this study is probably that mentioned by Mulligan at 60°43'N, 132°31'W. Recent work (Harms, 1992) has shown that more extensive volcanics are found immediately south of the area mapped in the Thirtymile Range for this study.

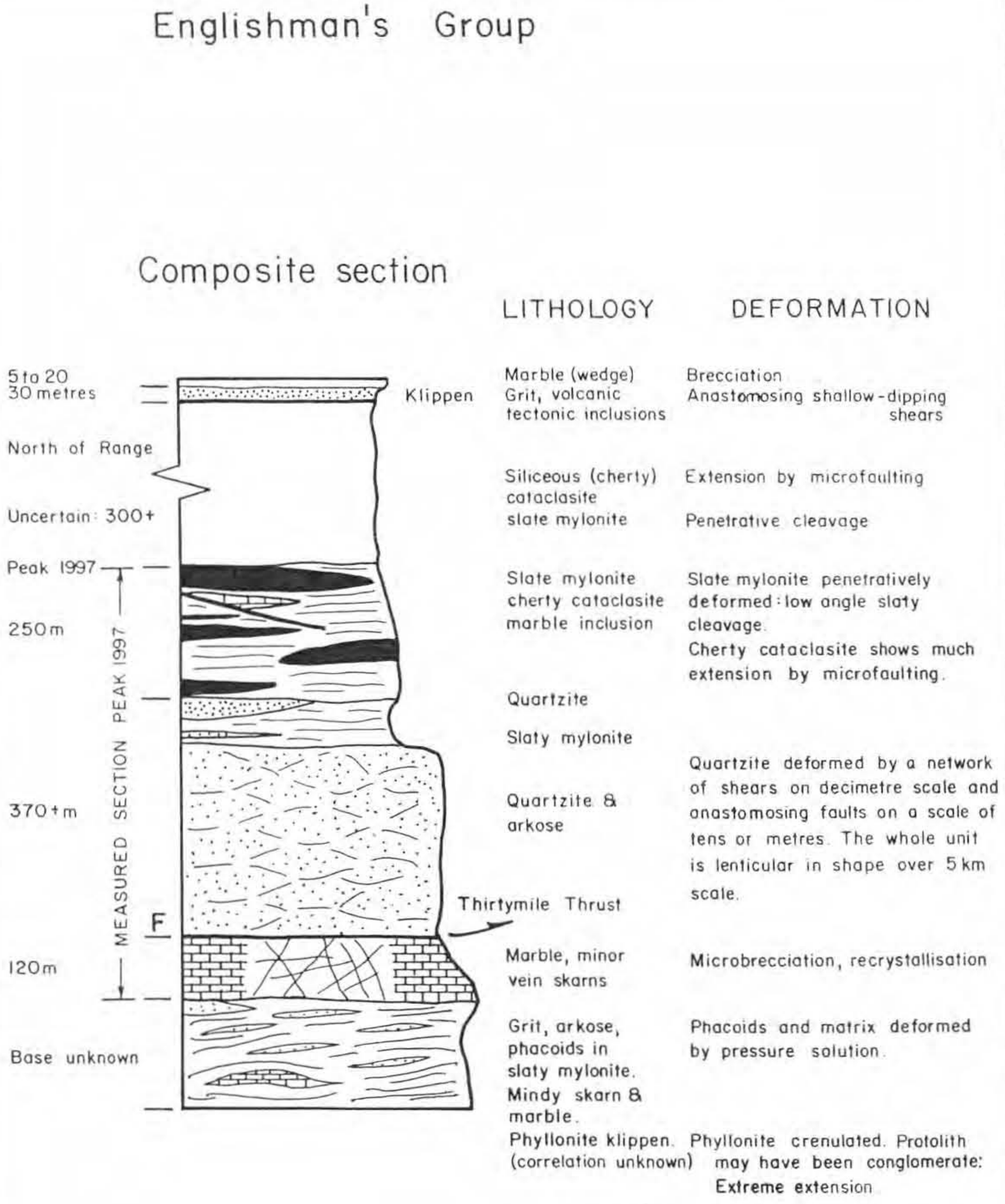

Figure 3·1

THIRTYMILE RANGE TECTONIC STRATIGRAPHY & DEFORMATION STYLE

CROSS SECTION THROUGH THE THIRTYMILE RANGE FACING NNW

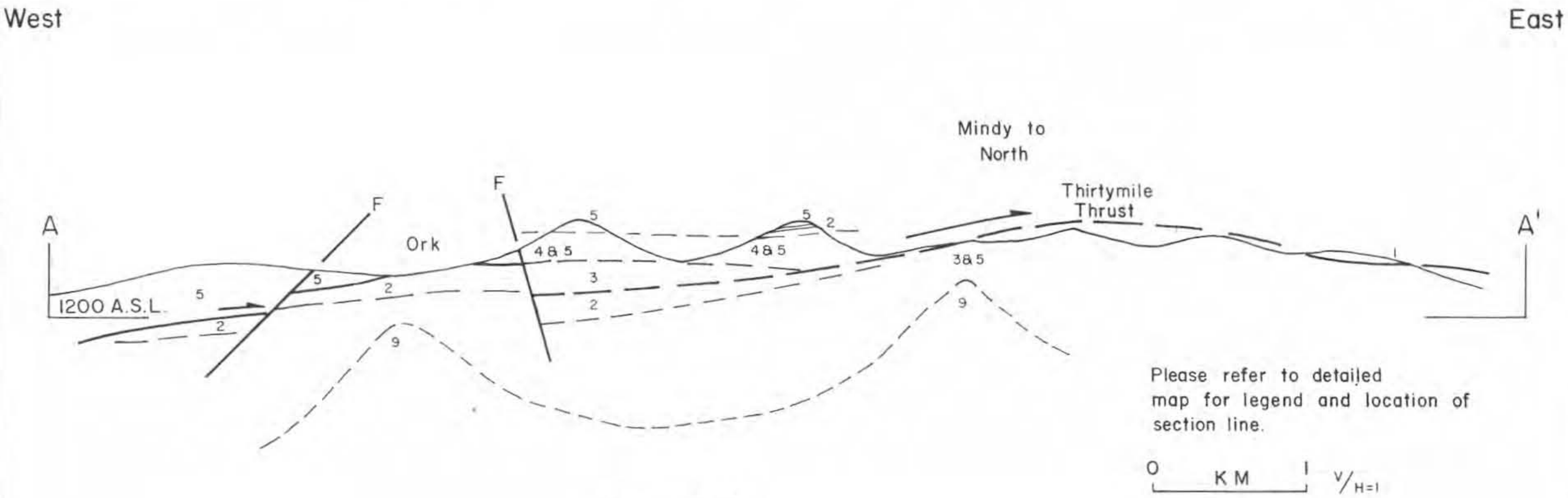

Please refer to detailed map for legend and location of section line.

Fig. 3·2

T.Liverton, January 1990.

3.2.2 TECTONIC STRATIGRAPHY: CENTRAL THIRTYMILE RANGE

The cataclasite-mylonite-siliciclastic sequence, representing unit 3 of Mulligan (1963) has been mapped in this study (Appendix B.1). Coordinates given are for the abbreviated 1000 metre UTM grid as shown on 1:50,000 scale map sheets 105C-9,10 (Appendix B.2). The sequence is summarised in Fig. 3.1 and a cross-section through the Thirtymile Range is shown in Fig. 3.2.
The following map units have been identified:

A) The topographically lowest unit mapped consists of quartzite (lithology 3 on the 1:25,000 scale map: Appendix B.1), occurring east of the Mindy prospect and in the felsenmeer (subcrop) of the spurs to the east. As do all quartzite (mega-phacoid) units within the tectonic sequence, this shows considerable small-scale shearing. A low angle pressure solution (PS) cleavage is visible in places. Since the base of this unit is not exposed thickness can merely be expressed as ≥100 m.

B) In the immediate region of the Mindy Prospect the sequence consists of sheared silty metasediments containing clasts and phacoids of quartzite and sub-arkose from a few centimetres to several metres scale. In outcrop the dominant foliation is metamorphic (a pressure-solution cleavage at shallow dips). Bedding can be recognised in thin section as a grading in the disrupted sandy layers and is at a few degrees to the orientation of the pressure-solution cleavage. Two marble/skarn units are contained within this unit at the Mindy Prospect. The lower (main, mineralised) unit shows considerable variation in thickness along strike as indicated by diamond drill hole intersections and appears boudinaged on a scale of several hundred metres. This marble may not correlate with either the major carbonate unit to the NW or the minor marble unit found about 750 m west. Thickness of the unit was not measured, however the Mindy cliffs {464239} expose a section of 125 metres thickness and total thickness is estimated at ≥170 metres.

C) In the main range, below Peak 1997 {443248} quartzite, possibly correlating with unit (A) is overlain by a thick white totally recrystallised calcite marble of grains 2 to 5 mm in size and devoid of recognisable sedimentary structures. A measured section down the NE spur from this peak traversed a true thickness of 120 metres (Figs. 3.1 & 3.3). Cliff exposures on the north side of this peak reveal that the marble is extensively brecciated down to a centimetre scale (Fig. 3.5). Exposures west of the Ork prospect show a striking cataclastic texture (See Ch. 5). Minor wollastonite vein skarns are developed within the unit, notably at {443258}. The cliff exposure opposite (north of) Peak 1997 at {430261} shows considerable near horizontal foliation developed in a 3 m thick diopside rich zone at the top of the marble and chevron style folding in the lowest metre or two of overlying quartzite. These features are taken to indicate a thrust faulted contact, later than the main cataclasis of the Englishman's Group. This has been called the Thirtymile Thrust. To the west the top of the marble is bounded by a moderate angle fault. Thickness of this unit diminishes rapidly southeastward, i.e. toward the Mindy prospect. The fault is visible in Figs. 3.3 and 3.14.

D) A sequence of massive quartzite (290 m) overlain by quartzite and slate mylonite intercalated (80 m), measured down the NE spur of peak 1997. The quartzite shows brecciation and small shears spaced every few decimetres throughout the succession. The slaty rocks are mylonitic and show cleavage with rapid variation in dip. The somewhat chaotic foliation (Fig. 3.3) does not exceed 30° dip, however. The attitude of this foliation is not reflected in the sheet dip of the lithologic units: it is likely that the tectonic cleavage is folding around phacoids of the more competent lithology which are on the scale of tens of metres.

E) Above unit D massive chert and slaty mylonite are intercalated. On the NE spur of Peak 1997 some 240 metres are exposed. The thickness of individual "chert" units varies from 10 to 105 metres on the NW spur. One 5 metre thick tectonic slice of marble is exposed on the spur 80 metres NE of the peak. A marble/calc-silicate hornfels unit noted 4.5 km NW of the peak is also within the possibly equivalent chert/mylonite sequence to the north.

Figure 3.3 The Thirtymile Thrust: visible as the upper contact of the marble unit (white). Overlying quartzites show a mesoscopic-scale anastomosing foliation partly consisting of many small flat-lying faults. NE spur of Peak 1997. White patches are remnants of the winter snow pack. Photograph taken from {429262} looking SE.

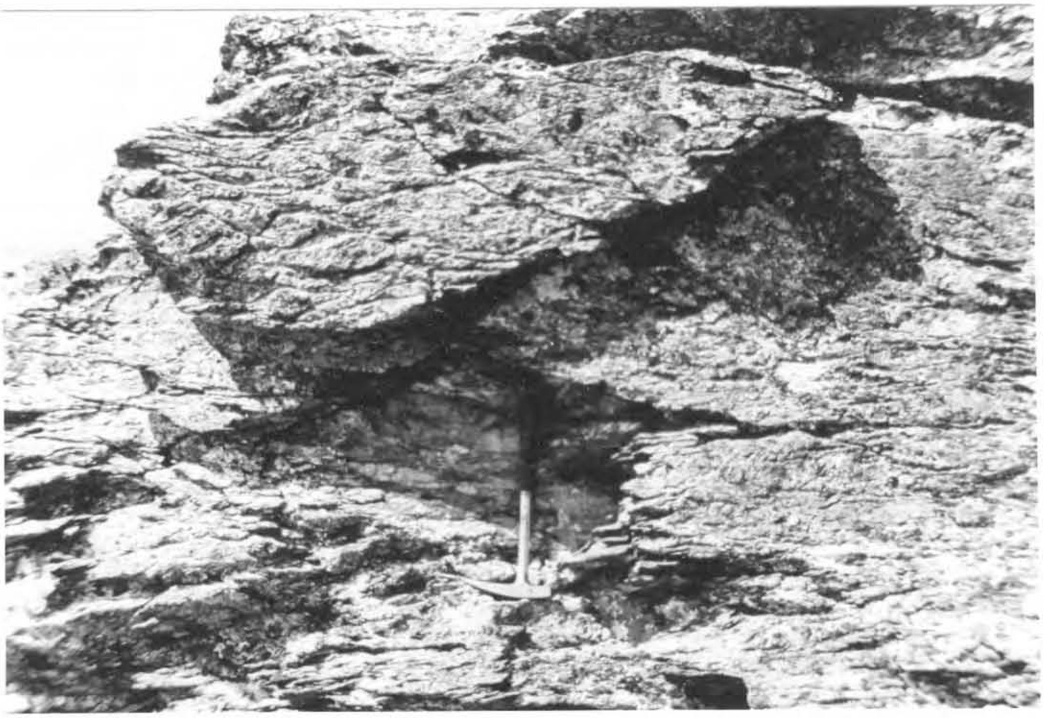

Figure 3.4 Anastomosing foliation in quartzite. Location {352339}, facing north westerly.

Figure 3.5 Brecciated marble. Mindy 3 prospect at {418265}.

F) In the NW of the map area {360330} slaty mylonite is overlain by a grit unit. Whether this represents a further (upper) clastic unit of the general tectonic stratigraphy is uncertain as lithologic correlation over the distance is questionable. This grit unit contains an intermediate volcanic unit, exposed over an outcrop length of 500 metres around {365328}. Sheared intermediate volcanics have also been noted as a tectonic inclusion (outcrop length of 10 metres) within grit at {402261}.

G) At {351339} a thin marble overlies the grit, which rapidly thickens toward the NE from 5 m to >20 m over a distance of 150 m. At least one of the contacts of this unit is likely to be faulted.

OTHER UNITS:

East of Mindy {473265 & 490247} highly deformed quartz-eye phyllonites overly the quartzite of unit (A). These show much open but disharmonic folding on a decimetre scale with sheet dips on these structures varying between individual exposures from 8° SW to 30° E. They are lithologically similar to the thick phyllonite sequence that outcrops west of Thirtymile Lake (105 C-15, UTM 270420), however their relationship to the general tectonic stratigraphy is uncertain.

3.2.3 NORTHWEST THIRTYMILE AREA

The region west of Thirtymile Lake (Map Sheet 105C-15, Fig. 3.7) shows excellent exposures along ridges of phyllonite and phyllite for an outcropping distance of 7 km from NE to SW. The phyllonite unit shows little variation in mineralogy, consisting of quartz layers up to 6 mm thick interspersed with mica-rich layers. A few exposures show little quartz and are best termed phyllite, as the micas are up to millimetre scale. Mesoscopic and macroscopic folding on a kink geometry is ubiquitous. A major quartz vein exposed for 150 m length and over 5 m wide forms the western boundary of the smaller hornblende granodiorite stock and is interpreted as a fault zone. Phyllonite separates this igneous body from the larger stock. To the SW {214417} a tiny marble exposure separates the phyllonite unit from amphibolite and foliated leucogranite which shows a foliation at 90° to the constant strike of the former unit. These metamorphics are considered to be the eastern edge of the Big Salmon Complex i.e. the Teslin suture zone.

3.3 STRUCTURAL GEOLOGY.

3.3.1 CATACLASITES: STYLE OF DEFORMATION

GENERAL COMMENTS:

The style of deformation within the siliciclastic units is universal throughout the area mapped: competent lithologies tend to form lenticular phacoids within pelitic material. This structure has been observed on the scale of a thin section, outcrop scale and variation in attitude of foliation of slaty mylonite below peak 1997 is interpreted as being the curving of the slaty mylonite around quartzite phacoids on a 5-30 m scale. Fig. 3.3 shows the anastomosing foliation in the cliff face below this peak. On an even larger scale the major stratigraphic units, particularly the marble, unit C, thins rapidly from 120 m below peak 1997 to ±15m near Mindy at {460252} and it is likely of similar geometry to the microscopic and macroscopic scale phacoids.

RESPONSE OF VARIOUS LITHOLOGIES TO DEFORMATION

Thick quartzite units show anastomosing fractures often spaced down to decimetre scale (Fig. 3.4). The major marble unit, C: 120 m thick below Peak 1997, is thoroughly recrystallised to from 1 to 6 mm sized calcite crystals. It does, however show frequent evidence of brecciation and shearing. Fig. 3.5 shows outcrop at {418265} and Fig. 3.6 {424235} shows the texture of sheared dolomitic breccia that has been preserved by contact metamorphism, the dolomitic portion is converted to diopside: lenticular calcite phacoids, showing pressure shadows are distributed throughout a magnesian calc-silicate matrix. Clear evidence of boudinage of one smaller carbonate unit is provided by the Mindy marble/skarn unit. (Ch. 5). The slaty mylonite on peak 1997 has a flat-lying penetrative cleavage. Cherts, which are intercalated with the slaty mylonite are predominantly massive and no mesoscopic scale folding was observed. At the few exposures where bedding is evident, as at {439232} it is planar and shows no small-scale folding. At locality {443271} what appears to be banded chert at first glance is a mylonite that shows later brittle fracture: steeply-dipping fractures are suggestive of

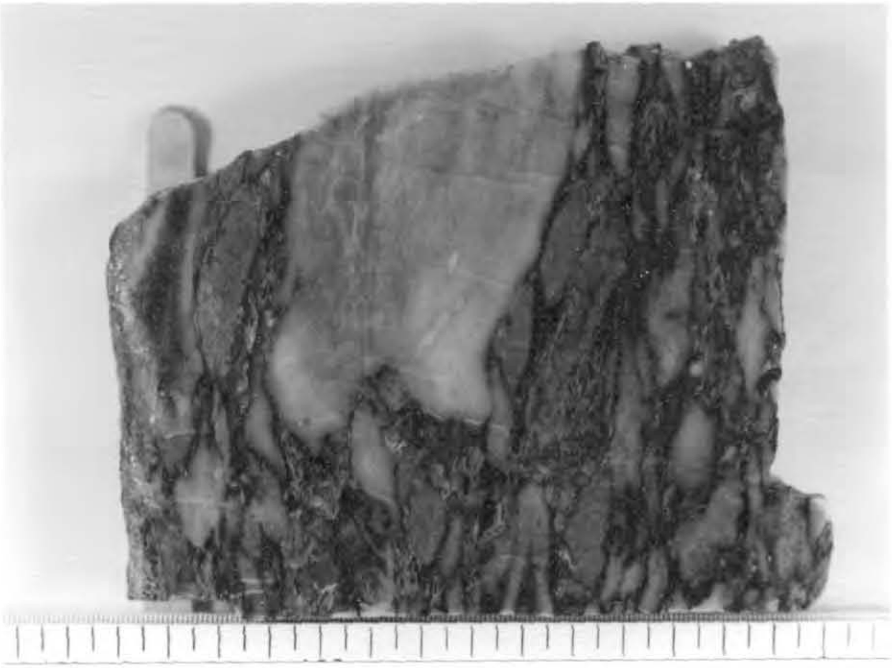

Figure 3.6 Ork area sheared marble breccia from {424235}: sawn and polished slab.

later brittle extension (Fig. 3.8).

Phyllonites universally show centimetre-scale crenulation or mesoscopic scale folding. Fold style differs somewhat between exposures east of Mindy {485245} and that of the NW Thirtymile area (Fig. 3.8). Fig. 3.9 shows quartz-rich mylonite with sheared-out limbs on one side of isoclinal folds {276455} and Fig. 3.10 the locality near Mindy {486245}, where folding consists of a disharmonic crenulation at a scale of a few centimetres wavelength, the enveloping surface of which is gently folded with amplitude of 0.1 to 0.5 metres and wavelength of 1 to several metres.

FOLDING: CENTRAL THIRTYMILE RANGE

Small-scale folding is only commonly observable in the phyllonite lithologies of the main Thirtymile Range. Consequently, few measurements of fold hinges appear on the 1:25,000 scale map. Attitude of the measured axes is mostly within 10° of N-S, with a predominant northerly plunge of up to 10°. Two steeper attitudes only were measured at

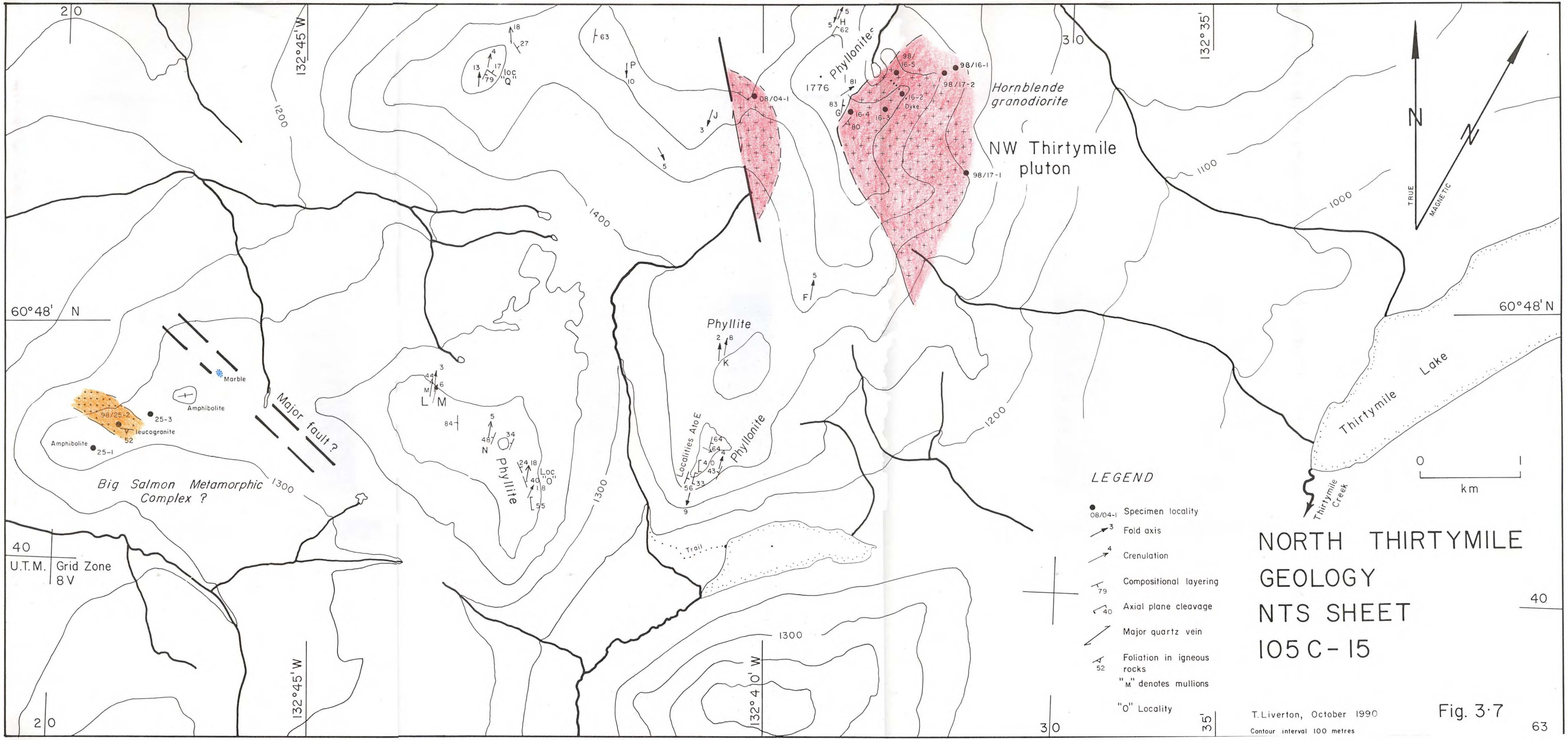
NORTH THIRTYMILE
GEOLOGY
NTS SHEET
105 C - 15
T. Liverton, October 1990
Contour interval 100 metres
LEGEND
08/04-1 Specimen locality
Fold axis
Crenulation
Compositional layering
Axial plane cleavage
Major quartz vein
Foliation in igneous rocks
"M" denotes mullions
"O" Locality
Hornblende granodiorite
NW Thirtymile pluton
Phyllonites
Phyllite
Phyllonite
Localities A to E
Loc "Q"
Loc "O"
Major fault ?
Big Salmon Metamorphic Complex ?
Marble
Amphibolite
leucogranite
98/25-2
25-3
25-1
08/04-1
98/16-5
98/16-1
98/17-2
16-2
16-3
16-4
Dyke
98/17-1
1776
Thirtymile Lake
Thirtymile Creek
Trail
60°48' N
132°45' W
132°40' W
132°35'
U.T.M. Grid Zone 8V
20
30
40
1000
1100
1200
1300
1400
N
TRUE
MAGNETIC
0
1
km

Fig. 3·7

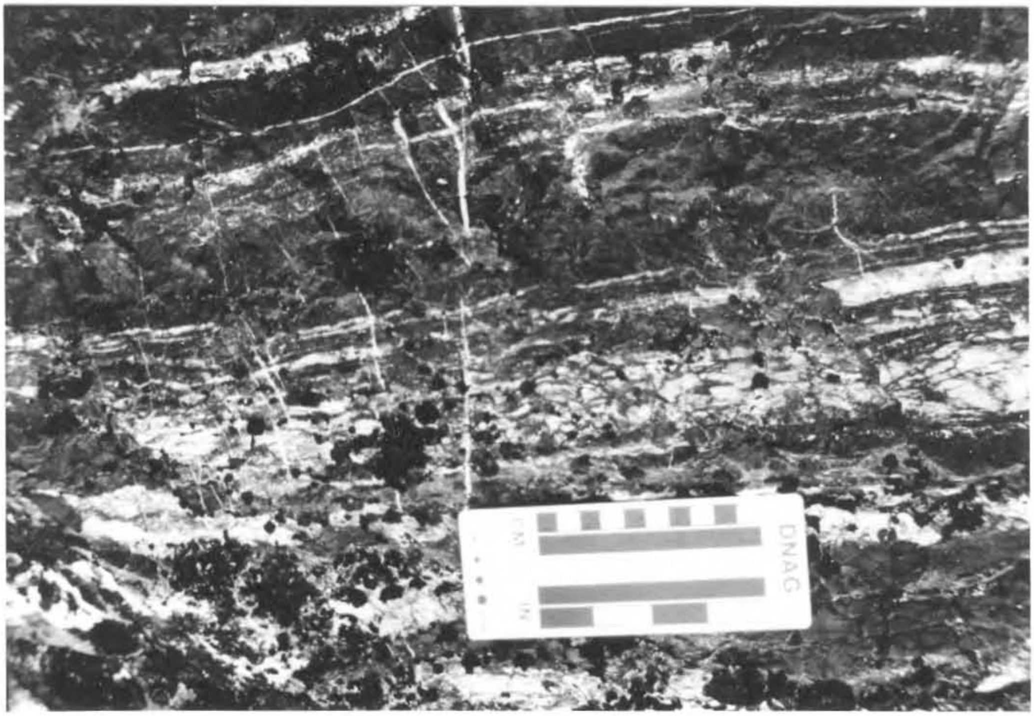

Figure 3.8 Boudinage in siliceous mylonite. Locality {443272}. Foliation dips 35° towards 335°.

Figure 3.9 Asymmetric folds with sheared-out limbs in phyllonite. NW Thirtymile area locality {276455}.

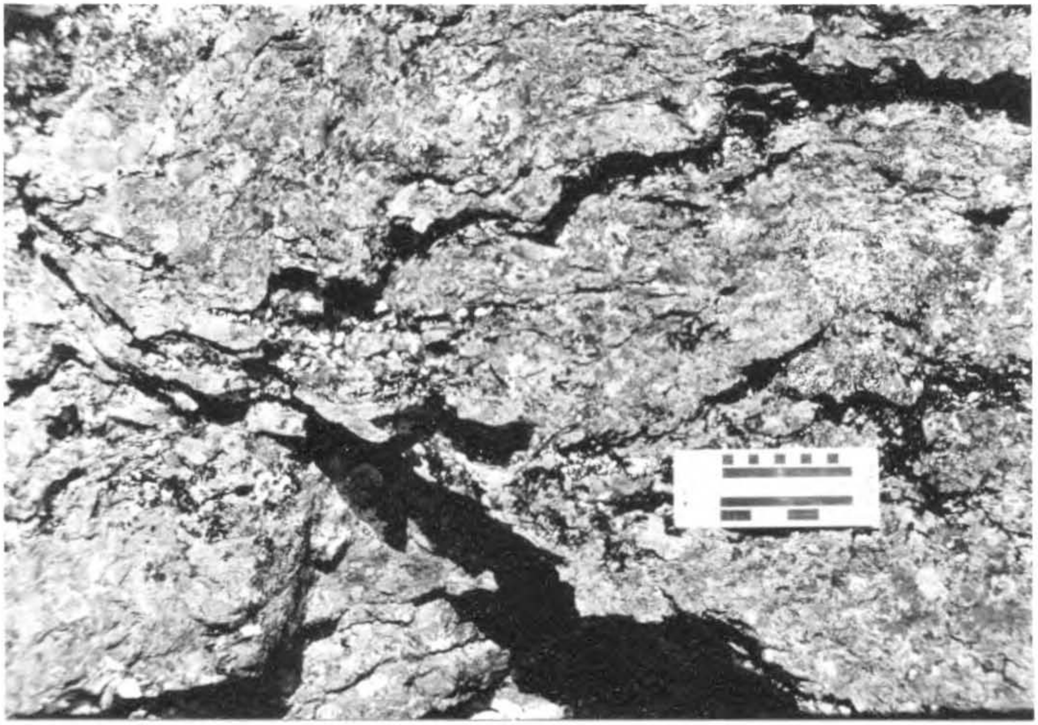

Figure 3.10 Open folding in phyllonite NE of the Mindy prospect. Locality {486245}.

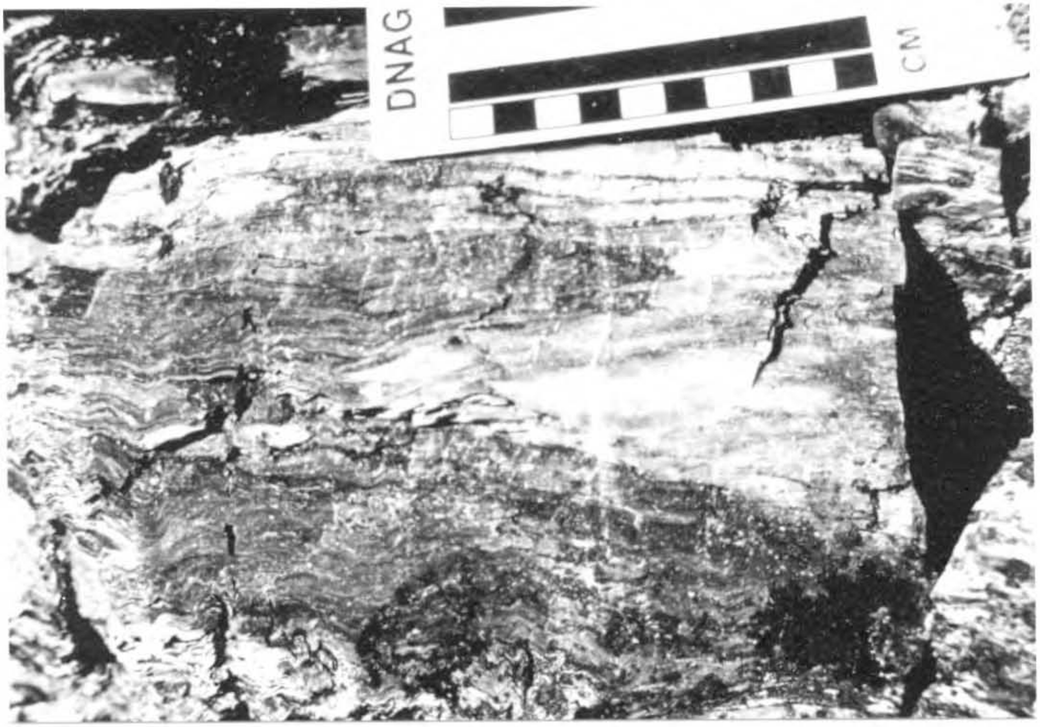

Figure 3.11 Crenulated siliceous mylonite. Locality {266410}. NW Thirtymile area.

the NW corner and east edge of the map sheet.

FOLDING: NW THIRTYMILE

In the NW area the fold style in the phyllonites is always somewhat disharmonic and on a scale of a few metres assumes a kink geometry (well exhibited at {246410}: Fig. 3.12). This is particularly demonstrable at localities A to E of Fig. 3.13, where the large exposures show folds with long, steep east-dipping limbs and shorter limbs dipping west at around 45°. Comparison of attitudes of the individual exposures on this ridge may be used to interpret an overall larger kink structure with fold limbs in the order of 20 metres length. Orientation of hinges of small-scale folds, crenulation and the rare mullion are remarkably constant over the area traversed. The axes trend at around 010° True and plunges are within 10° of horizontal, either northerly or to the south.

Figure 3.12 Typical chevron-style folding in the phyllitic lithologies of the N.W. Thirtymile area: locality {246410}. Rule is opened to 18" (457 mm). Facing SSE.

CLEAVAGES: PRESSURE SOLUTION

A pressure solution cleavage is strongly developed in the units where quartzite and pelitic lithologies are interleaved. It is a spaced (5-10 mm), anastomosing cleavage often highlighted by a little iron oxide staining. It most often obliterates any bedding observable in outcrop. In thin section, however, bedding is sometimes observable as a grading of grainsize in the psammitic layers, often at a few degrees to the cleavage. Examples are described from the Mindy prospect: Ch. 5.

PENETRATIVE SLATY CLEAVAGE

A slaty cleavage is only developed in the thick, black slaty rock interpreted as mylonite found below Peak 1997 (Appendices B.1 & B.2). Its attitude is at low angles to the horizontal, as is the pressure solution fabric over most of the Range.

3.3.2 FAULTING: THRUSTS

One major lithologic boundary is recognised as a thrust plane:
the upper surface of the major marble unit, lithology 2. At locality {430261} the uppermost metre of the marble is distinctly foliated (the foliation being enhanced by garnet layers in the marble). The quartzite above shows chevron style folds with 0.2m length limbs for 3 m above the contact. Hinges plunge 10° to 190° true.
Quartz-feldspar-muscovite pegmatite dykes 0.15 metre wide, with steep dips cut the quartzite above and small sill-like bodies 0.4m thick intrude the contact in places. (Fig. 3.14). This folding just above the contact and the strong foliation below are interpreted as evidence of appreciable shear movement. The contact is here called the Thirtymile Thrust. Many or perhaps all of the major flat-lying lithological boundaries in the Thirtymile Range are likely to be thrust faulted: the ubiquitous flat-lying pressure solution cleavage throughout the Englishmans group in this region is probably indicative of shearing. Others are difficult to trace over any long distance, so they have not been shown as thrust surfaces in the mapping. Above the Mindy prospect the 500 m wide erosional surface forming a small plateau can be correlated with the extension of the surface that bounds the marble unit. The marble has thinned from 120 metres below the main peak 1997 to around ≤15 m at 1.5 km to the NW of the prospect. To the east of the Mindy prospect

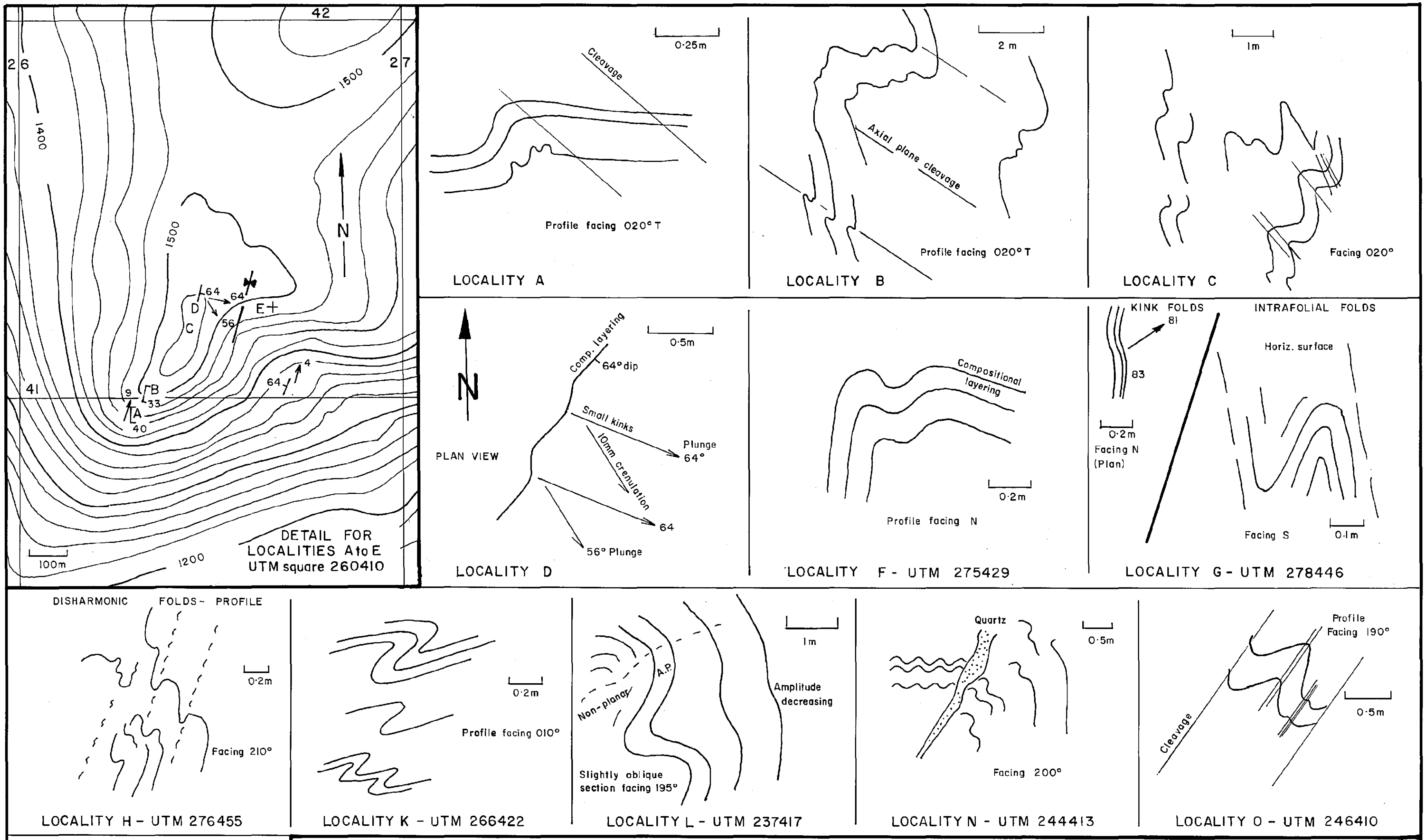

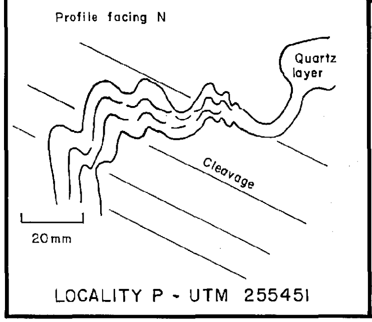

NORTH THIRTYMILE PHYLLONITE TECTONIC UNIT
SKETCHES OF MESOSCOPIC FOLD STRUCTURES
NTS 105 C-15

FOR LOCALITIES PLEASE REFER TO GEOLOGICAL MAP AT 1:25,000 SCALE

T. Liverton October 1990 Coordinates refer to UTM grid zone 8V

Fig. 3·13

Figure 3.14 The Thirtymile Thrust: Foliated marble (2 m) below; 1 metre of chevron-folded quartzite above. White dipping band is a pegmatite dyke. Locality {429261}, facing westward.

{485245 and 494247} two klippen of phyllonite are found overlying quartzite that is just below the Mindy stratigraphic level. The fault forming its lower contact may be correlated with the same thrust surface if a slight eastward roll is assumed (cross section: Fig. 3.2).

3.3.3 FAULTING: EXTENSIONAL

Brittle extensional faulting has disrupted the tectonic stratigraphy of the thrustbelt on a small scale. Evidence for ENE- to easterly- striking extensional faults abounds in the Thirtymile Range. Faults spaced from 0.2 to 1.5 km apart have been mapped throughout (Appendices. B.1 & B.2). Some have expression on aerial photographs as colour change or prominent saddles or 'notches' in ridge lines and appear as distinct lithologic differences across the saddles or zones of intense jointing or brecciation. Faults along the west side of the Thirtymile stock show prominent (small) throw displacement, but in most cases no obvious strike-slip movement of the granite contact. Some of the structures do continue as jointed zones in the granite, indicating slight movement after consolidation of the pluton, hence these faults are projected into the granite on the 1:25,000 scale map.

One fault does produce a mappable offset of the facies (Appendix B.2, 'E') in the stock at {412289}, so significant movement occurred at least here after pluton emplacement and consolidation. As occurs with many faults, at this locality there is a narrow zone (here 5-10 m wide) of no exposure, so any mylonitisation or gouge produced could not be observed.

It is suggested that this extensional faulting was the result of a regional tensional regime that allowed the emplacement of the granite plutons and immediately preceded intrusion, with some movement continuing after emplacement. Movement on these faults has produced relatively minor throw components- mostly under 50 metres.

3.3.4 HORST STRUCTURE AND MAJOR OBLIQUE FAULT

Two NNW striking faults are found either side of the Ork prospect (Append. B.2, 'O' & 'M'). These are particularly observable at {4242232 and 437234} and form a horst structure. This horst allows the broad outcrop of carbonate up the full extent of the Ork valley. This structure is interpreted as being consequential to the emplacement of the Ork stock. At the NW extremity of the area mapped in the central Thirtymile Range (105C-9) a NW trending fault is indicated (Append. B.2, 'A'). This structure is inferred from observations made from the cliffs at {352342} that the stratigraphy at this locality is not observable on the mountain to the northeast. It is likely therefore that this fault is one of the few extensional structures in the region with a major throw component of displacement.

3.3.5 FAULTING AND DISTRIBUTION OF SKARNS

Skarns developed in the marble units have been noted at {400281}, ≈3m thick garnet jasperoid skarn, outcropping over 50 metres length; at {403277}; at {418266}- the Mindy 3 prospect; as wollastonite veins at {443258} and at {446253}; as sporadic wollastonite and garnet at {459251}; at {453236} and at the Ork and Mindy showings. The first four mentioned occurrences indicate a broad metamorphic aureole above the Thirtymile and Ork stocks. No outcropping intrusion occurs at the Mindy prospect. The position of carbonate horizons was controlled first by thrusting and accompanying extension and boudinage of competent lithologies then by displacements during the extensional faulting. This extensional faulting has the further control of providing a conduit for mineralising fluids as may be seen around locality {453238} and is also discussed in the Mindy section of this work (chapter 4).

3.4 GRANITE PLUTONS OF THE THIRTYMILE RANGE

3.4.1 THIRTYMILE AND ORK STOCKS: LITHOFACIES

The Thirtymile stock has been mapped in detail. It is a roughly elliptical stock 6 Km across (Append. B.1, Figs. 3.15 & 3.16 show sampling locations). A low angle dip at the western contact is taken to infer that the present exposures on the centre ridge may be within 300 vertical metres of the original roof of the pluton. The stock is considered to be an apophysis of a large batholith underlying the whole range and connecting with the Hake Batholith (the large pluton at the east edge of the Teslin map sheet (Fig. 1.3). Four lithofacies are recognised in the Thirtymile Stock. In probable order of emplacement they are:

a) Porphyry: mingled with deep grey, seriate-textured granodiorite, it exists as isolated remnants within microgranite.

b) Even-grained microgranite.

c) Megacrystic granite occupying a little more than half of the exposed pluton.

d) Leucocratic topaz-fluorite bearing lithium mica microgranite occurring as a facies marginal to the main stock, as adjacent sills in the overlying metasediments, and as a separate stock and dykes on the west side of the Thirtymile and at the Ork prospect to the south at {428241 to 429236, 436247, 438237 and 437232}.

3.4.2 FIELD OCCURRENCE: MAP SHEET 105C-9

PORPHYRY: The Thirtymile Stock is represented in Fig. 3.15. The porphyry is found in sizable outcrop at three localities and as large xenoliths at two other localities at the SW margin of the pluton. At the two localities at the margin the facies appears as a reddish distinctly porphyritic rock, with K feldspar phenocrysts reaching 10 mm across and round quartz phenocrysts occurring with far less frequent plagioclase in a fine

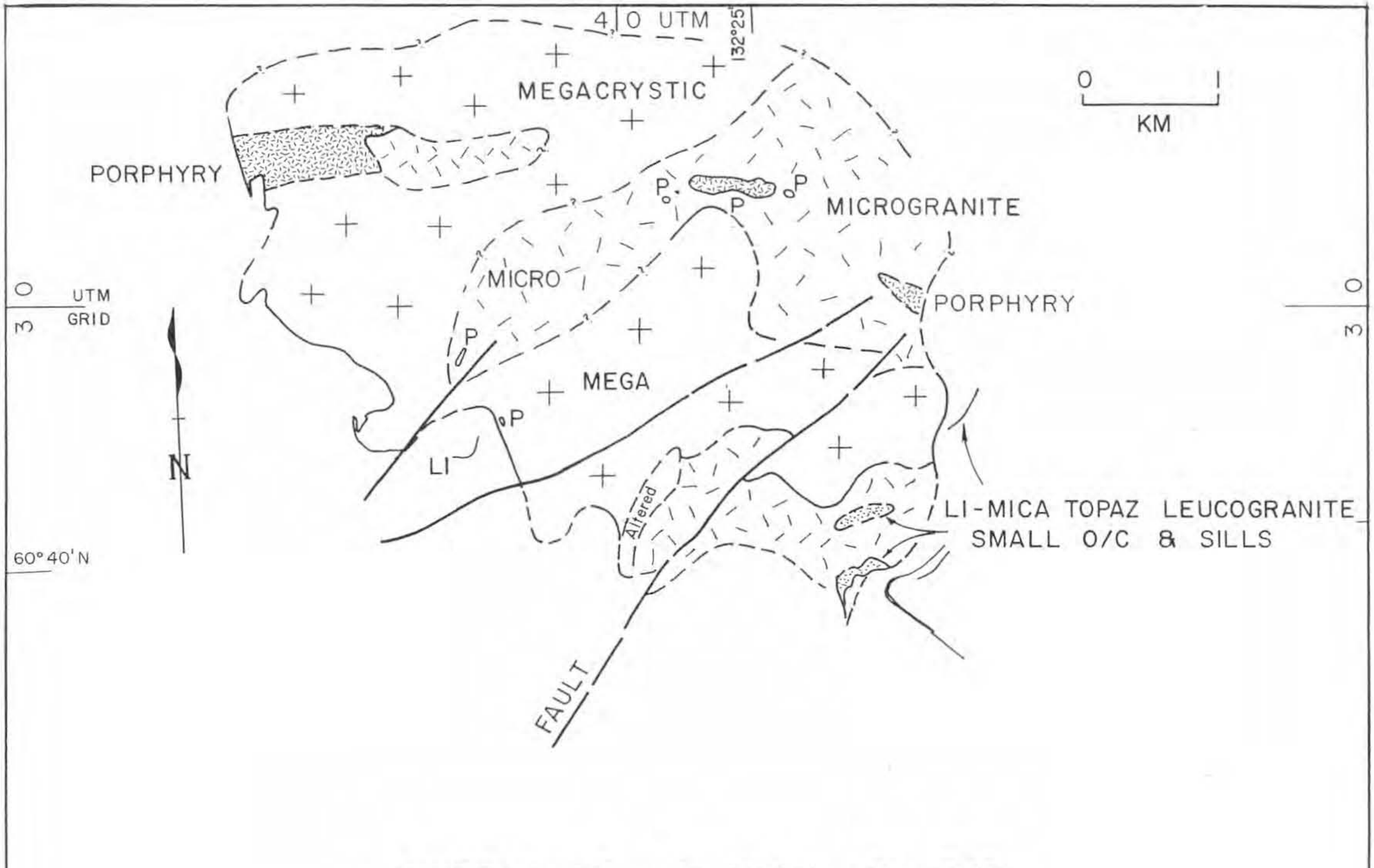

THIRTYMILE PLUTON Fig. 3·15

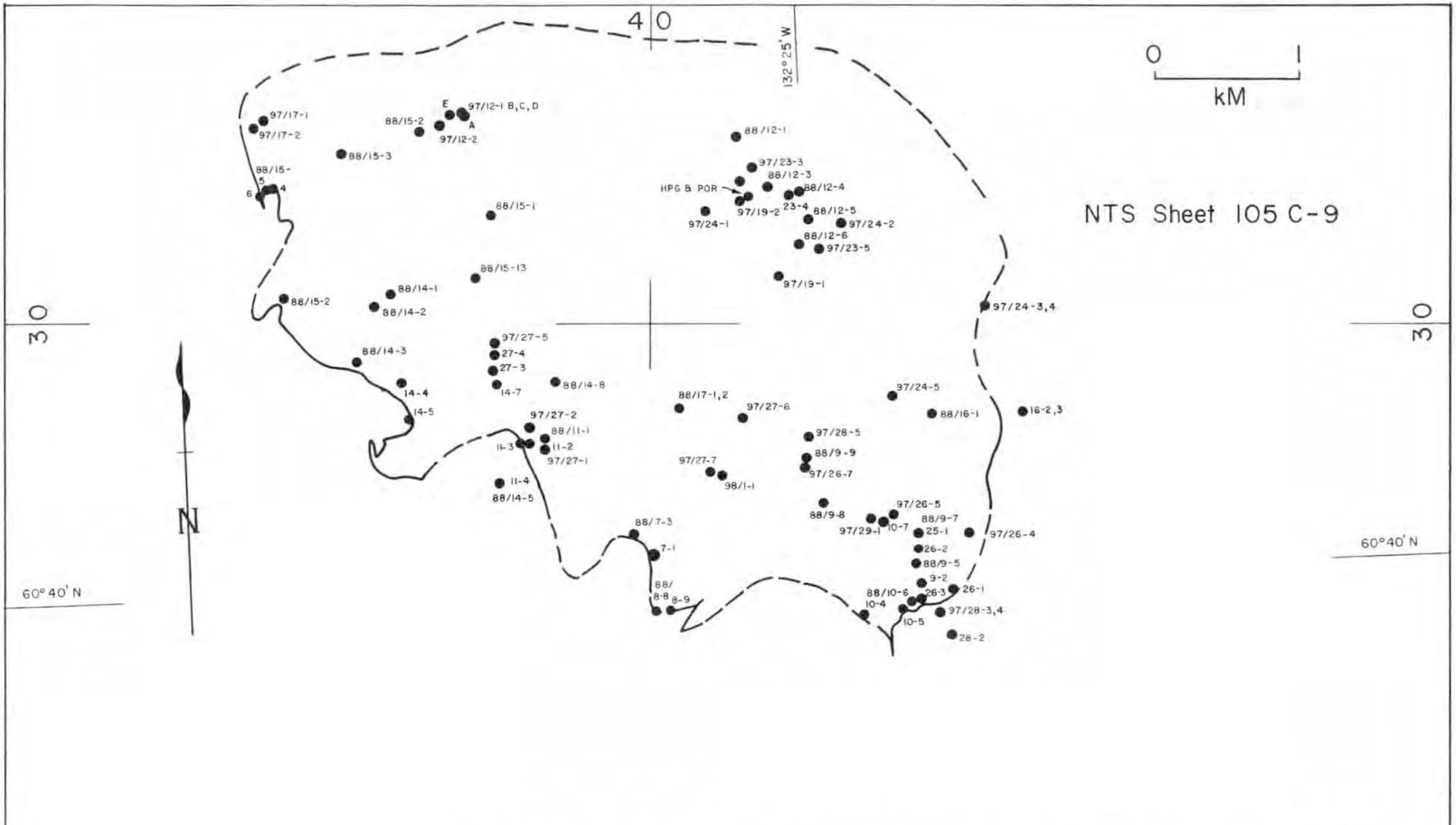

SAMPLING OF THE THIRTYMILE PLUTON Fig. 3·16 grained (often 1 mm) groundmass which contains hornblende and biotite (colour index ≈20). At the central ridge the body is similar to this in the two large xenoliths in microgranite and at the west end of the linear body, but rapidly becomes mixed with a more melanocratic rock to the east. Rounded enclaves of a fine grained (1 mm grainsize) granodioritic rock are found within the porphyry. A few slightly coarser (to 2 mm grainsize) round diorite enclaves, a few centimetres across, are found within the granodiorite. To the east the amount of granodiorite rapidly increases within this body. Rounded enclaves of porphyry are found within granodiorite and at the east end only the fine grained granodiorite occurs. Porphyry is found at the exposure at the east margin of the stock. Figs. 3.17 & 3.18 show typical enclaves.

EVEN-GRAINED MICROGRANITE: the microgranite occurs as irregular shaped bodies within the pluton. It is a white to pink granite which often has grainsize around 5 mm and biotite as the ferromagnesian present. It contains the porphyry as enclaves from 1 to 15 metres across and surrounds the larger central body of porphyry. Enclaves of porphyry within the microgranite are also found at {389296}. The contact between this facies and the megacrystic facies is fairly sharply defined across the central ridge, along its east side {411304} and at {412289}. The facies is without foliation for most of the pluton, the exception being locality 97/25-1: UTM {418285}.

MEGACRYSTIC GRANITE: occupies slightly less than half the outcrop area of the stock. Grainsize varies considerably, with pink potash feldspar up to 20 mm grainsize. Biotite mica the only ferromagnesian present. The megacrystic facies includes some blocks of the microgranite on the central ridge and also at 405289 (head of glacier) at the contact with that facies. At this locality the megacrystic facies also contains enclaves of the finer-grained lithology within the 'porphyry' facies (Fig. 3.18) and tiny (10 cm wide) aplite dykes that are displaced by microfaulting. Since the rock surface at this locality is a smooth glaciated form no sampling was possible. At the SW corner of the pluton, around {401285}, a few decimetre-sized chert xenoliths are found in the megacrystic facies with occasional 20 mm sized miarolitic cavities containing mostly quartz with a few black tourmaline crystals. No discernible foliation was noted in this facies. A large enclave of the porphyry within the megacrystic facies has been mapped at

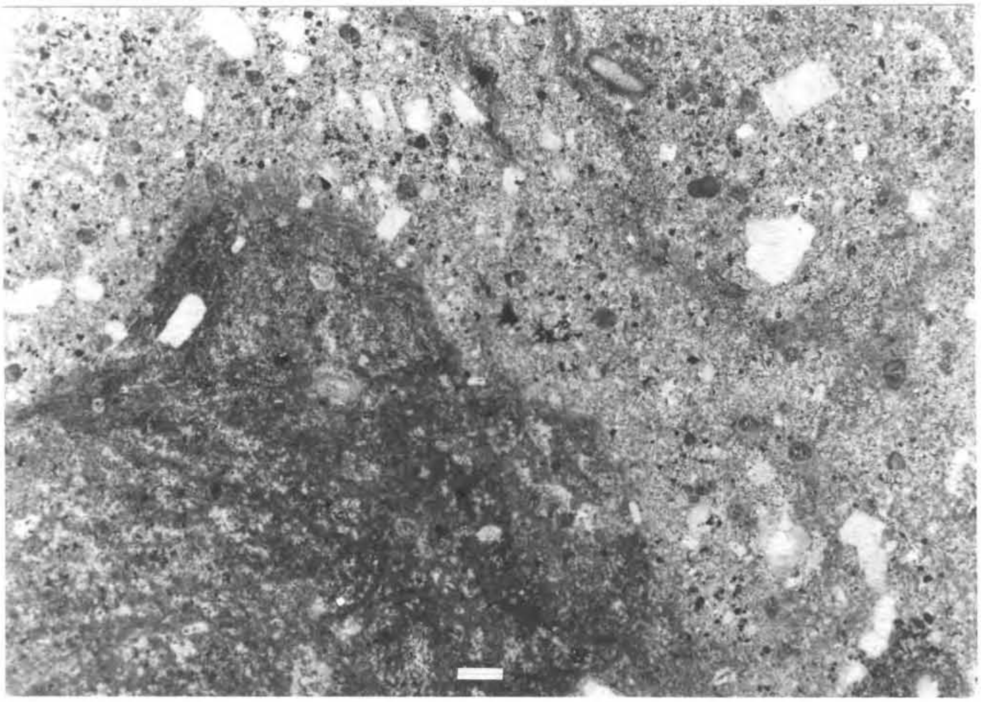

Figure 3.17 Enclave: central porphyry exposure of the Thirtymile stock at {407309}. Porphyritic granite displaying an embayed contact with surrounding fine-grained facies (similar to that of Fig. 4.4). The darker material is only slightly more mafic than the porphyritic variety. Analyses HPG and POR (App. C.1) are from this locality. Sawn slab: 10mm white scale shown.

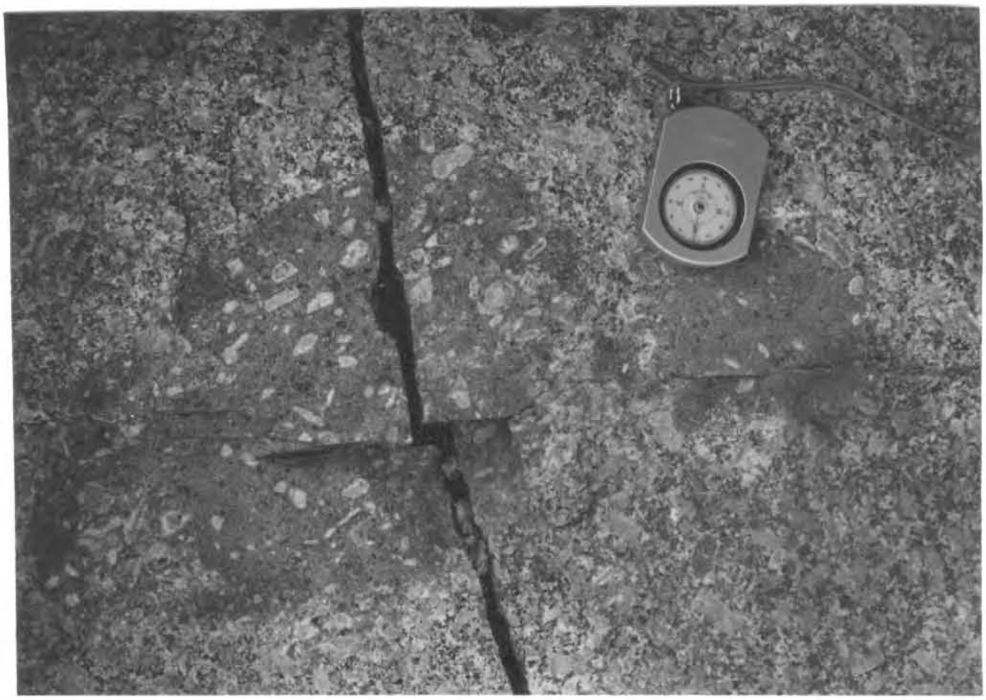

Figure 3.18 Enclave of porphyry in megacrystic granite (glaciated rock face). Thirtymile stock at {405288}. Compass is 75 mm long.

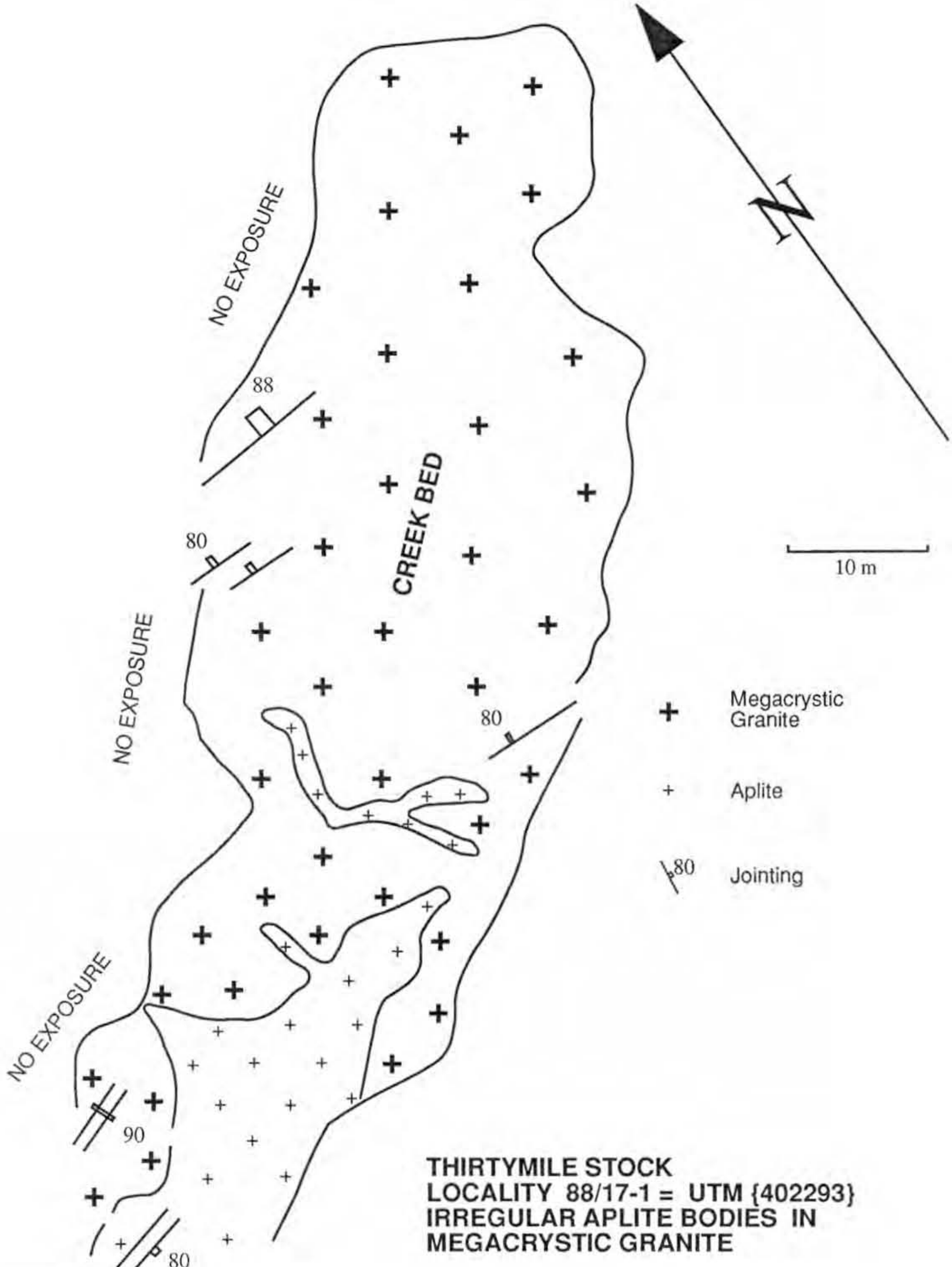

THIRTYMILE STOCK
LOCALITY 88/17-1 = UTM {402293}
IRREGULAR APLITE BODIES IN MEGACRYSTIC GRANITE

Figure 3.19

{392292}. Irregular masses of a finer grained aplitic facies, a few tens of metres across are also found within the megacrystic granite (Fig. 3.19). Enclaves of biotite microgranite have been noted within the megacrystic facies. If this microgranite represents the same facies as the even-grained granite then the megacrystic facies is the younger. At the contact between the two facies at {405289} the megacrystic facies does appear to have intruded the finer-grained granite.

LITHIUM MICA TOPAZ LEUCOGRANITE

This facies is found as two small bodies at the SE margin of the Thirtymile stock {418285 & 419281}, as three sills above this area, only two of which are of sufficient extent to be shown on the map; a sill and dyke on the the west side {390289 & 378297} and a further sill to the east {427293}; in the Ork stock {429235 & 438237} and two nearby dykes {433247 & 437232). It is a very white, fine grained rock, of rarely more than 4 mm grainsize. The texture in hand specimen is dominated by round quartz phenocrysts that are often coarser than euhedral feldspar laths. Orthoclase, which is subordinate in quantity and often grainsize to the plagioclase is anhedral. The ferromagnesian present is a dull grey lithium mica. At specimen locality 97/25-1: UTM {418285} microgranite with distinct biotite schlieren is cut by the leucogranite (Fig. 3.20). Spectacular miarolitic cavities and pod pegmatites up to 2 metres long are found in this region (Fig. 3.21). Smoky quartz and feldspars with a little mica are the principal minerals in the pod pegmatites, but the occasional tourmaline crystal may be seen. The dykes and sills are up to 4 metres thick and often show a foliation parallel to the contacts produced by preferred orientation of the feldspars. The sill has parts that in hand specimen are very obviously topaz-rich.

GREISEN VEINS, HAEMATITE VEINS AND PEGMATITE DYKES

At the SE corner of the Li-mica leucogranite exposure in the Thirtymile stock {421280}, frequent 5-10 mm wide steeply-dipping greisen veins cut the leucogranite. These consist mostly of quartz, topaz and zinnwaldite. One 10 mm thick vein of yellow beryl crystals was also noted. On the spur immediately west of this locality {421281}, adjacent to the southernmost contact of the microgranite, 2 mm wide joints with a coating of specular haematite are found in an attitude approximately normal to the contact and

Figure 3.20 Thirtymile stock, SE corner: biotite-rich layers of the Even-grained facies truncated by Li-mica leucogranite. Locality {418284}: fractured boulder.

Figure 3.21 Pod pegmatite (Coarse feldspar, quartz and occasional tourmaline crystals) in even-grained facies. Locality {418284}. Scale division on clino-rule is in inches.

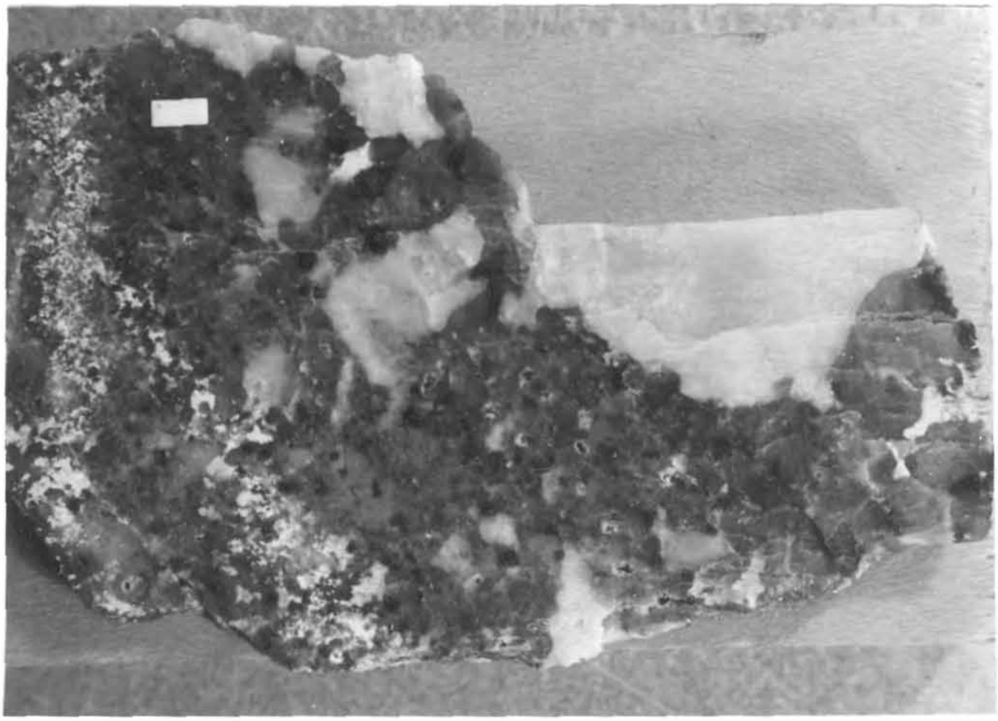

Figure 3.22 Ork pegmatite: sawn slab showing coarse amazonite feldspar, quartz and topaz with Li-mica leucogranite at the left edge. 10 mm white scale bar shown.

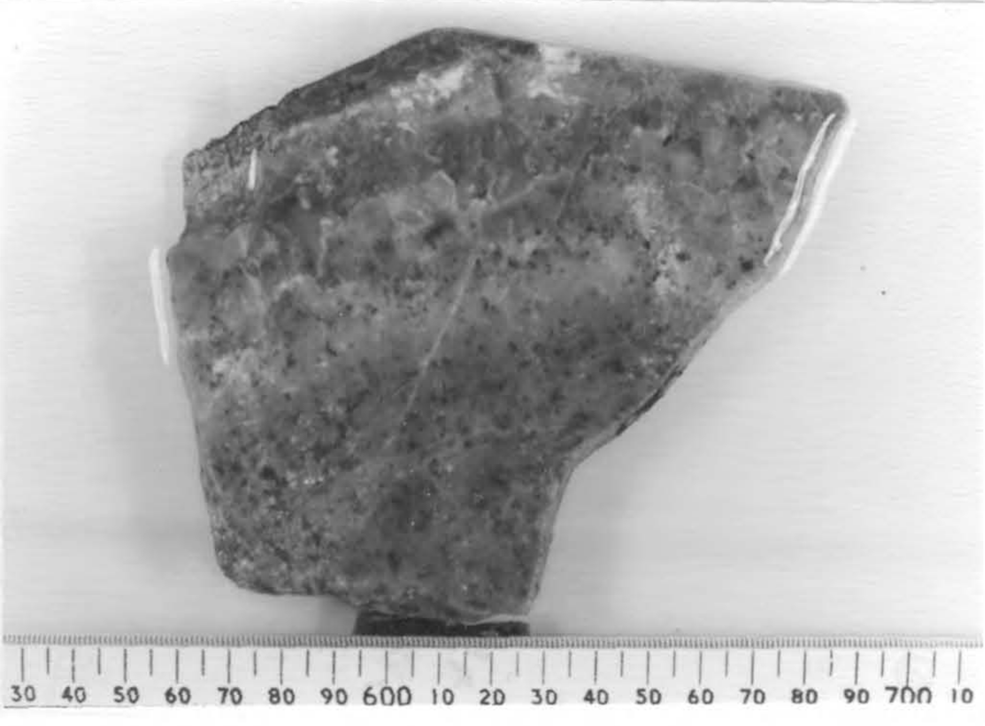

Figure 3.23 Ork contact in one hand specimen. Li-mica leucogranite nearest the scale (5 mm coarse division), plagioclase-fluorite endoskarn for 10 mm, then vesuvianite-malayaite exoskarn with a final 8 mm cebollite layer at the top of the photograph.

steeply dipping. Dip of the contact is about 45° to the SE. The contact at the Ork prospect {429235} is the one locality found where significant sized pegmatite dykes occur. One 1 metre wide, E-W striking dyke forms the steeply south-dipping contact between the Li-mica topaz leucogranite and white, coarsely crystallised marble for a few metres strike length in the creek bed. A further dyke of similar width and attitude is found approximately 15 metres to the north. Both dykes are composed predominantly of brilliant green perthite crystals, up to 200 mm across with grey (presumably zinnwaldite) mica. Subordinate interstitial (anhedral) topaz and quartz complete the mineral assemblage (Fig. 3.22). No cassiterite or wolframite were noted in the exposures of these dykes.

3.5 CONTACT METAMORPHISM

3.5.1 FIELD OBSERVATIONS

The Thirtymile stock has intruded mostly chert or quartzite cataclasites. Contact metamorphism is not readily observable in its aureole since grade indicator minerals that might have been produced in pelitic lithologies are absent except for the rare locality. The hornfelsed metasediments do, however, show a purple colouration close to the granite. An example is the peak at {397281} which is composed of chert with one minor skarn lens at about 1640 metres elevation on its SE side. The siliceous metasediments are distinctly purple for the total section exposed (180 metres vertical). On the ridge 500 metres SE the colouration is only obvious at its northern extremity. The rare pelite horizons present within the cherts do show development of biotite and rarely andalusite as at UTM {420280}. All marble horizons between the Thirtymile stock, Ork area and Mindy show coarse calcite crystals and occasional garnet-diopside±vesuvianite layers or vein skarns of wollastonite. Examples are:

(1) At {403277} 5-8 mm sized garnets and a little aphanitic green diopside occur as layers in white marble. At {418266}, the Mindy 3 prospect, minor calcite-diopside skarn, 0.5m thick, is developed at the quartzite/base of marble contact with discontinuous wollastonite skarn containing 10 mm diameter pods of vesuvianite and actinolite continuing over an outcropping strike length of 25 m. Wollastonite is found at the upper contact of this marble. Most of the intervening marble section is brecciated, but shows no calc-silicates.

(2) At {443258} near vertical wollastonite vein skarns up to 0.8 m wide and striking ≈120° True, cut 0.5 mm grainsize white marble.

(3) At {446253} the main marble unit has 4 m of fine grained diopside-garnet skarn, containing 20 cm diameter masses of vesuvianite crystals, is developed at the contact with the overlying quartzite. A pyrrhotite bearing diopside hornfels band from 1 to 3 m thick is found below the skarn at the immediate locality.

(4) At {460252} the hill is of white marble, of up to 8 mm grainsize, which shows some decimetre-thick diopside skarns and the occasional 10 cm thick layer of wollastonite in crystals up to 20 mm long.

(5) At {454235} massive actinolite skarn 5 m thick is developed at the upper surface of a minor marble unit, approximately 10 metres thick at its southern limit of exposure, which is about 70 metres long at the ridge top, before scree obscures on-strike extension to the west. This skarn zone is considered to be a manto-like body developed out from the two nearby extensional fault zones. Immediately to the NNE, at {454238} calcite-diopside-wollastonite skarn-breccia is developed in the fault zone. The breccia contains pyrrhotite and scheelite mineralisation.

(6) Contact metamorphism is quite evident in the pelitic horizons immediately above the Mindy prospect. The hornfelses are quite purple and under the microscope are seen to have a biotite-rich composition. (See Mindy, Chapter 5).

3.5.2 THE ORK CONTACT

The granite contact at the Ork prospect is surprisingly sharp and can literally be observed over the length of one thin section (see Fig. 3.23). The leucogranite shows no particular reduction in grainsize right up to the marble contact. A 10 mm wide zone of plagioclase feldspar and purple fluorite mark the contact. Pale brown vesuvianite in crystals up to 8 mm long follow for 35 mm, then a 5 mm layer of fibrous cebollite (an alteration product of melilite) is sharply terminated by coarse (6 mm) calcite marble. Just 50 metres to the SW the granite/marble contact is marked by the previously described pegmatite dyke. On the west side of the valley, above {425235}, the marbles are more dolomitic and are sheared breccias in part (see Ch. 5). In the breccias compositional differences are highlighted by the silicate skarn minerals produced: calcite lenses (phacoids) are surrounded by aphanitic diopside hornfels. Occasionally these lenses also show rims of axinite crystals. Fluorite veins, 5 mm wide and near vertically dipping cut the marble at {425234}. In calc-silicate hornfels above the marble, roughly 60 metres topographically higher, steep-dipping joints are filled with axinite crystals up to 15 mm long. At {436237}, adjacent to a small apophysis of the leucogranite, approximately 20 metres of marble are continuously exposed. Coarse calcite is ubiquitous, but the main evidence of contact metasomatism is the frequent occurrence of millimetre sized axinite veins. These localities demonstrate that the Ork stock has introduced much boron and fluorine into its aureole.

Description of the Mindy skarn mineral assemblages are given in chapter 5.

3.6 NW AND SW THIRTYMILE STOCKS

3.6.1 SW THIRTYMILE STOCK (SWTM): MAP SHEETS 105C-9 and 10

A range of lithologies have been observed in the SW Thirtymile area from gabbro to granodiorite. Two igneous bodies have been partially mapped and sampled: a gabbro-diorite body that is only just exposed by erosion and a (contiguous) leucocratic granodiorite body to the west that is well dissected. Work was concentrated on the basic body since time spent at the locality was severely limited by helicopter availability. The granodiorite body, being very leucocratic and slightly foliated, was thought at that time to be related to the Big Salmon Metamorphics (i.e. of the Teslin Suture) rather than the Middle Cretaceous plutons. Geochemical data now obtained would suggest that the granodiorite is indeed related to the basic intrusives (see Chapter 4).

The intermediate-composition portion of the stock has an irregular L-shaped outcrop (Fig 3.24) and the southern part is only exposed in a deep valley due to its shallow-dipping contacts. The northern tongue of the body climbs the ridge sharply and must have fairly steep angled contacts. Country rocks are massive fine-grained (>0.3 mm grainsize) quartzite on the NE side with massive quartzite, slate and a sheared quartzite (marked cataclasite on the sketch) to the south. Bedding and cleavages have shallow dips to the north and south.

Specimens 08/18-1 to 18-3 were taken from exposures of quartz diorite, 18-1 being

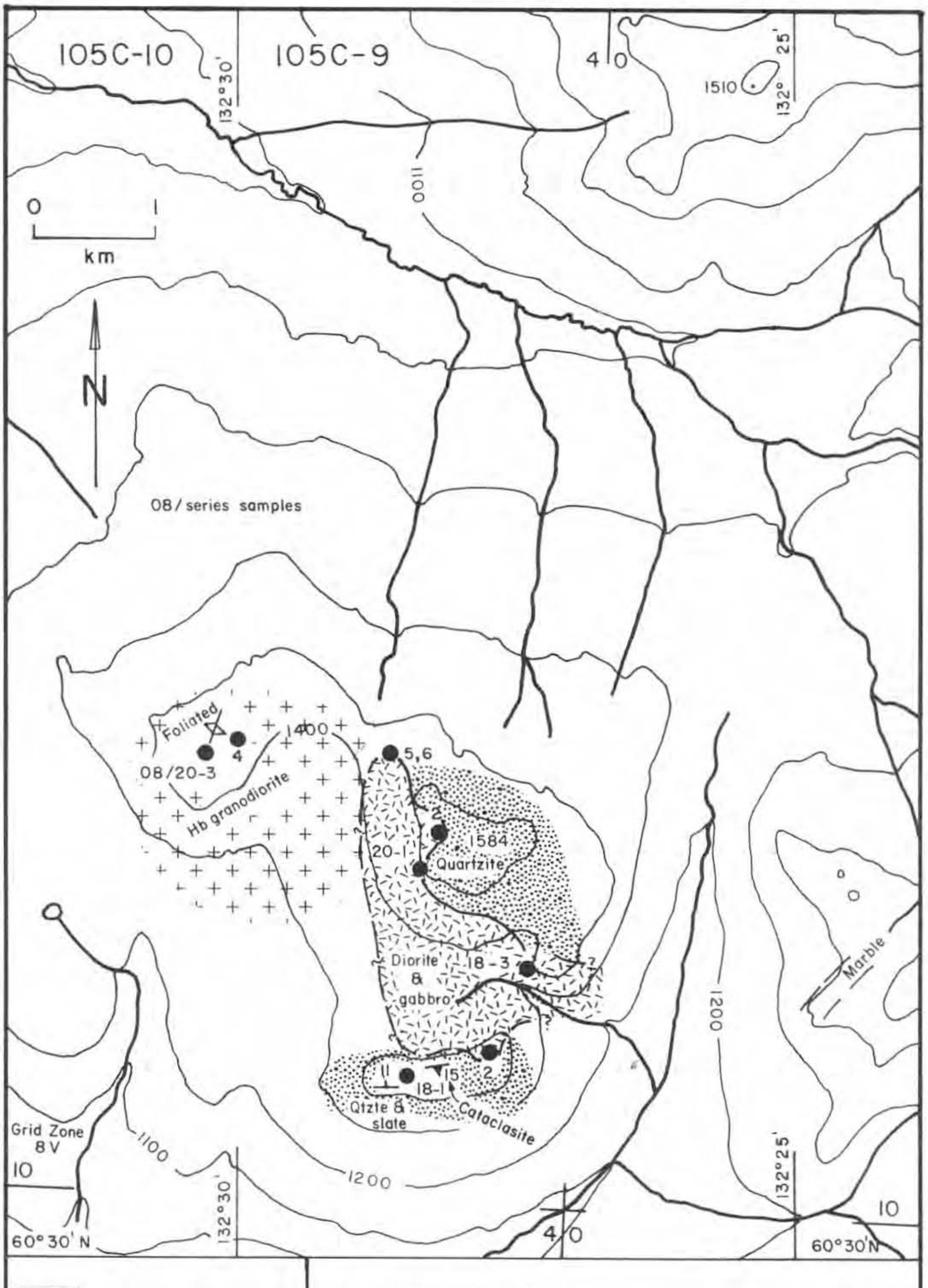

SOUTHWEST THIRTYMILE STOCK: GEOLOGY AND SPECIMEN LOCATIONS

1:50,000 Scale map sheets
105C-9 and 105C-10

T. Liverton, October 1990

Fig. 3·24

from a 2m wide vertical N-S trending dyke and has a fine-grained groundmass. Exposure is sparse, but the rock is not deeply weathered. At locality 18-3 small enclaves, 50 mm across of slightly finer-grained rock than the host diorite were noted. Exposures of the northern tongue of the body (some 100m topographically higher than those in the valley) are of augite-hornblende gabbro (20-2 and 20-6), although the pyroxene content has only been recognised in thin section). Grainsize of all the abovementioned lithologies is mostly ≤2 mm, with only occasional hornblende phenocrysts to 4 mm long. The adjacent hill to the west (localities 20-3 and 20-4: Fig 3.24) displays abundant exposure of pink hornblende granodiorite of ≈5 mm grainsize. A faint vertical N-S foliation is found at the summit. The exact location of the contact with the diorite is not exposed, however specimen 20-5 was taken from within 20 metres (horizontally) of it. The exposures of the contact zone are intermediate in colour index between those of the granodiorite and gabbro.

3.6.2 NW THIRTYMILE STOCK (NWTM): MAP SHEET 105C-15.

Location of the NW Thirtymile stock is shown in Fig. 1.3. and sample locations are given in Fig. 3.7. The traversed portion of the stock is entirely of pink hornblende granodiorite, that is mostly under 4 mm grainsize, with the occasional potash feldspar megacryst to 8 mm long. No reduction in grainsize or foliation in the intrusive was noted at the western contact with phyllonites. At a local scale (500 metres) in the cirque above specimen locality 98/16-5 (Fig 3.7) the contact is somewhat irregular and dips northwesterly at an angle of at least 60°.

The second body of granodiorite to the west around locality 08/04-1 is poorly exposed, however very fresh material was obtained from a grizzly-bear's dig in the saddle. The western limit of this intrusion is bounded by a prominent massive white quartz vein which is exposed for a width of 10 metres and over a length of 60 metres, which strikes about 170° True. This quartz vein is considered to represent a steeply-dipping fault zone (see also Mulligan, 1963).

A further granitic intrusion was briefly examined at {205412}: locality 98/25-2. Published 1:250,000 scale mapping (Mulligan, 1963) suggests that this body is related to the Cretaceous plutons. Lack of water in the area after an exceptionally dry Summer

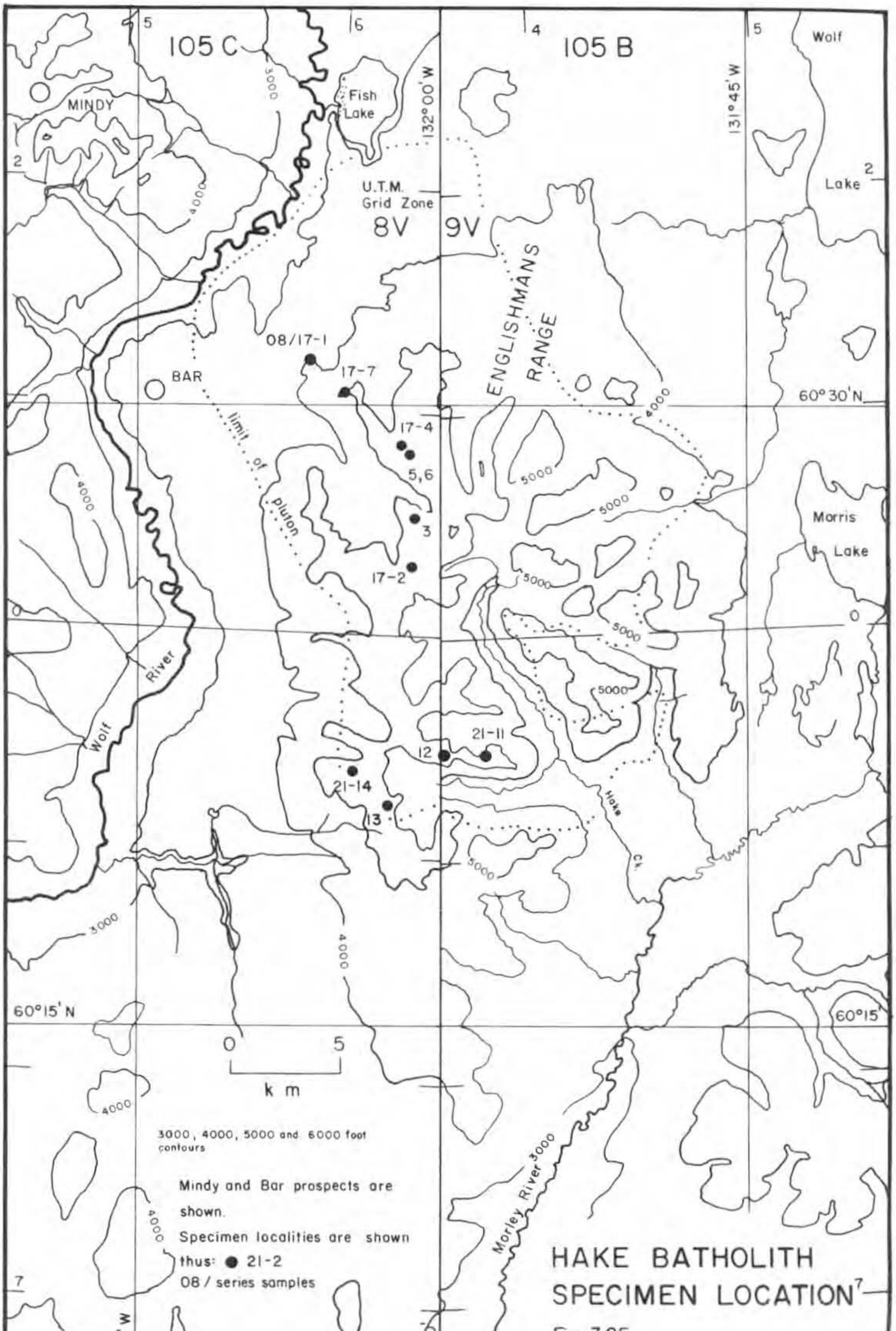

HAKE BATHOLITH SPECIMEN LOCATION

Fig. 3·25

prevented any extensive mapping. Observations consist of a ridge traverse showing a 300 metre-wide body of foliated, pink hornblende leucogranite of 4 mm grainsize that is bounded by foliated amphibolite. These metamorphics are considered in this study to represent the easternmost edge of the Big Salmon Complex. At {216418} an exposure of grey, massive marble, 5 metres across, is found on a small knoll which is separated from the phyllonites to the east by a region of no exposure. This swampy saddle would mark the location of a major fault zone bounding the Big Salmon Complex.

3.7 BATHOLITHS

3.7.1 THE HAKE BATHOLITH

No mapping was attempted over the Hake batholith. Specimens were collected from localities that were easily accessible to a helicopter and which had much exposure, hence the prospect of obtaining fresh material (Fig. 3.25). These localities, except for two, showed K-feldspar megacrystic granite with euhedral K-feldspar often up to 15 mm long

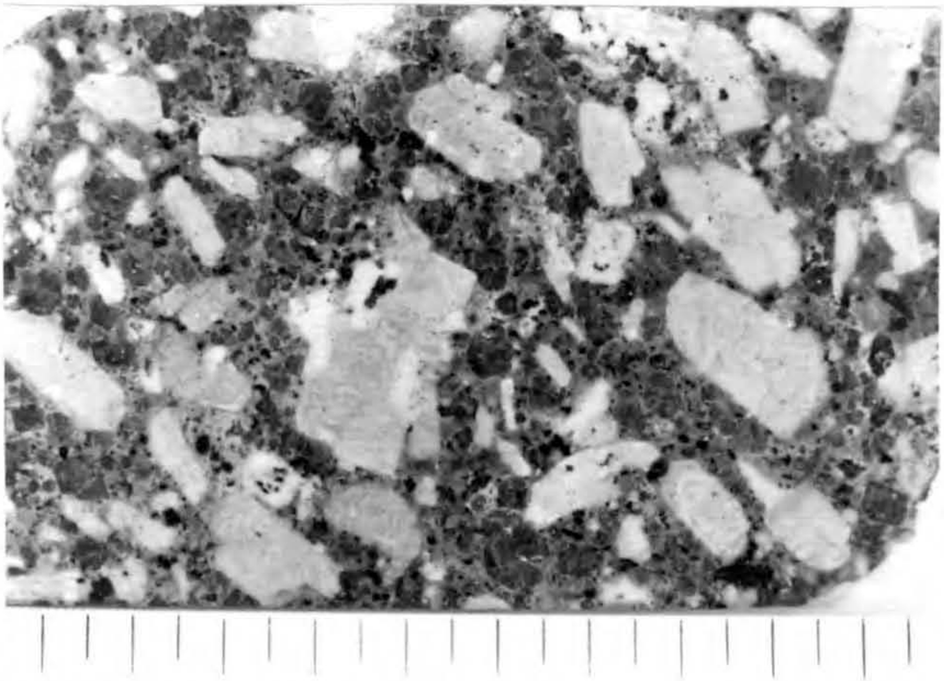

Figure 3.26 Hake batholith megacrystic granite: sawn slab of specimen 08/17-2 from {638030} showing a predominance of orthoclase microperthite megacrysts which have partial plagioclase mantles, small round quartz phenocrysts, some plagioclase and biotite. Scale division is 5 mm.

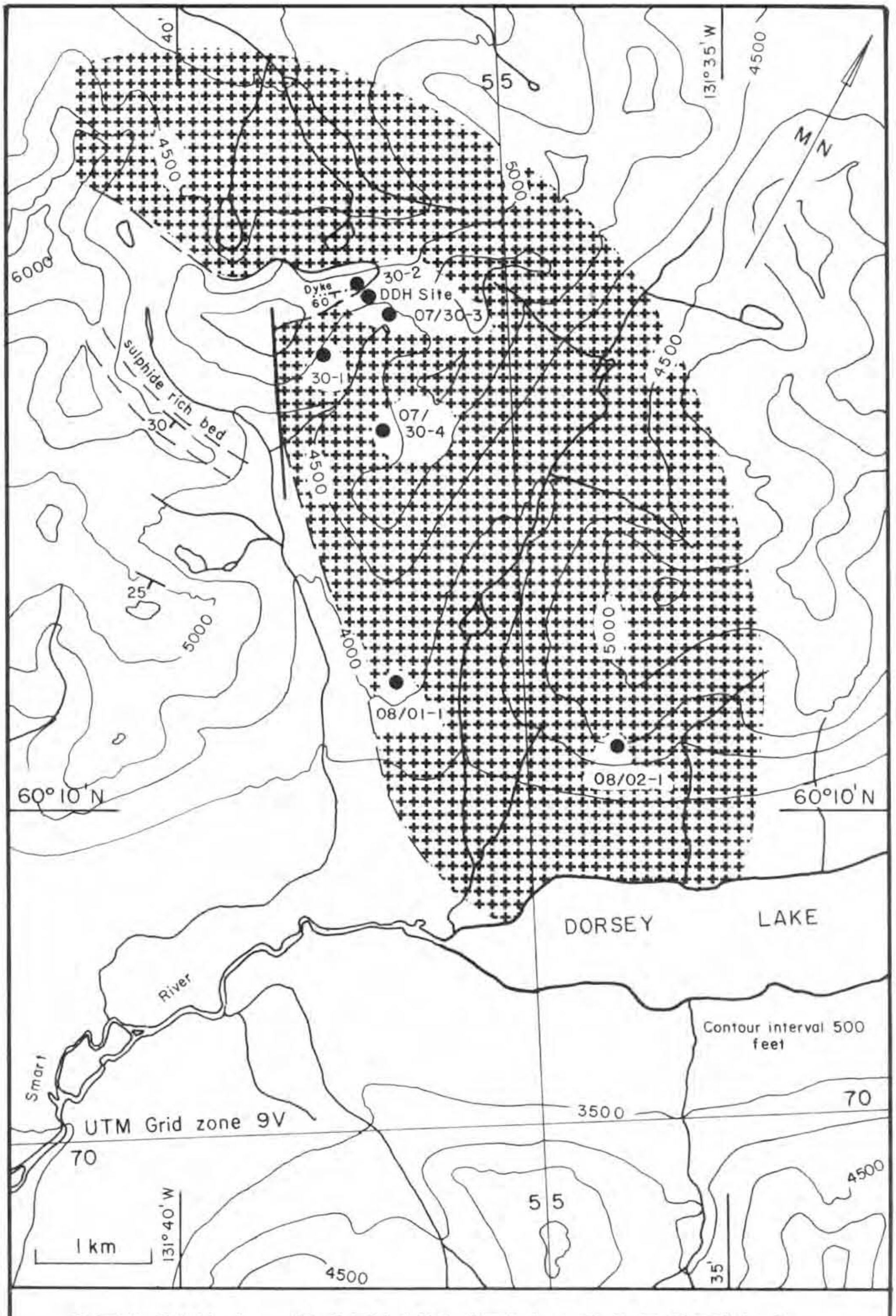

SEAGULL BATHOLITH: DORSEY L. AREA - SAMPLING, GEOLOGY.

NTS SHEET 105 B - 4.

T. Liverton, October 1990. Drill site shown is the DU prospect.
Figure 3·27

and occasionally mantled by a thin rim of plagioclase (especially rapakivi granite 08/17-2: Fig. 3.26). Plagioclase is always finer grained (often ≤5 mm) and subhedral to euhedral. Quartz and biotite are anhedral, the mica constituting <5% of the rock. In the specimen that is perhaps nearest to the contact of the batholith (08/17-1) a distinctly porphyritic texture was noted: 15 mm perthite megacrysts, round to hexagonal section quartz to 8 mm and similar sized subhedral plagioclase occurring in a 0.5 mm sized groundmass of feldspars, quartz and biotite. The round quartz is reminiscent of the textures common in the Seagull batholith. A microgranite (08/21-12) of ≤1.5 mm grainsize, containing approximately 5% biotite was sampled at the SW part of the batholith. The outcrop extent of this facies has not been determined, but it is at least several hundred metres across. A dyke, approximately 5 metres wide, containing <<1% biotite was sampled at locality 08/17-6. In thin section this rock is seen to contain an appreciable amount of fluorite.

3.7.2 THE SEAGULL BATHOLITH

Due to logistical problems the Seagull batholith was sampled in two regions only: Dorsey Lake and south of the Swift River. The Dorsey Lake area (Fig. 3.27) was examined by making a traverse to the west contact of the batholith from the lake. The DU cassiterite-bearing quartz vein prospect is at this northern contact. It was hoped to also traverse west to the JC tin skarn prospect, but the terrain proved too difficult to cross in the allotted time. The part of the batholith east of Seagull Creek, together with a small associated stock (locality 07/21-1) were sampled by walking from the Munson trail and by single use of a helicopter to gain access to the higher ridge.

The localities visited are of even-grained biotite granite with rarely more than 8 mm grainsize, containing only very occasional K-feldspar megacrysts to 18 mm and certainly not the commonly rapakivi megacrystic granites as shown by the Hake batholith. The quartz is often seen as occasional large subhedral crystals. In the Seagull Creek region the saddle immediately north of southernmost exposures visited (08/21-03: Fig. 3.28) shows two 3 to 5 metre wide, near vertical zones of microgranite which contain decimetre-sized miarolitic cavities of quartz crystals. The mining claim map 105B-3 indicates that the slopes to the west are the location of a claim which yielded large topaz crystals, presumably from similar cavities.

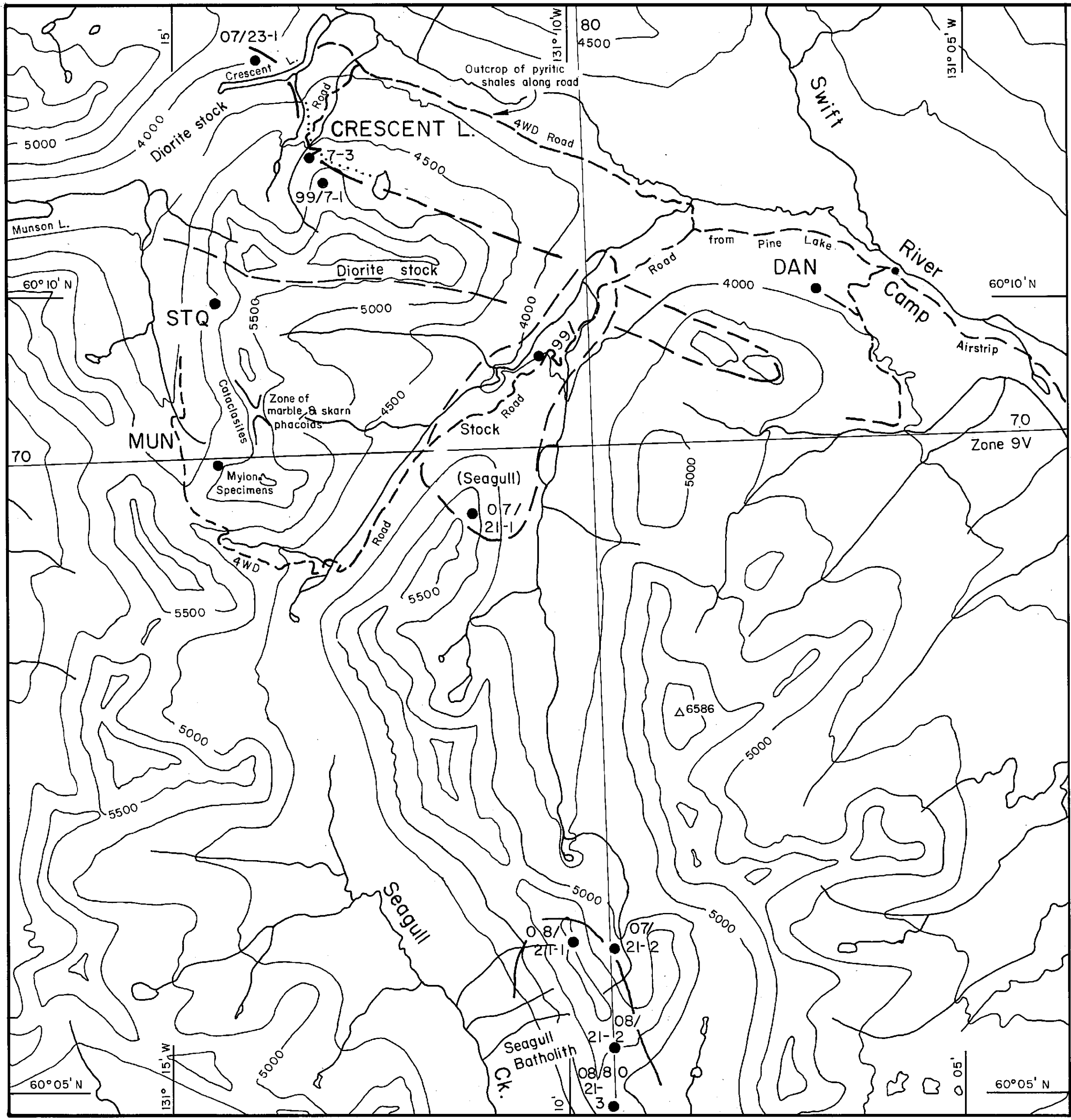

Fig. 3·28

SEAGULL BATHOLITH

AND DIORITE STOCK: LOCATION OF SPECIMENS.

Some geological notes and the location of the Dan, Crescent Lake, STQ and Munson prospects are shown.

In the region north of Dorsey Lake the granite contact is near vertical west of loc. 07/30-1 (Fig. 3.27) and is interpreted as being faulted. Around the DU prospect exposures of quartzite along the ridge top, with granite only a few metres vertically below indicate a shallow NE dip. In the eastern region sampled (locality 07/21-2, Fig. 3.28) the contact of the batholith is near vertical. The STQ tin stockwork prospect is located on the north side of the batholith, above a just-buried stock that has been intersected by diamond drilling. Cassiterite-bearing quartz veins were the exploration target. The core from the very felsic ('alaskite') stock and two outcropping dykes was sampled.

3.8 DISCUSSION

3.8.1 STRUCTURAL SUMMARY

The structural events affecting the Thirtymile allochthon may be summarised as:

1) Thrust faulting:

The stratigraphy of the Thirtymile Range is tectonic succession. Many, if not all major lithological boundaries are liable to be thrust faults, although only one such fault has been defined and named the Thirtymile Thrust since it is the one surface that can be readily traced for some distance. Thrusting of the Carboniferous sequence of the Englishmans Group eastward resulted in imbrication, very variable deformation throughout the tectonic units, and repetition of the stratigraphy. The major lithologies of the Range, i.e. Unit 3 of the Englishmans Group, are quartzite with lesser subarkose and conglomerate units, chert with chert-pebble conglomerate and black slaty pelite that is interpreted as being mylonite in part. Marble occurs as one major and at least three small tectonic units and intermediate volcanics form rarer thin tectonic slices. All units are continuous only over <5 km distance. Sheet dips of units in the central Thirtymile Range define a gentle cylindrical antiformal structure (following the NW-SE trend of the Range). In this study the Thirtymile Thrust is correlated with the base of the phyllonite sequence (klippen) east of the Mindy prospect (Fig. 3.2; Appendices B.1 & B.2) , which is consistent with mapped sheet dips. Very variable amounts of strain are (qualitatively) indicated by the textures of the various lithologies: quartzites show evidence of fracturing and slight extension, with anastomosing shear systems. Marbles show frequent evidence of brittle fracture as well as extensive recrystallisation of the marble with overall lensoid shape that may be a result of large-scale boudinage on a scale of hundreds of metres to perhaps a >1 km. A flat-lying pressure-solution cleavage is variably developed in the siliciclastic lithologies and a penetrative slaty cleavage is developed in black pelites that are interpreted as mylonites. Phyllonites alone show evidence of extreme extension. They are interpreted as deformed quartzites. Quartz layers in these have length-to-width ratios in excess of 50:1 and, if they are deformed cobbles, are indicative of high strain rates in these localised units.

Mesoscopic-scale structures:

Crenulation, where observed in these phyllonites has a fairly constant N-S strike and shallow dips in either sense. Mineral elongation is rarely visible, but when seen is parallel to crenulation axes. C-S fabrics have been observed at Mindy and are consistent with a top-to-the-east shear sense. Axes of mesoscopic kink folds and similar centimetre-scale crenulation in phyllonite in the North Thirtymile area have similar orientation. These fabrics are consistent with a general east to NE transport direction of thrust-faulted units. In the SW Thirtymile area the undeformed intermediate stock cuts penetratively-deformed siliciclastic metasediments. The age of this pluton, therefore, places an upper limit on timing of the penetrative deformation (see Ch. 4).

(2) Extensional faulting and granite intrusion:

The tectonic stratigraphy is disrupted on a comparatively small scale by E-W to NE-SW striking, steeply-dipping extensional faults. The undeformed Thirtymile granitic stock intrudes the thrust-faulted sequence. Only one extensional fault produces a minor mappable offset of granite lithofacies. Contact-metasomatic mineralisation at Mindy is faulted. The extensional faulting is interpreted as having preceded granite intrusion and continued on a small scale during final emplacement of the stocks. Two NNW-SSE striking faults in the Ork valley are interpreted as being directly related to granite intrusion. This small-scale movement along the extensional faults during consolidation and cooling of the granites provided the pathways for fluid circulation, retrograde metamorphism and mineralisation.

(3) No evidence for later deformation of the Thirtymile range has been found. It is possible that the whole Thirtymile Range and its plutons were detached from lower

crustal units during later thrust faulting.

3.8.2 LITHOLOGIC CORRELATION

The siliciclastic and marble units described here are unfossiliferous. Obvious lithologic correlation of a coarse siliciclastic unit in the Cordillera is with the Upper Proterozoic Windermere Group or Devono-Mississippian assemblages. The lithologies described here are very similar to those reported from the Indigo Lake area by Gordey (1981). In that region the "Black Clastic unit", uDMps consists of slate, greywacke, chert-pebble conglomerate of about 500 metres thickness. All these lithologies are represented in the Thirtymile Range, in a variably deformed condition: conglomerate is sparse in the central region, being represented mostly at the Mindy prospect, but extensive outcrops are reported from some 5-6 km SE (Mulligan, 1963; Gordey, 1992 pers. comm.; Harms, 1992). The rare volcanics found as minor slices amongst the clastics during the present mapping may be horses of Siluro-Devonian. Gordey's (1981) unit Mt: chert could well correlate with the repeated chert horizons of the Thirtymile Range. He notes general correlation of the Indigo Lake area stratigraphy with the McDame and Kechika map areas of northern British Columbia (Gabrielse, 1962 and 1963, see also McClay et al., 1989). The phyllonites of the klippen East of Mindy and the NW Thirtymile may correlate with Yukon Schist allochthons of the Indigo Lake area, which are considered to have been derived from Devono-Mississippian strata (Tempelman-Kluit, 1976).

3.8.3 IMPLICATIONS OF THE CORRELATION

Implications of these speculative correlations are:

Elsewhere in the Cordillera, Lower palaeozoic clastic sediments deposited in rifts were followed by carbonates of Tournaisian to Visean age (McClay et.al., 1989). If this postulated correlation is correct, then:

(1) the clastics of this study (Mulligan, 1963: Unit 3) are older than the carbonates (Mulligan, 1963: Unit 2) and hence represent structural superposition by major thrusting.

(2) Rocks of the Thirtymile Range, although they may be thrust over younger carbonates,

have not been displaced a great distance eastward and are essentially para-autochthonous North American margin rather than an accreted terrane as suggested in Wheeler and McFeely (1992).

3.8.4 IGNEOUS PLUTONS: TECTONIC SIGNIFICANCE

Two lithologically different plutonic intrusions are present in this mountain range: The one-mica granites of the Thirtymile stock and hornblende-rich gabbro to granodiorite lithofacies of the NW and SW Thirtymile stocks. Both truncate the thrust-faulted and penetratively deformed metasediments but are themselves undeformed. Chemical and isotopic evidence will be presented in Chapter 4 to demonstrate that these are igneous suites of differing origin and age.

3.8.5 THIRTYMILE STOCK: SEQUENCE OF INTRUSION

Sequence of emplacement of the various facies in this stock has been deduced largely by means of observations of one facies forming xenoliths within another, as follows:

1) The porphyry, both tonalitic and highly porphyritic facies, exists as isolated bodies within the megacrystic and even-grained bodies and has been found as enclaves from a few metres to decimetre size at more widely separated localities. (Refer to Appendix B.1).

2) Relative timing of emplacement of the even-grained and megacrystic facies is perhaps questionable. Geometry of the contact at one locality and rare enclaves have been used to infer intrusion of the megacrystic facies into the even-grained.

3) Nowhere has the Li-mica topaz bearing facies been seen included in the other facies and at one locality the Li- mica facies does truncate layering in the even-grained lithofacies. It is fairly certain, therefore, that this facies is the last to have been emplaced.

3.8.6 THIRTYMILE STOCK: SIGNIFICANCE OF THE PORPHYRY

The various unconnected porphyry bodies form a slightly curved trend across the width of the pluton, being truncated by the other facies. Since the exposed contacts of the granites are dipping very flatly on the west it is suggested that present exposures at the centre of the stock are likely to have been at no great distance from the roof of the stock. Three scenarios are considered to explain the occurrence of this facies:

(1) The porphyry might represent a dyke-like body that was the precursor to emplacement of the main body of granite, which is now exposed as a roof pendant. One objection to this hypothesis is that the porphyry does not penetrate the country rocks past the contact of the stock. The very western end of the porphyry exposures, however, has not been accurately mapped, merely the eastern end of that outcrop, but it can be stated confidently that the igneous body does not form a dyke in the metasediments.

(2) An alternative hypothesis is that the porphyry is a remnant of a pressure-quenched carapace that occupied only at the very uppermost portion of the stock. The western exposure would fit such a model, being along the crest of a prominent ridge. The central exposures are slightly north of the crest of the topographic dome. For the porphyry to have a shallow depth as such a model requires would mean that the body had a trough-like geometry. The texture of the rock (coarsely porphyritic in places with euhedral quartz phenocrysts, some adcumulate texture and much fine groundmass) does bear a striking similarity to the description of a pressure-quenched carapace given by Plimer (1987).

(3) A third hypothesis is that the porphyry represents a large disaggregated synplutonic dyke (Vernon, 1986). For the same contact relationships to be produced this origin would require the whole pluton to have forcibly intruded the country rock en-masse which, considering the presence of a generally low-angle western contact to the pluton, also might require considerable plastic deformation of the whole upper region of the stock in order to accommodate the changes in (plan) area. No evidence of deformation, such as foliation or schlieren has been observed in the stock, but this is most plausible interpretation.

3.8.7 THIRTYMILE STOCK AND ORK STOCKS: Li-MICA FACIES

Evidence has been presented that suggests that the Li-mica topaz leucogranite was the last facies to be emplaced. It occurs as a marginal zone to the Thirtymile stock, as two apophyses in the Ork area, and as several small sills and dykes. These dykes and sills are under 4 m thick, yet penetrate the country rock for up to 900 metres from the contact of the stock. No significant chilling along their margins was seen. This field evidence can be used to deduce two facts: the aureole of the granite was comparatively large (at least to a temperature of perhaps 400°C for ≈1 km laterally from the granite contact) and that the Li facies magma had a comparatively low viscosity. Although no exposure of granite exists at the Mindy Prospect or was intersected in the 1981 drilling programme a stock must exist at a shallow depth beneath the skarns. The B/F metasomatism occurring in the skarns makes it likely that this Li-mica facies forms such an apophysis.

3.8.8 CONTACT METAMORPHISM IN THE CENTRAL THIRTYMILE RANGE

The siliceous nature of the metasediments precludes the mapping of metamorphic indicator minerals such as cordierite or andalusite. Some occurrences of these minerals have been noted, but they are rare. The main signs of a metamorphic aureole in the cherty metasediments are the development of a distinct purple colouration within a few hundred metres of the granite. Wherever marble units are in contact with chert a bimetasomatic skarn is developed for a metre or so width, as is well demonstrated at the SW side of the Thirtymile stock and east of peak 1997 {403277 & 446253}(Append. B.2). The contact skarn at the Ork stock is very narrow, but wider zones are developed in the intercalated marble breccia and hornfels around {425284}. Wollastonite and diopside vein skarns are developed at widespread locations in the thick marble unit. These observations are interpreted as indicating development of a contact metamorphic aureole of up to 1 km extent around the Thirtymile granite stock.

3.8.9 FAULT CONTROL OF MINERALISATION

The introduction of mineralisation and formation of calc-silicate mineral assemblages along the extensional faults is well illustrated by scheelite-pyrrhotite mineralisation and diopside-szaibelyite developed in carbonate fault breccia at {454238} (Append. B.2), west of Mindy. The same fault passes immediately north of the skarn exposures and it, plus parallel structures, are believed to be crucial in localisation of the principal mineralisation at the prospect by acting as 'plumbing' for hydrothermal and meteoric circulation.

CHAPTER 4

PETROGRAPHY AND GEOCHEMISTRY OF THE JURASSIC AND CRETACEOUS INTRUSIONS

CHAPTER 4: PETROGRAPHY AND GEOCHEMISTRY OF THE JURASSIC & CRETACEOUS INTRUSIONS

4.1 INTRODUCTION:

4.1.1 AIMS

The field relationships of the various lithofacies comprising the Thirtymile Stock, the granites of the Hake and Seagull batholiths and the hornblende diorite to granodiorite facies of the NW Thirtymile and SW Thirtymile stocks have been described in chapter 3. Analytical data is presented and discussed in this chapter.

It is intended to show that two separate suites of intrusions occur in the study area: the granites and the hornblende-bearing intermediate to granodiorite stocks. Genesis of the biotite granites is from a mostly I-type source as a result of crustal thickening and that of the anomalous leucogranites is consistent with production by extreme fractionation of the biotite granite magma under conditions of high halogen concentrations in an apophysis of the batholith. These granites compare chemically with many other 'tin-granites'.

4.1.2 CONTENTS OF THIS CHAPTER

This chapter will present the following petrographic and analytical data:

1) Petrography of each pluton and lithofacies.

2) Modal compositions for the finer-grained lithologies.

3) Major and trace element geochemistry. The biotite granites of the Seagull, Hake and Thirtymile plutons are shown to represent one evolutionary trend toward silica enrichment and mild increase in K/Na. The Li-mica leucogranites are shown to represent a change in the trend leading to crystallisation of albite with lowered silica contents on increased fractionation which matches published experimental studies on F-enriched

granite melts. The specimens from the Northwest and Southwest Thirtymile stocks are shown to produce separate geochemical trends from those demonstrated by the granites.

4) Mica major and trace element compositions are given for the Fe-Li micas separated from granites of the Thirtymile stock, Hake batholith and Seagull batholith.

These analyses are shown to demonstrate a simple progression in major and trace element mica compositions through the biotite granites, leading to most evolved compositions in the Seagull granite, that match the rock chemical trends for most elements. A sharp change in trace contents is shown from the lithian biotites of the granites to zinnwaldite or lepidolite in the leucogranite.

5) Ammonium content of these intrusions is presented and shown to be surprisingly low compared to published data from other granites. This is consistent with an I-type source.

5) Rb/Sr whole-rock isotopic data is presented for the Thirtymile granite. The age obtained is shown to be complementary to that published for the Seagull batholith. Geochronology of the SW Thirtymile stock is shown to yield a significantly older age and lower Sr initial ratio, thereby providing further evidence that the SW and NW Thirtymile stocks are of a separate plutonic suite to the granites.

Topics of discussion are:

1) The Seagull-Thirtymile granites: their predominantly I-type nature as indicated by major, trace element, Sr-isotopic compositions and mineralogy; the likelihood that the granites represent one plutonic suite; reduced nature of the granite magma as indicated by mineralogy and mica chemistry; evidence for derivation of this suite in a continental collision setting and production of the leucogranites by extreme fractionation.

2) The NW and SW Thirtymile stocks: their being a separate, older plutonic suite with compositions indicative of a subduction-related magmatic component.

3) Comparison is made between the Seagull-Thirtymile suite, 'HHP' Sn-U granites and the granites of the nearby W-related Selwyn suite.

4) The petrogenesis of Li-F-B enriched granites is considered and the 'ultrafractionation' process is proposed for the Thirtymile granites.

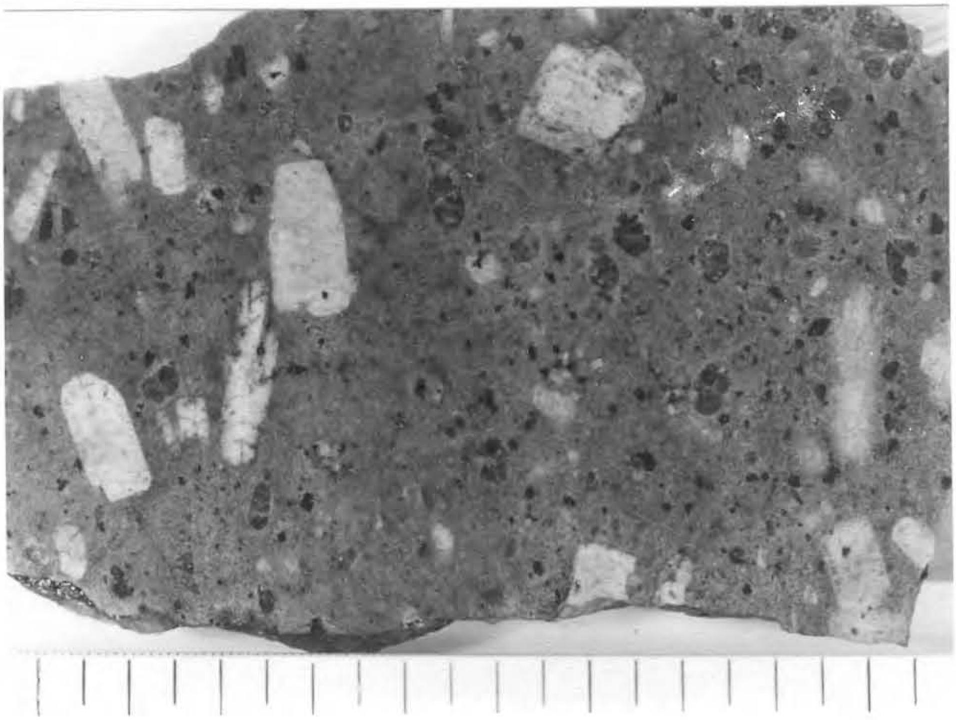

Figure 4.1 Porphyry: sawn slab showing coarse orthoclase phenocrysts (one with a Rapakivi rim), plagioclase and round quartz in a fine-grained feldspar-quartz-biotite-hornblende groundmass. Specimen 97/12-1D from {387315}. Scale division 5 mm.

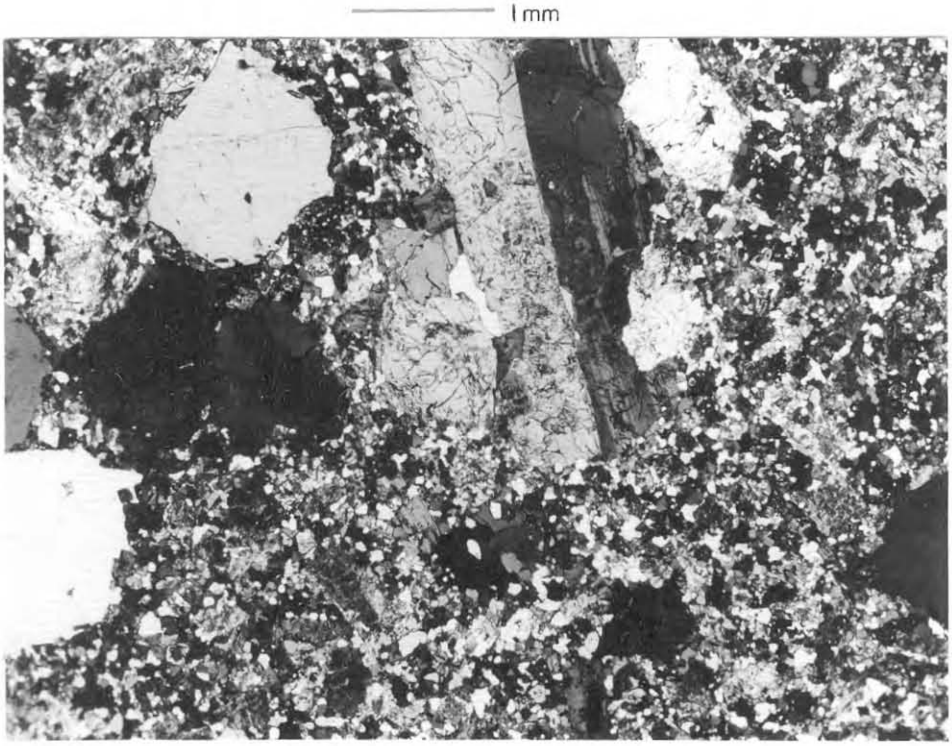

Figure 4.2 Porphyry: specimen 88/15-2 from the Thirtymile stock in thin section under crossed polarisers. Shows large embayed quartz phenocrysts with plagioclase in a quartz-feldspar-biotite groundmass. Locality {386314}.

4.2 PETROGRAPHY

4.2.1 THE LITHOFACIES OF THE THIRTYMILE STOCK

A general description of each facies follows:

PORPHYRY

At the western end (Appendices. B.1 & B.2) of the exposure {407309} the predominant lithology is very porphyritic- the texture is frequently dominated by euhedral to subhedral equant quartz phenocrysts, some with their margins intergrown with the grains of the groundmass. Single-twinned perthite phenocrysts from 4 to 10 mm long which are anhedral to euhedral often occur in clusters with very little interstitial quartz (adcumulus texture) and occasionally show rapakivi texture. Plagioclase is finer grained (2 to 4 mm), subhedral to rarely euhedral, often twinned on both Albite and Carlsbad-Albite laws and is frequently oscillatory zoned. Rare subhedral hornblende xenocrysts, often altered to biotite and chlorite, are up to 3 mm long. Deep brown, often chloritised and very ragged biotite forms phenocrysts to 2 mm size and smaller (0.5 mm) grains in the groundmass. The micas contain some euhedral zircon inclusions and rarely are intergrown with anhedral monazite. Occasional clusters of biotite, very fragmented hornblende (0.5 mm), monazite, pyrite and apatite may be seen. Monazite and allanite are common in the groundmass as very anhedral grains to 0.8 mm size and subhedral to euhedral crystals to 1 mm long respectively. Quartz and K feldspar form the bulk of the groundmass. Quartz is the prominent mineral of the groundmass, with grainsize of approximately 0.5 mm and it tends to poikilitically enclose the feldspar. The porphyry contains frequent rounded enclaves up to 0.5 metres across of a dark grey fine grained seriate-textured granitic composition rock, which in turn contains centimetre sized darker rounded dioritic enclaves. Similar shaped enclaves have been interpreted as clear evidence of magma mixing in the literature (Chandra Kumar, 1988; Vernon, 1983; Vernon, Etheridge and Wall, 1988). Fig. 4.1 shows a sawn slab of porphyry and Fig. 4.2 a thin section. At the east of this exposure the body is entirely of the fine-grained variant. Chemical data presented later in this chapter will demonstrate that although the two end-members of the mixed porphyry body are visually quite different, there is little difference in composition. Enclaves of this lithofacies (both fine-grained and porphyritic

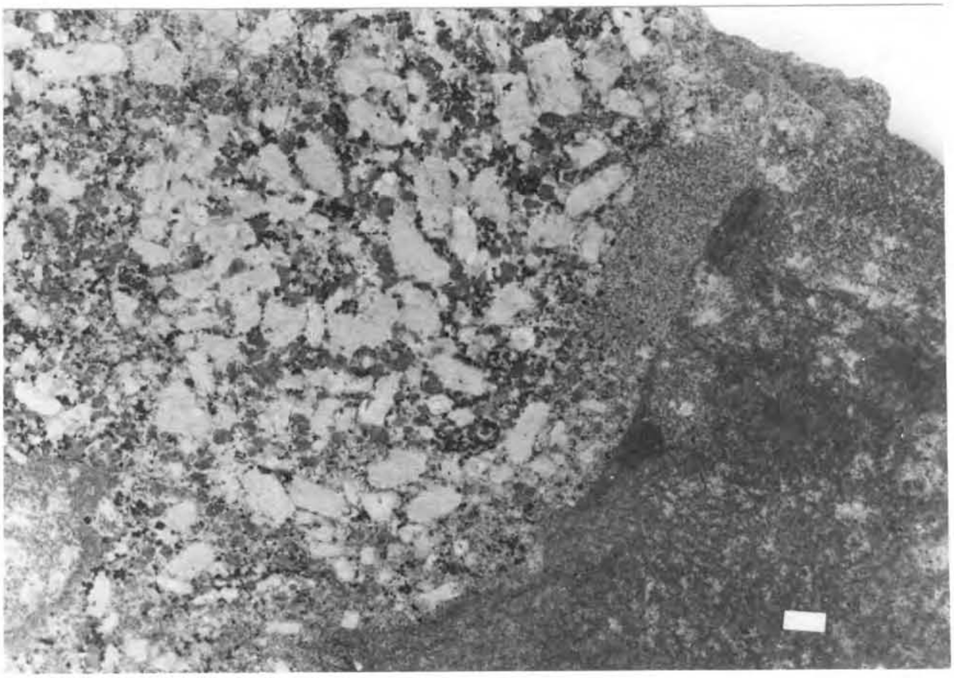

Figure 4.3 Enclave: sawn slab of finer-grained variety of porphyry (under white 10 mm long scale bar) in megacrystic granite. Specimen 88/14-2 from locality {390296}.

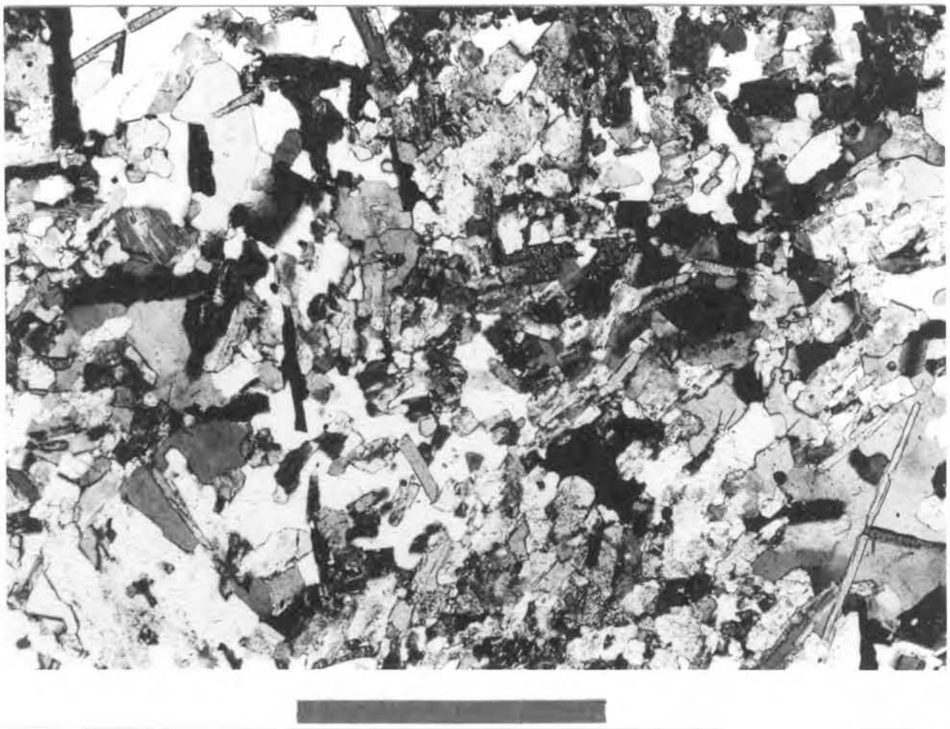

Figure 4.4 Enclave: photomicrograph of seriate-textured porphyry 88/14-2 under crossed polarisers showing very elongate biotite cryatals in a two-feldspar quartz groundmass.

varieties) are found in both the microgranite and megacrystic granite in widely separated localities (Appendix B.1; Figs. 3.17, 3.18, 4.3 & 4.4), so the porphyry body is possibly the earliest intruded facies (see discussion in Ch. 3).

EVEN-GRAINED MICROGRANITE

Gradations exist from a rock with 0.2 to 0.5 mm grainsize range to more porphyritic and coarser varieties. Perthite constitutes from 30 to 40% of the bulk, plagioclase 10 to 15% (sometimes as large euhedral phenocrysts that show concentric cracks: Fig. 4.5) and quartz 40 to 55%. Micas are sparse: 1% or less is common and 5% rare. A chloritised, deep coloured biotite is found in this facies. Accessory minerals present are occasional fluorite, monazite, zircon, allanite and pyrite.

At the southern contact a distinctly reddened alteration zone is found: this is essentially the same lithology as the even-grained facies except that the rock is deep red in hand specimen and under the microscope the feldspars show considerable sericitisation and kaolinisation. Sericite and opaques are all that remain of any micas. Blocks of microgranite have been observed within megacrystic granite near their contact.

MEGACRYSTIC GRANITE

This lithofacies is coarse grained with potash feldspar megacrysts typically from 6 to 15 mm long. These are subhedral, micro-perthitic and often zoned, some zones being altered to a red sericite-iron oxide mixture. Plagioclase feldspar is finer grained (1 to 8 mm), zoned and often shows cloudy cores. Zoning is optically distinct and analysis by microprobe indicates compositional of An_5 in the groundmass and variation from core to rim of An_{47} to An_{28} in coarse phenocrysts. Quartz is usually anhedral and forms phenocrysts up to 5 mm across. The mica present is a deep red-brown biotite up to 2 mm with very ragged margins, often containing much included apatite and very fine grained zircon which produces prominent pleochroic halos (Fig. 4.6), some to 0.05 mm radius from the inclusion. It can occasionally be seen to pseudomorph hornblende and occurs also as clusters to 4 mm diameter. The groundmass of this facies is from 0.5-1 mm grainsize and subordinate in quantity to the phenocrysts. Accessory minerals present are apatite, monazite, zircon, allanite (rarely in 2 mm long euhedral crystals) and, less frequently, pyrite and interstitial topaz or fluorite. Alteration is ubiquitously present, but

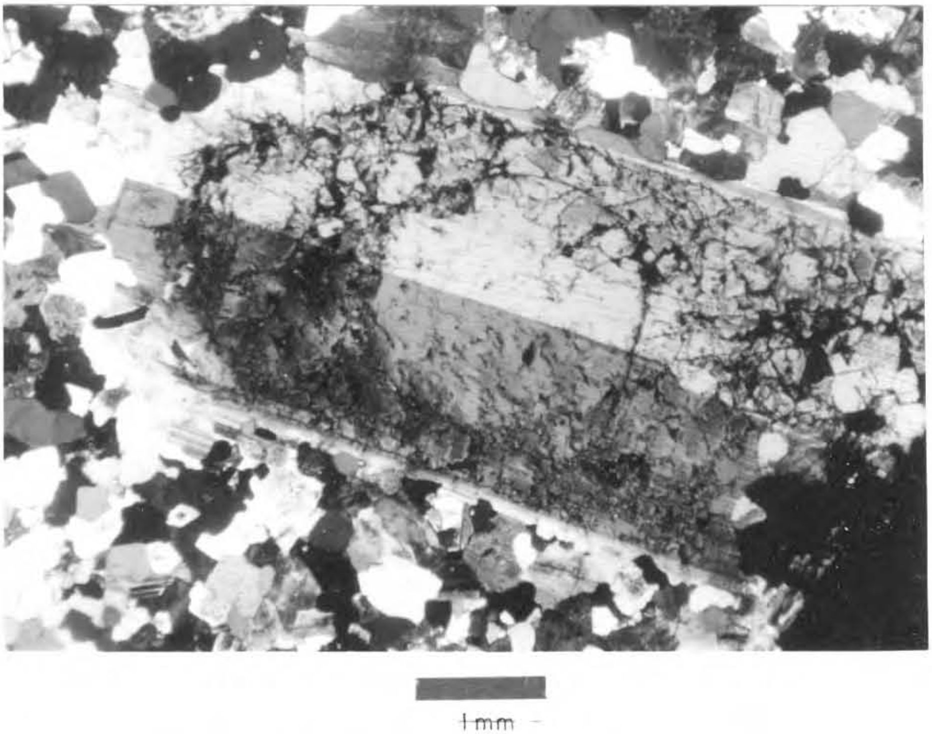

Figure 4.5 Even-grained granite: specimen 88/14-8 from {394296}. large cracked and altered plagioclase phenocryst. Thin section under crossed polarisers.

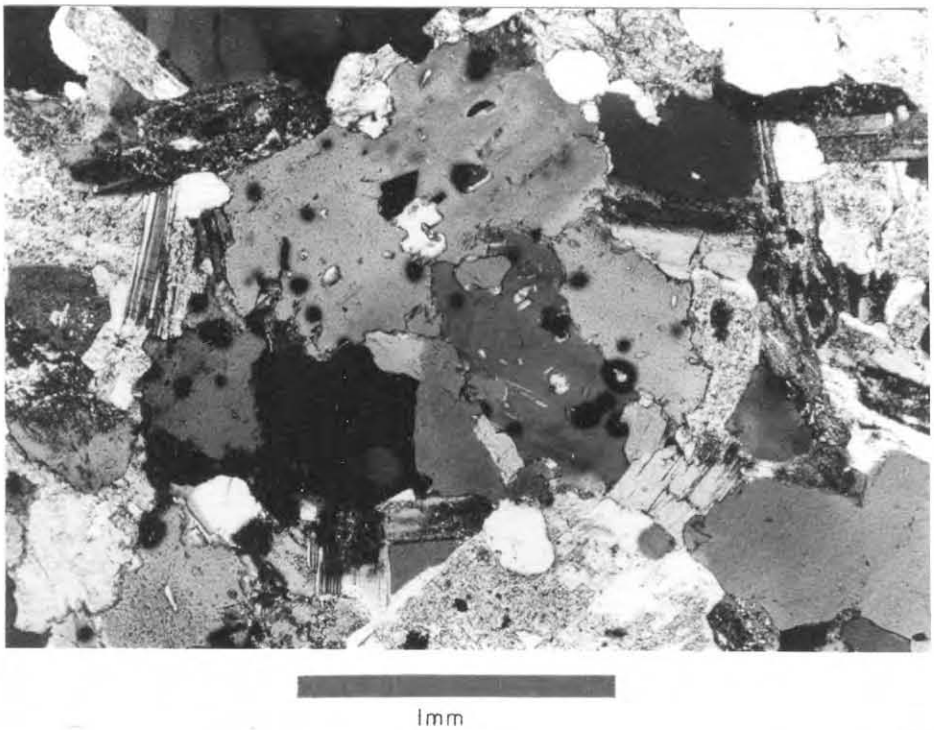

Figure 4.6 Cluster of very red biotite grains containing many zircon inclusions (restite?) in megacrystic granite 88/15-6 from {373309}. Thin section under crossed polarisers.

is limited to slight kaolinisation of feldspars, the perthite being most affected. Mineral proportions vary from: perthite 30-40%; plagioclase 20-10%; quartz 40- 45% and micas <1 to 5%.

Occasional centimetre-sized miarolitic cavities, containing quartz and tourmaline have been seen close to the margins of the pluton.

Li-MICA TOPAZ LEUCOGRANITE

This lithology has a striking texture dominated by equant quartz phenocrysts 2 to 4 mm across in a groundmass that is most commonly 1 mm long subhedral to euhedral plagioclase (some are poikilitically included in the quartz), although some localities show a predominance of perthitic orthoclase in the groundmass. A pale lithium mica is present as anhedral, often quite skeletal phenocrysts 1 to 4 mm across. Accessory minerals are rarely included in this mica. It forms a maximum of 15% of the bulk of the rock, but is often present to only 1%. Proportions of the other minerals vary greatly between

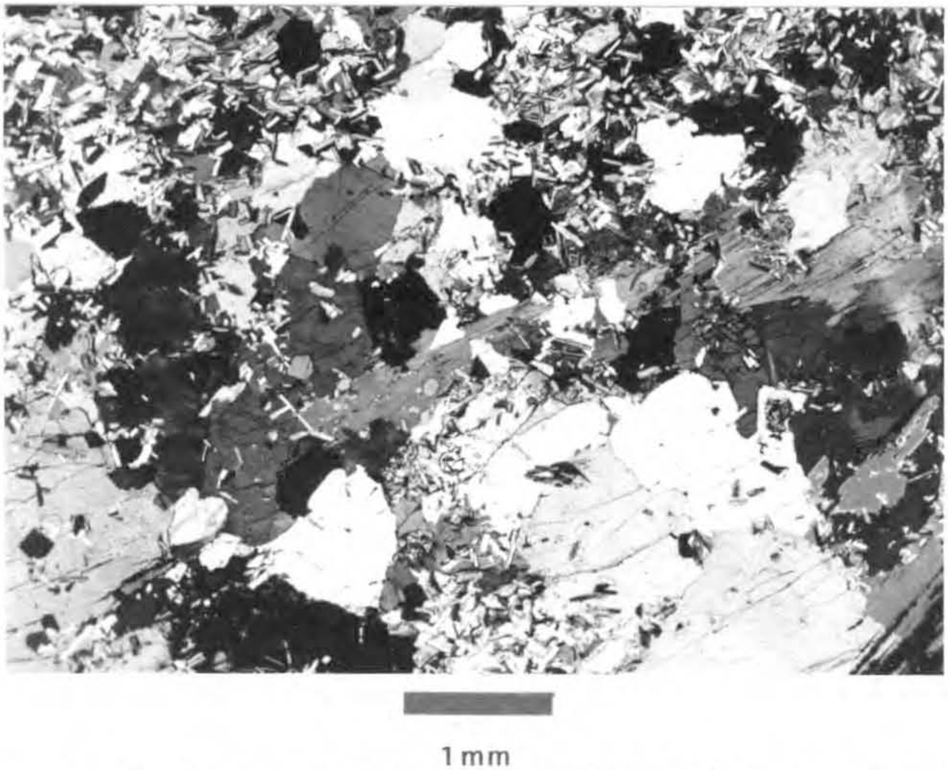

Figure 4.7 Ork contact: photomicrograph of pegmatite (here quartz and topaz) with coarse zinnwaldite) in contact with the leucogranite. Locality {429235}. Crossed polarisers.

localities (K feldspar 10 to 50%, plagioclase 60 to 30%). Topaz is a common interstitial mineral and may constitute 3% of the bulk by volume. Fluorite is also common in this facies. Schorl, apatite and allanite are occasional accessories. Surprisingly, the K-feldspar is the only mineral showing slight alteration. Where this facies forms sills (as at 421279) the plagioclase laths show a preferred orientation (flow foliation). Fig. 4.7 shows a thin section of the facies in contact with a pegmatite dyke.

GREISEN

At the SE corner of the Thirtymile stock the Li-mica leucogranite is cut by close-spaced joints, from 2 to 20 cm apart and steeply-dipping, that carry a greisen-type mineralogy. Li-mica which is coarser than the surrounding microgranite and showing a slight purple hue in thin section is common, together with topaz and quartz as irregular masses. The veins are commonly only 6 mm thick. The mica in these zones contains frequent tiny acicular crystals of an opaque mineral which produces distinct pleochroic halos and is possibly uranophane. Adjacent to the veins, irregular masses of blue tourmaline a few millimetres across are seen in the microgranite.

PEGMATITE

The one locality where pegmatite crops out is the Ork stock contact exposed in the creek (Appendix B.1; Fig. 4.7). Two metre-wide dykes are exposed, one which forms the contact between the marble and microgranite for a short distance (striking E-W and near vertical) and the other, a parallel structure about 5 metres into the pluton. The pegmatite is composed chiefly of brilliant green microperthitic orthoclase in subhedral crystal to 150 mm long with a roughly equal amount of 15 mm crystals of quartz and topaz with finer (5-10 mm) grey mica. No accessory minerals were noted in hand specimen or in one 75 x 50 mm thin section prepared from the pegmatite. The contact with the microgranite is very sharp and easily distinguished in section.

4.2.2 PETROGRAPHY OF THE NW THIRTYMILE STOCK

The NW Thirtymile stock is fairly mineralogically homogeneous. Hornblende dominates the texture of the rock, being in mostly euhedral form and up to 3 mm long. It is occasionally markedly zoned and can contain some round epidote masses (especially specimen 98/16-3). Plagioclase is oscillatory zoned in the larger, untwinned forms which can reach 2.5 mm length. Smaller, subhedral forms are Carlsbad-Albite twinned. K-feldspar is present as microperthite and lesser amounts of microcline and is mainly anhedral. It can form a few megacrysts up to 7 mm long. Quartz is always anhedral and shows common fluid inclusions in linear arrays (healed fractures). Biotite is not plentiful and occurs as very ragged interstitial grains. Sphene is quite noticeable in some specimens (98/16-1: 1 mm euhedral crystals, some in aggregates with opaques, apatite and some small hornblendes). Apatite is present in every specimen as stumpy crystals to 0.3 mm long. Where microcline is present a little granophyre often mantles it (in 98/17-1 particularly). Modal analyses of specimens from this pluton are presented in table form in appendix C.4 and microphotographs are shown as Figs. 4.8 to 4.10.

4.2.3 PETROGRAPHY OF THE SW THIRTYMILE STOCK

The SW Thirtymile intrusion presents a range of basic to intermediate compositions in one body (gabbro to hornblende quartz diorite) with a separate body of more felsic composition. Specimens from the southern portion of the diorite body (08/18-2 and 18-3), see Fig. 3.24, show much subhedral hornblende up to 3 mm long; subhedral plagioclase, which may be strikingly normal zoned, twinned and up to 3 mm long in (18-2): see Fig. 4.11; with minor ragged biotite to 0.8 mm; very subordinate microperthite and interstitial quartz. Sphene and apatite are prominent accessory minerals and opaques are in clusters with the apatite in (18-3). Specimen (18-1) is from a 2m wide dyke in quartzite close to the diorite contact. It shows euhedral equant Hornblende crystals to 3 mm which are enclosed in euhedral plagioclase (Carlsbad-Albite twinned) to 8 mm long, and together with apatite needles to 0.7 mm long they form aggregates. Smaller separate euhedral plagioclase crystals to 1.2 mm are cracked, have altered cores and show striking normal zoning. The majority of a (felsic) groundmass is ≤0.1 mm

Figure 4.8 NW Thirtymile hornblende granodiorite 98/16-5 from {282450}. Thin section under crossed polarisers showing a large zoned and single-twinned microperthite phenocryst with euhedral hornblende in a plagioclase-quartz groundmass.

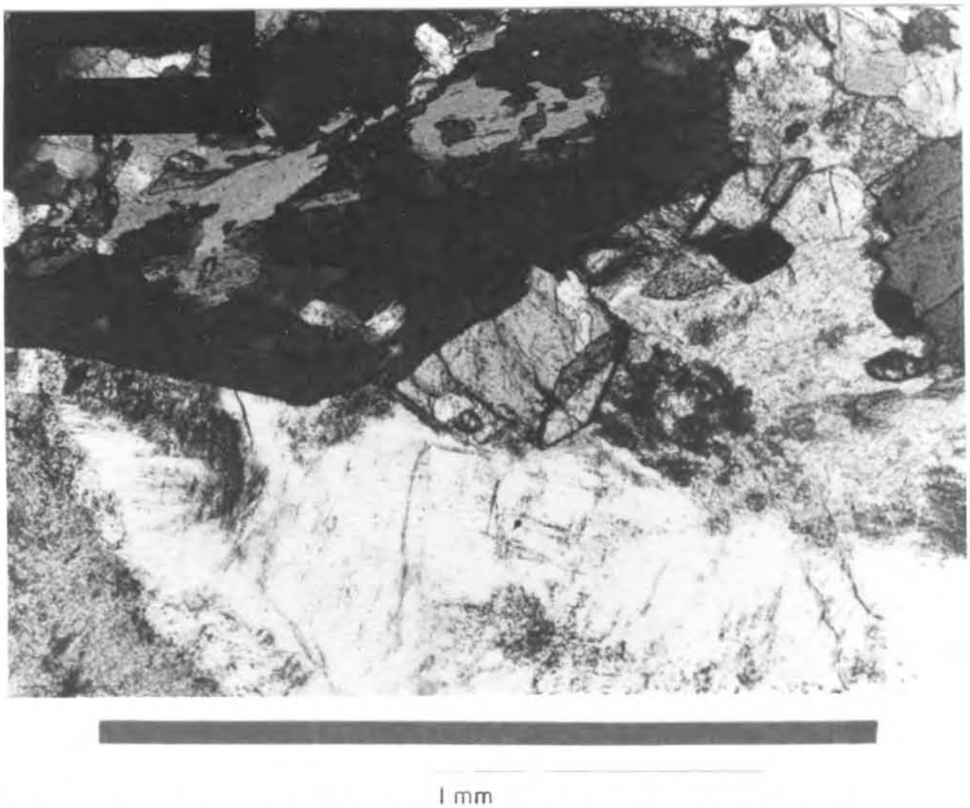

Figure 4.9 NW Thirtymile granodiorite 98/16-3 from locality {281446} under plain polarised light showing hornblende associated with yellow epidote and euhedral sphene.

grainsize- 55% of the volume. No obvious quartz is present.

At the contact of the NW portion of the stock the rock (08/20-1) shows 1 mm long, thin, kinked pale brown mica grains in a groundmass of 0.15 mm plagioclase laths and carbonate (Fig. 4.12). Apatite, as 0.1 mm equant crystals is prominent in this groundmass. A 10 mm xenolith of quartz (originally quartzite) has embayed margins. Exposure at this particular locality is limited, however it is obvious that this forms a very small body, possibly a dyke of only 1 metre width. It is interpreted to be a lamprophyre, the mineralogy being not unusual for the calc-alkaline lamprophyres (see Rock, 1987: Table 1). At locality 08/20-2 subhedral pink augite, 1.5 mm long is sometimes enclosed in biotite (to 1.5 mm long) and occurs with subhedral plagioclase (to 1.5 mm) in a groundmass of fine plagioclase. It also has clusters of opaques (0.5 mm) and a few 0.05 mm long apatites. (Gabbro: Fig 4.13).

The two northernmost specimens (08/20-5, 6) have no obvious quartz in thin section. The first shows anhedral hornblende containing some remnant pyroxene, anhedral biotite containing prismatic apatite to 0.3 mm (biotite to 2 mm) and occasional separate subhedral augite to 5 mm long which is rimmed by hornblende in an anhedral plagioclase groundmass (plagioclase is 0.5-3 mm long). The second is an altered gabbrowhich has much very chloritised augite (1 mm) and with some hornblende and ragged biotite (0.5 mm), interstitial microperthite and very sericitised plagioclase. Some prominent apatite is up to 0.2 mm long. Two specimens were sectioned from the western diorite to granodiorite body. The granodiorite is represented by 08/20-3 which has anhedral hornblende 1 mm long which includes apatite, sphene and opaques. It occurs with subhedral plagioclase in 1 mm laths and interstitial quartz and microcline. Specimen 08/20-4 contains an enclave of diorite in granodiorite. The granodiorite is reminiscent of the Northwest Thirtymile pluton. It has subhedral phenocrysts of 3 mm long hornblende poikilitically enclosing subhedral 0.5 mm apatite, 1 mm plagioclase and 1 mm sphene. Other phenocrysts of ragged biotite clusters to 1 mm and microcline (3 mm), are in a finer quartz and altered 1 mm plagioclase lath groundmass. Some yellow epidote is included in the hornblende. An enclave is much finer: anhedral very green hornblende; a little subhedral 0.2 mm augite with ragged 0.3 mm biotite in a microcline-plagioclase groundmass containing some round quartz grains and ragged 0.3 mm biotite.

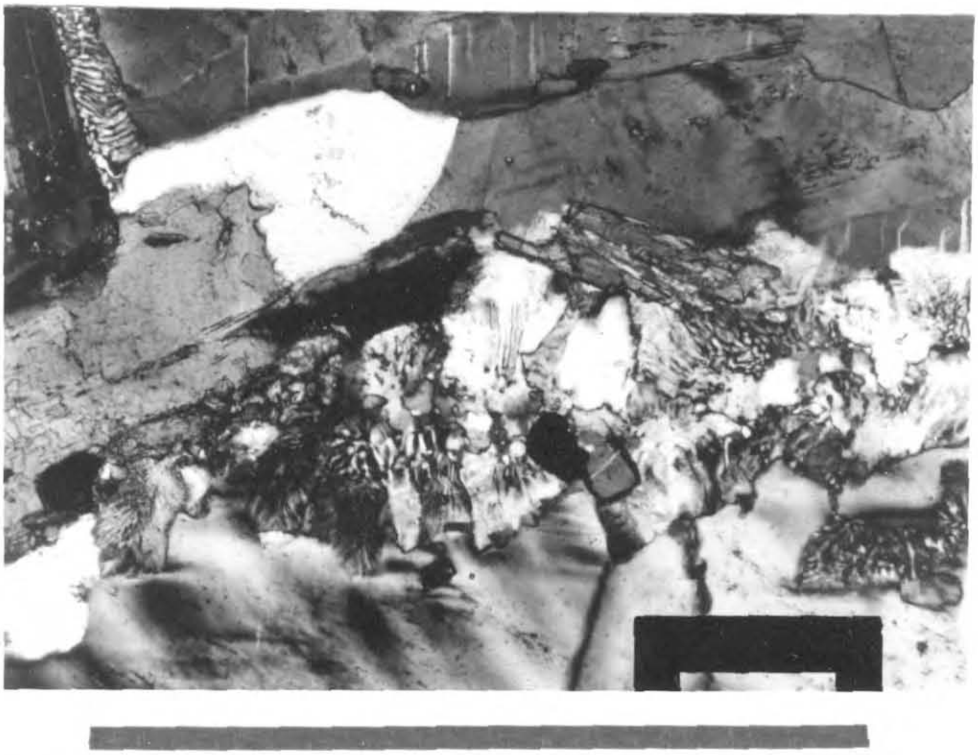

Figure 4.10 NW Thirtymile granodiorite 98/16-1: section under crossed polarisers showing granophyre development.

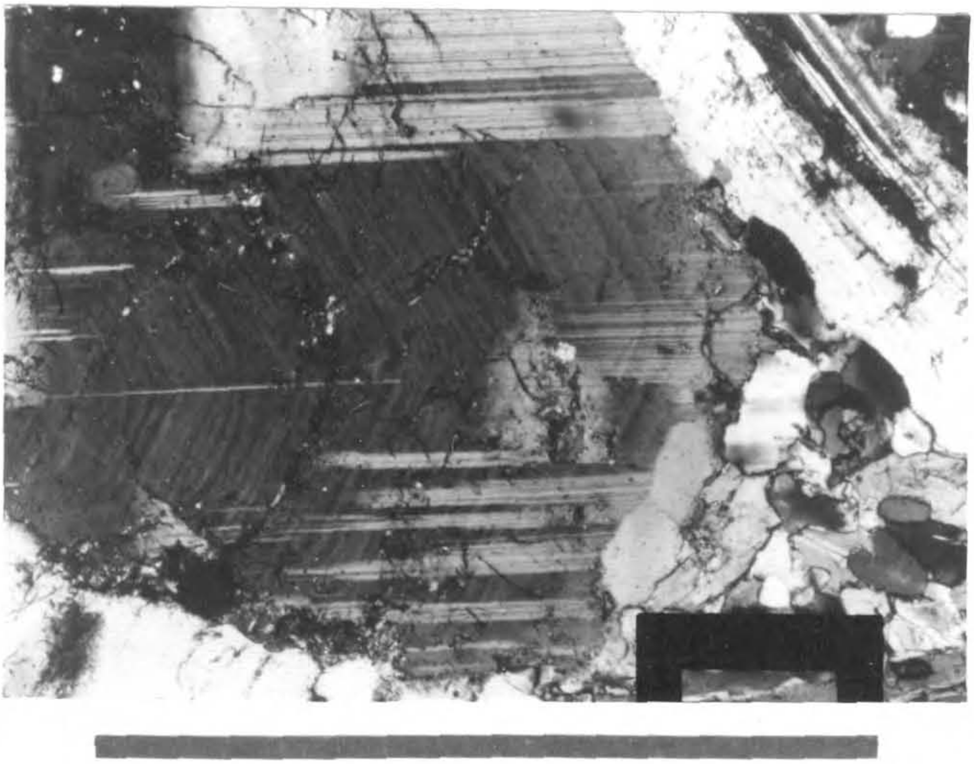

Figure 4.11 SW Thirtymile diorite 08/18-2 from locality {393112}.
Thin section under crossed polarisers showing zoned and twinned plagioclase and hornblende.

4.2.4 THE HAKE BATHOLITH

The granites of the Hake batholith exhibit two textural types: those with prominent rounded quartz phenocrysts and a K-feldspar megacrystic type. Sample locations are shown on Fig. 3.25. The specimens (08/17-1 & 4) which show the round quartz and 08/17-3, which has in addition a distinct granophyric texture, are in the NW portion of the batholith and may represent a lithofacies at the margin of the pluton. The very limited sample density precludes the possibility of judgment as to whether a particular mappable zoning actually exists. These granites show round polygonised quartz grains up to 8 mm size with the occasional subhedral perthite megacryst to 12 mm long. Plagioclase is around 2 mm grainsize and Carlsbad-Albite twinned. Biotite is always golden-brown, ragged and interstitial to the feldspars. It contains occasional zircon inclusions. A few grains of fluorite (0.5 mm) were noted with the mica in (17-1).

Specimen 08/17-4 is a porphyritic type intermediate between the two in having 8 mm quartz ocelli, clusters of 5 mm perthite and antiperthite crystals with 2 mm plagioclase phenocryst in a finer groundmass of 0.1-0.2 mm quartz, untwinned feldspar and 0.5 mm biotite.

The megacrystic specimens (08/17-2, 5, 7 and 08/21-11, 13, 14) show microperthite megacrysts up to 20 mm long with usually finer (rarely 16 mm but usually 6 mm in the coarser varieties and 1-2 mm in others) carlsbad-albite twinned plagioclase, anhedral quartz to 6 mm and always ragged golden brown to dark brown biotite. Specimen 21-13 was the only one to exhibit relatively coarse (1 mm) zoned subhedral allanite. Occasional granophyric intergrowths rim the K-feldspars (especially in 08/17-5) and is probably the rapakivi texture noted in hand specimen. Rare antiperthite has been noted only in this specimen.

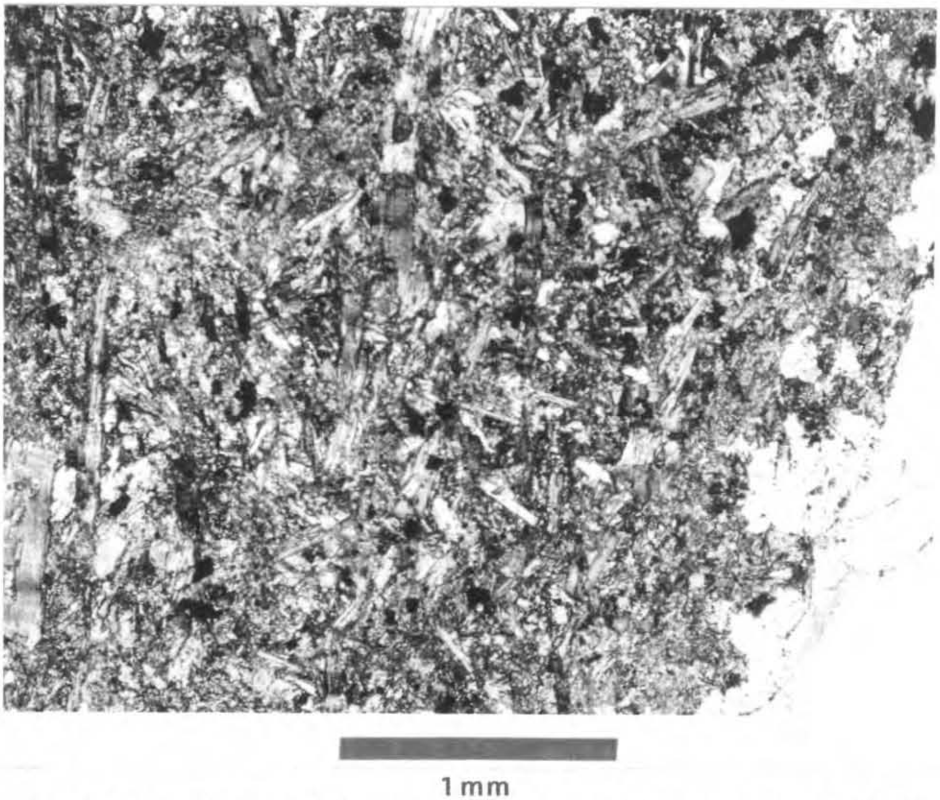

Figure 4.12 SW Thirtymile area: phlogopite-rich lamprophyre 08/20-1 found adjacent to the contact of the basic stock at {387128}. Photmicrograph taken under crossed polarisers shows kinked mica flakes in a plagioclase-carbonate groundmass in contact with a quartzite or chert xenolith.

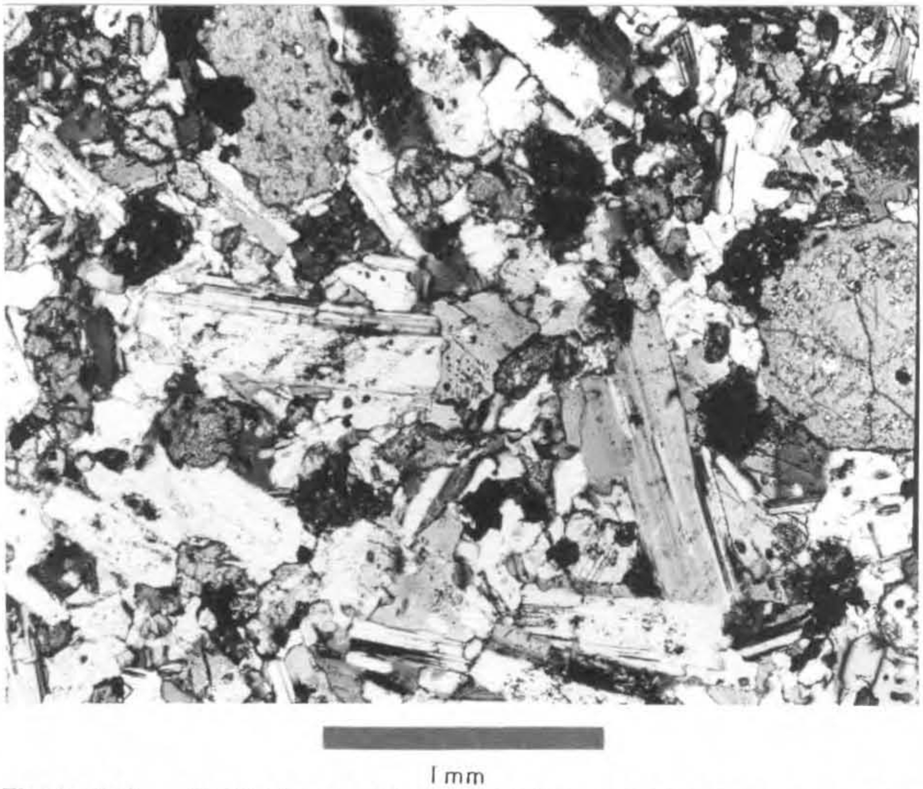

Figure 4.13 SW Thirtymile gabbro 08/20-2 from {388131}. Thin section under crossed polarisers showing titanaugite, plagioclase and a little olivine.

4.2.5 THE SEAGULL BATHOLITH

The portions of the Seagull batholith examined are mostly finer and more even-grained than the Hake granites. Localities (Figs. 3.27 & 28) that showed a very even-grained lithology are 07/21-1, 2, and 07/30-1. These showed only the rare perthite megacryst (8 mm) and were mostly 1-2 mm in grainsize. The rather ragged biotite is a 'foxy-red', i.e. indicative of reducing conditions in the magma (White, 1990) and contains frequent zircon inclusions that produce small pleochroic halos. Some secondary muscovite accompanies the biotite. Blue tourmaline, fluorite and topaz are frequent, though small, accessory minerals.

The coarser-grained specimens (07/30-3 and 08/03-1, from the Dorsey Lake area in the NW) are somewhat different. The first has 15 mm clusters of plagioclase and perthite with some granophyric margins in a groundmass of around 1 mm grainsize composed of quartz, feldspars with red biotite as 2 mm clusters containing much zircon. Some interstitial fluorite is noticeable in the groundmass. The second specimen has round quartz phenocrysts and 10 mm perthite megacrysts in a 1 mm grainsize quartz-plagioclase-orthoclase groundmass which contains a few very ragged chloritised hornblende relicts (0.3 mm) and brown biotite which containing zircon. A little fluorite is visible. Three specimens from the STQ tin stockwork are included in the analytical data. These rocks are fine grained (<2 mm grainsize) and felsic, being virtually devoid of micas. One specimen ('STQ') is of drillcore from the buried stock and the others are from dykes that outcrop at the surface.

4.2.6 MODAL COMPOSITIONS

The modal compositions of a selection of specimens from each facies of the Thirtymile stock (see appendix C.4) plot in the granite field of a Streckeisen diagram (Fig. 4.14). The coarser granites (megacrystic facies) do, however, show a considerable difference between results obtained from sections cut at different orientations (Appendix C.4). For this reason point counting was not employed for the granites of the batholiths. The specimens from the hornblende-bearing stocks fall in the granite, granodiorite and quartz monzodiorite/gabbro fields of this classification scheme.

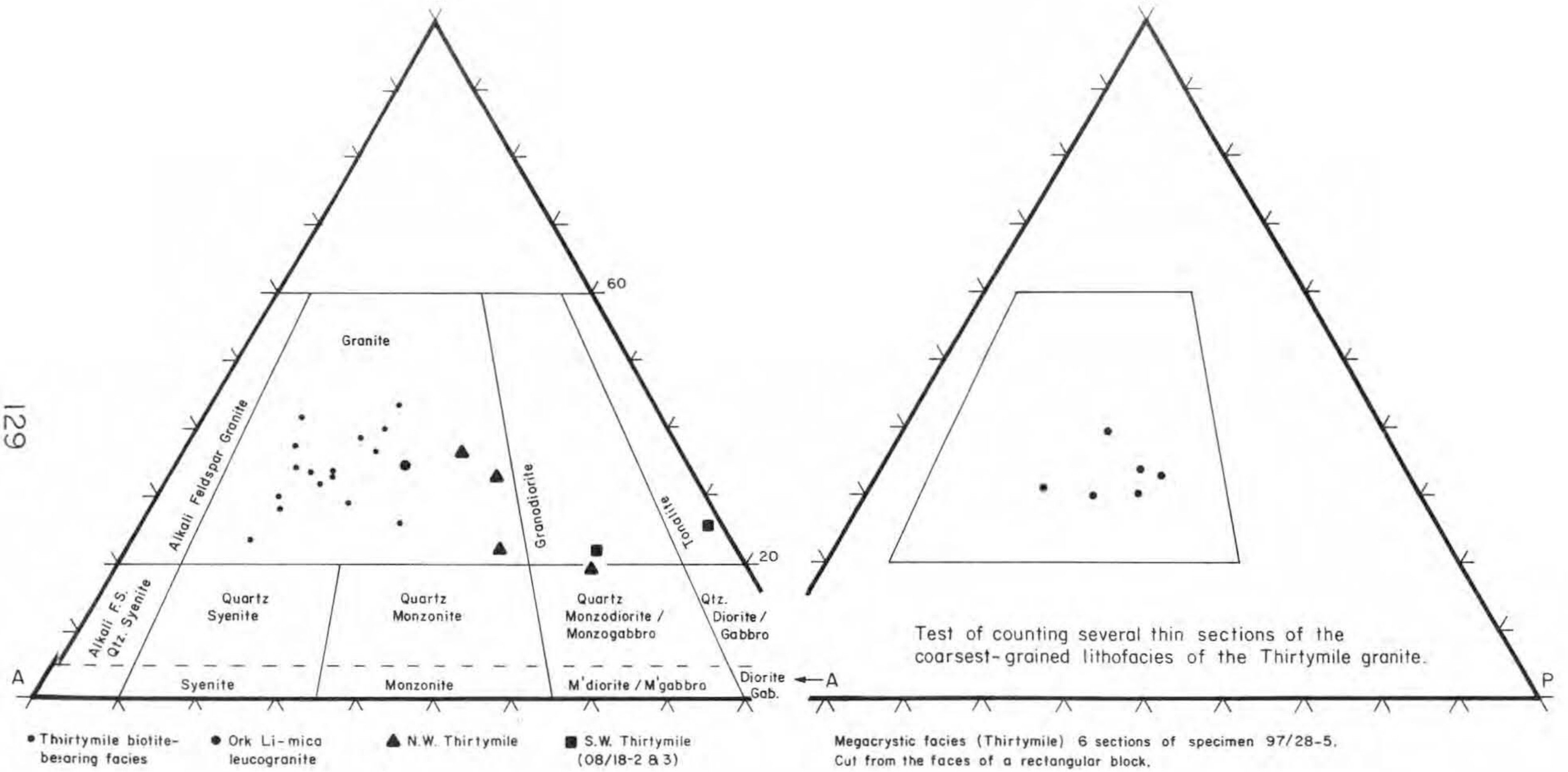

Test of counting several thin sections of the coarsest-grained lithofacies of the Thirtymile granite.

Megacrystic facies (Thirtymile) 6 sections of specimen 97/28-5. Cut from the faces of a rectangular block.

STRECKEISEN DIAGRAMS (MODAL QUARTZ-PLAGIOCLASE-ALKALI FELDSPAR) FOR SPECIMENS FROM THE THIRTYMILE STOCK, WITH A FEW SPECIMENS FROM THE N.W. & S.W. THIRTYMILE STOCKS.

Fig. 4.14

4.3 GEOCHEMISTRY OF THE PLUTONS

4.3.1 ANALYSIS

Chemical data obtained from the granites is of the following forms:

1) Whole-rock analysis for major elements: X-ray fluorescence (XRF) analysis of fused borate glass beads was employed for the Thirtymile suite of specimens and Inductively Coupled Plasma Emission Spectrometry (ICP) analysis of nitric acid digested borate fusions was used for specimens from the other plutons.

2) Trace element analysis of pressed rock powder disks was achieved using X-ray fluorescence (XRF) analysis for all rocks. A few rock specimens were also analysed by ICP (yielding their Li content), for F and for H_2O^+ (see following methods).

3) Mica analyses were made to test whether their composition would provide an indication of fractionation or 'specialisation' of the stanniferous plutons. Recent work (Scott, 1988) has shown that tin-bearing granites may have biotite compositions considerably richer in Fe than adjacent unmineralised plutons. Micas were separated from powdered granite of the Thirtymile and batholith facies by magnetic techniques. These specimens were analysed by ICP for both major and trace elements. Since spectrometric techniques do not differentiate the oxidation state of elements titration was employed on cold HF digested specimens to determine the Fe^{2+} content (Wilson method). Water was determined as H_2O^- by gravimetry and as H_2O^+ by the Penfield tube technique. F was determined by sodium carbonate fusion and the colourimetric method of Hall and Walsh (1969), Cl by sodium carbonate fusion then ion-selective electrode and Rb by atomic absorption spectrophotometry.

4) A limited number of specimens of granite were analysed under the electron microprobe (energy dispersive analysis) to determine variations in composition of the feldspars.

5) Granite from the Thirtymile stock was analysed with the mass spectrometer to obtain a whole-rock Rb/Sr isochron and initial Sr ratio.

4.3.2 MAJOR ELEMENT GEOCHEMISTRY

Major and trace element analyses for the various stocks and the two batholiths are tabulated in appendix C1. The data in this table have been presented to show all major element analyses as water-free, i.e. corresponding to ignited rock, with the combined water as an additional amount shown after the total, as is the custom with determinations at the R.H.B.N.C. XRF laboratory. A normalisation calculation (the "Ignite" programme of Dr. M.F. Thirlwall) was applied to those analyses obtained by ICP to achieve uniformity.

AVERAGE COMPOSITION

Average compositions (Table 4.1) for the four Thirtymile lithofacies, the two batholiths and the highly leucocratic STQ stock, associated with the Seagull batholith, show that these granites are all particularly silica-rich (i.e. >72.7%) and low in Mg-Fe (i.e. 3.04-0.56% [Mg+Fe]). They are highly fractionated granites (Larsen Index= 14.13-16.82), which have appropriate ranges of trace element contents: high alkalis (especially Rb, Li) and HFSE elements Nb and Th, and low Sr and Ba. They compare well in trace element contents with the Sn-U enriched 'high heat production' (HHP) granites of the Caledonian and Variscan terranes of Europe and the highly evolved tin granites of Alaska (Table 4.2). They are more felsic than the average granite and the than the usual calc-alkaline batholith (Table 4.3), which have average compositions ranging from tonalite to adamellite (quartz-monzonite in North American parlance).

The NW Thirtymile stock and leucocratic (west) part of the SW Thirtymile stock have compositions intermediate between the average granodiorite and tonalite with the east part of the SW stock being somewhat more basic than the average diorite (Fig. 4.15 to 17). Average trace element contents of these stocks are characterised by low Rb, Nb with high Sr and Ba that compare with the calc-alkaline suites shown.

NORMATIVE COMPOSITION

CIPW norms have been calculated from the analyses and are presented in the appendix. A glance at these norms will reveal that the various Thirtymile stock facies have low normative anorthite; are mostly metaluminous (with the Li-mica facies being the

SEAGULL-THIRTYMILE PLUTONIC SUITE: SEAGULL & HAKE BATHOLITHS, THIRTYMILE STOCK

FACIES	SiO2	Al2O3	Fe2O3	MgO	CaO	Na2O	K2O	TiO2	MnO	P2O5	Total
Li-mica (7)	75.11±1.85	14.75±1.23	0.54±0.24	0.02±0.04	0.11±0.09	5.44±0.92	4.02±0.51	0.01±0.01	0.05±0.01	0.02±0.01	100.07
Even-Gr. (12)	76.64±1.32	12.58±0.29	1.46±0.62	0.12±0.15	0.62±0.16	3.71±0.47	4.90±0.37	0.14±0.09	0.03±0.01	0.03±0.02	100.22
STQ (3)	76.48±0.59	13.02±0.51	1.14±0.22	0.14±0.02	0.43±0.14	3.37±0.15	4.64±0.26	0.06±0.00	0.01±0.00	0.02±0.01	99.31
Seagull b. (11)	76.41±0.95	12.49±0.31	1.52±0.17	0.08±0.05	0.57±0.12	3.34±0.21	5.10±0.31	0.11±0.04	0.02±0.01	0.03±0.01	99.65
Hake b. (11)	76.04±1.67	12.57±0.54	1.76±0.46	0.23±0.09	0.71±0.19	3.21±0.21	5.22±0.39	0.20±0.08	0.03±0.01	0.05±0.03	100.00
Mega. (8)	75.21±1.54	13.09±0.44	1.78±0.55	0.23±0.14	0.92±0.22	3.68±0.25	4.89±0.25	0.24±0.09	0.04±0.01	0.07±0.03	99.93
Porphyry (7)	72.72±1.95	13.67±0.58	2.61±0.52	0.43±0.13	1.16±0.24	3.50±0.27	5.36±0.30	0.40±0.09	0.05±0.01	0.10±0.02	100.00
	Rb	Sr	Ba	Li	Nb	Th	Pb	Cr	Ni		
Li-mica (5)	2074±812	0.9±0.7	16±4	626±188 (3)	71±32	17±8	37±5	3±3	4±1		
Even-Gr. (11)	496±113	23±12	92±53	147±92 (3)	74±9	61±5	38±14	2±1	3±0.4		
STQ (3)	886±36	13±8	35±7	n.d.	114±3	72±16	28±7	1±0.5	4±0.3		
Seagull b. (10)	499±148	16±17	123±144	n.d.	59±9	69±21	32±3	2±0.5	4±0.4		
Hake b. (11)	424±69	50±30	192±120	76 (1)	63±25	71±11	31±10	2±0.8	4±0.6		
Mega. (8)	392±72	71±32	318±171	88±47 (2)	59±6	51±11	44±54	4±3	4±0.7		
Porphyry (7)	304±58	124±25	737±277	78±6 (2)	54±5	46±7	37±17	6±5	4±0.6		

HORNBLENDE-BEARING STOCKS: NORTHWEST & SOUTHWEST THIRTYMILE

STOCK	SiO2	Al2O3	Fe2O3	MgO	CaO	Na2O	K2O	TiO2	MnO	P2O5	Total
NWTM (5)	62.00±1.62	15.50±0.20	6.43±0.76	2.40±0.35	4.81±0.45	3.67±0.05	3.75±0.16	0.62±0.07	0.14±0.02	0.31±0.03	99.63
SW (D+G) (5)	57.20±4.39	15.17±1.45	7.97±2.46	4.77±2.13	7.19±1.67	3.28±0.44	2.97±0.52	0.67±0.20	0.13±0.03	0.33±0.11	99.68
SW (Gr) (2)	60.67±1.81	16.29±0.11	5.82±0.80	2.51±0.28	4.65±0.30	4.44±0.13	4.29±0.16	0.49±0.01	0.11±0	0.26±0.04	99.53
	Rb	Sr	Ba	Li	Nb	Th	Pb	Cr	Ni		
NWTM (6)	88±13	913±106	2073±167	11 (1)	9±2	7±1	32±11	17±3	11±1		
SW (D+G) (5)	67±9	638±37	1290±222		5±2	2±2	19±6	136±99	51±33		
SW (Gr) (2)	98±6	961±0	1345±218		7±2	4±0.6	24±17	46±8	22±4		

Number of specimens is shown in brackets and one standard deviation is given after the mean NWTM= NW Thirtymile; SW= SW Thirtymile; D= diorite; G= gabbro; Gr= granodiorite.

Table 4. 1 **Average compositions for each igneous lithofacies: major and selected trace elements.**

SOURCE	SiO_2	Al_2O_3	Fe_2O_3	MgO	CaO	Na_2O	K_2O	TiO_2	MnO	P_2O_5	Total
A (Calc-Alk.)	70.02±1.62	15.37±0.68	2.04±0.70	0.73±0.30	2.53±0.53	4.16±0.39	3.51±0.62	0.32±0.12	0.03±0.02	0.12±0.04	98.83
B (Calc-Alk.)	62.08±1.87	16.61±0.09	4.63±1.39	2.23±0.63	4.68±0.61	3.95±0.28	3.04±0.29	0.78±0.18	0.07±0.03	0.30±0.06	98.37
C (9)	63.19±2.49	16.42±0.52	5.81±0.47	1.96±0.29	4.76±0.72	3.99±0.15	2.21±0.31	0.65±0.14	0.15±0.05	0.19±0.06	99.33
D (174)	63.41	15.70	5.55	2.71	5.70	3.45	1.69	0.64	0.09	0.10	
E (149)	66.05	16.23	3.79	1.49	4.41	3.82	2.26	0.65	0.06	0.15	
F (Evolved)	75.90	13.10	1.48	0.02	0.86	3.82	4.48	0.04	0.04	0.05	99.70
G (Cornwall)	72.43	15.03	1.96	0.44	0.84	3.11	5.06	0.21	0.04	0.25	99.37
H (Cornwall)	71.10	16.11	1.25	0.09	0.59	3.73	4.84	0.06	0.07	0.50	98.34
I (HHP) (5)	76.3±1.24	13.00±0.44	1.11±0.38	0.17±0.09	0.45±0.24	3.69±0.34	4.90±0.30	0.13±0.07	0.05±0.03	0.04±0.01	99.84

	Rb	Sr	Ba	Li	Nb	Th	Pb	Cr	Ni
A (Calc-Alk.)	92±25 (7)	576±170	1328±373	n.d.	9±4 (5)	6±3 (5)	19±4 (5)	5±2 (5)	3±1 (5)
B (Calc-Alk.)	86±12 (3)	768±206 (3)	1217±224	n.d.	15±5 (3)	12±5 (2)	25±12 (2)	38±19 (2)	27±17 (2)
C (9)	64±13	372±38	890±95	n.d.	14±1	n.d.	n.d.	9±3	5±4
D (174)	49	268	451	n.d.	5	6	8	67	18
E (149)	73	501	863	n.d.	9	9	12	24	6
F (Evolved)	320	38	172	34	25	18	31	5	4
G (Cornwall)	419	94	196	280	n.d.	n.d.	46	n.d.	n.d.
H (Cornwall)	1218	61	204	1260	93	22	16	n.d.	n.d.
I (HHP) (5)	449±96	47±27	n.d.	n.d.	36±10	36±14	33±4	n.d.	n.d.

A= Biotite granodiorites, B= Hornblende-biotite granodiorites: Chemehuevi Suite (John & Wooden, 1990); C= Quartz diorite to granodiorite Puscao Gp.2 (Bussell, 1988); D= Peninsular Ra. West, E= East, (Silver & Chappell, 1988); F= Fairbanks average late granite (Newberry et al., 1990); G= Bodmin 'B', H= Tregonning 'E' (Stone, 1985); I= Cairngorm Main Granite (Webb et al., 1985). Average value ± 1 standard deviation is shown.

Table 4.2 Average compositions of Calc-alkaline, Evolved Alaskan, Cornish and 'HHP' granites.

	AVERAGE ROCK COMPOSITIONS							
LITHOLOGY	SIO2	Al2O3	Fe2O3	MgO	CaO	Na2O	K2O	TIO2
Granite (2485)	72.04	14.42	3.09	0.71	1.82	3.69	4.12	0.30
Adamellite (135)	69.51	14.76	4.20	1.11	2.55	3.51	4.14	0.51
Granodiorite (885)	66.80	15.99	4.71	1.80	3.92	3.77	2.79	0.54
Tonalite (97)	63.04	16.68	6.16	2.78	5.42	3.64	1.99	0.73
Diorite (872)	58.58	16.98	8.25	3.73	6.66	3.60	1.81	0.96

The numbers in brackets indicate size of the database. From LeMaitre, (1976).

Table 4.3 **Average composition of felsic to intermediate plutonic rocks.**

only one with normative corundum exceeding 1%); have some normative clinoenstatite/ortho-ferrosilite, magnetite and ilmenite. Some normative apatite also appears, but no sphene.

The Hake and Seagull batholiths show slightly higher normative corundum than the biotite-bearing facies of the Thirtymile stock and also slightly more normative clinoenstatite/ orthoferrosilite, magnetite, ilmenite and apatite. The Li-mica leucogranite stands alone as having the largest range of values of normative corundum, with some specimens being obviously peraluminous. In the classification of O'Connor (1965) the Thirtymile stock, Hake and Seagull lithofacies are granites (Figs. 4.15 & 4.16).

The two hornblende-bearing stocks are markedly different to the Thirtymile stock and batholiths: the NW Thirtymile shows lower normative quartz and higher anorthite indicating an intermediate composition; no normative corundum; significant normative clinoenstatite/ clinoferrosilite and orthoenstatite/orthoferrosilite components; olivine components in some; magnetite; ilmenite and apatite. The Ti modally present in sphene appears in the ilmenite fraction of the norm calculation. The SW Thirtymile granodiorite has a modal range overlapping that of the NW Thirtymile. The diorites show lower normative orthoclase and quartz; higher anorthite; higher pyroxene components; similar magnetite, ilmenite and apatite to the NW Thirtymile. No normative olivine appears. Specimens 08/20-2 and 6 show no quartz; a marked decrease in orthoclase and albite plus appearance of normative olivine indicating that they are of gabbroic composition. The NW Thirtymile and western (leucocratic) specimens from the SW Thirtymile stock are predominantly granodiorites in the O'Connor normative classification (Fig. 4.17).

When the CIPW normative quartz, orthoclase and albite components (Q-Or-Ab) of the batholiths and Thirtymile stock are plotted on a ternary diagram (Fig. 4.18) two clear trends result:

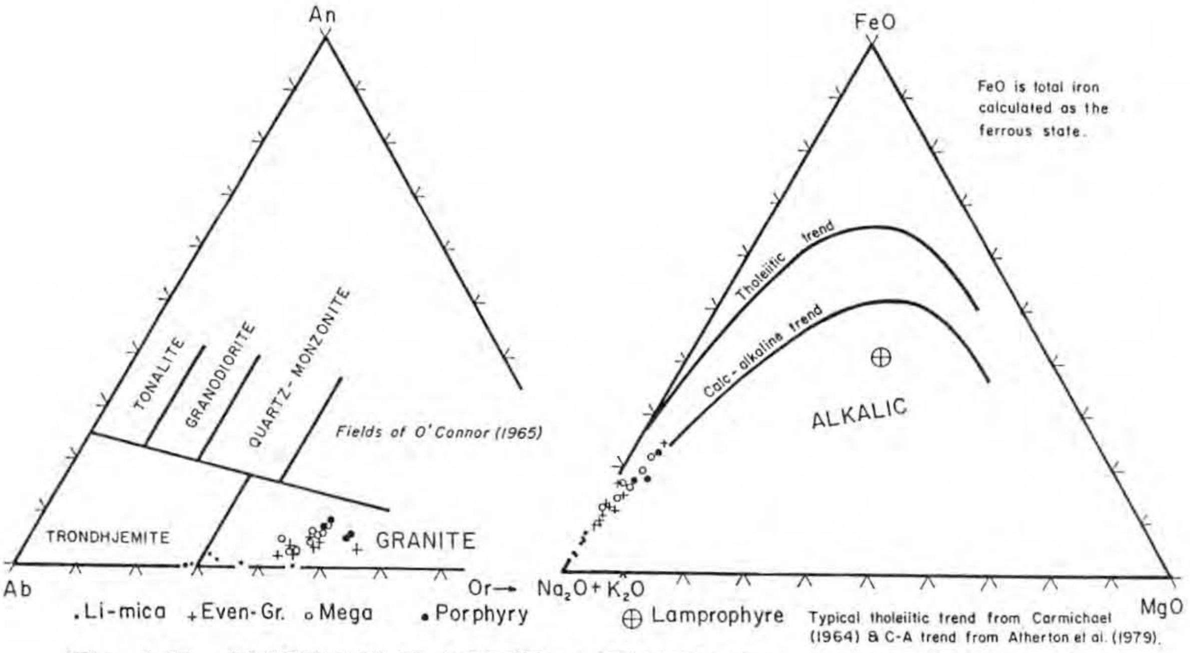

Fig. 4·15 THIRTYMILE STOCK LITHOFACIES: CIPW NORMATIVE Albite-Anorthite-Orthoclase & AFM DIAGRAMS.

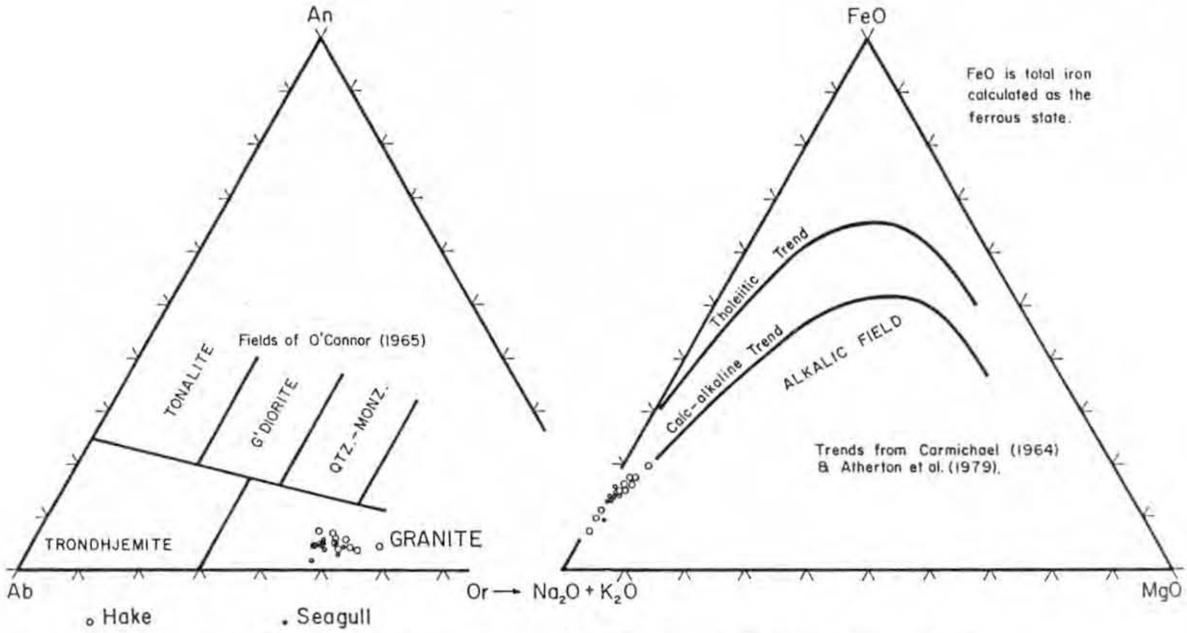

Fig. 4·16 HAKE & SEAGULL GRANITES: CIPW NORMATIVE Albite-Anorthite-Orthoclase & AFM DIAGRAMS

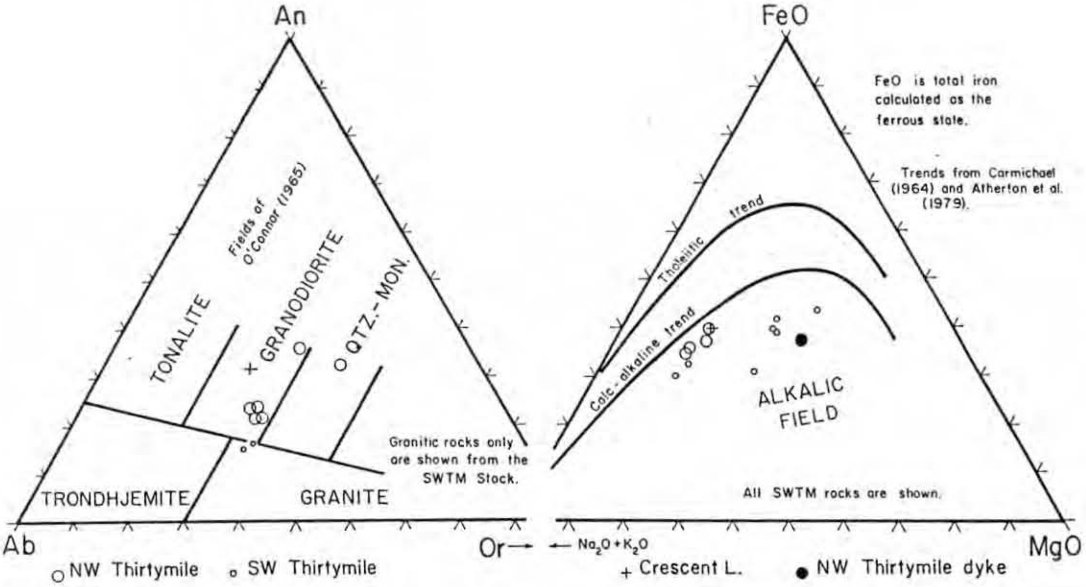

Granitic rocks only are shown from the SWTM Stock.

FeO is total iron calculated as the ferrous state.

Trends from Carmichael (1964) and Atherton et al. (1979).

All SWTM rocks are shown.

Fig. 4·17 N.W. & S.W. THIRTYMILE STOCKS: CIPW NORMATIVE Albite-Anorthite-Orthoclase & AFM DIAGRAMS.

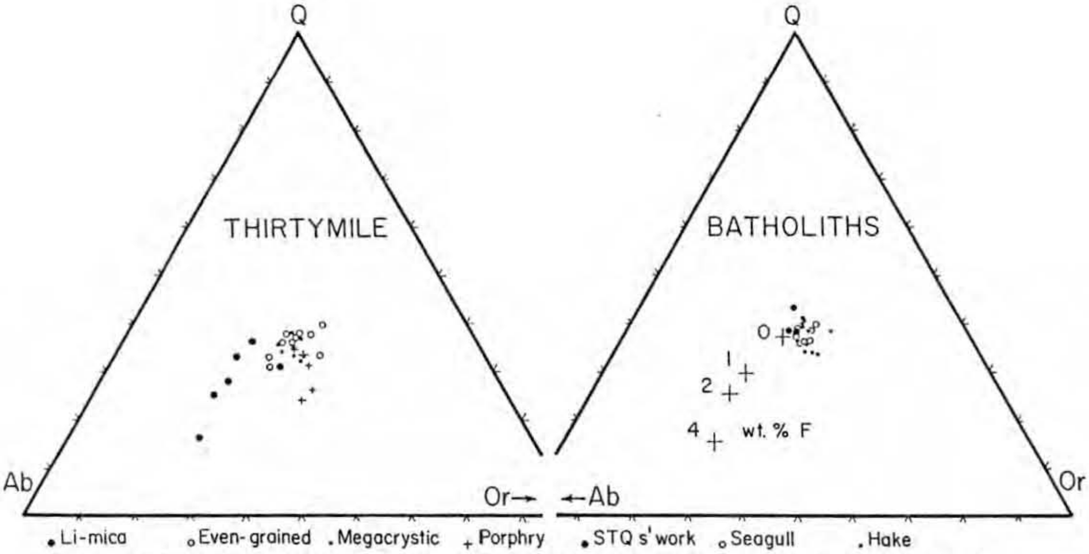

Points labelled 0, 1, 2, 4 represent minimum melting compositions for the quartz-orthoclase-albite system at 1kbar as reported in Manning (1982).

Fig. 4·18 Quartz - orthoclase - albite C.I.P.W. normative components for the granites of the Seagull - Thirtymile plutonic suite.

(1) A trend toward silica enrichment that progresses from the porphyry through the megacrystic and even-grained facies of the Thirtymile stock to the batholiths, with the most quartz-rich specimen being the alaskitic intrusion below the STQ tin stockwork, which is associated with the Seagull batholith. A very slight increase in orthoclase component over the albite component is indicated.

(2) A trend away from quartz enrichment and towards significant increase in the albite component in the leucogranites. The significance of these trends will be discussed in sections 4.7.6 and 6.4.3.

MAJOR ELEMENT TRENDS: VARIATION DIAGRAMS

The various facies of the Thirtymile stock show some sensible chemical trends when variation diagrams are examined. The clearest linear variation is exemplified by Harker plots of Al_2O_3, CaO, TiO_2, MnO and P_2O_5. These are reproduced in Figs. 4.19-20. There is a progression in composition from Porphyry through Megacrystic to Even-grained and (sometimes) Li-mica facies. The batholiths follow the same trends, overlapping the values of the Thirtymile megacrystic and even-grained facies. These trends are:

1) Al_2O_3 shows a very linear decrease with silica increase from the Porphyry to Even-grained and Seagull granites, which overlap. The Li-mica leucogranites, however, occupy a separate linear field which is higher in Al_2O_3 than the main trend. In fact, the highest Rb-bearing specimens plot as the highest Al_2O_3 types. If the Rb content is indicative of degree of fractionation, then this distribution indicates a reverse direction to that of the batholith-stock trend.

2) CaO and TiO_2 show some scatter, but do define a linear trend between the Thirtymile Porphyry and the Seagull granite. The Li-mica leucogranites show the lowest contents and, because of a spread in silica content, fall below the values shown in the biotite-bearing facies.

3) MnO distribution shows a less-well defined though still obvious trend. The Li-mica facies is generally higher in this element than the biotite granites of similar silica content.

4) P_2O_5 distribution defines a linear trend with the Seagull granites showing some scatter, but the Li-mica leucogranites are in a separate field of the lowest values,

irrespective of silica content.

5) The alkalis show a broad spread on a Harker plot: K_2O does, however, generally increase in the facies with higher silica content. The Li-mica leucogranites show the most alkali enrichment. The NW Thirtymile and SW Thirtymile stocks do not correspond to the linear trends indicated by CaO and TiO_2 plots for the Thirtymile stock and batholiths (TiO_2 shown in Fig. 4.21 c), clearly occupying separate fields on the Harker diagrams.

4.3.3 TRACE ELEMENT GEOCHEMISTRY

TRACE ELEMENT VARIATION

The following trace element analyses are presented in the form of Harker diagrams.

1) Rb shows (Fig. 4.19 d) a gradual increase through the Thirtymile facies from porphyry to even-grained facies then to granites of the Seagull batholith, as the most evolved lithofacies. Analyses from the Hake batholith overlap the fields of the megacrystic and even-grained facies. Those of the Seagull batholith overlap the range of the even-grained facies. The Li-mica facies displays spectacular (non-linear) enrichment in Rb.

2) A Sr plot (Fig. 4.19 f) demonstrates a wide range of values in the Thirtymile stock, from 150 to <1 ppm, which plot as a linear trend, including the leucogranites as well as the biotite-bearing facies. The same trend is occupied by the batholiths, with the specimens from the eastern part of the Seagull granite having the lowest contents. Significantly, the STQ dyke/stock specimens, which are highly leucocratic facies of the Seagull batholith associated with a tin stockwork, are not among the most evolved if depletion of this element is taken as an indicator (STQ Range 7-22 ppm compared to Seagull NW of 1-45 ppm and Seagull east range 2-13 ppm: see Append. C1).

The NW Thirtymile and SW Thirtymile stocks plot as broad separate fields, which require considerable imagination to correlate with the batholith trend (Sr to Ba is shown in Fig. 4.21b).

3) Ba distribution: The Thirtymile facies show a linear distribution from over 1100 ppm in the porphyry to <50 ppm in the Li-mica (Fig. 4.19e). The batholiths show somewhat greater scatter, but cover portion of the same field. The NW and SW Thirtymile stocks

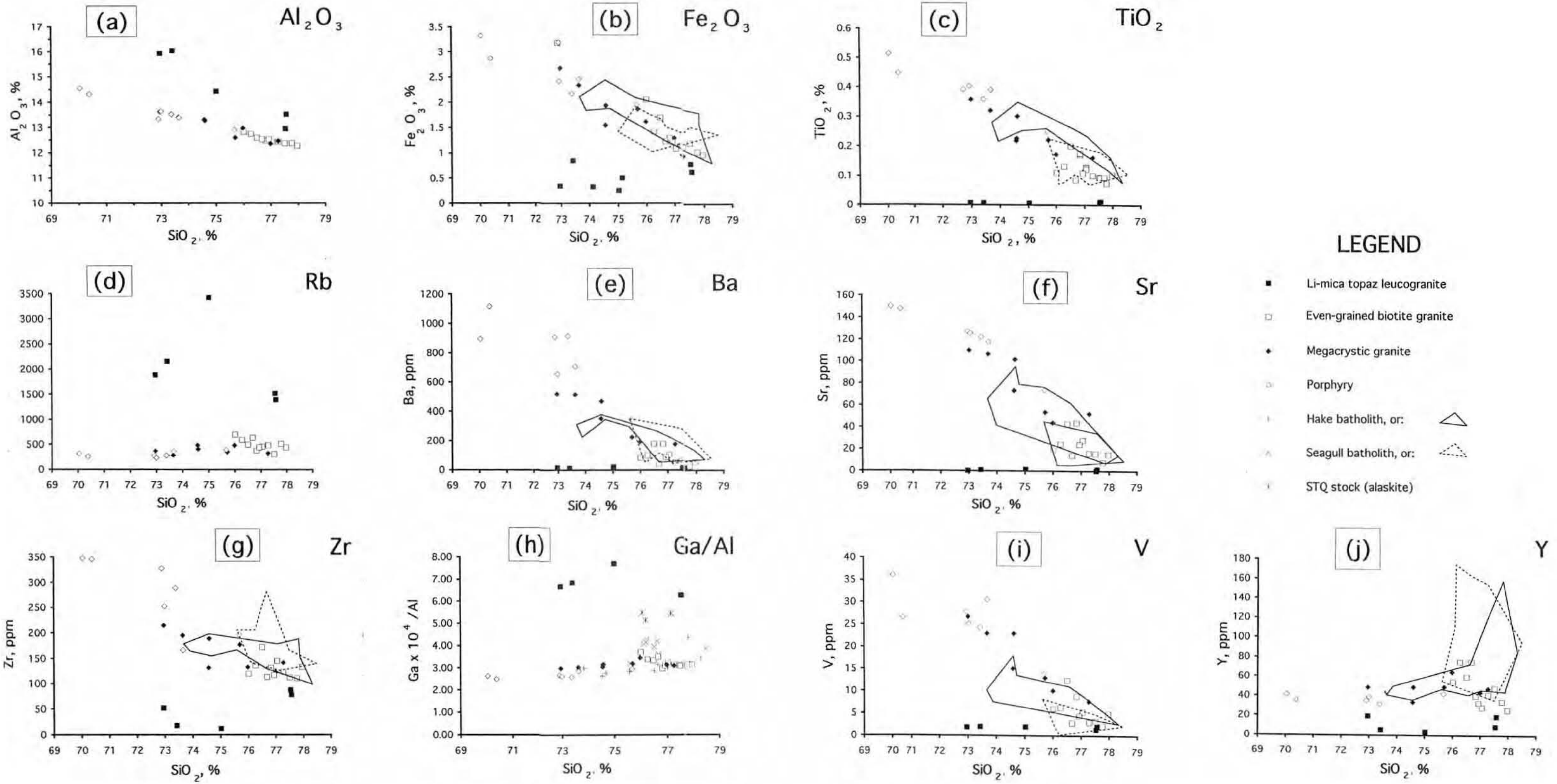

Figure 4.19. Thirtymile stock, Hake and Seagull batholiths: Harker variation diagrams for Al_2O_3 Fe_2O_3 TiO_2 ; Rb; Ba; Sr; Zr; Ga/Al; V and Y.

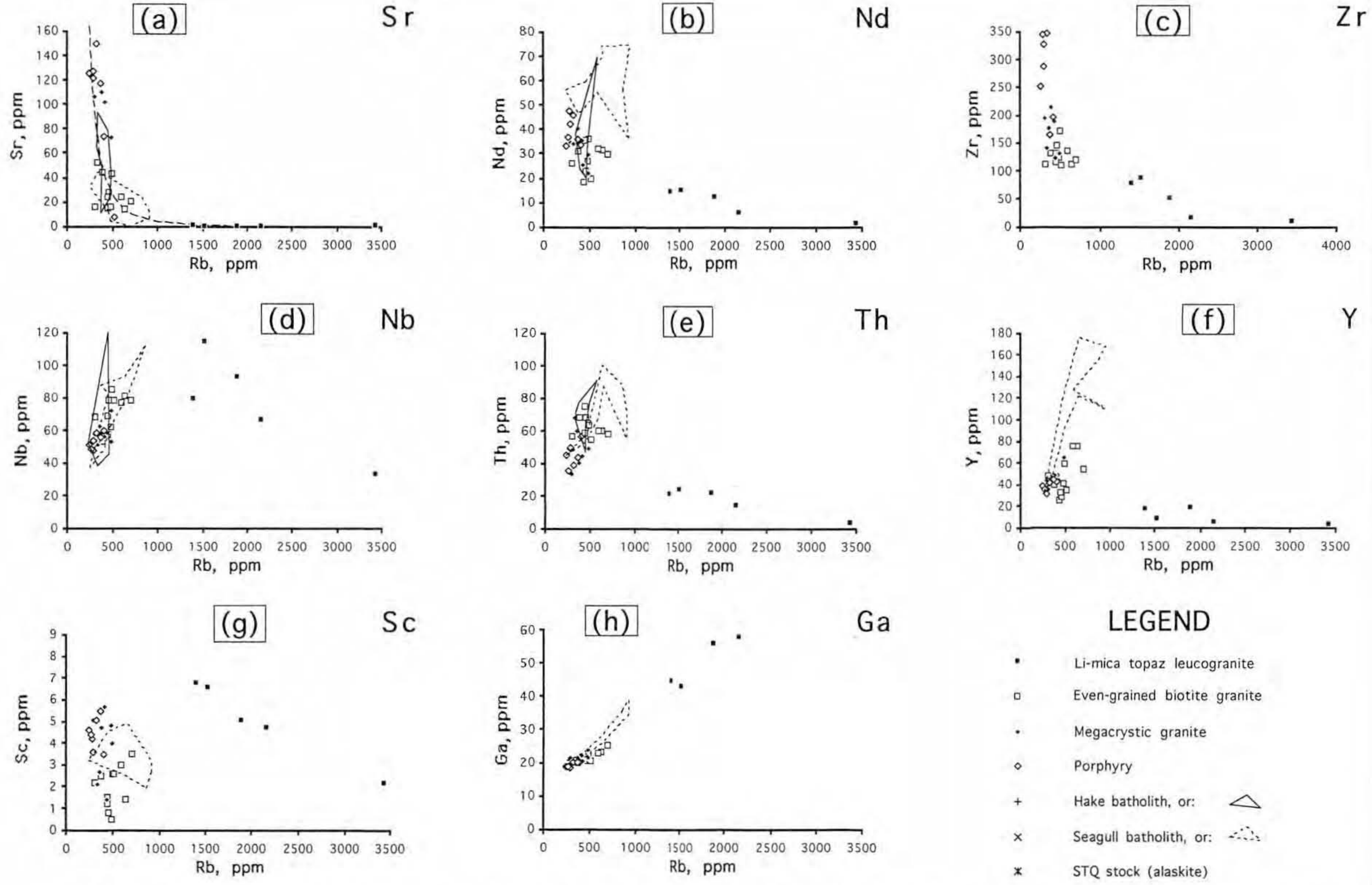

Figure 4.20. Thirtymile stock, Hake and Seagull batholiths: Rb variation diagrams for trace elements Sr; Nd; Zr; Nb; Th; Y; Sc and Ga.

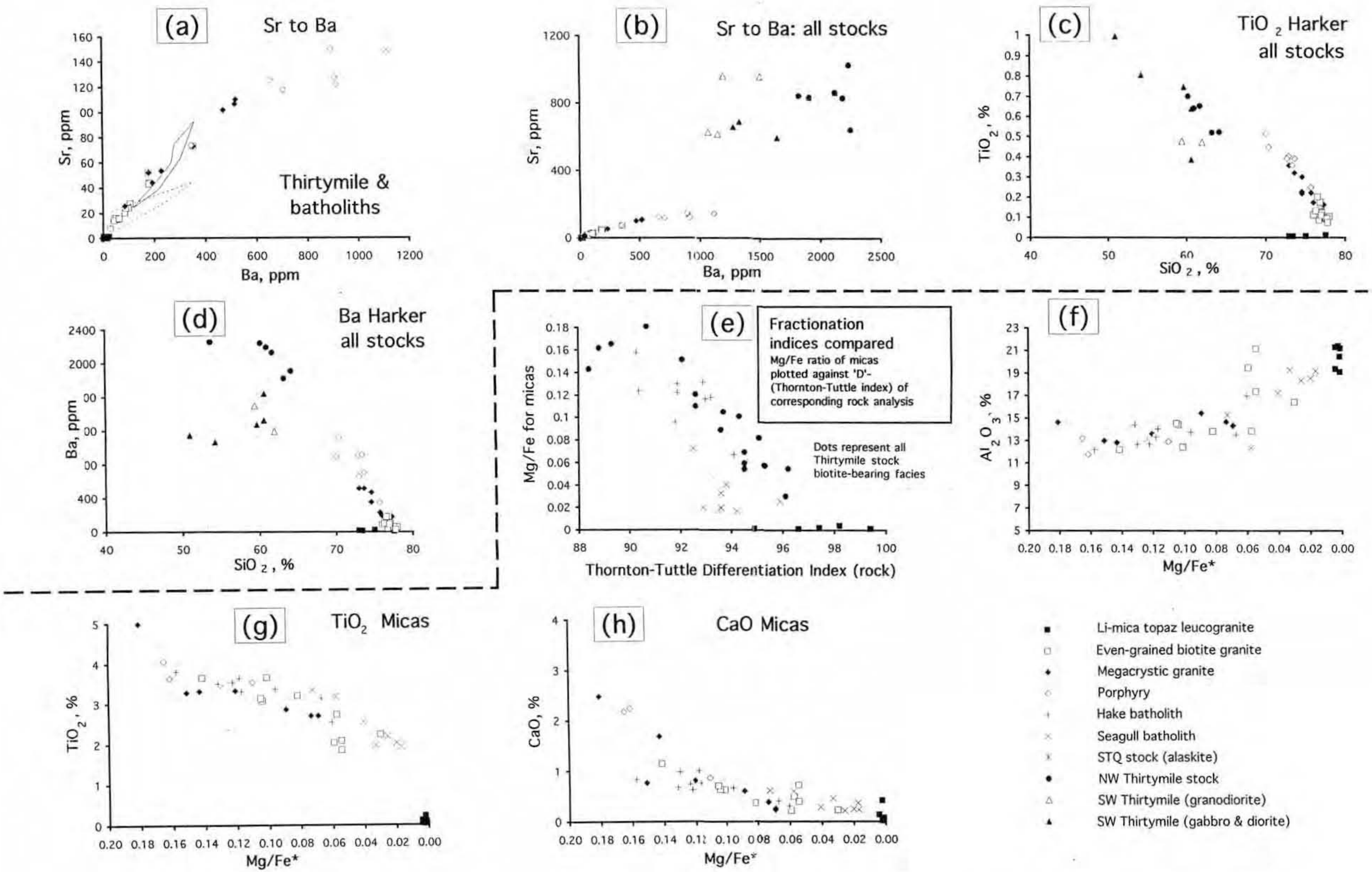

Figure 4.21. Thirtymile stock: Sr to Ba diagram; Thirtymile & NW-SW Thirtymile stocks: Sr to Ba, Harker TiO$_2$ Ba plots for rock; Seagull-Thirtymile suite micas: Al$_2$O$_3$ TiO$_2$ CaO to Mg/Fe.

N.B. Plots (a) to (d) are ROCK; (f) to (h) are MICA

display entirely different ranges of values, with a great scatter (Fig. 4.21d).

4) V: A linear variation exists (negative correlation with silica content), with the batholiths overlapping the field of the Thirtymile facies. V content decreases toward the evolved facies. The Li-mica leucogranites stand out by reason of their showing little variation with silica content. The field of the Seagull batholith extends over portion of the Li-mica facies range (Fig. 4.19i).

5) Ga: This element shows little variation through the plutons, except in the Seagull batholith and Li-mica leucogranite, where it is decidedly enriched showing a wide spread of values. Depicted as the Ga/Al ratio (Fig. 4.19h), which follows the Ga pattern, a slight increase in ratio from 2.5 to 3.2 is noted through the Thirtymile biotite-bearing facies. The Li-mica facies occupies a Ga-enriched field and the Seagull granites show erratic values intermediate between the two linear trends.

6) Pb shows very little change from one facies to another (not shown).

7) Other trace elements Sc, Cr, Zn, Nb, Nd, Zr and Cl show a wider scatter.

8) Y is perhaps significant in that slight enrichment is indicated through the Thirtymile porphyry and less-evolved even-grained facies, then a sharp decrease in the most-evolved even-grained granites and it is depleted in the Li-mica leucogranites. The batholiths display spectacular erratic enrichment of this element (Fig. 4.19i), after the manner of Ga (c.f. Fig. 4.19h, since Ga/Al depicts this trend), but this latter element is enriched in the leucogranites, whereas Y is depleted. This behaviour of Y is particularly obvious when increasing Rb is used as an indicator of evolution of the granites (Fig. 4.20f): two distinct fields being produced. Y is therefore displaying a behaviour nearest to that of the HFSE elements Th and Nb rather the REE, which it would be expected to mimic. The micas, which are the mineral likely to contain Y are still able to contain significant concentrations even in zinnwaldite (see batholith concentrations in Fig. 4.26). The inflection indicated by the Thirtymile trend (Fig. 4.19i) is interpreted as being due to sharp change in bulk K_d of the element once halogens were concentrated in the upper part of the plutons (see 4.7.2).

9) High field strength elements (Nb & Th are shown in Fig. 4.20 d & e) produce Rb plots indicative of enrichment of these elements through the biotite-bearing lithofacies, then show a sharp depletion through the leucogranites.

The relation of Ba to Sr (Fig. 4.21a, b) is fairly linear for porphyry then the more evolved lithofacies of the Thirtymile stock and the batholiths, an inflection in gradient occurring between the fields of the porphyry and megacrystic facies. The Seagull batholith overlaps the field of the Thirtymile stock facies (not shown on Fig. 4.21 to avoid clutter), however the gradient shown by the Hake granites is more consistent with that of the Thirtymile porphyry. Lowest Ba and Sr contents in the batholiths are shown by the specimens from the eastern part of the Seagull batholith, which almost correspond to those of the Li-mica leucogranites. The separate fields for the NW and SW Thirtymile stocks are quite accentuated on such a plot (adjacent plot on Fig. 4.21).

Using high Rb or low Sr or Ba as an indicator of evolution of the various facies, it may be seen that the Thirtymile Porphyry represents the least fractionated and the Seagull granite the most, with the biotite granites of the Hake batholith being compositionally similar to the Even-grained facies of the Thirtymile stock. For several elements the Li-mica leucogranites show extreme values but do not always follow the general trend of the batholith-Thirtymile facies, which show variation of major and trace elements as a linear function of silica content.

TRACE ELEMENTS AND TWO IGNEOUS SUITES

Nb and Th contents of the various plutons dramatically separate the Thirtymile stock and batholiths from the NW and SW Thirtymile stocks. Mean values are presented in Table 4.4. It will be obvious that with the large standard deviations shown for the means from the batholiths that their values overlap those of the Thirtymile facies. There is an indication of a general increase in both these elements from the porphyry to the even-grained facies, with the Seagull granite and its evolved stock (STQ) showing the highest. The Li-mica facies is erratic in Nb and Th content and low in Th compared to the Seagull granite. The much lower contents of the NW and SW Thirtymile stocks contrast with those of the granites.

Sr values are ≤150 ppm in the porphyry and fall to <1 ppm in the Li-mica facies, whereas in the SW Thirtymile stock they are from 598 to 961 ppm and in the NW Thirtymile the range is from 641 to 1070 ppm. Rb values range from 280 to 731 ppm in the porphyry, megacrystic, even-grained, Hake and Seagull specimens. The Li-mica specimens have significantly more Rb: from 1374 to 3540 ppm. The SW Thirtymile and

NW Thirtymile stocks are similar with the range from 64 to 171 ppm.

V contents further show the contrast between the two groups of plutons: the Thirtymile facies and both batholiths show a range of 0 to 36 ppm; the NW Thirtymile and SW Thirtymile cover a range of 131 to 324 ppm.

PLUTON	Nb	σ	Th	σ
Porphyry	54	4.8	46	7.1
Megacrystic	58	6.3	52	11.3
Even-gr.	71	10.6	63	6.0
Li-mica	77	30	17	8.1
Hake	63	25	71	10.7
Seagull	73	20	68	20
STQ	114	2.9	72	15.7
NW Thirtymile	9	2.0	7	1.2
SW Thirtymile	5	1.8	3	1.5

Values of Nb and Th are in ppm. σ is one standard deviation for the mean values quoted.

Table 4.4 MEAN VALUES FOR Nb and Th FOR THE PLUTONS

CHONDRITE-NORMALISED TRACE ELEMENT DIAGRAMS

Trace elements from all the plutons have been plotted in the form of chondrite-normalised diagrams calculated according to values published in Sun (1980). The graphs for individual specimens belonging to each facies have been combined in the one plot showing maximum and minimum curves. Each facies (with the exception of the megacrystic granite of the Thirtymile stock) or pluton is represented in Figs. 4.22 to 4.25. The megacrystic facies has been omitted since its range is similar to that of the even-grained granites.

The various Thirtymile facies all show prominent negative Ba and Sr anomalies. The magnitude of the Ba anomaly increases drastically from Porphyry through Even-grained granite to the Li-mica leucogranite, as does the Sr anomaly. (Note that these three plots cover logarithmic scales of from 3 to 7 cycles, so the visual magnitude of the change in size of the anomaly is belittled). A negative Nb anomaly is evident in the plot depicting Porphyry which diminishes in the Even-grained facies and is imperceptible in the Li-mica facies. Both the Hake and Seagull batholiths show distributions that overlap the Even-grained facies: the same distinct negative Ba and Sr anomalies are seen.

The NW and SW Thirtymile stocks have chondrite-normalised trace element distributions which are quite distinct from those of the Thirtymile stock or batholiths. The plots show positive Rb-Ba and Sr anomalies and strong negative Th-Nb anomalies, particularly in the SW Thirtymile stock.

4.4 MICA MINERALOGY AND GEOCHEMISTRY

4.4.1 MICA OPTICAL MINERALOGY

The micas of the granites in the Thirtymile stock and batholiths, with the exception of the Li-mica topaz leucogranite, are biotite. Only very subordinate quantities of secondary white-mica have been noted in specimens from the batholiths, particularly those from the Seagull granite, and this is likely a Li-mica. No difference in colour is discernible in hand specimen between the various biotites: they are uniformly black. Micas of the Li-bearing facies of the Thirtymile and Ork stocks, the Ork pegmatite and greisen veins are a steel-grey. In thin section there is a range of colours:

PLUTON/FACIES	COLOUR	ESTIMATED FROM ISOGYRE
Seagull batholith:	Pleich. "foxy" red to pale yellow	2V<< 5°
Hake batholith:	Pleich. in pale bronze shades	2V< 5°
TM Porphyry:	Mostly deep bronze, rare "foxy" red	2V << 5°
TM Megacrystic and Even-grained:	Light to deep bronze varieties, with rare red-brown	2V 0-10°
TM Li-mica leuco:	Colourless in section	2V << 5°
TM Greisen	Faintly violet in section	2V << 5°

Table 4.5 Optical mineralogy of micas in the Thirtymile facies and batholiths.

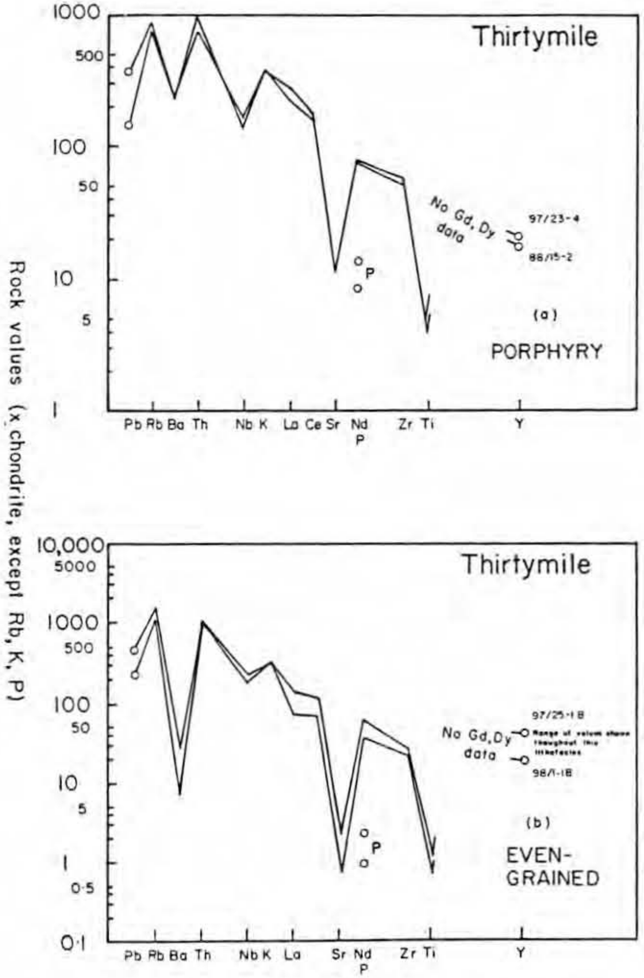

Figure 4·22 Chondrite-normalised trace-element diagrams for the Thirtymile Stock porphyry and even-grained lithofacies.

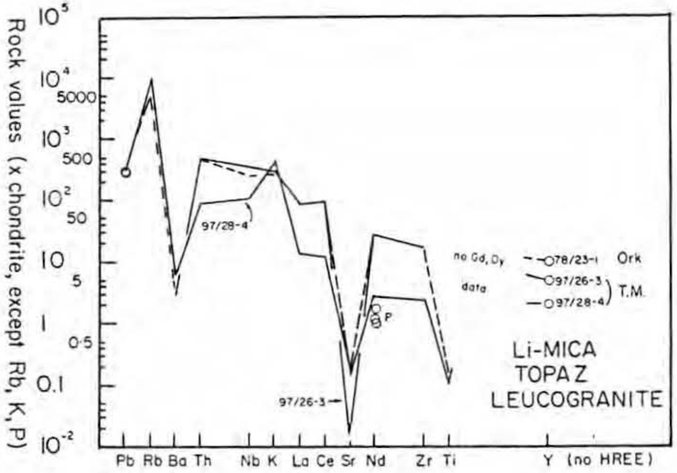

Figure 4·23 Chondrite-normalised trace-element diagrams for the Li-mica topaz leucogranites of the Thirtymile and Ork stocks

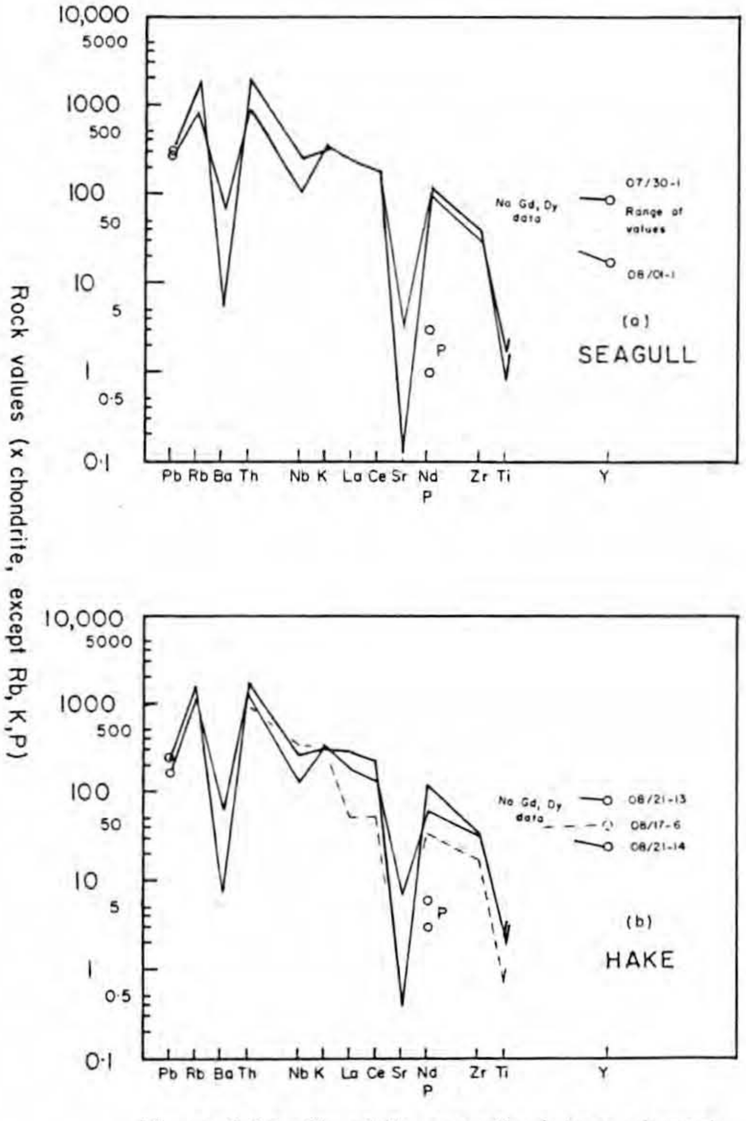

Figure 4·24 Chondrite-normalised trace-element diagrams for the Hake and Seagull Batholith.

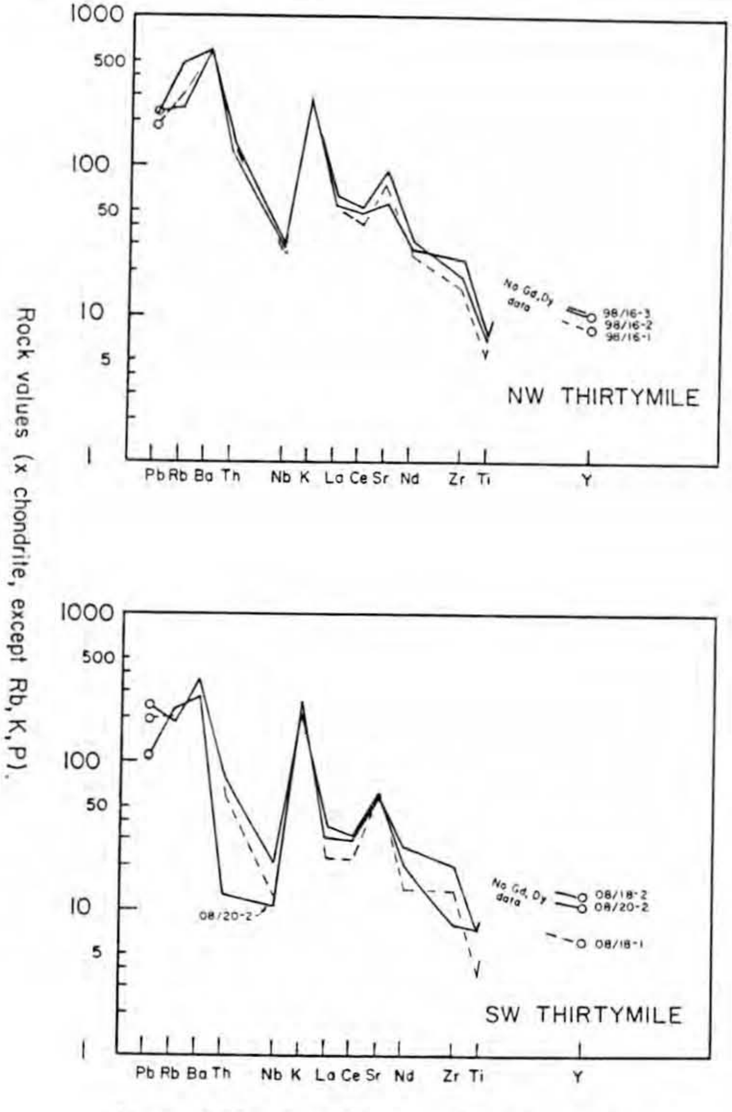

Figure 4·25 Chondrite-normalised trace-element diagrams for the NW and SW Thirtymile stocks.

4.4.2 MICA CHEMISTRY: THIRTYMILE STOCK, SEAGULL BATHOLITH AND HAKE BATHOLITH.

METHODS:

Mica concentrates were prepared by crushing 52 specimens, sieving to limit the range of size fractions and three stages of magnetic separation: a rough separation of a 'magnetic' concentrate using a Davis non-entraining rotary separator, further cleaning of the concentrate on a traditional Frantz-type isodynamic machine and final preparation of a >98% pure concentrate on a Frantz 'Barrier' instrument. Specimens that did not clean-up readily on the isodynamic machine were passed through a bromoform/acetone heavy liquid separation process. Hand picking of quartz and feldspar contamination in the concentrates was employed before analysis, resulting in material of usually better than 99.5% purity for the +250-500μ size fractions. Two preparations were made from each concentrate whenever quantity permitted and several size fractions were analysed when available. The fractions >500μ may carry a little feldspar contamination as tiny fragments attached to the mica flakes, to perhaps 1%. The two preparations used for ICP analysis were a lithium metaborate fusion followed by nitric acid digestion ('majors' programme, which allows silica determination) and a direct hydrofluoric/perchloric digestion ('traces' programme, which may not dissolve all Mo or Zr). Absorbed water and combined water were also determined and the analyses presented as being 'wet-rock' rather than ignited material as in the XRF whole-rock analysis (Appendix A).

The micas from the batholiths and Thirtymile stock exhibit regular variation in both major and trace element contents according to facies, often showing less spread than corresponding whole-rock trace elements. Attempts at correlating the amount of silica in the rock and mica composition show considerable spread, however if Mg/Fe* ratio of the micas is compared to the Thornton-Tuttle differentiation index, a good linear distribution results for all of the Thirtymile facies and the micas chosen from the Hake batholith (Fig. 4.21e). A Pearson correlation coefficient of 0.84 was obtained for the 34 micas (other than Seagull) shown in this plot. Some of the differences in the Li-mica leucogranites compared to the batholith-Thirtymile trend are particularly well demonstrated by the mica analyses.

LEGEND

◇	Porphyry	Thirtymile & Ork stocks
◆	Megacrystic	
□	Even-grained	
■	Li-mica	
×	Seagull	Batholiths
+	Hake	

(except for figure 4·26c, where an open square depicts F and a filled square Cl)

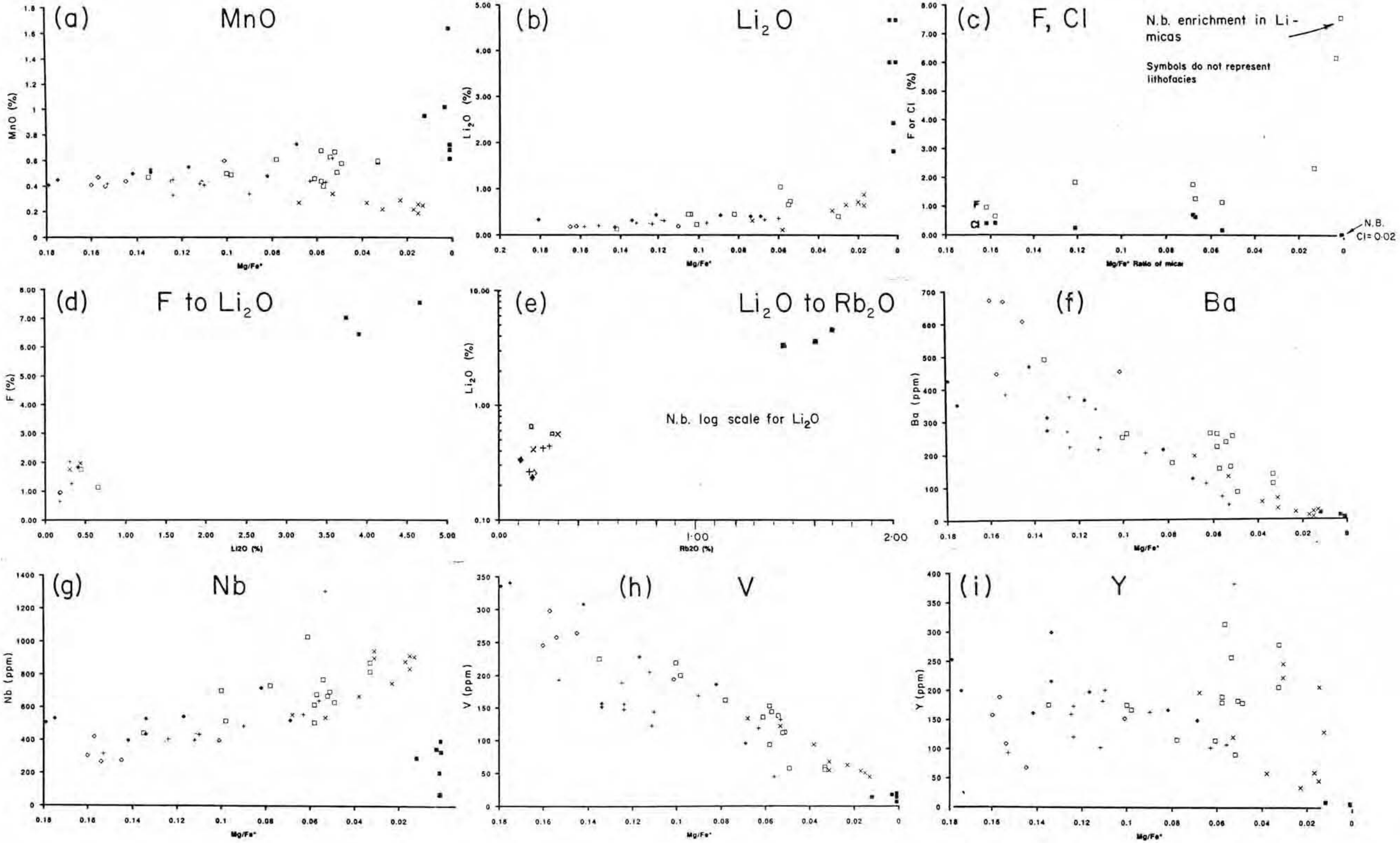

Figure 4.26 Major & trace element variation in Seagull-Thirtymile micas: MnO, Li_2O, F, Cl, Ba, Nb, V, Y to Mg/Fe; F to Li_2O, Li_2O to Rb_2O.
Symbols used for lithofacies are the same as in Figures 4·19 and 4·20.

MICAS: MAJOR ELEMENTS

If Mg/Fe* (Fe* being total Fe) is employed as a parameter to express the mica composition then it may be seen (Appendix C.2) that K_2O decreases slightly with increase in the ratio and Al_2O_3 shows a continuous range from 11 to 20%, the Al content being inversely proportional to Mg/Fe*. Such regular variation is to be expected for substitutions in the mica structure over a range of biotite compositions. CaO, although not normally considered a component significant in biotite micas, shows a steady decrease with corresponding Mg/Fe* decrease (i.e. the progression toward the evolved granite facies), which, when compared with the amount present is interpreted as actual mica content rather than possible feldspar contamination of the concentrate. TiO_2 content decreases similarly (Fig. 4.21g). Li, which petrographically (as an indicator of micas found in a greisen environment) may be considered a measure of 'specialisation' of the granite shows a slight but regular increase through the micas of the stock and batholith facies, then increases exponentially in the Li-mica topaz leucogranite (Fig. 4.26). The same trend is indicated when Li is plotted against Al_2O_3 (i.e. either Al_2O_3 or Mg/Fe* is an indicator of mica composition for these micas).

Each of these plots (Figs. 4.21 & 26) shows a range of mica compositions from the three biotite-bearing facies of the Thirtymile stock, with the Hake batholith overlapping portion; more extreme values in the Seagull granites; and the most extreme values in the Li-mica facies. The gradual changes in Li observed from the micas of the Porphyry to Even-grained facies are interpreted as a regular substitution of the Li for Al in the octahedral site of the mica. Ranges of values are shown in Table 4.6. The regular change in major element composition is well demonstrated in the Si-Fe-Al ternary diagram of Fig. 4.27.

FACIES	Li, from	Li, to	Mg/Fe*, from	Mg/Fe*, to
Porphyry	0.04%	0.09%	0.101	0.160
Megacrystic	0.08%	0.20%	0.082	0.179
Even-grained	0.06%	0.48%	0.033	0.135
Hake	0.06%	0.17%	0.056	0.125
Seagull	0.05%	0.41%	0.013	0.068
Li-mica	0.85%	2.17%	0.001	0.003

Table 4.6 Mica compositions of the various Thirtymile lithofacies.

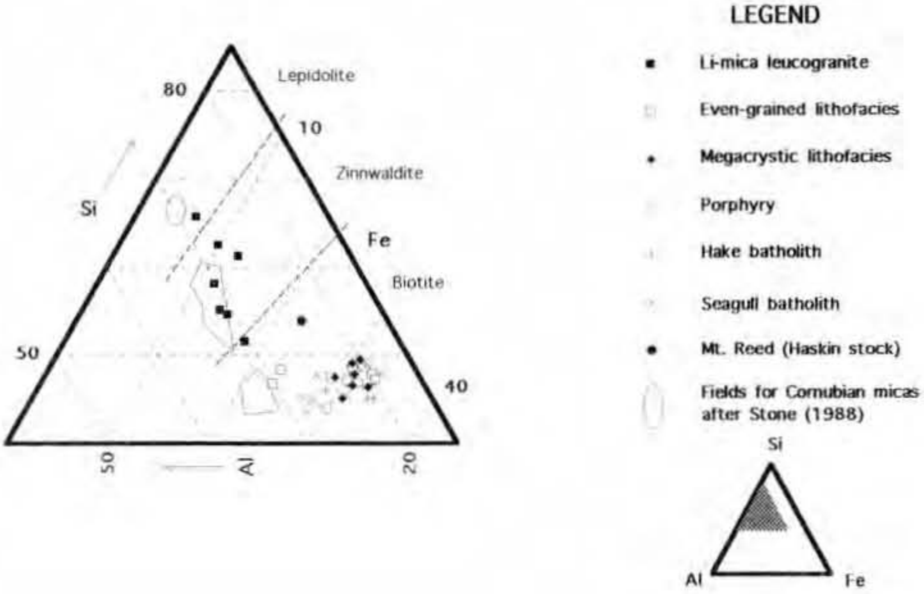

Fig. 4.27 CATION PROPORTIONS: Si-Fe-Al IN MICAS FROM THE SEAGULL-THIRTYMILE SUITE GRANITES & MT.REED INTRUSION (CASSIAR).

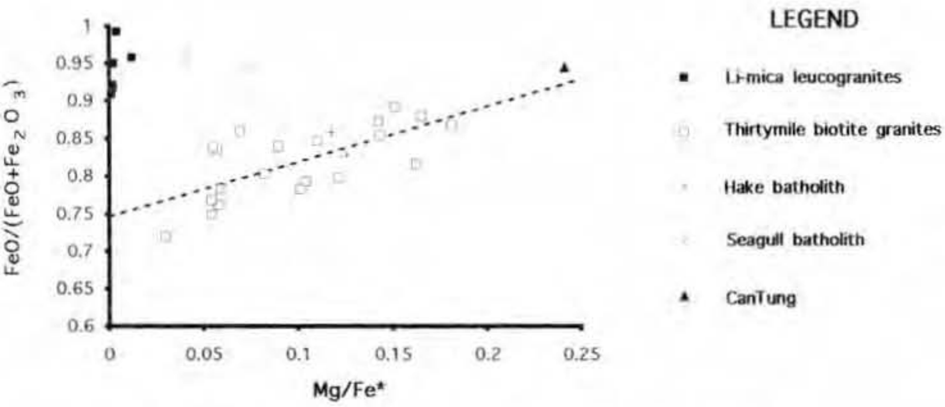

FACIES	FeO/(FeO+FE2O3) MEAN	σ	n
Porphyry	0.876	0.025	4
Megacrystic	0.847	0.025	6
Even-grained	0.787	0.041	11
Li-mica	0.921	0.021	5

Fig. 4.28 OXIDATION STATE OF MICAS AS INDICATED BY FERROUS/FERRIC IRON CONTENT

The low Mg content of these micas, combined with high (Fe^{+2}+Fe^{+3}) allow them to be classified as lepidomelanes and in particular close to the siderophyllite end-member (Deer et al, 1962 V. 3, p. 57).

Structural water and halogen content also vary according to composition. Table 4.7 shows the results from the various Thirtymile facies that were analysed for H_2O^{+}, F and Cl. It will be noted that the biotite micas from the Even-grained and Megacrystic facies have from 1.14 to 4.21% structural water whilst the Li-micas have from 0.33 to 0.77% structural water. Fluorine content increases from 0.96% in those from the porphyry to 1.76-2.33% in the Seagull micas and 6.46-7.55% in the Li-micas of the leucogranites.

Table 4.7 Average Mg/Fe* ratio & Nb contents with ranges of F, Cl & combined water of micas from the Seagull-Thirtymile suite & Mt. Reed.

FACIES	Mg/Fe* Av.	Nb Av. (ppm)	F (%)	Cl (%)	H2O (%)
Li-mica	0.003 (7)	275 (6)	6.16-7.55 (4)	0, 0.02 (2)	0.33-0.77 (4)
Seagull	0.031 (9)	790 (9)	1.76-2.33 (3)	0.41, 0.70 (2)	1.23-1.55 (3)
Even-grained	0.067 (12)	671 (12)	1.14, 1.76 (2)	0.17, 0.42 (2)	1.14-3.30 (4)
Hake	0.108 (16)	525 (11)	0.65-2.03 (3)	0.41-0.63 (3)	1.18-2.82 (4)
Megacrystic	0.128 (7)	524 (8)	1.65, 1.84 (2)	0.25, 0.34 (2)	1.24-4.21 (4)
Porphyry	0.143 (5)	349 (6)	0.70-0.96 (3)	0.26, 0.40 (2)	1.05, 2.30 (2)
Mt. Reed	0.395 (1)	248 (1)	2.4 (1)	0.02 (1)	0.94 (1)

Number of analyses are shown in brackets.

The FeO/(FeO+Fe_2O_3) ratio of the micas is high (i.e. >0.8), possibly decreasing slightly with evolution of the biotite granites, but is much higher (>0.9) in the Li-mica leucogranites, indicating decidedly reducing conditions during crystallisation of this lithofacies (Fig. 4.28).

MICA TRACE ELEMENTS

Some trace elements in the micas show linear relationships to the Mg/Fe* content of the mica. These are:

1) Ba contents have positive correlation with Mg/Fe*, i.e. Ba decreases toward the Li-Mica leucogranites (Fig. 4.26f).

2) Ni contents also have positive correlation with Mg/Fe*; the Li-Mica facies occupies a distinct field of low content in this element.

3) Y contents have good positive correlation with Mg/Fe*, decreasing linearly toward the Li-Mica facies.

4) V contents have good positive correlation with Mg/Fe*, i.e. decreasing through the Thirtymile and batholith biotite-granites (Fig. 4.26h).

5) Nb contents have good negative correlation with Mg/Fe*. The Li-Mica facies occupies a separate field (Fig 4.26g).

Others (notably the 'ore' metals) show a spread through the Thirtymile biotite-bearing facies but no systematic increase and a larger spread of values for the Seagull specimens. Zn content changes little in the Thirtymile facies (including Li-mica) and Hake granites, but shows a wide scatter in specimens from the Seagull granite, possibly indicating proximity to mineralisation associated with hydrothermal activity above the batholith. The rare earths, Ce, Dy, Sm show some scatter and no large change. It should be noted that whereas the Y contents of the whole-rock vary greatly, indicating a general increase toward the Hake granite and even-grained facies, then an erratic concentration through the Seagull specimens, those in the micas show a fairly regular linear decrease toward the evolved facies. Ba/Sr ratio of the micas shows a regular variation throughout the facies, decreasing towards the evolved facies. The ratio of La/Dy (light to heavier rare earths), which might be expected to be an indicator of fractionation shows a wide scatter about a constant of 7, but the Seagull granites are clearly higher (i.e. the heavier element is relatively depleted). Surprisingly, the Li-mica facies is notably lower in this ratio than the next most evolved granite (Seagull).

4.4.3 COMPARISON OF ELEMENTAL TRENDS IN MICAS WITH THOSE OF THE WHOLE-ROCK.

Trends in micas compared to whole-rock contents are compared using decreasing (Mg/Fe*) value for the mica as corresponding to increasing silica in the rock. The following elemental trends compare:

(1) CaO and TiO_2 in the mica decrease with decreasing (Mg/Fe*), as does the CaO content of the rock toward the evolved facies.

(2) K_2O, Li and F content of the mica increases toward the evolved facies, following the general rock trend.

(3) MnO decreases in Harker diagrams for the Thirtymile and batholith granites, with considerable spread due to the low contents and possible analytical uncertainty at this

level. MnO content of the micas (Fig. 4.26) indicates a similar decrease in the more evolved granites of the batholiths, however those micas from the Thirtymile stock demonstrate a slight increase toward the low Mg/Fe* biotites and decided enrichment in the Li-micas.

TRACE ELEMENTS:

(4) The trace elements Ba, Sr and Ni and V particularly demonstrate a positive correlation between contents in mica and whole-rock.

The following elements show some differences between trends in rock and mica, often highlighting the Seagull granite and Li-mica leucogranites as peculiar to the general trend:

(5) Nb increases toward the evolved facies in rock values, with much scatter in the Seagull and Li-mica leucogranites. The values in the micas show a very linear distribution, again with enrichment toward the Seagull granite. This trace element in micas from the Li-mica leucogranites plots as a separate field of lowest contents.

(6) Zr decreases in both whole-rock and micas toward the leucogranites, however the micas of the Seagull granites show erratic values covering the full range of the other granites.

(7) Zn in both rock and mica from the Seagull granites has erratic elevated values compared to the other granite facies.

4.4.4 MICA COMPOSITION AND EVOLUTIONARY TRENDS

Much of the mica contained in the granites of the Seagull suite is interstitial to the other minerals, although some clustered biotite in the porphyry of the Thirtymile stock may represent restitic material. The micas are, therefore, a mineral phase that has sampled the fluids residual to what was largely solidified granite. Concentration of the lithophile/hygrophile elements in the Li-mica facies of the Thirtymile stock is shown by the modal presence of zinnwaldite, topaz and fluorite. The Li-enrichment of the associated micas is obvious. Mica chemistry is a clear indication of the most evolved granites of this suite, with a progression toward high Al, high Li and F, low Mg/Fe* ratio (but actually lower total Fe) types i.e. zinnwaldite. The association of micas containing high Fe/(Fe+Mg+Mn) with stanniferous granites is in agreement with

Table 4.8 Ammonium contents of granites and related rocks.

Specimen	NTS map sheet	UTM coordinates	NH_4^+ (ppm)	Petrographic comments
Thirtymile pluton				
HPG	105C-9	407309	1.1	Porphyry
97/29-1	105C-9	415286	1.1	Even-grained facies
TOR	105C-9	408303	2.0	Megacrystic facies
97/28-5	105C-9	411292	0.7	Megacrystic facies
97/26-3	105C-9	419280	1.4	Li-mica border facies
97/26-3 (repeat analysis)		419280	1.8	"
97/28-4	105C-9	420279	8.5	Li-mica facies, sill
78/23-1	105C-9	429235	3.1	Li-mica facies, Ork stock
Ork stock				
78/23-1	105C-9	429235	3.1	Li-mica facies at contact
Hake batholith				
08/17-1	105C-9	589123	2.5	Granite porphyry
08/17-2	105C-8	638030	2.3	Granite, coarse-grained
08/17-3	105C-8	636055	5.2	Granophyre
08/17-5	105C-8	634084	3.1	Granite, coarse-grained
08/21-3	105C-8	630925	2.7	Granite, coarse-grained
08/21-14	105C-8	614938	4.3	Granite, coarse-grained
Seagull batholith				
07/21-2	105B-3	800042	5.5	Granophyre, near contact
08/21-2	105B-3	800630	2.9	Microgranite
07/30-1	105B-4	534765	3.5	Microgranite
07/30-4	105B-4	539759	1.9	Microgranite
08/02-1	105B-4	557728	1.9	Granite porphyry
Southwest Thirtymile stock				
08/18-3	105C-9	396119	4.3	Diorite, fine-grained
08/20-4	105C-10	371138	3.5	Diorite, coarse-grained
08/20-2	105C-9	388131	2.4	Gabbro, fine-grained
08/20-6	105C-9	384137	15.2	Gabbro, slightly hydrothermally altered.

analytical data presented by Scott (1988). Enrichment in F in micas from the even-grained facies and Seagull granites compared to the porphyry is obvious. The Li-micas have extreme F enrichment, with contents up to 7.5% F (Table 4.7).

4.5 AMMONIUM

4.5.1 AMMONIUM CONTENTS OF THE THIRTYMILE FACIES, HAKE AND SEAGULL BATHOLITHS

Ammonium contents of some selected specimens were determined by Dr. A. Hall as a reconnaissance exercise for this part of the Cordillera (Hall and Liverton, 1992). Results are shown in Table 4.8. Ammonium contents in this suite of specimens are the lowest yet reported from granites. It will be noted that the only amounts of ammonium above background are in specimens 97/28-4 and 08/20-6: the Li-mica facies specimen from the sill at the SE margin of the Thirtymile stock and a gabbro from the north margin of the SW Thirtymile stock. The other specimens show some detectable ammonium, but nothing that could be considered significant if a value of 30 ppm is taken as the average for granites generally.

Ammonium occurring in granites has its chief origin in organic compounds in source material. Low values may therefore reflect an originally low-N source, or loss of the ammonium by boiling-off or oxidation. Higher values may indicate derivation from the aureole or by hydrothermal activity. This is discussed at the end of this chapter.

4.6 Sr ISOTOPES

4.6.1 Rb/Sr-ISOTOPE ANALYSES

Six specimens were chosen for whole-rock Rb/Sr isotope analysis as an initial attempt at determining an isochron for the Thirtymile pluton and the initial $^{87}Sr/^{86}Sr$ ratio. The specimens analysed, their Rb and Sr contents as determined by XRF analysis and the $^{87}Sr/^{86}Sr$ ratios are shown in Table 4.9. The first five of these specimens were chosen from particularly fresh rock of the same facies (megacrystic), giving a range of Rb/Sr ratios. The sixth is from the porphyry.

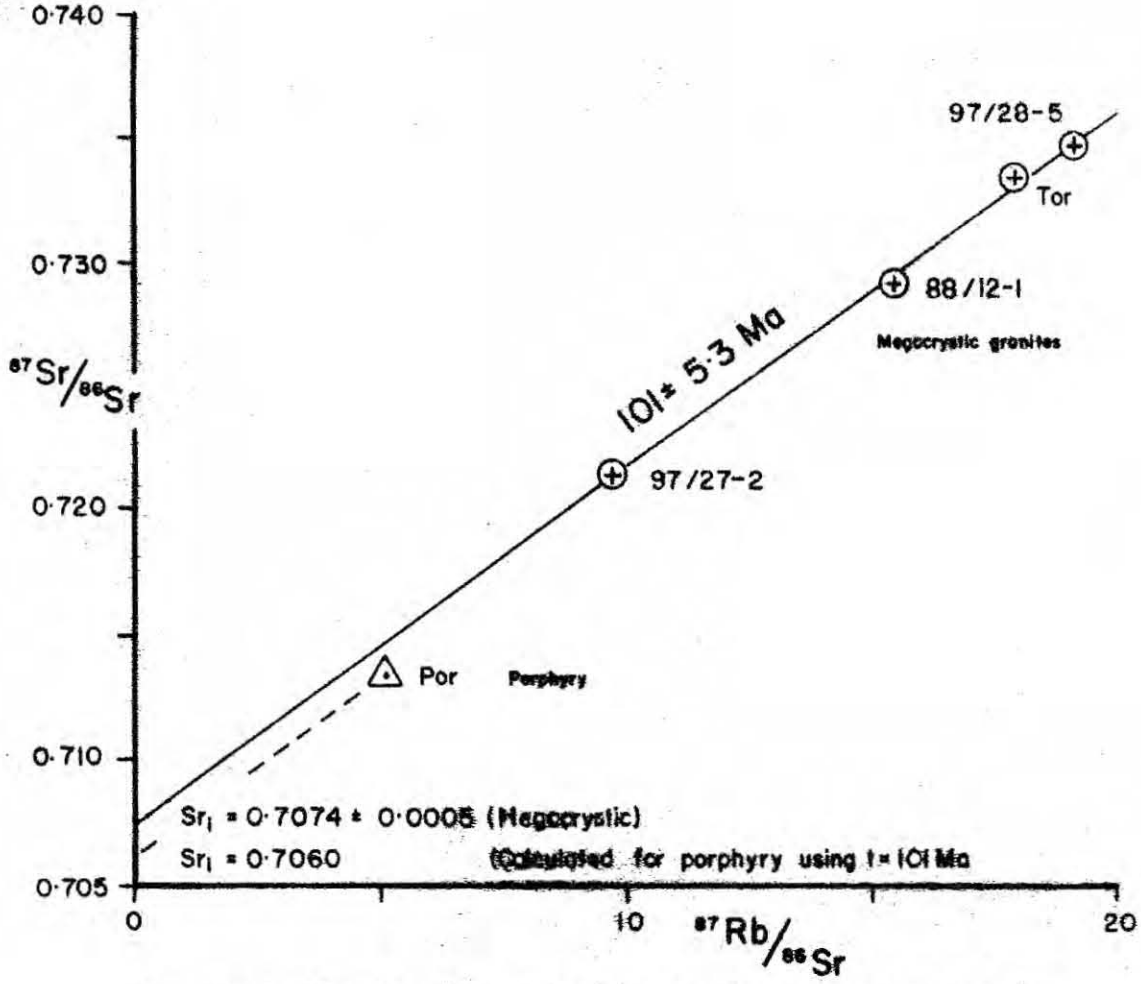

Figure 4·29 Rb / Sr whole-rock isochron diagram for the Thirtymile Stock megacrystic lithofacies.

Table 4.9a Sr-Isotope whole-rock determinations for the Thirtymile Megacrystic facies and Porphyry.

SPECIMEN	**Rb (XRF)**	**Sr (XRF)**	**Rb/Sr**	**^{87}Sr/^{86}Sr ±2 S.E.**
97/24-5	497.3	43.1	11.54	Filament failed
97/28-5	482.6	73.2	6.59	0.734721± .000012
88/12-1	393.7	73.9	5.33	0.729086± .000018
97/27-2	370.4	110.2	3.36	0.721347± .000011
Tor	323.3	52.2	6.19	0.733384± .000009
Por	260.8	147.4	1.77	0.713364± .000015

A York regression for the four megacrystic specimens yields an age of 101.0±5.3 (York II) Ma with an initial ^{87}Sr/^{86}Sr ratio of 0.7074±0.0005 (2σ) and MSWD of 4.6549. Calculation of the initial ratio of porphyry sample Por using a 101 Ma age yields 0.7060.

Table 4.9b Sr Isotope-dilution (I.D.) determinations on micas for the Thirtymile leucogranite & Hake batholith, with mica and whole-rock values for the SW Thirtymile granodiorite.

SPECIMEN	**Rb (I.D.)**	**Sr (I.D.)**	**^{87}Rb/^{86}Sr**	**^{87}Sr/^{86}Sr**	**Age (Ma±2s)**
Leucogranite:					
97/28-2 (Mica)	14,699	---	---	---	
97/28-4 (Mica)	15,491	6.69±0.1	94,379	135±5	100±4*
Hake granite:					
08/17-2 (Mica)	1,478.9	7.38±0.02	627.4	1.586±1	98.3±2.9*
08/17-5 (Mica)	2406.8	---	---	---	
SW Thirtymile:					
08/20-2 (Mica)	379.38	---	---	---	
08/20-4 (Mica)	403.98	69.25±0.01	16.89	0.74836±8)	181.5±2.5
08/20-4 (Rock)	102.1 (XRF)	960.7 (XRF)	0.3063	0.70529±1)	

* Assuming initial ^{87}Sr/^{86}Sr of 0.7074. The SW Thirtymile granodiorite (08/20-4) biotite/whole-rock calculation gives a Sr_i ratio= 0.70450±00003 (2s). XRF indicates analysis by X-ray fluorescence spectrometry for the rock.

4.7 DISCUSSION

4.7.1 THE SEAGULL-THIRTYMILE PLUTONIC SUITE

CLASSIFICATION

Mineralogy and relative proportions of the mineral components of igneous rocks are guides to the source of the parent magma. A classification should be capable to some extent of distinguishing genetic types (see Lameyre and Bowden, 1982). Classifications of igneous rocks have been proposed by means of modal mineral proportions (Streckeisen, 1974) and chemical composition (Streckeisen and LeMaitre, 1979; Le Bas and Streckeisen, 1991). There are practical problems inherent in the application of either scheme and in making comparison between the two. A modal classification is only reliable when the grainsize of the rocks is sufficiently coarse to allow point counting (i.e. ideally >0.2 mm if thin sections are used or >2 mm if sawn slabs of rock are used for estimation by grid counting), but increase in grainsize require a commensurate increase in counting area for the result to be representative. The feldspars present must be readily distinguished (potash vs. plagioclase feldspar) or stained and sufficient area counted to obtain a representative specimen. Problems arise in counting only one thin section of a granite. The coarsest-grained facies counted in this study (megacrystic lithofacies, specimen 97/28-5) showed considerable variation in feldspar contents between individual sections prepared from the faces of a rectangular parallelepiped due to the influence of some large orthoclase crystals (Appendix C.4). Biotite and accessory minerals varied very little. Even with the likelihood of some deviation of an individual specimen from a completely representative sample, all Thirtymile specimens that were counted plot as granites on the Streckeisen diagram. Only the NW and SW Thirtymile stocks contain rocks that are modally classified as granodiorite, tonalite or quartz monzogabbro (Fig. 4.14).

The division between granites and granodiorites on the Streckeisen diagram has been criticised since many monzogranites from the Lachlan Fold Belt of SE Australia straddle this boundary (White, 1990). White divides granite-granodiorite and quartz monzodiorite at 25% quartz rather than 20%, arguing that this division follows the chemical definition of diorite and andesite more closely (i.e. 56> Qtz <62 %). Such a shift in the division would classify some Thirtymile rocks as quartz syenite and quartz monzonite. The simple quartz-alkali feldspar-plagioclase distinction does differentiate between possible genetic types (Lameyre and Bowden, 1982).

Problems arise when comparing chemistry with modal schemes (Streckeisen and Le Maitre, 1979). If CIPW normative components are plotted on a Streckeisen diagram, the decision to include the albite component with the alkali feldspar may lead to the plotted composition being closer to the alkali apex than the modal proportions would indicate. If normative values of quartz, orthoclase and plagioclase for the Thirtymile stock granites are plotted as in the modal subdivisions they would still fall within the granite classification, except for some of the Li-mica leucogranites which would fall within the granodiorite field.

A simple CIPW modal scheme for the granitic rocks was proposed by the U.S. Geological Survey (O'Connor, 1965), but has not been universally employed. If normative feldspar proportions are used for classification (as by O'Connor) the Thirtymile lithofacies are shown to be granites (Fig. 4.15). More recent chemical classifications (Streckeisen and LeMaitre, 1979; Le Bas and Streckeisen, 1991) employ Barth-Niggi molecular norms. These are most applicable to the fine grained volcanic rocks and are complementary to the cationic scheme proposed by Debon and LeFort (1988). The Streckeisen and O'Connor classifications (Figs. 4.14 to 4.17) are employed in this study since they are a simple, consistent method that is applicable to granites.

THE THIRTYMILE, HAKE AND SEAGULL GRANITES

The Seagull/Hake/Thirtymile granites have the following characteristics:

(1) MINERALOGY: modally the Thirtymile stock and batholiths (Fig. 4.14) plot in the granite field of the IUGS classification (Streckeisen 1974). Mineralogically they are biotite-only granites devoid of any primary muscovite and containing significant hornblende only in the porphyry. No peraluminous-type minerals such as andalusite, sillimanite, cordierite or garnet have been noted. Evidence of hydrothermal alteration, which is very slight, is present mainly in the Seagull granite as traces of secondary lithium mica accompanied by tourmaline and fluorite.

(2) MAJOR ELEMENT CHEMISTRY: the Seagull-Thirtymile granites are metaluminous to slightly peraluminous. The peraluminous compositions are found in the highly evolved Li-mica facies. Substantial amounts of topaz cause the excess aluminium, rather than mica content. Clear trends are shown on Al_2O_3, CaO, Fe_2O_3*, MnO, P_2O_5 and TiO_2 Harker variation diagrams for the biotite-bearing facies. The Hake specimens overlap the middle Thirtymile stock field and those from the Seagull batholith plot with the extreme even-grained specimens. The Li-mica facies occupies a separate field that suggests a reversal of the main trend (especially when viewed using Rb contents as an indicator of evolution). Clear chemical trends throughout the granites of the Thirtymile stock facies and the Seagull and Hake batholiths, plus similar age dates (below) are interpreted as indicating that these granites form one plutonic suite: here called the Seagull-Thirtymile Suite.

(3) Rb/Sr ISOTOPES: the Thirtymile and Hake specimens have given Rb/Sr ages of 101.0±4.6, 100±4 and 98.3±2.9 Ma and with $^{87}Sr/^{86}{}_i$ from 0.7052 to 0.7074. Published Rb/Sr data for the Seagull granite is 100 Ma age with $Sr_i = 0.712$ (Sinclair, 1986), which is in excellent agreement with the age determined by this present work.

(4) TRACE ELEMENTS: on Harker plots many trace elements show a regular progression of values from the porphyry, through the megacrystic to even-grained and Li-mica facies. Plots of Sr & Zr to Rb (Fig. 4.20) have hyperbolic distributions, which are to be expected if a fractionation (e.g. crystal-liquid or Rayleigh) process has been dominant in the production of these granites. Nb is concentrated with silica or Rb increase from Thirtymile porphyry to the Seagull granites, but is at particularly low levels in the Li-mica leucogranites. Attempts to use trace element levels as indicators of S or I nature of the granites give equivocal results: Cr contents are very low with mean values of 4 ppm for the Thirtymile; 1.8 ppm for the Seagull and 2.4 ppm for the Hake, (c.f. White, 1990: average for S-types= 46 and for I-types= 27). Mean Pb content is considerably higher at 35 ppm for the Thirtymile and 31 ppm for both batholiths than White's criterion of 27 ppm and 16 ppm for average S- and I-types respectively; but this may reflect mineralisation near the top of the intrusions. Sr content is low: for the Lachlan

Fold Belt, White (1990) gives averages of 253 and 139 ppm for I- and S-types and argues that the lower Sr in S-types results from release of that element on K-feldspar weathering in production of source sediments. The least evolved facies of the Seagull-Thirtymile suite (porphyry) has an average Sr content of 129 ppm.

(5) AMMONIUM CONTENT: The biotite granites have an average ammonium content of 1.2 ppm which is the lowest level yet reported in granites. A level of 30 ppm is typical (Hall and Liverton, 1992). Higher values are found in two of the Li-mica leucogranites, but not the third specimen analysed. The origin of ammonium in S-type igneous rocks is considered to be nitrogenous organic material in the source sediment that has been incorporated into silicate minerals as the ammonium ion substituting for potassium during diagenesis and metamorphism. A small sedimentary component is still likely for I-type granites: if the calc-alkaline magma suite is derived from subducted oceanic crust, some organic input is possible. The various processes that are likely to affect NH_4 content of a magma at the site of intrusion are crustal contamination, loss of volatiles if the intrusion is near-surface and late-stage hydrothermal activity (Hall and Liverton, 1992). If any organic matter is present in the country rocks it is likely to raise the level of NH_4 in the magma, except for marginal reduction effects (Gastil et al., 1990). Hydrothermal activity has been observed to cause significant increase in content (Hall, 1988, Bencini and Hall, 1988). Low content of NH_4 would most likely arise where shallow depth of emplacement of the intrusion allowed volatile loss, however the exsolution of magmatic water may not cause great loss (Hall and Neiva, 1990). It is suggested that some ammonium may have been lost during volatile release from the Thirtymile-Seagull magmas, but the low contents encountered reflect similar content in the original magma, thus providing some evidence for a predominantly I-type source for the granites.

(6) MICA COMPOSITIONS:

Micas from these granites are all high in total Fe and low in Mg: they range from lepidolite through zinnwaldite to siderophyllite according to the classification used by Foster (1965). A continuous substitution series is exhibited throughout the range of corresponding biotite mica/lithofacies compositions, Mg/Fe* or Al_2O_3 content varying regularly in a progression from the least to most evolved facies in the Thirtymile stock. The Mg/Fe* ratio of the mica has a fair correlation (coefficient= 0.801) with the Thornton-Tuttle differentiation index of the rock (Fig. 4.26), hence increasing Fe/(Mg+Fe) ratio or decreasing Mg/Fe* (as has been used for diagrams here) is a means of depicting evolution of the granite series. The compositions observed for the Hake batholith overlap the middle of the Thirtymile field and those of the Seagull plot with the higher Li biotite granites of the even-grained facies.

Some, but not all (notable the compatible) trace elements in the micas exhibit a clear linear trend through the various facies, showing less spread than many whole rock trace element contents. Of particular interest is Nb, which might be expected to be enriched in the most fractionated lithofacies. An enrichment trend is observable throughout the biotite-bearing facies (Fig. 4.26), but the extremely fractionated leucogranites have low contents of Nb, which matches the rock trend. These trends are considered to be the result of 'ultrafractionation' (Newberry et al., 1990) and are further discussed in Section 7.2.2.

(7) OXIDATION STATE OF THE MAGMA: ILMENITE AND MAGNETITE SERIES

Two granite types are recognised (Ishihara, 1977) that show a clear association with various types of mineralisation: magnetite-bearing (oxidised) versus ilmenite-(reduced) type: the latter carrying few opaque minerals (<1%), most of which is ilmenite. Mo, porphyry copper and base metal deposits are found in direct association with the magnetite series and tin (greisens) with ilmenite series (Ishihara, 1977). Takahashi et al. (1980) compared this twofold distinction with Chappell and Whites' S or I scheme using molar ACF ternary composition diagrams of published analyses from plutons (where a clear magnetite/ilmenite classification was established). All magnetite series granites correspond to I-types but ilmenite series granites may include both S and I types.
The criteria for recognition of the two types are (Ishihara, 1981):

Magnetite Series :

(1) Magnetite >0.1% volume; (2) Magnetic susceptibility $>1x10^{-4}$emu g^{-1};

(3) $Fe_2O_3/FeO >0.5$;

(4) Depleted lithophile elements; (5) Accessory magnetite 0.1-2.0 vol. %, plus ilmenite, haematite, pyrite and chalcopyrite; (6) Biotite with high Fe_2O_3/FeO and low refractive index; (7) Intrusive sequences in which Fe/(Fe+Mg) in biotite and amphiboles decreases with increasing SiO_2 of the rock.

Ilmenite series :

(1) Magnetite and ilmenite, 0.1 % vol; (2) Magnetic susceptibility <1x10-4 emu g^{-1}; (3) Fe_2O_3/FeO <0.5; (4) Enrichment in lithophile elements; (5) Accessory ilmenite, pyrrhotite, graphite, ±monazite±garnet, muscovite; (6) Biotite with low Fe_2O_3/FeO and high refractive index and (7) Intrusive sequences in which Fe/(Fe+Mg) in biotite and amphiboles increases with increasing SiO_2 of the rock (see Ch. 6).

Gastil et al., (1990a) report a clear division within the Peninsular Ranges batholith from the western (gabbro to monzogranite, largely magnetite-bearing part) to the eastern region, which lacks magnetite and varies from leucotonalite to monzogranite. Some western magnetite-bearing plutons have magnetite-free margins, however. An increase in Fe/Mg, Fe^{2+}/Fe^{3+} and NH_4^+ in these margins is reported and the lack of magnetite is explained by reducing reaction with country rocks. The totally magnetite-free plutons do not show evidence of wall-rock interaction.

In continental SE Asia ilmenite-type granites tend to occur to the west of the magnetite types i.e. toward the continent as is the case in California. A model for the generation of Ilmenite-type magma at a specific depth along a subduction zone has been proposed, where f_{H_2O} would be higher due to dehydration of ferromagnesians and f_{O_2} would be lower than at either side of this critical zone (Gastil et al., 1990b).

THE SEAGULL-THIRTYMILE GRANITES

In the Seagull-Thirtymile granites opaque minerals present are largely those other than magnetite, judging from the low amounts encountered during magnetic separation of micas for analysis. There are some sulphides. The total amount of opaque minerals is generally <0.2%. The ratio of Fe^{2+} to Fe* in the micas gives an indication of oxidation state of the granite magma (van Middelaar and Keith, 1990). All of the micas from the Thirtymile stock have most of their Fe in the Fe^{2+} state (>0.7, see Fig. 4.28), indicating a reduced nature for these granites. A slight trend toward increasing oxidation in the magma is indicated by the lowered FeO/(FeO+Fe_2O_3) ratio from the porphyry to even-grained biotite granites. The Li-mica leucogranites, however, have very high $FeO/(FeO+Fe_2O_3)$ ratios (>0.9); a further reversal to add to chemical trends shown by the biotite granites. A distinct red colour in thin section of some of the batholith biotites (the 'foxy-red' of White, 1990) is consistent with such generally reduced nature. Further evidence that the granite magma had a low f_{O_2} is provided by skarn mineralogy at the Mindy prospect (see Ch. 5). The granites are therefore distinctly of the ilmenite-type. The trend of decreasing Mg/Fe* ratio of the biotites is also typical for an ilmenite-series granite suite (Ishihara, 1980).

(8) SOURCE REGION: A BRIEF REVIEW

Granites found in a continental setting are ideally of three principal chemically and isotopically distinctive types: S-, I- and A-type. The S-I distinction is based on the hypothesis that these types reflect an origin due to partial melting of sedimentary- or igneous-derived crustal material. Due to the removal of Na and Ca from feldspathic source rocks during weathering and preferential transport of lighter isotopes, sedimentary sources are expected to be initially peraluminous and to produce granites with higher $^{87}Sr/^{86}Sr$ ratios than an igneous source (Chappell and White, 1974; White and Chappell, 1988; Clemens, 1988). $^{87}Sr/^{86}Sr$ ratios greater than 0.706 are considered indicative of magma genesis involving older continental crust (Armstrong, 1988), which may reflect either anatexis of metasediments or assimilation of such material into a magma (e.g. Kistler, 1990; Silver and Chappell, 1988).

Compositional variation in these two granitic types is envisaged as resulting from variable degrees of mixing and subsequent partial or complete homogenisation of a felsic melt produced under conditions of 'ultrametamorphism' (White and Chappell, 1977) and refractory, i.e. granulitic, residue (restite). Mineralogically, S-type granites will contain both muscovite and biotite micas, frequent Al_2SiO_5 minerals and often garnet. 'Restite' will appear as metasedimentary xenoliths in S-types and as mafic hornblende-rich xenoliths in I-type granites (White and Chappell, 1977). Hornblende is derived from residual pyroxene by its equilibration with OH-bearing material as magma rises and a_{H_2O} increases. Complex zoned and twinned plagioclase phenocrysts in S-type granites are interpreted by White and Chappell as modified restite. In peraluminous granites muscovite can appear in either oxidised or reduced types but garnet is to be expected particularly in the reduced type. Cordierite is the obviously peraluminous mineral found commonly in reduced types, but also rarely in oxidised types. S-type granites are commonly associated with the major Sn-W greisen and stockwork deposits of the World, and it has been claimed that the largest Sn deposits will only be found in proximity to this type (A.J. White, pers. comm. 1990).

The metaluminous (i.e. $Al_2O_3/[Na_2O + K_2O + CaO] < 1$ but $Al_2O_3/[Na_2O + K_2O] > 1$) nature of I-type granites is reflected in their biotite-only or hornblende± biotite ferromagnesian content. I types are expected to be more homogeneous than S types since they are derived from igneous sources, hence their variation diagrams frequently show less spread than those of S-types.

The chemically and mineralogically distinct A-type granites are described from continental extensional tectonic settings (see following section).

Experiments and thermodynamic modelling indicate that granitic composition melts may be formed from quartzofeldspathic rock by melting generated by muscovite and biotite breakdown at $T \leq 850°C$, $p \geq 4$ kb; for amphibole breakdown to be an important mechanism higher temperatures are required (Clemens and Wall, 1981; Clemens and Vielzeuf, 1987). Potassic, biotite-rich compositions are the most fertile source. Chemical trends in crystallising S-type magmas have been experimentally investigated by Clemens and Wall, 1981, who demonstrate that fractionation of garnet would lead to a decrease in the Fe/(Fe+Mg) of the residual liquid, whereas cordierite fractionation would have the opposite effect and result in late crystallisation of almandine garnet .

Experiments of crystallisation of intermediate composition (≈65 wt% SiO_2) I- and S-type melts, at f_{O_2} close to the QFM buffer were performed by Conrad et al (1988). These indicated that the higher silica melts formed at low a_{H_2O} and at minimum normative An / maximum normative Or melt compositions.

Strong peraluminosity is not conclusive evidence of a pelitic source-rock for granitic melts as the restite hypothesis might suggest. If garnet is consumed in the reaction:

Garnet + Qtz = Orthopyroxene + Sillimanite

in a silica-saturated magma, then even non pelitic sources could produce very strongly peraluminous melts at the appropriate p/T conditions (Clemens and Wall, 1988). Indeed, few strongly peraluminous igneous rocks may have had a pure pelitic source. The isotopic signatures of the Phanerozoic strongly peraluminous igneous rocks show E_{Nd}/E_{Sr} trends more consistent with a primary crustal composition than a distinctly pelitic source (Miller, 1985). Rb is high in pelites. If much mica remains in the residue from melting the liquid will not be enriched. Sr is expected to be the same in the melt as in the pelite because of low abundance of feldspar in the expected residue. Ba should be lower than the original pelite (partition coefficient <1 because of abundance of mica and K feldspar). The Rb/Ba ratio may be distinctive (pelites have ≈0.25, melts will be higher) and $^{87}Sr/^{86}Sr_i$ should be ≥0.71. Pelites are considered unlikely sources for most granites of the North American Cordillera (Miller, 1985).

ANOROGENIC or A-TYPES

These are chemically and hence mineralogically distinctive (peralkaline, with low CaO and Al_2O_3 content and high Fe/Fe+Mg and K_2O/Na_2O). The A-types are enriched in Zr, Nb, Ta and low in the elements compatible in mafic minerals (Co, Sc, Cr, Ni) and feldspars (Ba, Sr, Eu). Initial Sr ratios range from 0.703 to 0.712. They have high F contents and distinctively contain sodic pyroxene or amphiboles. Associated Sn-Ta mineralisation is common. An origin involving basaltic magma interacting with a depleted granulitic crustal component or fractionation directly from basalt without contamination has been suggested (Loiselle and Wones, 1979; Collins et al., 1982).

TECTONIC SETTING

The various granite types recognised (Chappell and White 1974; White and Chappell, 1977; Loiselle and Wones, 1979; Collins et al., 1982) may be generally related to their tectonic setting (Pitcher, 1982). Particularly diagnostic properties of the various types (Table 4.10) are $^{87}Sr/^{86}Sr$ initial (Sr_i) ratios; peraluminosity (in this particular classification defined as Al/[Na + K + Ca/2]); mineralogy and nature of xenolithic material. Both Cordilleran (oceanic plate subduction) and Caledonian (continent-continent collision) magmatism will produce I-type intrusions. The Cordilleran types often contain megacrystic K-feldspars and have consistently lower (Sr_i) values (<0.706) than the continental types (Pitcher, 1982: see Table 4.10). The I-Cordilleran type granites (gabbro-quartz diorite-tonalite suite) are associated with the major porphyry Cu-Mo deposits, whereas the Caledonian type (granodiorite suite) are much less commonly

M-type	I- (Cordilleran) type	I- (Caledonian) type	S-type	A-type
Plagiogranite subordinate to gabbro	Tonalite dominant but broad compositional spectrum — diorite to monzogranite — with wide SiO_2-range. Major association with gabbro	Granodiorite-granite in *contrasted* association with minor bodies of hornblende diorite and gabbro	Granites with high but narrow range of SiO_2. Leucocratic monzogranites predominate but granitoids with high biotite content locally important	Biotite granite in evolving series with alkalic granite and syenite. Highly contrasted acid–basic relationship
Hornblende and biotite; pyroxene	Hornblende and biotite; magnetite, sphene	Biotite predominates; ilmenite and magnetite	Muscovite and red biotite; ilmenite, monazite, garnet, cordierite.	Green biotite. Alkali amphiboles and pyroxenes in alkalic types, astrophyllite.
K-feldspar interstitial micrographic	K-feldspar interstitial and xenomorphic	K-feldspar generally interstitial and invasive. Often quartz-rich	K-feldspar often as megacrysts with protracted history. Autometasomatic variants	Perthites
Basic igneous xenoliths	Dioritic xenoliths; may represent restitic material	Mixed xenolith populations	Metasedimentary xenoliths predominant	Cognate xenoliths, also basic magma blebs
Typical initial $^{87}Sr/^{86}Sr$ ratios $<0{\cdot}704$	$\mathrm{Al}/\left(\mathrm{Na}+\mathrm{K}+\frac{\mathrm{Ca}}{2}\right)<1{\cdot}1$ (often <1) $<0{\cdot}706$	$\mathrm{Al}/\left(\mathrm{Na}+\mathrm{K}+\frac{\mathrm{Ca}}{2}\right)$ *ca.* 1 $>0{\cdot}705 \quad <0{\cdot}709$	$\mathrm{Al}/\left(\mathrm{Na}+\mathrm{K}+\frac{\mathrm{Ca}}{2}\right)>1{\cdot}05$ $>0{\cdot}708$	Peralkaline, relatively rich in F. Considerable range, 0·703–0·712
Small, quartz diorite-gabbro composite plutons	Great multiple, linear-batholiths with arrays of composite cauldrons	Dispersed, isolated complexes of multiple plutons and sheets	Multiple batholiths, plutons and sheets, less voluminous and more commonly diapiric than I-types	Multiple, centred, cauldron-complexes of relatively small volume
Associated island-arc volcanism	Associated with great volumes andesite and dacite	Sometimes associated basalt–andesite lava "plateaux"	Can be associated with cordierite-bearing lavas but characteristically lacking in voluminous volcanic equivalents	Associated with caldera centred alkalic lavas
Short, sustained plutonism	Very long-duration episodic plutonism	Short, sustained plutonism; postkinematic	Sustained plutonism of moderate duration; syn- and post-kinematic	Short-lived plutonism
Oceanic island arc	Andinotype marginal continental arc	Caledonian-type post-closure uplift	Hercynotype continental collision. Also encratonic ductile shear-belts	Post-orogenic or anorogenic situations
Open folding: burial-type metamorphism	Vertical movements, little lateral shortening: burial-type metamorphism	Dip-slip and strike-slip faulting: retrograde metamorphism	Much shortening; low-pressure metamorphism in slate belts; part of a *Granite Series*	Doming and rifting
Porphyry-Cu, Au, mineralization	Porphyry-Cu, Mo, mineralization	Rarely strongly mineralized	Sn and W-greisen and vein-type mineralization	Columbite, cassiterite and fluorite

Table 4.10 **The Pitcher classification of granites** (after Pitcher, 1982)

mineralised (Pitcher, 1982; Ishihara, 1980).

S-type granites are found in a Hercynian type continent- continent collision tectonic setting (Pitcher, 1982) or, when associated with continental-margin orogeny, occur further onboard the craton than the I-type batholiths where S- and I-types form paired magmatic arcs (Takahashi et al., 1980; Ishihara, 1981). The common occurrence of megacrystic K-feldspar in this granite type may be a result of both magma chemistry and emplacement or cooling history . K-feldspars may not nucleate well in the less-potassic melts. Magma is only likely to be saturated in K-feldspar at temperatures close to the solidus and crystallisation would be fastest in water-undersaturated melts, i.e. those where large amounts of melt are still available at that temperature (Vernon, 1986; Winkler and Schultes, 1982).

A-type or anorogenic granites are volumetrically inferior to I- and S-types and are found entirely in a continental setting. They are associated with extensional tectonics and crustal melting due to tectonic decompression and intrusion of basic magma.

The M-type are plagiogranites typical of island arcs in a setting where subduction involves only oceanic crust or where mantle-derived magma may have differentiated to form the acid magma (Pitcher, 1982).

THE SEAGULL-THIRTYMILE SUITE

The Seagull-Thirtymile granites are not distinctly S-type (mineralogy, metaluminous composition and the Sr_i ratio suggest this). The Sr_i ratio is slightly higher than the range indicated for Cordilleran I-types in the scheme of Pitcher (1982), but is similar to the Caledonian types. The mineralogy suggests a largely I-type magma. Peraluminous magmas may not even require a pelitic source rock (Clemens and Wall, 1981; Miller et al., 1985): feldspar-rich metagreywackes or even some metaluminous igneous rocks are suitable sources, therefore no great sedimentary input to the region of magma generation is needed to produce $Sr_i = 0.707$. The reduced (i.e. ilmenite-type) magma indicated by relatively high $[FeO/(FeO+Fe_2O_3)]$ contents of the biotites is consistent with their being derived from an I-type source.

(9) MAGMA TYPE: Comparisons of granite compositions with the discrimination diagrams for alkalic, calc-alkaline and tholeiitic magma series show them to be on a highly evolved calc-alkaline trend (Fig. 4.30-32). Alkali-silica plots (c.f. Irvine and Baragar, 1971: see Fig. 4.29) show the Seagull-Thirtymile suite, to have calc-alkaline affinity. One specimen only: a Li-mica leucogranite crosses the boundary and this is interpreted as being due to the high albite component in this lithofacies. The ferromagnesian-silica diagram (c.f. Miyashiro, 1974: see Fig. 4.31) is not diagnostic.

(10) COMPARISON WITH CHEMICAL TECTONIC CLASSIFICATIONS:

The use of purely chemical parameters to define the setting of magmatism in the Thirtymile Range does discriminate the Seagull-Thirtymile suite plutons from the hornblende-rich NW and SW Thirtymile stocks and also demonstrates some differences between these granites and the W-related Selwyn plutonic suite. Rb-Ba-Sr relationships (Fig. 4.32) just cross the within-plate/collision boundary, but do suggest a largely within-plate environment source for the magma. This suite does contrast with more Sr-rich compositions of the Mactung Selwyn Suite W-related pluton. A plot of (Y+Nb) to Rb (c.f. Pearce et. al., 1984: see Fig. 4.33) shows the suite to fall in the 'within-plate' field, except for the very fractionated leucogranites, which have too much Rb enrichment to be able to reliably use this criterion. It is suggested that the Thirtymile-Seagull suite was derived from a predominantly I-type, but continental-crustal source. The lack of any distinct negative Nb anomaly on the 'spidergrams' (c.f. Figs. 4.22-25) indicates little subduction-related component to these magmas.

4.7.2 ULTRAFRACTIONATION TRENDS

Li enrichment in a facies of almost pegmatitic composition is understandable, but depletion of Nb compared to the next most fractionated lithofacies is not so readily explained, particularly since the most fractionated granite at the east side of the Seagull batholith (Rb-Ba-Sr diagram: Fig. 4.32) is little different chemically. Reversal shown by other major-element trends, when Rb is used as an indicator of fractionation (Fig. 4.20) further suggests that a drastic change in processes occurred to form these F-rich leucogranites. It is suggested that once water vapour loss occurred in the magma at the onset of 'second-boiling' (Burnham and Ohmoto, 1980) a drastic change in the bulk K_d of many trace elements was produced (Newberry et al., 1990). Nb would have been scavenged from the magma by Cl-rich magmatic fluids in the same manner that Sn is transported most efficiently by Cl-complexes (Barsukov and Kuril'chikova, 1966; Stemprok, 1982). The Nb was then transported from the intrusion to form mineralisation above. This ultrafractionation model adequately explains the crystallisation trend of the leucogranites away from the quartz field (Fig. 4.18) and toward the albite field. Both albite and orthoclase crystallisation under such F-rich conditions is to be expected (Manning, 1982).

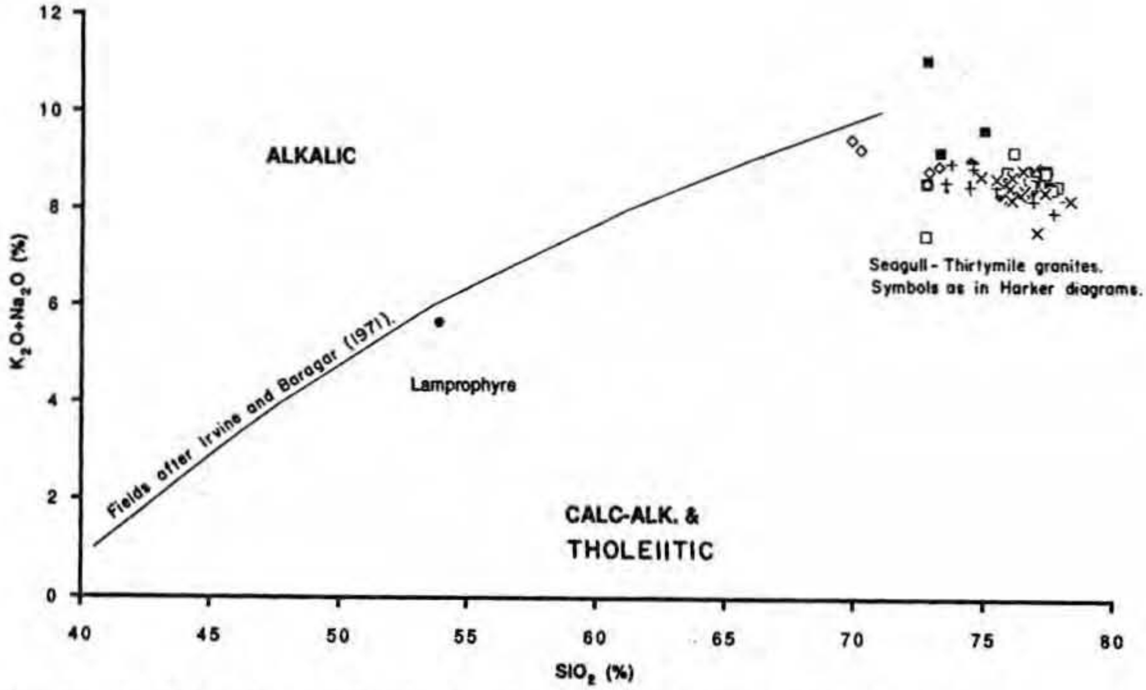

Figure 4·30 Seagull-Thirtymile plutonic suite: Alkali variation diagram.

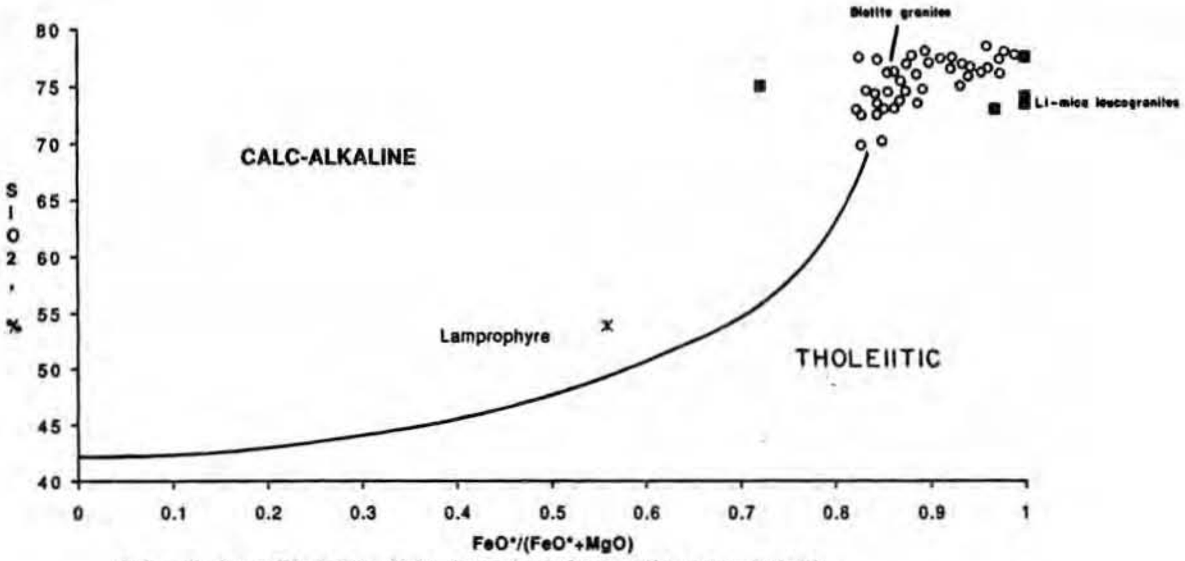

Calc-alkaline / Tholeiitic field boundary from Miyashiro (1974).

SEAGULL-THIRTYMILE PLUTONIC SUITE: MIYASHIRO VARIATION DIAGRAM

Fig. 4·31

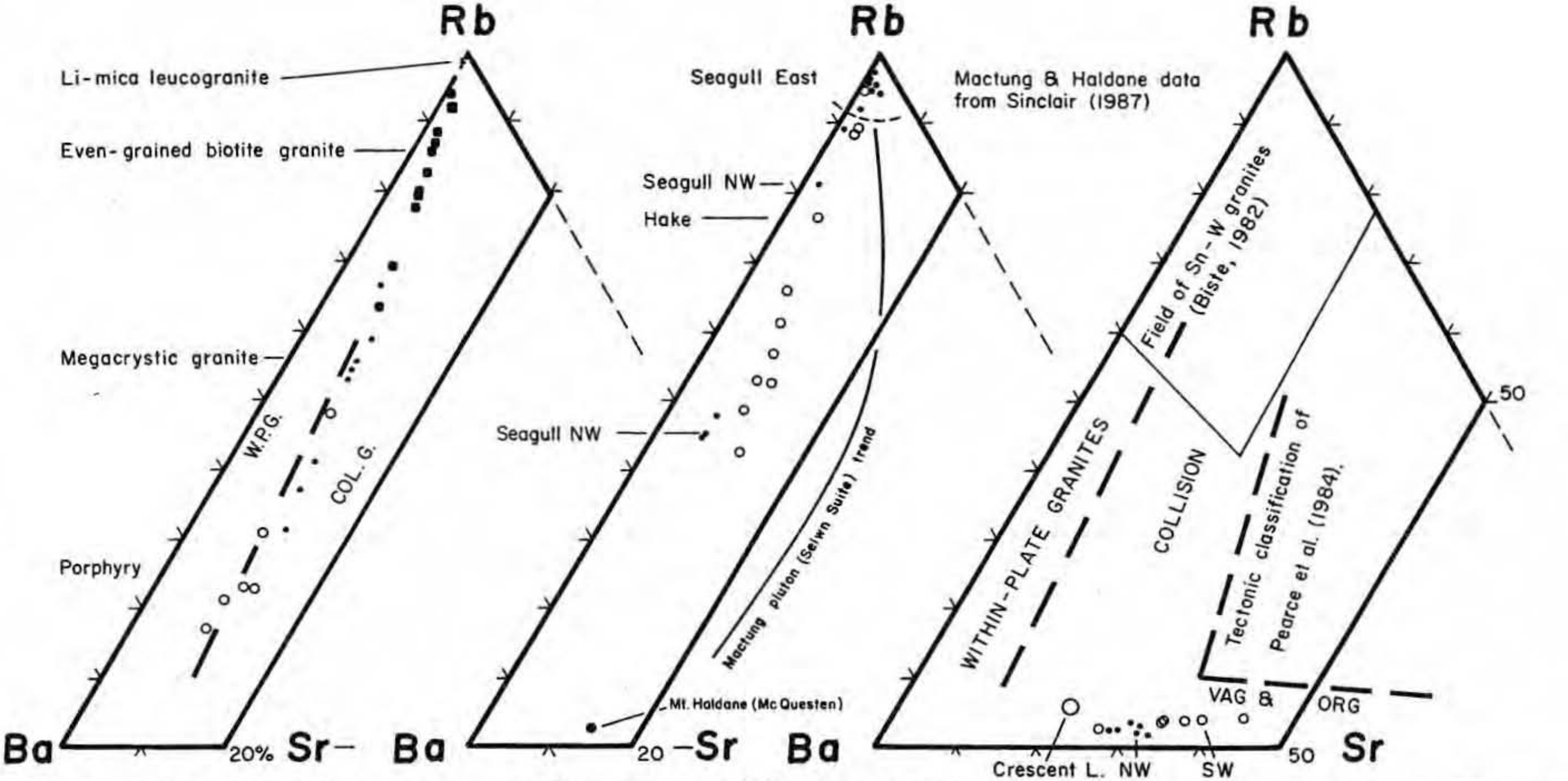

THIRTYMILE & ORK STOCKS

BATHOLITHS & COMPARISON

DIORITE & GABBRO STOCKS WITH TECTONIC CLASSIFICATION. Northwest & Southwest Thirtymile, Crescent Lake.

Ba-Rb-Sr Ternary Diagrams for the Seagull-Thirtymile Suite and Diorite Stocks.

Fig. 4·32

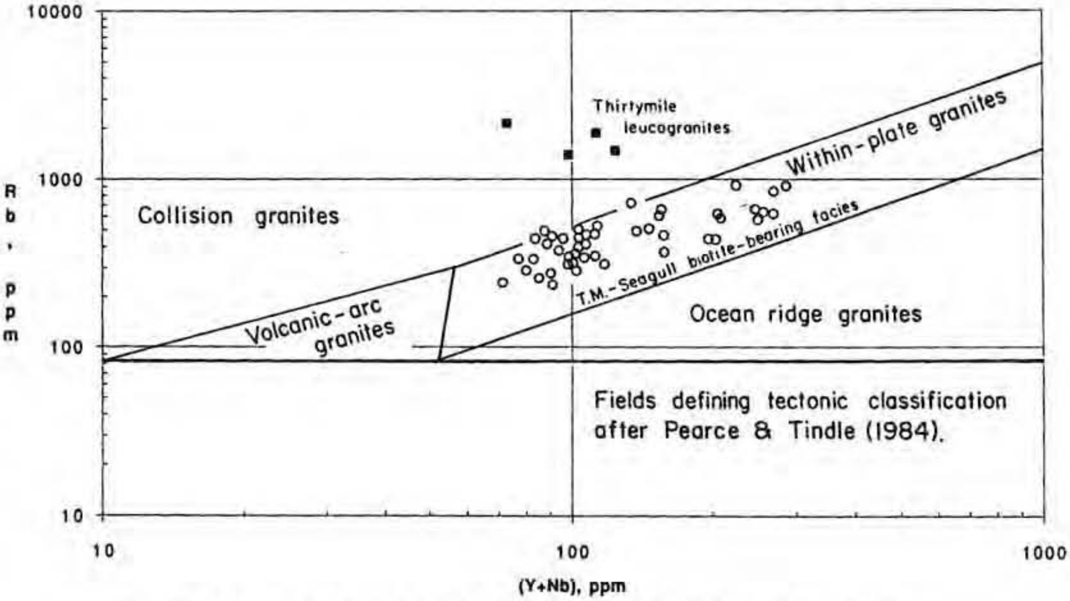

Fig. 4.33 Rb to (Y+Nb) DISTRIBUTION OF THE SEAGULL-THIRTYMILE GRANITES.

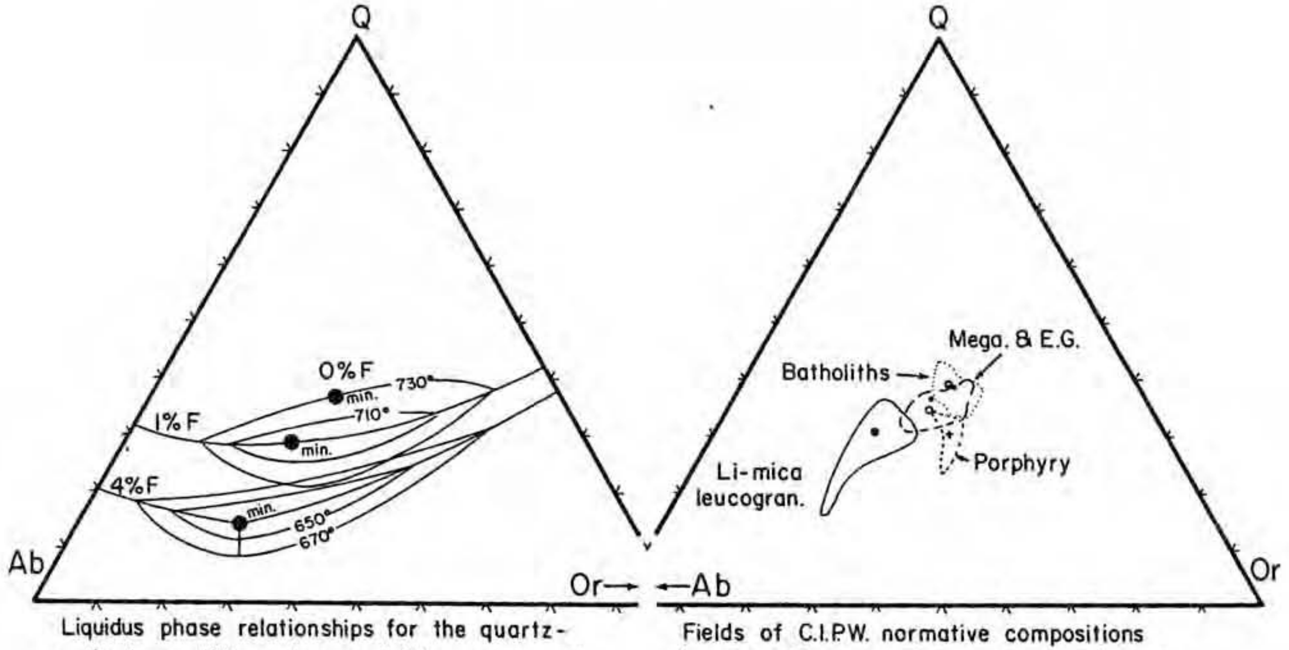

Liquidus phase relationships for the quartz-orthoclase-albite system containing excess water and 1% / 4% F by weight at 1 kb· pressure. After Manning (1982).

Fields of C.I.P.W. normative compositions (quartz-orthoclase-albite components) of the granites from the Seagull-Thirtymile plutonic suite. Average composition for each facies/pluton is shown.

Fig. 4·34

4.7.3 THE HORNBLENDE RICH STOCKS

The SW Thirtymile stock has compositions ranging from gabbro to hornblende diorite and monzo-granodiorite (the latter most felsic component falling on the granite/granodiorite boundary on an O'Connor diagram: Fig. 4.17). The presence of enclaves of diorite in the granodiorite, plus similar trace element contents to the diorite are considered reasonable evidence for the adjacent bodies being comagmatic, rather than the possibility of the more leucocratic facies being related to older intrusions of the Big Salmon complex (i.e. the Teslin suture zone). The NW Thirtymile stock is uniform in modal composition, being a monzogranodiorite from modal composition or granodiorite from normative feldspar ratios. All these lithofacies are rich in hornblende and often sphene and contain epidote.

In Harker variation diagrams the SW Thirtymile and NW Thirtymile stocks occupy fields that cannot be readily correlated with the batholith trends (Figs. 4.21 b,c,d). Differences between the two groups of plutons are more accentuated when chondrite-normalised incompatible trace element patterns are compared: positive Ba and Sr anomalies and strong negative Nb anomalies (Fig. 4.25) do not change markedly despite a range of composition from gabbro to monzo-granodiorite, with no evidence for pronounced feldspar fractionation trends. Such patterns are similar to that of the Crescent Lake diorite stock at the Swift River, which is perhaps correlable with other diorites previously considered to be of late Jurassic to early Cretaceous in age (Poole et al., 1960; Abbott, 1981) and which intrude the Yukon Cataclastic complex (i.e. Dorsey terrane). These fields of trace element composition which are quite separate from the clear trends on variation diagrams shown by the Seagull-Thirtymile granites are interpreted to show that the hornblende-rich stocks represent a separate less-evolved magmatic suite. The Rb-Ba-Sr ternary plot (Fig. 4.32) also distinguishes the hornblende-rich stocks from the Seagull-Thirtymile suite and the (Y+Nb) content falls within the volcanic-arc granite field (Fig. 4.35). Chondrite-normalised 'spidergrams' (Fig. 4.25) show distinct positive Ba and much more obvious negative Nb anomalies than the Seagull-Thirtymile suite granites. A negative Th anomaly is pronounced for the SW specimens, but less obvious for the NW stock, perhaps a result of the more evolved composition of the NW Thirtymile stock. The ferromagnesian content (Miyashiro, 1974) suggests that these

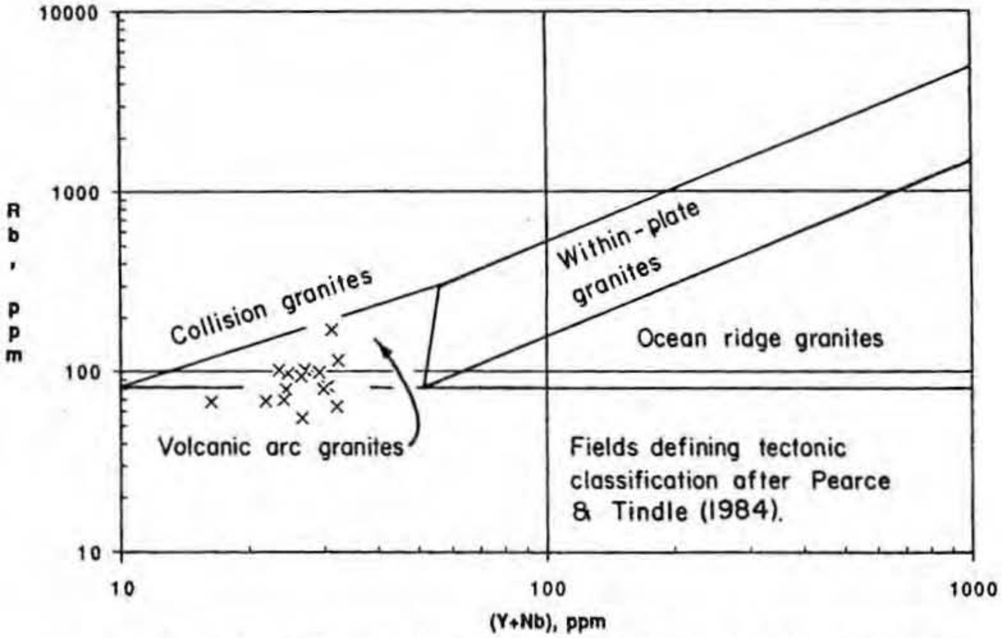

Fig. 4·35 Rb to (Y+Nb) DISTRIBUTION OF THE SW & NW THIRTYMILE STOCKS.

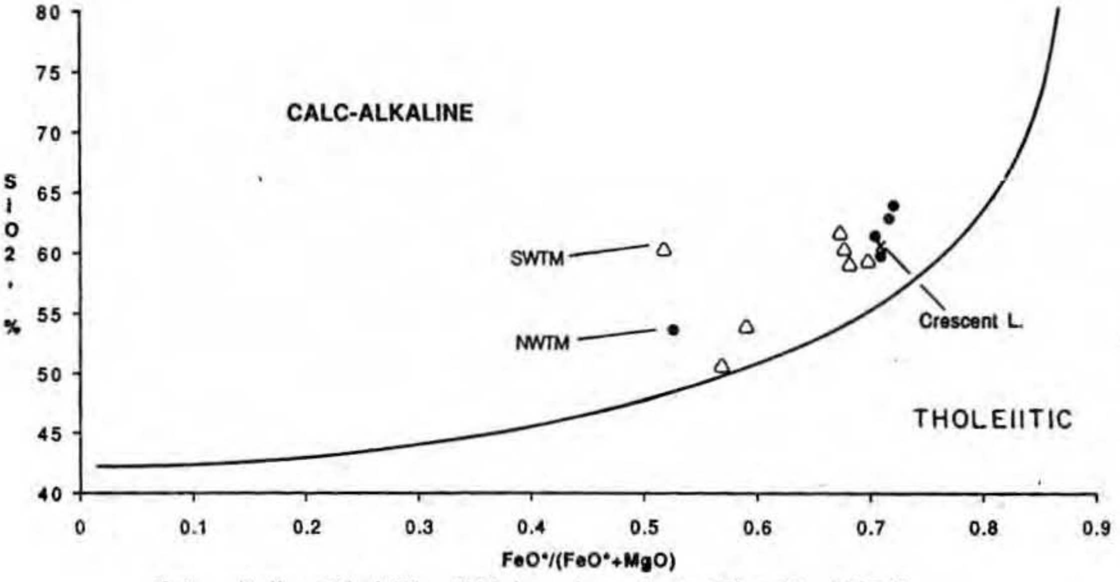

Calc - alkaline / tholeiitic field boundary from Miyashiro (1974).

NW & SW THIRTYMILE & CRESCENT LAKE STOCKS: MIYASHIRO VARIATION DIAGRAM.

Fig. 4·36

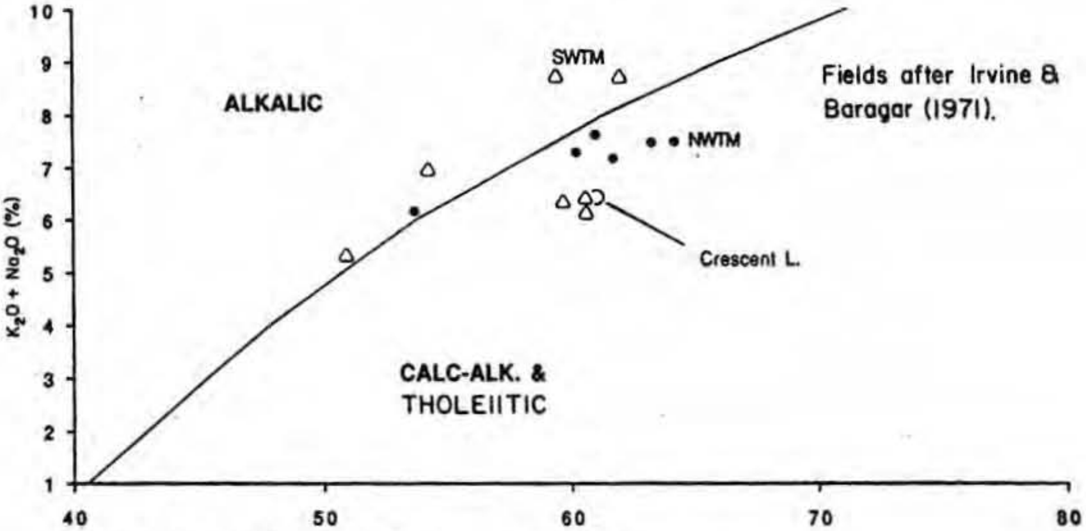

NW & SW THIRTYMILE & CRESCENT LAKE STOCKS: ALKALI VARIATION DIAGRAM.

Fig. 4·37

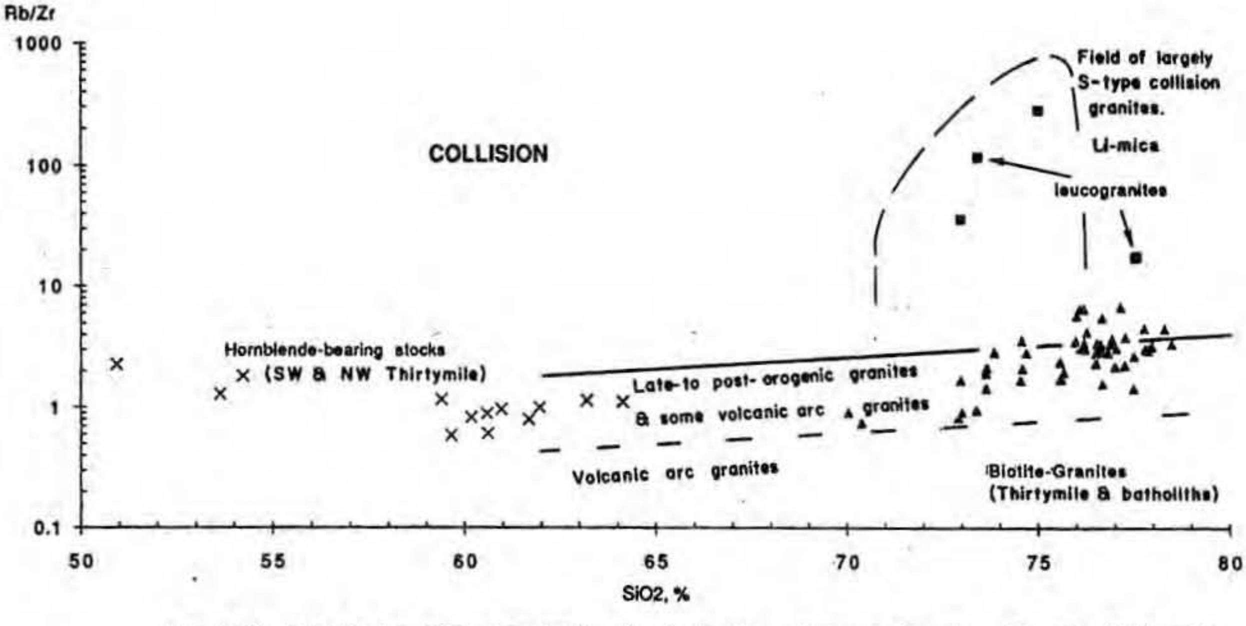

Fig. 4·38 Rb/Zr to SiO_2 Tectonic discrimination diagram for the Seagull - Thirtymile Suite and the hornblende - bearing stocks (c.f. Harris et al., 1986).

stocks were derived from calc-alkaline magma (Fig. 4.36), however alkali content (Irvine and Baragar, 1971) is not diagnostic: the range of compositions spans the alkalic/calc-alkaline or tholeiitic boundary (Fig. 4.37) and they plot towards the alkalic field on an AFM diagram (Fig. 4.17). It is postulated that this suite was derived from subduction-related magma.

AMMONIUM CONTENTS: The ammonium contents of the hornblende-rich stocks have a range similar to those of the Seagull-Thirtymile suite, i.e. they are particularly low when compared to granites elsewhere (Hall and Liverton, 1992). One specimen from the contact zone of the SW Thirtymile stock (08/20-6), see Fig. 3.24, is markedly higher in ammonium (Table 4.8). This particular rock is somewhat hydrothermally altered. Such alteration is adequate to explain an increased NH_4^+ level (Hall, 1988) and interaction with country-rocks is also capable of increasing the levels (Gastil et al, 1990; Cooper and Bradley, 1990). The mechanisms capable of lowering ammonium contents at the level of emplacement of a pluton are oxidation and loss due to boiling-off of volatiles from shallow intrusions. There is no field evidence to suggest that much fracturing of the country-rocks took place. The presence of frequent magmatic epidote in the two stocks (and particularly in the NW pluton) tends to indicate that these bodies were crystallised at some depth in the crust. The low ammonium contents are interpreted to indicate a low content in the magma. Low NH_4^+ magma levels are likely to indicate derivation from an igneous (either a substantial mantle derived component or an I-type) source or from high-grade metamorphics that had previously lost their NH_4^+ content (Hall and Liverton, 1992).

4.7.4 H.H.P. GRANITES AND CORDILLERAN/CALEDONIAN TYPES

The Seagull-Thirtymile granites are chemically and isotopically quite similar to the Caledonian and Hercynian High-Heat-Production ('HHP') granites. Granites which carry high amounts of the radioactive elements (particularly the U and Th decay series and ^{40}K) have been shown to be associated with long-lived hydrothermal activity, Sn mineralisation, and elevated geothermal gradients: hence they are 'HHP'. These include both S- and I-types. HHP granites may be generated either as evolved calc-alkaline magmas distal to subduction zone trenches (as in the case of Bolivia) or late in orogenic cycles (Plant et al., 1985; see also Fig 4.37). Their characteristics are defined as follows:

1) Moderate to low Fe enrichment accompanying SiO_2 increase.

2) High K, Rb, Ba, Sr and Th.

3) High Ba/Sr, Rb/Sr, and low K/Rb and Na/K ratios.

4) High LIL/HFS element ratios showing complex enrichment and depletion patterns as compared to tholeiitic suites where both LIL and HFS behave incompatibly.

5) They sometimes show negative Nb anomalies on mantle-normalised plots.

In particular, the HHP (Sn-U) granites of the British Hercynian and Caledonian have particularly high Rb, Nb, Y and Li and very low Ba, Sr, Ni and Cr. (Plant et al., 1985). Comparison of the chondrite-normalised trace-element diagrams of the Seagull-Thirtymile suite with distributions illustrated by those authors shows that the Thirtymile granites compare well with the Cairngorm granite: (Fig. 4.39; see also Watson et al., 1984). The pattern of trace elements is mirrored by the Cornubian Batholith, with similar contents of Ba and Sr to Cairngorm. The principal differences between the Thirtymile-Seagull suite and the HHP types are the range of Ba and Sr anomalies (Thirtymile porphyry has Sr approximately 10x chondrite and the Li-mica facies has contents falling almost to 10^{-2} of chondrite) and slight Fe-enrichment with increase in silica in the latter, which is seen only in the Li-mica lithofacies of the Seagull-Thirtymile suite (and that is a trend contrary to the Rb-enrichment direction).

Comparison with the Pitcher (1982) tectonic classification shows that the characteristics of this suite are closer to his I-Caledonian type than the typical Cordilleran granites: with Al/(Na+K+Ca/2)= 0.953 to 0.992 for the Thirtymile biotite-bearing facies and the batholiths and 1.046 and 1.090 for the very evolved Li-mica and STQ facies respectively; $^{87}Sr/^{86}Sr_i$ of 0.705-0.707 and biotite >> hornblende mafic contents.

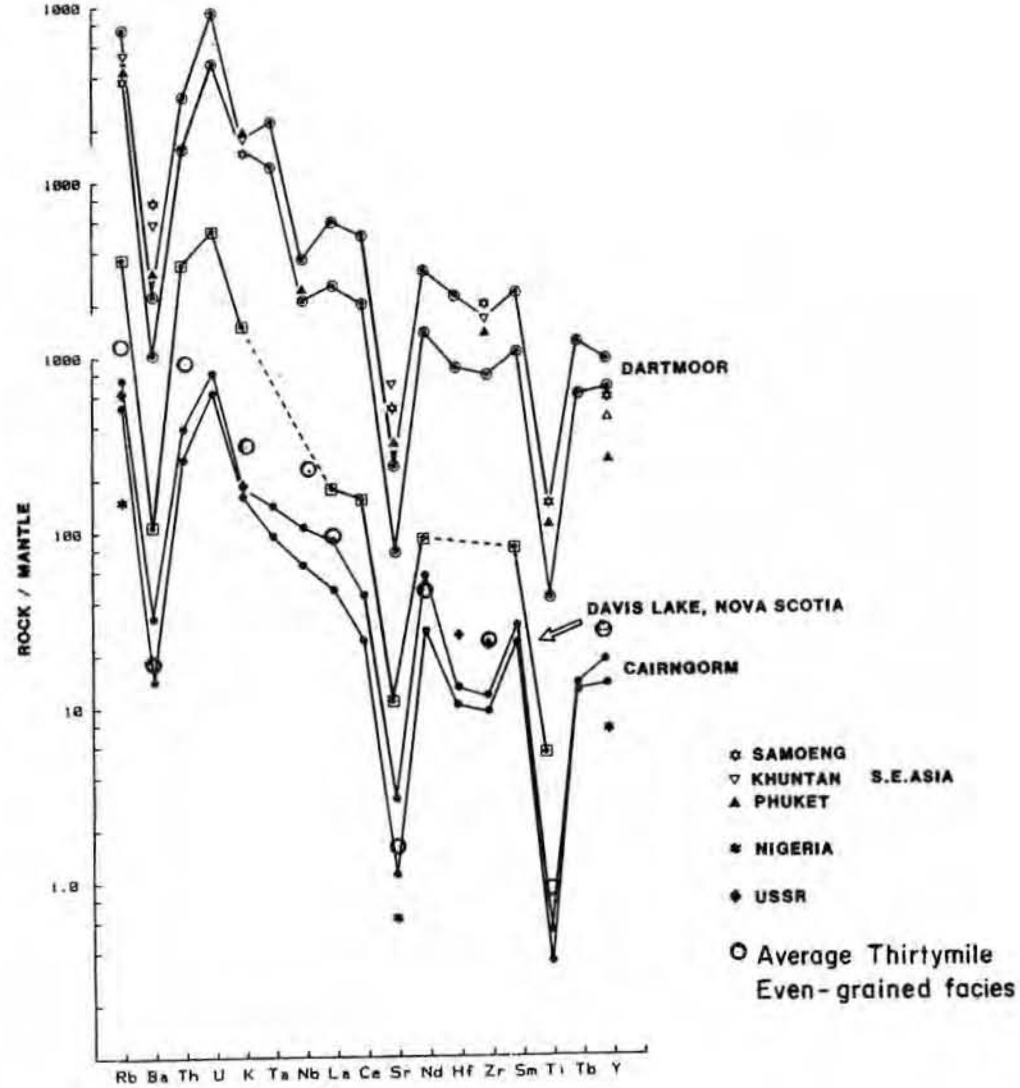

Figure 4·39 Primordial mantle-normalised trace element diagrams for HHP granites (after Plant et al., 1985).

4.7.5 DISTINCTIONS BETWEEN Sn- AND W-BEARING GRANITES

Many granitic plutons of the Northern Cordillera have associated scheelite-type mineralisation, providing carbonate sediments are found in their contact aureoles (Union Carbide Exploration Corp., 1972-1983, unpublished data). Few regions have known tin occurrences. These are, from north to south: McQuesten area (Emond, 1986); Kalzas Twins (inferred buried pluton: Lynch, 1985); Seagull batholith (Abbott, 1981; Layne and Spooner, 1987; this study); Cassiar Batholith (Ash Mountain: Mulligan, 1969) and Mt. Reed (Canadian Superior Exploration, unpublished exploration reports). Some distinction may be made between stanniferous and tungsten-bearing granites on the basis of petrographic characteristics: the Selwyn suite stocks, which are associated with the Cantung and Lened deposits are frequently, but not exclusively, coarsely K-feldspar megacrystic (Anderson, 1983; Union Carbide Exploration Corp., unpublished data), whereas the Sn-associated facies of the Seagull-Thirtymile suite and Mt. Reed are predominantly either even-grained granite or granite-porphyry with distinctive large subhedral quartz phenocrysts (this study). Such a distinction, however, is difficult to quantify and perhaps not very diagnostic, although Newberry et al. (1990) have correlated the largest outcrop area of equigranular granite with the highest tin content on the Seward Peninsula.

Both S- and I-type granites are found associated with W and Sn mineralisation in both Cordilleran and continental settings.

Continental examples are:

1) The I-type Elizabeth Creek granite of the Herberton tinfield of Queensland (White, pers. comm., 1990) is associated with frequent small tin deposits in the south and west at Herberton, Irvinebank and Stannary Hills, major W-greisen at Wolfram Camp to the east and small W-greisens at Tungsten Hill to the NW (J. Ransley and T. Liverton, 1965 unpublished report: Metals Exploration N.L.). Potentially large tin prospects are associated with S-type granite further to the north near Cooktown (White, pers. comm. 1990).

2) The Western Tasmanian tin granites are of both S- and I-type (Sawka et al., 1990).

3) The Cornubian batholith has an S-type signature indicated by comparatively high initial Sr_i ratios (average 0.7119: Stone and Exley, 1985), yet trace element contents have been

used to argue against an entirely S-type source (Plant et al., 1985). It is associated with widespread lode Sn and less frequent skarn W mineralisation.

4) The Erzgebirge muscovite granites (Dill, 1985) show mineralogy that is consistent with a largely S-type source. Similar mineralogies in the Hercynian granites of Portugal suggest a largely S-type source.

Cordilleran examples are fewer:

1) Fairbanks-Circle, Alaska: I-type, ilmenite-series granites (Newberry et al., 1990).

2) Seagull batholith: Largely I-type, ilmenite-series (this study).

A wide range of isotopic and chemical compositions of granites associated with both W- and Sn-skarns has led various workers to suggest that source material of the intrusion is less important for development of mineralisation than cooling history (Keith et al., 1990; Newberry et al., 1990; Swanson et al., 1990; Kwak, 1987). Both unevolved and relatively evolved granites may be associated with W-skarns (Ch. 6), but the Sn-F skarns are associated with particularly evolved types. F content of the W-related plutons and that of their biotite micas decreases with increase in differentiation index; those of the Sn-related plutons increase in almost exponential fashion. (Newberry et al., 1990). Tin granites also tend to be metaluminous to peraluminous, with >67% silica content (Griffiths and Godwin, 1983).

The W-related plutons will show only moderately evolved compositions (Rb to perhaps 450 ppm and Sr >120 ppm; low F content, but may have $K_2O/Na_2O > 1$ and SiO_2 to 72%). Oxygen fugacity, as indicated by the proportions of ferrous to ferric iron in biotites, in the W-related granite magmas is higher in these than for most Sn-related intrusions (Kwak, 1987). Sn-related plutons may have similar major-element compositions, but often reach extremes in SiO_2 (78%).

Trace-element indicators of fractionation (high Rb/Sr, low Ba/Rb and K/Rb) in the Sn-granites will far exceed those of the W-granites. These differences are considered here to be a reflection of the degree of evolution (or fractionation) that the granite has undergone and hence a direct function of depth of emplacement of the pluton which, in a rapidly uplifted and eroded Cordillera, is a function of timing (see also arguments in Newberry et al., 1990).

The extremely evolved, lithophile element-rich nature of late-stage lithofacies of the Sn granites is the obvious distinguishing chemical feature from the literature. Granites that carry amazonite feldspar and lithium mica have been recognised as being widespread in the upper portions of 1-10 km^2 section plutons in the USSR. A progression from porphyritic biotite granite with 0.04-0.45% Li_2O in the mica through leucogranites with 0.5-1.0% Li_2O and amazonite- protolithionite-bearing facies with 1.3-1.7% Li_2O to final apical facies with 4.5-5.0% Li_2O contents in their micas has been described by Zalashkova and Gerasimovskii (1974). The setting of many tin deposits above stocks and apophyses of batholiths indicates a relative depth control on mineralisation.

4.7.6 PETROGENESIS OF 'SPECIALISED' TIN GRANITES

Experimental data show that the addition of a small amount of F to a granitic magma will quite dramatically lower the minimum liquidus temperature and composition. The composition will change from Qtz_{37}-Ab_{34}-Or_{29} to Qtz_{15}-Ab_{58}-Or_{27} with addition of 4 wt% F to the system and the minimum temperature will fall from 730°C to 630°C at I kbar pressure (Manning, 1981). At certain compositions some 2 alkali feldspar-qtz-melt-vapour phase mixtures can co-exist at 550°C at p= 1 kbar. Mechanisms of reduction of the minimum liquidus temperature may theoretically be of three kinds: reaction of F with Si-O-Si bonds in the melt forming Si-F bonds; hydrolysis of Si-F bonds to release F; reaction of Al and F to form aluminofluoride complexes. The $(AlF_6)^{3-}$ complex is stable at high temperature. In F-rich granites both albite and orthoclase feldspars are present. Equilibrium between the two phases will be favoured as long as melt is present, so it is possible that two very different compositions may crystallise before the solidus is reached. Because of the asymmetry of the alkali feldspar solvus, in which the albite limb is much steeper than the K-feldspar limb, subsolidus exsolution will be more marked for the potassium-rich phase, so an assemblage consisting of albite and perthitic K-feldspar may be formed. Li and B will add to the effect of F on the solidus (Manning, 1982).

Similar experimental results are reported by Luth and Muncill (1989): a reduction of 350°C in the granite solidus temperature from volatile-free compositions is reported when molar F/(F+O)= 0.56 at 2 kb pressure. Boron will have a similar effect on the reduction of temperature of the minimum-melting composition granite. The addition of 4.5 wt% B to a granite melt results in the lowering of the solidus temperature to 660°C at 1 kbar (Manning and Pichavant, 1984) and results in a sodic peralkaline vapour phase (Pichavant, 1981) that carries boron in roughly the same concentration as the melt phase (Pichavant, 1983).

TWO MODELS FOR GENERATION OF HIGH F Sn-RELATED GRANITES

Different processes have been proposed as mechanisms for the generation of the Cornubian F-Li-rich granites and Cordilleran types such as those in central Alaska. The chemical enrichment in both types (with perhaps the exception of Nb trends) is very similar.

(1) THE CORNUBIAN MODEL

Six facies of granite are recognised from the Cornubian granite, 3 biotite-bearing lithofacies, 2 Li-mica-fluorite-bearing types and a muscovite-fluorite facies (Stone, 1985). Various ion-exchange reactions between F-rich fluid and biotite granite magma are suggested as the origin of the chemically distinct leucogranites. Production of the equigranular Li-mica granite ('E') (containing 9% mica, fluorite and apatite 2%, topaz 3%) from the main biotite-granite ('B') magma is envisaged by a process of albitisation caused by F-rich fluid phases causing conversion of biotite to zinnwaldite by Li-Al exchange for Mg-Fe. The high F content of the transformed magma would result in remobilisation (Stone and Exley, 1985). Production of type 'F' fluorite granite (containing muscovite 6%, fluorite 2%, topaz 1% and apatite <1%) by plagioclase, zinnwaldite and topaz breakdown, releasing Ca, Li and F is suggested by Manning and Exley (1984).

Mechanisms to produce sub-solidus alteration reactions (Manning and Exley, 1984) are: Breakdown of topaz in two reactions:

$$Al_2SiO_4F_2 + H_2O = Al_2SiO_4(OH)_2 + 2HF$$

$$3/2Al_2SiO_4(OH)_2 + 3/2SiO_2 + K^+ = KAl_3Si_3O_{10}(OH)_2 + H^+$$

to form muscovite plus the breakdown of Li-mica:

$$K_2(FeLi_3Al_2)Si_7AlO_{20}F_4 + 2H_2O = K_2(FeLi_3Al_2)Si_7AlO_{20}(OH)_4 + HF$$

and $$K_2(FeLi_3Al_2)Si_7AlO_{20}(OH)_4 + 6H+ = KAl_3Si_3O_{10}(OH)_2 + 4SiO_2 + 4\,H_2O + K^+ + Fe^{2+} + 3Li^+$$

and $$Ca^{2+} + 2HF = CaF_2 + 2H^+$$

to form muscovite and fluorite. An alteration of alkali feldspar to sericite is expected to accompany the above reactions (Manning and Exley, 1984).

The topaz granites are chemically distinct from the biotite granites and peculiar in their association with marginally-located tourmaline-bearing pegmatites. Nb and Rb contents are increased dramatically (c.f. an opposite trend for Nb in the Thirtymile pluton). An origin independent from that of the biotite granites has been suggested by Manning and Hill (1990), who advocate a process of low degrees of partial melting of granulitic residue from the earlier magma generation. Heat input to the lower crust is assumed to be by intrusion of potassic basic magma, which contributed to the chemistry of the topaz granites.

(2) EXTREME FRACTIONATION

Alkali-F-rich aplitic segregations are reported from Missouri (Nabelek and Russ-Nabelek, 1990) in which enrichment in the alkalis and F is a result of crystallisation of feldspars and quartz from granitic magma producing residual liquids rich in these elements. Enrichment in F leads to crystallisation away from the quartz field (i.e. towards albite, c.f. Manning, 1982).

Theoretical studies (Nekvasil and Burnham, 1987) suggest that an increase in water content at constant pressure will also cause contraction of the quartz field during crystallisation of granitic magma. Recent experimental data (Webster and Holloway, 1990) indicate that at pressures between 0.5 and 5 kbar and temperatures from

775-1000°C in metaluminous F-bearing haplogranite melts, Cl is partitioned into the aqueous phase rather than the melt. Increase in water activity, pressure, temperature, Cl content in fluid and a decrease in F activity cause increase in Cl partitioning toward the fluid phase. If F content is >7 wt %, Cl ≤1200 ppm, p= 2 Kbar and T= 1000°C the relationship is reversed, i.e. the Cl partitions toward the melt and F partitions toward the fluid phase. Estimates made by modelling using K_d values from those experiments for a magma of topaz-rhyolite composition show that in such a magma, initially containing low amounts of water, CaO, FeO and MgO with >1.25 wt% F and >1500 ppm Cl, crystallisation will lead to evolution of a Cl-rich fluid before the residual melt reaches 1 wt % Cl concentration (i.e. at 90% crystallisation). Removal of the CaO, MgO and FeO will produce a residuum saturated in topaz (Webster and Holloway, 1990).

The Fairbanks tin granites were produced by large degrees (85-90%) of crystal-liquid fractionation followed by vapour loss from magma producing F-enrichment in the residual magma: the F content of the W-related plutons and that of their biotite micas decreases with increase in differentiation index; those of the Sn-related plutons increase in almost exponential fashion. ('Ultrafractionation': Newberry et al., 1990). Vesiculation of an aqueous phase late in the consolidation of a magma has been recognised as an important process in concentration of F, Cl, B, Li, Rb, Cs and Sn-W-Mo (Eugster and Wilson, 1985).

The role of B in reduction of granite solidus and transport of Sn in a magma has been briefly discussed by Charoy (1982). Ryabchikov et al (1974) quote experimental data indicating that boron is capable of extracting Sn from melts, besides compounding the effect of fluorine on lowering of minimum melting point of granites. Experimental data show that the addition of a small amount of F to a granitic magma will quite dramatically lower the minimum liquidus composition and temperature. The plagioclase composition for minimum temperature melts will change from $Ab_{34}$to Ab_{58} with 4 wt% F in the system and the minimum liquidus temperature will fall from 730°C to 630°C at I kbar pressure (Manning, 1981). The shift in plagioclase composition toward albite is significant in consideration of the petrogenesis of the Thirtymile granites: the Li-mica topaz leucogranite has plagioclase of composition near the albite/oligoclase boundary; fluorine is visible modally as fluorite or topaz and evidence of much boron having been released by the Ork stock is found in the amount of axinite in the aureole and Li is obvious as the zinnwaldite mica. The facies therefore represents an extreme enrichment in those elements which lower the melting-point of a granite.

From this evidence it seems that it is possible to produce high-silica, albite-rich topaz granites (and the corresponding rhyolitic volcanics) simply by extreme fractionation of a low-Ca magma, without the requirement of a separate heat-source produced by intrusion of basic magma into the batholithic source region. This mechanism may only be capable of forming comparatively small volumes of these 'specialised' topaz granites, but if cupolas are developed above batholiths the amount of leucogranite generated is likely to be adequate to form the small stocks as found in Alaska and the southern Yukon.

Mineralogical arguments against the Cornubian-type alteration reactions having occurred in the Thirtymile magma to form the Li-mica topaz leucogranite are:

(1) Grainsize: the Li-mica facies is considerably finer-grained than the even-grained or megacrystic facies. It is impossible to envisage how smaller euhedral feldspars could form by such a process or even from remobilisation of an already crystal-laden melt;

(2) Feldspars are generally quite fresh, certainly not extensively sericitised;

(3) Muscovite is a rare alteration product in the Thirtymile facies,

(4) Topaz is quite common and interstitial to the feldspar in the Li-mica facies: it appears to have crystallised last, with the fluorite (after zinnwaldite);

(5) The magma forming this facies was quite mobile as is demonstrated by its intrusion as small sills and dykes that penetrate the country-rock for up to 1 km;

(6) The occurrence of quartz-zinnwaldite-topaz greisen in close-spaced veins ≤10 mm wide that cut the Li-mica facies in the SE corner of the Thirtymile stock does indicate that hydrothermal processes may produce zinnwaldite, but here not at the expense of the topaz and:

(7) Some trace element chemical trends of the Thirtymile granites differ from those of the Cornubian granites: although the HFSE (notably Nb) are concentrated with evolution of the biotite granite lithofacies, there is a sharp decrease in contents of this element through the Li-mica facies. Lehmann (1987) postulated that tin concentration in granites was due to change in distribution coefficient between that element and the granitic melt. Rapidly changing distribution coefficients of many elements are a feature of the models proposed in Newberry et. al. (1990).

It is entirely possible that the small amount of accessory topaz noted in the granites of the Seagull batholith might have arisen from hydrothermal alteration: there some sericitisation of the alkali feldspars is quite evident and minor Li-mica alteration of biotite may be seen.

It is here postulated that both mechanisms are likely in the production of F-Li-enriched granites: the ultrafractionation mechanism (Newberry et al., 1990) operating in the uppermost regions of plutons in a Cordilleran tectonic setting and the deeper Li-exchange metasomatism mechanism (Stone et. al., 1988) operating in large batholiths emplaced in a continental collision setting, where underplating of the crust by basic magma may occur under an extensional stress regime late in the orogenic cycle.

CHAPTER 5

SKARNS OF THE THIRTYMILE RANGE

CHAPTER 5: SKARNS OF THE THIRTYMILE RANGE

5.1 INTRODUCTION

5.1.1 TIN AND TUNGSTEN PROSPECTS

Tin-tungsten mineralisation in the Thirtymile Range is found entirely in skarns with proximity to the granite stocks. No wolframite- or cassiterite-quartz stockworks have yet been found. This chapter describes the two mineral prospects: 'Ork' and 'Mindy'. Much of the section will be concerned with the Mindy prospect, since this is the largest mineral prospect. It has been studied in detail by surface mapping, sampling and study of the sections of core that are preserved from nine diamond drill holes that were used for assessment work on the property in 1981. A total of 1025 metres was drilled and roughly a quarter of the core is preserved in usable form. All major skarn intervals, with the exception of wollastonite and a few massive garnet veins within the thick marble intersections, were available for study. Much of the intervening core of siliciclastic metasediments was unidentifiable. Company drill logs are available (Nebocat, 1981) and were of some use in identifying the unmineralised marble intersections.

5.1.2 TERMINOLOGY

Two terms will be used in this thesis to describe contact-metamorphosed carbonates that contain calc-silicate mineral assemblages: skarn and calc-silicate hornfels. The usage follows that common in the mining industry in North America. A skarn is any rock of calc-silicate or magnetite-rich mineral assemblage that has a grainsize easily visible in hand specimen, i.e. roughly ≥0.1 mm, and has resulted from thermal metamorphism/metasomatism of carbonate-rich sediments. Calc-silicate hornfels is used to describe a rock that is completely aphanitic in hand specimen. Often calc-silicate hornfelses (CSHF) are pink or green, reflecting garnet- or pyroxene-rich mineralogies. Since they are likely derived from siliceous, calcareous sediments or may be products of bimetasomatism (Kwak, 1987), the examples of this study may carry scapolite or even some wollastonite. The term is equivalent to the British 'calc-flinta'. CSHF can bear mineralisation, although it is rarely of the same tenor as in the coarser skarns.

5.2 THE ORK CONTACT

The creek exposure of the Ork stock {429235} reveals an amazingly sharp contact, as has been described in section (3.5.2). The transition from granite through skarn to marble can be observed over the length of a thin section. Toward the contact the last 10 mm of granite is composed mostly of plagioclase with fine purple fluorite i.e. is an endoskarn. Coarse vesuvianite exoskarn follows which contains some fluorite and a few sphene crystals. It was noted in hand specimen that some fine-grained (<<1 mm) minerals which fluoresce yellow under shortwave ultraviolet light were present. This would suggest that some of the sphene may be the malayaite variety (attempts at mineral separation from a powdered specimen were not successful). After approximately 15 mm thickness of vesuvianite a mineral that is brown and of turbid appearance in section is the last calc-silicate phase. In hand specimen it is a green-brown 6 mm thick resistant-weathering 'rind' that marks a sharp transition to unaltered marble. An X-ray powder diffractogram (Appendix D) was obtained and the mineral identified as cebollite: composition published as [$Ca_5Al_2(OH)_4Si_3O_{12}$], an alteration product of melilite (Winchell and Winchell, 1961). Unaltered white marble, commonly of 5 mm grainsize, continues up the creek section for hundreds of metres. In places decimetre-sized masses of bright pink calcic plagioclase are developed at the contact. Fig. 3.23 shows a slab of the entire contact. XRD data for the cebollite and plagioclase are presented in the appendix. Sn and W soil geochemical anomalies discovered in the region (Stephen, 1981) were never investigated.

5.3 THE MINDY PROSPECT

5.3.1 DISCOVERY AND DEVELOPMENTAL WORK ON THE MINDY DEPOSIT

During the 1972 to 1981 decade large prospecting programmes were carried out throughout the Canadian Cordillera by many companies searching for scheelite skarn deposits. Methodology was simple, being nothing more elaborate than the methods employed by prospectors since the Californian Gold Rush. The use of helicopters for rapid transport allowed large areas (often one or more 1:250,000 map sheets per season) to be sampled. However, since all information was proprietary, no results are publicly accessible. Typical methods employed were to collect a few kilogrammes of gravel of sand-sized active stream sediment and concentrate the heavy minerals by hand panning. Examination of dried concentrates under short-wave ultraviolet (U.V.) light allowed recognition of scheelite by its intense blue-white or cream coloured fluorescence, depending upon molybdenum content of the mineral.

The Mindy prospect was discovered as a tungsten prospect by the efforts of crews from Newmont Exploration of Canada Limited and the Ork prospect by JC Stephen Explorations Ltd. for the DC (DuPont-Cominco) Syndicate (Stephen and Mysyk, 1980; Campbell and Stephen, 1982). At the Mindy prospect the lower skarn horizon was found as magnetite-rich skarn float. Subsequent assays revealed significant tin content (T.N. Macauley, pers. comm.). Dr. D. Sinclair of the Geological Survey of Canada identified the borate minerals fluoborite, hülsite and vonsenite from such material.

Subsequent investigation of the Mindy Claims was as a tin prospect. A Maxmin II ground horizontal loop E.M. and magnetic survey was performed over a grid and float/exposure geology mapped (Limion, 1979; Nebocat, 1981). Nine BQ sized (36.5 mm diameter core) diamond holes were drilled in 1981 at angles from 50° to 90° to the horizontal. These holes penetrated the lower skarn horizon but did not intersect any igneous intrusion. Drilling was stopped as soon as the hole penetrated siliceous lithologies below the skarn/marble unit. Recent accurate surveying (this study) has shown that the drillholes did not penetrate (topographically) deeper than the northernmost carbonate/ skarn outcrop on the property, since all holes were collared on top of the Mindy plateau.

For the present study remapping of the Mindy prospect was performed (Appendices B.3 & B.4). It was obvious than neither the Newmont nor JC geologists had recognised the extent of cataclasis and small-scale faulting in the Thirtymile Range. Examination of the Newmont drill logs showed that the skarn intersections could not be interpreted as one continuous horizon. Mapping and drillhole layout by Newmont staff had relied on Brunton compass and tape for survey control, so reduced levels indicated on their plan were suspect. During the 1989 field season key exposures and recognisable drill collars were surveyed using theodolite tachymetry. A horizontal closure error of 1 part in 400 was obtained with vertical closure of 0.24 metres over the 1.48 km traverse. Reduced levels, which are referred to an assumed elevation for the Mindy tarn, are therefore accurate to a small fraction of a metre.

During the 1981 diamond drilling programme core from mineralised skarn intervals was shipped to Vancouver by Newmont and stored after being split for assay at the site. This material was subsequently kindly made available for study. All remaining core was stacked on the property. During the eight years between drilling and commencement of this study the local Marmots' appetite for plywood resulted in many core boxes being overturned and core markers lost, so the siliciclastic sequence between and above the skarns could not be continuously re-logged. All identifiable core, with the exception of DDH 7 which is entirely of siliciclastic metasediments, was recovered, flown to Whitehorse during the 1989 season and stored in the H.S. Bostock Core Library.

5.3.2 SURFACE GEOLOGY

SKARNS

Two significant skarn horizons crop out at the Mindy prospect (Fig. 5.1). The upper skarn is exposed at the base of the cliff at {152S, 137W}, 1989 grid. The metre-thick skarn consists of red garnet and olive green radiating crystals of vesuvianite up to 50 mm long (Fig. 5.1). The skarn becomes finer grained near the upper contact, grading to aphanitic green diopside hornfels within 15 cm of the overlying quartzite.The skarn is displaced by small extensional faults spaced every metre or two (Fig. 5.2). Apparent throws on these faults are from 10 to 80 cm.

The lower skarn/marble unit is exposed at the SW and NE extremities of the area

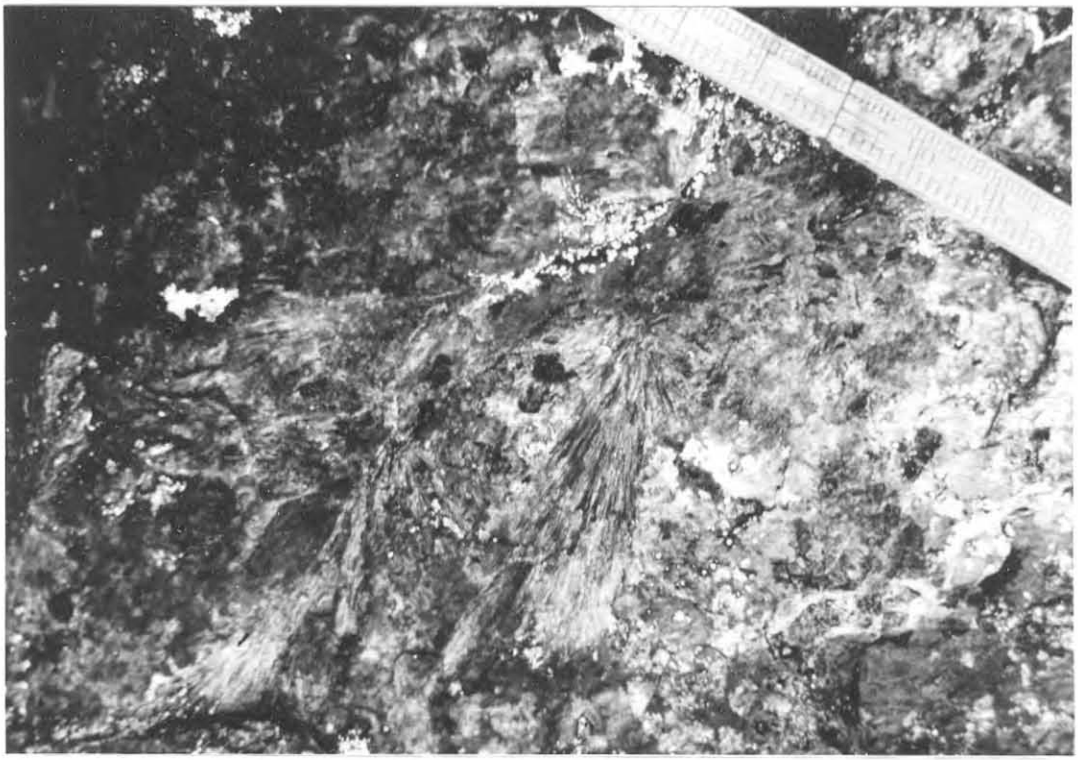

Figure 5.1 Mindy prospect: upper skarn exposure in cliff (see App. B.3) showing vesuvianite crystals up to 50 mm long. Ruler is divided in inches (i.e. ≈0.15 metres of rule is showing).

Figure 5.2 Mindy prospect: upper skarn exposure in cliff showing one of many small faults with apparent throws of ≤1 metre. Facing SE. Rule is opened to 18" (i.e. 0.46 metres). 1989 survey coordinates 150S, 140W (App. B.3).

mapped and appears as sporadic float between the two. At the southern end, around 1989 coordinates: {680S, 170W} three exposures give a vertical skarn thickness of 29 metres. The mineralogy is a massive 1-2 mm grainsize diopside-actinolite-calcite skarn containing some pyrrhotite. Thin section examination has shown frequent fluorite grains and chondrodite-humite series minerals. To the north this unit grades to magnetite-borate rich mineralogies as seen in float at {78S, 193W}. Massive magnetite and coarse (5 mm radiating crystals) ludwigite-vonsenite with smaller masses of greenish fluoborite may be seen in hand specimen. The northern extremity of the exposure of this unit {95N, 25W} is an outcrop of dark grey calc-silicate marble breccia.

Float of pyrrhotite-rich diopside skarn was noted to the NE of the mapped cliffs {UTM 465242}. This has been interpreted as continuation of the lower skarn as a downthrown block on the north side of the extensional fault (See 1:25,000 scale map, Appendix B.1; sections: App. B.4).

Figure 5.3 Mineralised fractures in drillcore: alizarin/ ferricyanide stained dolomitic marble from DDH 81-8, 87.90 m showing magnetite mineralisation and pyrrhotite vein in siliciclastic sediment with a distinct bleached selvedge from 81-4/ 14.58 m.

SILICICLASTIC METASEDIMENTS

Exposures on the cliff face above the upper skarn outcrop {1989 grid: 170S, 130W} show lenticular quartzite or chert phacoids up to 0.5 m long surrounded by biotite-rich pelite. Gently east dipping iron-stained pressure-solution cleavage may be seen in the quartzite. Steeply-dipping fractures carrying weathered sulphide (pyrrhotite?) are common at this locality. Disturbance of the outcrop by frost wedging prevents accurate measurement, but angles of the bounding faces of blocks indicate that strike of these veins is variable. Such veins are likely of the same nature as those sulphide bearing veins with bleached selvedges noted in fresh drill core (Fig. 5.3). A strong cleavage is also evident at the north end of the cliff {70S, 25W}: see Appendix B.3.

5.3.3 STRUCTURAL INTERPRETATION FROM DRILL LOGS

The structure of the skarn/marble unit at the Mindy prospect has been interpreted from surface and drillhole data as a gently easterly dipping, boudinaged tectonic unit (Appendix B.4). Where vertical holes are projected onto the plane of the longitudinal section, the distance projected is shown and points of intersection of inclined holes with this section plane are indicated by circles. Projection distances of the top and bottom of the skarn unit are also indicated.

Mapping at 1:25,000 scale and interpretation of 1:2000 scale mapping and drill logs has shown the existence of an ENE striking extensional fault system adjacent to the prospect. Parallel minor structures have been interpreted using drill logs. The fault system is considered to have played an important role in circulation of mineralising fluids and proximity to the fault system would have a major control on skarn chemistry. Three extensional faults are postulated to allow correlation of the lower skarn horizon between adjacent drillholes. A fourth fault, the projection of the main ESE trending fault zone for the ridge to the west, is also shown. Throw on this fault has been estimated by correlating pyrrhotite skarn float found further down the Mindy cirque (off the detailed map) with the main horizon. Considerable change in thickness of the marble/skarn unit is evident. According to the logs of Nebocat (1982) and an examination of core from DDH 7, which was complete, the skarn is absent at this position. Rapid change of thickness and discontinuity of the unit is interpreted in this study as due to mega-boudinage.

5.3.4 MINERALOGY AND TEXTURE OF THE SKARNS

SURFACE EXPOSURES

Exposure of the skarn/marble units is limited to the extreme southern and northern ends of the main (lower) unit, with some sporadic float in the central region. Surface exposures show mineralogies that vary from diopside-actinolite-pyrrhotite-scheelite to magnetite-vonsenite- fluoborite to calc-silicate marble along the strike of the main skarn horizon (section Appendix B.3).

Surface exposures form the southern limit of the known skarn. At {670S, 180W} (1989 Coords.) 28.8 vertical metres of skarn are exposed. Nebocat (1982) reports significant amounts of scheelite at this outcrop, quoting an assay giving >0.3% WO_3 over 15m. No tin minerals are identified from this exposure although sampling was sporadic due to extreme hardness of the rock. Examination of thin sections shows that the rock is composed of subhedral hedenbergite, chondrodite-humite series minerals with masses of actinolite crystals (replacing the former) and interstitial fluorite. Pyrrhotite content is very variable. An analysis of the hedenbergite (average of 29 microprobe determinations) is shown in Table 5.1.

	SiO_2	CaO	MgO	FeO	MnO	Total
Hedenbergite	47.56	22.90	0.00	24.73	4.79	99.98

Analysis by microprobe of pyroxene in skarn from Mindy {670S, 180W}.

	SiO_2	CaO	MgO	FeO	MnO	Total
Diopside	59.52	17.43	23.87	-	-	100.82
Andradite	38.11	34.40	-	27.84	0.44	100.79

Microprobe analyses of skarn minerals for surface specimen 270N, 285W

Table 5.1 Electron microprobe analyses of Mindy surface specimens

Float specimens in the northern part of the prospect at {80S, 195W} i.e. Newmont grid {685N, 290W}, have remnant diopside with minor garnet which has been replaced by fluoborite and szaibelyite. Bands of massive magnetite and vonsenite

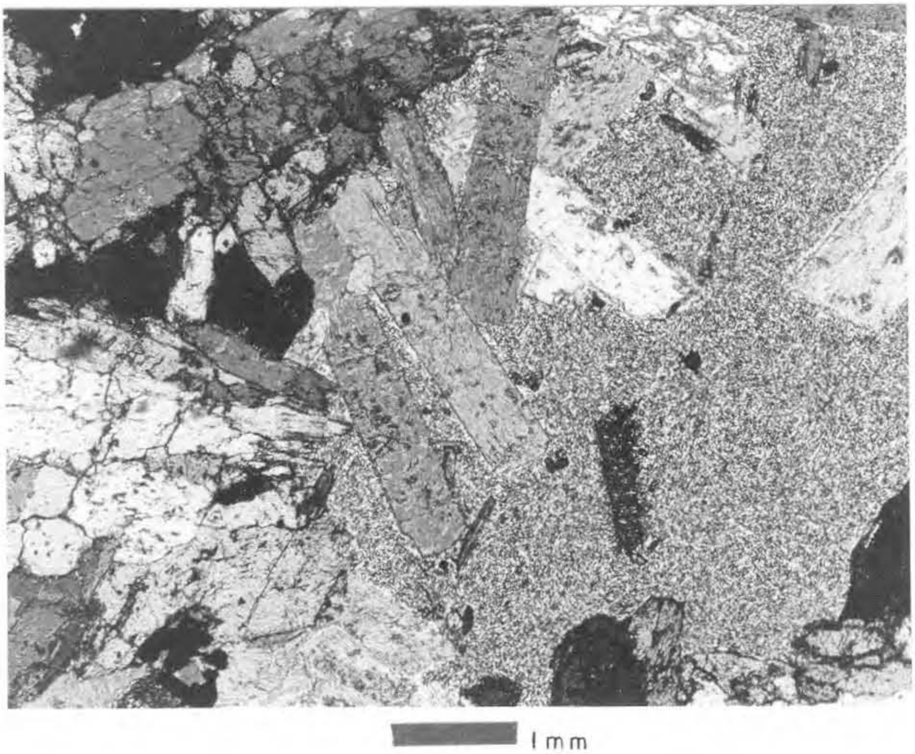

Figure 5.4 Borate & hydrous alteration: photomicrograph under crossed polarisers of diopside skarn replaced by fluoborite (prismatic crystals) and serpentine. Mindy surface specimen 670N, 285W (Newmont grid coordinates).

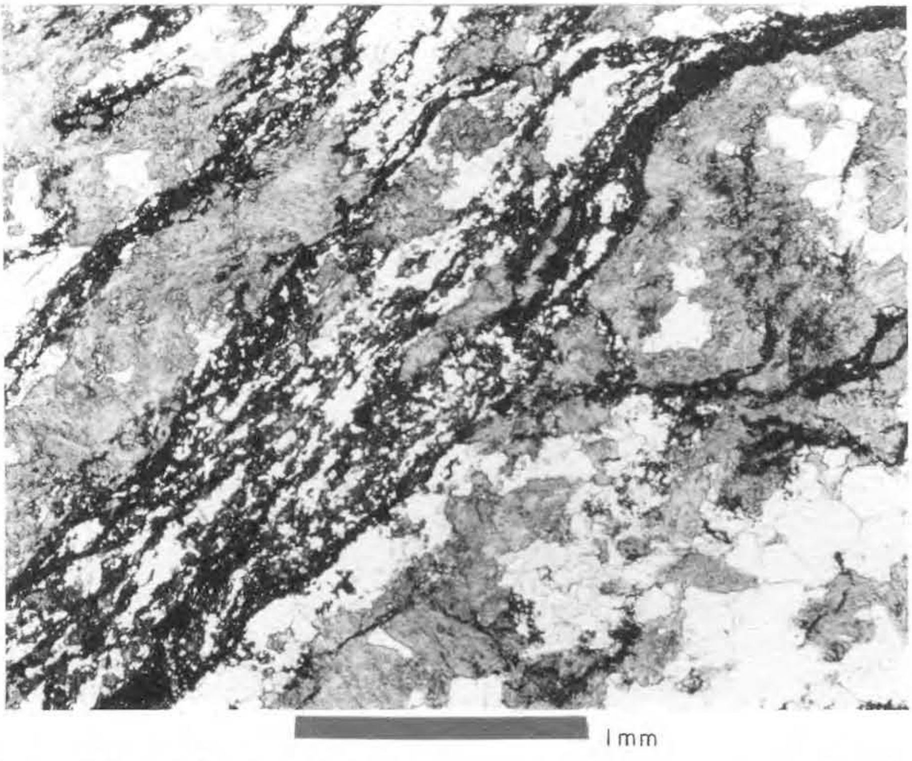

Figure 5.5 Calc-silicate marble showing relict pressure-solution fabric. Mindy surface 920N, 165W (Newmont grid). Photomicrograph under plain polarised light (Epidote/chlorite/opaques/carbonate).

≥0.2m thick cut the pyroxene. Microprobe analysis indicates that the pyroxene is pure diopside and the garnet andradite.

The diopside has very obviously been replaced by fluoborite: euhedral crystals of the pyroxene have ragged ends where they project into a mass of fluoborite (Fig. 5.4). From an adjacent locality {82S, 203W}, or Newmont coordinates {685N 290W} float of pelite was noted which bears a strong pressure-solution fabric and contains clasts of carbonate around 8 mm long and carbonate layers to 7 mm thick. This grades to a coarse chlorite-calcite-epidote skarn with some very ragged remnant diopside grains up to 1.5 mm long. This material represents the lower contact of the marble/skarn unit.

At {107N, 19W} or Newmont {95N, 25W} a prominent outcrop of black impure marble containing 20x50 mm clasts of quartzite and showing a strong pressure-solution cleavage dipping easterly at 9° is found overlying pelite. The marble also displays a pressure-solution cleavage which is marked by opaque minerals. Coarse calcite grains (2 mm) alternate with chlorite and fine quartz layers (Fig. 5.5).

DIAMOND DRILL CORE

Diamond drilling performed by Newmont has provided complete sections through the main skarn in three holes (DDHs 1, 2, 3) and, due to lack of preservation of core, sections through skarn and partial marble sections in holes 4, 5B, 6 and 8. Sections are shown in Appendix B.4, graphic logs in Appendices 2.5-10, and sketches of mineral textures in Figs. 6.6 to 6.8. Logging of the core shows that major borate-rich skarn intervals are developed in the northern part of the property where thickness varies from 16 to 40 metres (holes 1 to 3). This location is likely influenced by the proximity of the E-W striking extensional fault system (Section 3-3-5).

The skarns may be broadly grouped into the following types:

(1) Massive diopside-hedenbergite skarn: Subhedral pyroxene with a little calcite or quartz remaining and minor quantities of the chondrodite-clinohumite group minerals.

(2) Garnet-vesuvianite skarn with varying amounts of pyroxene present.

(3) Banded pyrrhotite skarn: 1 mm thick pyrrhotite bands alternating with pyroxene, clinohumite group minerals and often fluorite.

(4) Wrigglite: finely laminated, intricately convoluted magnetite-fluorite rich skarns with varying amounts of pyrrhotite also present. These carry both oxide and borate tin

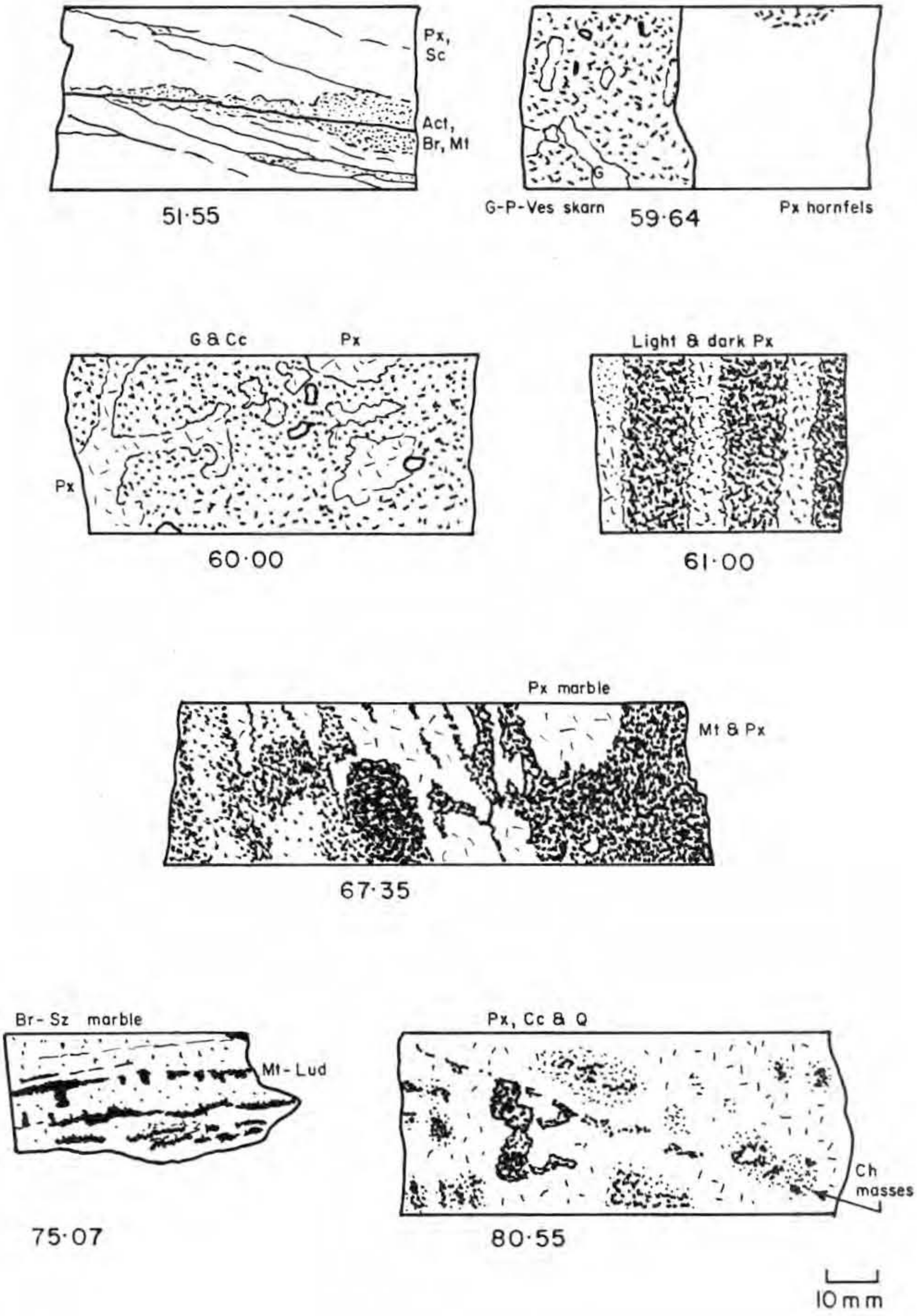

Br = brucite
Act = actinolite
Ch = chlorite
Lud = ludwigite
Px = diopside-hedenbergite

Cc = calcite
G = garnet
Mt = magnetite
Sz = szaibelyite
Sc = scapolite

Ves = vesuvianite

SKETCHES OF SPLIT DIAMOND DRILL CORE. DDH 81-3

FIG. 5·6

T. Liverton June 1991

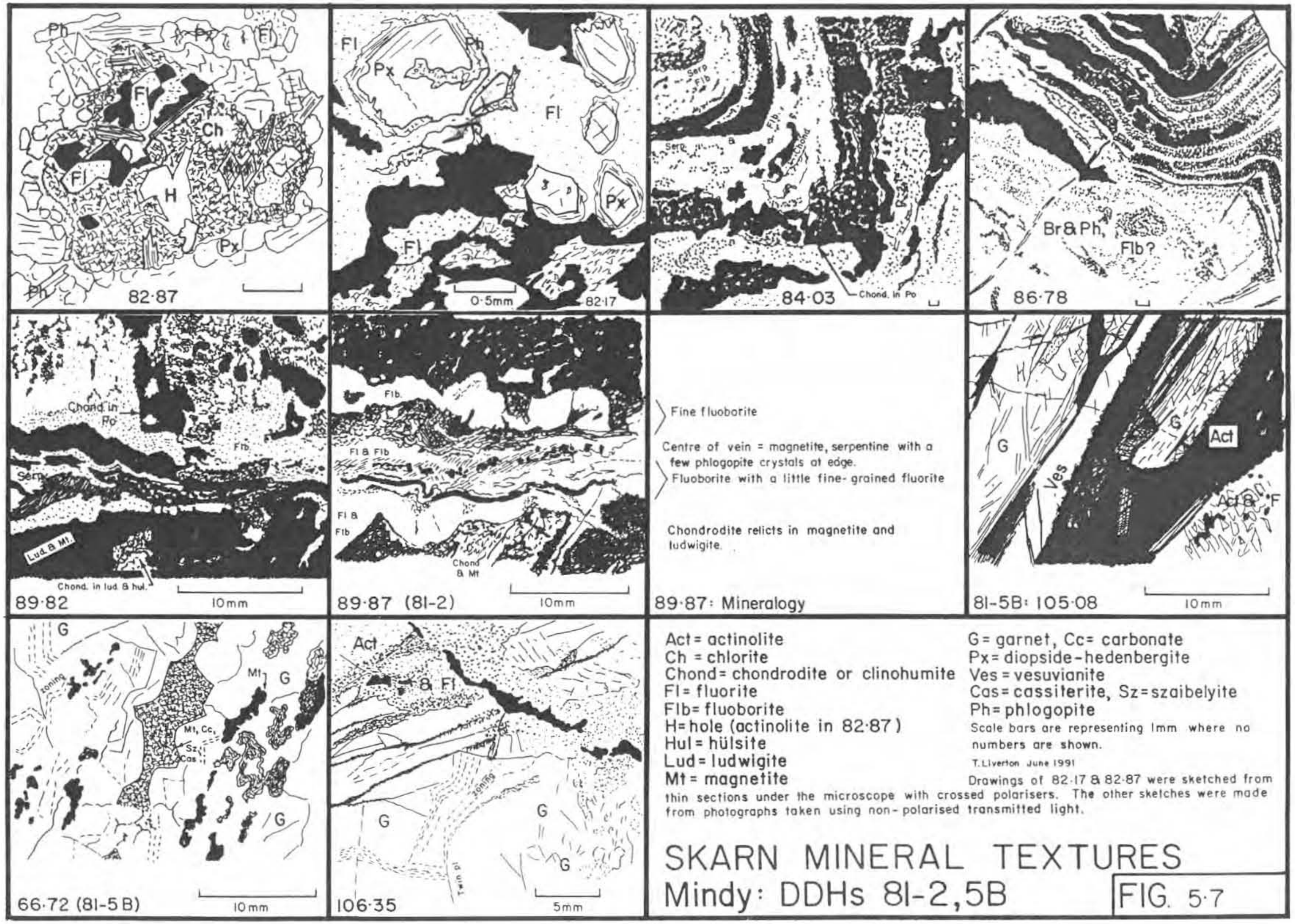

Fine fluoborite

Centre of vein = magnetite, serpentine with a few phlogopite crystals at edge.

Fluoborite with a little fine-grained fluorite

Chondrodite relicts in magnetite and ludwigite.

Act = actinolite
Ch = chlorite
Chond = chondrodite or clinohumite
Fl = fluorite
Flb = fluoborite
H = hole (actinolite in 82·87)
Hul = hülsite
Lud = ludwigite
Mt = magnetite
G = garnet, Cc = carbonate
Px = diopside-hedenbergite
Ves = vesuvianite
Cas = cassiterite, Sz = szaibelyite
Ph = phlogopite

Scale bars are representing 1mm where no numbers are shown.

T. Liverton June 1991

Drawings of 82·17 & 82·87 were sketched from thin sections under the microscope with crossed polarisers. The other sketches were made from photographs taken using non-polarised transmitted light.

SKARN MINERAL TEXTURES
Mindy: DDHs 81-2,5B

FIG. 5·7

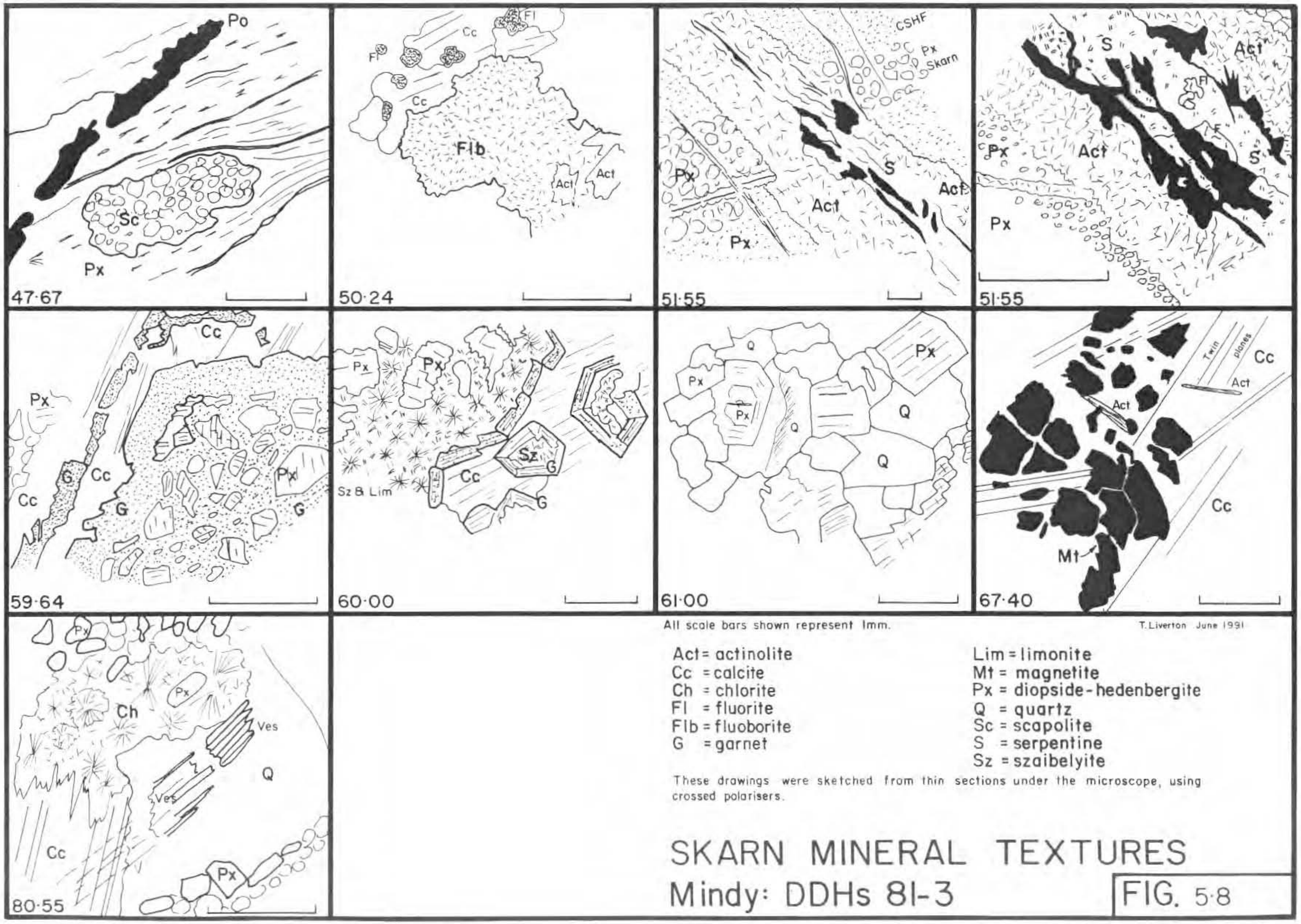

All scale bars shown represent 1mm.

T. Liverton June 1991

Act = actinolite
Cc = calcite
Ch = chlorite
Fl = fluorite
Flb = fluoborite
G = garnet

Lim = limonite
Mt = magnetite
Px = diopside-hedenbergite
Q = quartz
Sc = scapolite
S = serpentine
Sz = szaibelyite

These drawings were sketched from thin sections under the microscope, using crossed polarisers.

SKARN MINERAL TEXTURES
Mindy: DDHs 81-3

FIG. 5·8

mineralisation.

(5) Retrograde skarns: actinolite, chlorite or phengite minerals developed along fracture systems in the preceding types.

(6) Vein skarns: predominantly wollastonite or green andradite skarn (never together) in pure marble.

INTERSECTIONS WHERE MARBLE PREDOMINATES

In the central portion of the prospect (holes 4 to 8) a greater thickness of marble and skarn is present (>60 m), with white calcite marble predominating. Skarn is developed near the margins of the marble body and as irregular wollastonite layers, which transgress the faint pressure- solution fabric (where visible) of the marble by up to 40° and also follow smaller irregular fractures that dip from 45° to 70° to the horizontal (App. B.8a: sketch 81-4, 101.20). Andradite vein skarns with crystals up to 20 mm across are found within the marble, but are mostly only in the order of 20 cm thick (Figs. 5.9, 10).

GENERAL MINERALOGY: NORTHERN SKARNS DDHs 1 to 3

Silicate skarn developed at the northern end of the property is predominantly of diopside-hedenbergite. The contact with overlying siliceous sediments is usually marked by a varying thickness (decimetres to several metres) of aphanitic green or pink calc-silicate hornfels, which consists primarily of diopside-hedenbergite, with occasional scapolite augen or crystals and garnet layers. In the coarse skarns calcite may remain in minor quantities and varying amounts of pyrrhotite appear, together with rare chalcopyrite, often as alternating layers of silicate and sulphide. The maximum amount of pyrrhotite is present at 81-1, 76.52 m, where perfectly euhedral diopside is enclosed in pyrrhotite. This particular texture can only be readily explained by the hypothesis of pyroxene having been formed by replacement of dolomitic marble, with later total replacement of remaining carbonate by the sulphide. Very minor amounts of pyrite and chalcopyrite been noted associated with pyrrhotite.

Vesuvianite is found as massive coarse (often 5 mm) crystals in layers that alternate with the diopside. Often a little andradite is present with the vesuvianite, the usual paragenesis being garnet replaced by vesuvianite. Forsterite or chondrodite/humite group minerals are seen only occasionally, in massive skarn or with magnetite (81-3,

Figure 5.9 Mindy vein skarn: DDH 81-8, 59.4 m, sawn and polished core showing green andradite crystal with fine-grained honey-coloured garnet containing arsenopyrite crystals. Scale division is 5 mm.

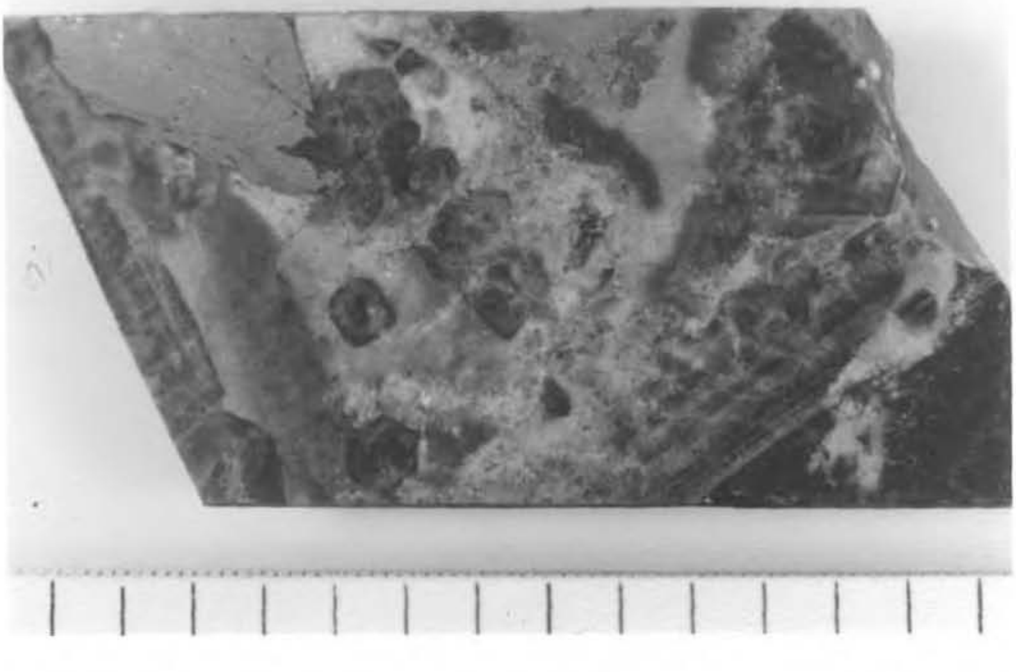

Figure 5.10 Vein skarn: DDH 81-8, 83.36 m, sawn and polished core showing zoned green and brown andradite with calcite, diopside (pale green) and arsenopyrite. 5 mm scale division.

60.50; and Fig. 5.11). Fluorite usually accompanies the latter minerals. Actinolite is found as irregular masses within the diopside skarn, most often associated with interstitial fluorite. Often it can be seen to replace early skarn minerals along closely-spaced fractures. Chlorite is not plentiful in this deposit but is seen to replace amphibole, particularly along fractures. Magnetite and the borate minerals, vonsenite and hülsite, which are occasionally associated with cassiterite and rare nordenskiöldine (see Fig. 5.12) form irregular layers replacing earlier diopside. Where fluoborite is present it either replaces diopside and pyrrhotite interstitially, or where large quantities occur, it forms 'wrigglite' (Kwak and Askins, 1981). The 'wrigglite' is a very finely banded (often ≤1 mm layers) magnetite-vonsenite±hülsite-fluorite-phlogopite-fluoborite rock that shows most intricate and disharmonic convolutions (Figs. 5.13 & 14).

MINERAL FORMULA			**REFERENCE**
Fluoborite		$Mg_3(F,OH)3BO_3$	Winchell and Winchell (1961)
Szaibelyite		$2MgO.B_2O_3.H_2O$	Watanabe (1953)
Warwickite		$(Mg,Fe)_3 TiB_2O_8$	Watanabe (1954)
Ludwigite		$(Mg,Fe)_2Fe^{3+}BO_5$	Bonazzi and Mencetti (1989)
Hülsite	from	$Mg_2(Fe^{3+},Sn^{4+})BO_5$	Kwak (1987)
"	to	$Fe^{2+}(Fe^{3+},Sn^{4+})BO_5$	Kwak (1987)
Malayaite		$CaSnSiO_5$	Kwak (1987)
Nordenskiöldine		$CaSnB_2O_6$	Kwak (1987)
Bandylite		$CuClBO_2.2H_2O$	Winchell and Winchell (1961)
Hydrochlorborite		$Ca_4B_8O_{15}Cl_2.21H_2O$	Bayliss et al., (1986)

Table 5.2 Rare skarn minerals at Mindy

CENTRAL MARBLE AND SKARNS

Massive white calcite marble predominates in the region of drillholes 4, 5 and 8 it is cut by irregular vein skarns of wollastonite, decimetres thick; millimetre-scale talc, brucite or serpentine veins and rare ≤1 mm veins of ludwigite mineralisation (81-8 87.90). Grainsize of the marble varies from under 1 mm to around 6 mm maximum. The marble is largely structureless, but occasional sections do retain evidence of brecciation of the original limestone (see following sections). In this central section some minor diopside or garnet skarns are found within the marble, but the prominent mineralised interval occurs at its base. Both magnetite- and pyrrhotite-rich skarn, bearing ludwigite and hülsite mineralisation is found within massive garnet skarn. Two generations of garnet are evident at some intervals: at 81-8, 59.4 m (Figs. 5.9 and 5.10) euhedral zoned green garnet is fractured and enclosed by light brown massive garnet containing arsenopyrite crystals 6 mm long. Some of the brecciation, however, has occurred during contact metamorphism: one likely example is at 81-4, 101.20, where sharp fractures cut the marble at low angles to the core (vertical) and wollastonite has formed along a fracture.

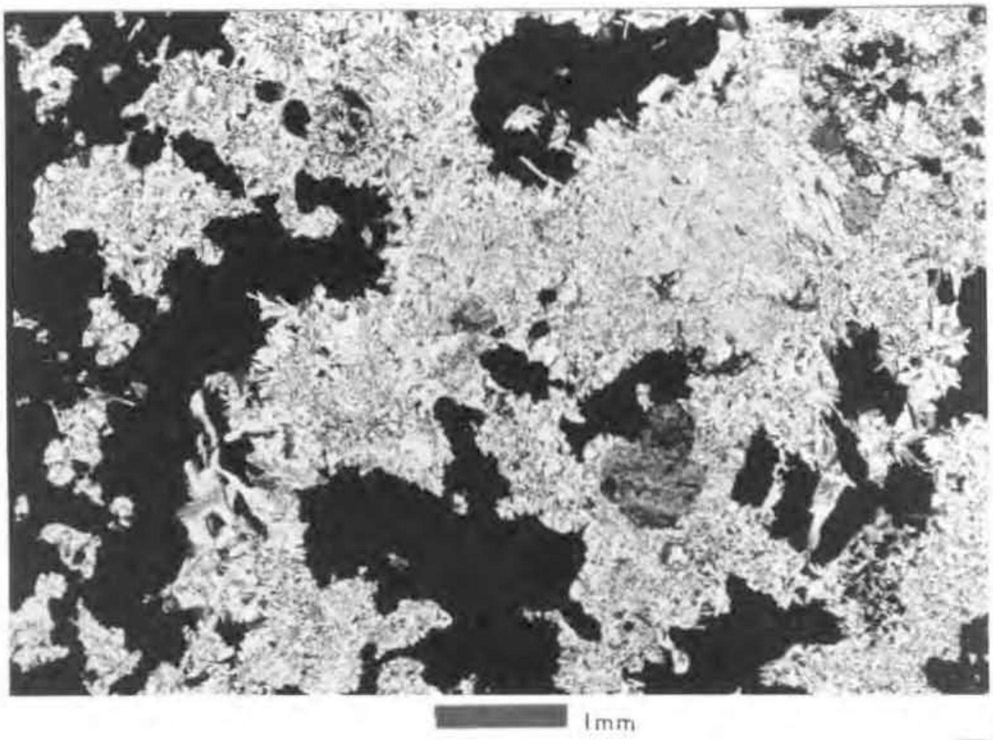

Figure 5.11 Mindy prospect wrigglite: DDH 2, 92.84 m. Thin section under crossed polarisers shows chondrodite-humite group mineral relicts in phlogopite-fluorite-magnetite 'wrigglite' greisen-skarn.

5.3.5 MINOR OCCURRENCES OF UNUSUAL OR RARE MINERALS

Several unusual minerals have been encountered during the study of the Mindy skarns:

(1) HYDROCHLORBORITE: identification is on the basis of XRD powder patterns. It is a pale green biaxial mineral occurring with fluorite in veins 2-3 mm wide has been noted in DDH 81-2 at 97.44 metres. Pleochroism is from pale green to colourless and it occurs in a prismatic habit which shows a good cleavage (Fig. 5.16). X-ray powder diffraction data has been obtained, using both 114.59 mm Ø Gandolfi and Phillips type Debye-Scherrer cameras from a small amount of the mineral that was carefully excavated from a thin section. Diffraction data are presented in Appendix D.

(2) BANDYLITE: one occurrence, identification is on the basis of optical properties. The mineral is possibly too fine-grained for good separation and X-ray diffraction. It has been recognised only in DDH 81-4 at 148.50 metres depth. It occurs as tiny anhedral grains entirely enclosed in ferrophengite. Its optical properties are quite striking: it is pleochroic from indigo blue to colourless.

(3) WARWICKITE: one occurrence, identification is optical, by comparison with material from Hol Kol (see Watanabe, 1954). Warwickite has been noted at one interval only (DDH 3, 75.07-75.14).

Thin sections from the Hol Kol, Korea material of Professor Watanabe (Watanabe, 1954) from the Harker collection, Cambridge, were lent for comparison by Dr. S.O. Agrell. The mineral is found around the margin of ≤1 mm wide magnetite veins in marble that has been heavily replaced by szaibelyite.

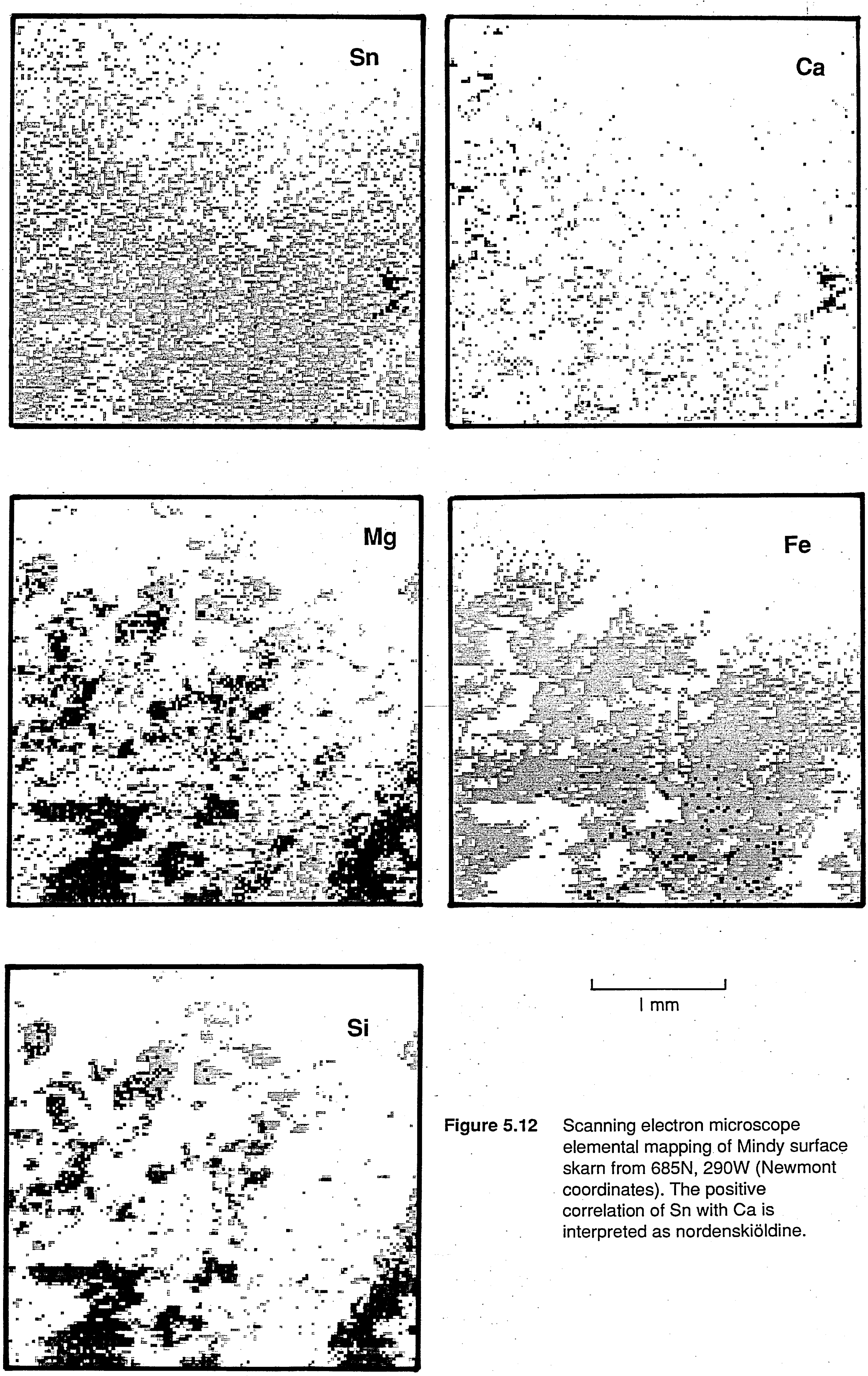

Figure 5.12 Scanning electron microscope elemental mapping of Mindy surface skarn from 685N, 290W (Newmont coordinates). The positive correlation of Sn with Ca is interpreted as nordenskiöldine.

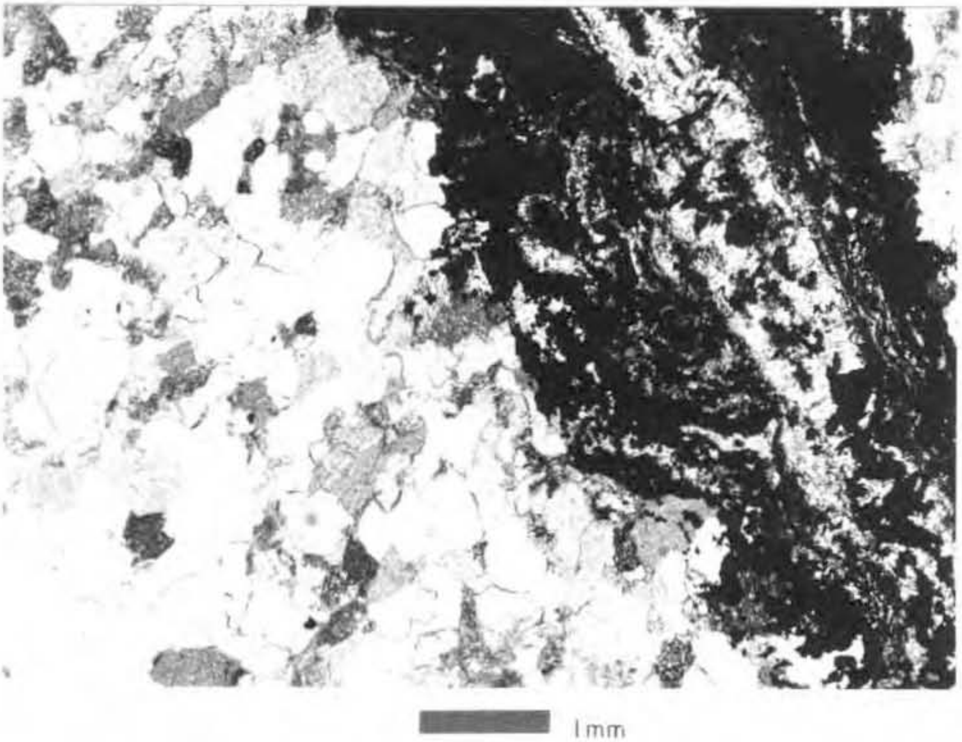

Figure 5.13 Wrigglite: DDH 81-8, 90.02 m. Finely banded magnetite vein with a fluorite-phengite core in marble. Thin section under crossed polarisers.

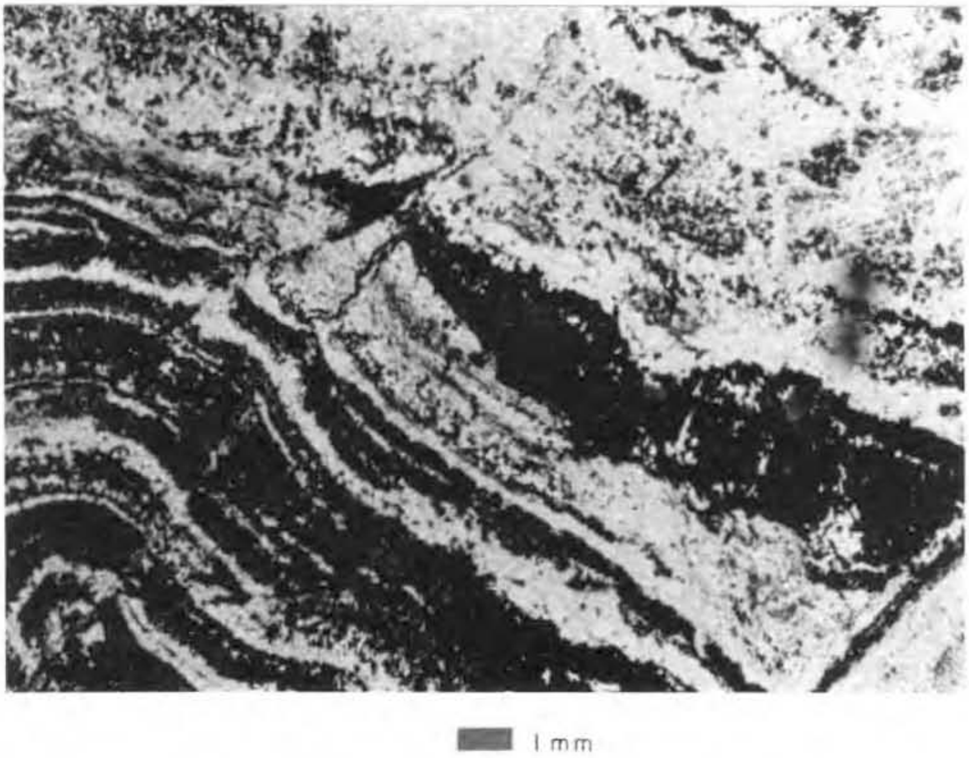

Figure 5.14 Magnetite-talc-fluoborite wrigglite with late fractures: DDH 81-2, 86.78 m. Thin section under plain polarised light.

(4) **FERROPHENGITE**: identification is definite from microprobe analysis, optics and XRD powder patterns. Although this mineral is not especially rare, it is a particularly Fe-rich variety (c.f. Deer et al., 1963 V.3), which is occasionally seen in the wrigglite. At 81-5B, 106.75 it is found in the fluorite bands adjacent to warwickite which rims euhedral magnetite. It also occurs along fractures. At 81-4, 148.50, the wrigglite contains a phengite which encloses crystals of the rare copper borate/chloride bandylite. It occurs as euhedral crystals whose hexagonal basal sections (around 0.2 mm size) are prominently zoned (Fig. 5.15), or in prismatic sections which show zoning in an 'hourglass' pattern. Pleochroism from deep green to almost colourless is striking. Basal sections give a uniaxial (-) interference figure. Microprobe analysis of this mineral is shown below.

SiO_2	CaO	FeO	MnO	Al_2O_3	K_2O	Na_2O	TOTAL
37.21	0.13	29.37	2.17	18.39	9.09	0.29	96.64

Table 5.3 Microprobe analysis (mean of 8 determinations) of ferrophengite from DDH 81-5B 106.75 m.

(5) FERROAN CLINOCHLORE: veins (0.5 mm wide) have been noted in hand specimen of core at 81-8, 93.21m. This green mineral is so brilliantly coloured that it was originally mistaken for dioptase. X-ray diffraction data is presented in Appendix D.

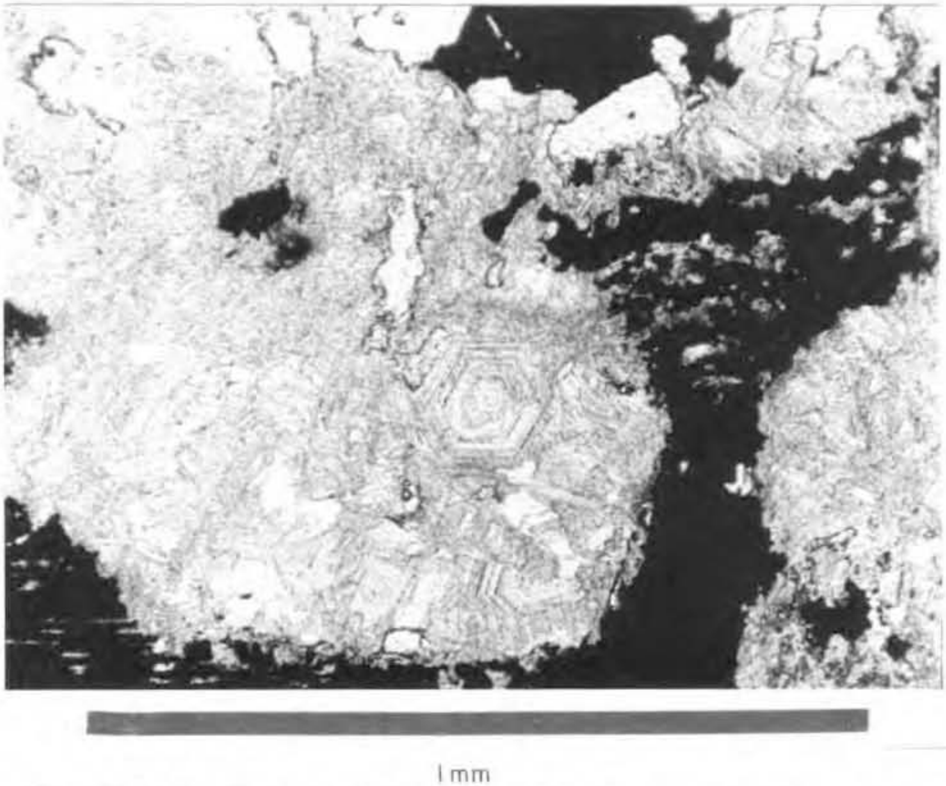

Figure 5.15 Skarn minerals: ferrophengite with magnetite and fluorite in wrigglite. Thin section under plain polarised light showing the striking zoning in this mineral.

Figure 5.16 Rare mineral: thin section from DDH 81-2, 97.44 m under crossed polarisers showing a vein of hydrochlorborite (magenta interference colours) in corroded diopside-hedenbergite.

5.3.6 FRACTURING OF MARBLE AND SKARNS

Evidence of two episodes of brecciation and fracturing in the marble/skarn unit is found:

(1) BRECCIATION OF MARBLE: THRUST-RELATED

Brecciation of dolomitic carbonates representing original cataclasis of the carbonate unit during imbrication of the Thirtymile allochthon has been preserved in calc-silicate mineral assemblages, particularly at 81-3, 64.3-66.2 m (Figs. 5.17, 18). Brecciation of the original limestone (81-4, 137.47; 81-8, 58.5 m) is visible once the core is stained with alizarin/ferricyanide. Other sections show equidimensional clasts of calcite marble enclosed in diopside-andradite skarn, as in 81-4, 133.2 m, the interval 131.5 to 133.55 m, where white calcite marble clasts with subrounded form and approximately 20 cm across are found surrounded by fine-grained diopside hornfels showing irregular foliation which is defined by yellow garnet layers curving around the clasts. Other layers are wollastonite-rich and masses of green andradite several centimetres across may be seen. The texture of this rock is very similar to that seen in sheared marble breccia from the Ork area, where clasts of calcite marble (showing distinct calcite pressure-solution 'tails') are found in diopside hornfels (Fig. 5.17). See also 81-8, 85.04 m (Fig. 5.18). Such examples of brecciation are likely to be remnants of cataclasis of the carbonate unit synchronous with that of the enclosing siliciclastic sediments. It is concluded that such mineralogy reflects original chemistry of the marble breccia, the diopside skarn having replaced the dolomitic matrix of the breccia. Two intervals of core were observed where lenticular clasts of chert are enclosed in marble: 81-8, 58.52 m and 81-8, 87.78. In the latter example a selvedge of actinolite up to 10 mm wide has formed as a 'bimetasomatic skarn' (c.f. Kwak, 1987) around the clast (Fig. 5.18). The calc-silicate hornfelses occasionally show pressure-solution cleavage and C-S fabric that are preserved in silicate minerals (Fig. 5.19 a &b). In this particular case use of the prevailing dip direction of the pressure-solution cleavage to obtain a rough orientation of the vertical core yields a top-to-east sense of shear, which is in agreement with the vergence of the thrust-stack.

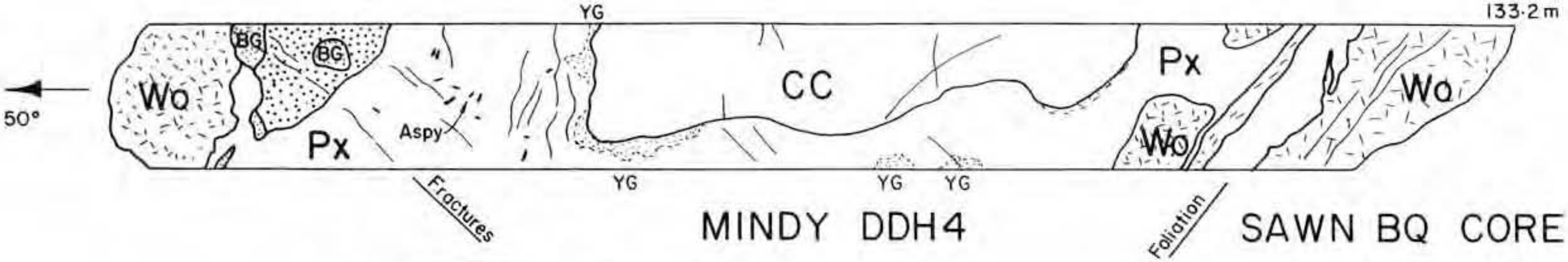

MINDY DDH4

SAWN BQ CORE

36·5mm diameter.

CC= Calcite
Px = Pyroxene
Bg = Brown garnet
G = Green (andradite) garnet
YG= Yellow garnet
Aspy= Arsenopyrite

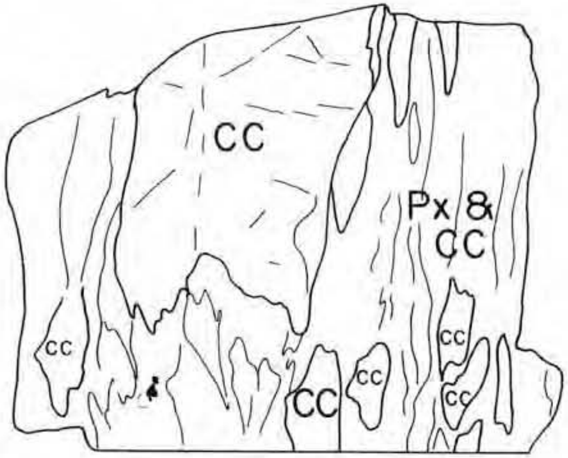

ORK AREA 424235

0 100
mm

POLISHED SLAB

COMPARISON OF CATACLASTIC TEXTURE IN BRECCIATED, SHEARED MARBLE AT THE ORK AUREOLE WITH SKARN FROM THE MINDY PROSPECT.

T.Liverton, March 1990

Fig. 5·17

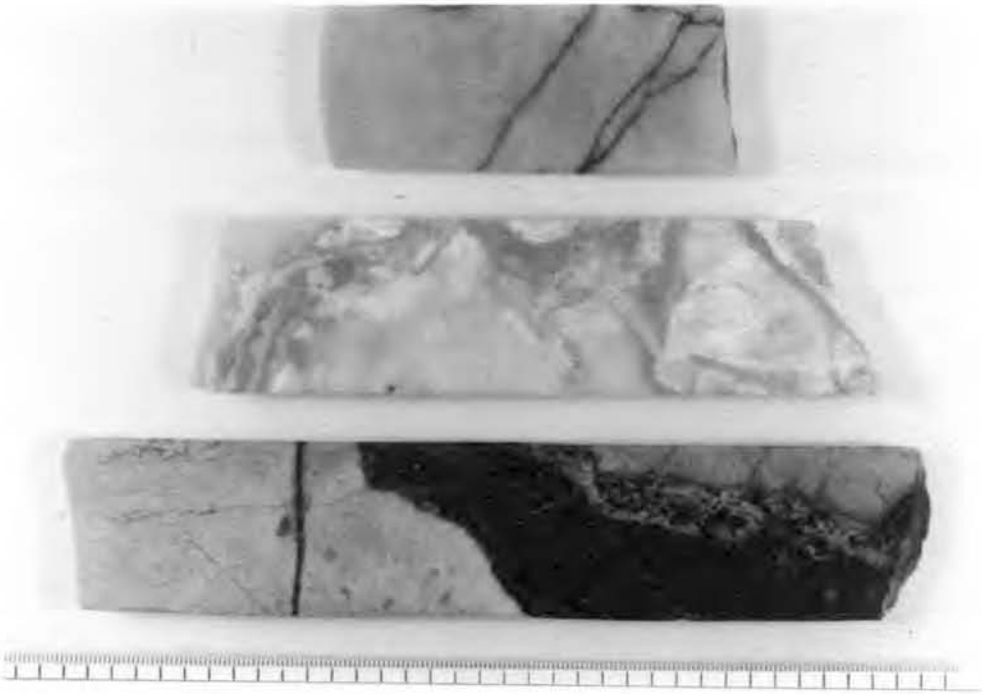

Figure 5.18 Mindy marbles: alizarin/ferrocyanide stained, sawn core from DDH 81-8, 50.81 m showing calcite marble with magnetite veins; 85.04 m showing dolomite breccia partially replaced by diopside (green) and 87.78 m, a clast of chert (dark) in marble with a bimetasomatic amphibole skarn developed around its margin. Coarse scale division 5 mm.

(2) FRACTURING: RELATED TO EXTENSIONAL FAULTING AND CRYSTALLISATION OF THE GRANITE BELOW

Fracturing and comminution of early formed diopside or andradite-vesuvianite skarns may be observed. Some pyroxene skarns have been fractured and show zones of brecciation over centimetre-scale widths. Evidence of fracturing of marble and primary skarns which has allowed either retrograde contact metamorphism or replacement by sulphide or fluoride/borate mineralisation is also common.

Examples from thin sections of the drill core are: 81-3, 47.67 m- where aphanitic diopside hornfels is cut by irregular pyrrhotite mineralised fractures which dip at 70° (Fig. 5.19b). The steeply-dipping (skarn-related) pyrrhotite vein clearly cuts the early formed calc-silicate assemblages. At 48.33 m the fractures carry hydrochlorborite. Immediately below the veined skarn (especially at 64.60m) brecciation is obvious in hand

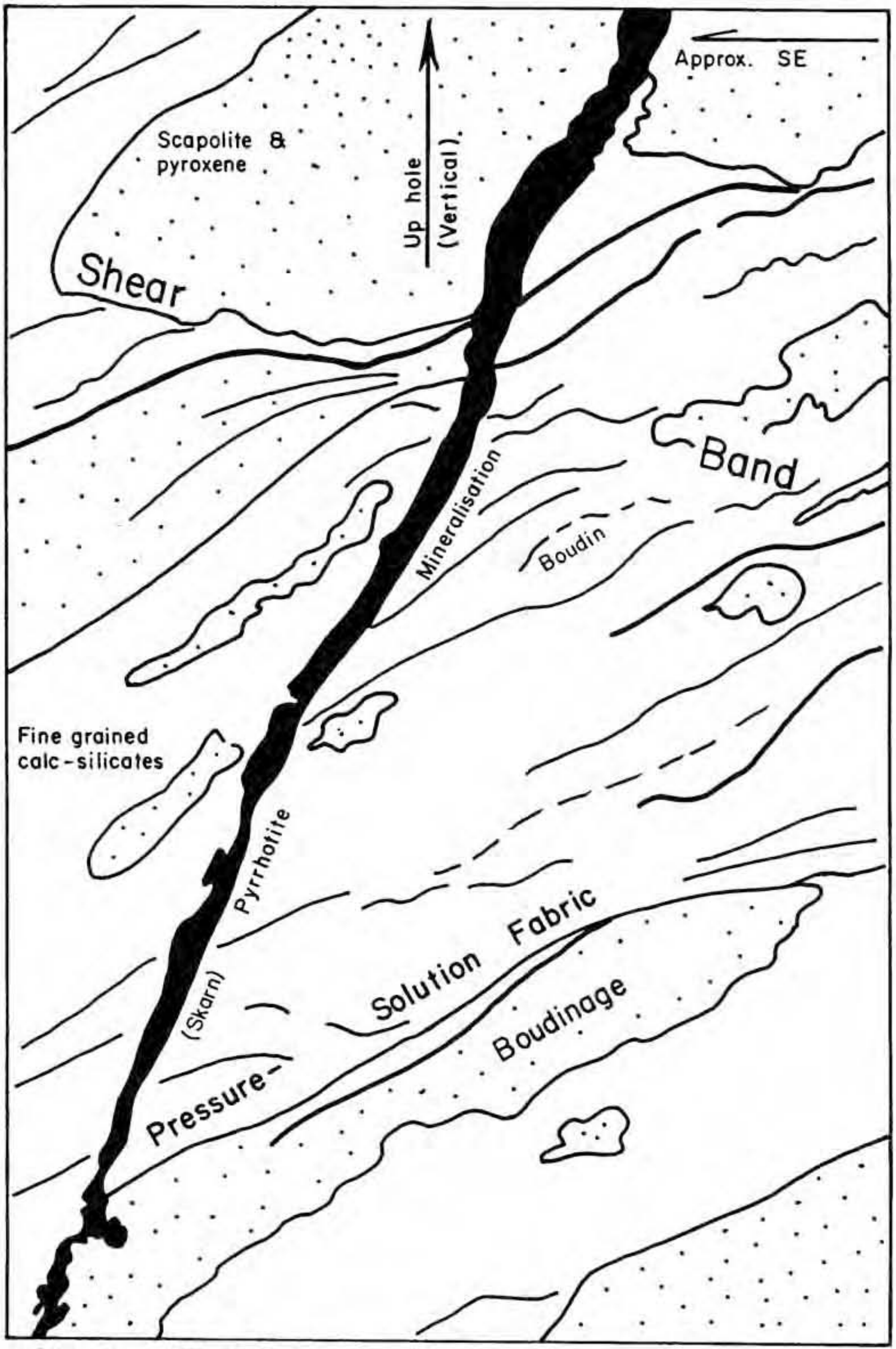

81-3, 47·67 m

Calc-silicate hornfels showing preservation of C-S fabric and a cross-cutting sulphide vein.

Thin section photographed in transmitted light.

FIG. 5·19a

Figure 5.19b Scapolite is concentrated in the porphyroclasts and diopside in the fine-grained matrix. The core is vertical and the section faces approximately SE, hence a top-to-the- east shear sense is indicated. The opaque vein is skarn-related pyrrhotite mineralisation.

specimen. Clasts of aphanitic diopside-hedenbergite hornfels are found in a matrix of pyroxene skarn.

Marble is fractured by many tiny near-vertical veins which bear fluorite, fluoborite and ludwigite in DDH 81-8 at 90.02 m. Fracturing and mineralisation are frequently evident Appendix B.10).

In DDH 81-5B at 106.35 m garnet is much fractured and at 105.08 garnet-vesuvianite skarn is cut by many subparallel fractures which introduce first actinolite and later serpentine (Appendix B.9). Retrograde assemblages are introduced along fractures also at 108.10 m. Later B-F metasomatic skarns are also brecciated and fractured: 81-2 89.82 shows two generations of chlorite introduced along fractures which cut magnetite-fluorite skarn with relict clinohumite; scheelite is found in the veins at this interval and in DDH 81-2 at 86.78 wrigglite is obviously fractured (Fig. 5.14, Appendix B.6).

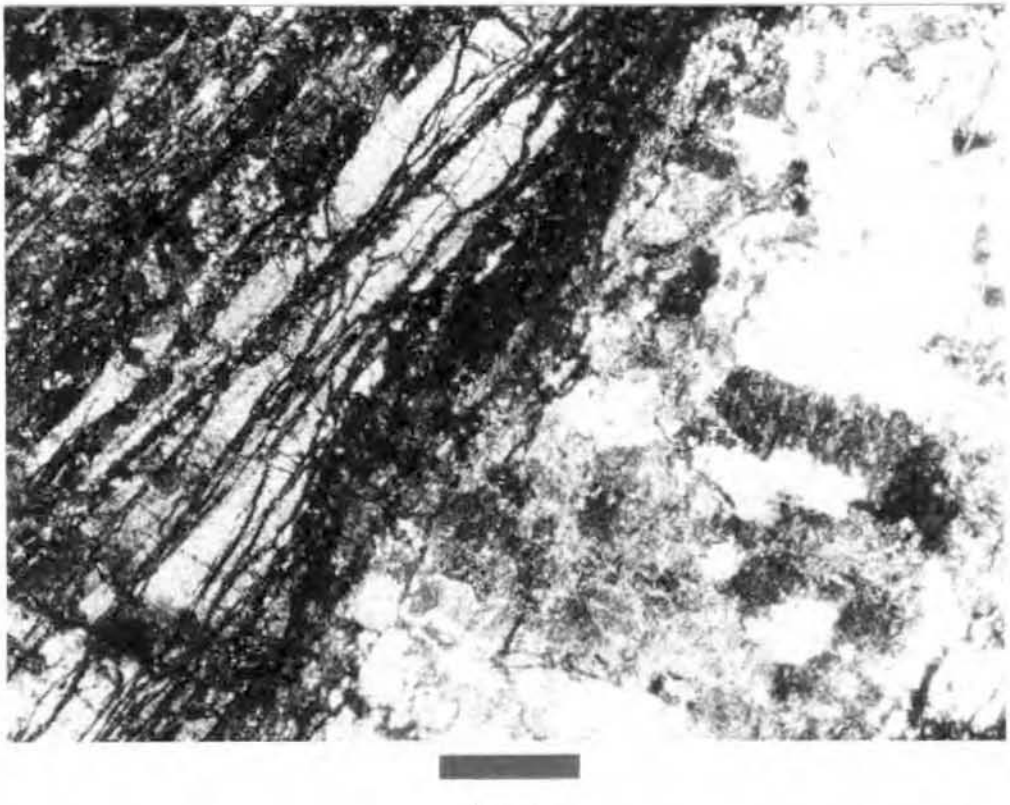

Figure 5.20 Shearing in primary skarn: drillcore from DDH 81-5B, 105.08 m. Vesuvianite and garnet are altered to actinolite along fractures. Thin section under crossed polarisers.

5.3.7 CHEMISTRY OF SKARN MINERALS

Analysis of individual minerals, primarily from diamond drill core, by electron microprobe was performed in order to investigate chemical variation in the skarns. Rock analysis was not attempted due to the rapid variation in mineral content of the skarns and occurrence of frequent alteration or mineralisation along veins. Any such analysis would merely reflect the sampling interval and would have required continuous sampling for the whole skarn intersection, which was no longer available since the core had been originally rather inexpertly split and fairly coarsely sampled by Newmont staff for assay, their crushed samples having been destroyed many years ago.

Microprobe analyses have been obtained for a large number of pyroxenes from drillholes 81-1 and 81-3, together with analyses of various garnets, amphiboles, scapolite, vesuvianite, chondrodite-humite group minerals, carbonate and phengite from these holes and also DDH numbers 5B and 8.

PYROXENES

Pyroxene compositions determined cover the full range from diopside to pure hedenbergite. Some specimens show little variation in pyroxene composition over the scale of the one thin section whilst others are quite variable. Specimens collected from drill core of holes 1 and 3 have been analysed. Those from DDH 1 show little compositional variation, falling in the field of diopside or magnesian salite (Fig. 5.21), with one exception. Pyroxenes from DDH 3, however show much more variation in Mg:Fe content, both over the scale of individual thin sections and through the whole skarn intersection (Figs. 5.22, 23). The compositions have been shown as atomic proportions of the Mn, Fe and Mg components since these skarn pyroxenes are predominantly diopside-hedenbergite, with no significant Al content, but with a small johannsenite component (maximum Mn proportion compared to Mg and Fe being ≈11% in all of the analyses made of drillcore and 25% in one specimen from the southernmost surface exposure). In some cases, e.g. 81-3: 61.00m, the small-scale compositional variation may be seen to follow colour-banding in the specimen that highlights fracture-controlled pyroxene development (Figs. 5.6; 5.23). Maximum compositional variability occurs between 54.14 and 62.60m in DDH 3. Increase in Fe content in the

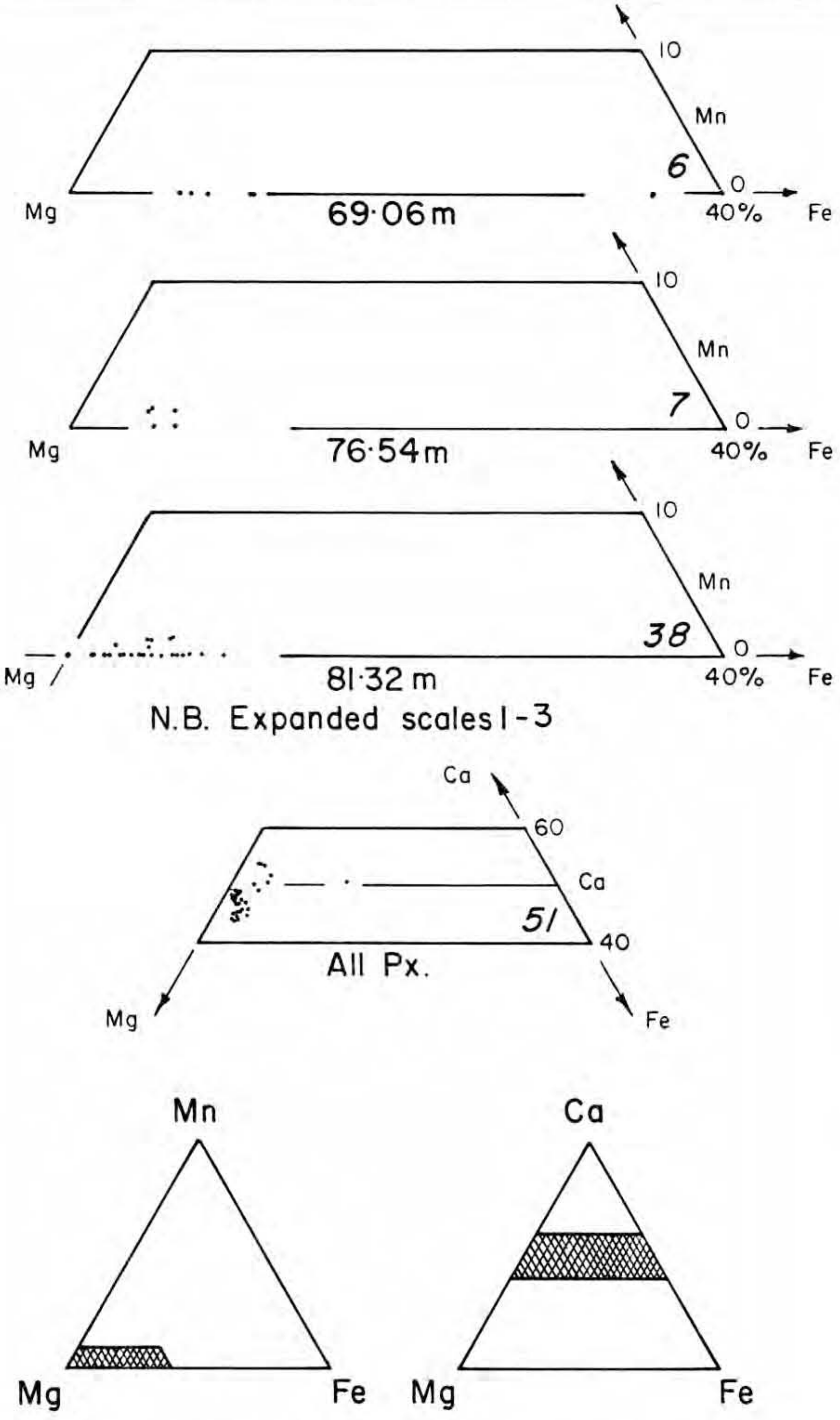

PYROXENE COMPOSITIONS:
ATOMIC PROPORTIONS OF
Mn-Fe-Mg & Ca-Fe-Mg. DDH 81-1.
Fig. 5·21

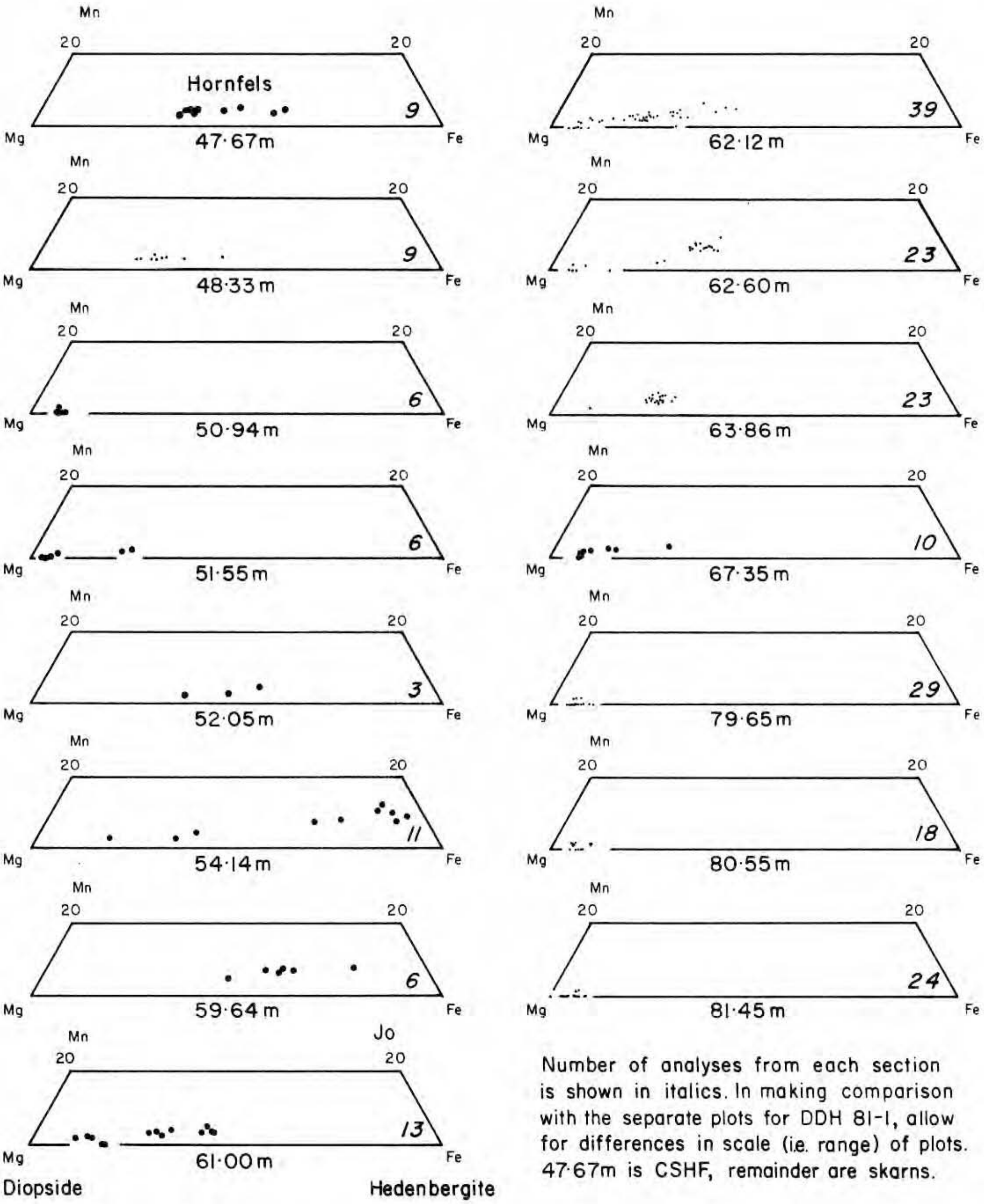

Number of analyses from each section is shown in italics. In making comparison with the separate plots for DDH 81-1, allow for differences in scale (i.e. range) of plots. 47·67m is CSHF, remainder are skarns.

PYROXENE COMPOSITIONS SHOWN AS ATOMIC PROPORTIONS OF Mn, Fe & Mg FOR MINDY SKARN INTERSECTION IN D.D.H. 81-3.

Fig. 5·22

T.L. March 1992.

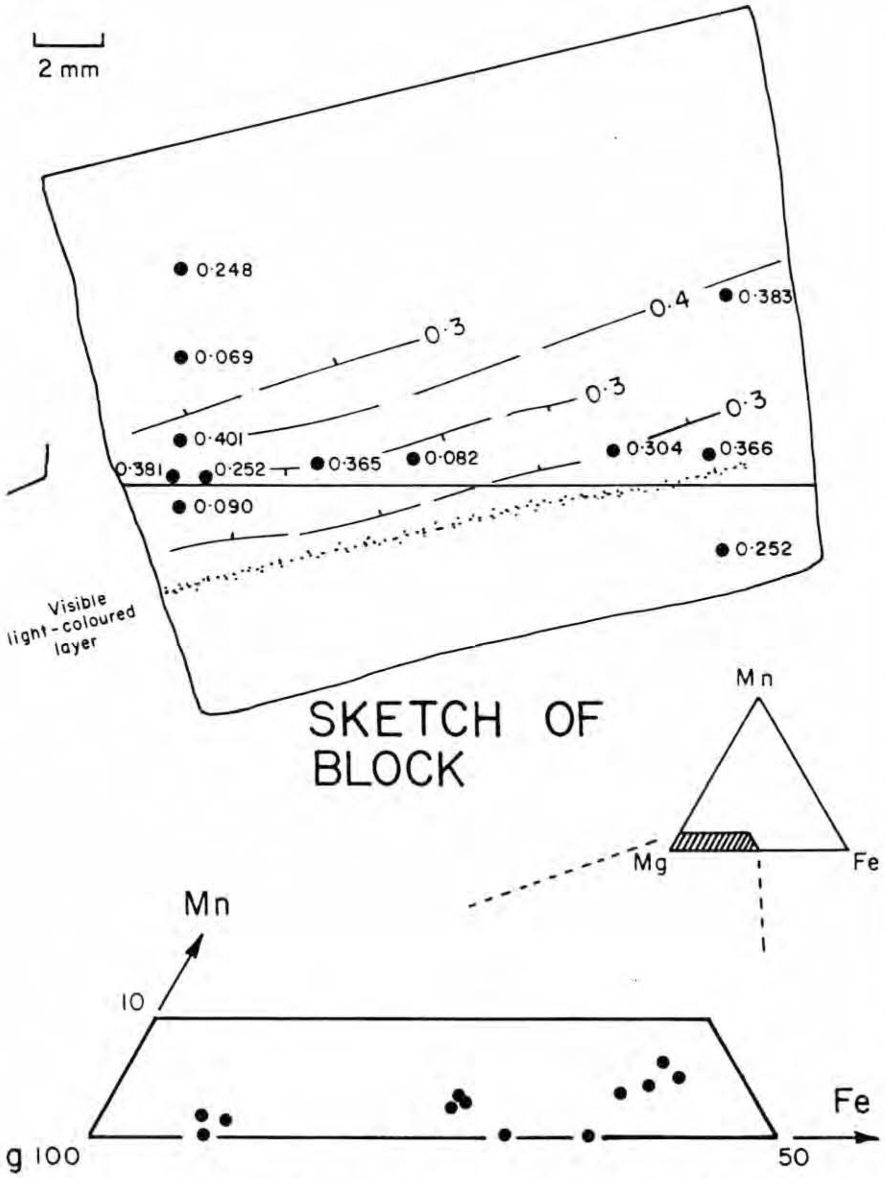

SKETCH OF BLOCK

PYROXENE COMPOSITION

The sketch shows position of the microprobe analyses and Fe/(Mg+Fe+Mn).
Contours at 0·3 and 0·4 Fe ratio are shown.

MINDY SKARN: PYROXENES FROM FROM FRACTURE-REPLACEMENT ZONE. D.D.H. 81-3, 61·00m.

Fe-rich zones are 2·5 to 3mm wide.

Fig. 5·23

T.L. Mar.'92.

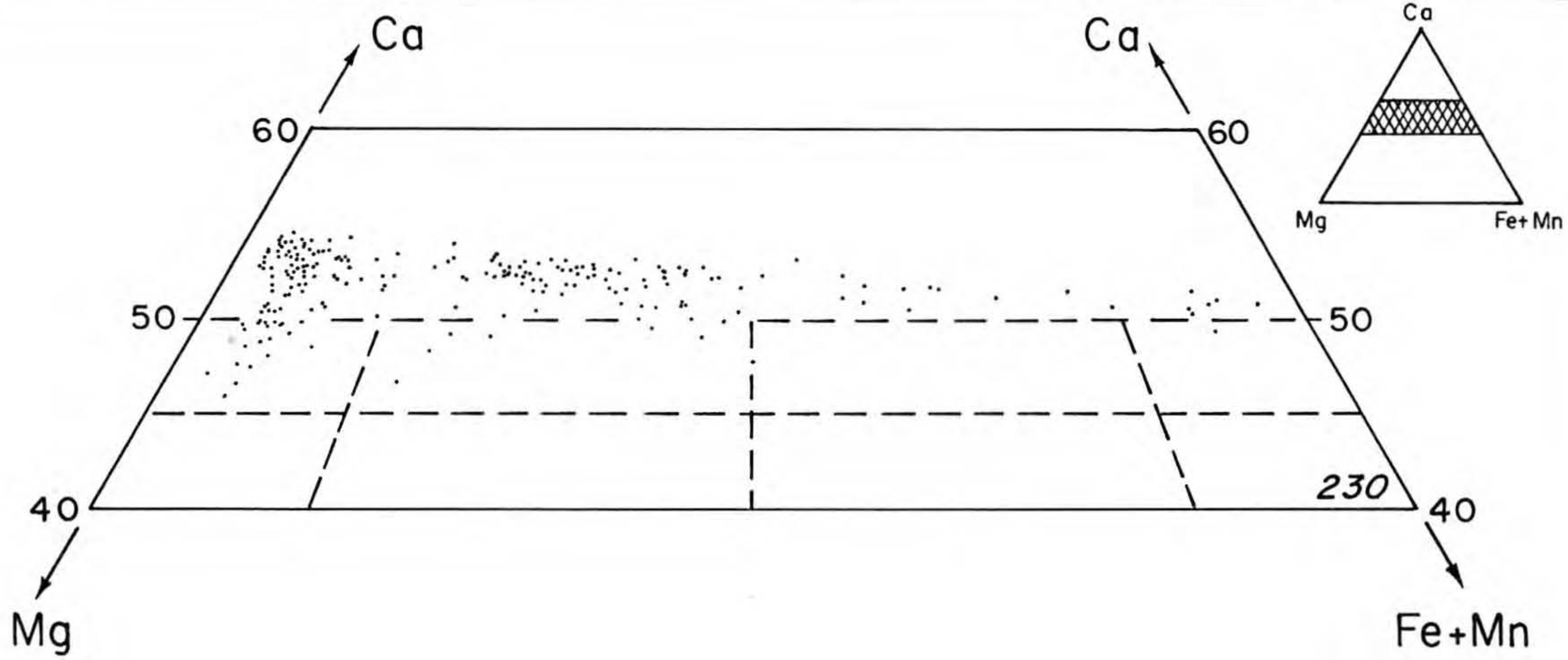

COMPOSITIONS OF ALL PYROXENES ANALYSED BY MICROPROBE FROM MINDY D.D.H. 81-3, ATOMIC PROPORTIONS OF Ca-(Fe+Mn)-Mg. Fig. 5·24

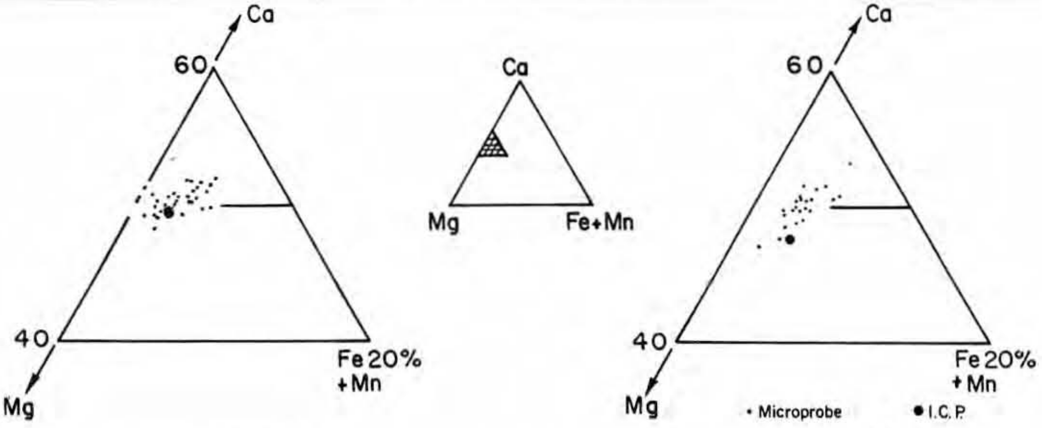

81-1, 81·32 m

81-3, 79·65 m

COMPARISON OF ATOMIC PROPORTIONS OF Ca-(Fe+Mn)-Mg

FROM SPOT ANALYSES BY MICROPROBE TO I.C.P. ANALYSIS OF MINERAL SEPARATES FOR MINDY SKARN DIOPSIDES.

Fig. 5·25

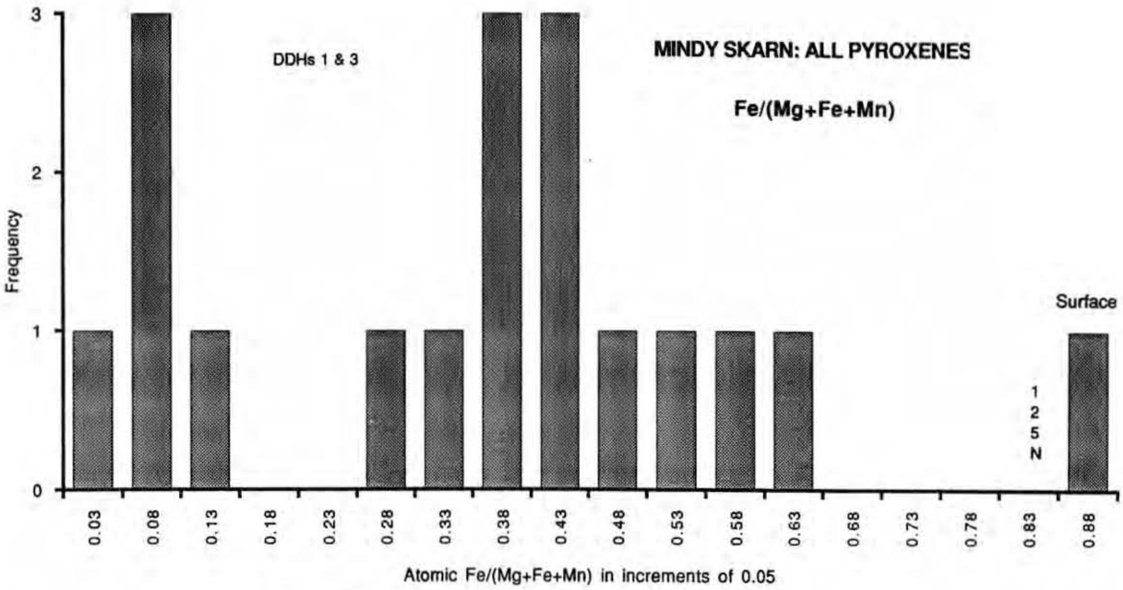

Figure 5.26 Histogram of average pyroxene compositions from Mindy skarns.

pyroxenes is accompanied by greater small-scale variability in composition (note the ranges indicated in Appendix B.7).

All analyses from both drillholes have also been presented as Ca-(Fe+Mn)-Mg components (Figs. 5.21; 5.24), as is the more common representation of pyroxene compositions. It will be noted that many of the ratios fall above the 50% Ca ratio. As a check on microprobe calibration, two specimens that showed small spreads in spot analyses were used to prepare mineral separates which were analysed by I.C.P. Comparison between the results of the two techniques (Fig. 5.25) indicates that the microprobe results do perhaps overestimate the Ca content and underestimate Mg, but the net effect on a plot is only a shift of <2% toward the Ca apex. These minerals are therefore richer in the Ca component than the usual 50% level used in pyroxene classification. This is also indicated in some analyses in the compilation presented in Deer et al. (1963): V.2, p. 5.

The plot of all pyroxene compositions from DDH 3 gives a suggestion of a bimodal distribution. Since the number of spot analyses from individual specimens varies greatly and might have produced this bias, the average composition from each specimen from core and surface specimens were plotted on a histogram (Fig. 5.26). This plot confirms the mostly bimodal distribution. One grouping with very high Fe content forms a separate mode . It is hedenbergite-johannsenite from the surface specimen at {125N, 110W} (Newmont coords.). The diopside (Fe/Mg+Fe+Mn= 0.05-0.10) is interpreted as being the original contact-metamorphic/metasomatic pyroxene, and the salite, (Fe/Mg+Fe+Mn= 0.35-0.45) as being the most frequent composition resulting from the later metasomatism that immediately preceded magnetite-Sn mineralisation. A trend towards increasing Fe content during skarn alteration has also been reported from W-skarns (Zahm, 1987). The contrast in variability in compositions of pyroxenes between drillholes 1 and 3 is interpreted as being due to relative proximity to the fault zone that was the main local conduit for SiO_2 and $FeCl_2$ bearing hydrothermal fluids during early metasomatism.

GARNETS

Green, yellow and brown garnet found in the lower skarn horizon and in vein skarns in marble (81-8, 57.3m and 83.4m) is andradite with no appreciable aluminium content (See Appendix C.3). The X-ray spectra obtained indicated no appreciable Sn content (i.e. <<0.2%). The very low grossular component of this garnet contrasts with those minerals in the W-skarn deposits (e.g. Zahm, 1987).

SCAPOLITE

Scapolite has been analysed from aphanitic pyroxene-scapolite hornfels in DDH 81-3, at 47.67 m. The composition varies little over the one section, SiO_2 varying from 43.95% to 46.45%; CaO varying from 19.07 to 20.70%; maximum Na_2O being 1.41%; Al_2O_3 from 27.15 to 35.39%; FeO* varying up to 3.03% and MgO being up to 2.56%. Most of the microprobe analyses showed Na and K contents within the analytical error range, i.e. indicating composition close to that of the meionite end member (Deer et al., 1963: V.4, p. 326), however one analysis (LIV820) indicated 1.0% K_2O and 4.07% Na_2O content i.e. a 60% meionite component, so considerable variation in composition may occur in this skarn. The mineral has not been recognised from the coarser skarns, probably reflecting the absence of aluminium in the marble protolith. No appreciable Sn content was detected. The development of Al-rich skarn mineralogies that preserve original cataclastic fabric is interpreted as indicating that diffusion transport of chemical components in these skarns was limited to a very small scale (i.e. ≤ 1 mm).

AMPHIBOLES

Amphiboles analysed from the Mindy skarns are restricted to the calcium amphiboles. MgO or FeO* content varies by no more than 2% in the one specimen, but the range of compositions throughout the skarns is considerable: the ratio Fe/(Mg+Fe+Mn) varies from 0.275 to 0.484 in the actinolite of DDH 81-3/48.33m, 50.94m and 51.55m; is 0.061 in tremolite of 62.60m, but in ferroactinolite of 54.14m it is 0.773 (Fig. 5.27). The ferroactinolite occurs in zones of cataclasis and replacement of the pyroxene skarn.

VESUVIANITE

Vesuvianite has been analysed from 81-3, 81.45 m. Five analyses show less than 1% variation in any constituents, whereas one single analysis indicates increase in TiO_2

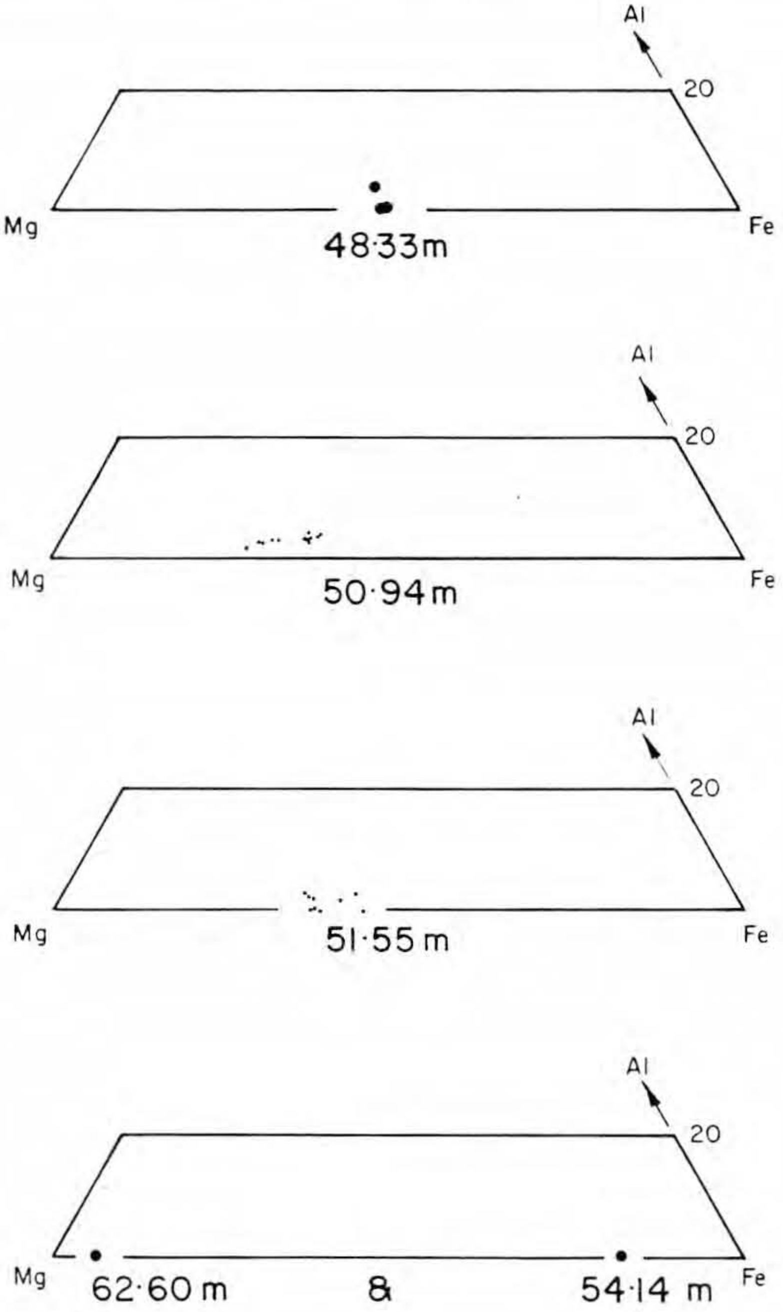

AMPHIBOLE COMPOSITIONS: ATOMIC PROPORTIONS OF Al-Fe-Mg FOR MINDY SKARN INTERSECTION IN D.D.H. 3.
Fig. 5·27

from around 1.4% to 3.76%, with corresponding decrease in Al_2O_3. An average for the five analyses and the high Ti analysis are reproduced in Table 5.3. No significant amount of Sn was noted in this mineral.

DRILL HOLE	FILE NO.	SIO2	CaO	MgO	FeO	MnO2	Al2O3	TiO2	Cl	TOTAL
81-3 81.45	LIV882	38.66	36.43	1.94	3.34	0.26	17.24	1.26	0.64	99.77
81-3 81.45	LIV883	37.78	36.36	2.77	4.22	0.49	13.31	3.76	0.70	99.38
81-3 81.45	LIV884	38.10	37.37	1.88	3.47	0.16	16.35	1.13	0.65	99.10
81-3 81.45	LIV885	38.59	37.03	1.44	4.29	0.04	16.53	1.44	0.71	100.09
81-3 81.45	LIV892	37.95	36.89	1.90	3.33	0.42	17.00	1.17	0.74	99.40
81-3 81.45	LIV895	38.76	36.89	1.72	3.73	0.39	16.81	1.36	0.72	100.38

Table 5·4 ELECTRON MICROPROBE ANALYSIS OF VESUVIANITE

HUMITE GROUP MINERALS

The humite group minerals chondrodite and clinohumite have been recognised optically (by fine lamellar twinning and euhedral crystal shape in some cases) and by X-ray diffraction, particularly in the Fe/F-rich skarns. No microprobe analyses have been obtained from these minerals.

EFFECT OF BRECCIATION AND FRACTURING OF SKARNS

Each of the specimens from DDH 81-3 that show great variation in pyroxene compositions over centimetre-scale distances (54.14; 61.00; 62.12 and 63.86 metres) shows either evidence of cataclasis (grain size reduction) of pyroxene skarn in narrow (5-10 mm wide) zones or veining of slightly different coloured pyroxene every 20 mm or less (Fig. 5.6), these structures dipping at a shallow angle to the horizontal. Some tiny (<<1 mm) fractures at high angles to the horizontal cut the low-angle veining. The brecciation process has obviously allowed introduction of successively more Fe into the skarn system as metamorphism continued.

5.3.8 PARAGENESIS: SKARN MINERALS

The silicate mineral paragenesis is fairly well definable from the study of mineral assemblages present in the thin sections, however the corresponding timing of oxide and sulphide phase introduction is less accurately defined, partially due to their occurrence with a wide range of the silicate phases or as cross-cutting vein minerals. The

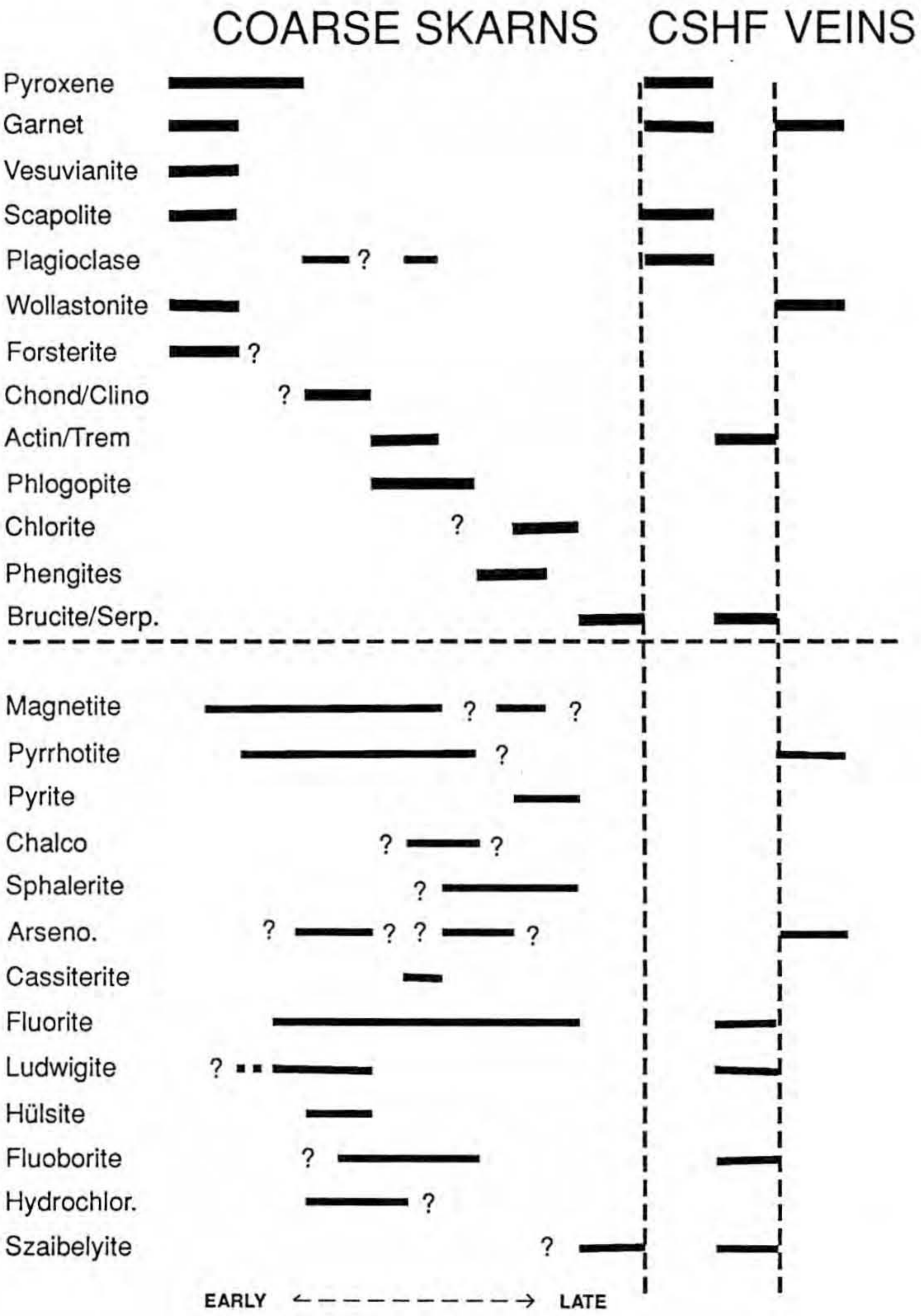

Fig. 5. 28 Paragenesis of Mindy skarn minerals.

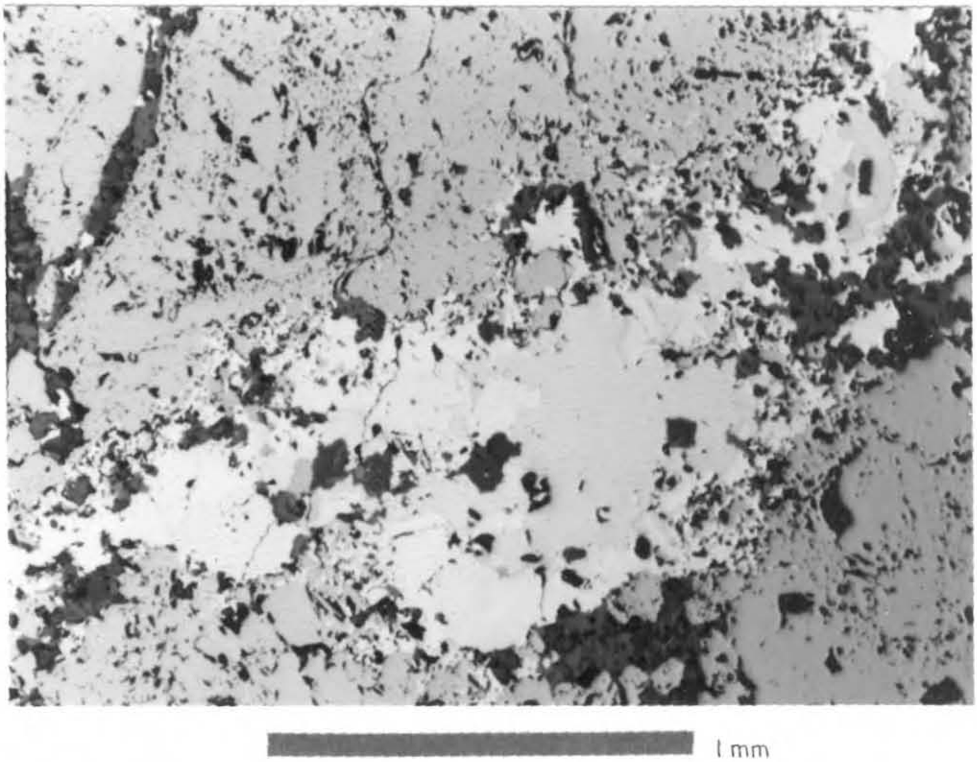

Figure 5.29 Mindy DDH 81-5B, 108.87 m: pyrrhotite-chalcopyrite vein (white and yellow) in magnetite (grey). Some of the deep brown is probably cassiterite. From a magnetite-phengite greisen-skarn. Polished block under plain-polarised reflected light.

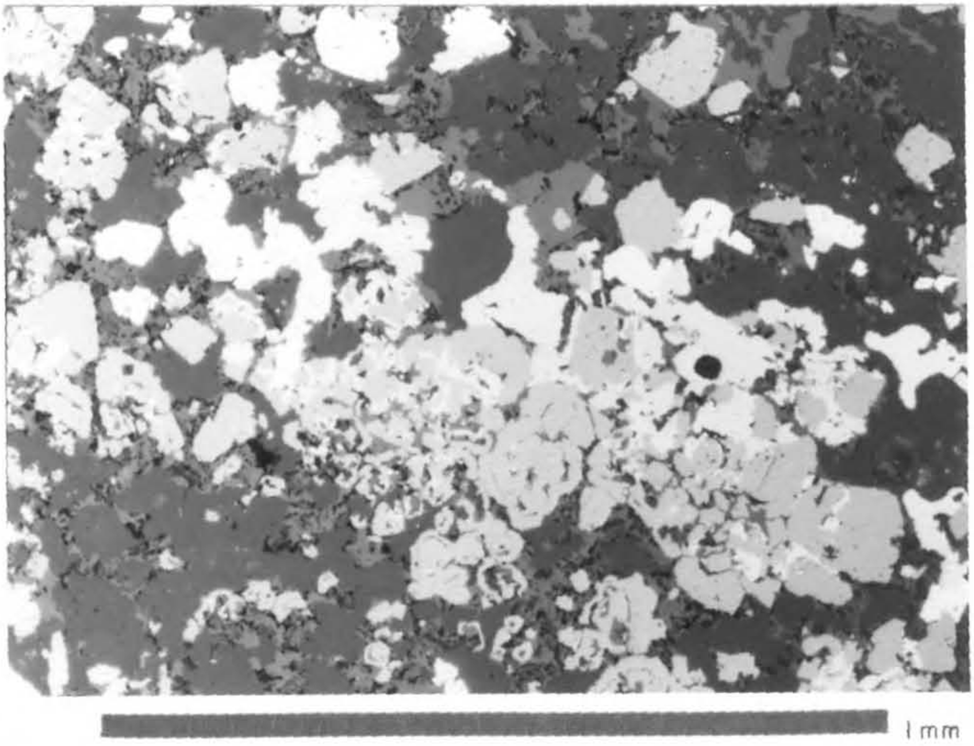

Figure 5.30 Mindy DDH 81-4, 148.50 m. Concentrically formed magnetite crystals (grey) with pyrrhotite (white) in andradite skarn which has been heavily replaced by actinolite. Polished block in plain-polarised reflected light.

following generalisations regarding mineral occurrence may be stated:

Diopside-hedenbergite is found with both garnet and vesuvianite, as subhedral to euhedral inclusions in garnet, as interstitial anhedral forms in the garnet-rich skarn and intergrown with the vesuvianite.

Forsterite has been rarely recognised, but when it has been observed it occurs with the pyroxene. The clinohumite-chondrodite group minerals are observed in hedenbergite skarn at surface (Newmont coordinates {125N, 110W}) but mainly as coarse grains in the magnetite and fluorite-rich skarns as quite corroded relicts, sometimes occurring with diopside-hedenbergite. A few crystals have been noted in the diopside-calcite skarns, particularly as euhedral forms projecting into the carbonate.

Scapolite is found only in the very fine-grained calc-silicate hornfels as remnant porphyroclasts (Fig. 5.19b). Wollastonite is observed only in virtually monomineralic skarns developed in pure marble. Amphibole, covering the range from tremolite to actinolite is found both as irregular masses of tiny acicular crystals replacing pyroxene and (more commonly) along fracture systems from a millimetre to several centimetres wide (Figs. 5.7, 5.8 & 5.20).

Phlogopite and phengites are associated with alteration along fracture systems and occur as discreet bands in the 'wrigglite' skarns, the phengite also forming cores to alteration veins.

Brucite and serpentine form the cores of the wider alteration veins. Some brucite is also seen in fracture systems that cut the pure marbles, but bear little mineralisation.

SULPHIDE/OXIDE MINERALISATION

Both magnetite and pyrrhotite are found occurring together alongside a wide range of silicate mineralogies. Pyrrhotite occurs in the pyroxene skarn as disseminations, as at surface {680S, 180W}, or as layers in the fluorine-rich skarns (DDH 81-2, 82.17) and finally in subordinate quantity in the magnetite-rich wrigglite. Magnetite persists in vein-type alteration, occurring with serpentine. Pyrite and chalcopyrite have been noted with pyrrhotite where it occurs as bands in the wrigglite. Sphalerite has been identified only rarely associated with the other sulphides. The coarsest material seen is associated with magnetite replacement of garnet-diopside (81-5 B, 104.40) or of wrigglite (81-4, 70.40): Figs. 5.29 & 30.

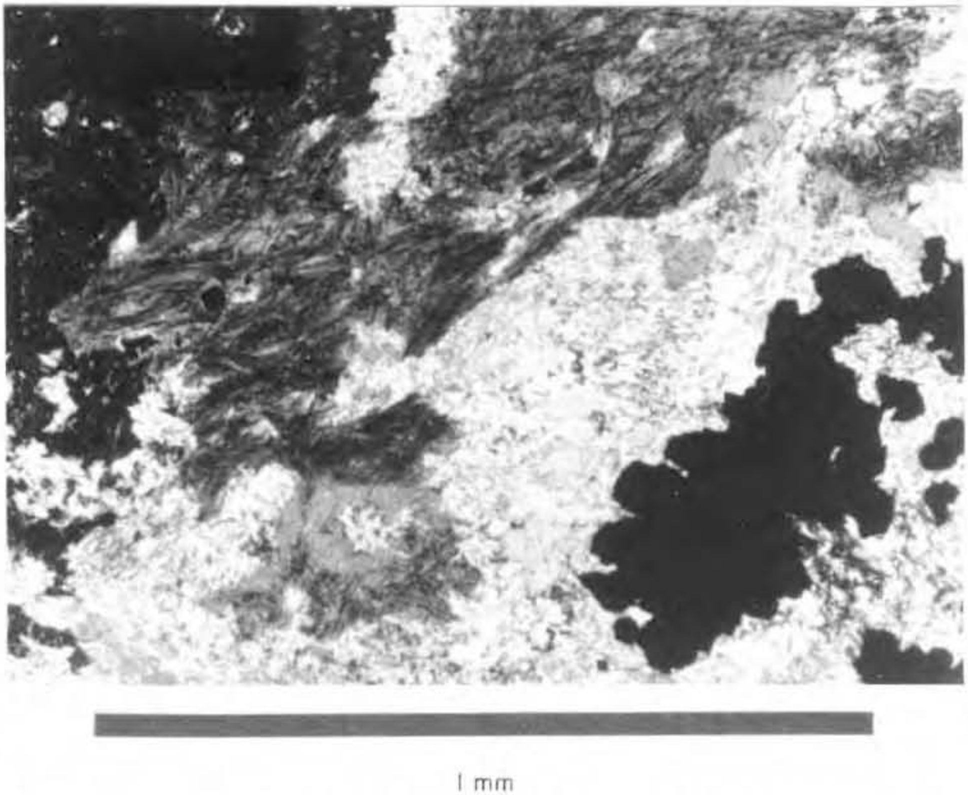

Figure 5.31 F-B rich skarn: DDH 81-1, 77.60 m. Thin section under crossed polarisers showing calcite, fluoborite (blue interference colour), szaibelyite (brownish highly birefringent mineral) and magnetite.

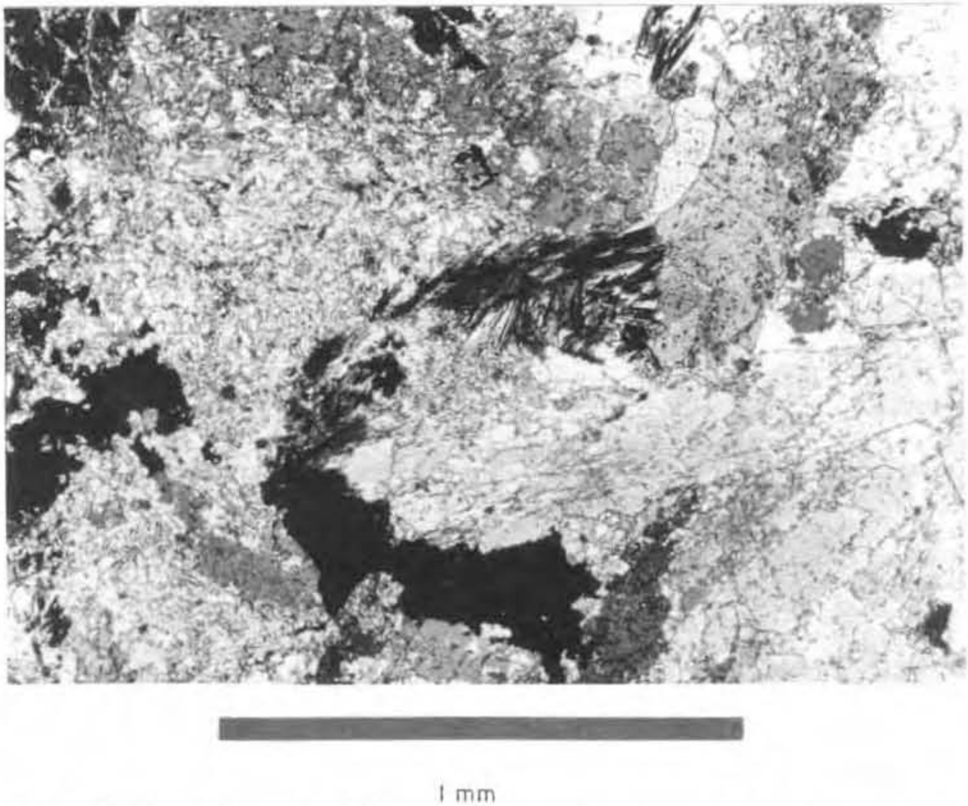

Figure 5.32 Alteration: DDH 81-1, 75.30 m. Diopside-hedenbergite replaced by ludwigite (acicular opaques), fluoborite and talc. Thin section under crossed polarisers.

Arsenopyrite has been noted in veins: as fine fractures that cut wrigglite in 81-2, 89.7 m and pyrrhotite-diopside skarn in 81-8, 46.3m and in the coarse vein skarns developed in marble, where coarse crystals of the arsenopyrite are found with euhedral andradite (Fig. 5.10). Cassiterite is found with fluorite in the magnetite-rich wrigglite and occasionally in veins and its appearance likely immediately preceded the appearance of the tin borates.

FLUORINE AND BORON MINERALS

Fluorite occurs throughout the sequence of silicate minerals from pyroxene skarn to wrigglite and with the phengite veins. Fluoborite appears somewhat later with actinolite and wrigglite skarns and alters to szaibelyite. The Fe-Mg-(Sn) borates, the ludwigite-vonsenite series and hülsite are found in quantity in the wrigglite and occasionally in the small crosscutting veins. Boron metasomatism likely persisted somewhat later than fluorine since szaibelyite is seen to occur as selvedges to brucite veins in marble. Figures 5.31-33 show occurrences of szaibelyite, ludwigite and fluoborite. Ludwigite accompanies either talc-brucite alteration of pyroxene skarn or chondrodite development in marble (Fig. 5.33).

TIN MINERALS

Cassiterite (Fig, 5.34) and the borates hülsite and ludwigite are the major Sn-bearing phases recognised at the Mindy deposit. Nordenskiöldine has been recognised in only one specimen (Fig. 5.12) and malayaite is absent. The absence of malayaite is understandable since it is stable under high T, high pH conditions only (Burt, 1978).

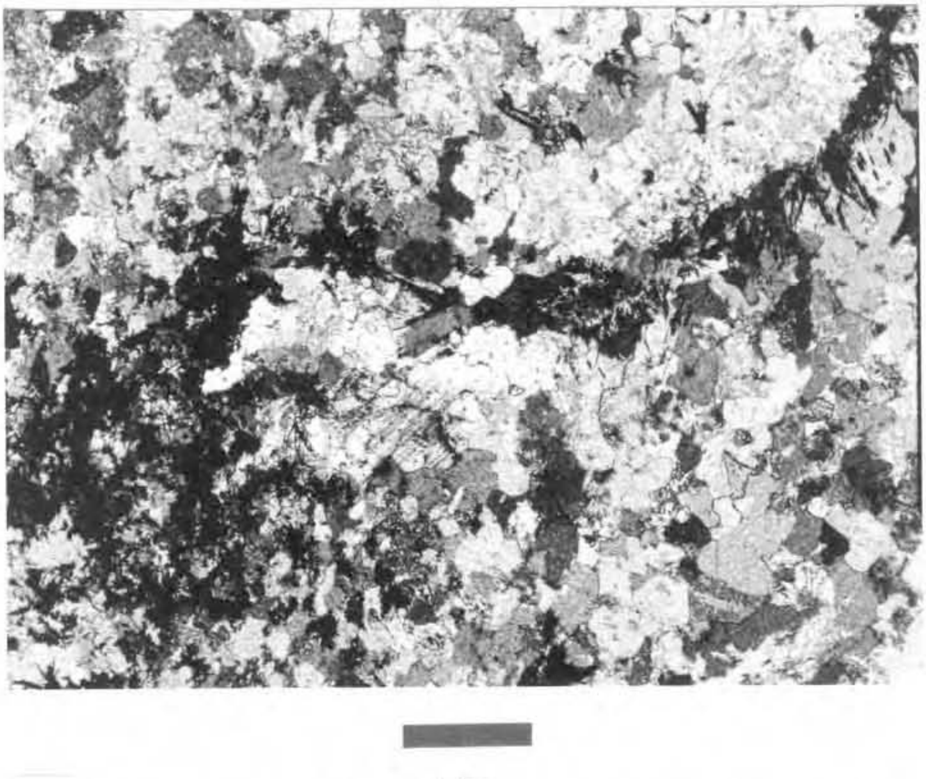

Figure 5.33 Thin section under crossed polarisers of core from DDH 81-2, 92.00 m showing a ludwigite vein in marble with a chondrodite selvedge (yellow interference colour).

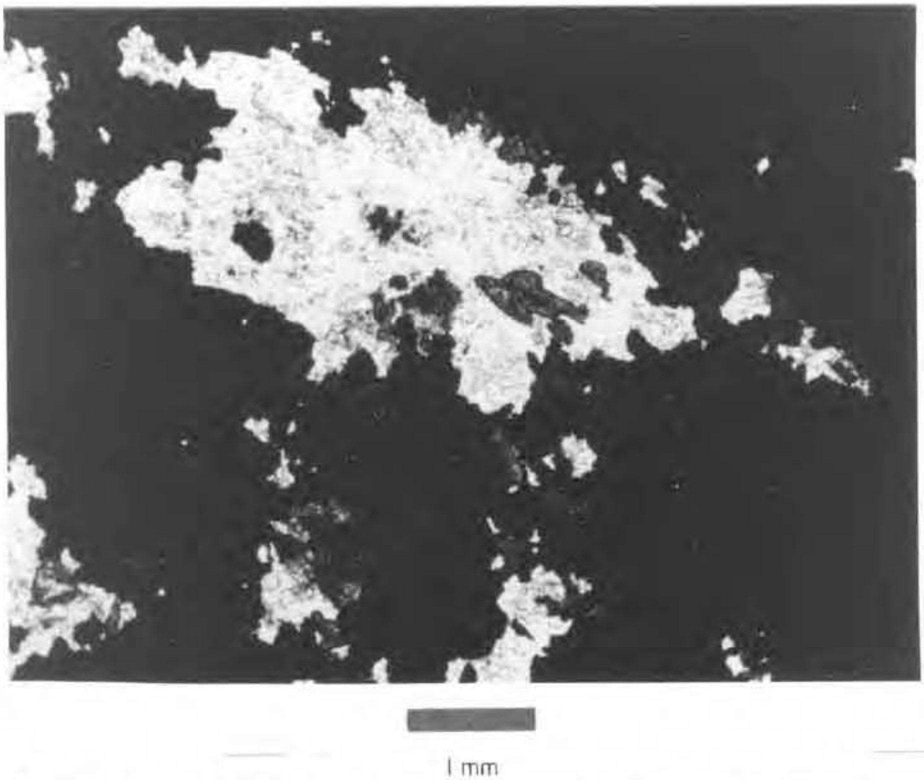

Figure 5.34 Cassiterite mineralisation: marble from DDH 81-1, 73.4 m in thin section under crossed polarisers showing magnetite, talc and cassiterite (yellow-brown).

The following general sequence of skarn development is:

1) Prograde skarn:

  a) Diopside-hedenbergite skarns developed in magnesian host.

  Successively more Fe- rich pyroxene produced with time.

  Pyrrhotite probably precedes much magnetite introduction.

  b) Andradite-vesuvianite skarn developed in calcic host.

2) Magnetite skarn: timing overlaps (3)

  a) Massive magnetite-cassiterite mineralisation in calcic marble.

  b) Ludwigite and hülsite accompany magnetite in the magnesian skarns.

3) Greisening:

  a) Phlogopite replacement of pyroxene and humite-group minerals.

  b) Ferrophengite development along fractures.

  Minerals such as bandylite ($CuClBO_2 \cdot 2H_2O$) formed by alteration of sulphides.

  c) Serpentine formed in some wrigglite.

4) Hydrous skarn, fracture-controlled: stages 2-3

  a) Tremolite-actinolite, progressively more Fe-rich.

  b) Chlorite minerals.

  c) Serpentine.

5.3.9 METASOMATIC TRENDS IN THE MINDY SKARNS

The stages of skarn formation at the Mindy deposit may be summarised as:

1) Formation of diopside or diopside-forsterite skarn in a dolomitic protolith / andradite-diopside or andradite-vesuvianite in calcic protolith. Scapolite/pyroxene developed in fine-grained hornfelses.

2) Early fluorite/pyrrhotite mineralisation

3) Brecciation of skarn: formation of more Fe-rich pyroxenes. Scheelite mineralisation at south end of Mindy carbonate horizon.

4) Local replacement of pyroxenes by chondrodite/clinohumite.

Continuing fluorite/pyrrhotite mineralisation.

5) Development of wrigglites, as veins and mantos from the main extensional fault system: massive Fe/F mineralisation (F/B metasomatism accompanying greisen-skarn development). Cassiterite appears to accompany first magnetite.

6) Continued F/B introduction: fluoborite/complex Sn borate mineralisation.

7) Fracture-controlled alteration of pyroxene and garnet assemblages to amphiboles of actinolite to ferroactinolite composition. Cu-Zn sulphide mineralisation. Phlogopite and talc production. Phengite in some wrigglite, but mostly introduced along fractures.

8) B metasomatism continued as local szaibelyite replacement of marbles, again along fractures.

5.4 DISCUSSION

5.4.1 THIRTYMILE SKARN TYPES

Several skarn types are recognisable in the Thirtymile Range. These are:

1) Endoskarn. This type has only been observed at the Ork prospect as a 10 mm wide zone marking the sharp granite contact.

2) Proximal exoskarns: skarns formed close to the outcropping granite contact are seen only in 3 localities: (a) Ork: vesuvianite-cebollite exoskarn. (b) Locality {400281}: massive garnet-jasperoid skarn is developed in a 4m wide zone over about 30 m strike length (Appendix B.2). (c) Skarns in the main marble unit at the Ork area are pyroxene-garnet CSHF in impure carbonates and diopside-axinite skarn in the sheared marble breccia (Ch. 4). The principal example is the Mindy deposit (below).

3) Distal skarns: massive pyroxene skarn is developed high in the Thirtymile range at {453235}, adjacent to an extensional fault. The neighbouring extensional fault zone carries some diopside skarn or pyrrhotite-szaibelyite-scheelite skarn developed in its breccia {454238} (Ch. 3).

4) Bimetasomatic skarns are seen at the contacts of the marble units with the overlying siliceous sediments, notably at {446253} and for several hundred metres either way along strike. Garnet-pyroxene or vesuvianite rich assemblages are developed for 1-2 metres thickness. The upper skarn exposure at the Mindy prospect is a further example.

5.4.2 COMPARISON WITH OTHER SKARN MINERALOGIES

The Mindy skarns have many similarities to other Sn-bearing skarn deposits. The broad characteristics of the various ore-bearing skarns have been summarised by Einaudi et al. (1981). The prograde and retrograde mineralogies of the Mindy skarns bear features in common with both his calcic and magnesian Sn types. The tectonic setting of continental margin and late orogenic (at least relative to the first phase of crustal thickening) timing is appropriate to his classification.The particular mineralogies quoted by those authors (their table 1) have some relevance: for the prograde calcic skarns grandite and vesuvianite (idocrase) are prominent at the Mindy, however malayaite has only been seen at the Ork prospect and the calcium borate danburite or the hydrous borosilicate datolite have not been recognised. The magnesian prograde assemblages quoted are well represented: forsterite, phlogopite, magnetite, humite group minerals and ludwigite. Of the retrograde assemblages quoted amphibole, mica, chlorite and fluorite are common in the magnesian sections, only tourmaline being absent from the calc-silicates and cassiterite, fluoborite, magnetite, micas and fluorite are all represented. Stannite is the only ore mineral quoted for both the magnesian and calcic skarn assemblages that has not been seen in the Mindy deposit.

A table setting out the various mineral assemblages reported in the literature is presented as Appendix B.11. Of the magnesian skarns shown in this table early-formed assemblages are forsterite/spinel±diopside. The humite group minerals and magnetite follow later and the garnet/ vesuvianite association is also reported as replacing the first assemblage. Some localities lack forsterite or spinel (e.g. Yerington, JC and Mt. Bischoff), reflecting lower contact metamorphic grades. Retrograde hydrous phases reported are calcic amphibole, followed by chlorite, talc, then serpentine or brucite. References are given in the table.

At St. Dizier cassiterite is reported to accompany the forsterite/diopside/magnetite assemblage but most of the references cited in this table show the oxide tin mineralisation to accompany magnetite/fluorite or magnetite/fluoborite. In this example it should be noted that the tin appears as the fluo-borate, hülsite at the later stage of mineralisation.

This relationship of initial oxide tin mineralisation followed by fluo-borates is also observed at the Mindy prospect: coarse cassiterite is found clustered around magnetite, and ludwigite is a later replacement of the marble, particularly in DDH 81-1 around 73.4 metres, whilst at 76.52 metres massive hülsite accompanying pyrrhotite replaces most of the calcite interstitial to pyroxene.

At Iten'yurginsk both fluorite and fluoborite accompany cassiterite; at Brooks Mt. only fluorite is reported and at the JC fluorite accompanies cassiterite mineralisation. In the Mindy deposit fluorine appears as fluorite throughout retrograde metamorphism and mineralisation (including being a core to late serpentine alteration veins), whereas fluoborite accompanies the main iron-tin mineralisation episode. Boron mineralisation continues late in the sequence as occasional szaibelyite alteration around fluorite veins.

On Skye the borate minerals ludwigite, fluoborite and szaibelyite are reported from magnetite-bearing 'ore' skarns and there accompany chondrodite. Some possibly relict diopside-magnetite-grossular- vesuvianite skarn is reported from this particular locality (Tilley, 1951 p. 628). Although ludwigite is plentiful no Sn content was reported in the analyses, so it is presumably the Fe-rich variety.

5.4.3 CLASSIFICATION OF THE MINDY SKARNS: PROXIMITY TO INTRUSION AND OXIDATION STATE

The classification of skarns according to their dominant mineralogies allows inferences to be made as to chemical conditions prevailing during late-stage crystallisation of the associated granite magma. The scheme of Einaudi has been expanded by Kwak (1987) to emphasise ore mineralogy and oxidation state in the W-Sn skarns (Table 5.5).

W-SKARNS WITH LITTLE OR NO Sn

1) OXIDISED RELATED TO GRANITOIDS
  - a) Magnetite-andradite type
  - b) Andradite

2) REDUCED RELATED TO GRANITOIDS
  - a) Grossularite (-almandine or andradite) type
  - b) Grossularite-almandine type

3) POLYMETALLIC (±W) RELATED TO GRANITOIDS

4) REGIONAL METAMORPHIC TERRAINS
  W- skarns unrelated to intrusions

Sn-SKARNS ± HIGH W

A: PROXIMAL, HIGH T, NON-GREISEN
  - 1) OXIDISED
    - a) Magnetite type
    - b) Andradite type
  - 2) REDUCED
    - a) Magnetite-fluorite-vesuvianite type
    - b) Forsterite-pyroxene-spinel type

B: PROXIMAL, HIGH T, GREISEN (USUALLY)
  - 1) GREISENISED SKARN TYPE
  - 2) GREISEN SKARN TYPE

C: DISTAL, LOW T, NON-GREISEN
  - 1) MAGNETITE TYPE
  - 2) PYRRHOTITE TYPE
  - 3) PYRITE TYPE

Table 5.5 W-Sn Skarn classification of Kwak (1987)

		PRIMARY		RETROGRADE				
		I A	I B	II A	II B	II C	II D	
	Garnet	• • • • • •						
	Pyroxene	• • • • • •						
	Vesuvianite	• • • • • •						
	Magnetite/Ilm	•••	• • • • • • •	•				
3	Wollastonite	• • • • • •						
3	Malayaite/Sph	• ••	•• •					
	Fluorite	•	• • •	• • •	• • •	• • •	• •	
1	Fe-amphibole			• • • • • •				
1	Epidotes			• • • • • •				
1	Ilvaite			• •	• • • • • • •	•		
1	Fe-biotite				• • • • • •			
1	Chlorite					• • • • • •		
2	Axinite			• • ••	•• • •	•		
2	Nordenskiöldine				• • •	••••	•	
2	Datolite				•	• • • • • •	•	
2	Danburite				•	• • • • • •	•	
	Quartz	• • •	• • •	• • •	• • •	• • •	• • •	
	Carbonate	• • •	• • •	• • •	• • •	• • •	• • •	
	Cassiterite	• •	• •			•• •		
	Scheelite	•• •	•• •	•• •	•			
	Sulphides		•	• • • • • •	• • • • • • •	•		
	Zeolites					•	• • • • • •	
	Varlamoffite						• • •	•

1= hydrous retrograde overprints (stage 2, low B); 2= borate retrograde overprints; 3= wollastonite skarns at skarn/marble contacts.

Table 5.6 General paragenetic sequence for calcic W- & Sn- skarns (After Kwak, 1987).

		PRIMARY		RETROGRADE				
		I A	I B	II A	II B	II C	II D	II E
	Forsterite	• • • • • •						
	Mg-spinel	• • • • • •						
	Pyroxene	Diops.	Heden.					
	Calcite	• • • • • •				• •	• • • • • • •	• •
	Garnet		• • • • • •					
	Magnetite	•	• • • • • • •	• • •				
	Mont./chond.	•	• • • •					
1	Serpentine		•	• • • • • • •	• • •			
1	Mg-amphibole			• • • • • •				
1	Talc			• •	• • • • • • •	• • •		
1	Phlogopite		•	• • ••	••• •			
2	Fluorite/sellaite		•	• • • • • •	• • • • • • •	• • • • • • •	• • • •	• • •
2	Humite gp.		•	• •••	••• •	•		
3	Fe-amphibole			• • • • • •				
3	Epidotes			• • • • • •				
3	Chlorite					• • • • • •		
4	Ludwigite		•	• • • • • • •	• •			
4	Hülsite			• • ••	•••• •			
4	Pageite		•	• •••	• •			
4	Fluoborite		•	••••	• •			
4	Suanite		•	• • •	• • •			
4	Kotoite		•	• • • • • • •	• •			
4	Szaibelyite			•	• • • • • • •	•		
	Cassiterite	•	• • •	• • •	• • •	• • •	• •	
	Scheelite	• • •	• • •	• • •	•			
	Siderite		• •	• • • • • •	• • • • • • •	• • •	•	
	Quartz	• • •	• • •	• • •	• • •	• • •	• • •	•
	Sulphides			• • • • • •	• • • • • • •	• • • • • • •		
	Sn hydroxides						• • • • • •	
	Apophyllite						• •	•
	Zeolites						• •	• ••
	Varlamoffite						•	• • •

1= Hydrous retrograde products (low F & B); 2= Fluoride-rich retrograde products; 3= Hydrous retrograde products after IIB calcic assemblages; 4= Borate-rich retrograde products.
Mont./chond.= monticellite/chondrodite.

General paragenetic sequence for proximal magnesian W- and Sn-skarns

The Mindy deposit, despite there being no exposed granite, shows the features of a proximal tin skarn. It should be noted that the Newmont diamond drill holes were terminated immediately siliceous metasediments were encountered and did not penetrate any deeper into the mountain than the topographically lowest marble outcrop on the claims (see Appendix B.3). In general proximal deposits are found within 300 metres of a major pluton (Kwak, 1987). Extensive biotite-cordierite development in the pelitic country rocks around the Mindy prospect is good reason to expect an intrusion at shallow depth beneath the lower skarn unit.

Both magnesian and calcic skarns are found at the prospect. The silicate mineralogies can highlight original brecciation of the dolomite/ limestone protolith (section 5.3.6). The amount of transport of Mg throughout these carbonates is unknown, but such textures are interpreted as indicating that skarn chemistry will greatly approximate to the Ca/Mg composition of the protolith.

MINERAL PARAGENESIS AT MINDY

The Mindy mineralogy is typical of the proximal high temperature reduced skarn type: (vesuvianite-magnetite-fluorite and pyroxene±forsterite assemblages), with vein andradite skarns possibly reflecting more oxidised conditions (compare Fig. 5.28, Tables 5.5, 5.6,). Cataclasis of some of the diopside skarn is evident as centimetre-wide, low angle, somewhat irregular zones where grainsize reduction is obvious. Bands of Fe-rich pyroxene skarn are seen to cut early diopside skarns. That is, there is a trend towards higher Fe content in successive prograde skarns.

Coarse chondrodite or clinohumite appear as occasional crystals in the diopside skarn, where it can sometimes be seen to clearly have replaced the pyroxene. Very coarse material is only seen as remnant, highly corroded layers in the fluorite-rich wrigglite or greisen-overprinted phengite-rich skarn, formed at a later stage than the pyroxene. Actinolite and chlorite are developed as replacements of both pyroxene and garnet-vesuvianite (non-wrigglite) skarns along fractures: all compositions in the tremolite-actinolite series are represented.

It will be noted that the Mindy skarn mineralogies are similar to both types 2a and b of Table 5.5, which is likely to have been governed by initial carbonate chemistry and that a late type B1 greisen overprint occurs as phlogopite-phengite veins. The deposit therefore has many similarities to reduced Sn skarns. The scheelite-bearing (0.3% WO_3) skarn at the south end of the prospect has hedenbergite-johannsenite pyroxene, chondrodite or clinohumite, a little forsterite, a little pyrrhotite and fluorite. This mineralogy indicates a reduced skarn type (Einaudi et al., 1981). No Sn minerals have been detected at this end of the skarn unit, reinforcing the observation of a generally antithetic relationship between local Sn and W occurrences.

The reduced-type mineralogy at Mindy is in accordance with the ilmenite-type nature of the Thirtymile granites: reduced-type granites are expected to produced reduced skarns. Physical conditions existing during skarn formation have been estimated from the data of Burnham and Ohmoto (1980) and Einaudi (1981) by Kwak (1987) to compare with possible fO_2 and temperature existing during granite emplacement (see 6.5.4). Oxidation state of magmas is reflected in the Fe-sulphide phase found as accessory minerals in the intrusion. Reduced ilmenite-type or S-type granites have pyrrhotite, whilst magnetite-series and most I-types have pyrite. (White, 1990; Burnham and Ohmoto, 1980; Kwak,1987). Reactions involved in the magma are likely to be:

Low fO_2 magmas: S occurs as H_2S or HS^-

$FeCl_2 + H_2S = FeS + 2HCl$

The FeS is deposited as pyrrhotite (in the intrusion), leaving S-deficient solution and melt (since the solubility of S is <100 ppm in such magma: Burnham and Ohmoto, 1980). Aqueous fluids will be high in Fe, explaining the usually high Fe content of proximal Sn skarns.

The progressive increase in Fe content of pyroxenes has been demonstrated at Mindy (Figs. 5.21-26), where channelling of fluid circulation along fault zones appears to have been important in localising metasomatism.

SKARN PRODUCTION RESULTING FROM THESE REACTIONS:

Acid solutions will be capable of producing pore space in carbonates by production of $CaCl_2$, water and CO_2, which, provided there are pathways, will be released as saline fluids and gas. Production of the usual silicate/magnetite skarn mineral assemblages will be typically as:

$$3FeCl_2 + 4H_2O = Fe_3O_4 + 6HCl + H_2$$

$$3CaCO_3 + 3H_2O + 6SiO_2 + 3FeCl_2 = 3CaFeSi_2O_6 + 3CO_2 + 6HCl$$

(Diopside etc.)

$$3CaCO_3 + 2FeCl_3 + 3SiO_2 + 3H_2O = Ca_3Fe_2Si_3O_{12} + 3CO_2 + 6HCl$$

(Andradite etc.)

Acidic exhaust solutions from the skarn production will further react with carbonates to form pore spaces and chloride-rich solutions. Whether volume changes during skarn formation are important is debatable. The process may be constant-volume, despite theoretical considerations that would indicate that silicate assemblages, of higher density than carbonate, occupy less volume (Kwak, 1987). For loss of volume in formation of skarn minerals to occur there must be either an increase in pore space in the rock or structural adjustment in the surroundings. In working almost entirely from drill core no estimate as to whether there has been any volume change at the Mindy prospect can be made. One general observation is possible: in the massive diopside-hedenbergite skarn pyroxene crystals are mostly subhedral to anhedral until a calcite mass is encountered, where euhedral forms somewhat coarser than the rest are developed. The texture suggests very rapid replacement of carbonate. Later retrograde (actinolite) or fluoborite assemblages are developed along pyroxene grain boundaries or cleavages and rapidly diminish away from fracture zones, indicating that the primary skarns were a very 'tight' rock.

WRIGGLITE

At the Mindy prospect finely banded magnetite±vesuvianite+cassiterite+fluorite wrigglite skarn is associated with fracture systems. Kwak (1987) explains the rhythmic alternation of mineralogies in wrigglite skarn as being due to sealing of rock at the carbonate/skarn interface by the rapid formation of fluorite:

$$2HF + CaCO_3 = CaF_2 + CO_2 + H_2O$$

The high pressures of CO_2 evolved are then thought to cause micro-fracturing and repetition of the cycle. This is essentially similar to the fracture-reaction-seal mechanism described by Bucher-Nurminen (1989). It differs somewhat from the original explanation of wrigglite as a chemically produced texture analogous to the Liesegang ring diffusion phenomenon produced in some experimental gels (Tilley, 1951).

5.4.4 GREISENING AND 'GREISEN-SKARN'

Greisen development in the Erzgebirge is recognised as being in two stages which are recognisable by their Li contents and hence mica mineralogy: an early Zinnwaldite to protolithionite mica greisen which is restricted to within 200-300 m from the granite contact and a low-Li later stage with phengitic muscovites (Wasternak et al., 1974). Only a Li-rich stage of greisening is visible at the margin of the Thirtymile stock, however the late-stage 'wrigglite' magnetite-phlogopite or phengite skarns of the Mindy would be considered to be 'greisenised-skarn' in the classification of Kwak. Four types are recognised (Kwak, 1987):

1) Proximal retrograde skarns, usually fault controlled, phyllosilicate- rich which have a range of silicates and sulphides where temperatures indicated by fluid inclusions are <350°C and salinities low.

2) Distal skarns, formed in unaltered limestone which can be kilometres laterally and >500 m vertically from a large intrusive and contain low salinity fluid inclusions indicating temperatures of 240-350°C. They may be stratiform or irregular and are related to vein stockworks.

3) Greisenised skarn, formed from proximal primary skarn, perhaps within 500 vertical metres of a contact in the 300-500°C temperature range and at moderate salinity of fluid. High Ca, Fe, F, Be, Li are common.

4) Greisen-skarn proper, formed mostly directly from a carbonate precursor in both proximal and distal environments under the same fluid conditions as (3). High in Sn, B, F, Be, Li.

Phlogopite-fluorite banded skarns (wrigglite) are a representation of skarn type 3 at the Mindy prospect, whereas the ferrophengite veins may be the retrograde equivalent (type 1).

5.4.5 TIN MINERALISATION

Many tin skarns contain appreciable amounts of Sn in their early-formed silicate phases (Kwak, 1987), but this does not seem to be the case at Mindy. Due to problems with the electron microprobe, quantitative analyses of the garnets, pyroxenes, amphiboles and vesuvianite did not include Sn. The amount of Sn present in any of these phases is judged to be low (<0.2% Sn) from examination of the X-ray spectra. Although cassiterite and ludwigite-vonsenite are both present no textural evidence of a retrograde reaction to produce a late-stage cassiterite mineralisation has been noticed (as in Kwak, 1987 p. 283):

$$(Fe^{2+},Mg)_2(Fe^{3+},Sn^{4+})BO_3 + HF + 6H_2O = Mg_3BO_3(F,OH)_3 + Fe_3O_4 + SnO_2 + 6H_2$$

Sn-ludwigite Fluoborite Magnetite

5.4.6 EVOLUTION OF METASOMATISM IN THE MINDY SKARNS

The Mindy paragenesis is indicative of the following trend in composition of metasomatising fluid:

(1) Si±Fe-bearing fluids: Initial diopside skarn could have been produced by addition of silica to a dolomitic protolith. Increasing amounts of Fe introduction with the silica is indicated by the more hedenbergite-rich pyroxenes found along fracture systems. This skarn development is consistent with conditions of >570°C if p= 1kb. In other deposits successive increase in Fe content of pyroxenes has been correlated with decreasing pH of the hydrothermal fluids (Zharikov, 1970b).

(2) F±S, accompanying later Si-Fe bearing fluids: Early F introduction is evident in both the Sn- and W-bearing skarn as chondrodite or clinohumite, accompanied by fluorite. Relatively minor sulphide (as pyrrhotite) introduction occurred at this stage.

(3) Acid high Fe±F±Sn solutions: a massive introduction of Fe (as $FeCl_2$) is indicated by the fracture-controlled magnetite mineralisation (wrigglite), which contains F as fluorite. Cassiterite was formed possibly later in this stage. In other deposits fluid

inclusion studies have indicated temperatures of formation for wrigglites ≤ 530°C, with NaCl equivalent salinities of >26 wt% (Kwak and Askins, 1981). Such salinities are in accordance with the transport of Sn by Cl-complexes. The probable range of pH during Sn deposition is 3.9-5.4 (Wilson and Eugster, 1990).

(4) High F-B±Fe±Sn solutions: wholesale replacement of early silicate assemblages by fluoborite. Sn deposited as hülsite and ludwigite-vonsenite. Fracture-controlled.

(5) Alkali-bearing fluids: minor Na-K introduction is indicated by the association of vesuvianite with the wrigglite-skarn. Larger amounts of K introduction are indicated by the phlogopite-ferrophengite vein formation i.e. greisen-skarn replacement. These mineralogies indicate a progressive reduction in pH of the circulating fluids.

(6) Lower temperature Si-F±B bearing fluids are indicated by serpentine, talc and szaibelyite veining.

5.4.7 STRUCTURAL CONTROLS

The importance of an active fault system at Mindy during contact metamorphism and mineralisation cannot be overemphasised. The very location of the prospect alongside an extensional fault (that has been shown to be a conduit for mineralisation to the west) demonstrates that hydrothermal and probably later meteoric fluid flow concentrated in such 'plumbing'. The fracturing of the siliciclastics and early prograde skarns (Figs. 5.19b & 5.20) to form retrograde assemblages, continued activity of fractures shown by development of mineralised discordant vein skarns in the marbles all demonstrate that faulting was active until very late in the mineralisation process.

CHAPTER 6

DISCUSSION

CHAPTER 6 DISCUSSION

6.1 INTRODUCTION

This chapter discusses the implications of the structural geology of the study area, possible correlation of rock units and their relation to tectonics of the northern Canadian Cordillera. A hypothesis for the metallogeny of tin in this region is proposed. The origin of the geochemically anomalous leucogranites is discussed and comparison made between their chemistry and metasomatism at the Mindy skarns. Some quantitative parameters for recognition of tin granites are suggested. The effects of different redox conditions in magmas on mineralisation are discussed. Recommendations are made concerning mineral exploration in the Thirtymile Range.

6.2 THE THIRTYMILE AND ENGLISHMAN'S RANGES

6.2.1 GEOLOGY OF THE THIRTYMILE RANGE: SUMMARY

The Thirtymile Range is underlain by the Englishman's Group succession of siliciclastic metasediments and carbonates of Unit 3 in the original regional mapping by Mulligan (1963). Rather than being a simple sedimentary sequence, the succession is an east-verging, low metamorphic grade thrust belt. It has been intruded by Middle Cretaceous granite stocks, which are undeformed. The siliceous metasediments are quartzite, minor subarkose, chert and quartz-rich pelite. Carbonates are dolomitic to pure calcite marble. Rare tectonic inclusions of sheared andesitic volcanics have been observed. The entire sequence is disrupted by low angle thrust faulting.

The style and amount of deformation of individual lithologic units are variable: much of the tectonic succession shows evidence of either small anastomosing shears, a penetrative flat-lying pressure-solution cleavage (rarely with C-S fabric developed) or brittle fracture, that are indicative of comparatively small amounts of strain. Less common, fault-bounded phyllonite units are interpreted as being developed from highly-strained conglomerate protoliths.

No single lithologic unit can be reliably traced for more than 5 km strike length. Any gross 'stratigraphy' now visible is a tectonic layering. Many lithological boundaries are faults and the common (sectional) geometry of units is lenticular. Local zones of mylonite have been identified and the pelitic lithologies exhibit a flat-lying penetrative cleavage that appears as a slaty or pressure-solution fabric, depending on the protolith.

Pelitic lithologies show the characteristics of L-S tectonites: small-scale folds and crenulations are parallel to (rarely visible) stretching lineation and roughly normal to the possible transport direction. Shear sense criteria (C-S fabric) observed are in accordance with movement of top-to-the east. The presence of identifiable mylonite zones and differing styles of deformation between individual units are used to infer the presence of many possible thrust surfaces in what might be termed a tectonic mélange using the broad definition of Raymond (1984).

Extensional faulting, which strikes predominantly ESE, largely preceded emplacement of small granitic stocks into the Englishman's Group. These plutons developed proximal and distal skarns that carry W and Sn mineralisation wherever a marble unit was within their aureole and particularly where an extensional fault allowed fluid transfer.

REGIONAL TECTONIC SETTING

The Englishman's Group (Dorsey terrane) is the westernmost limit of Palaeozoic sediments in this portion of the Omineca Belt, i.e. the early Mesozoic North American continental margin. Immediately west are the amphibolite grade metamorphics and deformed granitic plutons of the Teslin Suture Zone: the Big Salmon Metamorphics. West of the Suture are Mesozoic island arc volcanics and sediments of the Intermontane Belt. The entire Palaeozoic sedimentary package is imbricated for 100 km eastward from the Teslin Suture, forming the Yukon Cataclastic Complex (Abbott, 1981).

6.2.2 CORRELATION

Regional correlations are very much debatable. The Dorsey terrane has been considered to be allochthonous (Wheeler and McFeely, 1991), however this present study and other current work would suggest that it is parautochthonous (Gordey, 1992; Harms, 1992; see Fig. 6.1). A lack of palaeontological evidence as to the age of the upper portion of the Englishmans Group complicates matters. The published age

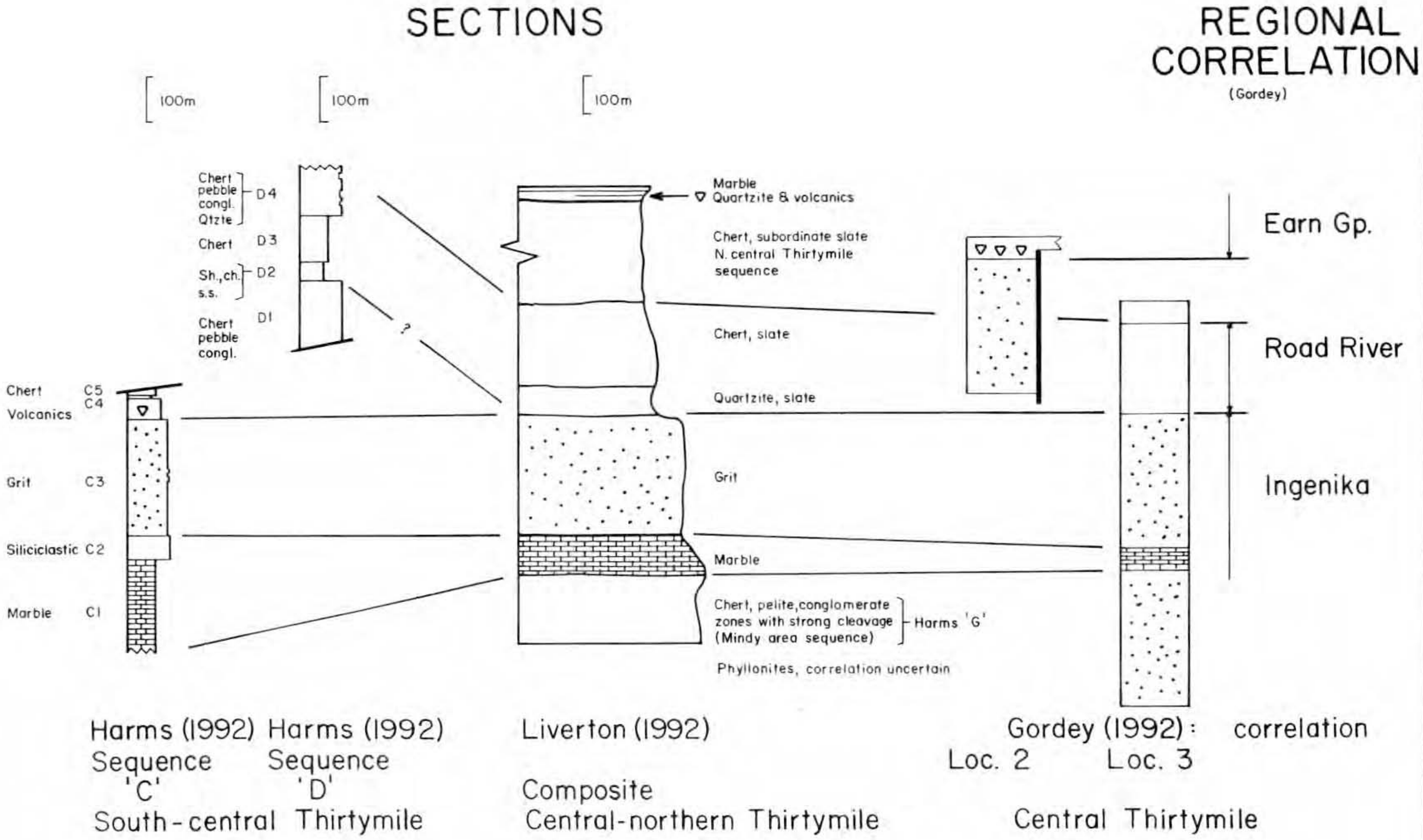

Fig. 6·1 STRATIGRAPHIC SECTIONS & REGIONAL CORRELATION

(Mississippian) of the Englishmans Group is based on macrofossils reported in Mulligan (1963) from the thick carbonate succession (Unit 2) that underlies the siliclastics of the Thirtymile Range. Although in this study three localities were selected from the carbonate lenses within the siliciclastics for collection of carbonates to allow a search for microfossils, none were found.

Coarse siliciclastic sediments are uncommon in the southern Yukon. Tempelman-Kluit (1979) has noted arkoses in the klippen some 45 km NE of the Thirtymile Range and suggested correlation between the two purely on lithologic grounds. Similarity exists between the lithologies mapped in this study and part of the succession reported in the Indigo Lake area by Gordey (1981) (see section 3.8.2). It is entirely possible that the clastic upper portion of the Group is older than Carboniferous. Thick successions of grit in the Selwyn Basin are late Proterozoic in age (Gordey, 1979; Gordey, 1992), however coarse clastics are known from the Cambrian and Devono-Mississippian sequences also. Black clastics are typical of the Silurian Road River group and chert and chert pebble conglomerate sequences are typical of the Devonian-Mississippian Lower Earn Group (see McClay et al, 1990). Mississippian carbonates overly the clastics in the continental sequences of northern British Columbia.

It is here postulated that much of the black slate and chert succession of the Thirtymile (i.e. Mulligan's Unit 3) correlates with the Road River and Lower Earn Groups. Quartzites could be Windermere equivalent or also Devono-Mississippian. Thickness of the quartzites in the Thirtymile Range indicate that the Upper Proterozoic (Windermere equivalent) correlation is most likely.

There are some differences in local interpretation between the mapping of this study and the later mapping of Gordey (1992) and Harms (1992). Gordey recognises basic volcanics at the top of quartzite at his locality 2 (i.e. approximately {420231} of Append. B.2), which is correlated with the Earn Group (Fig. 6.1). An aphanitic, black, slightly foliated rock was noted at the top of the measured section of this study. This was considered to be a sediment in hand specimen. If this unit is volcanic, then it more likely correlates with unit C4 of Harms. Faulting shown as separating sections 2 and 3 of Gordey is consistent with the extensional faults mapped in this study (Ork horst: faults 'O' & 'M' of Append. B.2). This study indicates (using the main marble unit as a datum) that displacement between the two sections (Gordey 2 & 3) is relatively minor. No thrust fault at the top of the marble is recognised by Gordey. This study interprets the contact as being a a fault purely on evidence of deformation observed. The extensional fault ('O' of Append. B.2) mapped in this study has not been recognised by Harms. The fieldwork of this study, however, indicated that the upper contact of the carbonates (loc. 9 of Append. B.2) is discordant with bedding below and has been interpreted as an extensional fault. Fault 'M' (Append. B.2) of this study has been confidently mapped and is also indicated in the mapping of Harms. Differences exist in interpretation of structure, stratigraphy and correlation in the Thirtymile Range. Only much more widespread detailed mapping (and palaeontology) will resolve the issue and allow confident regional correlation.

If the preceding regional correlation is correct, then the underlying carbonates (Mulligan Unit 2) would be younger and a major thrust fault must separate the two units (Fig. 6.2).

6.2.3 TECTONIC IMPLICATIONS

The individual lithologic units of the Thirtymile show some variation in style of deformation but linear fabric elements have remarkably constant orientation. The thicker marble units, which have been deformed by a myriad of small shears have a generally lenticular geometry. This is illustrated by the rapid thinning of the major carbonate unit towards the SE and by the thickness changes in the lower carbonate/skarn unit at Mindy. Exact (plan) geometry of these carbonates is not known, but it is possible that the apparent boudin axes strike almost E-W (and are parallel to small fold axes in the pelites). Phyllonites east of Mindy have ribbons of quartz that are very elongate when seen in the NW-SE oriented rock faces of that locality and which show N-S trending crenulation axes.

Wherever a crenulation has been observed in pelitic lithologies the axes trend between 360-180° and 010-190° true, with plunges usually 0-10° in either direction and rarely up to 28°. In the NW Thirtymile area the extensive phyllite unit shows mesoscopic-scale kink folding as well as millimetre-scale crenulation. Both hinges of metre-scale kink folds and millimetre-scale crenulation axes show N-S to NNE-SSW trends, with plunges being 0-18° in either direction. Axial planes of the crenulation (i.e. an incipient cleavage) is near vertical. In the rare cases where mineral elongation lineations have been observed (one example just north of Peak 1997 and some examples in the phyllonites of the NWTM area) they are parallel to crenulation axes. Only a few observations have been made in hand specimen and thin section as to sense of shear in the Thirtymile metasediments, C-S fabric being rare. The material examined from the Mindy prospect indicates a dextral shear sense (in section looking northward).

Published petrofabric analysis (Hansen, 1986a and b) of the metamorphics in the Teslin Suture Zone has shown that there is a dominantly NNW-SSE striking, near vertical foliation, with well-developed C-S fabric in places. Two generations of stretching lineation have been recognised: an early moderately steep westerly plunging fabric which parallels isoclinal fold axes; and a gently NNW to SSE plunging structure. Interpretation is that early motion (Mid Triassic) was contractional movement at a high angle to the continental margin and that later motion (perhaps early Jurassic) was almost parallel to the continental margin and in a dextral sense (Hansen, 1986a and b).

The orientation of the mesoscopic-scale linear fabric in the Englishmans Group is consistent with its having been generated by oblique collision at the Teslin suture: The general problem of orientation of lineation relative to layer-parallel extension in a convergent wrench setting has been considered by many authors. In transpressive regimes the orientation of fold axes marginal to the main fault is at 45° to that structure and a simple shear model for deformation has been suggested (Jamison, 1991) . Purely convergent terranes (pure shear) produce fold axes parallel to the fault. Odonne and Vialon (1983) carried out analogue modelling of transpression that produced a similar result. During progressive development of folds, their axes become rotated toward the fault from the initial 40-45° angle. Fold axes are curved and at some distance from the fault remain at the initial angle of close to 45° to the strike of the fault. Axial planes of folds become progressively flatter away from the fault i.e. they fan out.

In zones of ductile deformation mineral lineation is often parallel to the extension direction. Eisbacher (1970) carried out a thorough petrofabric study of a mylonite zone in Nova Scotia and found that mineral lineation was parallel to extension direction and interpreted the lineation as representing laminar (ductile) flow lines that were oriented at 45° to flow. Escher and Watterson (1974) proposed that L-S tectonite fabrics in which the planar element dips at a low angle away from the foreland and in which the stretching element is transverse to the boundary of the belt originate in simple shear deformation.

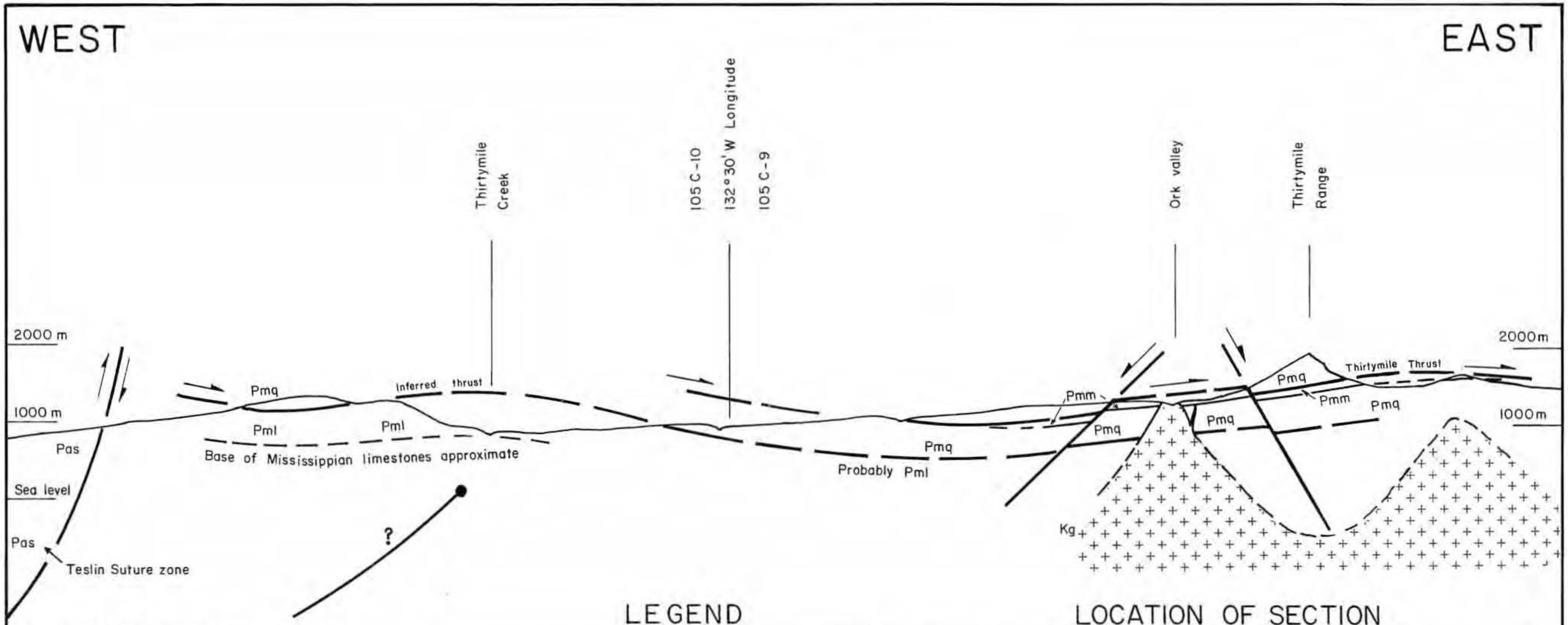

Vertical / horizontal = 1

LEGEND

Kg	Cretaceous		Granite
Jg	Middle		Granite, granodiorite
Jd	Jurassic		Gabbro, diorite
Pml	Mississippian	Dorsey Terrane (Englishmans Gp.)	Fossiliferous limestone
Pmm	Palaeozoic	Dorsey Terrane " "	Marble
Pmq	Palaeozoic	Dorsey Terrane " "	Quartzite, chert, pelite, mylonite
Pph	Palaeozoic	Dorsey Terrane " "	Phyllite & phyllonite
Pas	Lower Pal?	Teslin-Taylor Mountain Terrane?	Amphibolite & schist.

Fault (nature unknown) — Fault (thrust)

Fault (normal) — Contact (uncertain)

Antiformal axis — Synformal axis

0 5 10 Scale of map, km

0 1 2 3 Scale of section, km

LOCATION OF SECTION

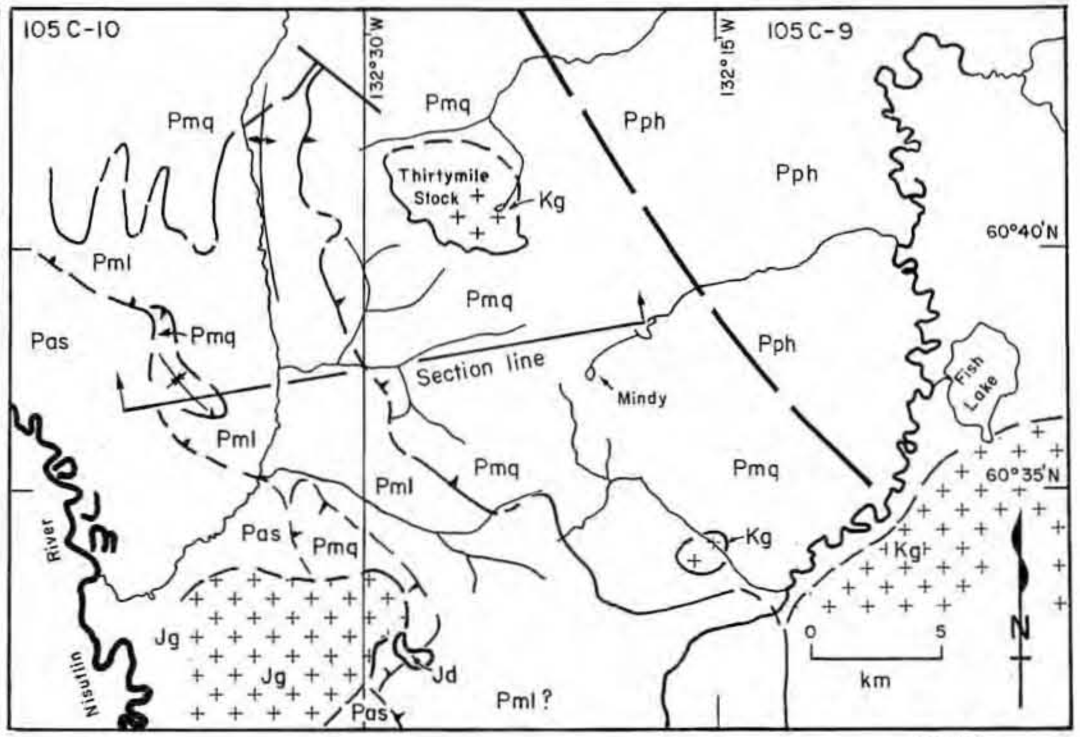

CROSS SECTION THROUGH THE ENGLISHMANS GROUP (WEST EDGE OF THE DORSEY TERRANE) ON 080°, WITH REGIONAL GEOLOGICAL MAP.

Fig. 6·2

Geology after Mulligan (1963) & Liverton (1992).

T. Liverton May 1992.

Early formed folds would be rotated into an orientation close to the stretching lineation. Malavieille et al. (1984) noted a regional consistency in stretching lineations (associated with boudinage, sheath folds, stretched pebbles) in the Western Alps and interpreted the deformation as simple shear in a ductile regime. In Corsica stretching lineation is parallel to sheath folds and the transport direction (hence normal to the major fold axes). Again, a simple shear model is proposed (Mattauer et al., 1981).

Boudinage and C-S fabric observed in the Thirtymile Range are considered to be indicative of layer-parallel extension in sheared lithologic units. Mechanisms of such foliation boudinage formation as a layer-parallel extension phenomenon have been discussed by Platt and Vissers (1980): extension along a foliation results in brittle failure (shear band development). Where the deformation is non-coaxial an asymmetric boudinage is produced (Fig. 6.3). The cleavage orientation does not appear to be related directly to axes of finite strain.

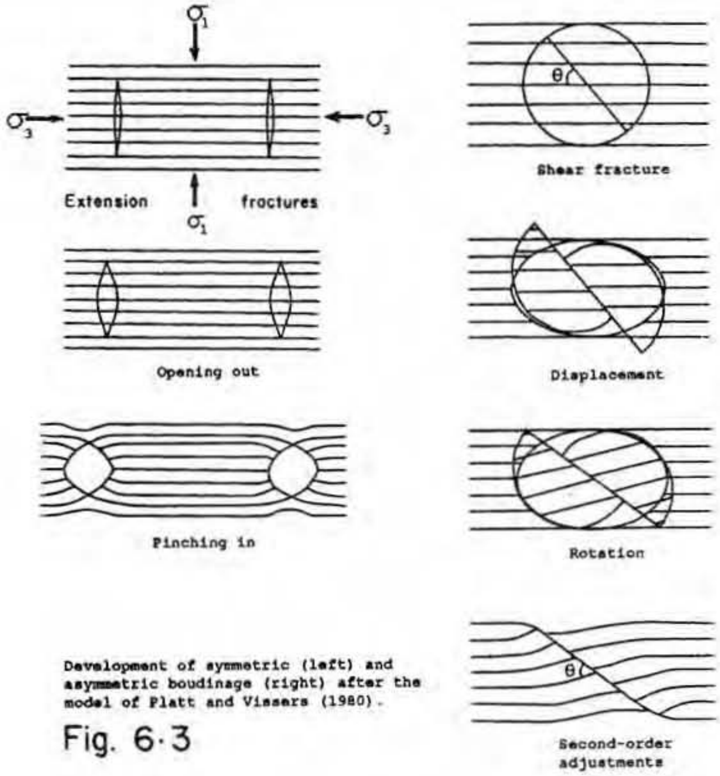

Development of symmetric (left) and asymmetric boudinage (right) after the model of Platt and Vissers (1980).

Fig. 6·3

Fig. 5.19 shows asymmetric boudinage developed in what were calcareous pelites at Mindy and which have since been contact metamorphosed to hornfelses. Layer-parallel extension is thus a component of the deformation of parts of the Thirtymile allochthon. A model of transpression as a result of oblique collision at the Teslin suture could thus explain the orientation of fold axes observed in the Thirtymile Range, i.e. roughly at 45° to the strike of the suture zone.

UPLIFT OF THE TESLIN SUTURE METAMORPHICS:

One obvious feature of the regional geology requires thought: there is a sudden change from amphibolite-grade metamorphics in the suture to lower greenschist grade metasediments to the east (the Englishman's Group). Development of a pressure-solution cleavage in these sediments requires perhaps 7 km of burial to provide adequate hydrostatic pressure. Geobarometric/thermometric estimates for the Teslin Suture are up to 625°C temperature and $p= 8$ kbar for silicate assemblages (i.e. ≈ 26 km depth) and a temperature range of 350-500°C for carbonates (Hansen, 1986b). The lower temperatures for the carbonates are said to reflect a lower temperature regime necessary for ductile flow and recrystallisation in marble. Higher pressures are quoted for eclogite tectonic inclusions within the Nisutlin Allochthon (Tempelman-Kluit, 1979). Much uplift (≈ 20 km) of the core of the suture is therefore apparent. A mechanism for this is provided in Hansen's tectonic model of a change from compression to transcurrent movement. Transpression would provide the necessary uplift of the metamorphic core of the suture (by oblique thrust faulting). Gentle folding of thrust-bounded units of the parautochthonous continental Englishmans group in the Thirtymile area could be produced by blind thrust faulting associated with the major fault bounding the suture zone (Fig. 6.2).

Timing of at least the initial uplift of the western part of the suture is provided by the isotopic work of Hansen et al. (1989). The tectonites west of the d'Abbadie fault in the suture zone were uplifted and cooled through 350° during the Early Jurassic. Rocks east of the fault did not cool through 300°C (K-Ar biotite) until the Middle Cretaceous. Hansen considered that Early Jurassic thrusting caused burial of the footwall (eastern) rocks and proposed a crustal-thickening model after the scheme of England and

Thompson (1984). Rocks of the suture zone are considered to be both from the accreted terranes and essentially autochthonous North American continent (Hansen, 1992): peraluminous granites give U-Pb zircon ages of 355±25 Ma and orthogneiss yields Sm-Nd model ages of 2.0-2.3 Ga, which are consistent with other North American crustal ages (Hansen et al., 1989).

A constraint to the upper limit for the timing of penetrative deformation in the Englishmans Group is the cooling age of the SW Thirtymile stock. The stock is undeformed, yet it intrudes metasediments with a well-developed flat-lying pressure-solution fabric (Fig. 3.24). The Rb/Sr biotite/whole-rock age determined for the western granodioritic intrusion was 181 Ma, i.e. Middle Jurassic. Deformation and transport of the sililiclastic metasediments must therefore predate this time and coincide with either initial deformation of the continental margin (Late Triassic) or uplift of the Teslin suture tectonites (Lower Jurassic).

6.3 PLUTONS

6.3.1 THE SEAGULL-THIRTYMILE PLUTONIC SUITE

The Seagull Batholith, Hake batholith and Thirtymile stock are considered to form one plutonic suite. Evidence for this is:

1) The batholiths are elongated bodies that follow the NW-SE macroscopic fabric of the Northern Cordillera and the Thirtymile stock is on the same trend. The presence of a small stock between the Thirtymile stock and the Hake batholith {60°34'N,132°16'W} (see Mulligan, 1963), plus metamorphism (J. Morin, pers. comm., 1987) at the Bar prospect {60°31'N, 132°16'W} would suggest that the Hake batholith continues NW at relatively shallow depth below the present level of exposure.

2) The Rb/Sr ages of 101.0±4.6 and 100±4 Ma obtained for the Thirtymile stock and an age of 98.3±2.9 Ma for the Hake batholith correlate with the published values of 101±4 and 100±4.3 Ma for the Seagull batholith (Sinclair, 1987).

3) Major and trace element whole-rock geochemistry show linear trends encompassing compositions of all the bodies. There is a progression in composition demonstrated by the various facies of the Thirtymile stock from porphyry through megacrystic and even-grained granites to the Li-mica topaz leucogranite. Compositions of the Hake batholith overlap the ranges of the megacrystic and even-grained facies. Those of the Seagull fall at the more evolved end of the even-grained granite range. Chondrite-normalised 'spidergrams' show similar profiles for each lithofacies, with progressive increase in the size of negative Ba and Sr anomalies toward the more leucocratic facies. Both major- and many trace-element contents of the biotite mica in the granites follow tight linear trends with distinct ranges for each facies. The three Thirtymile biotite-bearing facies are therefore considered to be a serendipitous sampling of the components that formed the underlying batholith. These granites have a potassic low Ca calc-alkaline composition (the H_{LO} notation of Barbarin, 1990), with low Sr content (Fig. 4.32, centre), which separates them from the major W-related Selwyn plutonic suite of the N.W. Territories (Fig. 2.1) and the hornblende-rich gabbro to monzogranodiorite suite of the Thirtymile Range (see 6.3.2 below).

6.3.2 NW AND SW THIRTYMILE HORNBLENDE-RICH STOCKS

These stocks are amphibole-rich intrusions containing epidote and much sphene, and which show alteration of early-formed clinopyroxene first to hornblende then biotite. They are older than the Seagull-Thirtymile granites at Middle Jurassic age (181.5±2.5 Ma). Chemically they are distinct from the Seagull-Thirtymile granite suite, the NW and SW stocks showing volcanic arc-type compositions (Figs. 4.32 & 4.35) and distinct negative Nb anomalies with positive Sr and Rb anomalies on chondrite-normalised trace element diagrams (Fig. 4.25). There is a chemical resemblance of these intrusions to the diorite of the Crescent Lake stock. Their mineralogy and composition is consistent with the low-K high Ca Calc-alkaline (H_{CA}) classification (Barbarin, 1990), indicating a mixed mantle-crustal source and usually associated with generation by subduction. The low Sr initial ratio for the granodiorite of the SW Thirtymile stock (Sr_i= 0.7045) is consistent with derivation by melting of subducted oceanic crust, as are the prominent negative Nb and Th anomalies shown by chondrite-normalised trace element plots.

6.3.3 TECTONIC SETTING OF MAGMATISM IN THE STUDY AREA

TIMING AND TECTONIC PLATE MOTION:

If the SW and NW Thirtymile (plus Crescent Lake diorite) magmas were generated by subduction of oceanic crust, then a comparatively rapid change in polarity of subduction zones from westward subduction of the North American continental margin beneath the island arc terrane to eastward subduction of the Pacific plate beneath both the accreted arc terrane and continental margin is indicated. The Middle Jurassic age (181.5±2.5 Ma) obtained in this study for the SW Thirtymile stock is interpreted to indicate the onset of subduction-generated magmatism at the North American margin. Comparison of this age with the Early Jurassic cooling age of the Cassiar terrane-related tectonites of the Teslin suture (uplift interpreted as being due to A-type subduction-related crustal thickening: Hansen, 1992) indicates that a comparatively short period of time was required for a change in polarity and, presumably a westward jump, of subduction to that of the ancient Pacific plate eastward (Fig. 6.4).

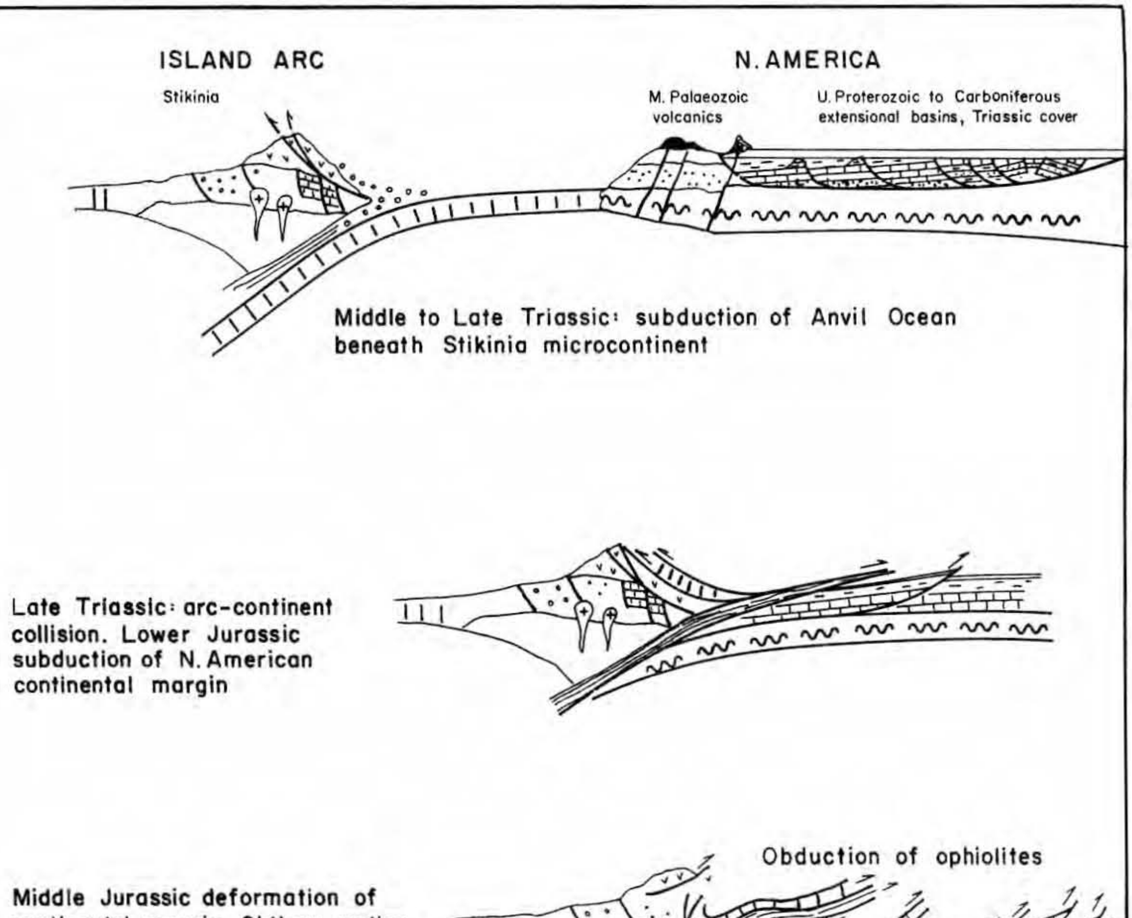

Middle to Late Triassic: subduction of Anvil Ocean beneath Stikinia microcontinent

Late Triassic: arc-continent collision. Lower Jurassic subduction of N. American continental margin

Middle Jurassic deformation of continental margin. Oblique motion along suture. Intrusion of small-volume intermediate-acid plutons in Omineca. No penetrative deformation of westernmost plutons. Rocky Mountain thrust faulting may have commenced.

Cretaceous crustal thickening. Eastward subduction of the Pacific crust beneath accreted & continental terranes. Peak of granite intrusion at 105-95 Ma. Dextral transcurrent faulting (Tintina).

TECTONIC MODEL FOR THE SOUTHERN YUKON

Figure 6·4

(Not to scale)

Adapted from Tempelman-Kluit (1979).

The timing of purely granitic plutonism in the southern Yukon (Albian: ≈105 Ma for the Cassiar and 101 Ma for the Seagull batholith) coincide with estimates of commencement of transcurrent motion on the Tintina Fault by mid Albian time (Gabrielse, 1985) and with change in the plate motion vector of the Farallon Plate with respect to North America from a minor near orthogonal convergent motion to an accelerated dextral strike-slip motion (Engebretson et al., 1985), which would provide a mechanism for local extension. Recent work has shown evidence for major mantle plume activity starting in the Pacific during the Mid Cretaceous, which would produce this acceleration of Farallon plate motion (Larson, 1991).

If, as Price and Carmichael (1986) advocate, small-circle motion along a transcurrent structure resulted in oblique subduction in the southern parts of the Rocky Mountain Fault and transcurrent movement in the Tintina Fault section, a narrow regime of local transtension in the northern Omineca Belt is feasible for that time. Any regional extension following Jurassic to Early Cretaceous crustal thickening by obduction of the imbricated continental margin and accreted terranes accompanied by under thrusting would provide the environment for granitic plutonism. Models for crustal thickening differ according to the part of the Northern Cordillera being considered. Tempelman-Kluit (1979) proposed subduction of the island-arc (later termed Superterrane 1) beneath the continental margin, which agrees with the observed geology in the southern Yukon.

For the region at the latitude of Quesnel, B.C. (some 1025 km SE of this study area), Brown et al. (1986) propose a crustal thickening and wedging model (i.e. underthrusting of continental crust) for the Cordilleran Hinterland. The amount of crustal thickening that occurred at the latitude of the study area during the Cretaceous is unknown. Hansen (1990) notes that whereas the hinterland of the Mackenzie fold and thrust belt was thickened to the extent that orogenic collapse occurred in the Middle Cretaceous, with extension resulting in exposure of underthrust continental wedges, this has not been documented from the Omineca rocks in the southern Yukon. Local extension and uplift of metamorphics in the Horseranch Range core complex due to dextral oblique-slip on a NW-striking normal fault zone has been demonstrated, but not until Eocene time (Plint et al., 1992). This strike-slip faulting was active from mid Cretaceous to Oligocene, and peak metamorphism in that core complex occurred at late

Early Cretaceous time. The timing of peak metamorphism probably indicates maximum crustal thickening in the region. A crustal thickening process, followed by transtension, given sufficient time for melt generation to occur, is likely to provide a magma with a distinct crustal signature which is the case with the Seagull-Thirtymile suite.

ISOTOPIC and CHEMICAL EVIDENCE:

The initial $^{87}Sr/^{86}Sr$ ratio obtained for the Thirtymile granite (porphyry to megacrystic facies= 0.7060-0.7074) of this study agrees well with the distribution of isotopic ratios for Mid to Late Cretaceous magmatism shown by Armstrong (1988, Fig.18). The $^{87}Sr/^{86}Sr_i$ compositions of igneous rocks of the Insular, Coast and Intermontane belts are usually <0.704 and those of the Omineca are notably higher. There is evidence for a Precambrian basement component in Alexander Terrane magmas, and generally higher initial ratios in the Yukon are used as evidence for very variable and, from Middle Cretaceous times, large crustal components in magmas. The $^{87}Sr/^{86}Sr_i$ ratios for the Seagull batholith are 0.712, overlapping the range normally considered to define S-type granites, and for the Selwyn Suite $Sr_i = 0.723-0.739$ (Sinclair, 1987). The ratio for the Thirtymile stock (0.706-0.707) is sufficiently high to require a minor sedimentary component to the magma. The Seagull-Thirtymile granites are closer to the Pitcher I-Caledonian type than to Cordilleran types and are interpreted as reflecting a crustal-thickening origin of magmatism. A time-lag is necessary between thickening of crustal sections and generation of magma (Zen, 1988). Magma may have been generated during the thickening event, requiring the later onset of local extension to provide the mechanics of emplacement and hence giving rise to the seemingly late-tectonic chemical signature (c.f. Pitcher, 1982), with some trace elements falling into the fields normally associated with A-type granites (high Nb content, high Ga/Al ratio).

The hornblende-bearing stocks show a subduction-related composition, and are at least similar in composition to other diorite stocks in the Swift River area. The major intrusion in that region (the Ram stock) has previously been considered to be possibly Jurassic in age due to its altered and deformed nature (Poole et al., 1960; Abbott, 1981). The Crescent Lake stock also has a foliated and altered margin (this study). Such fabric is not conclusive evidence of greater (i.e. synchronous with thrust-faulting) age since intrusion of a pluton into an active shear zone will produce just such effects (Hutton, 1988), however chemical similarity of the SW Thirtymile and Crescent Lake stocks might indicate that the intrusions are consanguineous.

6.4 TIN METALLOGENY

6.4.1 DISTRIBUTION OF MINERALISATION IN THE NORTHERN CORDILLERA

In the northern Cordillera (apart from the plutonic suite presently studied with distinct geochemical 'collision' signature: see also Sinclair, 1987: Fig. 10), tin granites are only known from (a) McQuesten-Mayo district in the Yukon (450 km NNW of the Thirtymile Range: see Emond, 1986; Dick, 1979, and Kwak, 1987: p. 210); (b) the Seagull-Thirtymile suite; and (c) very minor occurrences associated with the western margin of the Cassiar Batholith where the Sn is found largely in silicate minerals, 50 km south of the Yukon border (Blue Light prospect and Ash Mountain area: Mulligan, 1969; Mt. Reed, near Cassiar, B.C.). To the north (150 km) of the Seagull batholith are Mo skarns (Stormy Mountain). Further north, and further inland on the continental margin are the large W deposits associated with the Selwyn plutonic suite: MacTung, CanTung and Lened-Rudy (Emond, 1986; Sinclair, 1986: see Fig. 2.1). Many much smaller W-skarn prospects are known associated with Mid to Late Cretaceous granites that follow the NW-SE Cordilleran trend, immediately SW of the Selwyn Suite plutons, especially associated with the Billings Batholith: Bailey etc. A very broad regional metallogenic distribution thus exists in the Northern Cordillera: Sn-related plutons (lacking a distinct subduction-related signature) were emplaced in the thickened crust at the outboard edge of the craton, minor W- or Mo-related plutons immediately inboard of these and the strongly discordant plutons associated with major W-deposits some 150 km further inboard on the craton.

A sedimentary component to granitic magma is desirable if an inheritance origin for tin in granitic magmas is to be adhered to (Lehmann, 1987). If tin-bearing granites reflect a particularly anomalous source region for magma, then the distribution of such Sn-associated granites poses a perplexing problem of distribution in that they are decidedly sparse, but are known throughout the length of the North American Cordillera.

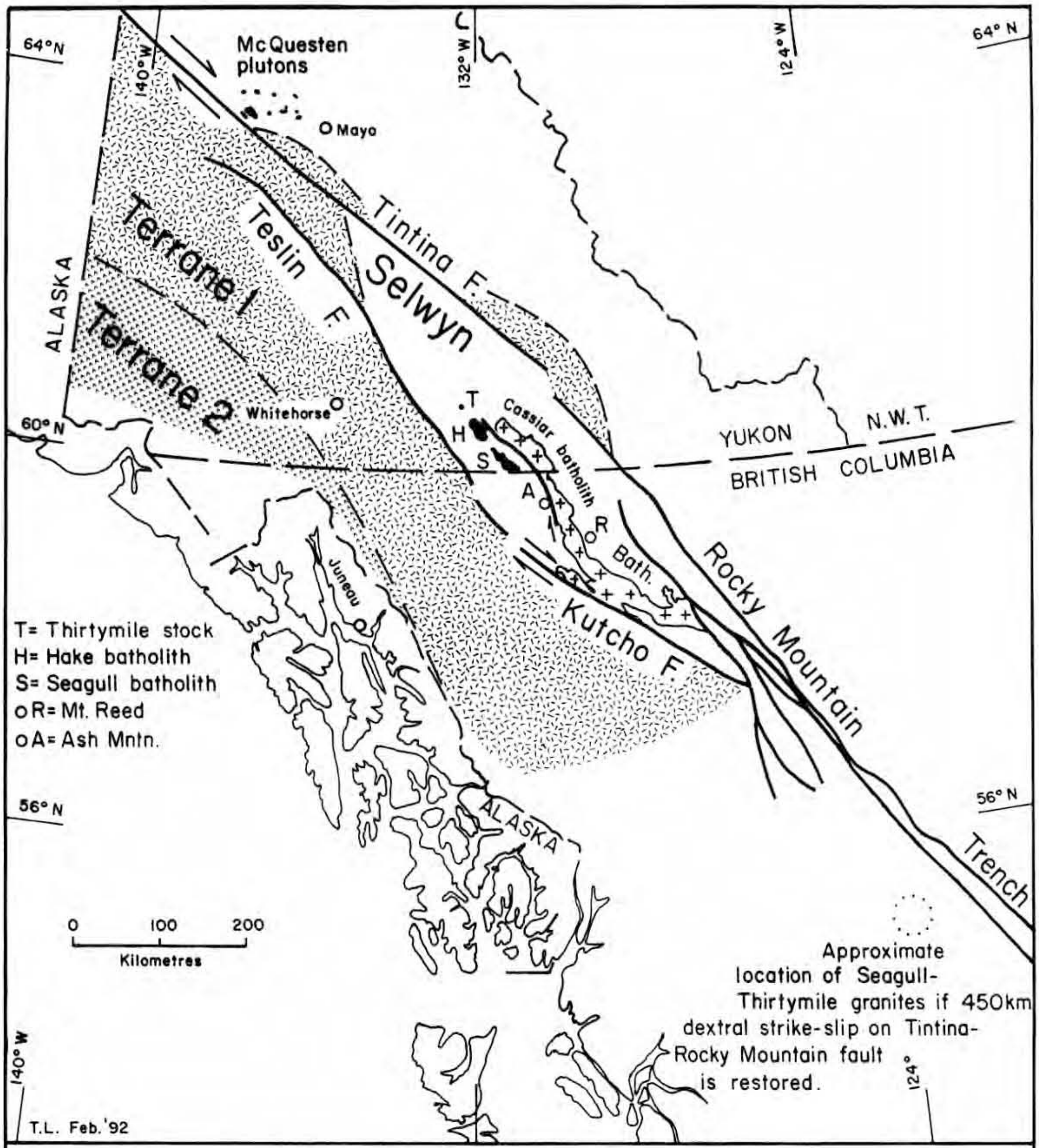

THE TWO GROUPS OF TIN-RELATED PLUTONS IN THE NORTHERN CANADIAN CORDILLERA: McQUESTEN AND THE SEAGULL-THIRTYMILE SUITE.

Geology after Tipper et al. (1981), Hansen (1990) and Emond (1986). Fig. 6·5

For this study region construction of pre-transcurrent Tintina Fault positions (Sinclair, 1986) shows that the McQuesten River and the Seagull Batholith Sn districts are at the very edge of the (preserved) Mesozoic N. American craton (Fig. 6.5). At the time of emplacement they would have been up to 1200 Km apart.

Extremely high Sr_i ratios of the Selwyn suite some 150 km further inboard on the craton suggest a source in the Proterozoic (metasedimentary) lower crust, although considerable contamination of mantle-derived magmas has been suggested (Godwin et. al., 1980; Sinclair, 1986). The lower isotopic ratios of the Seagull suite are consistent with a mixed but mainly I-type source. The I-type Sn-granites have formed at the outer edge of the continent, in the margin thickened by imbrication. Thickening of the continental crust as a result of oblique compressional movement at the Teslin suture (see Ch. 2) is adequate to explain the source region of these magmas and their possible tin-inheritance. No clear evidence for eastward subduction of Pacific terranes before Late Cretaceous-Early Tertiary time exists. The tectonic model proposed by Hansen (1990) requires perhaps minor modification to explain this ≈100 Ma age plutonism: eastward-directed subduction of the accreted terranes beneath the craton may not have commenced until late Middle Cretaceous time (i.e. after 100 Ma).

6.4.2 GRANITE PLUTONS AND TIN DEPOSITS

Plimer (1987) defines five parameters that describe the setting of most tin deposits in terms of tectonics, timing and chemistry:

1) A common association with late, or post-tectonic intrusions in either extensional or shear stress regimes;

2) Source granites appear to have been water-poor low-viscosity melts whose ascent to shallow crustal levels is fracture-controlled;

3) The granites have an anomalous geochemistry;

4) Solidification inward from a pressure-quenched carapace produces multiphase crystallisation and causes retention of volatiles in cupolas;

5) Fluid release is structurally controlled and occurs late in the consolidation of the pluton:

Above 5 km depth in the crust a crystallising hydrous magma will expand due to 'secondboiling', the release of vapour once crystals separate from the melt. At 0.5 kbar pressure the expansion is 60% (Burnham and Ohmoto, 1980). This produces adequate pressure to fracture any consolidated carapace around the pluton and the surrounding country rocks (Plimer, 1987).

Many of these criteria are applicable to the Seagull batholith and Thirtymile stocks. The timing of plutonism coincides with a change from clearly compressive to a transtensional stress regime. Shallow level of crystallisation is indicated by the presence of miarolitic cavities in both the Thirtymile stock and the Seagull batholith. The anomalous geochemistry is very obvious in the Seagull batholith, Thirtymile and Ork stocks. Evidence for a carapace having formed is tenuous for the Thirtymile (depending on interpretation of the nature of the porphyry) and conjectural for the Seagull batholith due to the limited amount of the pluton that was examined (the porphyritic granites with round quartz phenocrysts may be a remnant). Evidence of structural control on the channelling of very late-stage magmatic fluids exists in the distribution of skarns in the Mindy area of the Thirtymile Range.

6.4.3 HIGHLY EVOLVED GRANITES: THE Li-MICA FACIES.

Petrogenesis of the Li-mica topaz leucogranites has been discussed in Ch. 5. An 'ultrafractionation' (Newberry et. al., 1990) process is considered a feasible model for the origin of such chemically anomalous lithofacies, without the need for a unique sub-batholithic source for such magma as has been postulated for Cornwall (Stone and Exley, 1985). In the Alaskan tinfields granites enriched in the lithophile elements and halogens are the latest-intruded facies, as is the case with the Seagull-Thirtymile suite (Puchner, 1986; Swanson et al., 1988).

6.4.4 CONCENTRATION OF Sn IN A GRANITE PLUTON: TIN HERITAGE

The geochemical peculiarities (or 'specialisation") of tin granites are enrichment in Sn, F, B, Rb, Li and Cs with depletion in Ba, Sr, Zr, and Ti. Rayleigh fractionation modelling of such elements has been used both as evidence for and against the derivation of tin granites from sources originally anomalous in Sn (Lehmann, 1982; Pollard et al., 1982), although the final consensus seems to be in favour of the anomalous source region model (Lehmann, 1987). Fractional crystallisation processes may merely concentrate levels of tin in a magma.

Tin and tungsten are the only ore metals in the Cornish mineral field that are likely to have had a largely magmatic source. A study of fluid inclusions and their hydrogen/oxygen isotopic ratios from various stages of mineralisation and alteration associated with the Cornubian granites has shown that the fluid inclusions associated with Sn-W mineralisation have ∂D and $\partial^{18}O$ values that partially overlap the field of K-silicate alteration and that estimated for the magmatic fluids (Alderton and Harmon, 1991). This would suggest that the early mineralisation was formed entirely by magmatic fluids and that some mixing with meteoric water occurred to produce the later Sn mineralisation.

Contents of the Cornubian granites are between 12 and 54 ppm Sn (Alderton, 1981) which, if a value of approximately 10 ppm (e.g. Lehman, 1987) is taken to be the threshold for anomaly, makes them clearly anomalous. A study of trace elements in these granites indicates an evolution toward the Li-mica granite lithofacies enriched Sn in the magma (Stone, 1982). Other 'ore' elements were not concentrated in the granite, but in the aureoles during movement of water accompanying granite emplacement i.e. meteoric circulation. Examples of enrichment in other granites are Portuguese Sn granites (35 ppm); evolved granites of the Krusné Hory Mountains (≤350 ppm). An average for the SW of England is 45 ppm (Stone, 1982). Economic (c.f. merely anomalous) concentrations of Sn in the aureole of the Cornubian batholith may have been formed by later processes: a time span of ≥20 Ma between emplacement of the granite and development of the lode systems is indicated by radiometric ages (Dodson and Rex, 1981 and Hawkes et al, 1975: see Stone, 1982). Remobilisation of the Sn derived from the granites with addition of the other ore metals from the country rocks is implied.

If the initial concentration of Sn in a granite magma is only in the order of 10 ppm (Lehmann, 1987), then efficient means are necessary to concentrate the values even to the highly anomalous levels of 350 ppm such as in the Erzgebirge and much more efficient processes are required to extract the tin and deposit it in economic quantities. Tin is not likely to be transported in magmas simply as the fluoride, even if the presence of F increases the solubility of Sn in silicate melts. High pH values might encourage the concentration of the element into a liquid phase as a hydroxyl-fluoride complex, albeit at only in the order of perhaps ≤10 ppm concentration and the presence of B might further aid the partitioning (Stemprok, 1982; Barsukov and Kuril'chikova, 1966; Eugster and Wilson, 1985; Charoy, 1982). The presence of Cl^- in the system might actually concentrate (i.e. scavenge) Sn under hydrothermal conditions (see Manning and Pichavant, 1984). The second-boiling phenomenon (Burnham and Ohmoto, 1980) provides the trigger for onset of the ultrafractionation process and tin concentration into the fluid phase of the magma system. A shallow emplacement level of the pluton is therefore the most critical necessity for the development of tin concentrations.

6.4.5 GEOCHEMICAL RECOGNITION OF 'SPECIALISED' TIN GRANITES

PREVIOUS STUDIES (ROCK ANALYSIS)

Granitic plutons with an obvious spatial relation to Sn mineralisation are seen to contain extremely fractionated facies or extensive greisenisation (see Smith and Turek, 1976 for discussion), leading to anomalous geochemistry, typically: high SiO_2 content, K/Na ratio, Rb, Li, F and marked depletion in Ba. Whereas elemental ratio trends are inherently difficult to interpret in terms of geochemical models (degrees of partial melting, Rayleigh or crystal-liquid fractionation), the empirical study of these also shows important distributions. There are several studies reported in the literature that have identified numerical parameters that differentiate (tin) ore-bearing granites from barren plutons with varying degrees of certainty. Major element composition, trace elements that change markedly in evolved granites (Li, Rb, Ba and Sr) and trace 'ore' metals have been used.

Tauson and Kozlov (1973) have examined trace elements of various granite types from the USSR. The "plumasitic" leucogranites, which are small, shallow (3-4 km depth of emplacement) bodies considered to be acid differentiates (or perhaps more correctly nowadays, highly fractionated granites) derived from large "palingenic" batholiths, formed as large melt fractions from metamorphic terraines, and show distinct trace-element signatures. Fluorine is up to 5 times higher in the plumasitic type than the palingenic types. Li, Rb, Be, Sn, W, Nb, Ta, and REE are noticeably higher than in the larger batholiths.

The most striking difference is variance (σ^2) of Li and Sn contents shown between unmineralised and mineralised granites of the one region reported by those authors. The values of (σ^2) for Li are reported to be 25 times greater in mineralised plutons compared to that in barren granites. Tin variance is shown to be from 18 to 77 times greater for the ore-bearing plutons. Of the trace elemental ratios they show that Ba/Rb is the most dramatically changed parameter in fractionated, mineralised leucogranites. Examples given are changes from 15 to 0.26 (a decrease of 57x) in unmineralised and mineralised Czechoslovakian granites and from 2.5 to 0.03 (decreasing by 83x) in Mongolian examples. Li/K is reported to be highest (i.e. $>2\text{x}10^{-3}$) in the F-associated plutons, i.e. those likely to be associated with Sn.

Smith and Turek (1976) tested the use of the preceding parameters in a study of three Nova Scotia granites. The New Ross pluton, which is considered by them to have the highest potential for significant tin mineralisation shows a Ba/Rb ratio that decreases 20 times; Li/K is given as $>5\text{x}10^{-3}$. Obvious Rb enrichment and increased variance of Li, Rb, Zn and Sn are demonstrated for this pluton. In contrast the West Dalhousie pluton displays Ba/Rb ratios that decrease only 3.3 times and Li/K $\leq 2.4\text{x}10^{-3}$ with a correspondingly lower amount of Rb enrichment. Intermediate values are shown in the third pluton.

Hesp and Rigby (1974) examined a large number of analysed granites from the Lachlan Fold Belt of eastern Australia using the Kohler-Raaz indices as compositional parameters. They specify a narrow range of compositions that contain 80% of the Sn-bearing leucogranites of their data set, corresponding to high SiO_2 types. They also note that levels of Sn content of the rocks is an additional parameter to be considered in recognition of the ore-bearing granites since some barren plutons will also have similar Kohler-Raaz indices to the less-fractionated tin granites.

The mineralised Jurassic biotite granites of Nigeria have elevated SiO_2 (75.49 vs. 71.52) compared to unmineralised hornblende-bearing facies (but here silica content alone is not diagnostic since the unmineralised peralkaline riebeckite granites are also quite silica-rich); Larsen Index is 15.12 compared to 14.20 and K/Na is not significantly changed. Rb is higher; Sr is lower; Ba is markedly lower than the hornblende-facies and also than unmineralised biotite facies; Li is roughly double; Zr is depleted; Zn and Pb are higher and Cu shows no significant trend (Olade, 1980).

Alkali ratios (Li/K and K/Na) are broadly indicative of Sn-related granites. Ryabchikov et al. (1974) note that in continental margin plutonic belts a lateral zonation toward increasing K_2O content of plutons is evident and suggest that it might reflect depth and degree of partial melting of source regions, particularly melting of biotite. They also comment that biotite is also the principal silicate phase in which F and Sn are likely

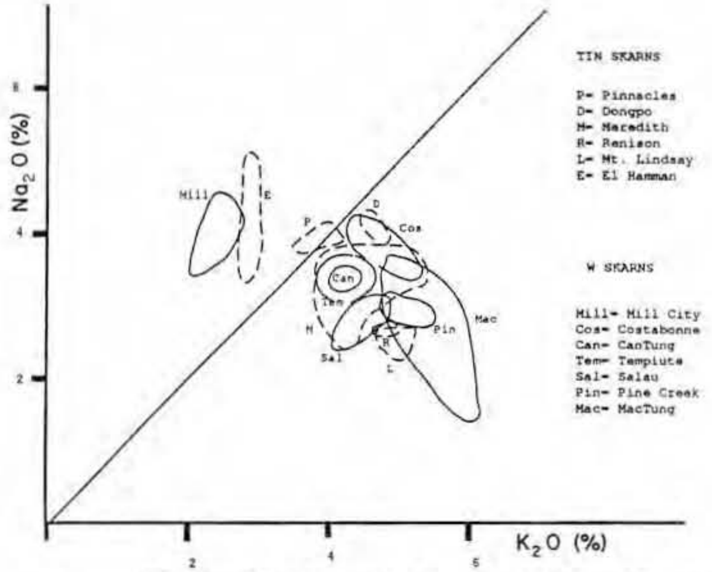

Ratio of alkalies for granites associated with Sn and W skarns
After Kwak (1987).

Fig. 6.6

to be found. These observations are used to explain the correlation of Sn with relatively high K granites. The average major-element composition of granites associated with both W and Sn skarn deposits have been compiled by Kwak (1987). Relative enrichment in K for the Sn-granites is indicated by plots of Na_2O to K_2O: the W granites have composition that fall either side of the 1:1 line but those of the Sn association are decidedly skewed toward higher K values (Fig. 6.6). Higher silica contents and low Fe* and Mg are generally found in granites associated with B-F bearing Sn-skarn deposits compared to those proximal to W-skarns (Table 6.3).

In general, whole-rock tin content of obviously mineralised granites is not necessarily greatly elevated, but a threshold of 10-15 ppm Sn does often identify stanniferous plutons. Tin-mineralised plutons do show a great range of metal contents: some may not appear anomalous whilst others will have hundreds of ppm of Sn (see Tauson and Kozlov, 1973). Nova Scotian granites do show slightly higher values in the more evolved New Ross granite (Smith and Turek, 1976). Similarly, the stanniferous plutons of the Tasman geosyncline are generally anomalous in Sn (Hesp and Rigby, 1974), although individual analyses may not be (Flinter et al., 1972).

The choice of analytical data to use for comparative study is to a large extent dictated by laboratory practice and economics: Li is not determined in XRF analyses and has only been available for the present work because of the use of ICP analysis in addition to XRF; Mo presents potential difficulty of incomplete digestion if HF digestion is used as in the ICP 'traces' programme used in this study, as does Zr. F, B and Be require separate techniques and trace W and Sn require the use of instrumental neutron activation analysis (INAA), the latter being particularly time-consuming, since a radiochemical separation is required after irradiation of the specimen (Alderton and Moore, 1981). Analyses showing all of these elements are rarely published.

Highly evolved stanniferous plutons are most easily recognised when a number of trace-element analyses that span the complete compositional range in a magmatic suite are available. One or two specimens may not prove diagnostic. The trends toward Rb enrichment and corresponding depletion in Sr and Ba in these intrusions result in an extreme range in elemental ratios, particularly K/Rb and Ba/Rb and often Ba/Sr that far exceeds the range of these ratios in 'normal' granites. These ratios may be used to identify potentially tin-bearing granites particularly when considered in conjunction with range of silica content; differentiation index; Rb, HFSE, Li and F content; and mica composition (Swanson et al., 1990; Nedachi, 1980; Scott, 1988; Imeokparia, 1982). This study also demonstrates the validity of these criteria.

A version of the Larsen index has been used in this study for simplicity of calculation from other workers' data. The Thornton-Tuttle index (defined as the sum of CIPW normative Quartz+Orthoclase+Albite+ Nepheline+Leucite+Kalsilite) has been shown to be equally useful (Swanson et al., 1991, Nakapundgrat, 1981) as well as the Kohler-Raaz indices (Hesp and Rigby, 1974).

Selection of suitable ranges of chemical parameters for recognition of tin granites will be influenced by the possible depth to which that pluton has been eroded: those that have only just been exposed will show their apical portions that may well be expected to be the most enriched in halogens, LIL, incompatible and alkali elements. More deeply exhumed granites would not be expected to demonstrate such extreme chemistry (see discussion in Smith and Turek, 1976), even if they are tin granites. Since many tin deposits are grouped directly above apophyses, or at least lateral to cupolas (e.g. Cornwall), the more deeply eroded granites may have had the bulk of their Sn-mineralisation already removed and may not have potential for significant remaining mineralisation.

ROCK ANALYSIS: THIS COMPARATIVE STUDY

Various parameters have been calculated from data published and that obtained in this study (Appendix B.12, summary table 6.1). Suitable parameters for recognition of the 'specialised' plutons are:

(1) Sn-mineralised granites are silica-rich (>71% SiO_2).

(2) K/Na is not always diagnostic, but is often >1. Mineralised plutons do have high K (i.e. $0.92 \leq K/Na \leq 2.3$) but so do some S-type granitoids of the Massif Centrale, where no mineralisation is obvious (this may have existed and been subsequently eroded).

(3) Rb contents are higher in the mineralised examples. The unmineralised Massif Centrale examples considered here have <294 ppm, the mineralised examples of this study (Appendix B.12) have >253 ppm. A level of >300 ppm is suggested as approximate threshold for anomaly. Relative Rb enrichment is obvious when Sr is plotted against Rb. The two elements follow a generally hyperbolic distribution (as might be

expected if a fractionation process is dominant), with the plutons of the Sn deposits falling toward the low Sr/higher Rb field (Fig. 6.7).

(4) Ba contents are very variable. In the Massif Centrale examples the range is from 484-927 ppm. In the mineralised granites Ba content can be >700 ppm, but ranges down to <30 in the suites examined. A large range in the one plutonic suite, with values dropping to a few tens of ppm indicates highly fractionated plutons.

(5) Sr contents are also quite variable (144-513 ppm in the Massif Centrale examples) but in the mineralised areas (Cornubia; Sardinia; Torington, N.S.W) are <175 ppm and may drop to <1 ppm. Very low Sr levels are considered to be diagnostic of tin-potential.

(6) K/Rb ratio shows a general decrease with increasing Rb in the unmineralised examples, but by a factor of about 0.8. The mineralised examples show greater reduction (by a factor of 0.6 to 0.14).

(7) Ba/Rb may decrease by a factor of about 0.25 in the unmineralised example, but in the mineralised examples it is < 0.03. This parameter seems especially useful in defining the 'ultrafractionated' plutons.

8) Ba/Sr may increase or decrease.

Pluton	SiO2	L	K/Na	Rb	K/Rb	Ba/Rb	Ba/Sr
Guéret	63.50-71.72	9.50-13.82	1.63-1.42	184-216	205.7-173.5	5.33-2.30	1.8-3.0 (Var.)
Millevaches	65.61-71.26	10.79-14.00	1.20-2.03	179-233	223.6-183.2	4.20-3.26	1.6-3.4 (Var.)
Margeride	65.65-72.56	10.82-13.59	1.65-1.83	198-294	187.8-140.2	4.42-1.07	3.1-1.9 (Clear)
Lachlan F.B.	67.15-74.87	8.31-15.16	0.81-2.42	92-526	156.5-798.6	5.38-0.37	1.2-3.2
Sardinia	65.5-74.5	>10->15.5	0.98-1.95	253-493	162-96	1.54-0.54	7.7-18.0
Mole	75.75-78.09	15.37-16.36	1.43-1.96	379-817	117.8-49.2	0.36-0.01	4.1-1.6 (Var.)
Seagull Suite	72.70-75.61	14.70-15.07	1.72-0.92	304-2087	160.2-17.1	2.76-0.01	3.6-22.1 (Clear)
Cornubian	71.10-74.20	13.68-17.34	1.28-2.03	419-2293	100.2-14.3	0.86-0.02	0.7-20.6

Table 6.1 Selected elemental ratios for unmineralised & mineralised granites.

From this very limited data set it appears that a 'specialised' tin granite suite might be expected to show: SiO_2 >71%; high Rb= >250 ppm, with increase in the one plutonic suite by >2x; very variable Ba, by a factor ≈30x; very variable Sr but probably= <175 ppm; K/Rb ratio decreasing by a factor of ≥0.6x with increase in Rb; Ba/Rb ratio in particular showing spectacular decrease with increasing Rb: by a factor of <0.1x throughout a stanniferous granite suite. The large range of elemental ratios and contents is perhaps the most useful indication of the highly fractionated granites. In order to use trace

SOURCE	REGION	TYPE	MICA	F (%)	Mg/Fe*	Li_2O (%)
Nedachi (1980)	Kyushu, Japan	Unmineralised	Biotite	0.21-0.52	0.607-0.263	Not given
Nedachi (1980)	Kyushu, Japan	Pb-Zn	Biotite	0.41-0.85	0.309-0.249	Not given
Nedachi (1980)	Kyushu, Japan	Sn	Biotite	0.5-2.11	0.463-0.114	Not given
Scott (1988)	N.S.W., Aust.	Unmineralised	Biotite	Not given	>0.54	Not given
Scott (1988)	N.S.W., Aust.	Sn-mineralised	Biotite	Not given	<0.33	Not given
Stone et al., 1988	Cornubian	Granite 'B'	Biotite	0.77-4.53	0.224-0.034	0.57-1.59
Stone et al., 1988	Cornubian	Granite 'E'	Li-mica	4.75-7.31	0.046-0.000	2.61-4.02
Stone et al., 1988	Cornubian	Granite 'G'	Li-mica	6.17-7.41	0.078-0.000	4.43-5.81
This study	Yukon	Por. & Mega.	Biotite	0.96-1.84	0.165-0.089	0.09-0.43
This study	Yukon	Hake	Biotite	0.65-2.03	0.158-0.060	0.17-0.37
This study	Yukon	Seagull	Biotite	1.76-2.33	0.073-0.013	0.11-0.88
This study	Yukon	Li-mica leuco.	Zinnwaldite	6.46-7.55	0.004-0.001	1.83-4.67

Table 6.2 F and Li contents & Mg/Fe* ratios for micas from Sn-mineralised and unmineralised areas.

TYPE OF SKARN ASSOCIATED	SiO_2, Range	SiO_2	Al_2O_3	Fe_2O_3	FeO	MgO	CaO	Na_2O	K_2O	TiO_2	MnO	P_2O_5	H_2O	F	S	CO_2	TOTAL	Number
Proximal Sn skarn±F/B overprint	70.63-79.52	74.39	13.18	0.22	1.14	0.27	0.91	2.93	4.79	0.17	0.04	0.06	0.91	0.21	0.06	0.23	99.51	36
Proximal Sn skarn, high F/B	71.47-78.14	74.4	12.66	0.24	1	0.14	0.52	3.28	4.68	0.08	0.03	0.01	1.12	0.15	0.01	0.37	99.03	20
Proximal Sn-W skarn with economic W>Sn	66.74-75.31	72.62	12.53	0.6	1.95	0.93	1.92	3.03	4.46	0.34	0.07	0.1	0.96	0.49	0.02	0.1	100.25	11
Distal Sn skarn	67.32-74.65	72.64	13.47	0.45	1.55	0.41	1.32	2.88	4.96	0.2	0.04	0.11	0.9	0.2	0.09	0.34	99.56	25
Meinert average of Sn skarns	75.4-78.0	76.6	12.6	0.4	1	0.2	0.5	2.8	4.6	0.03	0.1	0.01	x	x	x	x	98.84	9

Table 6.3 Average compositions of granites associated with various Sn skarn types (after Kwak, 1987).

'ore' metal contents as indicators of economic potential (as in Tauson and Kozlov, 1973) a large number of samples from any one magmatic suite is required in order to examine the variance rather than absolute levels.

MICA ANALYSIS

Mica compositions from 'specialised' granites are quite distinctively enriched in Li, F and have low Mg/Fe* ratios (although Fe* content may be lower in the mineralised examples). Scott (1988) has shown that of all plutons examined in his broad regional study, those unaltered plutons with associated Sn mineralisation have a Fe/(Fe+Mg+Mn) >0.75. This is approximately equivalent to Mg/Fe* <0.33. The micas of this study are within this range, with the one exception of those from the Mt. Reed W±Sn-related stock, which have high F, but also high Mg/Fe* (see Section 6.5.3).

6.5 TIN SKARNS

6.5.1 STRUCTURAL CONTROLS ON TIN/TUNGSTEN MINERALISATION IN THE THIRTYMILE RANGE

The location of mineralisation is entirely controlled by the structural history of the Thirtymile Range. The following parameters are required for skarn-type tin mineralisation:

(1) Proximity to the upper part of a pluton that is an HHP or 'specialised' granite and which carries anomalously high Sn contents. Concentration of the Sn into the apex of the pluton by halogen- or B-complex transport is also required. Sudden pressure release (hydrofracturing of the consolidated granite 'carapace' and aureole is therefore required. This places depth limitations on level of emplacement of these plutons, i.e. perhaps <3 km.

(2) Carbonate sediments must be within the contact aureole or convection cell of magmatic/meteoric fluids.

(3) Adequate permeability must exist in the cover rocks to allow protracted circulation of such magmatic and meteoric water sources.

Structural control on mineralisation in the Thirtymile consists of distribution of the marble units, which was determined during thrusting and shearing of the allochthon and in the extensional faulting which accompanied granite emplacement. This faulting not only allowed initial injection of magmatic fluids into the carbonates, but continued fault movement fractured early formed skarns and permitted the formation of a wide range of retrograde silicate skarn assemblages as well as extensive localised B/F metasomatism and greisen-skarns. This continued fracturing is perhaps one element of Sn skarn deposits that is underestimated in importance and rarely emphasised in the literature. In the prograde skarn early-formed pyroxenes are diopside; later replacement along fracture systems is by predominantly salitic pyroxene, but which may cover a range to hedenbergite- johannsenite. The abundance of Fe-rich fracture-introduced pyroxenes in DDH 3 compared to the diopside of the intersection in adjacent DDH 1, only 50 metres away is evidence of very limited transport of metasomatic fluid by percolation through the unfractured marble.

As a general observation the W skarns of the Cordillera have some fracturing present, but its importance in mineralisation is much less obvious. Good grades of scheelite mineralisation are possible in 'tight' host rocks.

6.5.2 Sn-SKARNS: GENERAL CHARACTERISTICS AND COMPARISONS.

Some general observations can be made regarding proximal Sn and W skarns (after Kwak, 1987):

(1) Primary skarns may be oxidised (Fe^{2+}/Fe^{3+} low), reduced or mixed in one deposit.

(2) Both calcic and magnesian types are found. In calcic types substitution of Sn into silicate phases is common. In the magnesian types a separate Sn phase is usual. Proximal magnesian types are rarely economic, even though assay grades are high as Sn concentrates into metallurgically refractory minerals.

(3) Sn skarns are associated with reduced, ilmenite-series granites.

On a worldwide scale granites associated with these skarns are predominantly S-type.

(4) Molybdoscheelite is associated mainly with oxidised Fe^{3+}-rich skarns whilst pure scheelite is found in reduced skarn. Magnetite-series granites may have either type associated, but the ilmenite types tend to have scheelite only (exceptions are rare).

(5) W skarns are never greisened.

(6) W skarns are predominantly silicate-rich. Sn skarns may have silicate-, magnetite- or sulphide-rich varieties.

(7) Many Sn skarns are wrigglites. These textures are unknown in W types.

(8) No correlation exists between Sn content of skarns and magnetite or sulphide content. When magnetite occurs most of the Sn occurs with it.

(9) Sn skarns of ore grade rarely produce W as well (the inverse grade relationship is demonstrated at Mindy).

(10) Sn minerals formed early (in primary skarn) in the proximal skarns are usually re-dissolved during retrograde alteration or greisening and may be lost.

(11) Sn-andradite garnet skarns are sub-economic: the garnet concentrates most of the Sn.

(12) Sn content of greisen exo-skarns is high (2-10%). Greisen-altered skarns that are phyllosilicate rich are typically of low grade.

The Mindy skarns have many features in common with several other Sn-skarns.

(1) Oxidation state, pH and mineralogy: Both calcic and magnesian mineralogies are present. Textures indicate that this bulk chemistry is largely remnant from shearing of the marble protolith during deformation of the Englishmans Group. An association with an ilmenite-series granite is inferred from the nearest outcropping intrusion (the Ork stock). Skarn mineralogy (Ch. 5) is further evidence of the reduced nature of the intrusion (see Table 2.6 & Fig. 4.2 of Kwak, 1987). Where scheelite is found on the surface it is always the blue-fluorescing variety i.e. virtually Mo-free, similarly indicating reducing conditions during deposition. Progressively more Fe-rich pyroxene replacement in the high-temperature skarns likely indicates a gradual decrease in pH of the hydrothermal fluid. K-metasomatism (phlogopite-phengite greisen-skarn overprint) immediately following a massive Fe and Sn mineralising episode indicates further increase in acidity of the fluids.

(2) Tin mineralisation: early-deposited Sn occurs as cassiterite with magnetite. No high Sn grades in silicate phases have been found. The highest assay grades (Appendices B.5 & B.7) are found where appreciable amounts of Fe-Mg borate minerals occur. It is estimated that >50% of the Sn in this prospect is contained in hülsite and ludwigite. No

significant Sn mineralisation has been noted to be associated with the phlogopite or ferrophengite greisen overprint that followed the wrigglite development.

6.5.3 TIN IN SILICATE MINERAL PHASES AND GRANITE TYPE

Some skarn deposits which carry the higher grades of Sn in a silicate mineral rather than cassiterite are associated with the tungsten-bearing granites that have a less-evolved composition than those associated with more widespread Sn occurrence. The reasons for partitioning of tin into early-formed silicate skarn minerals are unclear, but are likely to reflect the nature of the granite magma and relative timing of release of volatiles into the aureole of the intrusion. One readily accessible Sn-silicate occurrence was sampled in this study for purposes of comparison of a W±Sn-related intrusion with the Sn±W types: Mt. Reed, Cassiar district British Columbia. At this skarn scheelite prospect Sn is found only in andradite that forms discordant veins cutting marble approximately 15 metres from the contact of a leucocratic biotite granite stock. This garnet carries up to 3% SnO_2 (J. Watkins, Canadian Superior Exploration, pers. comm.). The granite at Mt. Reed is texturally similar to those of the Seagull batholith and to the Li-mica lithofacies of the Thirtymile stock, in that equant quartz phenocrysts are prominent. Chemically, however, the granite is not highly evolved: it has a low Rb/Sr ratio and comparatively high Ba/Rb and K/Rb ratios (Table 6.4). The biotite in the Reed granite has a composition comparable to that at the CanTung scheelite deposit (c.f. van Middelaar and Keith, 1990) and, although it contains a moderate F content (a level comparable to that in the megacrystic facies of the Thirtymile stock), the Cl content is very low. High F and low Cl contents are typical of the zinnwaldite in the Li-mica leucogranites of the Thirtymile that have been postulated to underlie the Mindy prospect and the low Cl content of the mica is interpreted as indicating the loss of much of the Cl from the magma during the 'ultrafractionation' and mineralising processes. The similarly low Cl content at Mt. Reed is considered indicative of the early release of a mineralising hydrothermal fluid from the apical portion of this stock. It is postulated that comparatively low f_F conditions in this magma prevented any major Sn concentration prior to transport into the aureole as Cl-complexes. No determination of Fe^{2+} is available for the mica of this granite, however the high Mg/Fe* ratio of the mica is interpreted to indicate that the granite is a magnetite-series pluton (Ilmenite-series plutons have decreasing Mg/Fe* with increasing fractionation and magnetite-series granite show the opposite trend: Ishihara, 1981), hence the f_{O_2} of its magma is expected to have been significantly higher than that of the Seagull-Thirtymile suite granites. The greater activity of oxygen may have an effect on the partitioning of the Sn into a silicate phase.

PLUTON	GRANITE:		FRACTIONATION INDICES		MICA
	L	Rb/Sr	Ba/Rb	K/Rb	Mg/Fe*
Seagull-Thirtymile suite	14.7-15.7	2.4-2300	2.75-0.01	160-17	0.001-0.179
Tin granites	12.5-17.3	10.2-48	0.95-0.01	153-33	
Unmineralised granites	8.3-15.1	0.23-8.6	5.38-0.37	799-140	
CanTung					0.279-0.330
Mt. Reed	14.2-14.6	1.3	2.4	140	0.395-0.409

Larsen Index, L= (1/3Si+K)-(Mg+Ca). Fe* is total Fe.
Sources: Tin- & unmineralised-granites: see Appendix 7.1; CanTung mica: van Middelaar & Keith (1990).

Table 6.4 Comparison of Mg/Fe* ratio of micas & fractionation indices of Mt. Reed granite with CanTung, tin mineralised & unmineralised granites.

6.5.4 SKARN AND GRANITE TYPE: THIRTYMILE RANGE

The unexposed stock beneath the Mindy prospect is likely to be similar to the F-rich leucogranites of the Ork stock and dykes, the nearest outcropping intrusions. The chemistry of this leucogranite is of the type expected to produce Sn-F skarns. It has high F content and the Rb/Sr ratio of these leucogranites (Fig. 4.32, Tables 4.7 & 6.4) exceeds any published analyses examined for the comparative study i.e. they are extremely evolved. Fe content is low and the Fe content of the micas is predominantly in the Fe^{2+} oxidation state (Fig. 4.28), indicating a reduced (ilmenite-type) magma. Skarn mineralogy also suggests formation under relatively reducing, high f_F conditions. These observations are consistent with the granite type normally found in association with high-F Sn-skarns (Fig. 6.7, 6.8, 6.9 & Tables 6.1 & 6.3). The chemistry of the F-B-rich skarns and the leucogranites is thus complementary.

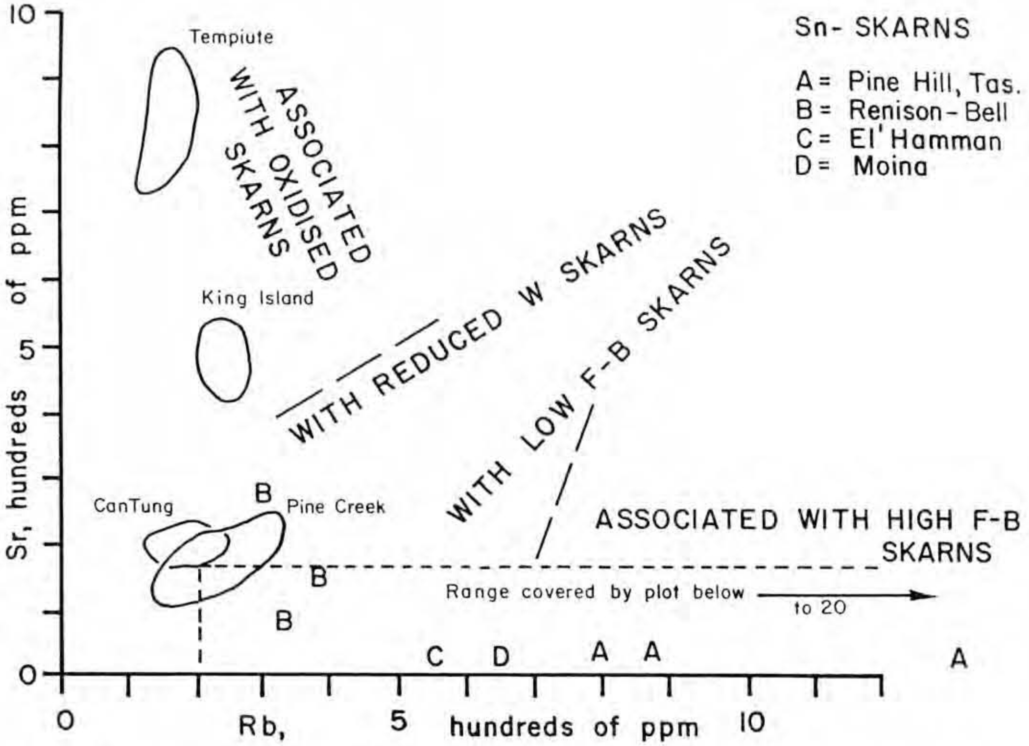

Rb - Sr variation of granites associated with various W & Sn skarn types (after Kwak, 1987).

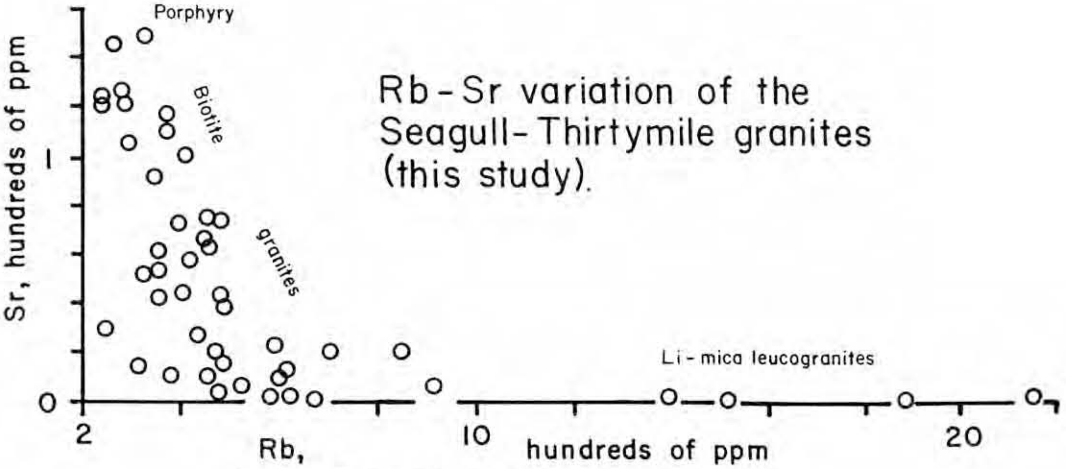

Rb - Sr variation of the Seagull - Thirtymile granites (this study).

Figure 6·7

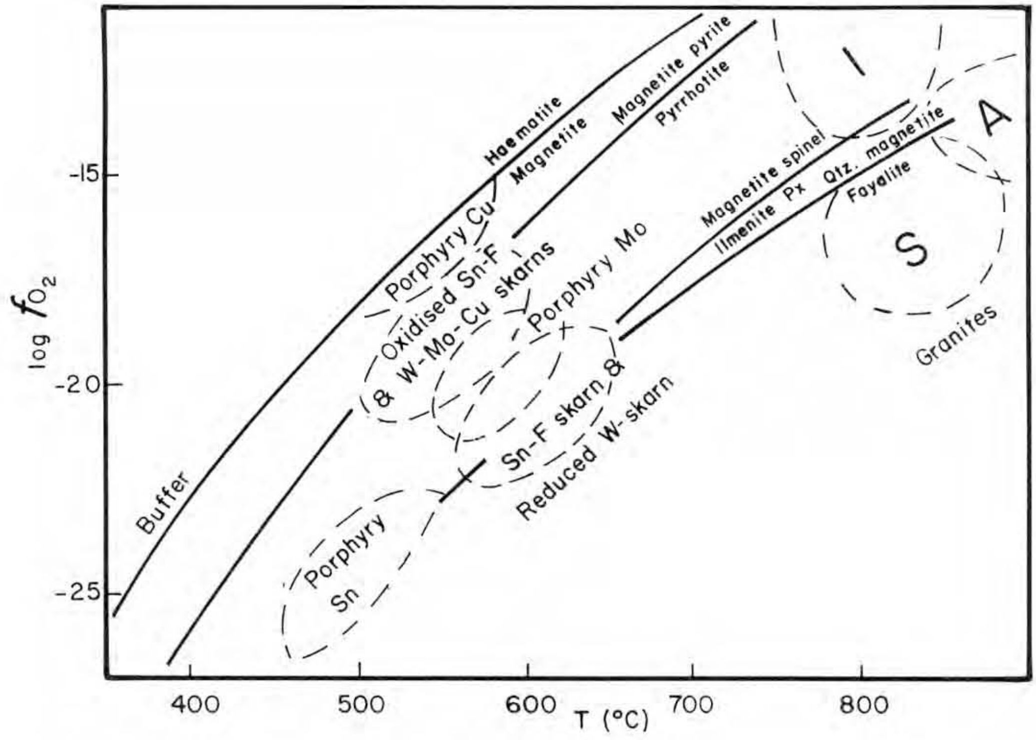

Figure 6·8 Temperature – log f_{O_2} diagram showing conditions of skarn formation at p=1 kb. (After Kwak, 1987)

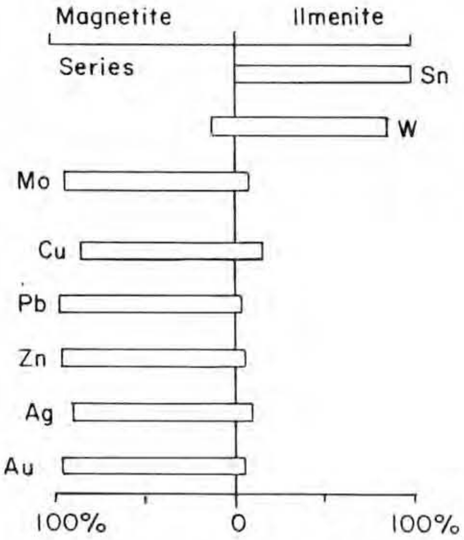

Figure 6·9 Types of mineral deposits associated with Japanese I- & S-type granites. After Ishihara (1980).

6.6 MINERAL EXPLORATION

6.6.1 RECOMMENDATIONS

The importance of active faulting on the development of the skarns at the Mindy prospect has already been postulated in Chapter 5. Metasomatism of the Mindy marble unit would have been very restricted without active fracturing. The main fracture systems are also possible exploration targets:

Steeply-dipping fractures that have penetrated the siliceous metasediments above both skarn horizons carry pyrrhotite mineralisation. Below the main skarn unit the few fractures that have been intersected in the short interval of drillhole to extend below the skarn level show tourmaline and fluorite mineralisation. These two levels of fracturing should be considered as exploration targets, as well as others:

1) Below the skarns- (depending on the depth to the intrusion): potential exists for stockwork cassiterite or even greisen zones along the granite margin.

2) Above and between the skarns the sulphide-filled fracture systems have potential to carry gold (no assays were made by the exploration company), particularly if meteoric circulation was important in the late-stages of hydrothermal activity.

3) The north side of the Mindy extensional fault system is covered by glacial débris for the whole width of the valley. Pyrrhotite-skarn float (see 1:25,000 scale map; Appendices B.1 & B.2) to the NE of the detail map area was used to infer a throw component on the northernmost fault shown on the longitudinal section (bottom of Appendix B.1) There is no reason why further tin mineralisation should not exist there.

4) Other unexposed highly fractionated granite apophyses may exist at a shallow depth beneath the southern part of the Thirtymile Range where, according to the regional mapping of Mulligan (1963), meta-conglomerate is the predominant lithology in the Englishmans Group. Coarse clastic sediments are the host rock to the larger tin veins at Irvinebank (Herberton tinfield), Queensland. Similar occurrences are possible in the Thirtymile Range. Systematic prospecting directly for tin has not been attempted in this mountain range.

CHAPTER 7

CONCLUSIONS

CHAPTER 7: CONCLUSIONS

7.1 REGIONAL GEOLOGY: THE DORSEY TERRANE

7.1.1 THE ENGLISHMAN'S GROUP

This study has shown that the upper, predominantly siliciclastic, sequence of the Englishman's Group (Unit 3 of Mulligan, 1963), is not a simple sedimentary succession as previously mapped. It is an east-verging low metamorphic grade thrust belt composed of discontinuous siliciclastic and carbonate units, that are mappable only for distances <5 km and which have undergone variable amounts and styles of deformation. The fabric of L-S tectonites within this succession is consistent with a generally ENE transport direction of the allochthon. Extension of the tectonites occurred normal to this transport direction and a (near horizontal) shear sense of top-to-the-east has been deduced. These fabrics are consistent with oblique collision of allochthonous terranes and the ancestral continental margin. A lithological correlation of part of this sequence with the Devonian Lower Earn Group and with units uDMps and Mt of Gordey (1981) in the Indigo Lake map area is proposed. No fossils were found within this sequence. The Mississippian (Mulligan, 1963: Unit 2) carbonates which crop out to the west of the Thirtymile Range may correlate with the carbonates overlying the Lower Earn Group in the Kechika area (McClay et al., 1989). If this is so, then unit 3 is older than 2 and thrust over it. This interpretation would imply that the Dorsey terrane is not an accreted terrane, but is parautochthonous North American North American continental margin.

7.1.2 INTRUSIONS: TWO SUITES

Two undeformed plutonic suites have intruded the imbricated Englishmans Group and the Palaeozoic sediments of the Yukon Cataclastic Complex in the Englishman's and Dorsey Ranges:

1) The Thirtymile stock (of four lithofacies: porphyry; even-grained granite; megacrystic granite and Li-mica leucogranite), Hake batholith and Seagull batholith form one suite,

here called the Seagull-Thirtymile Suite. These one-mica granites display an evolutionary trend from biotite-hornblende granite to highly evolved Li-mica topaz-fluorite leucogranites that are proximal to Sn±W-bearing skarn mineralisation. They are ilmenite-series, calc-alkaline I-type intrusions with much similarity to HHP (U-Sn mineralised) granites. Rb-Sr whole-rock and biotite (isotope-dilution) isochrons have been obtained for the Thirtymile stock giving ages of 101.0± 4.6 Ma with a Sr_i ratio= 0.707 for the megacrystic lithofacies; 100±4 Ma for the Li-mica lithofacies and a Sr_i ratio= 0.705 calculated for the porphyry. Biotite-wholerock Rb/Sr dating for the Hake batholith gives an age of 98.3±2.9 Ma. Their trace-element chemistry is consistent with a within-plate tectonic setting and is distinct from the major W-related Selwyn suite granites found ≈150 km further inboard of the N. American craton. The latter suite has greatly elevated Sr_i ratios and distinctly higher Ba relative to Rb+Sr contents in their least evolved lithofacies.

2) The NW and SW Thirtymile stocks are hornblende-rich stocks displaying gabbro to monzogranodiorite lithofacies. Their major and trace element compositions cannot be readily correlated with the trend of the previous suite, but there is similarity with the Crescent Lake diorite stock in the Swift River area, 75 km SE. They display a calc-alkaline trend, as do the Seagull-Thirtymile granites, but one that is more consistent with derivation in a subduction-related environment. Biotite-wholerock Rb/Sr dating of the granodiorite of the western part of the SW Thirtymile stock gave an age of 181.5±2.5 Ma and Sr_i ratio= 0.70450±3, thereby providing clear evidence of this pluton being from a magmatic suite different to the Thirtymile stock. It is postulated that these intrusions were derived from magmas generated early in the subduction of ancestral Pacific oceanic crust beneath the accreted Terrane 1 and the North American continental margin.

7.1.3 TECTONIC MODEL

The sequence of structural events directly affecting the Thirtymile Range is:

1) Imbrication and brittle-ductile deformation of the mid Palaeozoic sediments in the thrustbelt of the Yukon Cataclastic Complex. Formation of local mylonites.

2) Intrusion of Middle Jurassic subduction-related intermediate to acid magma as small stocks.

3) Extension producing mainly ENE-WSW striking minor faults.

4) Intrusion of the Middle Cretaceous Seagull-Thirtymile plutons with continued very minor post-emplacement extensional fault movement. Contact metamorphism and metasomatism.

These observations are consistent with the tectonic models of Tempelman-Kluit (1979), Monger et al. (1982), Price and Carmichael (1986) and Hansen (1990): the Englishmans group parautochthon (portion of the Dorsey terrane) represents distal N. American strata that were deformed and transported to the ENE during collision of Terrane 1 with the N. American continent. Timing of initial penetrative deformation during thrust transport is at the latest ≈181 Ma (undeformed granites and brittle extensional faults cut the thrust stack: this study). The earliest likely transport is Early Jurassic (closure of the ocean basin: Hansen, 1990). These conclusions, however, imply that the Dorsey terrane is not accreted (Wheeler and McFeely, 1991) but is parautochthonous.

Generation of the Seagull-Thirtymile granite magmas in continental crust thickened by underthrusting (e.g. Brown et al., 1986, England and Thompson, 1984) is consistent with their chemistry and their Sn-bearing character. An extensional environment for emplacement of these plutons may have been provided by the onset of transcurrent motion along the Tintina-Rocky Mountain fault system.

7.2 CORDILLERAN TIN METALLOGENY

7.2.1 TINFIELDS

Only two tinfields of any areal extent have been recognised in the northernmost Canadian Cordillera (McQuesten and Seagull-Thirtymile). It is suggested that these plutonic suites have had distinct crustal sources for their magmas, i.e. a tin inheritance, that was different from the W-related granitic suites to the east. These plutons may be related to magma generation from crustal thickening by underthrusting rather than subduction, hence timing and location relative to the ancient continental margin may have contributed to the scarcity of these 'specialised' granites.

7.2.2 THE SEAGULL-THIRTYMILE SUITE: ULTRAFRACTIONATION

Generation of the Seagull-Thirtymile plutonic suite from a mixed I-type and metasedimentary source, with minimal or no subduction contribution, in continental crust thickened by contraction would supply an initially anomalous amount of Sn (i.e. >15 ppm) to the granitic magma. An ultrafractionation process is adequate to explain the origin of the Li-F-B-rich leucogranites in the Thirtymile Range, the concentration of halogens, B and Sn at the apex of the granite stocks. This requires that the stanniferous pluton be emplaced at a sufficiently shallow depth to allow hydrofracturing of any granite carapace and the country rocks to occur.

Trends in major and trace element chemistry shown by the Seagull-Thirtymile Suite are:

1) Biotite granites show chemical trends consistent with protracted feldspar fractionation from the source magma. Content of incompatible trace elements increases with silica content.

2) The leucogranites demonstrate a reversal of the trends from the elemental levels contained in the most evolved of the biotite granites. Although Rb contents are rapidly increased, Al_2O_3 and alkali trends are reversed. Some of the incompatible trace elements

(notably Nb), which are concentrated with evolution of the biotite granites, are depleted in the leucogranites. The composition of these leucogranites is consistent with experimental data for melting of granite systems which contain B and much F: increase in halogen content produces albite-rich granite. A drastic change in distribution coefficients of many elements is indicated by the chemical trends of these granites. Such changes are consistent with the ultrafractionation model of Newberry et al. (1990) and experimental data of Webster and Holloway (1990) for very F-rich granite melts. This process is adequate to explain the generation of these anomalous granites that occur at the apex of a cupola, without the need to consider a special magma source as in the case of the Cornubian Li-rich granites (Stone and Exley, 1985; Manning and Hill, 1990).

Emplacement and cooling history of the pluton are therefore more important to Sn metallogeny than the origin of the magma.

7.2.3 STRUCTURAL CONTROL ON MINERALISATION

Extensional faulting preceded and accompanied emplacement of the granite stocks in the Thirtymile Range. Outcropping Sn- and W-skarn mineralisation is adjacent to ENE striking faults. Continued faulting and small-scale fracturing (fracture-reaction-seal) of early prograde skarns at the Mindy prospect allowed development of progressively Fe-rich prograde pyroxene skarn followed by retrograde skarn mineral assemblages and structurally localised Sn mineralisation. Comparatively local transport of Fe-rich solutions away from fault zones is shown in resulting pyroxene compositions. Skarns developed in the thick marble as limited mantos out from the faults and as discordant small, irregular vein replacements.

7.2.4 CHEMICAL TRENDS IN SKARN FORMATION

The Mindy skarns show mineralogies that are consistent with
1) Primary skarn formation initially by addition of mainly silica to a dolomitic protolith. Compositions of pyroxenes progressed from pure diopside to ferrosalite with successive fracture-introduced mineralogies, indicating increased Fe introduction, which is consistent with gradual decrease in pH of hydrothermal fluids. Early F introduction

appears as clinohumite or chondrodite. More aluminous or calcic marble protoliths produced local andradite-vesuvianite skarn, scapolite in diopside calc-silicate hornfels and epidote minerals in marble. Some sulphide iron (pyrrhotite) has accompanied the early silicates. No major Sn-silicate mineralisation has been observed.

2) Massive Fe introduction, primarily in discordant skarn, as magnetite that partially replaces the pyroxenes of early-formed skarn and forms massive replacement in marble. Cassiterite mineralisation accompanies this stage, which is consistent with metal transport by a Cl-rich stage of fluid evolution.

3) F-B metasomatism. Development of Fe-Mg±Sn borates. Replacement of earlier-formed silicates.

4) K alteration as greisen replacement of skarns: phlogopite and minor ferrophengite. Fluorite is the main mineralisation introduced at this stage. Timing may accompany later stage (3).

5) Retrograde silicate alteration: amphibole/chlorite alters pyroxene, garnet and vesuvianite assemblages. Late fractures allow serpentine alteration, sometimes accompanied by late boron minerals (e.g. szaibelyite).

7.2.5 SKARN AND GRANITE TYPE

The chemistry of Sn-F skarns and highly evolved granites are complementary. The composition of the leucogranite of the Thirtymile Range is comparable to the types found elsewhere associated with Sn-F-B skarns. The extremely high Rb and very low Sr content of the granite; high F and Li content and low Mg/Fe* ratios of the micas are typical of such intrusions. The reduced nature of the granite magma is reflected in the high Fe^{2+}/Fe^{3+} content of the micas. The skarns show a corresponding F-rich reduced type mineral assemblage. Low content of Sn in early-formed skarn silicate phases is considered a result of comparatively reducing conditions prevailing during skarn formation i.e. a direct result of low f_{O_2} in the granite magma. A massive release of magmatic Cl is envisaged as causing the main Fe-Sn mineralising stage.

7.3 MINERAL EXPLORATION

7.3.1 RECOMMENDATIONS

Tin mineralisation in the Thirtymile Range consists of both cassiterite and Sn-bearing borates, these latter phases containing at least half of the Sn contained in the Mindy prospect. Since the borates are metallurgically refractory the Mindy is unlikely to be of major economic interest in the immediate future. Skarns that contain mainly cassiterite, as well as small cassiterite quartz stockworks are found peripheral to the Seagull batholith. There is potential for further mineralisation to exist in the Thirtymile as stockwork systems. The on-strike continuation of extensional fault systems has not been prospected, neither has much of the Range below the tree-line. The Range south of Mindy may well have unexposed granite apophyses at a shallow depth that carry surrounding Sn mineralisation as either stockworks or skarns.

7.3.2 RECOGNITION OF TIN GRANITES

A comparative study of published analytical data from tin-related granites shows that plutons associated with significant mineralisation are quite geochemically anomalous. There seems to be little difference between the chemical signature of Cordilleran and Continental types. It is suggested that late-stage magmatic processes are more important than source of magma in the generation of granites that are associated with economic-grade Sn mineralisation. From this very limited data set some parameters for recognition of these anomalous granites are suggested:

SiO_2 >71%; high Rb= >250 ppm, with increase in the one plutonic suite by >2x; very variable Ba, by a factor ≈30x; very variable Sr but contents <175 ppm; K/Rb ratio decreasing by a factor of ≥0.6x with increase in Rb; Ba/Rb ratio in particular showing spectacular decrease with increasing Rb: by a factor of <0.1 throughout a stanniferous granite suite.

The large range of these elemental ratios and contents is perhaps the most useful indication of the highly fractionated granites. In order to use trace 'ore' metal contents as indicators of economic potential (as in Tauson and Kozlov, 1973) a large number of samples from any one magmatic suite is required in order to examine variance rather than absolute level.

Mica composition also distinguishes the 'specialised' tin granites. Mg/Fe* ratio alone is distinctive. The micas from granites in this study have a range of Mg/Fe* from 0.165 to 0.001 for least to most evolved lithofacies. The threshold value of ≈0.33 (from Scott, 1988) for mineralised plutons would include all lithofacies analysed in this study; all Cornubian micas (Stone et al., 1990); some, but not all Kyushu Sn-mineralised granites (Nedachi, 1980) and some of the Selwyn Suite W-granites (van Middelaar and Keith, 1990, Keith et al., 1990). It is a very conservative level. A value of ≤0.15 would certainly discriminate the 'ultrafractionated' leucogranites. Li contents are obviously elevated in such granites, but the levels vary considerably between ore-fields. F content >0.6% in micas does discriminate most Sn-related plutons.

REFERENCES

REFERENCES

Abbey, S. (1983): Studies in "standard samples" of silicate rocks and minerals 1969-1982.
Geol. Surv. Can. Paper 83-15, pp. 114.

Abbott, J.G. (1981): Geology of Seagull tin district.
in: Yukon Geology and Exploration 1979-80: Exploration and Geological Services Division, Yukon, Indian and Northern Affairs Canada. p. 32-44.

Abbott, J.G. (1982): Structure and stratigraphy of the Macmillan fold belt; evidence for Devonian faulting.
in: Yukon Exploration and Geology 1981: Exploration and Geological Services Division, Yukon, Indian and Northern Affairs Canada. p. 22-33.

de Albuquerque, C.A.R. (1973): Geochemistry of biotites from granitic rocks, Northern Portugal.
Geoch. et Cosmochim. Acta, V. 37 p 1779-1802.

Alderton, D.H.M. and Harmon, R.S. (1991): Fluid inclusion and stable isotope evidence for the origin of mineralizing fluids in South-west England.
Min. Mag. V. 55 p. 605-611.

Alderton, D.H.M. and Jackson, N.J. (1978): Discordant calc-silicate bodies from the St. Just aureole, Cornwall.
Min. Mag. V. 42, p 427-434.

Alderton, D.H.M. and Moore, F. (1981): New determinations of tin and tungsten in granites from southwest England.
Min. Mag. V. 144, p 354-356.

Alderton, D.H.M., Pearce, J.A. and Potts, P.J. (1980): Rare earth element mobility during granite alteration: evidence from southwest England.
Earth Planet. Sci. Lett. v. 49, p. 149-165.

Aleinikoff, J., Dusel-Bacon, C., Foster, H.L. and Futa, K. (1981): Proterozoic zircon from augen gneiss, Yukon-Tanana Upland, east-central Alaska.
Geology, 9: p. 469-473.

Aleksandrov, S.M. (1985): Geochemistry and mineralogy of tin and boron in skarn deposits.
In: High heat production (HHP) granites, hydrothermal circulation and ore genesis. Inst. Min. Metall. London. p. 425-435.

Al-Saleh, S., Fuge, R. and Rea, W.J. (1977): The geochemistry of some biotites from the Dartmoor granite.
Proc. Ussher Soc. V.4, p. 37-48.

Ames, L.L. (1961): The metasomatic replacement of limestones by alkaline, fluoride-bearing solutions.
Econ. Geol. V.56 p. 730-739.

Anderson, J.L. and Bender, E.E. (1989): Nature and origin of Proterozoic A-type granitic magmatism in the southwestern United States of America.
Lithos, V.23, p. 19-52.

Anderson, R.G. (1983): Selwyn plutonic suite and its relationship to tungsten skarn mineralization, southeastern Yukon and district of Mackenzie.
in: Current Research, Part B, Geological Survey of Canada, Paper 83-1B, p. 151-163.

Arakawa, Y. (1990): Strontium isotopic compositions of Mesozoic granitic rocks in the Hida belt, central Japan: diversities of magma sources and of processes of magma evolution in a continetal margin area.
Lithos V. 24 p. 261-273.

Armstrong, R.L. (1988): Mesozoic and early Cenozoic magmatic evolution of the canadian Cordillera.
in: Clark, S.P., Burchfiel, B. and Suppe, J., eds. Processes in continental lithospheric deformation. Geol. Soc. Amer. Special Paper 218 p. 55-91.

Armstrong, R.L., Taubeneck, W.H. and Hales, P.O. (1977): Rb-Sr and K-Ar geochronometry of Mesozoic granitic rocks and their Sr isotopic composition, Oregon, Washington and Idaho.
Bull. Geol. Soc. Amer. V.88, p 397-411.

Ashley, P.M. and Plimer, I.R. (1989): "Stratiform skarns"- a re-evaluation of three eastern Australian deposits.
Mineral. Deposita. V.24, p 289-298.

Atherton, M.P. and Plant, J.A. (1985): Hight heat production granites and the evolution of the Andean and Caledonian continental margins.
In: High heat production (HHP) granites, hydrothermal circulation and ore genesis. Inst. Min. Metall. London. p. 459-478.

Atkinson, W.W. and Einaudi, M.T. (1978): Skarn formation and mineralization in the contact aureole at Carr Fork, Bingham, Utah.
Econ. Geol. V.73, p. 1326-1365.

Barbarin, B. (1990): Granitoids: main petrogenetic classifications in relation to origin and tectonic setting.
In: Atherton, M.P. and Naggar, M.H., eds., Granite. Symposium celebrating the 70th birthday of W.S. Pitcher. Geol. Jour. V. 25, p. 227-238.

Barr, S.M. (1990): Granitoid Rocks and terrane characterization: an example from the northern Appalachian Orogen.
in: Atherton, M.P. and Naggar, M.H. eds., Granite: Symposium celebrating the 70th birthday of W.S. Pitcher. Geol. Jour. V. 25, p. 295-304.

Barsukov, V.L. and Kuril'chikova, G.Ye. (1966): On the forms in which tin is transported in the hydrothermal solutions.
Geochem. Int. V.3, p 759-764.

Bartholome, P. (1970): Minerais et skarns dans les aureoles de metamorphisme.
Mineral. Deposita, V. 5, p. 345-353.

Bayliss, P., Erd, D.C., Mrose, M.E., Sabina, A.P. and Smith, D.K. (1986): Mineral powder difffaction file.
JCPDS- International Centre for Diffraction Data, Swarthmore, PA, U.S.A. pp. 467

Bencini, A. and Hall, A. (1988): A reconnaissance study of ammonium content in rocks of the Tuscan granitic province.
Periodico di Mineralogia, V. 57, p. 671-674.

Biste, M. (1982): Geochemistry of south Sardinian granites compared with their tin potential.
in: Evans, A.M. ed: Metallization associated with acid magmatism. Wiley p. 37-49.

Blusson, S.L. (1968): Geology, Frances Lake, Yukon Territory and District of Mackenzie.
Geol. Surv. Can. Map 6-1966.

Bonazzi, P. and Menchetti, S. (1989): Contribution to the crystal chemistry of the minerals of the ludwigite-vonsenite series.
Neu. Jahrb. Miner. Mh. 1989, H2, p 69-83.

Bowden, P. (1982): Magmatic evolution and mineralization in the Nigerian younger granite province.
in: Evans, A.M. ed., Metallization associated with acid magmatism. Wiley p. 51-61.

Bowden, P. and Kinnaird, J.A. (1984): Petrological and geochemical criteria for the identification of potential ore-bearing Nigerian granitoids.
Proc. 27th. Int. Geol. Cong., Moscow. Abstracts V.4, p. 271-272.

Bowman, J.R., Covert, J.J., Clark, A.H. and Mathieson, G.A. (1985): The CanTung E Zone orebody, Tungsten, Northwest Territories: oxygen, hydrogen, and carbon isotope studies.
Econ. Geol. V.80, p. 1872-1895.

Bremner, T. and Liverton, T. (1991): Crescent, Dan *property descriptions in:*
Yukon Exploration 1990. Exploration and Geological Services Division, Yukon, Indian and Northern Affairs Canada: p. 25-30.

Brown, I.J. and Nesbitt, B.E. (1987): Gold-copper-bismuth mineralization in hedenbergite skarn, Tombstone Mountains, Yukon.
Can. Jour. Earth Sci. V. 24, p. 2362-2372.

Brown, P.E., Bowman, J.R. and Kelly, W.C. (1985): Petrologic and stable isotopic constraints on the source and evolution of skarn-forming fluids at Pine Creek, California.
Econ. Geol. V.80, p. 72-95.

Brown, R.L. and Read, P.B. (1983): Shuswap terrane of British Columbia-a Mesozoic "core complex".
Geology, V.11, p. 164-168.

Brown, R.L., Journeay, J.M., Lane, L.S., Murphy, D.C. and Rees, C.J. (1986): Obduction, back-folding and piggy back thrusting in the metamorphic hinterland of the southeastern Canadian Cordillera.
Jour. Struct. Geol. V. 8 p. 255-268.

Bucher-Nurminen, K. (1989): Reaction veins in marbles formed by a fracture-reaction-seal mechanism.
Eur. J. Mineral. V.1 p. 701-714.

Burnham, C.W. (1967): Magmas and hydrothermal fluids.
in: Barnes, H.L. ed: Geochemistry of hydrothermal ore deposits, Holt, Rinehart & Winston, New York, p. 34-76.

Burnham, C.W. (1959): Contact metamorphism of magnesian limestones at Crestmore, California.
Bull. Geol. Soc. Amer. V.70, p. 879-919.

Burnham, C.W. and Ohmoto, H. (1980): Late-stage processes of felsic magmatism.
in: Ishihara, S. and Takenouchi, S: Granitic magmatism and related mineralization. Mining Geology Special Issue No.8.
Society of Mining Geologists of Japan. p. 1-11.

Burt, D.M. (1978): Tin Silicate-borate-oxide-equilibria in skarns and greisens- the system CaO-SnO_2-SiO_2-H_2O-B_2O_3-CO_2-F_2O_{-1}
Econ. Geol. V.73, p. 269-282.

Burt, D.M. (1982): Skarn deposits. Historical bibliography through 1970
Econ. Geol. V.77, p. 755-763.

Burt, D.M. (1984): Relation of lithophile element mineralization to acid magmatism, western U.S.A.
Proc. 27 Int. Geol. Cong. Moscow. Abstracts, V.4, p. 273.

Burt, D.M., Sheridan, M.F., Bikun, J.V. and Christiansen, E.H. (1982): Topaz rhyolites- distribution, origin, and significance for exploration.
Econ. Geol. V. 77, p. 1818-1836.

Bussell, M.A. (1988): Structure and petrogenesis of a mixed-magma ring dyke in the Peruvian Coastal Batholith: eruptions from a zoned magma chamber.
Trans. Roy. Soc. Edin. Earth Sciences. v. 79, p. 87-104.

Butler, R.F., Harms, T.A. and Gabrielse, H. (1988): Cretaceous remagnetization in the Sylvester Allochthon: limits to post 105 Ma northward displacement of north-central British Columbia.
Can. Jour. Earth Sci. V.25, No 8, p. 1316-1322.

Campbell, and Stephen, J.C. (1982): Unpublished report on file as assessment work (091364) at the Watson Lake mining Recorder's Office.

Campbell, K.B. Mountjoy, E.W. and Struik, L.C: Structural cross-section through south central Rocky and Cariboo Mountains to the Coast Range.
Geol. Surv. Can. OF844.

Castro, A. (1987): On granitoid emplacement and related structures. A review.
Geol. Rundschau V.76/1 p. 101-124.

Chandra Kumar, S. (1988): Microgranular enclaves in granitoids: agents of magma mixing.
Journal of Southeast Asian Earth Sciences V.2 Nos 3/4 p. 109-121.

Cook, F.A., Green, A.G., Simony, P.S., Price, R.A. Parrish, R.R., Milkerheit, B., Gordy, P.L., Brown, R.L., Coflin, K.C. and Patenaude, C. (1988): Lithoprobe seismic reflection structure of the southeastern Canadian Cordillera: initial results.
Tectonics V. 7 p. 157-180.

Chappell, B.W. and Stephens, W.E. (1988): Origin of infracrustal (I-type) granite magmas.
In: The origin of granites. Trans. Roy. Soc. Edin. V.79, p. 71-86.

Chappell, B.W., and White, A.J.R. (1974): Two contrasting granite types.
Pac. Geol. V.8 p. 173-174.

Chappell, B.W., White, A.J.R. and Hine, R. (1988): Granite provinces and basement terranes in the Lachlan Fold Belt, southeastern Australia.
Aust. Jour. Earth Sci. V.35, p. 505-521.

Chappell, B.W., White, A.J.R. and Wyborn, D. (1987): The importance or residual source material (restite) in granite petrogenesis.
Jour. Pet. V.28, p. 1111-1138.

Charoy, B. (1982): Tourmalinization in Cornwall, England.
in: Evans, A.M. ed: Metallization associated with acid magmatism.
Wiley. p. 63-70.

Chatterjee, A.K. and Strong, D.F. (1985): Review of some chemical and mineralogical characteristics of granitoid rocks hosting Sn, W, U, Mo deposits in Newfoundland and Nova Scotia.
In: High heat production (HHP) granites, hydrothermal Circulation and ore genesis. Inst. Min. Metall. London. p. 489-516.

Chernhall, B.E., Jones, B.G. and Carr, P.F. (1988): Contact metamorphism of pelitic, psammitic and calcareous sediments in the Southern Highlands of New South Wales.
Aust. Jour. Earth Sci. (1988) 35, p. 389-401.

Churkin, M., Foster, H.L., Chapman, R.H. and Weber, F.R. (1982): Terranes and suture zones in east central Alaska.
J. Geophys. Res. V.87, p. 3718-3730.
Clark, D.B. and Muecke, G.K. (1985): Review of the petrochemistry and origin of the South Mountain batholith and associated plutons, Nova Scotia, Canada.
in: High heat production granites, hydrothermal circulation and ore genesis. Institution of Mining and Metallurgy, London. p. 41-54.

Clark, J.R. (1965): Crystallographic data for the iron borate mineral hulsite.
Am. Mineral. V.50, p. 249-254.

Clemens, J.D. (1988): Volume and composition relationships between granites and their lower crustal source regions: an example from central Victoria, Australia.
Aust. Jour. Earth Sci. V. 35, p. 445-449.

Clemens, J.D. and Vielzeuf, D. (1987): Constraints on melting and magma production in the crust.
Earth Planet. Sci. Lett. V. 86, p. 287-306.

Clemens, J.D. and Wall, V.J. (1981): Origin and crystallisation of some peraluminous (S-type) granitic magmas.
Can. Mineral. V.19, p. 111-131.

Clemens, J.D. and Wall, V.J. (1988): Controls on the mineralogy of S-type volcanic and plutonic rocks.
Lithos, V. 21, p. 53-66.

Cocirta, C., Orsini, J.B. and Coulon, C. (1989): Exemples de mélange de magmas en contexte plutonique: les enclaves des tonalites-granodiorites du massif de Bono (Sardaigne septrionale).
Can. J. Earth Sci. V. 26, p. 1264-1281.

Collins, B.I. (1977): Formation of scheelite-bearing and scheelite-barren skarns at Lost Creek, Pioneer Mountains, Montana.
Econ Geol. V. 72, p. 1505-1523

Collins, P.L.F. (1981): The geology and genesis of the Cleveland tin deposit, Western Tasmania- fluid inclusion and stable isotope studies.
Econ. Geol. V. 76, p. 365-392.

Collins, W.J., Beams, S.D., White, A.J.R. and Chappell, B.W. (1982): Nature and Origin of A-type granites with particular reference to southeast Australia.
Contrib. Min. Pet. V. 80, p. 189-200.

Coney, P.J. (1980): Cordilleran metamorphic core complexes: an overview.
in: Crittenden, M.D., Coney, P.J. and Davis, G.H: Cordilleran Metamorphic Core Complexes. Geol. Soc. Amer. Memoir 153 p. 7-31.

Coney, P.J., Jones, D.L. and Monger, J.W.H. (1980): Cordilleran suspect terranes.
Nature, V.288. p. 329-333.

Conrad, W.K., Nicholls, I.A. and Wall, V.J. (1988): Water-saturated and undersaturated melting of metaluminous and peraluminous crustal compositions at 10Kb: evidence for the origin of silicic magmas in the Taupo volcanic zone, New Zealand and other occurrences.
Jour. Pet. V.29, p. 765-803.

Cooke, B.J. and Godwin, C.I. (1984): Geology, mineral equilibria, and isotopic studies of the McDame tungsten skarn prospect, north-central British Columbia.
Econ. Geol. V. 79, p. 826-847.

Czejtey, B., Cox, D.P., Evarts, R.C., Sticker, G.D. and Foster, H.L. (1982): The Cenozoic Denali fault system and the Cretaceous accretionary development of southern Alaska.
J. Geophys. Res. V.87, p. 3741-3754.

Daly, S.F. and Raefsky, A. (1985): On the pentration of a hot diapir through a strongly temperature-dependant viscosity medium.
Geophys. J. Roy. Ast. Soc. V.83, p. 657-682.

Dana, E.S: A Texbook of Mineralogy.
Fourth Ed. (1932) by Ford, W.E.
Wiley, New York. pp. 851.

Darbyshire, D.P.F., and Shepherd, T.J. (1985): Chronology of granite magmatism and associated mineralisation, SW England.
Jour. Geol. Soc. Lond. V. 142, p. 1159-1173.

Dawson, K.M. (1979): Regional metallogeny of the Northern Cordillera: recent stratiform base metal discoveries in Yukon Territory and District of Mackenzie.
in: Current Research: Geol. Surv. Can. Paper 79-1A, p. 375-376.

Dawson, K.M. and Dick, L.A. (1978): Regional metallogeny of the northern Cordillera: tungsten and base metal skarns in southeastern Yukon and southwestern Mackenzie.
In: Current Research Part A: Geol. Surv. Can. Paper 78-1A, p. 287-292.

Debon, F. and LeFort, P. (1988): A cationic classification of common plutonic rocks and their magmatic associations: principles, method, applications.
Bulletin Minéral. V.111, p. 493-510.

Deer, W.A., Howie, R.A. and Zussman, J. (1962): Rock forming minerals.
5 vols., Longmans, London.

Dick, L.A. (1979): Tungsten and base metal skarns in the Northern Cordillera.
In: Current Research Part A: Geol. Surv. Can. Paper 79-1A, p. 259-266.

Dick, L.A. and Hodgson, C.J. (1982): The Mactung W-Cu (Zn) Contact Metasomatic and related deposits of the Northeastern Canadian Cordillera.
Econ. Geol. Vol.77, p. 845-867.

Didier, J. (1987): Contribution of enclave studies to the understanding of origin and evolution of granitic magmas.
Geol. Rundschau 76/1, p. 41-50.

Dill, H. (1985): Granite-related and granite-induced ore mineralization on the western edge of the Bohemian Massif.
In: High heat production (HHP) granites, hydrothermal circulation and ore genesis. I.M.M. Lond., p. 55-70.

Dingwell, D.B., Harris, D.M. and Scarfe, C.M. (1984): The solubility of H_2O in melts in the system SiO_2-Al_2O_3-Na_2O-H_2O at 1 to 2 Kbars.
Jour. Geol. V.92. p. 387-395.

Dinman, Ye.N. and Nekrasov, I.Ya. (1965): Hydrothermal synthesis of Nordenskioldine and its analogues.
Doklady, Earth Sciences Section, V.164, p. 129-133.

Dobson, D.C. (1982): Geology and alteration of the Lost River Tin-Tungsten-Fluorine Deposit, Alaska.
Econ. Geol. 77 p. 1033-1052.

Dodson, M.H. and Rex, D.C. (1971): Potassium-argon ages of slates and phyllites from south-west England.
Q. J. Geol. Soc. Lond., V. 126, p. 465-499.

Douglas, R.J.W., Gabrielse, H.; Wheeler, J.O., Stott , D.F.and Belyea, H.R: Geology of western Canada.
In: Geology and Economic Minerals of Canada. Geol. Surv. Can., p. 367-488.

Eadington, P.J. (1983): A fluid inclusion investigation of ore formation in a tin-mineralised granite, New England, New South Wales.
Econ. Geol. V.78, p. 1204-1221.

Einaudi, M.T. (1977): Petrogenesis of the copper-bearing skarn at the Mason Valley Mine, Yerrington District, Nevada.
Econ. Geol. V.72, p. 769-795.

Einaudi, M.T. and Burt, D.M. (1982): Introduction- terminology, classification and composition of skarn deposits.
Econ. Geol. Vol.77, p. 745-754.

Einaudi, M.T., Meinert, L.D. and Newberry, R.J. (1981): Skarn Deposits.
Econ. Geol. 75th. Ann. Vol., p. 317-391.

Eisbacher, G.H. (1970): Deformation mechanics of mylonitic rocks and fractured granites in Cobequid Mountains, Nova Scotia, Canada.
Geol. Soc. Amer. Bull. V.81, p. 2009-2020

Eisbacher, G.H. (1974): Evolution of successor basins in the Canadian Cordillera.
S.E.P.M. Special pub. 19, p. 274-291.

Eisbacher, G.H. (1977): Mesozoic-Tertiary basin models for the Canadian Cordillera and their geological constraints.
Can. Jour. Earth Sci. V.14, p. 2414-2421.

El Sharkawi, M.A.H. and Dearman, W.R. (1966): Tin-bearing skarns from the north-west border of the Dartmoor granite, Devonshire, England.
Econ. Geol. V. 61, p. 362-369.

Emond, D.S., (1986): Tin and Tungsten veins and skarns in the McQuesten River area, central Yukon.
in: Yukon Geology, V. 1, Exploration and Geological Services Division, Yukon, Indian and Northern Affairs Canada, p. 113-118.

Escher, A. and Watterson, J. (1974): Stretching fabrics, folds and crustal shortening.
Tectonophysics V.22, p. 223-231.

Elliott, J.E. and Strnad, J. (1984): Tin and tungsten in skarns.
in: Stemprok, M. ed: Metallization associated with acid magmatism.
Ustredni ustav geologicky, Praha.

Engbretson, D.C., Cox, A., and Gordon, R.G. (1985): Relative Motions between oceanic plates and continental plates in the Pacific basin.
Geol. Soc. Amer. Special Paper 206, pp. 59.

England, P.C. and Thompson, A. (1984): Pressure-temperature-time paths of regional metamorphism. 1. Heat transfer during the evolution of regions of thickened continental crust.
Jour. Pet. V. 25, p. 894-928.

England, P.C. and Thompson, A. (1986): Some thermal and tectonic models for crustal melting in continental collision zones.
in: Coward, M.P. and Ries, A.C. eds: Collision tectonics. Geol. Soc. Lond. Special Pub. No.19, p. 83-94.

Ettlinger, A.D. and Ray, G.E. (1988): Gold - enriched skarn deposits of British columbia. British Columbia Ministry of Mines and Petroleum Resources Paper 1988-1, p. 263-279.

Eugster, H.P. and Wilson, G.A. (1985): Transport and deposition of ore-forming elements in hydrothermal systems associated with granites.
in: High heat production (HHP) granites, hydrothermal circulation and ore genesis. Inst. Min. Metall. Lond., p. 87-98.

Farmer, G.L. and DePaulo, D.J. (1983): Origin of Mesozoic and Tertiary granite in the western United States and implications for pre-Mesozoic crustal structure. 1. Nd and Sr isotopic studies in the geocline of the Northern Great Basin.
J. Geophys. Res. V.88, B, p. 3379-3401.

Flinter, B.H., Hesp, W.R. and Rigby, D. (1972): Selected geochemical, mineralogical and petrological features of granitoids of the New England Complex, Australia and their relation to Sn, W, Mo and Cu-mineralization.
Econ. Geol. V. 67, p. 1241-1262.

Flood, R.H. and Vernon, R.H. (1988): Microstructural evidence of orders of crystallisation in granitoid rocks.
Lithos, V.21, p. 237-245.

Floyd, P.A. (1968): Tin and lead in the Land's End aureole, Cornwall.
Proc. Ussher Soc. V.2, p 45-48.

Floyd, P.A. (1968): Copper content of metamorphic and metasomatic basic hornfelses, Land's End Aureole.
Proc. Ussher Soc. V.2, p. 49-51.

Fonteilles, M., Guy, B., Dubru, M., Fouillac, A-M., Kaelin, J-L., Le Guyader, R., Marke, G.V., Sheppard, S., Toulhoat, P., Treil, M. and Velde, B: (1983): A comparative study of tungsten bearing skarns in the Pyrenees: structural and geochemical controls of mineralisation; dynamics of metasomatism.
Final report for the Commission of the European Communities contract 080-79-7.

Förster, H. (1987): Ignimbritic cauldrons, alkali granites and mineral deposits in fault block mountains.
Geol. Rundschau V.76/2 p. 373-388.

Foster, M.D. (1960): Interpretation of the composition of trioctahedral micas.
U.S. Geol. Surv. Prof. Paper 354-B, p. 11-49.

**Gabrielse, H. (1985): Major dextral transcurrent displacements along the Northern Rocky Mountain Trench
and related lineaments in north-central British Columbia.**
Bull. Geol. Soc. Amer. V.96, p. 1-14.

Gabrielse, H., Tempelman-Kluit, D.J., Blusson, S.L. and Campbell, R.B. *comps.* (1980): Macmillan River.
Geol. Surv. Can. Map 1398A, Scale 1:1,000,000.

Gabrielse, H. and Yorath, C.J. (1989): DNAG 4. The Cordilleran orogen in Canada.
Geoscience Canada V.16, p. 67-83.
Gallagher, V. (1989): Geological and isotope studies of microtonalite-hosted W-Sn mineralization in SE Ireland.
Mineral. Deposita V.24, p. 19-28.

Gastil, R., Calhoun, J., Rector, R., Tainosho, Y. and Shimizu, M. (1990): The nature and origin of the magnetite-bearing/magnetite-free distinction between granitic rocks of Peninsular California.
Abstracts: Granite: a Symposium to Celebrate W.S. Pitcher's 70th birthday: University of Liverpool, 6-7 th. Jan.

Gastil, R., Diamond, J., Knaack, C., Walawender, M., Marshall, M., Boyles, C., Chadwick, B. and Erskine, B. (1990): The problem of the magnetite/ilmenite boundary in southern and Baja California, California.
in: Anderson, J.L. ed., The nature and origin of Cordilleran magmatism.
Geol. Soc. Amer. Memoir 174. p. 19-32.

Gerstenberger, H. (1989): Autometasomatic Rb enrichments in highly evolved granites causing lowered Rb-Sr isochron intercepts.
E.P.S.L. V. 93, p. 65-75.

Ghosh, S.K. (1982): The problem of shearing along axial plane foliations.
Jour. Struct. Geol. V.4, p. 63-67.

Glazner, A.F. (1991): Plutonism, oblique subduction, and continental growth: an example from the Mesozoic of California.
Geology V. 19, p. 784-786.

Godwin, C.I., Armstrong, R.L. and Thompson, K.M. (1980): K-Ar and Rb-Sr dating and the genesis of tungsten at the Clea tungsten skarn property, Selwyn Mountains, Yukon Territory.
C.I.M. Bull., V. 73, p. 90-93.

Gordey, S.P. (1979): Stratigraphy of southeastern Selwyn Basin in the Summit Lake area, Yukon Territory and Northwest Territories.
in: Current Research, Part A. Geol. Surv. CAn. Paper 79-1A p. 13-16.

Gordey, S.P. (1981): Stratigraphy, structure and tectonic evolution of southern Pelly Mountains in the Indigo Lake area, Yukon Territory.
Geol. Surv. Can. Bull. 318.

Gordey, S.P: Structure section - Mackenzie fold belt.
Geol. Surv. Can. Open File 809.

Gordey, S.P. (1992): Geological fieldwork in Teslin map area, southern Yukon Territory.
in: Current Research Part A. Geol. Surv. Can. Paper 92-1A. p. 279-286.

Gordey, S.P., Abbott, J.G. and Orchard, M.J. (1982): Devono-Mississippian (Earn Group) and younger strata in east- central Yukon.
in: Current Research, Part B. Geological Survey of Canada Paper 82-1B p. 93-100.

Gordey, S.P., Abbott, J.G., Tempelman-Kluit, D.J. and Gabrielse, H. (1978): "Antler" clastics in the Canadian Cordillera.
Geology V. 15 p. 103-107.

Gordey, S.P. and Irwin, S.E.B: Sheldon Lake (105J) and Tay River (105K) map areas, east central Yukon.
Geol. Surv. Can. map 19-1987.

Grant, J.N., Halls, C., Avila, W. and Avila, G. (1977): Igneous geology and the evolution of hydrothermal systems in some subvolcanic tin deposits of Bolivia.
in: Volcanic processes in ore genesis. Inst. Min. Metall. London, p. 117-126.

Greenwood, H.J. (1967): Wollastonite: stability in H_2O-CO_2 mixtures and occurrence in a contact-metamorphic aureole near Salmo, British Columbia, Canada.
Amer. Mineral. V.52, p. 1669-1680.

Griffiths, J.R. (1977): Mesozoic-Early Cenozoic volcanism, plutonism and mineralization in southern B.C.- a plate tectonic synthesis.
Can. Jour. Earth Sci. V. 14, p. 1611-1624.

Griffiths, J.R. and Godwin, C.I. (1983): Metallogeny and tectonics of porphyry copper-molybdenum deposits in British Columbia.
Can. Jour. Earth Sci. V. 20, p. 1000-1018.

Guy, B. (1979): Petrologie et geochimie isotopique (S, C, O) des skarns a scheelite de Costabonne.
Doctoral thesis: École Nationale Supérieure des Mines de Paris.

Guy, B. (1980): Conditions d'apparition de la scheelite dans les gisements de Costabonne.
in: Autran et al: Mineralisations liées aux granitoïdes, 2eme partie: La genese des skarns a tungstene dans les Pyrénées.
B.R.G.M. Memoire 99.

Hall, A. (1971): Greisenisation in the granite of Cligga Head, Cornwall.
Proc. Geol. Assoc. V.82, p. 209-230.

Hall, A. (1988): The distribution of ammonium in the granites of south-west England.
Jour. Geol. Soc. Lond. V. 144, p. 37-41.

Hall, A. (1990): Geochemistry of the Cornubian tin province.
Mineralium Deposita V. 25, p. 1-6.

Hall, A., and Liverton, T. (1992): Trace ammonium in granites of the southern Yukon and its petrogenetic significance.
Yukon Geology; V. 3. Exploration and Geological Services Division, Yukon, Indian and Northern Affairs Canada p. 45-51.

Hall, A. and Neiva, A.M.R. (1990): Distribution of the ammonium ion in pegmatites, aplites and their minerals from central northern Portugal.
Min. Mag. V. 54, p. 455-461.

Hall, A. and Walsh, J.N. (1969): A rapid method for the determination of fluorine in silicate rocks.
Anal. Chim. Acta, V. 45, p. 341-342.

Hansen, V.L. (1986a): Preliminary structural and kinematic analysis of mylonitic rocks of the Teslin Suture Zone, 105E, Yukon.
in: Yukon Geology, V. 1, Exploration and Geological Services Division, Yukon, Indian and Northern Affairs Canada p. 119-124.

Hansen, V.L. (1986b): Petrotectonic study of the Teslin Suture zone, Yukon: a progress report.
in: Yukon Geology, V. 1, Exploration and Geological Services Division, Yukon, Indian and Northern Affairs Canada. p. 125-130.

Hansen, V.L. (1990): Yukon-Tanana terrane: a partial acquittal.
Geology V. 18, p. 365-369.

Hansen, V.L. (1992a): P-T evolution of the Teslin suture zone and Cassiar tectonites, Yukon, Canada: evidence for A- and B-type subduction.
Journal of Metamorphic Geology, V. 10, p. 239-263.
Hansen, V.L. (1992b): Backflow and margin-parallel shear within an ancient subduction complex.
Geology V. 20, p. 71-74.

Hansen, V., Mortensen, J.K. and Armstrong, R.L. (1989): U-Pb, Rb-Sr, and K-Ar isotopic constraints for ductile deformation and related metamorphism in the Teslin suture zone, Yukon-Tanana terrane, south-central Yukon.
Can. J. Earth Sci. V. 26, p. 2224-2235.

Harms, T.A. (1992): Stratigraphy of the southern Thirtymile Range, Teslin map area, southern Yukon Territory.
in: Current Research Part A. Geol. Surv. Can. Paper 92-1A. p. 297-302.

Harris, N.B. and Einaudi, M.T. (1982): Skarn deposits in the Yerrington District, Nevada: metasomatic skarn evolution near Ludwig.
Econ. Geol. V.77, p. 877-898.

Harris, N.B.W., Pearce, J.A. and Tindle, A.G. (1986): Geochemical characteristics of collision-zone magmatism.
in: Coward, M.P. and Ries, A.C., eds: Collision Tectonics. Geol. Soc. Lond. Special Pub. No.19, p. 67-81.

Harwood, A. (1985): Tungsten-tin mineralization at Chojlla in the Taquesi batholith, Cordillera Réal, Bolivia.
in: High heat production (HHP) granites, hydrothermal circulation and ore genesis. Inst. Min. Metall. London, p. 549-561.

Hawkes, J.R., Harding, R.R. and Darbyshire, D.P.F. (1975): Petrology and Rb:Sr age of the Brannel, South Crofty and Wherry elvan dykes, Cornwall.
Bull. Geol. Surv. G.B. No. 52, p. 27-42.

Henderson, C.M.B. and Martin, J.S (1989): Compositional relations in Li-micas from S.W. England and France: an ion- and electron- microprobe study.
Min. Mag. V. 53, p. 427-449.

Hesp, W.R. and Rigby, D. (1974): Some geochemical aspects of tin mineralisation in the Tasman Geosyncline.
Mineral. Deposita, V. 9, p. 49-60.

Hibberd,M.J. (1981): The magma-mixing origin of mantled feldspars.
Contrib. Min. Pet. V.76, p. 158-170.

Holtz, F. (1989): Importance of melt fraction and source rock composition in crustal genesis- the example of two granitic suites of northern Portugal.
Lithos V. 24, p. 21-35.

Hosking, K.F.G. (1973): The primary tin mineralisation patterns of West Malaysia.
Geol. Soc. Malaysia, Bull. V. 6, p. 297-308.

Hughes, O.L., Campbell, R.B., Muller, J.E. and Wheeler, J.O (1969): Glacial limits and flow patterns, Yukon Territory, south of 65 degrees north latitude.
Geol. Surv. Can. Paper 68-34.

Huppert, H.E. and Sparks, R.S. (1988): The fluid dynamics of crustal melting by injection of basaltic sills.
In: The Origin of Granites. Trans. Roy. Soc. Edin. V.79, p. 237-243.

Hutton, D.H.W. (1982): A tectonic model for the emplacement of the Main Donegal Granite, N.W. Ireland.
J. Geol. Soc. Lond. V.139, p. 615-631.

Hutton, D.H.W. (1988): Igneous emplacement in a shear zone termination: the biotite granite at Strontian, Scotland.
Geol. Soc. Amer. Bulletin V.100, p. 1392-1399.

Hutton, D.H.W. (1988): Granite emplacement mechanisms and tectonic controls: inferences from deformation studies.
in: The Origin of Granites. Trans. Roy. Soc. Edin. V.79, p. 245-255.

Ihlen, P.M., Trønnes, R. and Vokes, F.M. (1982): Mineralization, wall rock alteration and zonation of pre deposits associated with the Drammen granite in the Oslo region, Norway.
in: Evans, A.M: Metallization associated with acid magmatism. Wiley, p. 111-136.

Ilton, E.S. (1990): Partitioning of base metals between silicates, oxides, and a chloride-rich hydrothermal fluid. Part II. Some Aspects of base metal fractionation durung isothermal metasomatism.
in: Spencer, R.J. and Chou, I-M., eds: Fluid mineral Interactions: a tribute to H.P. Eugster. Geochemical Society Special Publication No. 2, San Antonio, Texas, p. 171-178.

Imeokparia, E.G. (1982): Tin content of biotites from the Afu Younger granite complex, central Nigeria.
Econ. Geol. V. 77, p. 1710-1724.

Irvine, T.N. and Baragar, W.R.B. (1971): A guide to chemical classification of the common igneous rocks.
Can. Jour. Earth Sci., V. 8, p. 523-548

Irving, E. and Wynne, P.J. (1990): Palaeomagnetic evidence bearing on the evolution of the Canadian Cordillera.
Phil. Trans. Roy. Soc. Lond. A 331, p. 487-509.

Ishihara, S. (1981): The granitoid series and mineralisation
Economic Geology 75th Anniversary Volume, p. 458-484.

Ivanova, G.F., and Naumov,V.B. (1985): Geochemical inter-relations of rare-metal ore mineralization with granites.
in: High heat production granites, hydrothermal circulation and ore genesis. Inst. min. Metall. Lond., p. 155-162.

Jackson, L.E., Gordey, S.P., Armstrong, R.L. and Harakal, J.E. (1986): Bimodal Paleogene volcanics near Tintina fault, east-central Yukon, and their possible relationship to placer gold.
in: Yukon Geology, V.1; Exploration and Geological Services Division, Yukon, Indian and Northern Affairs Canada, p. 139-147.

Jackson, N.J. and Alderton, D.H.M. (1974): Discordant calc-silicate bodies in the Botallack area.
Proc. Ussher Soc. V.3, p. 123-127.

Jackson, N.J., Halliday, A.N., Sheppard, S.M.F. and Mitchell, J.G. (1982): Hydrothermal activity in the St. Just mining district, Cornwall, England.
In: Evans, A.M. ed: Metallization associated with acid magmatism. Wiley. p. 137-179.

Jackson, N.J., McMoore, J. and Rankin, A.H. (1977): Fluid inclusions and mineralisation at Cligga Head, Cornwall, England.
J. Geol. Soc. Lond. V.134, p. 343-349.

Jamison, W.R. (1991): Kinematics of compressional fold development in convergent wrench terranes.
Tectonophysics V. 190, p. 209-232.

Johannes, W. (1984): Beginning of melting in the granite system Qz-Or-Ab-An-H_2O.
Contrib. Min. Pet., V 86, p. 264-273.

Johnson, C.M., Czamanske, G.K. and Lipman, P.W. (1989): Geochemistry of intrusive rocks associated with the Latir volcanic field, New Mexico, and contrasts between evolution of plutonic and volcanic rocks.
Contrib. Min. Pet. V. 103, p. 90-109.

John, B.E and Wooden, J. (1990): Petrology and geochemistry of the metaluminous to peraluminous Chemehuevi Mountains Plutonic Suite, southeastern California.
In/ Anderson, J.L. ed: The nature and origin of Cordilleran magmatism.
Geol. Soc. Amer. Memoir 174. p. 71-98.

Jones, D.L. (1990): Synopsis of late Palaeozoic and Mesozoic terrane accretion within the Cordillera of western North America.
Phil. Trans. Roy. Soc. Lond. A331, p. 479-486.

Jones, D.L., Silberling, N.J., Hillhouse, J. (1977): Wrangellia a displaced terrane in northwestern North America.
Can. Jour. Earth Sci. V. 14, p. 2565-2577.

Jones, D.L., Silberling, N.J. and Coney, P.J. (1986): Collision tectonics in the Cordillera of Western North America: examples from Alaska.
in: Coward, M.P. and Ries, A.C. eds: Collision tectonics.
Geol. Soc. Lond. special pub. No.19. p 37-50. p 367-387.

Keith, J.D., van Middelaar, W., Clark, A.H. and Hodgson, C.J. (1990): Granitoid textures, compositions, and volatile fugacities asssociated with the formation of tungsten-dominated skarn deposits.
In: Whitney, J.A. and Naldrett, A.J. eds., Ore deposition associated with magmas, Reviews in economic geology V. 4, p. 235-250.

Kelly, W.C. and Turneare, F.S. (1970): Mineralogy, paragenesis and geothermometry of the tin and tungsten deposits of the eastern Andes, Bolivia.
Econ. Geol. V. 65, p. 609-680.

Kinnaird, J.A., Batchelor, R.A., Whitley, J.E. and MacKenzie, A.B. (1985): Geochemistry, mineralization and hyrothermal alteration of the Nigerian high heat producing granites.
In: High heat production (HHP) granites, hydrothermal circulation and ore genesis. Inst. Min. Metall., p. 169-195.

Kinnaird, J.A., Bowden, P., Ixer, R.A. and Odling, N.W.A. (1985): Mineralogy, geochemistry and mineralization of the Riruwai complex, northern Nigeria.
J. Afr. Earth Sci. V. 3, p. 185-222.

Kistler, R.W. (1990): Two different lithoshere types in the Sierra Nevada, California.
In: Anderson, J.L., ed: The nature and origin of Cordilleran Magmatism.
Geol. Soc. Amer. Memoir 174. p. 271-281.

Kukowski, N. and Neugebauer, H.J. (1990): On the ascent and emplacement of granitoid bodies- dynamic-thermal numerical models.
Geol. Rundschau V. 79/2 p. 227-239.

Kwak, T.A.P. (1987): W-Sn skarn deposits and related metamorphic skarns and granitoids.
Developments in Economic geology, 24 Elsevier, Amsterdam pp. 451.

Kwak, T.A.P. (1983): The geology and geochemistry of the zoned, Sn-W-F-Be skarns at Mt Lindsay Tasmania, Australia.
Econ. Geol. V. 78, p. 1440-1465.

Kwak, T.A.P. and Askins, P.W. (1981): Geology and genesis of the F-Sn-W (-Be-Zn) skarn (wrigglite) at Moina Tasmania.
Econ. Geol. V. 76, p. 439-467.

Kwak, T.A.P. and Nicholson, M. (1988): Szaibelyite and fluoborite from the St Dizier Sn-borate skarn deposit, NW Tasmania, Australia.
Min. Mag. V. 52, p. 716-717.

Kwak, T.A.P. and Tan, T.H. (1981): The geochemistry of zoning in skarn minerals at the King Island (Dolphin) mine.
Econ. Geol. V. 76, p. 468-497.

Kwak, T.A.P. and Tan, T.H. (1981): The importance of $CaCl_2$ in fluid composition trends- evidence from the King Island (Dolphin) skarn deposit.
Econ. Geol. V. 76, p. 955-960.

Lagarde, J.L. and Michard, A. (1986): Stretching normal to the regional thrust displacement in a thrust-wrench shear zone, Rehamna Massif, Morocco.
Jour. Struct. Geol. V. 8, p. 483-492.

Larson, R.L. (1991): Geological consequences of superplumes.
Geology V. 19, p. 963-966.

Lameyre, J. and Bowden, P. (1982): Plutonic rock type series and related rocks.
J. Volc. and Geothermal Res. V. 14, p. 169-186.

Layne, G.D. and Spooner, E.T.C. (1980): The JC Sn-Fe-F skarn Seagull Batholith area, southern Yukon.
in: Morin, J., ed: Mineral deposits of the Northern Cordillera.
G.A.C. Special Vol. 37, p. 266-273.

Leake, B.E. (1990): Granite magmas: their sources, initiation and consequences of emplacement.
J. Geol. Soc. Lond., V. 147, p. 579-589.

Le Bas, M.J. and Streckeisen, A.L. (1991): The I.U.G.S. systematics of igneous rocks.
Jour. Geol. Soc. Lond. V. 148, p. 825-833.

Lehmann, B. (1982): Metallogeny of tin: magmatic differentiation versus geochemical heritage.
Econ. Geol. V. 77 p. 50-59.

Lehmann, B. (1987): Tin granites, geochemical heritage, magmatic differentiation.
Geol. Rundschau V. 76/1, p. 177-185.

Limion, H. (1979): Report on geophysical surveys Mindy claims- Yukon Territory, August 20-23, 1979.
Unpublished report on file as assessment work (090647) at the Watson Lake Mining Recorder's Office.

Lin, C. (1987): Mineralization and alteration of a compound greisen and skarn deposit.
Pacific Rim Congress 1987, Proceedings. Aust. IMME, p. 279-281.

Lindgren, W. (1924): Contact metamorphism at Bingham, Utah.
Geol. Soc. Amer. Bull. 35, p. 507-534.

Lipman, P.W. (1988): Evolution of silicic magma in the upper crust: the mid Tertiary Latir volcanic field and its cogenetic granitic batholith, northern New Mexico, U.S.A.
in: The Origin of Granites. Trans. Roy. Soc. Edin. V.79, p. 265-288.

Lister, C.J. (1979): Luxullianite in situ with the St. Austell granite, Cornwall.
Min. Mag. 42, p. 295-297.

Lister, C.J. (1979): Luxullianite in situ with the St. Austell granite, Cornwall: a reply.
Min. Mag. 43, p. 442-443.

Liu, C., Zhu, J., Xu, X., Cai, D. and Yang, P. (1989): The Hercynian-Indosinian collision type granites of west Yunnan and their tectonic significance.
Jour. Southeast Asian Earth Sci. V. 3, p. 263-270.

Liverton, T. (1992): Tin-bearing skarns of the Thirtymile Range, N.T.S. sheet 105C 9: a progress report.
Yukon Geology V. 3. Exploration and Geological Services Division, Yukon, Indian and Northern Affairs Canada p. 52-70.

Loiselle, M.C. and Wones, D.R. (1979): Characteristics and origin of anorogenic granites.
Geol. Soc. Amer. Abstracts. V. 11, p. 468.

Lowell, J.D. and Guilbert, J.M. (1970): Lateral and vertical alteration-mineralization zoning in porphyry copper deposits.
Econ. Geol. V. 65, p.373-408.

Luth, R.W. and Muncill, G.E. (1989): Fluorine in aluminosilicate systems: Phase relations in the system $NaAlSi_3)_8$-$CaAl_2Si_2O_8$-F_2O_{-1}.
Geoch. et Cosmochim. Acta V. 53, p. 1937-1942.

Lynch, G.V. (1985): Mineralization and alteration zonation of the Kalzas wolframite vein-deposit, Yukon Territory.
Unpublished MSc thesis, Washington State University, Pullman, Washington. pp 123.

Macdonald, R. and Smith, R.L. (1988): Relationships between silicic plutonism and volcanism: geochemical evidence.
In: The Origin of Granites. Trans. Roy. Soc. Edin. V.79, p. 257-263.

MacLellan, H.E. and Taylor, R.P. (1989): Geology and geochemistry of the Burnthill Granite and related W-Sn-Mo-F mineral deposits, central New Brunswick.
Can. J. Earth Sci. V.26, p. 499-514.

McClay, K.R., Insley, M.W. and Anderton, R. (1989): Inversion of the Kechika trough, northeastern British Columbia.
in: Cooper, M.A. and Williams, G.D, eds: Inversion Tectonics.
Geol. Soc. Lond. Special Pub. No. 34, p. 235-257.

Magaritz, M. and Taylor, H.P. (1986): Oxygen-18/oxygen-16 and D/H studies of plutonic granite and metamorphic rocks across the Cordilleran batholiths of southern British Columbia.
J. Geophys. Res. V. 91, B2, p. 2193-2217.

Mahawat, C., Atherton, M.P. and Brotherton, M.S. (1990): The Tak batholith Thailand: the evolution of contrasting granite types and implications for tectonic setting.
Jour. S.E. Asian Earth Sci. V.4, No.1, p. 11-28.

Malavieille, J., Lacassin, R. and Mattauer, M. (1984): Signification tectonique des linéations d'allongement dans les Alpes occidentales.
Bull. Soc. Géol. France V. 26, p. 895-906.

Manning, D.A.C. (1981): The effect of fluorine on liquidus phase relationships in the system Qtz-Ab-Or with excess water at 1Kb.
Contrib. Mineral. Pet. V.76, p. 206-215

Manning, D.A.C. (1982): An experimental study of the effects of fluorine on the crystallisation of granitic melts.
In: Evans, A.M. ed: Metallization associated with acid magmatism.
Wiley. p. 191-203.

Manning, D.A.C., and Exley, C.S., (1984): The origin of late-stage rocks in the St. Austell granite; a reinterpretation.
Jour. Geol. Soc. Lond., V. 141, p. 581-591.

Manning, D.A.C. and Hill, P.I. (1990): The petrogenetic and metallogenetic significance of topaz granite from the southwest England orefield.
In: Stein, H.J., and Hannah, J.L., eds., Ore-bearing granite systems; petrogenesis and mineralizing processes. Geol Soc. Amer. Special Paper 246, p. 51-69.

Manning, D.A.C. and Pichavant, M. (1984): Experimental studies of the role of fluorine and boron in the formation of late-stage granitic rocks and associated mineralisation.
Proc. 27 Int. Geol. Cong. Moscow, Abstracts, V.4, p. 386.

van Marcke de Lummen, G. (1985): Mineralogical observations and genetic considerations relating to skarn formation at Botallack, Cornwall, England.
In: High heat production (HHP) granites, hydrothermal circulation and ore genesis. Inst. Min. Metall. Lond., p. 535-547.

van Marcke de Lummen, G. (1985): Mineralogy and geochemistry of skarn deposits in the Land's End aureole, Cornwall.
Proc. Ussher Soc. V. 6, p. 211-217.

van Marcke de Lummen, G. (1986): Geochemical evolution of the Land's End granite (south-west England) in relation to its tin potential in the light of data from western marginal areas.
Proc. Usher Soc. V. 6, p. 398-404.

Mathieson, G.A. and Clark, A.H. (1984): The CanTung E Zone scheelite skarn orebody, Tungsten, Northwest Territories: a revised genetic model.
Econ. Geol. V. 79, p. 883-901.

Mattauer, M. (1986): Intracontinental subduction, crust-mantle décollement and crustal-stacking wedge in the Himalayas and other collision belts.
in: Coward, M.P. and Ries, A.C. eds: Collision tectonics.
Geol. Soc. Lond. Special Pub. No.19, p. 37-50.

Mattauer, M., Fauré, M. and Malavieille, J. (1981): Transverse lineation and large-scale structures related to Alpine obduction in Corsica.
Jour. Struct. Geol. V.3, p. 401-409.

van Middelaar, W.T., and Keith, J.D. (1990): Mica chemistry as an indicator of oxygen and halogen fugacities in the CanTung and other W-related granitoids in the North American Cordillera.
In: Stein, H.J., and Hannah, J.L., eds., Ore-bearing granite systems; petrogenesis and mineralizing processes: Geol. Soc. Amer. Special Paper 246, p. 205-220.

Meinert, L.D. (1986): Gold in skarns of the Whitehorse copper belt southern Yukon.
in: Yukon Geology, V. 1, Exploration and Geological Services Division, Yukon, Indian and Northern Affairs, Canada, p. 19-43.

Miller, C.F., Stoddard, E.F., Bradfish, L.J. and Dollase, W.A. (1981): Composition of plutonic muscovite: genetic implications.
Can. Mineral. V. 19, p. 25-34

Miller, C.F., Watson, E.B. and Harrison, T.M. (1988): Perspectives on the source, segregation and transport of granitoid magmas.
in: The Origin of Granites. Trans. Roy. Soc. Edin. V.79, p. 135-156.

Miyashiro, A. (1974): Volcanic rock series in island arcs and active continental margins.
Am. Jour. Sci. V. 274, p. 321-355.

Möller, P., Mortiani, G. and Hoefs, J. (1985): REE and^{18}O/^{16}O distributions in altered Variscan granites of the western Harz, Germany and southrern Sardinia, Italy.
in: High heat production (HHP) granites, hydrothermal circulation and ore genesis. Inst. Min. Metall. Lond., p. 213-220.

Monger, J.W.H. (1989): Overview of Cordilleran Geology
in: Ricketts, B.D., ed., Western Canada Sedimentary Basin. A case History. Canadian Society of Petroleum Geologists, Calgary. p. 9-32.

Monger, J.W.H., Price, R.A. and Tempelman-Kluit, D.J. (1982): Tectonic accretion and the origin of the two metamorphic and plutonic welts of the Canadian Cordillera.
Geology, V.10, p. 70-75.

Monger, J.W.H., Souther, J.G. and Gabrielse, H. (1972): Evolution of the Canadian Cordillera: a plate tectonic model.
Am. Jour. Sci. V. 272, p. 577-602.

Moore, J. McM. (1982): Mineral zonation near the granitic batholiths of south-west and northern England and some geothermal analogues.
in: Evans, A.M. ed: Metallization associated with acid magmatism.
Wiley, p. 229-241.

Moore, J.N. and Kerrick, D.M. (1976): Equilibria in siliceous dolomites of the Alta aureole, Utah.
Am. Jour. Sci. V. 276, p. 502-524.

Morrison, G.W., Godwin, C.I. and Armstrong, R.L. (1979): Interpretation of isotopic ages and ^{87}Sr/^{86}Sr initial ratios for plutonic rocks in the Whitehorse map area, Yukon.
Can. Jour. Earth Sci. V. 16, p. 1988-1997.

Moseley, G. (1981): Petrochemical characterization of rare metal granitoids.
Unpublished MSc thesis, Imperial College of Science and Technology, University of London.

Mount, M. (1985): Geevor mine: a review.
in: High heat production (HHP) granites, hydrothermal circulation and ore genesis. Inst. Min. Metall. Lond., p. 221-238.

Mulligan, R. (1963): Geology of Teslin map area, Yukon Territory.
Geol. Surv. Can. Memoir 326. pp. 96.

Mulligan, R. (1969): metallogeny of the region adjacent to the northern part of the Cassiar Batholith, Yukon Territory and British Columbia.
Geol. Surv. Can. Paper 68-70.

Mulligan, R. (1984): Geology of Canadian tungsten occurrences.
Geol. Surv. Can. Economic Geology Report 32.

Mulligan, R., and Jambor, J.L. (1967): Tin-bearing silicates from skarn in the Cassiar district, northern British Columbia. Canadian Mineralogist, V.9, p. 358-370.

Munoz, J.L. and Ludington, S.D. (1974): Fluoride-hydroxyl exchange in biotite.
Am. Jour. Sci. V. 274, p. 396-413.

Murata, M. and Tetsumani, I. (1987): Sulfide and oxide minerals from S-type and I-type granitic rocks.
Geoch. et Cosmochim. Acta V. 51, p. 497-507.

Nabelek, P.I., and Russ-Nabelek, C. (1990): The fole of fluorine in the petrogenesis of magmatic segregarions in the St. Francois volcan-plutonic terrane, southeastern Missouri.
In: Stein, H.J., and Hannah, J.L., eds., Ore-bearing granite systems; petrogenesis and mineralizing processes: Geol. Soc. Amer. Special Paper 246, p. 71-87.

Nakapadungrat, S. (1982): Geochronology and geochemistry of the Thong-Lang granite complex, Central Thailand.
Unpublished PhD. Thesis, King's College, University of London. pp. 336.

Nebocat, J. (1981): Geochemical and geological survey on the Mindy 17-32 claims.
Unpublished report on file as assessment work (090776) at the Watson Lake Mining Recorder's Office.

Nebocat, J. (1982): Diamond drill logs from the Mindy prospect.
Unpublished report on file as assessment work (090987) at the Watson Lake Mining Recorder's Office.

Nedachi, N. (1980): Chlorine and fluorine contents of rock-forming minerals of the Neogene granitic rocks in Kyushu, Japan.
in: Ishihara, S. and Takenouchi, S., eds: Granitic magmatism and related mineralization. Mining Geology Special Issue No.8.
Society of Mining Geologists of Japan. p. 39-48.

Newberry, R.J. (1982): Tungsten-bearing skarns of the Sierra-Nevada. 1. The Pine Creek Mine, California.
Econ. Geol. V. 77, p. 823-844.

Newberry, R.J., Burns, L.E., Swanson, S.E. and Smith, T.E. (1990): Comparative petrologic evolution of the Sn and W granites of the Fairbanks-Circle area, interior Alaska.
In: Stein, H.J., and Hannah, J.L., eds., ore-bearing granite systems; petrogenesis and mineralizing processes: Geol. Soc. Amer. Special Paper 246, p. 121-142.

Neiva, A.M.R. (1982): Geochemistry of muscovite and some physico-chemical conditions of the formation of some tin-tungsten deposits in Portugal.
In: Evans, A.M. ed: Metallization associated with acid magmatism.
Wiley. p. 243-259.

Nekvasil, H. and Burnham, C.W. (1987): The calculated individual effects of pressure and water content on phase equilibria in the granite system.
In: Mysen, B.O., ed., Magmatic processes; physicochemical principles: The Geochem. Soc. Special Pub. 1, p. 433-445.

Noble, S.R., Spooner, E.T.C., and Harris, F.R. (1986): Logtung: a porphyry W-Mo deposit in the southern Yukon.
In: Morin, J., ed: Mineral deposits of the northern Cordillera.
C.I.M. Special Volume 37. p.

Norman, D.I. and Trangcotchasan, Y. (1982): Mineralization and fluid inclusion study of the Yod Nam tin mine, southern Thailand.
In: Evans, A.M. ed: Metallization associated with acid magmatism.
Wiley, p. 261-272.

Norton, D. (1988): Metasomatism and permeability.
Am. Jour. Sci. Vol.288, p. 604-618.

O'Connor, (1965): A classification for quartz-rich igneous rocks based on feldspar ratios.
U.S.G.S. Prof. Paper 525 B, p. 79-84.

Odonne, F. and Vialon, P. (1983): Analogue models of folds above a wrench fault.
Tectonophysics V. 99, p. 31-46.

Olade, M.A. (1980): Geochemical characteristics of tin-bearing and tin-barren granites, northern Nigeria.
Econ. geol., v. 75, p. 71-82.

Parrish, R.R., Carr, S.D. and Parkinson, D.L. (1988): Eocene extensional tectonics and geochronology of the southern Omineca belt, British Columbia and Washington.
Tectonics V. 7 p. 181-212.

Paterson, B.A., Stephens, W.E. and Herd, D.A. (1989): Zoning in granitoid accessory minerals as revealed by backscattered electron imagery.
Min. Mag. V. 53, p. 55-61.

Patterson, D.J., Ohmoto, H. amd Solomon, M. (1981): Geologic setting and genesis of cassiterite-sulfide mineralization at Renison Bell, western Tasmania.
Econ. Geol. V. 76, p. 393-438.

Pearce, J.A., Harris, N.B.W. and Tindle, A.G. (1984): Trace element discrimination diagrams for the tectonic interpretation of granitic rocks.
J. Pet. V. 25, p. 956-983.

Pesquera, A. and Pons, J. (1989): Field evidence of magma mixing in the Aya granitic massif (Basque Pyreneees, Spain).
N. Jb. Miner. Mh. Jg. 1989, H.10 p. 441-454.

Peterson, J.W. and Newton, R.C. (1989): Reversed Experiments on Biotite-Quartz-feldspar melting in the system KMASH: implications for crustal anatexis.
Jour. Geol. V. 97, p. 465-485.

Pichavant, M. (1981): An experimental study of the effect of boron on a water saturated haplogranite at 1kbar vapour pressure.
Contrib. Min. Pet. V. 76, p. 430-439.

Pichavant, M. (1983): Melt-fluid interaction deduced from studies of silicate B_2O_3-H_2O systems at 1 Kbar.
Bulletin de Minéralogie V. 106, p. 201-211.

Pigage, L.C. and Anderson R.G. (1985): The Anvil plutonic suite, Faro, Yukon Territory.
Can. Jour. Earth Sci. V. 22, p. 1204-1216.

van de Pijpekamp, B. (1982): petrological criteria for establishing the tin potential in granitoid complexes.
In: Evans, A.M. ed: Metallization associated with acid magmatism.
Wiley, p. 273-278.

Pitcher, W.S. (1979): The nature, ascent and emplacement of granitic magmas.
J. Geol. Soc. London, V.136, p. 627-662.

Pitcher, W.S. (1982): Granite types and tectonic environment.
in: Hsu, K.J. ed: Mountain Building Processes. Academic Press, London. p. 19-40.

Pitcher, W.S. (1987): Granites and yet more granites, forty years on.
Geol. Rundschau V. 76/1 p. 51-79.

Plant, J.A., O'Brien, C. and Hurdley, J. (1985): Geochemical criteria for the recognition of high heat production granites.
in: High heat production (HHP) granites, hydrothermal circulation and ore genesis. Inst. Min. Metall. Lond., p. 263-285.

Plant, J.A., Simpson, P.R., Green, P.M., Watson, J.V. and Fowler, M.B. (1983): Metaliferous and mineralised Caledonian granites in relation to regional metamorphism and fracture systems in northern Scotland.
Trans. Inst. Min. Metall. London. V. 92, B, p. 33-42.

Platt, J.P. and Vissers, R.L.M. (1980): Extensional structures in anisotropic rocks.
Jour. Struct. Geol. V. 2, p. 397-410.

Plimer, I.R. (1980): Exhalative Sn and W deposits associated with mafic volcanism as precursors to Sn and W deposits associated with granites.
Mineral. Deposita V. 15 p. 275-289.

Plimer, I.R. (1984): Malayaite and tin-bearing silicates from a skarn at Doradilla via Bourke, New South Wales.
Aust. Jour. Earth Sci. V. 31, p. 147-153.

Plimer, I.R. (1987) : Fundamental parameters for the formation of granite - related tin deposits.
Geol. Rundschau 76/1. p. 23-40.

Plimer, I.R. and Kleeman, J.D. (1985): Mineralization associated with the Mole Granite, Australia.
In: High heat production (HHP) granites, hydrothermal circulation and ore genesis. Inst. Min. Metall. Lond., p. 563-569.

Plint, H.E., Erdmer, P., Reynolds, P.H., and Grist, A.M. (1992): Eocene tectonics in the Omineca Belt: northern British Columbia, Canada: field, ^{40}Ar-^{39}Ar, and fission track data from the Horseranch Range.
Bull. Geol. Soc. Amer. V. 104, p. 106-116.

Pollard, P.J., Taylor, R.J., and Cuff, C. (1983): Metallogeny of tin; magmatic differentiation versus geochemical heritage- a discussion.
Econ. Geol. V. 78 p. 543-545.

Pollard, P.J. (1988): Petrogenesis of tin-bearing granites of the Emuford district, Herberton tinfield, Australia.
Aust. Jour. Earth Sci. V. 35, p. 39-57.

Poole, W.H., Roddick, J.A., and Greene, L.H. (1963): Wolf Lake Yukon Territory.
Geol. Surv. Can. Map 10-1960, scale 1:250,000.

Price, R.A. and Carmichael, D.M: (1986): Geometric test for Late Cretaceous-Palaeogene intracontinental transform faulting in the Canadian Cordillera.
Geology, V. 14, p. 468-471.

Pride, M.J. (1988): Bimodal volcanism along the Tintina trench, near Faro and Ross River.
in: Yukon Geology V. 2, Exploration and Geological Services Division, Yukon, Indian and Northern Affairs Canada p. 69-80.

Puchner, C. (1986): Geology, alteration, and mineralization of the Kougarok Sn deposit, Seward Peninsula, Alaska.
Econ. Geol. V. 81, p. 1775-1794.

Ramsay, J. (1980) The crack-seal mechanism of rock deformation.
Nature V. 284, p. 135-139.

Rankin, A.H. and Alderton, D.H.M. (1985): Fluids in granites from southwest England.
in: High heat production (HHP) granites, hydrothermal circulation and ore genesis. Inst. Min. Metall. Lond., p. 287-299.

Ray, G.E., Dawson, G.L.and Simpson, R. (1987): The geology and controls of skarn mineralisation in the Hedley gold camp southern British Columbia. British Columbia Ministry of Energy, Mines and Petroleum Resources, Paper 1987-1.

Ray, G.E., Dawson, G.L., Simpson, R. (1988): Geology, Geochemistry and metallogenic zoning in the Hedley gold skarn camp. B.C. Ministry of Mines and Petroleum Resources,
Paper 1988-1. p. 263-279.

Ray, G.E. McClintock, J. and Roberts, W. (1986): A comparison between the geochemistry of the gold - rich and silver - rich skarns of the Tillicum Mountain area (82F/13, 82K/4). British Columbia Ministry of Energy, Mines and Petroleum Resources Paper 1986 - 1.

Raymond, L.R. (1984): Classification of melanges.
In: Raymond, L.R., ed., Melanges: their nature, origin and significance. Geol. Soc. Amer. Special Paper 198. p. 7-20.

Reid, J.E. (1978): Skarn alteration of the Commercial Limestone, Carr-Fork area, Bingham, Utah.
Econ. Geol. V. 73, p. 1315-1325.

Rice, J.M. (1977): Contact metamorphism of impure dolomitic limestone in the Boulder aureole, Montana.
Contrib. Min. Pet. V. 59, p. 237-259.

Rottura, A., Bargossi, G.M., Caironi, V., Del Moro, A., Maccarrone, E., Macera, P., Petrini, R., Piccarreta, G. and Poli, G. (1990): Petrogenesis of contrasting Hercynian granitoids from the Calabrian Arc, southern Italy.
Lithos, V. 24 p. 97-119.

Ryabchikov, I.D., Durasova, N.A. and Barsukov, V.L. (1974): The rôle of volatiles in the mobilization of tin from granitic magmas.
In: Stemprok, M., ed., Metallization associated with acid magmatism. V. 1
Geological Survey of Czechoslovakia, Praha, p. 287-288.

Saavedra,J. (1982): Geochemistry of barren granites and those mineralized with tin and tungsten in west central Spain.
In: Evans, A.M. ed: Metallization associated with acid magmatism.
Wiley, p. 291-300.

Santarelli, F., Alderton, D. and Guy, B. (1988): Etude des fluides des skarns a tungstene de Costabonne (Pyrénées); analyses chimiques, minéraux fils: quelques résultats.
C.R. Acad. Sci. Paris, V. 307, Ser. 2 p. 1231-1236.

Savage, D., Cave, M.R. and Milodowski, A.E. (1985): Interaction of meteoric groundwater with Carnmellis granite at 250°C and 50MPa: an experimental study.
In: High heat production (HHP) granites hydrothermal Circulation and ore genesis. Inst. Min. Metall. London. p. 315-327.

Sawka, W.N. (1988): REE and trace element variations in accessory minerals and hornblende from the strongly zoned McMurry Meadows Pluton, California.
In: The Origin of Granites. Trans. Roy. Soc. Edin. V.79, p. 157-168.

Sawka, W.N., Heizler, M.T., Kistler, R.W. and Chappell, B.W. (1990): Geochemistry of highly fractionated I- and S-type granites from the tin-tungsten province of western Tasmania.
In: Stein, H.J. and Hannah, J.L. eds., Ore-bearing granite systems; petrogenesis and mineralizing processes.
Geol Soc. Amer. Special Paper 246, p. 161-179.

Sawka, W.N., Chappell, B.W. and Norrish, K. (1984): Light-rare-earth-element zoning in sphene and allanite during granitoid fractionation.
Geology, V. 12, p. 131-134.

Scott, K.M. (1988): Phyllosilicate and rutile compositions as indicators of Sn specialization in some southeastern Australian granites.
Miner. Deposita, V. 23, p. 159-165.

Sevigny, J.H., Parrish, R.R. and Ghent, E.D. (1989): Petrogenesis of peraluminous granites, Monasheee mountains, southeastern Canadian cordillera.
Jour. Pet. V. 30, p. 557-581.

Shaw, A.L. and Guilbert, J.M. (1990): Geochemistry and metallogeny of Arizona peraluminous granitoids with reference to Appalachian and European occurrences.
In: Stein, H.J., and Hannah, J.L., eds., Ore-bearing granite systems; petrogenesis and mineralizing processes.
Geol. Soc. Amer. Special Paper 246 p. 317-356.

Shepherd, T.J., Miller, M.F., Scrivenor, R.C. and Darbyshire, D.P.F. (1985): Hydrothermal fluid evolution in relation to mineralization in southwest England with special reference to the Dartmoor-Bodmin area.
In: High heat production (HHP) granites, hydrothermal circulation and ore genesis. Inst. Min. Metall. Lond., p. 345-364.

Silver, L.T. and Chappell, B.W. (1988): The Peninsular Ranges Batholith: an insight into the evolution of the Cordilleran batholiths of southwestern North America.
in: Origin of Granites. Trans. Roy. Soc. Edin. V. 79, p. 105-121.

Simony, P.S., Ghent, E.D., Craw, D., Mitchell, W. and Robbins, D.B. (1980): Structural and metamorphic evolution of northeast flank of Shuswap complex, southern Canoe River area, British Columbia.
Geol. Soc. Amer. Memoir 153 p. 445-461.

Sinclair, W.D. (1986): Molybdenum, tungsten and tin deposits and associated granitoid intrusions in the northern Canadian Cordillera and adjacent parts of Alaska.
In: Morin, J. ed: Mineral deposits of the northern cordillera. CIM special volume 37, p. 216-233.

Skippen, G.B. (1971): Experimental data for reactions in siliceous marbles.
Jour. Geol. V. 79, p. 457-481.

Skippen, G. (1974): An experimental model for low pressure metamorphism of siliceous dolomitic marble.
Am. Jour. Sci. V. 274, p. 487-509.

Slaughter, J., Kerrick, D.M. and Wall, V.J. (1975): Experimental and thermodynamic study of equilibria in the system CaO- MgO-SiO_2-H_2O-CO_2.
Am. Jour. Sci. V. 275, p. 143-162.
Smith, R.B. (1978): Seismicity, crustal structure and intraplate tectonics of the interior of the western Cordillera.
Geol. Soc. Amer. Mem. 152, p. 111-144.

Smith, T.E., Miller, P.M. and Huang, C.H. (1982): Solidification and crystallisation of a stanniferous granitoid pluton, Nova Scotia, Canada.
In: Evans, A.M. ed: Metallization associated with acid magmatism.
Wiley. p. 301-320.

Smith, T.E. and Turek, A. (1976): Tin-bearing potential of some Devonian granitic rocks in S.W. Nova Scotia.
Mineral. Deposita V. 11, p. 234-245.

Soler, P. and Fonteilles, M. (1980): Etude pétrologique du gisement de Salau et de son enveloppe immédiate.
in: Autran, A., Derré, M., Fonteilles, B., Guy, P., Soler, P. and Toulhoat, P:
Mineralisations liées aux granitoïdes, 2eme partie: La genese des skarns a tungstene dans les Pyrénées.
B.R.G.M. Memoire 99.

Sonnet, P.M. and Verkaeren, J. (1989): Scheelite-, malayaite-, and axinite-bearing skarns from El Hammam, Central Morocco.
Econ. Geol. V. 84, p. 575-590.

Souther, J.G., Brew, D.A. and Okulitch, A.V. comp., (1979): Iskut River.
Geol. Surv. Can. Map 1418A. 1:1,000,000 scale.

Speer, L.A., Naeem, A. and Almohandis, A.A. (1989): Small-scale variations and subtle zoning in granitoid plutons: the Liberty Hill pluton, South Carolina, U.S.A.
Chemical Geology V. 75, p. 153-181.

Stemprok, M. (1974): Relation of tin and tungsten metallogeny to acid magmatism in the Krushné Hory-Erzgebirge.
in: Stemprok, M. ed: Metallization associated with acid magmatism.
Ustredni ustav geologicky, Praha, p. 127-131.

Stemprok,M. (1982): Tin-fluorine relationships in ore-bearing assemblages.
In: Evans, A.M. ed: Metallization associated with acid magmatism.
Wiley. p. 321-337.

Stemprok,M. (1985): Vertical extent of greisen mineralization in the Krusné hory/Erzgebirge granite pluton of central Europe.
in: High heat production (HHP) granites hydrothermal Circulation and ore genesis. Inst. Min. Metall. Lond., p. 383-392.

Stephen, J.C. and Mysyk, (1980):
Unpublished report on file as assessment (090667) at the Watson Lake Mining Recorder's office.

Stephen, J.C. (1981):
Unpublished report on file as assessment (090886) at the Watson Lake Mining Recorder's office.

Stephens, W.E. (1988): Granitoid plutonism in the Caledonian orogen of Europe.
In: Harris, A.L. and Fettes, D.J. eds: The Caledonian-Appalachian Orogen. Geol. Soc. London. Spec. Pub. No. 38. p. 389-403.

Stern, C.R. and Wyllie, P.J. (1981): Phase relations of I-type granite with H_2O to 35 kilobars: the Dinkey Lakes biotite-granite from the Sierra Nevada.
J. Geophys. Res. V. 86, p. 10412-10422.

Stone, M. (1982): The behavior of tin and some other trace elements during granite differentiation, west Cornwall, England.
In: Evans, A.M., ed: Metallization associated with acid magmatism.
Wiley, p. 339-355.

Stone, M. (1988): The significance of almandine garnets in the Lundy and Dartmoor granites.
Min. Mag. V. 52, p. 651-658.

Stone, M. and Exley, C.S. (1985): High heat production granites of southwest England and their associated mineralization: a review.
In: High heat production (HHP) granites, hydrothermal circulation and ore genesis. Inst. Min. Metall. Lond., p. 571-593.

Stone, M. and Exley, C.S. (1986): High heat production granites of southwest England and their associated mineralisation: a review.
Trans. Inst. Min. Metall. Sect. B: 95, p. 25-36

Stone, M., Exley, C.S. and George, M.C. (1988): Compositions of trioctahedral micas in the Cornubian batholith.
Min. Mag. V. 52, p. 175-192.

Stormer, J.C. and Carmichael, I.S.E. (1970): Villiaumite and the occurrence of fluoride minerals in igneous rocks.
Am. Mineral., V. 55, p. 126-134.

Streckeisen, A.L. (1974): Classification and nomenclature of igneous rocks. Recommendations of the IUGS subcommission on the systematics of igneous rocks.
Geol. Rundschau V. 63, p. 773-786.

Streckeisen, A.L. and LeMaitre, R.W. (1979): A chemical approximation to the modal QAFP classification of the igneous rocks.
Neues Jahrb. Mineral. Abh. V. 136, p. 169-206.

Struik, L.C. (1987): The ancient western North American margin: an alpine rift model for the east-central Canadian Cordillera.
Geol. Surv. Can. Paper 87-15, pp. 19.

Sun, S-S. (1980): Lead isotopic study of young volcanic rocks from mid-ocean ridges, oceanic islands and island arcs.
Phil. Trans. Roy. Soc. Lond. A 297, p. 409-445.

Swanson, S.E., Bond, J.F., and Newberry, R.F. (1988): Petrogenesis of the Ear Mountain tin granite, Seward Peninsula, Alaska.
Econ. Geol. V. 83, p. 46-61.

Swanson, S.E., Newberry, R.J., Coulter, G.A. and Dyehouse, T.M. (1990): Mineralogical variation as a guide to the petrogenesis of the tin granites and related skarns, Seward Peninsula, Alaska.
In: Stein, H.J. and Hannah, J.L. eds., Ore-bearing granite systems; petrogenesis and mineralizing processes. Geol. Soc. Amer. Special Paper 246, p. 143-159.

Sylvester, P.L. (1989): Post-collisional alkaline granites.
Journal of Geology V.97, p. 261-280.

Symons, D.T.A. (1983): New paleomagnetic data for the Triassic Guichon batholith of south-central Brirish Columbia and their bearing on Terrane1 tectonics.
Can. Jour. Earth Sci. V. 20, p. 1340-1344.

Takenouchi, S. (1971): Hydrothermal Synthesis and consideration of the genesis of malayaite.
Mineral. Deposita 6, p. 335-347.

Takenouchi, S; Aramaki, S. and Ishihara, S. (1980):
Magnetite-series/ilmenite series vs. I-type/S-type granitoids.
in: Ishihara,S. and Takenouchi,S: Granitic magmatism and related mineralization. Mining Geology Special Issue No.8.
Society of Mining Geologists of Japan. p. 13-28.

Taylor, H.P. (1988): Oxygen, hydrogen and strontium isotope constraints on the origin of granites.
In: The Origin of Granites. Trans. Roy. Soc. Edin. V. 79, p. 317-338.

Taylor, W.P. (1976): Intrusion and differentiation of granitic magma at a high level in the crust: the Puscao pluton, Lima Province, Peru.
J. Pet. V.17, p. 194-218.

Tauson, L.V. and Kozlov, V.D. (1973): Distribution functions and ratios of trace-element concentrations as estimators of the ore-bearing potential of granites.
in : Jones, M.J., ed: Geochemical exploration 1972. Inst. Min. Metall. London, p. 37-44.

Tempelman-Kluit, D.J. and Wanless, R.K. (1975): Potassium-argon age determination of metamorphic and plutonic rocks in the Yukon Crystalline Terrane.
Can. Jour. Earth Sci. V12, p. 1895-1909.

Tempelman-Kluit, D.J. (1977): Stratigraphic and structural relations between Selwyn Basin, Pelly-Cassiar Platform, and Yukon Crystalline Terrane in the Pelly Mountains, Yukon.
in: Report of activities, Part A, Geol. Surv. Can. Paper 77 -1A, p. 223-227.

Tempelman-Kluit, D.J. (1979): Transported cataclasite, ophiolite and granodiorite in yukon: evidence of arc - continent collision. Geol. Surv. Can. Paper 79-14, pp. 27.

Tempelman-Kluit, D.J. (1979): Five Occurrences of transported synorogenic clastic rocks in Yukon Territory
Geol. Surv. Can. Paper 79-1a, p. 1-12.

Tempelman-Kluit, D.J. (1980): Evolution of physiography and drainage in southern Yukon.
Can Jour. Earth Sci. V.17, No 9, p. 1189-1203.

Thirlwall, M.F. and Marriner, G.F. (1986): A guide book to rock analysis using the Philips PW 1400 X-ray fluorescence spectrometer.
Department of Geology, Royal Holloway and Bedford New College, University of London. pp. 20 (unpublished).

Thompson, B., Mercier, E., and Roots, C. (1987): Extension and its influence on Canadian Cordilleran passive-margin evolution.
In: Coward, M.P., Dewey, J.F., and Hancock, P.L. eds., Continental Extensional Tectonics. Geol. Soc. Lond. Special Pub. 28. p. 409-417.

Tilley, C.E. (1951): The zoned contact-skarns of the Broadford area, Skye: a study of boron-fluorine metasomatism in dolomites.
Min. Mag. V. 29, p. 621-666.

Tindle, A.G. and Pearce, J.A. (1981): Petrogenetic modelling of in situ fractional crystallisation in the zoned Loch Doon pluton, Scotland.
Contrib. Min. Pet. V. 78, p. 196-207.

Tindle, A.G. and Pearce, J.A. (1983): Assimilation and partial melting of continental crust: evidence from the mineralogy and geochemistry of autoliths and xenoliths.
Lithos, V. 16, p. 185-202.

Tipper, H.W., Woodsworth, G.J. and Gabrielse, H. (1981): Tectonic assemblage map of the Canadian Cordillera and adjacent parts of the United States of America.
Geol. Surv. Can. Map 1505A. Scale 1:2,000,000.

Toselli, J.N., Rossi de Toselli, J.N., Saavedra, J. and Pellitero, E. (1989): Granitoids of the Tafi Megafracture (Sierras Pampeanas, Argentina): petrogenetic implications.
Jour. South Amer. Earth Sci. V. 2, p. 199-204.

Vernon, R.H. (1983): Restite, xenoliths and microgranitoid enclaves in granites.
Jour. Proc. Roy. Soc. N.S.W. V. 116, p. 77-103.

Vernon, R.H. (1986): K-feldspar megacrysts in granites- phenocrysts, not porphyroblasts.
Earth-Science Rev., V. 23, p. 1-63.

Vernon, R.H., Etheridge, M.A. and Wall, V.J. (1988): Shape and microstructure of microgranitoid enclaves: indicators of magma mingling and flow.
Lithos, V. 22, p. 1-11.

Wall, V.J., Clemens, J.D. and Clarke, D.B. (1987): Models for granitoid evolution and source compositions.
Jour. Geol. V. 95, p. 731-749.

Wang Shufeng (1983): Some problems concerning geochemistry of the Dading tin-iron ore deposits.
Bull. Inst. Min. Deposits, 9. Chinese Academy of Geological Sciences, Beijing.
Abstract in English p. 69-70.

Wasternack, J., Kühne, R. and Schulze, H. (1974): Late magmatic and high to medium temperature postmagmatic metasomatism in Saxonian Erzgebirge, G.D.R.
In: Stemprok, M. ed: Metallization associated with acid magmatism.
Ustredni ustav geologicky, Praha, p. 226-231.

Watanabe, T. (1953): Suanite, a new magnesium borate mineral from Hol Kol, Suan, North Korea.
Mineralogical Jour. V. 1, No.1, p. 54-62.

Watanabe, T. (1954): On the ocurrence of Warwickite $(Mg,Fe)_3TiB_2O_8$ at Hol Kol, Korea: a study of boron metasomatism.
Jour. Faculty of Science, Univ. Tokyo, Sect. 2, Vol 9, part 2, p. 337-349.

Watson, J.A., Fowler, M.B., Plant, J.A. and Simpson, P.R. (1984): Variscan-Caledonian comparisons: late orogenic granites.
Proc. Ussher Soc. V. 6, p. 2-12.

Webb, P.C., Tindle, A.G., Barritt, S.D., Brown, G.C. and Miller, J.F. (1985): Radiothermal granites of the United Kingdom: comparisons of fractionation patterns and variation of heat production for selected granites.
In/ High heat production (HHP) granites, hydrothermal circulation and ore genesis. Inst. Min. Metal. Lond. p. 409-424.

Webster, J.D. and Holloway, J.R. (1990): Partitioning of F and Cl between magmatic hydrothermal fluids and highly evolved granitic magmas.
In: Stein, H.J. and Hannah, J.L., eds., Ore-bearing granite systems; petrogenesis and mineralizing processes. Geol. Soc. Amer. Special Paper 246, p. 21-34.

Weidner, J.R. and Martin, R.F. (1987): Phase equilibria of a fluorine-rich leucogranite from the St Austell pluton; Cornwall.
Geoch. et Cosmochim. Acta V. 51, p. 1591-1597.

Wheeler, J.O. and McFeely, P. (comp) 1991: Tectonic assemblage map of the Canadian Cordillera and adjacent parts of the United States of America.
Geol. Surv. Can. Map 1712A. Scale 1:2,000,000.

White, A.J.R. (1990): Crustal protoliths of granites
Notes for the January 1990 meeting, University of St. Andrews. pp. 44.

White, A.J.R. and Chappell, B.W. (1977): Ultrametamorphism and granitoid genesis.
Tectonophysics, V. 43, p. 7-22.

White, A.J.R. and Chappell, B.W. (1988): Some supracrustal (S-type) granites of the Lachlan Fold Belt.
in: The Origin of Granites. Trans. Roy. Soc. Edin. V. 79, p. 169-181.

White, A.J.R., Clemens, J.D., Holloway, J.R., Silver, L.T., Chappell, B.W. and Wall, V.J. (1986): S-type granites and their probable absence in S.W. North America.
Geology, V.14, p. 115-118.

Wickham, S.M. (1987): The segregation and emplacement of granitic magmas.
J. Geol. Soc. Lond. V.144, p. 281-297.

Wilson, G.A. and Eugster, H.P. (1990): Cassiterite solubility and tin speciation in supercritical chloride solutions.
in: Spencer, R.J. and Chou, I-Ming, eds. Fluid mineral Interactions: a tribute to H.P. Eugster. Geochemical Society Special Publication No. 2, San Antonio, Texas, p. 179-195. Can. Jour. Earth Sci. V.13, p. 1007-1019.

Winkler, H.G.F. and Schultes, H. (1982): On the problem of alkali feldspar phenocrysts in granitic rocks.
Neues Jahrb. Mineral. Monatsch. H. 12, p. 558-564.

Witt, W.K. (1987): Fracture-controlled feldspathic alteration in granites associated with tin mineralisation in the Irvinebank-Emuford area, northwest Queensland.
Aust. Jour. Earth Sci. v.34 (4), p. 447-462.

Wyllie, P.S., Huang, W.-L., Stern, C.R. and Maaloe, S. (1976): Granitic magmas: possible and impossible sources, water contents and crystallisation sources.

Yorath, C.J., Green, A.G., Clowes, R.M., Sutherland Brown, A., Brandon, M.T., Kanasewich, E.R., Hyndman, R.D. and Spencer, C. (1985): Lithoprobe, southern Vancouver Island: seismic reflection sees through Wrangellia to the Juan de Fuca Plate.
Geology V. 13, p. 759-762.

Young, G.M. (1992): Late Proterozoic stratigraphy and the Canada-Australia connection.
Geology, V. 20, p. 215-218.

Zahm, A. (1987): The compositional evolution of calc-silicates from the Salau skarn-deposit (Ariège, Pyrénées).
Bulletin de Minéralogie V. 110 (6), p. 623-632.

Zalashova, N.E. and Gerasimovskii, V.V. (1974): Petrographic and geochemical features of rare-metal amazonite granites.
in: Stemprok, M., ed: Metallization associated with acid magmatism.
V1. IGCP: Geological Survey of Czechoslovakia, Praha, 232-236.

Zaw, U.K. and Clark, A.H. (1978): Fluoride-hydroxyl ratios of skarn silicates, Cantung E-zone scheelite orebody, Tungsten, Northwest Territories.
Can. Mineral. V.16, p. 207-221.

Zen, E-an (1988): Thermal modelling of stepwise anatexis in a thrust-thickened sialic crust.
In: The Origin of Granites. Trans. Roy. Soc. Edin. V.79, p. 223-235.

Zharikov, V.A. (1970a): Skarns (Part 1).
Internat. Geol. Rev. V. 12, p. 541-559.

Zharikov, V.A. (1970b): Skarns (Part 2).
Internat. Geol. Rev. V. 12, p. 619-647.

Zharikov, V.A. (1970c): Skarns (Part 3- Conclusion).
Internat. Geol. Rev. V. 12, p. 760-775.

Figure 1.2 The Thirtymile Range. A view looking south towards the highest peak (1997) from point {427276}. The top of the marble unit (and Thirtymile Thrust) is just visible as a lighter coloured area at the left hand base of this peak. Other marble exposures may be seen as white areas in the left middle distance.

Figure 3.3 The Thirtymile Thrust: visible as the upper contact of the marble unit (white). Overlying quartzites show a mesoscopic-scale anastomosing foliation partly consisting of many small flat-lying faults. NE spur of Peak 1997. White patches are remnants of the winter snow pack. Photograph taken from {429262} looking SE.

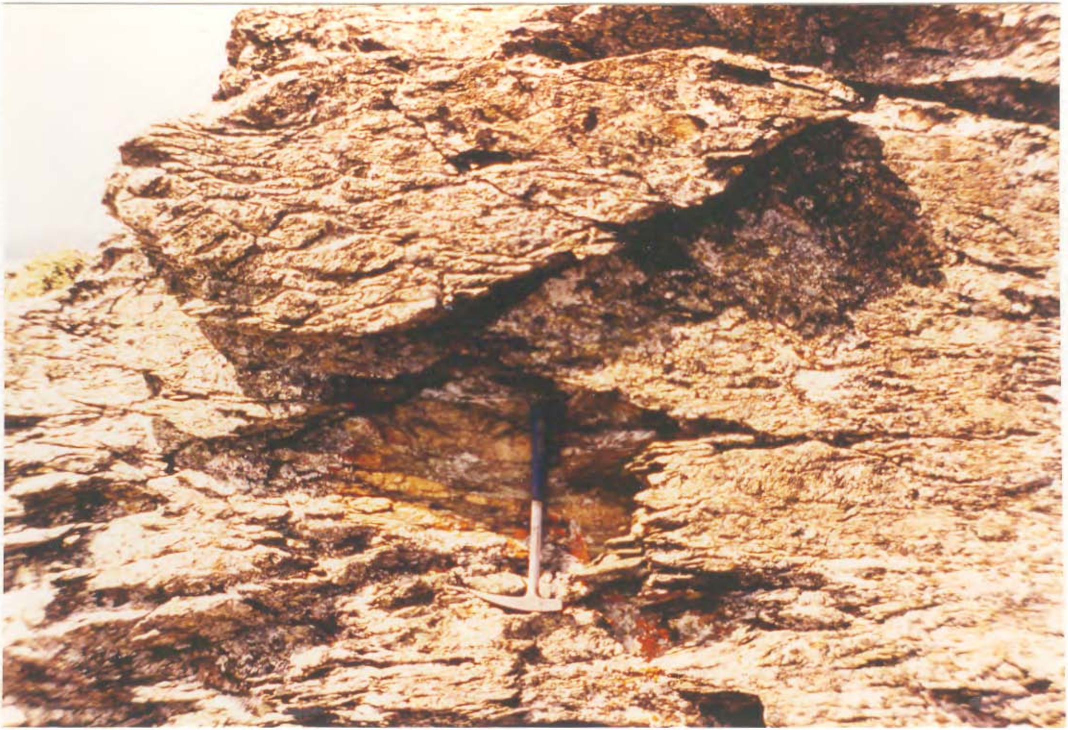

Figure 3.4 Anastomosing foliation in quartzite. Location {352339}, facing north westerly.

Figure 3.5 Brecciated marble. Mindy 3 prospect at {418265}.

Figure 3.6 Ork area sheared marble breccia from {424235}: sawn and polished slab.

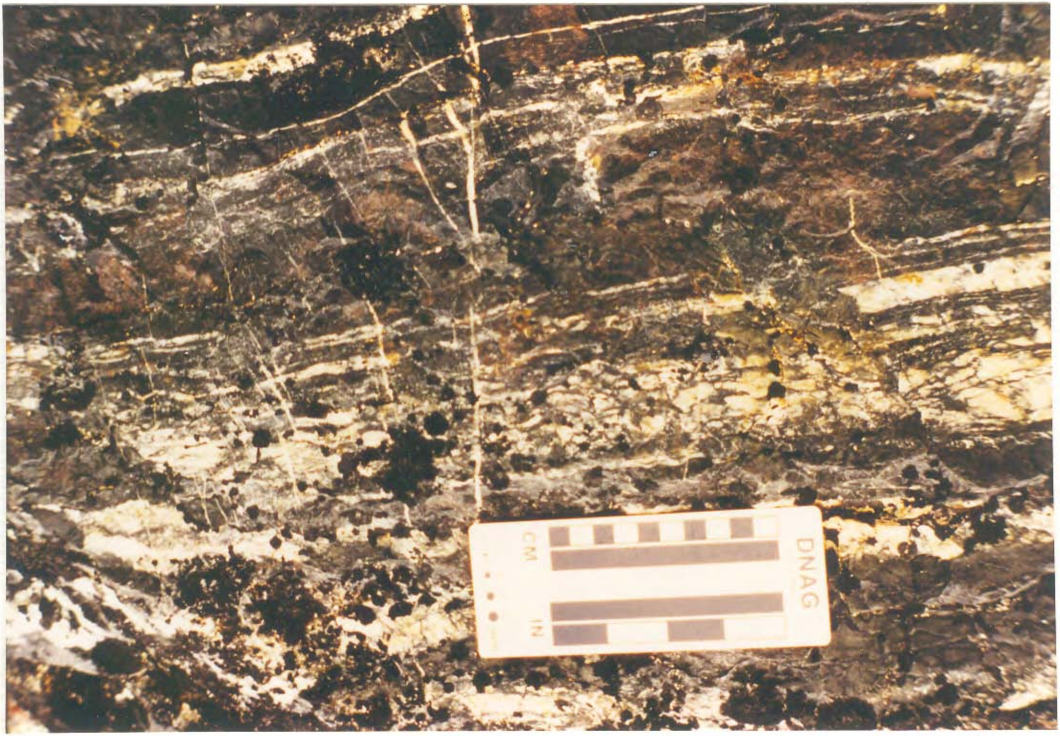

Figure 3.8 Boudinage in siliceous mylonite. Locality {443272}. Foliation dips 35° towards 335°.

Figure 3.9 Asymmetric folds with sheared-out limbs in phyllonite. NW Thirtymile area locality {276455}.

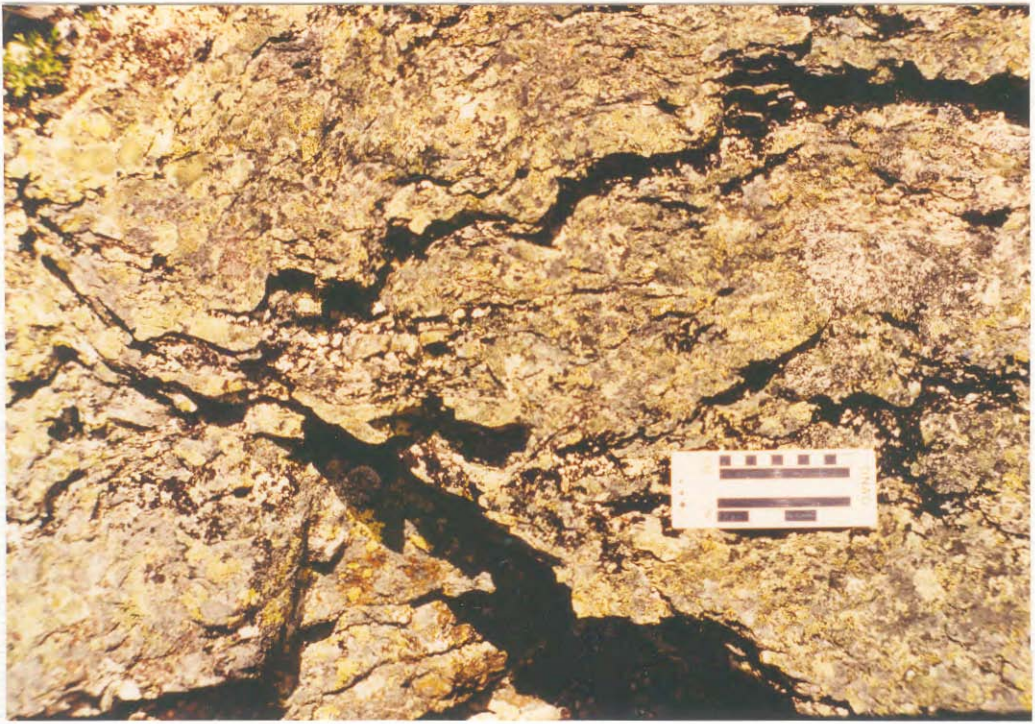

Figure 3.10 Open folding in phyllonite NE of the Mindy prospect. Locality {486245}.

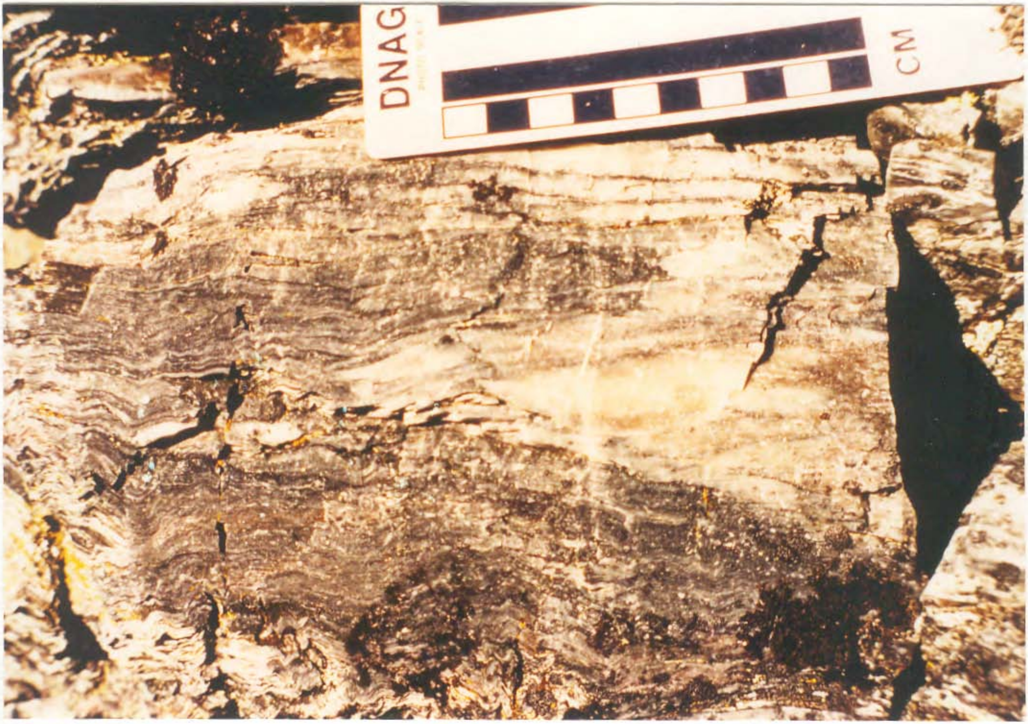

Figure 3.11 Crenulated siliceous mylonite. Locality {266410}. NW Thirtymile area.

Figure 3.12 Typical chevron-style folding in the phyllitic lithologies of the N.W. Thirtymile area: locality {246410}. Rule is opened to 18" (457 mm). Facing SSE.

Figure 3.14 The Thirtymile Thrust: Foliated marble (2 m) below; 1 metre of chevron-folded quartzite above. White dipping band is a pegmatite dyke. Locality {429261}, facing westward.

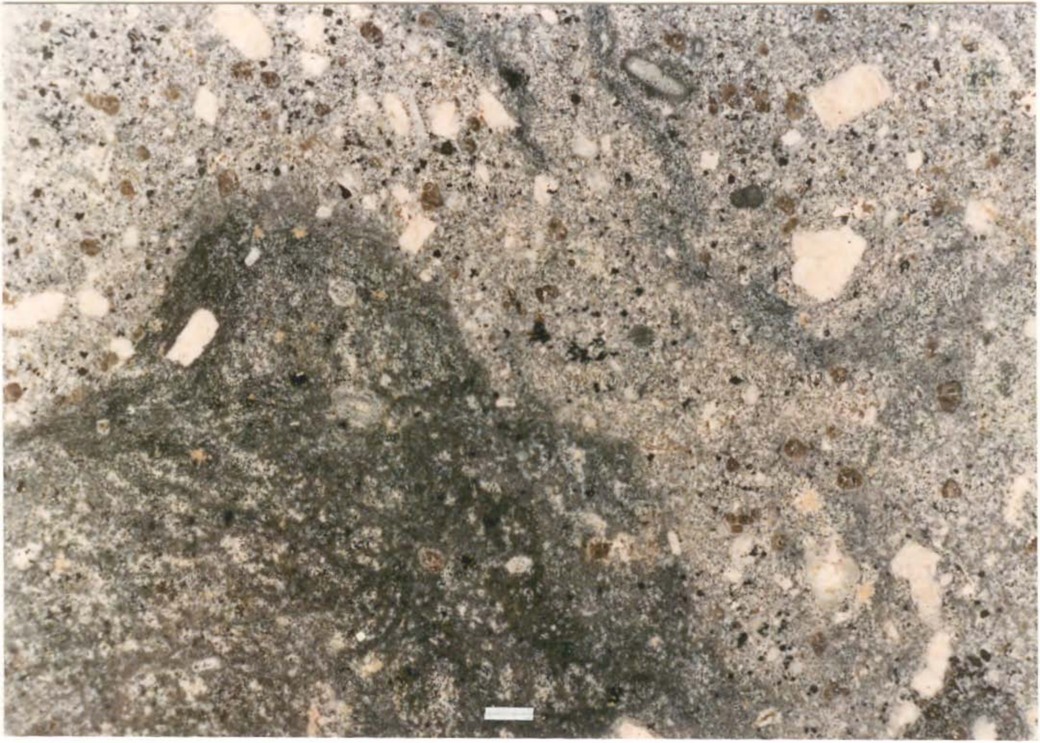

Figure 3.17 Enclave: central porphyry exposure of the Thirtymile stock at {407309}. Porphyritic granite displaying an embayed contact with surrounding fine-grained facies (similar to that of Fig. 4.4). The darker material is only slightly more mafic than the porphyritic variety. Analyses HPG and POR (App. C.1) are from this locality. Sawn slab: 10mm white scale shown.

Figure 3.18 Enclave of porphyry in megacrystic granite (glaciated rock face). Thirtymile stock at {405288}. Compass is 75 mm long.

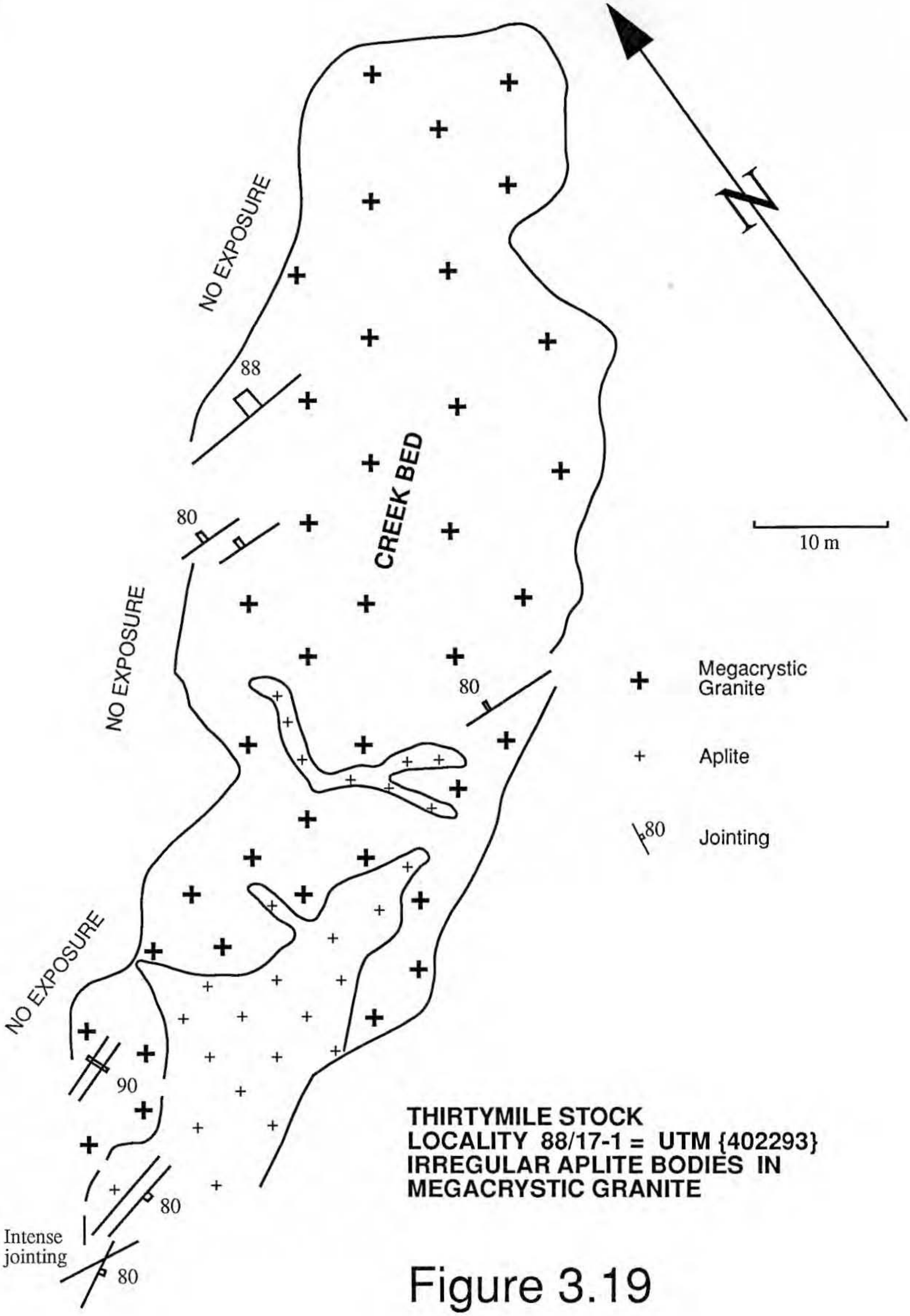

THIRTYMILE STOCK
LOCALITY 88/17-1 = UTM {402293}
IRREGULAR APLITE BODIES IN
MEGACRYSTIC GRANITE

Figure 3.19

Figure 3.20 Thirtymile stock, SE corner: biotite-rich layers of the Even-grained facies truncated by Li-mica leucogranite. Locality {418284}: fractured boulder.

Figure 3.21 Pod pegmatite (Coarse feldspar, quartz and occasional tourmaline crystals) in even-grained facies. Locality {418284}. Scale division on clino-rule is in inches.

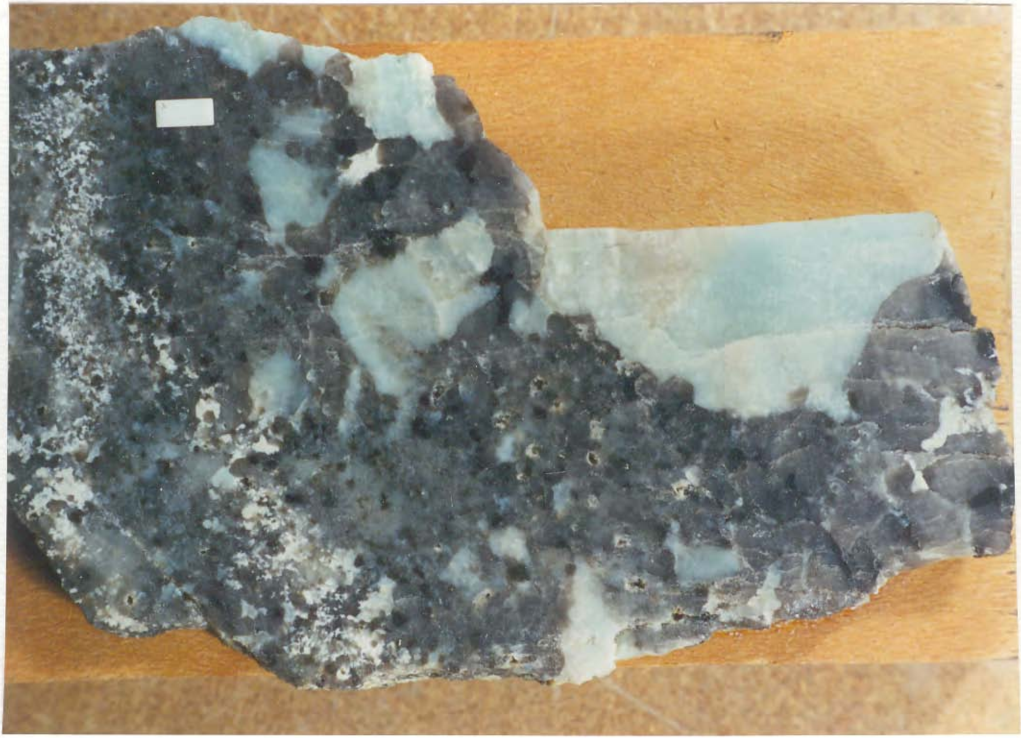

Figure 3.22 Ork pegmatite: sawn slab showing coarse amazonite feldspar, quartz and topaz with Li-mica leucogranite at the left edge. 10 mm white scale bar shown.

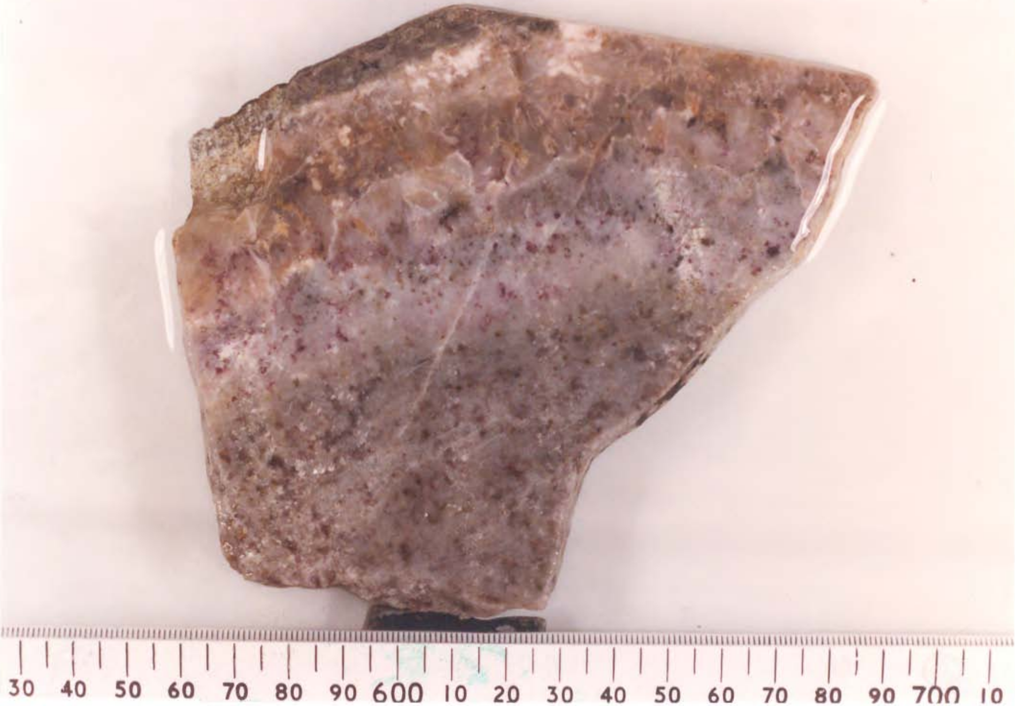

Figure 3.23 Ork contact in one hand specimen. Li-mica leucogranite nearest the scale (5 mm coarse division), plagioclase-fluorite endoskarn for 10 mm, then vesuvianite-malayaite exoskarn with a final 8 mm cebollite layer at the top of the photograph.

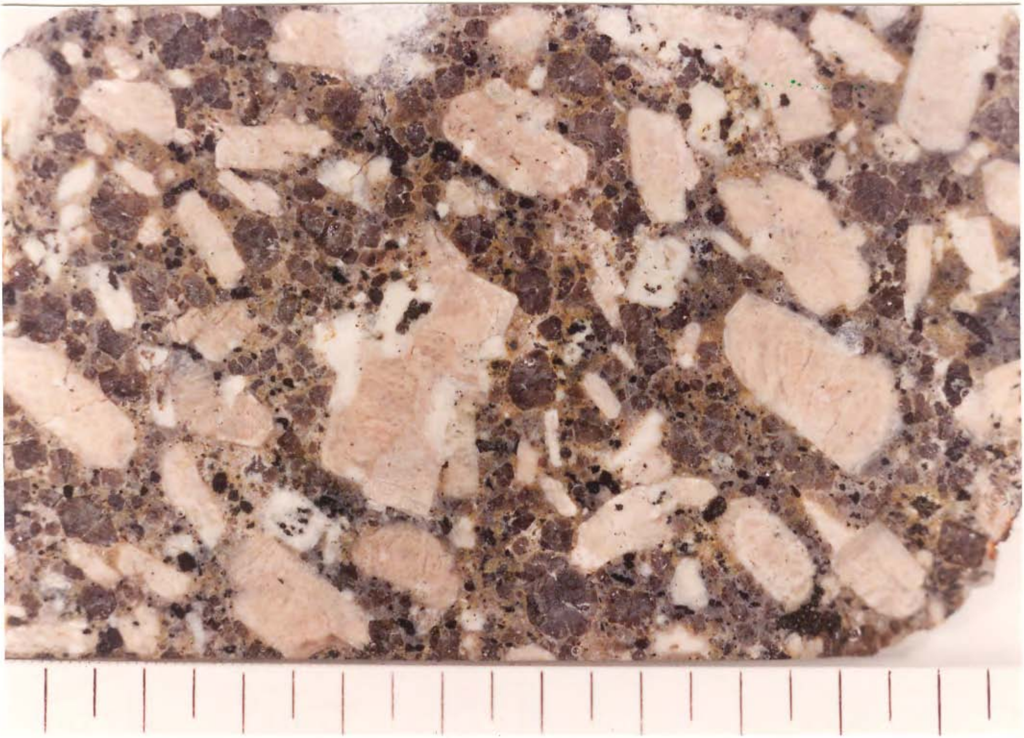

Figure 3.26 Hake batholith megacrystic granite: sawn slab of specimen 08/17-2 from {638030} showing a predominance of orthoclase microperthite megacrysts which have partial plagioclase mantles, small round quartz phenocrysts, some plagioclase and biotite. Scale division is 5 mm.

Figure 4.1 Porphyry: sawn slab showing coarse orthoclase phenocrysts (one with a Rapakivi rim), plagioclase and round quartz in a fine-grained feldspar-quartz-biotite-hornblende groundmass. Specimen 97/12-1D from {387315}. Scale division 5 mm.

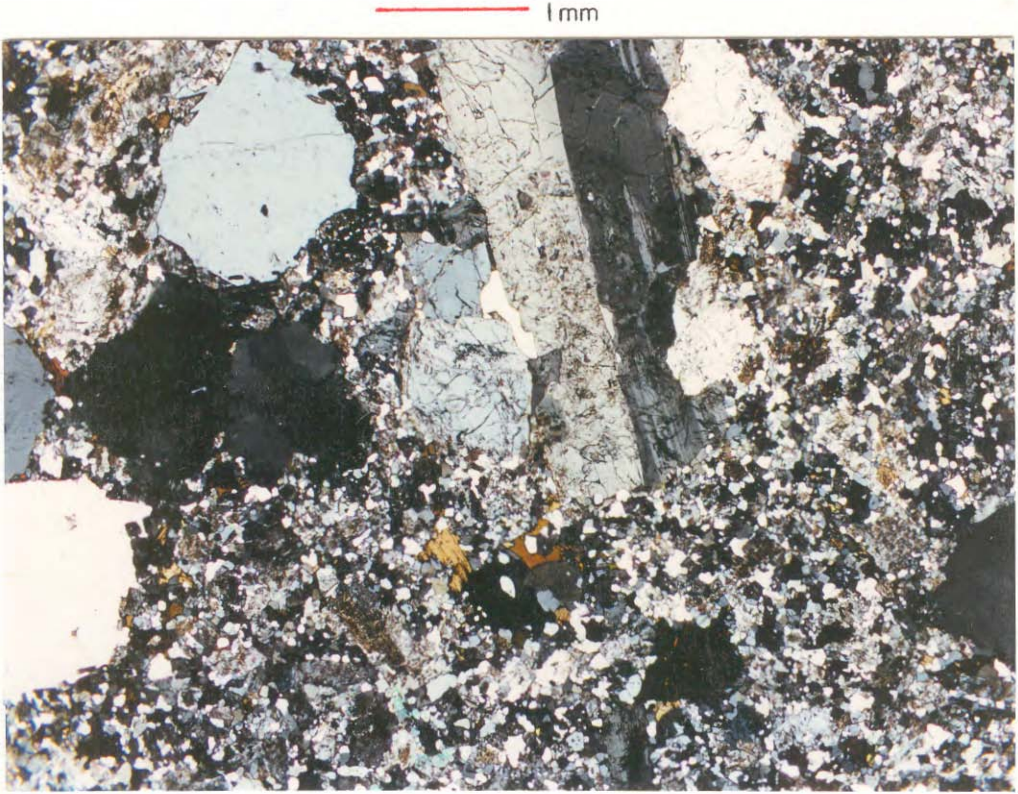

Figure 4.2 Porphyry: specimen 88/15-2 from the Thirtymile stock in thin section under crossed polarisers. Shows large embayed quartz phenocrysts with plagioclase in a quartz-feldspar-biotite groundmass. Locality {386314}.

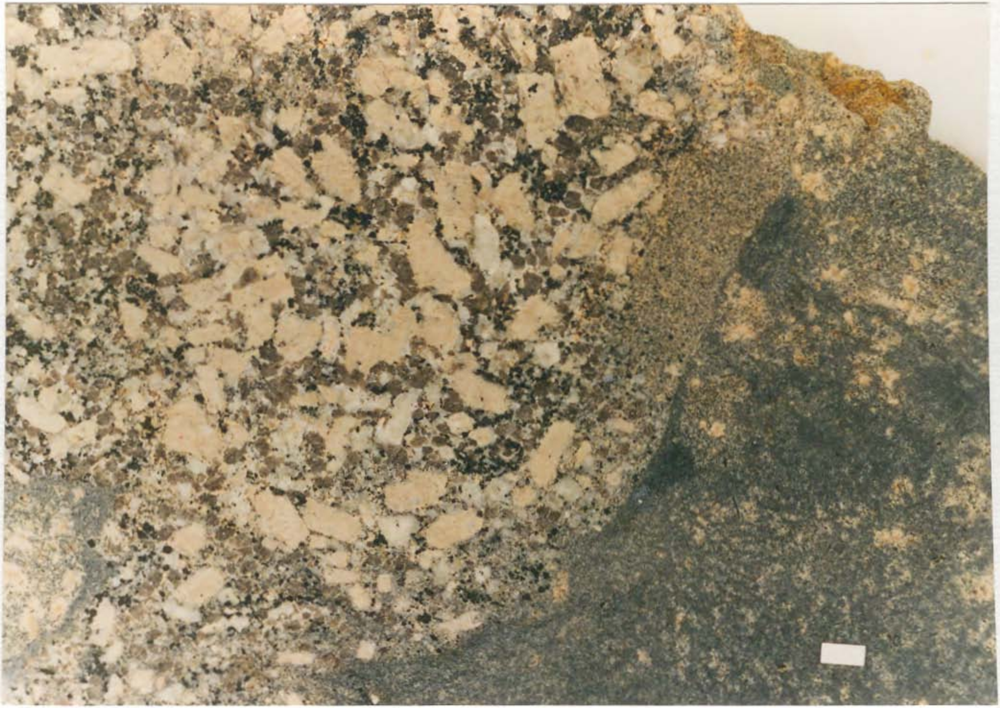

Figure 4.3 Enclave: sawn slab of finer-grained variety of porphyry (under white 10 mm long scale bar) in megacrystic granite. Specimen 88/14-2 from locality {390296}.

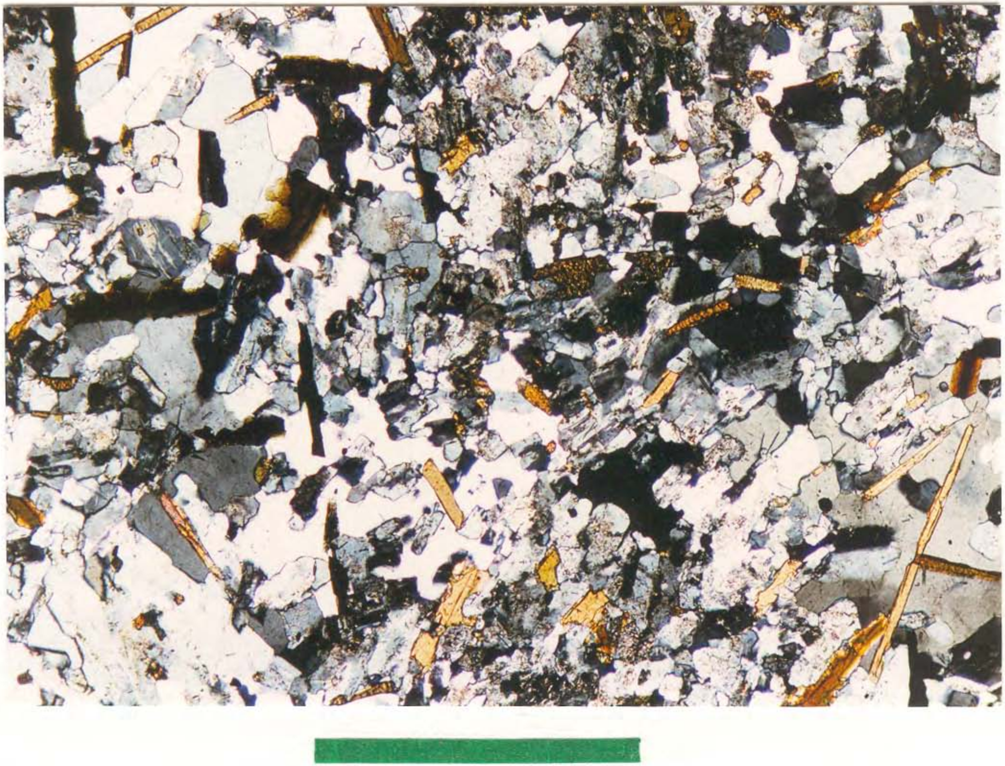

Figure 4.4 Enclave: photomicrograph of seriate-textured porphyry 88/14-2 under crossed polarisers showing very elongate biotite cryatals in a two-feldspar quartz groundmass.

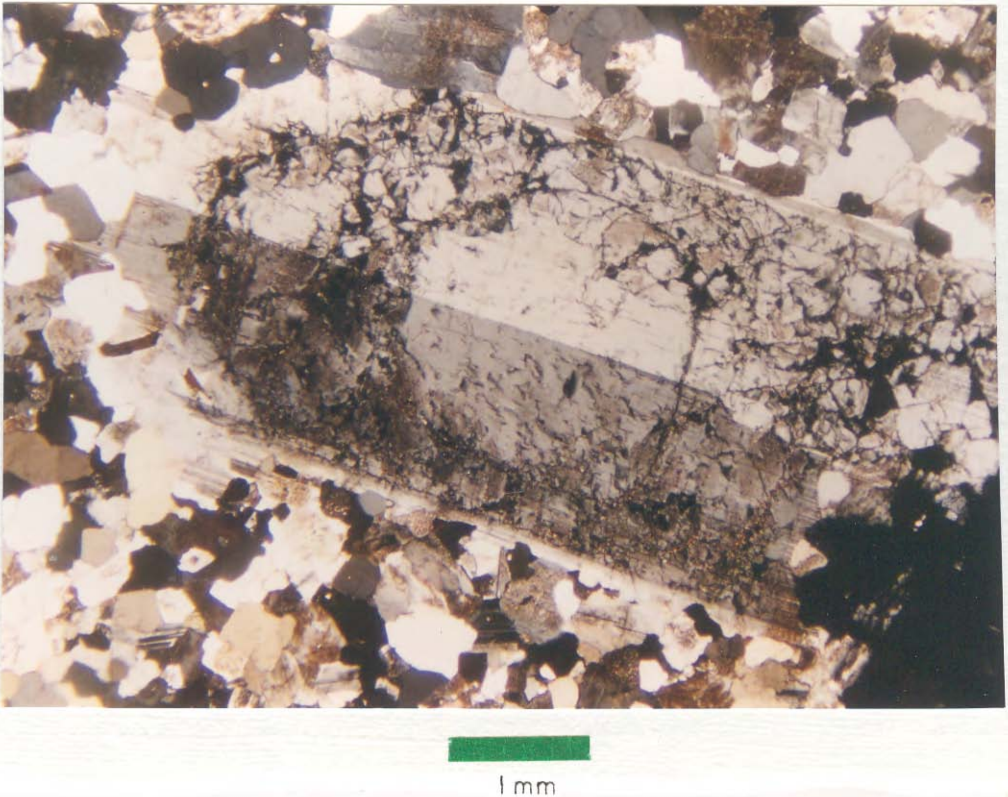

Figure 4.5 Even-grained granite: specimen 88/14-8 from {394296}. large cracked and altered plagioclase phenocryst. Thin section under crossed polarisers.

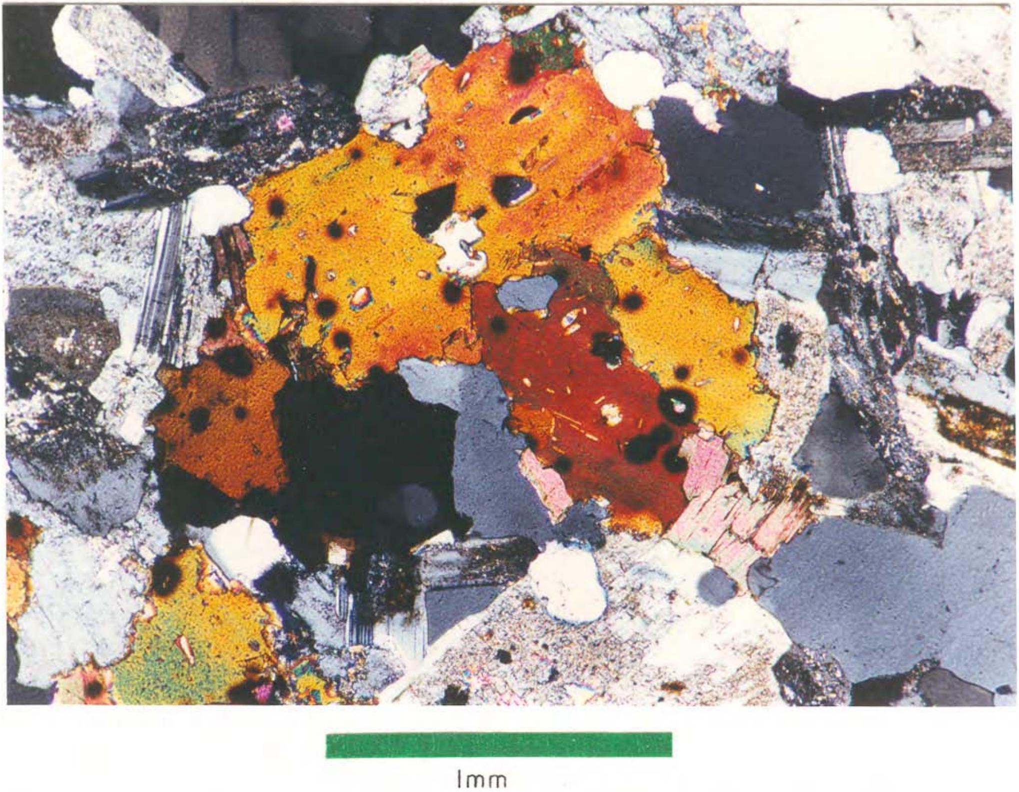

Figure 4.6 Cluster of very red biotite grains containing many zircon inclusions (restite?) in megacrystic granite 88/15-6 from {373309}.
Thin section under crossed polarisers.

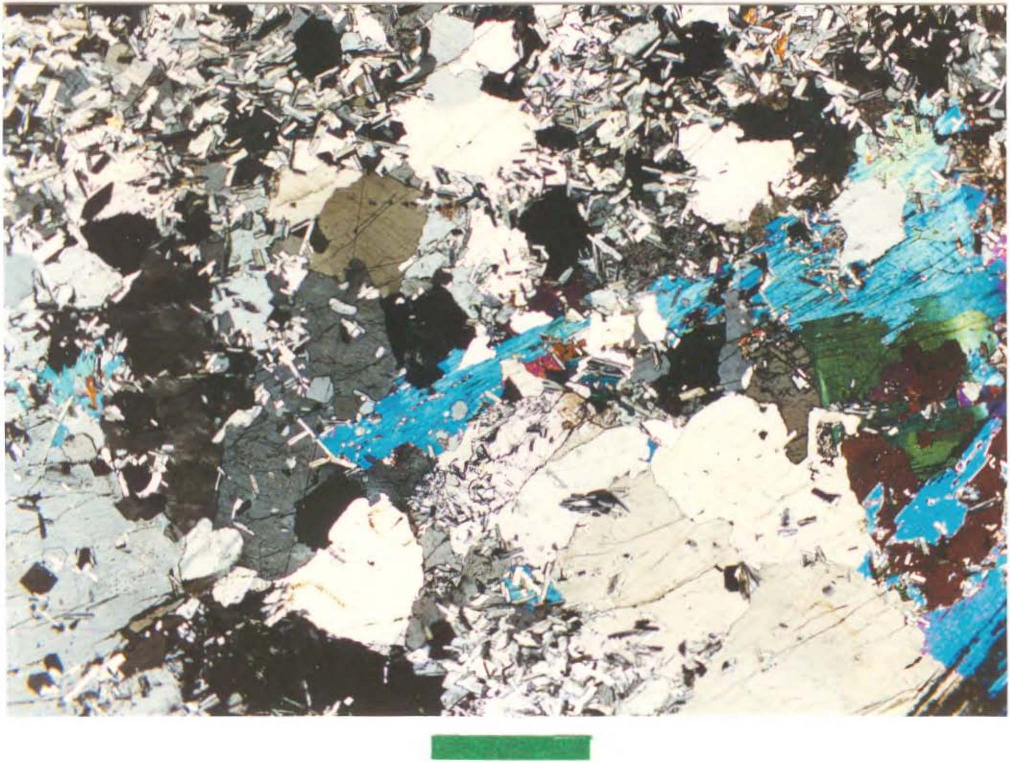

Figure 4.7 Ork contact: photomicrograph of pegmatite (here quartz and topaz) with coarse zinnwaldite) in contact with the leucogranite. Locality {429235}. Crossed polarisers.

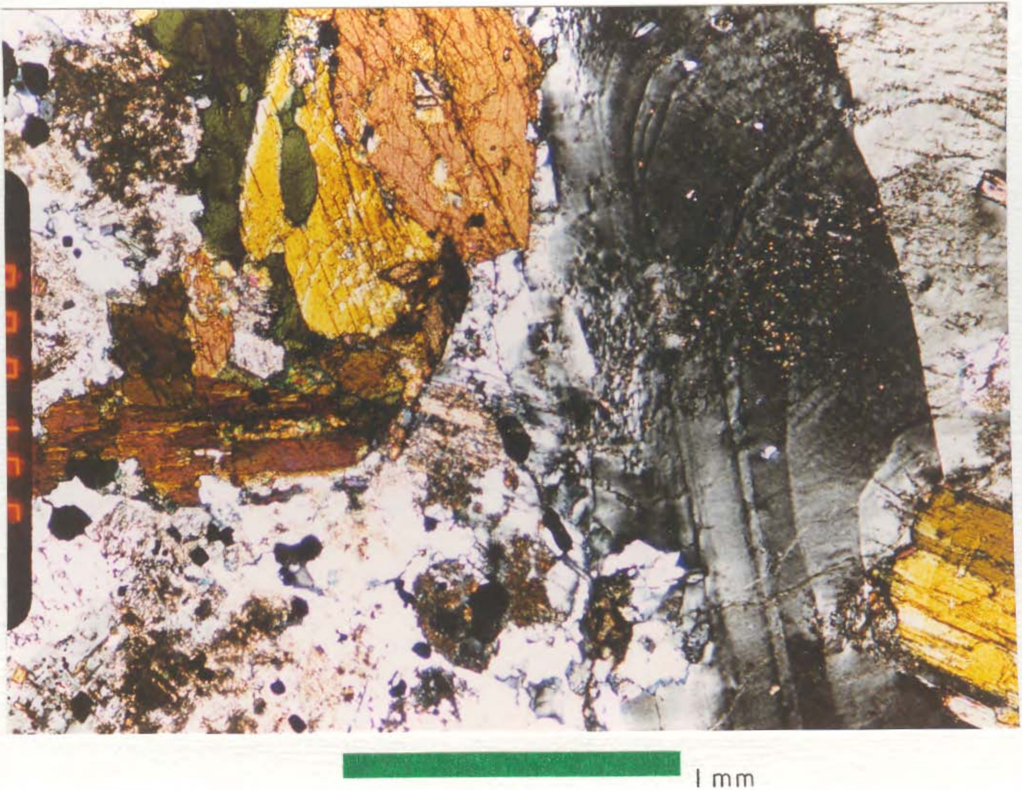

Figure 4.8 NW Thirtymile hornblende granodiorite 98/16-5 from {282450}. Thin section under crossed polarisers showing a large zoned and single-twinned microperthite phenocryst with euhedral hornblende in a plagioclase-quartz groundmass.

Figure 4.9 NW Thirtymile granodiorite 98/16-3 from locality {281446} under plain polarised light showing hornblende associated with yellow epidote and euhedral sphene.

Figure 4.10 NW Thirtymile granodiorite 98/16-1: section under crossed polarisers showing granophyre development.

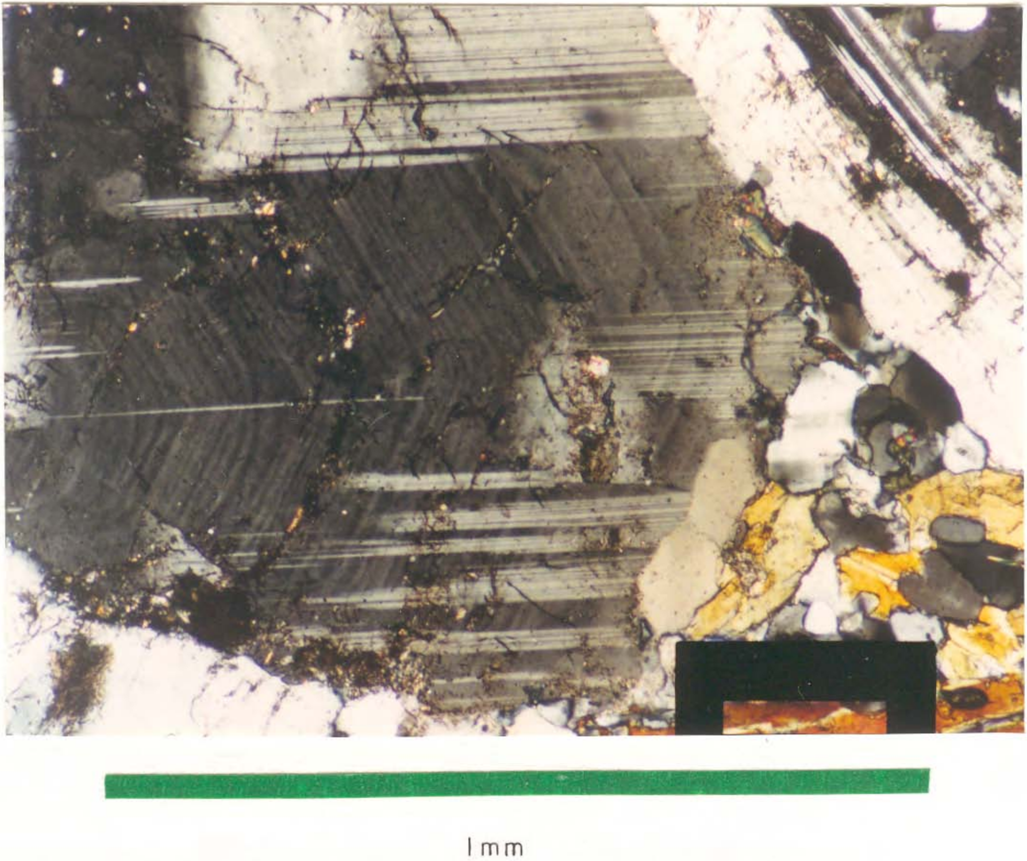

Figure 4.11 SW Thirtymile diorite 08/18-2 from locality {393112}.
Thin section under crossed polarisers showing zoned and twinned plagioclase and hornblende.

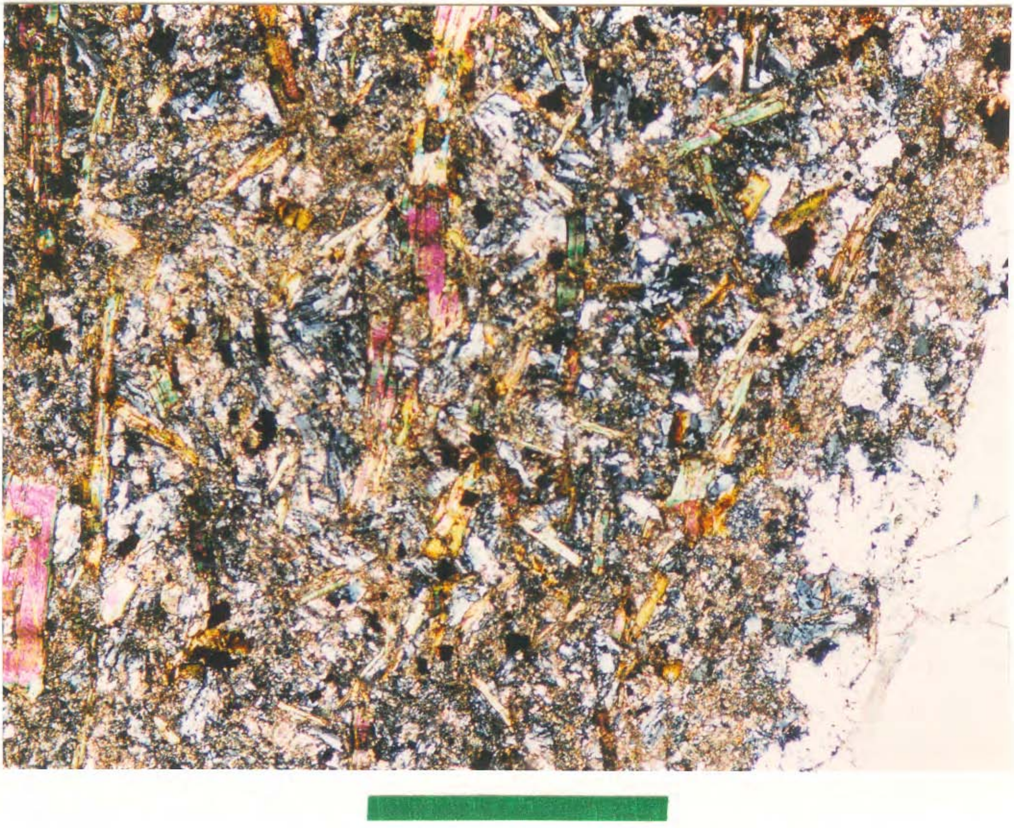

Figure 4.12 SW Thirtymile area: phlogopite-rich lamprophyre 08/20-1 found adjacent to the contact of the basic stock at {387128}. Photmicrograph taken under crossed polarisers shows kinked mica flakes in a plagioclase-carbonate groundmass in contact with a quartzite or chert xenolith.

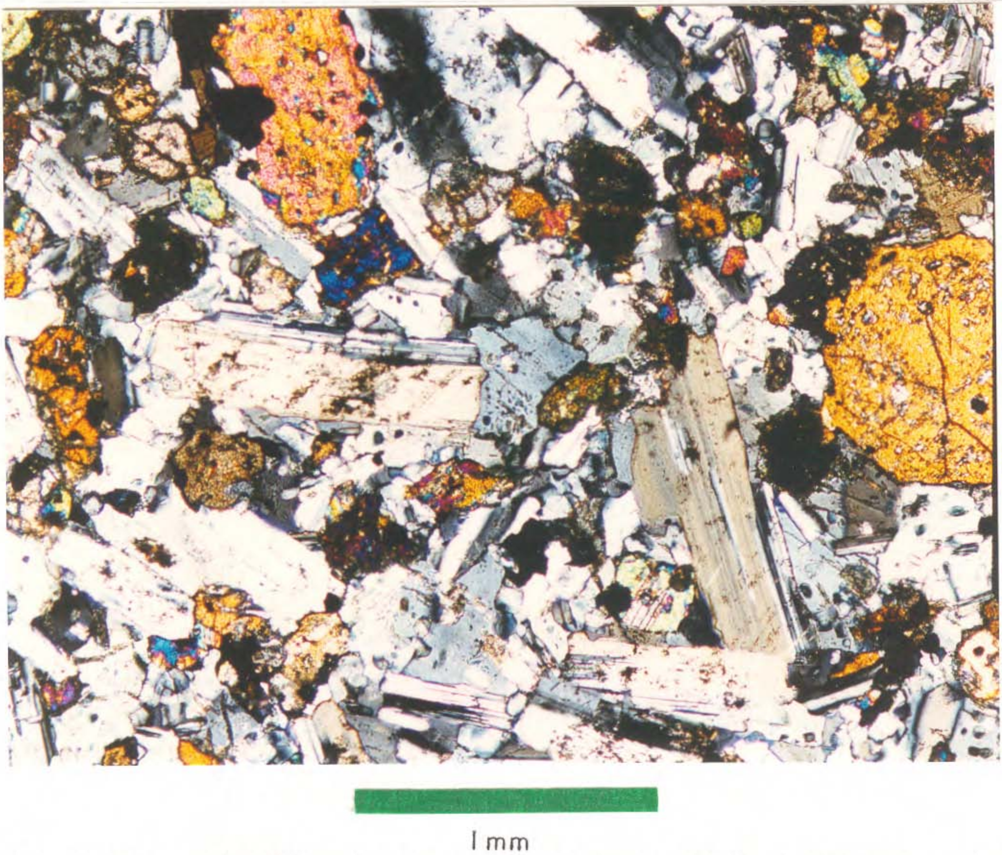

Figure 4.13 SW Thirtymile gabbro 08/20-2 from {388131}. Thin section under crossed polarisers showing titanaugite, plagioclase and a little olivine.

Figure 5.1 Mindy prospect: upper skarn exposure in cliff (see App. B.3) showing vesuvianite crystals up to 50 mm long. Ruler is divided in inches (i.e. ≈0.15 metres of rule is showing).

Figure 5.2 Mindy prospect: upper skarn exposure in cliff showing one of many small faults with apparent throws of ≤1 metre. Facing SE. Rule is opened to 18" (i.e. 0.46 metres). 1989 survey coordinates 150S, 140W (App. B.3).

Figure 5.3 Mineralised fractures in drillcore: alizarin/ ferricyanide stained dolomitic marble from DDH 81-8, 87.90 m showing magnetite mineralisation and pyrrhotite vein in siliciclastic sediment with a distinct bleached selvedge from 81-4/ 14.58 m.

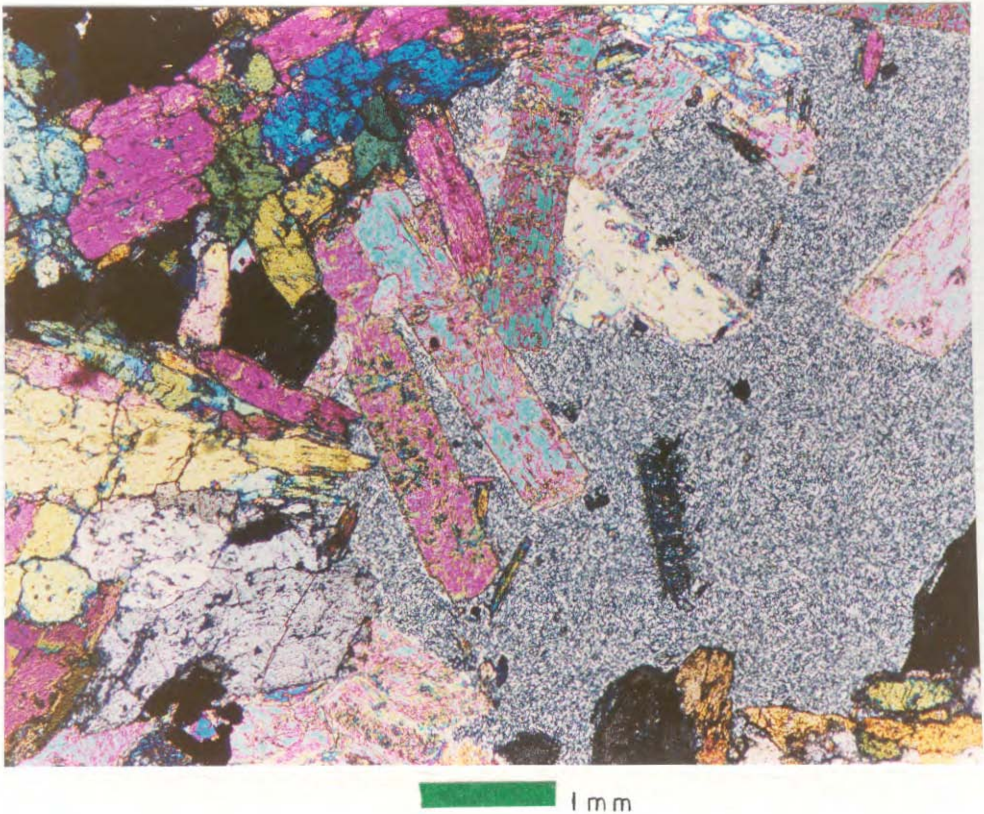

Figure 5.4 Borate & hydrous alteration: photomicrograph under crossed polarisers of diopside skarn replaced by fluoborite (prismatic crystals) and serpentine. Mindy surface specimen 670N, 285W (Newmont grid coordinates).

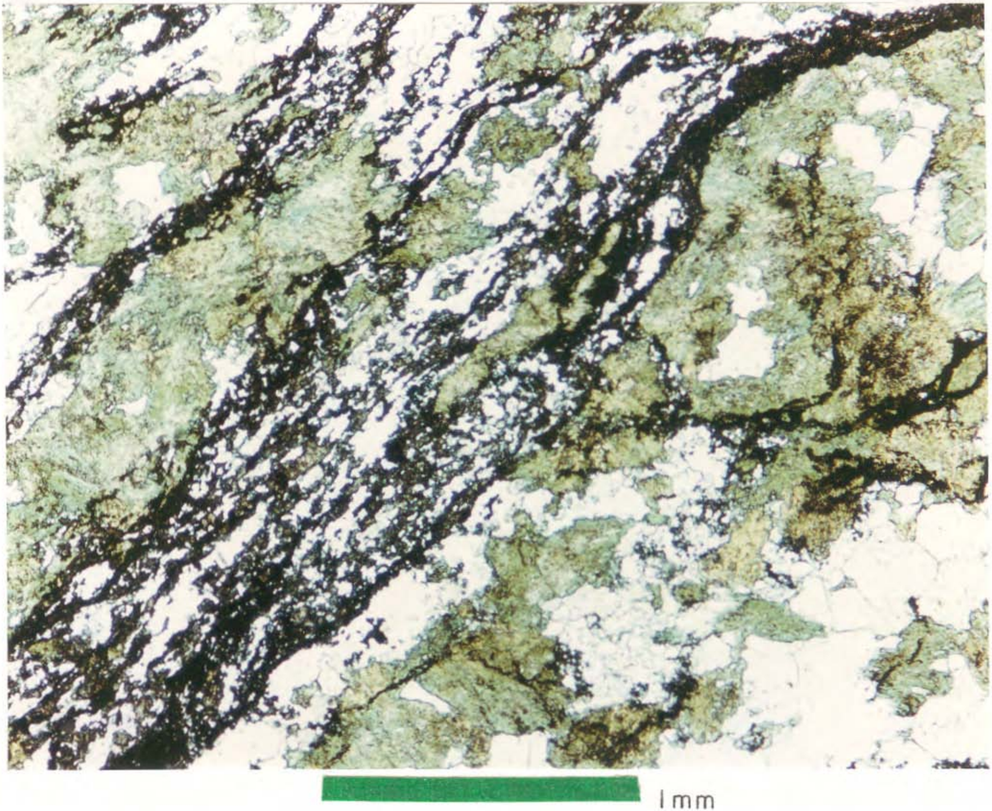

Figure 5.5 Calc-silicate marble showing relict pressure-solution fabric. Mindy surface 920N, 165W (Newmont grid). Photomicrograph under plain polarised light (Epidote/chlorite/opaques/carbonate).

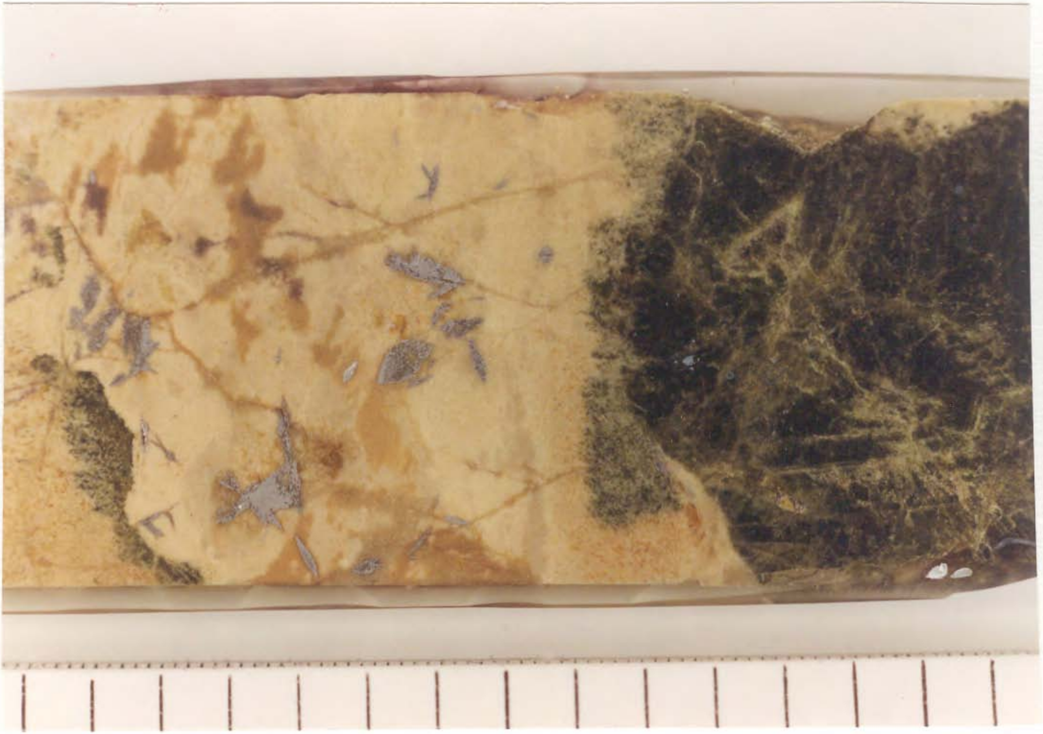

Figure 5.9 Mindy vein skarn: DDH 81-8, 59.4 m, sawn and polished core showing green andradite crystal with fine-grained honey-coloured garnet containing arsenopyrite crystals. Scale division is 5 mm.

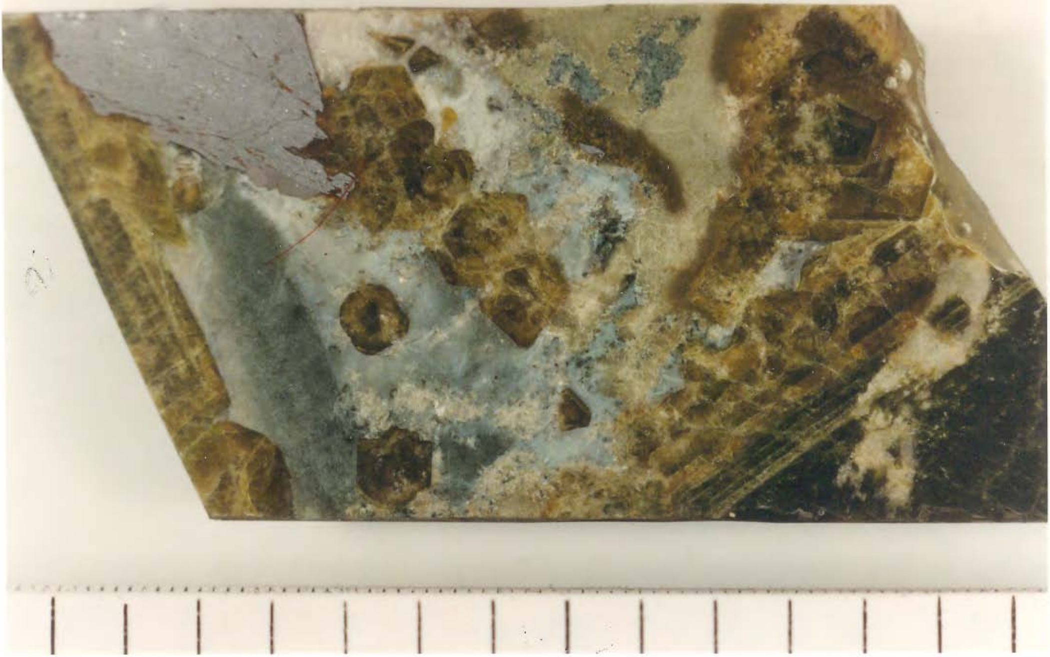

Figure 5.10 Vein skarn: DDH 81-8, 83.36 m, sawn and polished core showing zoned green and brown andradite with calcite, diopside (pale green) and arsenopyrite. 5 mm scale division.

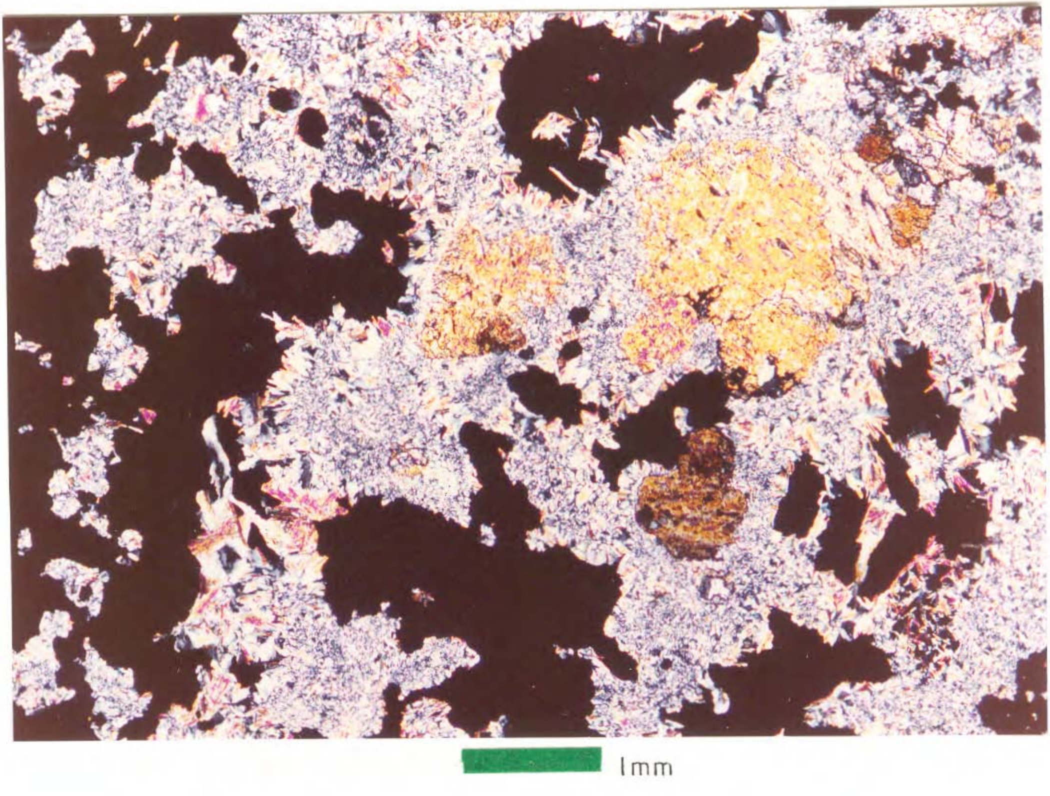

Figure 5.11 Mindy prospect wrigglite: DDH 2, 92.84 m. Thin section under crossed polarisers shows chondrodite-humite group mineral relicts in phlogopite-fluorite-magnetite 'wrigglite' greisen-skarn.

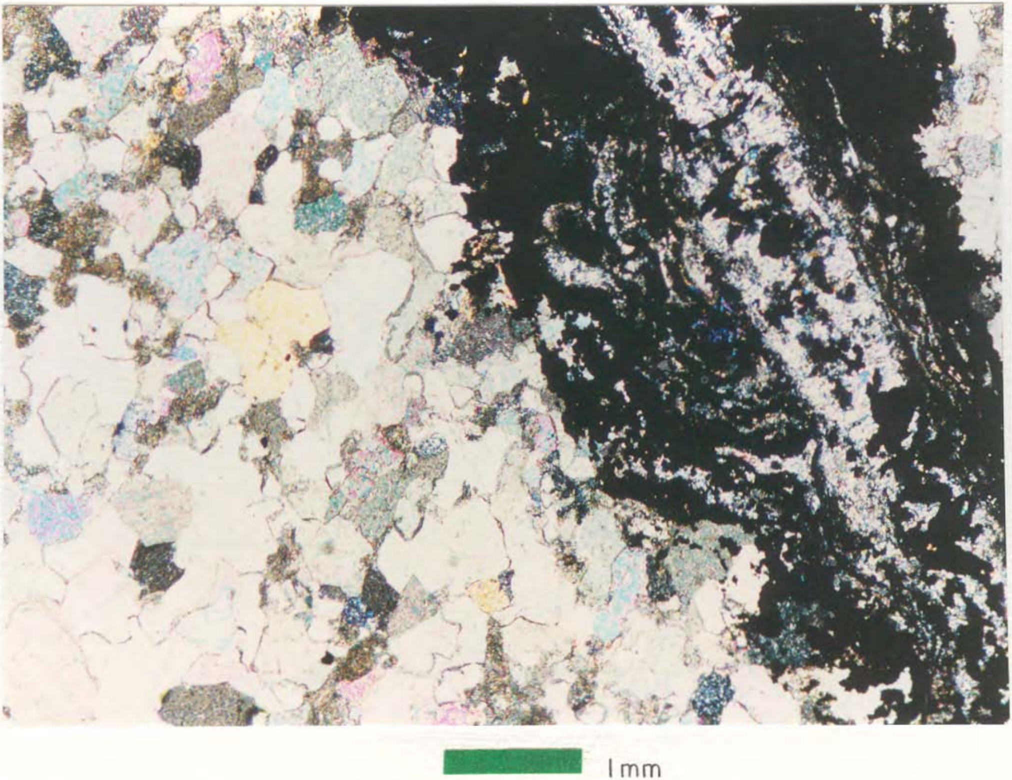

Figure 5.13 Wrigglite: DDH 81-8, 90.02 m. Finely banded magnetite vein with a fluorite-phengite core in marble. Thin section under crossed polarisers.

Figure 5.14 Magnetite-talc-fluoborite wrigglite with late fractures: DDH 81-2, 86.78 m. Thin section under plain polarised light.

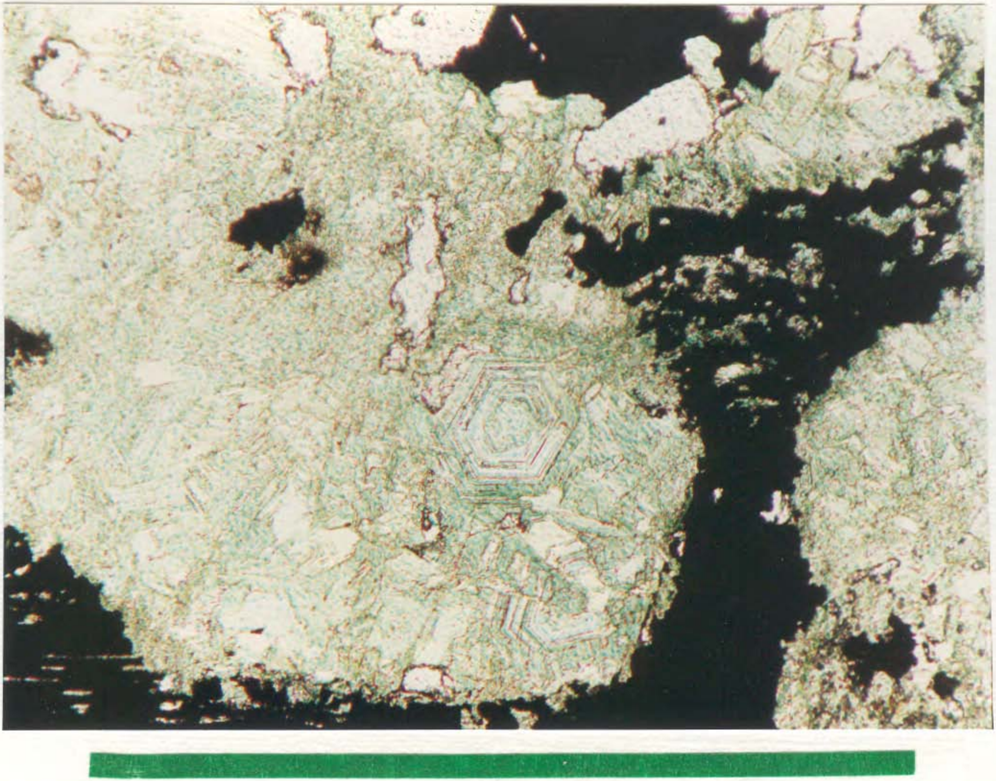

Figure 5.15 Skarn minerals: ferrophengite with magnetite and fluorite in wrigglite. Thin section under plain polarised light showing the striking zoning in this mineral.

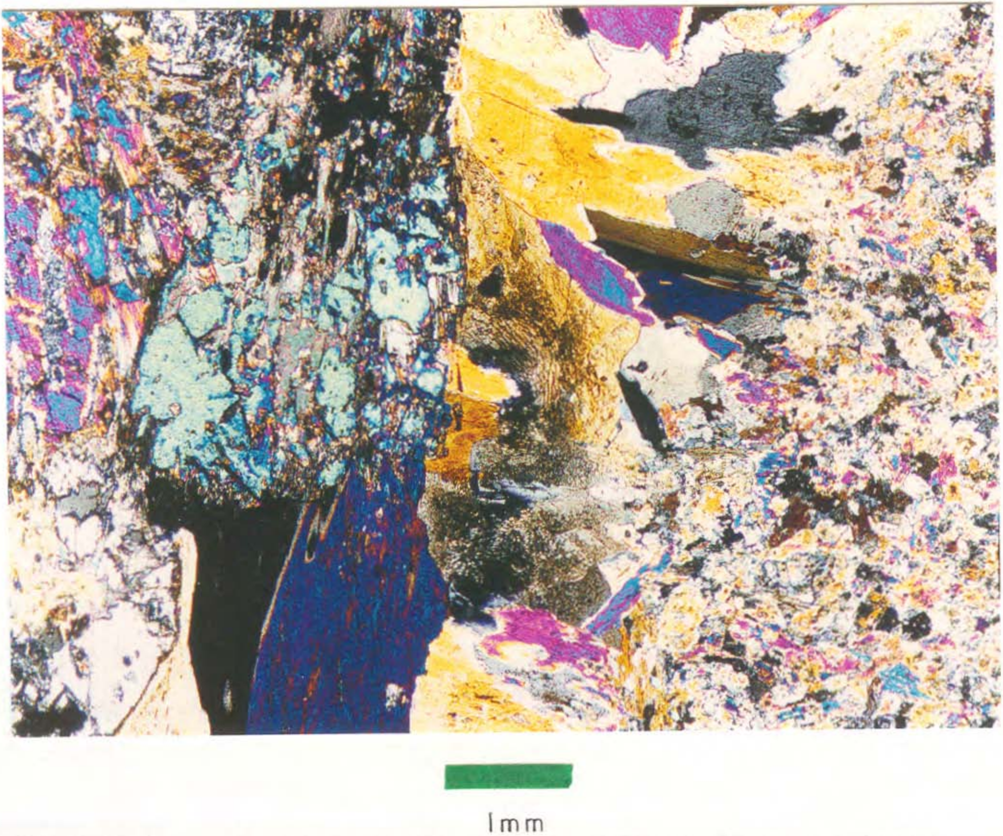

Figure 5.16 Rare mineral: thin section from DDH 81-2, 97.44 m under crossed polarisers showing a vein of hydrochlorborite (magenta interference colours) in corroded diopside-hedenbergite.

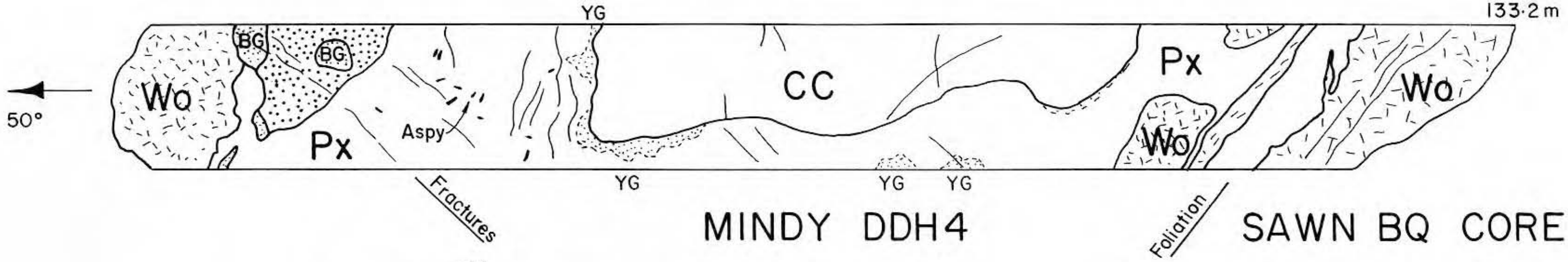

MINDY DDH4

SAWN BQ CORE

36·5mm diameter.

CC= Calcite
Px = Pyroxene
Bg = Brown garnet
G = Green (andradite) garnet
YG= Yellow garnet
Aspy= Arsenopyrite

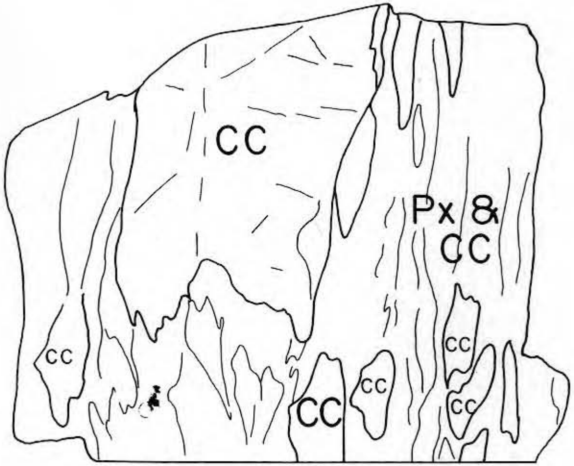

ORK AREA 424235

POLISHED SLAB

COMPARISON OF CATACLASTIC TEXTURE IN BRECCIATED, SHEARED MARBLE AT THE ORK AUREOLE WITH SKARN FROM THE MINDY PROSPECT.

T.Liverton, March 1990.

Fig. 5·17

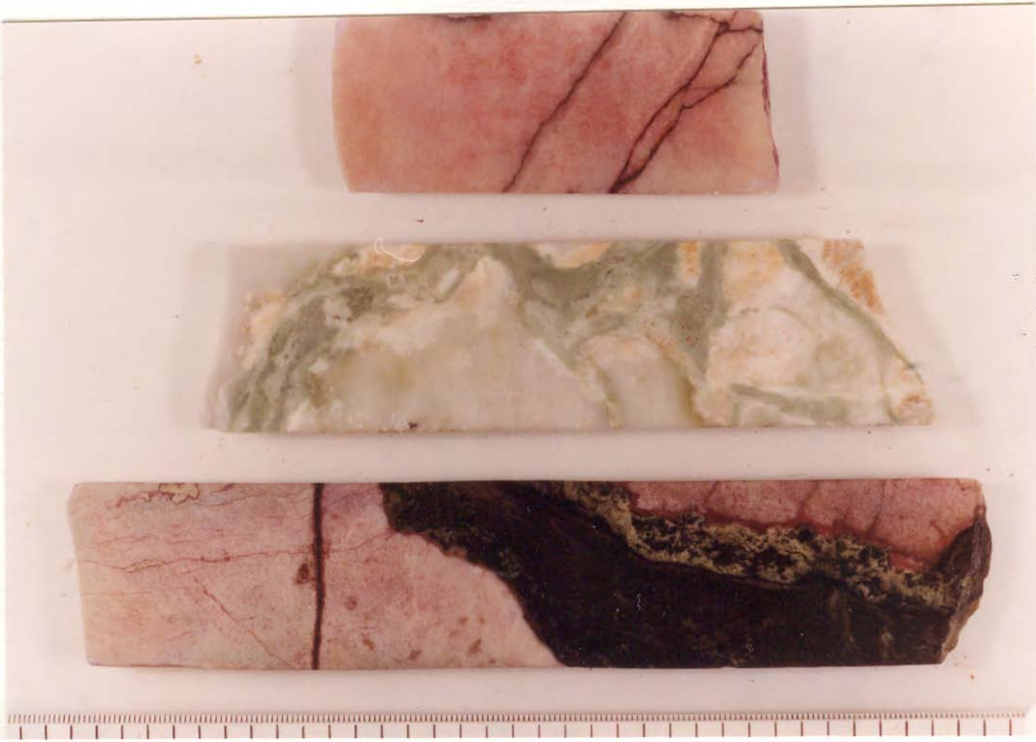

Figure 5.18 Mindy marbles: alizarin/ferrocyanide stained, sawn core from DDH 81-8, 50.81 m showing calcite marble with magnetite veins; 85.04 m showing dolomite breccia partially replaced by diopside (green) and 87.78 m, a clast of chert (dark) in marble with a bimetasomatic amphibole skarn developed around its margin. Coarse scale division 5 mm.

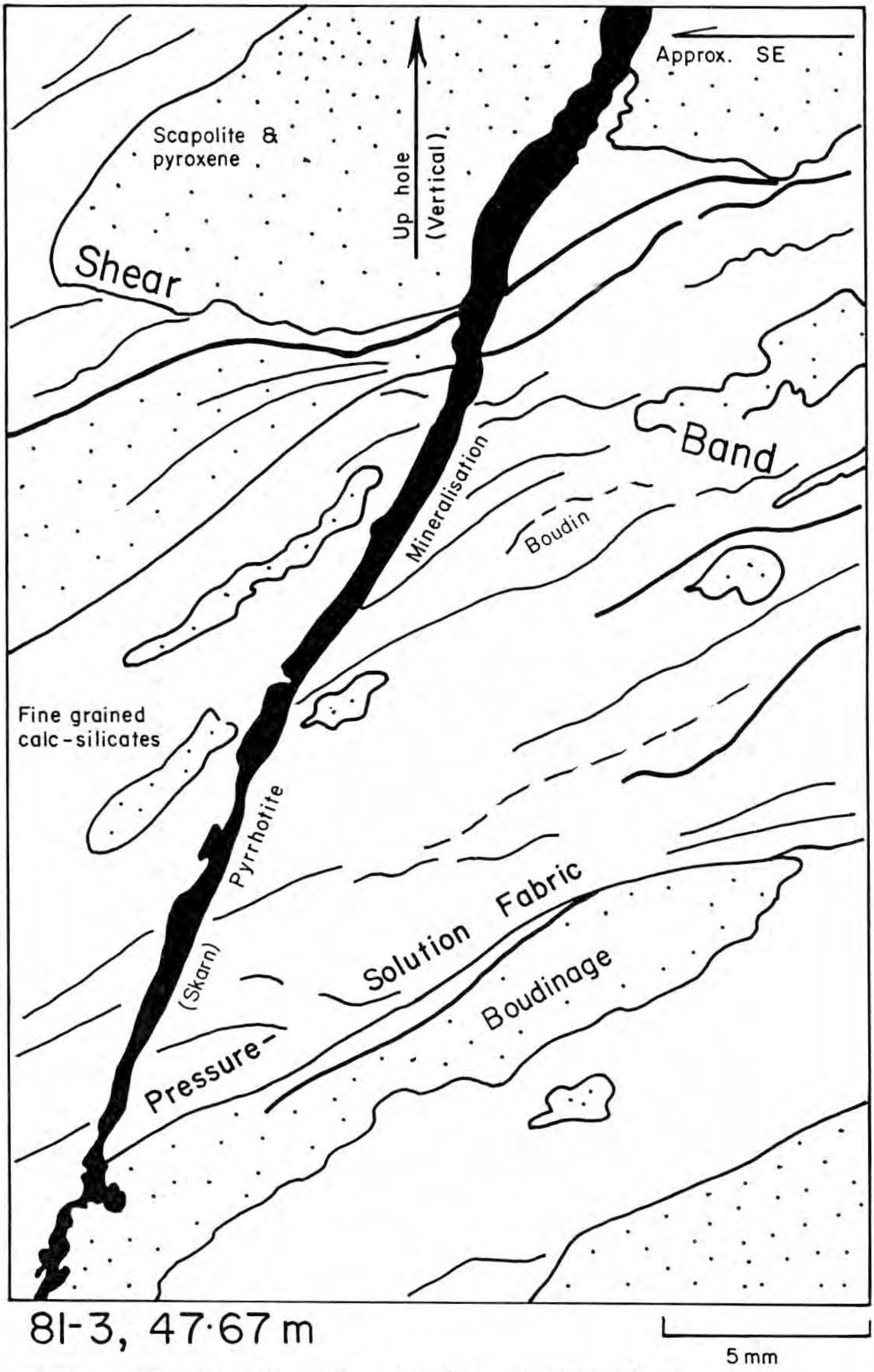

81-3, 47·67 m

Calc-silicate hornfels showing preservation of C-S fabric and a cross-cutting sulphide vein.

Thin section photographed in transmitted light.

FIG. 5·19a

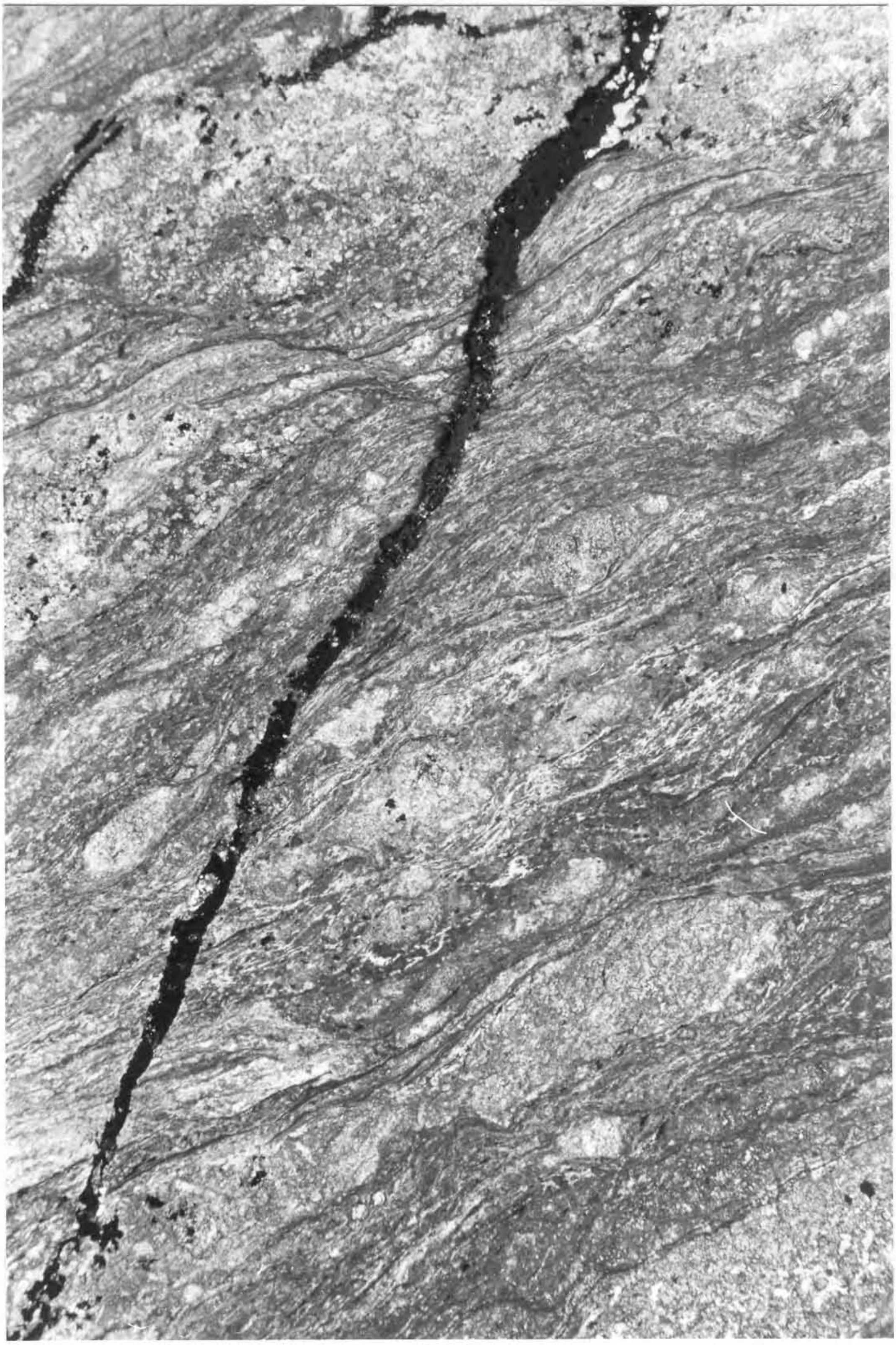

Figure 5.19b Scapolite is concentrated in the porphyroclasts and diopside in the fine-grained matrix. The core is vertical and the section faces approximately SE, hence a top-to-the- east shear sense is indicated. The opaque vein is skarn-related pyrrhotite mineralisation.

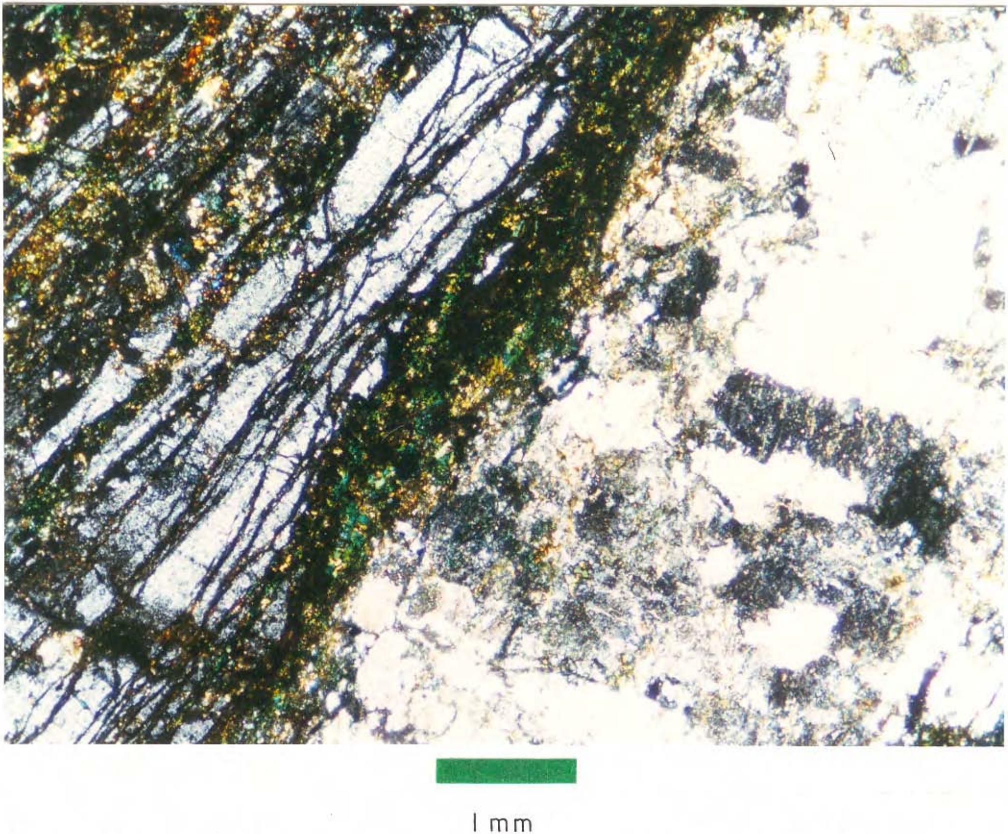

Figure 5.20 Shearing in primary skarn: drillcore from DDH 81-5B, 105.08 m. Vesuvianite and garnet are altered to actinolite along fractures. Thin section under crossed polarisers.

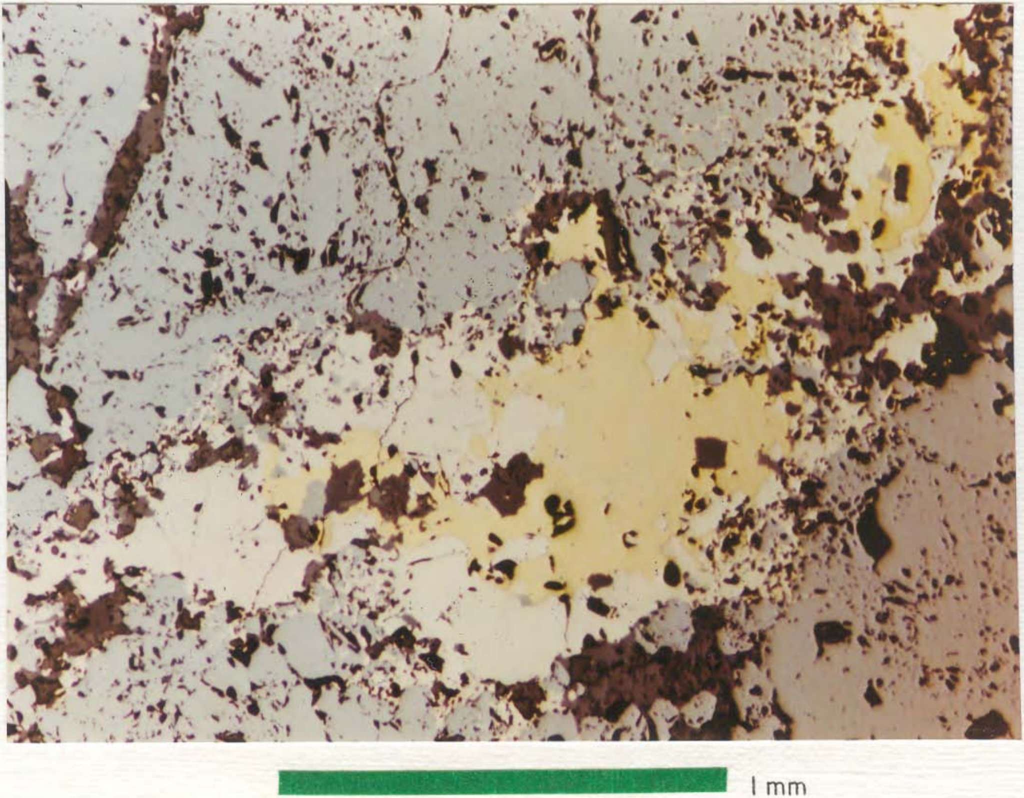

Figure 5.29 Mindy DDH 81-5B, 108.87 m: pyrrhotite-chalcopyrite vein (white and yellow) in magnetite (grey). Some of the deep brown is probably cassiterite. From a magnetite-phengite greisen-skarn. Polished block under plain-polarised reflected light.

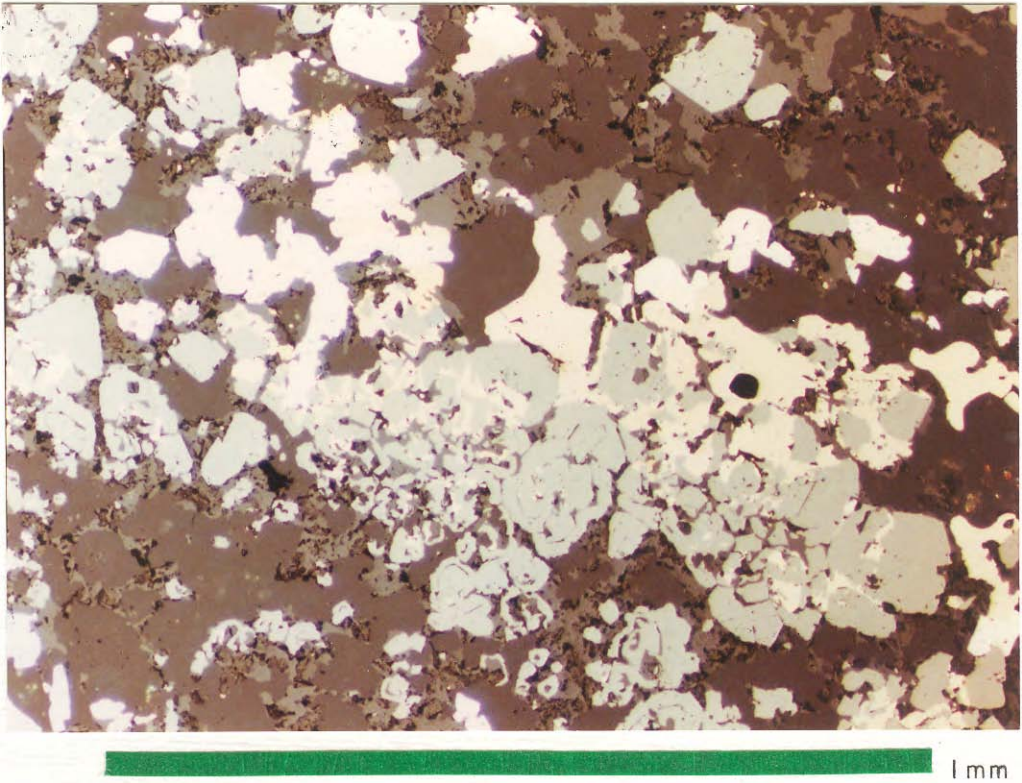

Figure 5.30 Mindy DDH 81-4, 148.50 m. Concentrically formed magnetite crystals (grey) with pyrrrhotite (white) in andradite skarn which has been heavily replaced by actinolite. Polished block in plain-polarised reflected light.

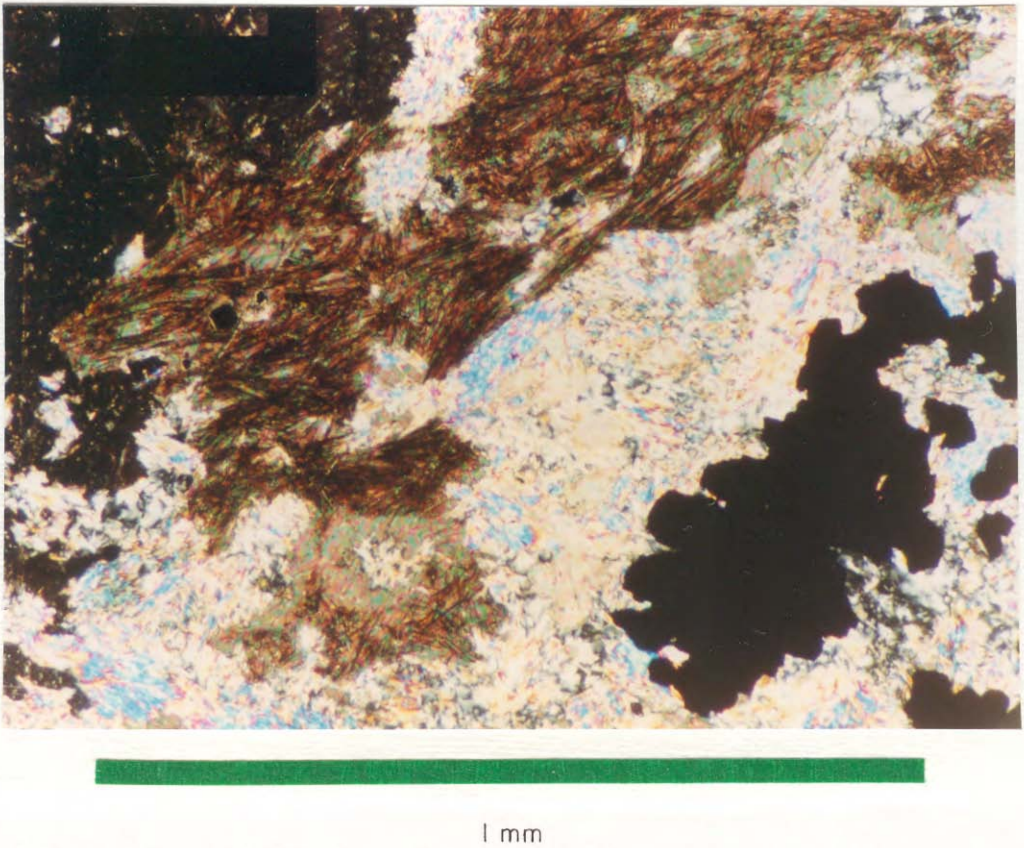

Figure 5.31 F-B rich skarn: DDH 81-1, 77.60 m. Thin section under crossed polarisers showing calcite, fluoborite (blue interference colour), szaibelyite (brownish highly birefringent mineral) and magnetite.

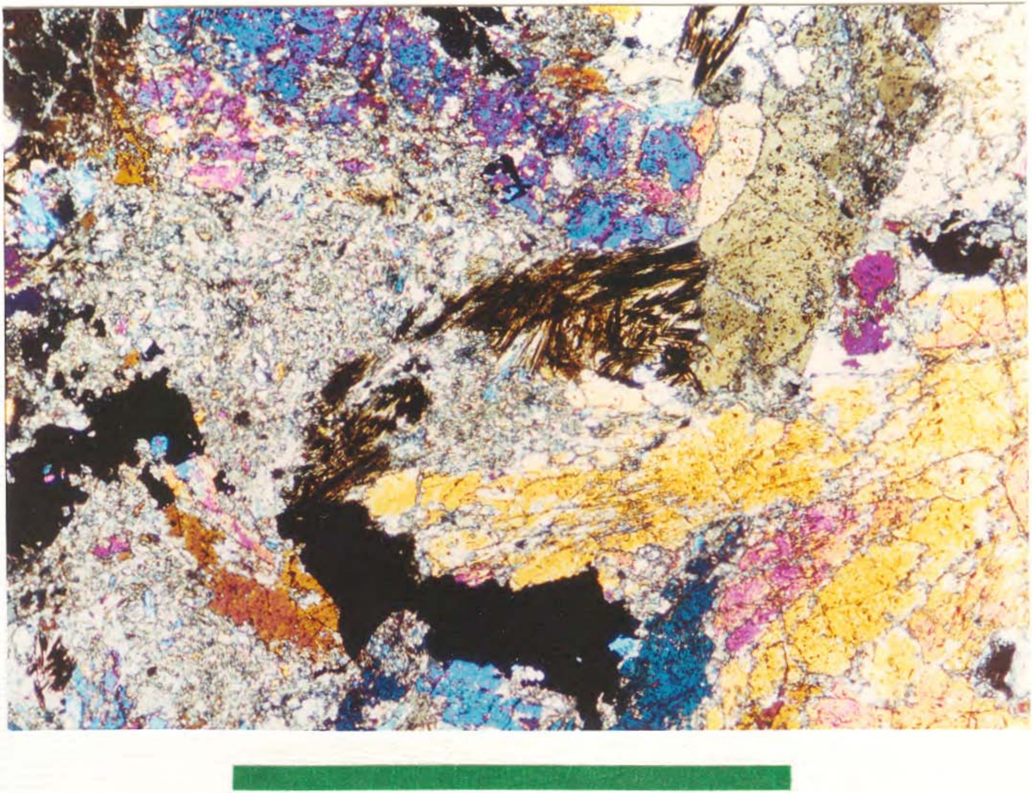

Figure 5.32 Alteration: DDH 81-1, 75.30 m. Diopside-hedenbergite replaced by ludwigite (acicular opaques), fluoborite and talc. Thin section under crossed polarisers.

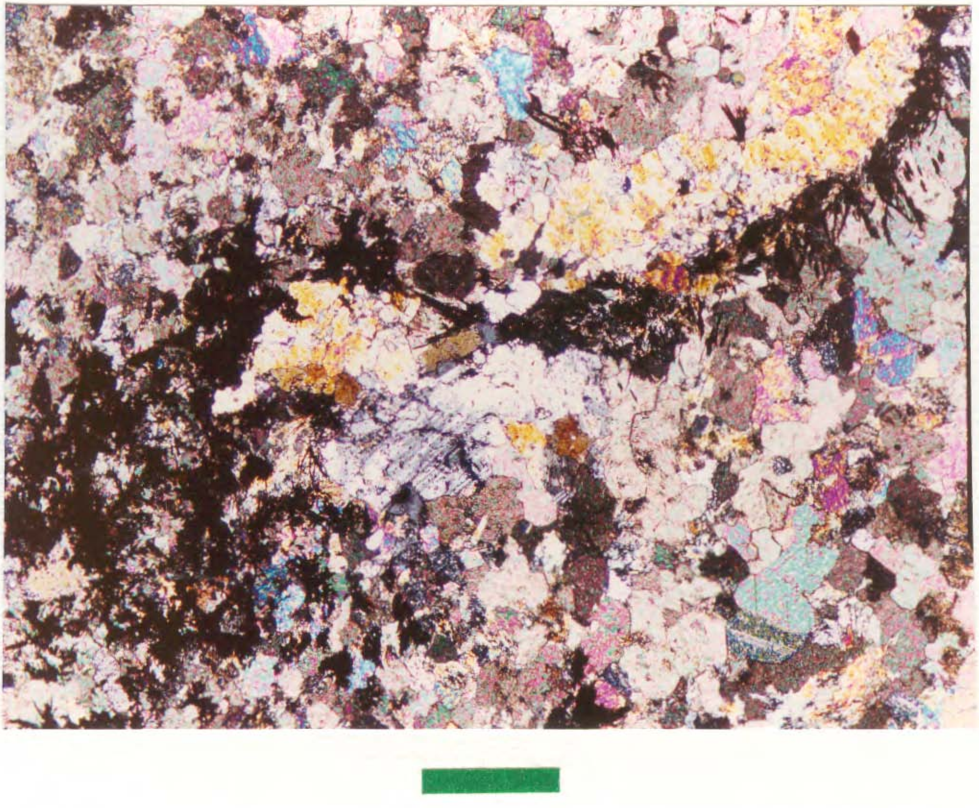

Figure 5.33 Thin section under crossed polarisers of core from DDH 81-2, 92.00 m showing a ludwigite vein in marble with a chondrodite selvedge (yellow interference colour).

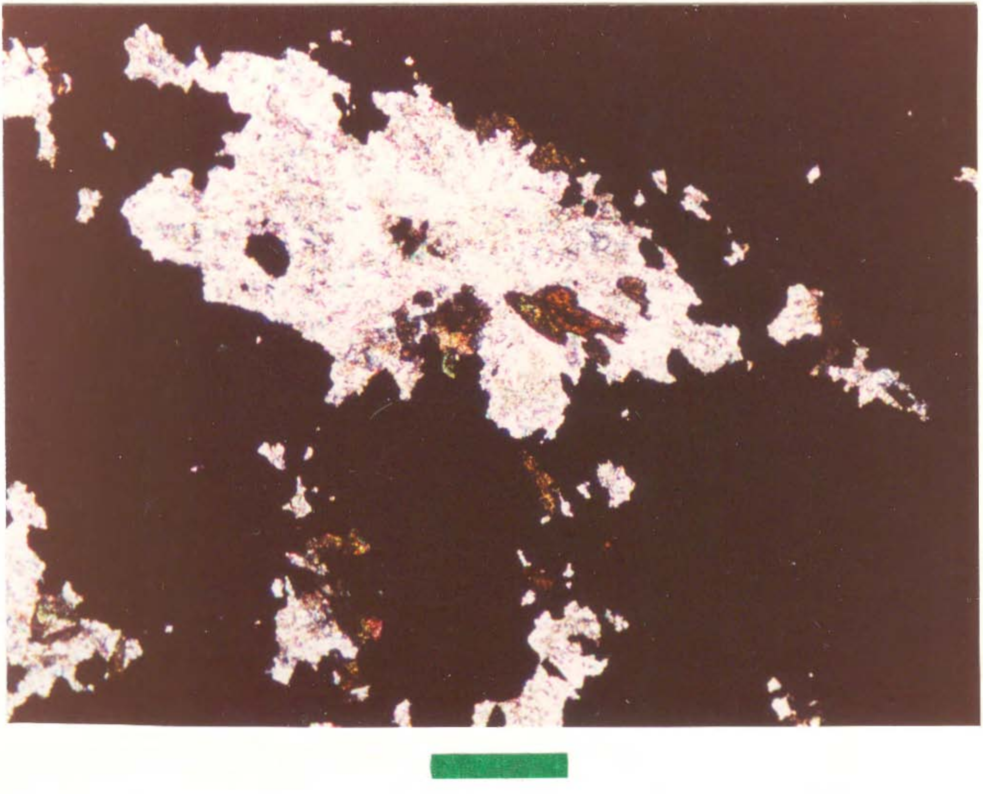

Figure 5.34 Cassiterite mineralisation: marble from DDH 81-1, 73.4 m in thin section under crossed polarisers showing magnetite, talc and cassiterite (yellow-brown).

BELT	DESCRIPTION
Rocky Mountain	Northeasterly tapering wedge of Mid-Proterozoic to Upper Jurassic (1500-150 Ma) miogeoclinal and platformal carbonates and cratob-derived clastics, and overlying Upper Jurassic to Paleogene exogeoclinal, cordillera-derived clastics; horizontally compressed and displaced up to 200 km NE onto the craton in Late Jurassic to Paleogene time.
Omineca Crystalline	Mid Proterozoic to Mid Palaeozoic miogeoclinal rock, Palaeozoic and Lower Mesozoic volcanogenic and pelitic rock, local Precambrian crystalline basement, highly deformed and variably metamorphosed (up to high grade) in Mid-Mesozoic to Early Tertiary and intruded by Jurassic and Cretaceous plutons.
Intermontane	Upper Palaeozoic to Mid-Mesozoic marine volvanic and sedimentary rock, mid-Mesozoic to Upper Tertiary marine and nonmarine sediments and volcanics; granitic intrusions comagmatic with the volcanics; deformed at various times (Early Mesozoic to Neogene)
Coast Plutonic Complex	Sedimentary and volcanic strata of known Late Palaeozoic to Tertiary age and probable Early Palaeozoic and Precambrian age, variably metamorphosed up to high grades and dominant, mainly Cretaceous and Tertiary granitic rock.
Insular	Upper Cambrian to Neogene volcanic and sedimentary strata, granitic rocks in part comagmatic with the volcanics; deformed at various times from Palaeozoic to Neogene

Table 1.1 Tectonic belts of the Canadian Cordillera

interpreted to be the result of a process of 'ultrafractionation', in common with Alaskan examples.

1.2 AIMS OF THIS RESEARCH

This research aims to:

1) Present a geological map of the central and northern portions of the Thirtymile Range; to determine the structure of the Englishman's Group and to correlate these with established sequences in the northern Canadian Cordillera and to elucidate the geological history of the region in terms of tectonic evolution of the Northern Cordillera.

2) To define the setting of tin-tungsten mineralisation in the Thirtymile Range in terms of tectonics and structural controls: to determine chemical trends in formation of the skarn mineralisation and compare the unusual chemistry of the metasomatic mineralisation with that of the adjacent intrusions.

3) To investigate rock and mineral chemistry and geochronology of the Thirtymile plutons. Sampling and analysis of the Hake and Seagull batholiths is to be undertaken on a reconnaissance scale to allow comparison. This data is to be used to infer the affinity of these intrusions with one another and these nearby granitic batholiths. Timing and structural controls of igneous intrusion are to be considered relative to northern Canadian Cordilleran tectonics. The chemical evolution of the various granite lithofacies is to be

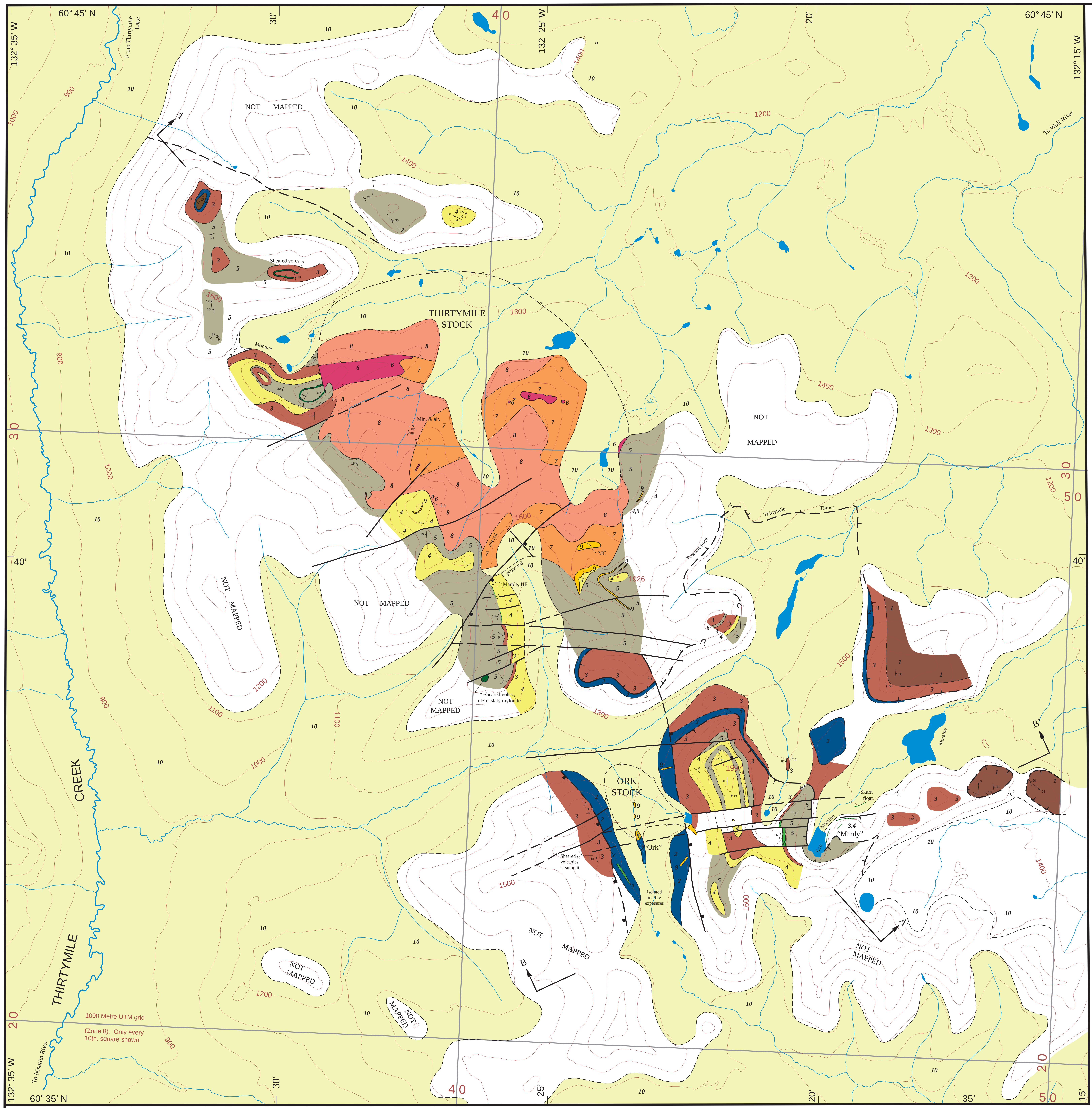

LEGEND

Quaternary

10 Glacial till, alluvium

Cretaceous

9 Li-mica topaz - bearing leucogranite. Exposed as a facies marginal to the main stock, as sills and as a separate stock and dykes at the Ork prospect.

8 Megacrystic biotite granite } Form the main stock

7 Biotite microgranite } Form the main stock

6 Porphyry: small E-W trending bodies and large xenoliths of granite to diorite composition.

U. Proterozoic to Mississippian: Englishmans Group: cataclasites

5 Highly foliated, fine-grained "slaty" cataclasite. Includes thin sheared volcanics = ■

4 Massive to banded chert. May include some quartz-ribbon mylonite.

3 Quartzite: brecciated and sheared: sometimes as phacoids in a slaty mylonitic matrix. Some arkosic material present.

2 Marble: brecciated and recrystallized. Includes skarn and hornfels = ■

1 Phyllonite: crenulated

Contact: dashed where approximate. Dots indicate a thin marble or sill.

Fault: thrust

Fault: moderate angle (45° to 60°) extensional

Fault: high angle

Foliation: slaty cleavage in cataclasite, enveloping surface of folds in phyllonite

Foliation: pressure solution cleavage, attitude of lithologic contact

Lineation: plunge of small-scale folds, crenulation

Attitude of jointing in the intrusives. Min= mineralized (sulphide), alt= altered
Prominent jointing in metasediments

Abbreviations: volcs. = (intermediate) volcanics; qtzte = quartzite; HF = hornfels
La = lamprophyre, MC = miarolitic cavities

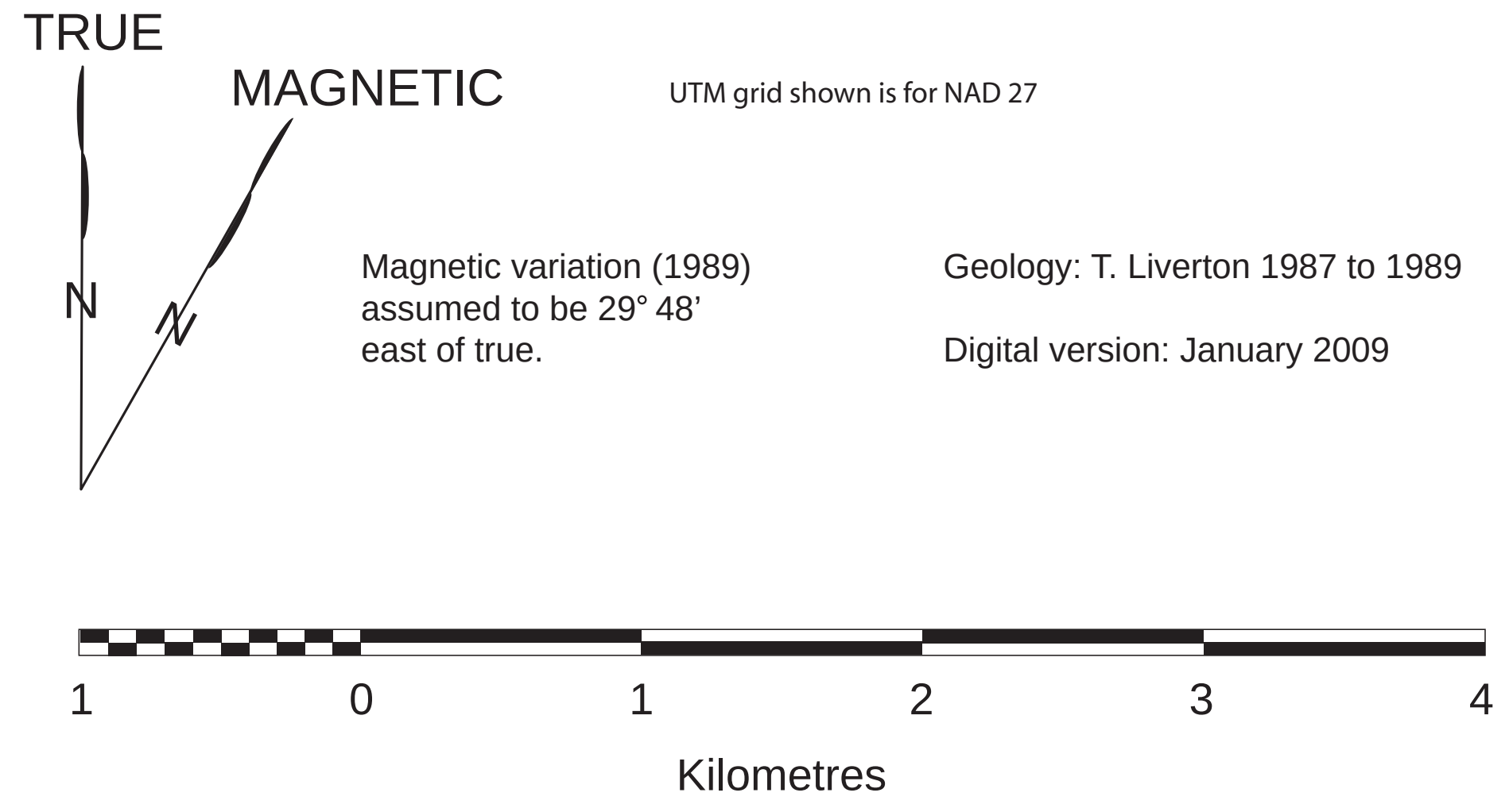

UTM grid shown is for NAD 27

Magnetic variation (1989)
assumed to be 29° 48'
east of true.

Geology: T. Liverton 1987 to 1989

Digital version: January 2009

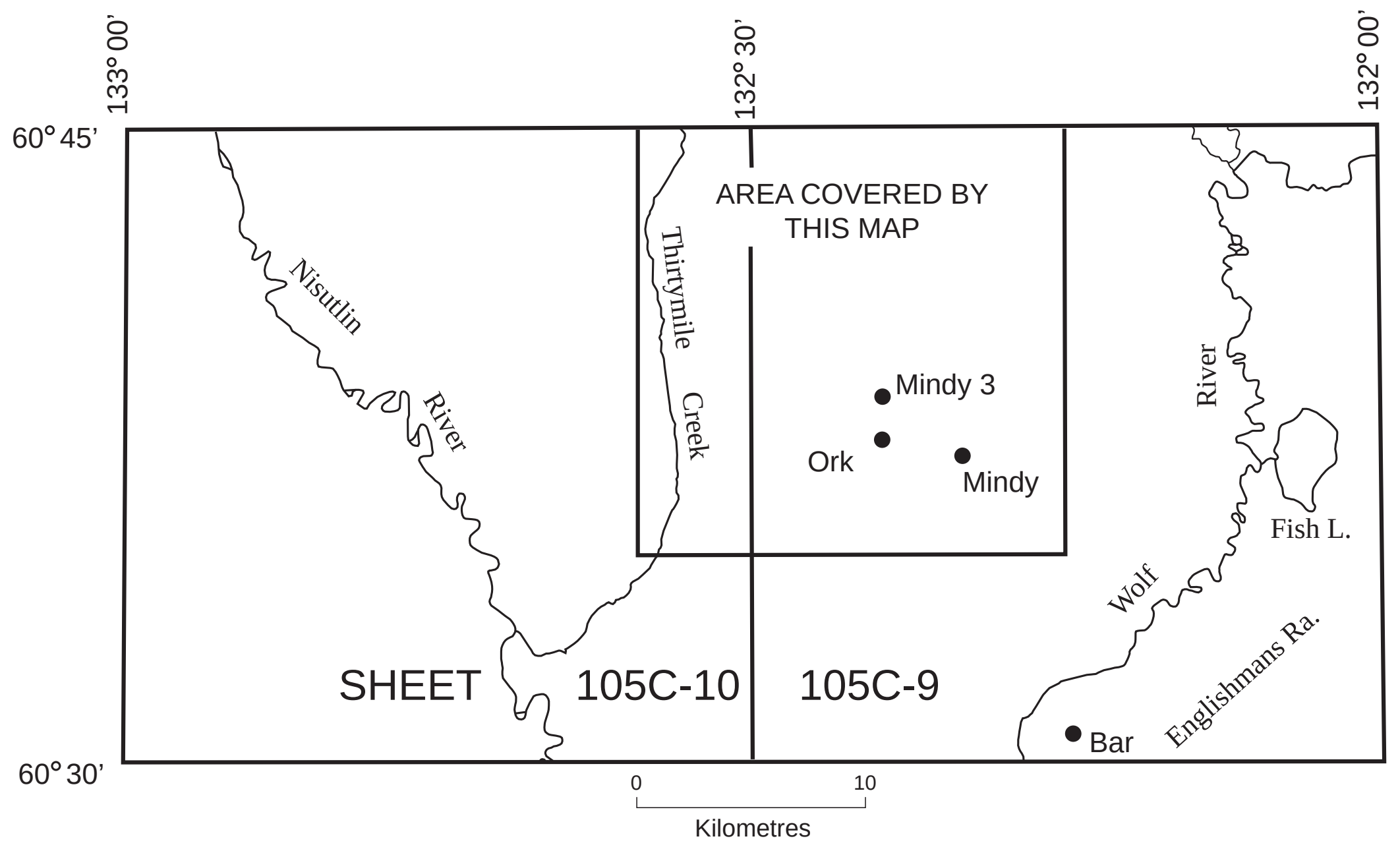

INDEX TO 1:50,000 SCALE TOPOGRAPHIC MAP SHEETS 105C-9, 10

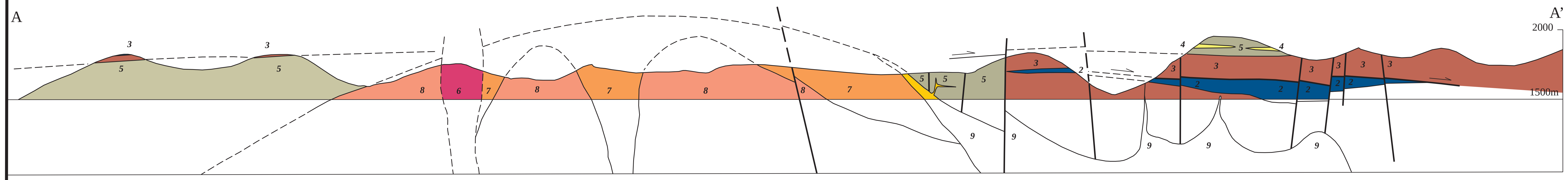

LONGITUDINAL SECTION THROUGH THE THIRTYMILE RANGE: Section A-A'

GEOLOGY OF THE THIRTYMILE RANGE

YUKON TERRITORY: NTS 105C 9 & 10

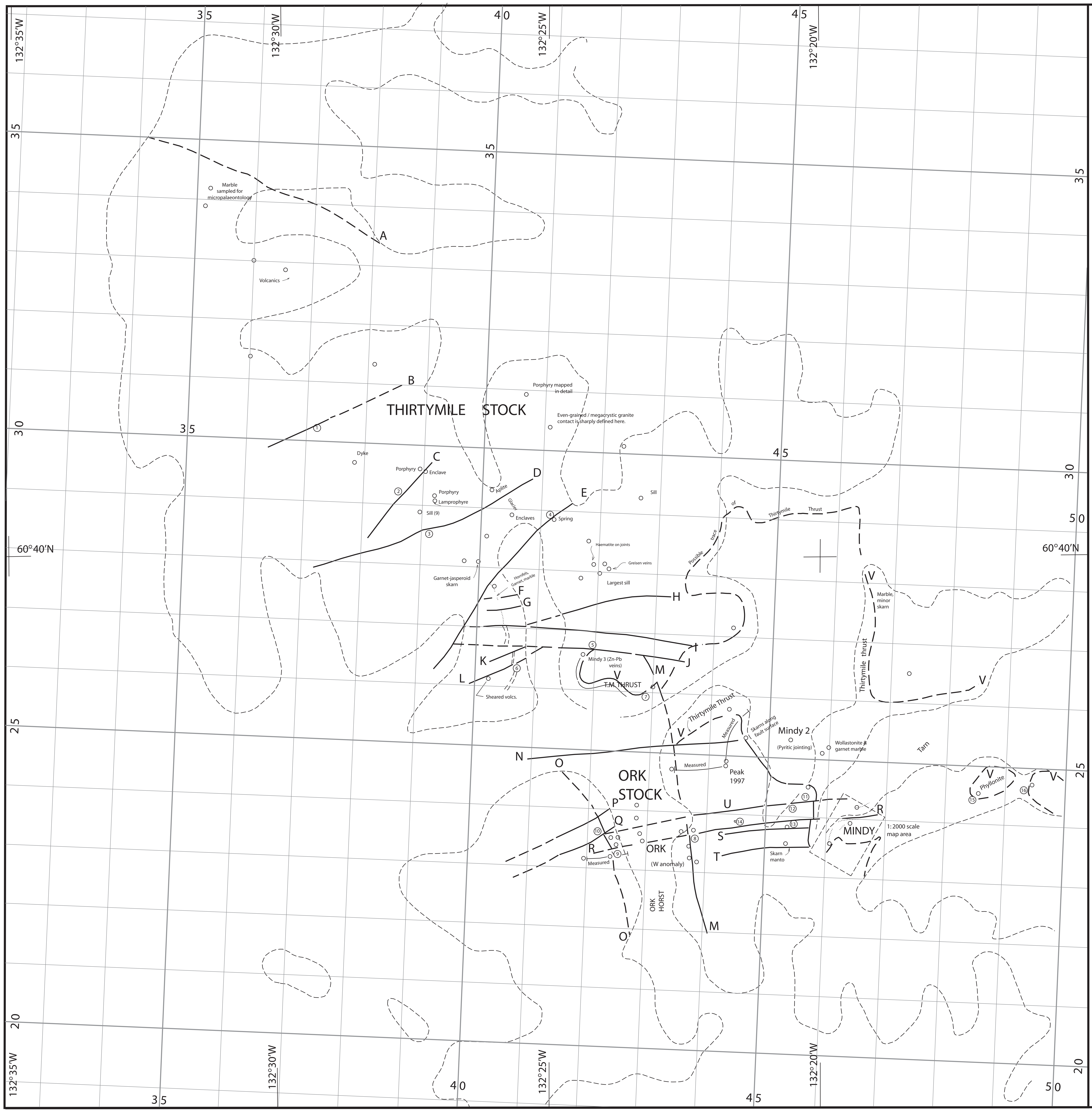

GEOLOGICAL NOTES
FAULTS

Fault 'A':	A topographic lineament. Stratigraphy of the metsediments does not correlate across this boundary. It is assumed to be a near-vertically dipping fault with a significant throw component.
Fault 'B':	Mapped - a break in stratigraphy is observed at loc. (1).
Fault 'C':	Mapped - a break in stratigraphy across this structure is observed at locality (2). Prominent jointing is found in the granites at the north end of this structure, so some movement has postdated granite emplacement.
Fault 'D':	Mapped - a distinct difference in stratigraphy and attitude of the metasediments is observed across the saddle (3).
Fault 'E':	Mapped - a displacement of the granite lithofacies is observable at locality (4)'
Fault 'F' Fault 'G':	Photo lineaments.
Fault 'H':	A photo-lineament. A slight displacement of the microgranite sill has been observed.
Fault 'J':	A prominent photo-lineament. Mapping reveals an abrupt termination of the marble u nit at locality (5), so this structure is interpreted to have an appreciable north-block down throw component.
Fault 'K' Fault 'L':	Photo-lineaments.
Fault 'M':	The eastward abrupt termination of the major marble unit against this structure has been mapped at locality (8). The northern extension of this fault is inferred to explain the lack of marble outcrop to the east.
Fault 'N':	Photo interpretation of strike. Mapped on ridge to north of Peak 1997.
Fault 'O':	Well exposed and mapped. The measured section crosses the fault at locality (9).
Fault 'P':	A prominent photo-lineament. No significant offset of fault 'O" has been observed in the field.
Fault 'Q':	An offset of fault 'O' has been mapped.
Fault 'R':	Mapped (east portion) and a photo-lineament. Shearing observed on the ridge at locality (14).
Fault 'S':	Mapped. Mineralized fault breccia has been observed at locality (13).
Fault 'T':	Interpreted. South limit of skarn unit.
Fault 'U':	The fault zone is obvious at locality (11). An offset of a quartzite unit has been mapped (12).
Fault 'V':	The Thirtymile Thrust. Shearing in marble and folding in quartzite at the base of the upper plate has been observed at locality (7). The NE continuation of the thrust has been correlated with the top of the marble unit and the base of the phyllonite klippen (15, 16).

Measured section are shown thus:

Sample localities and those mentioned in text shown: ○

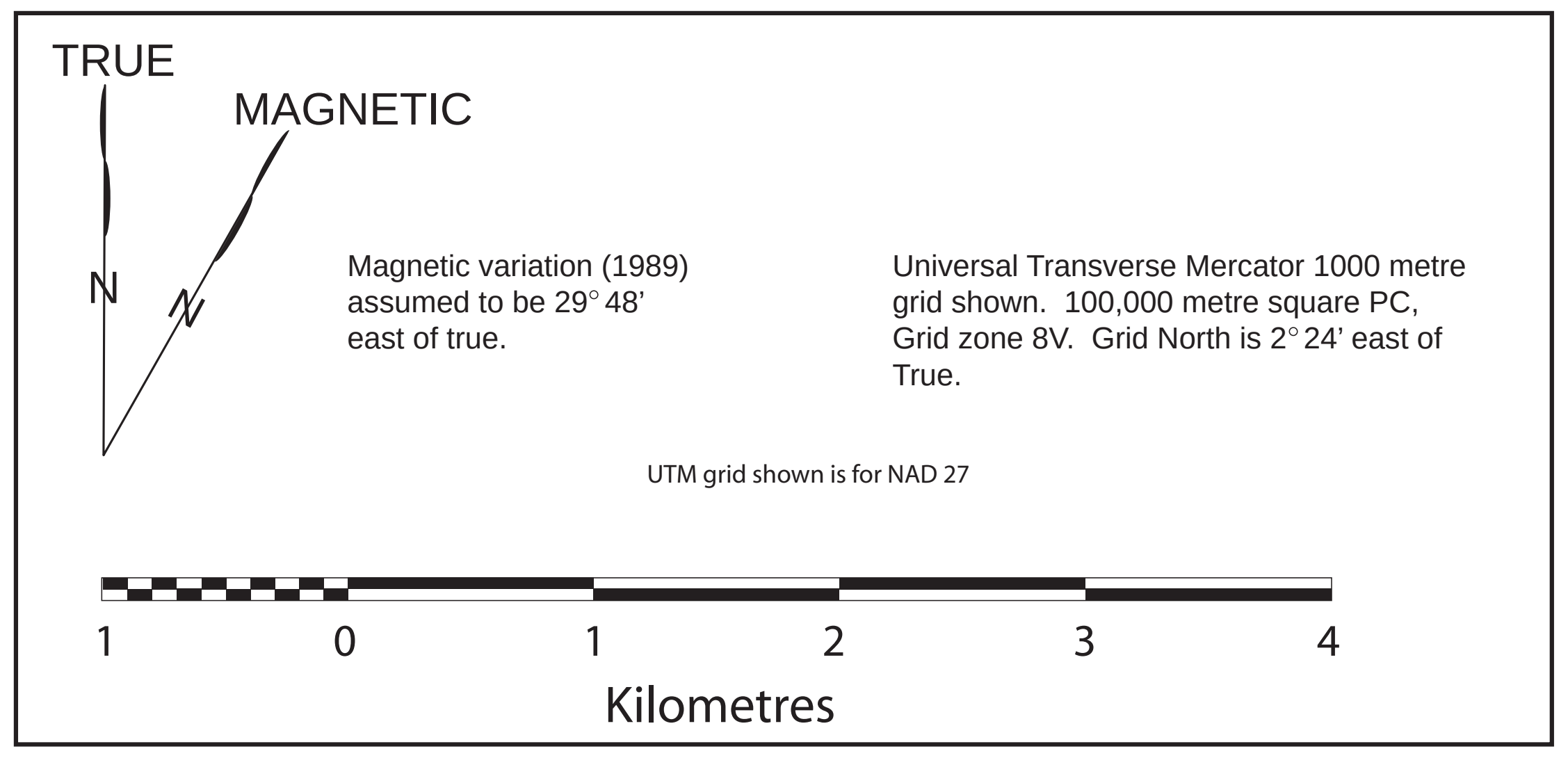

Magnetic variation (1989) assumed to be 29° 48' east of true.

Universal Transverse Mercator 1000 metre grid shown. 100,000 metre square PC, Grid zone 8V. Grid North is 2° 24' east of True.

UTM grid shown is for NAD 27

GEOLOGY OF THE THIRTYMILE RANGE

SKETCH SHOWING LOCALITIES MENTIONED
IN TEXT AND GIVING GEOLOGICAL NOTES

This sketch is intended to be read together with the geological map at the same scale
Original map: T. Liverton, February 1992. Digital version January 2009

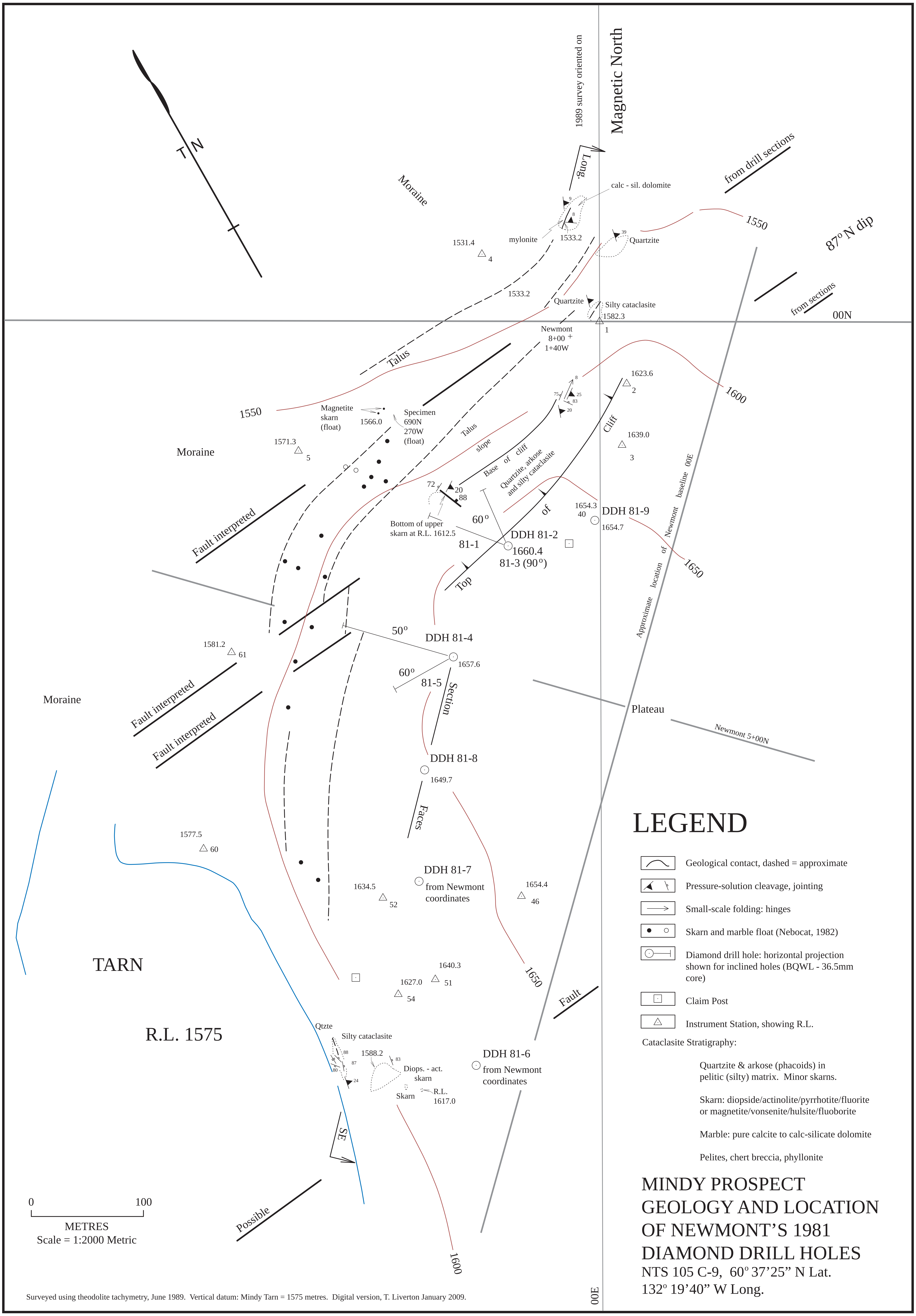

LEGEND

⌒	Geological contact, dashed = approximate
▲	Pressure-solution cleavage, jointing
→	Small-scale folding: hinges
● ○	Skarn and marble float (Nebocat, 1982)
⊙	Diamond drill hole: horizontal projection shown for inclined holes (BQWL - 36.5mm core)
▣	Claim Post
△	Instrument Station, showing R.L.

Cataclasite Stratigraphy:

Quartzite & arkose (phacoids) in pelitic (silty) matrix. Minor skarns.

Skarn: diopside/actinolite/pyrrhotite/fluorite or magnetite/vonsenite/hulsite/fluoborite

Marble: pure calcite to calc-silicate dolomite

Pelites, chert breccia, phyllonite

MINDY PROSPECT GEOLOGY AND LOCATION OF NEWMONT'S 1981 DIAMOND DRILL HOLES

NTS 105 C-9, 60° 37'25" N Lat.
132° 19'40" W Long.

Surveyed using theodolite tachymetry, June 1989. Vertical datum: Mindy Tarn = 1575 metres. Digital version, T. Liverton January 2009.

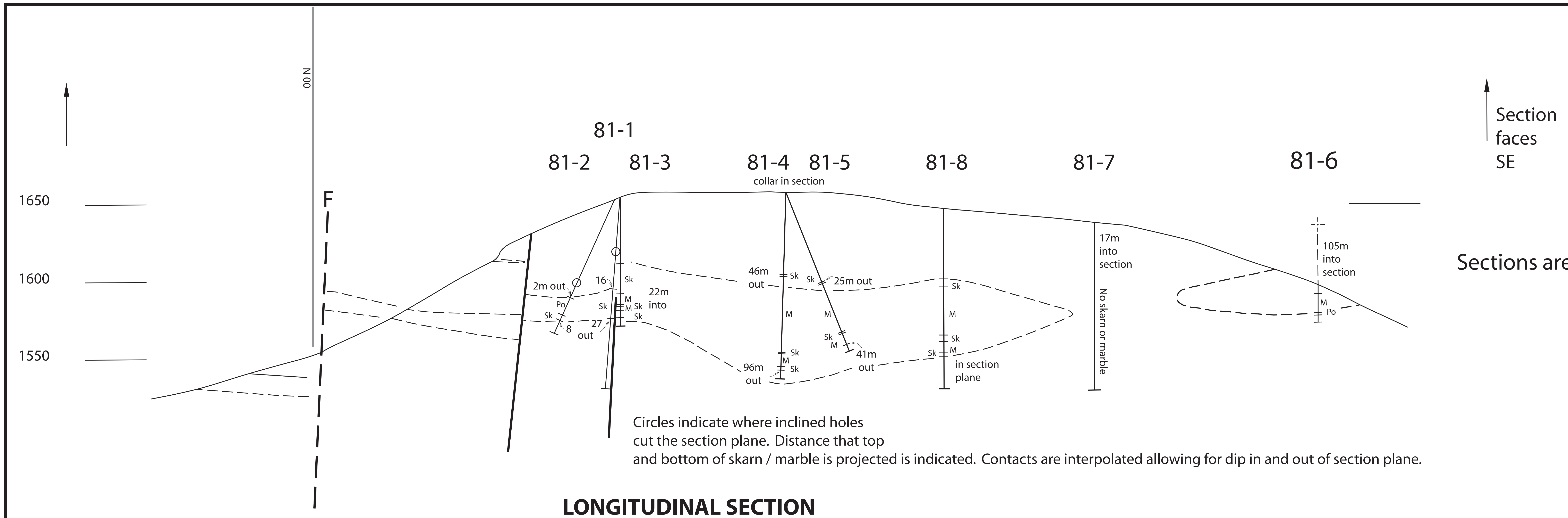

Sections are vertical

Circles indicate where inclined holes cut the section plane. Distance that top and bottom of skarn / marble is projected is indicated. Contacts are interpolated allowing for dip in and out of section plane.

LONGITUDINAL SECTION

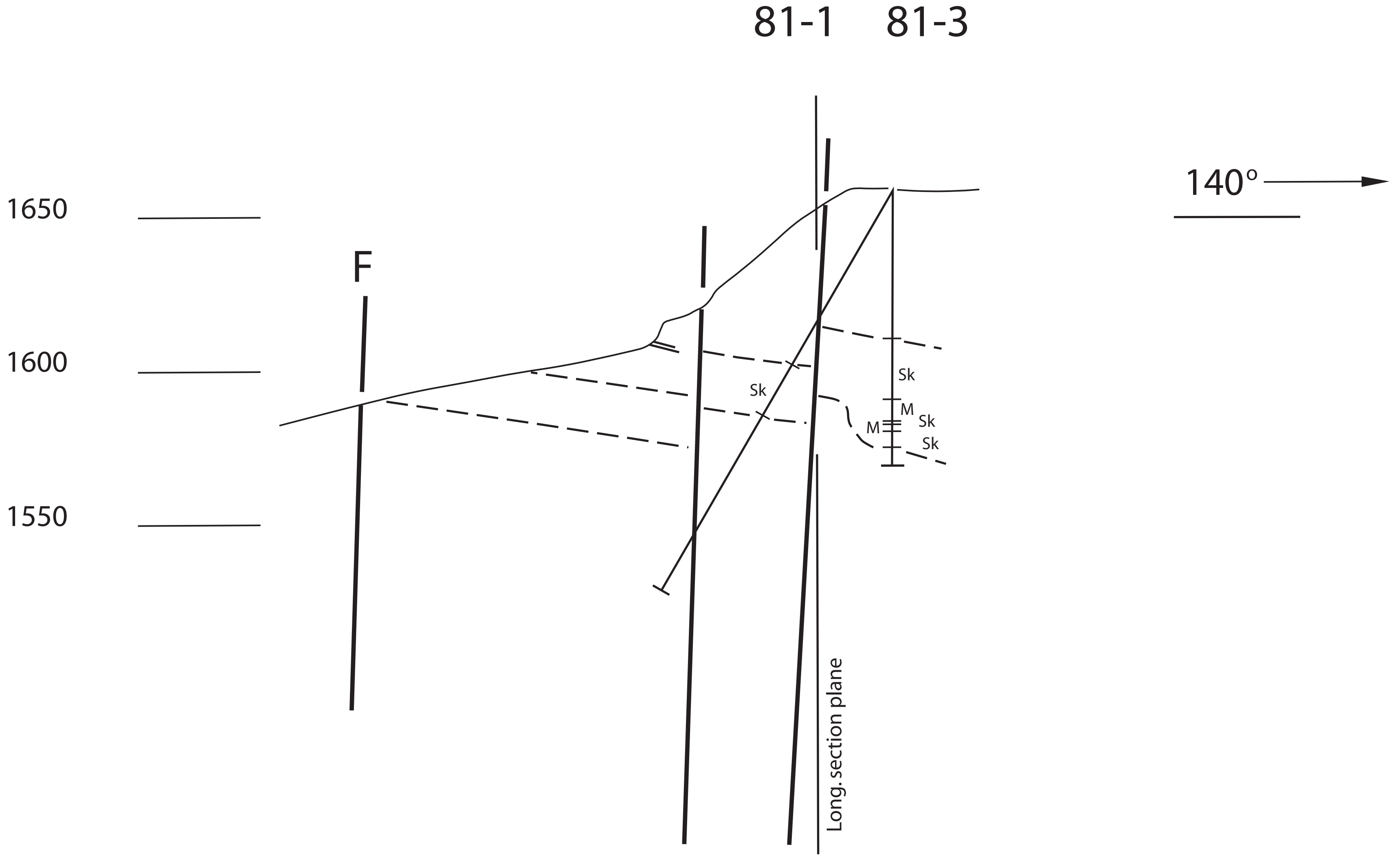

SECTION THROUGH DRILLHOLES 1 AND 3

FACING NE

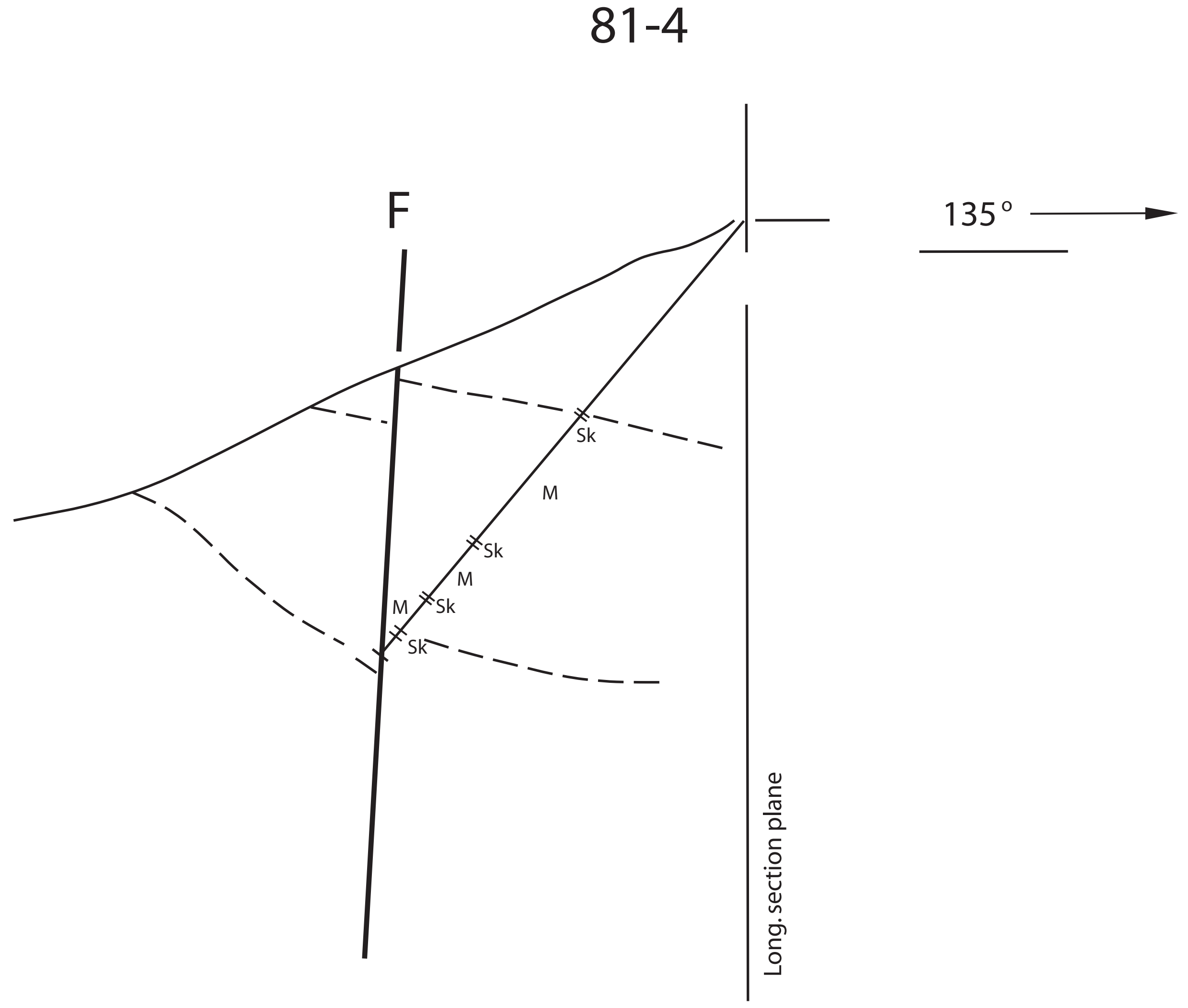

SECTION THROUGH DRILLHOLE 4

FACING NE

LITHOLOGIES

Sk = skarn (scale does not permit mineralogy to be shown)

Po = pyrrhotite rich sections

M = marble

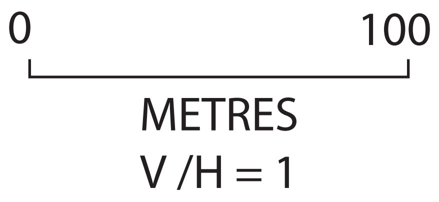

MINDY PROSPECT SECTIONS THROUGH DRILLHOLES 81-1 to 8

Scale = 1:2000
T. Liverton, Digital version Jan. 2009

FIELD LOG

Grey to purple pelitic metasediment-shows quartz layers of irregular thickness, often in S-folds. Has occasional 0·5-1·5mm thick pyrrhotite-filled fractures at 0 to 30°. Much pyrrhotite veining from 80·2 to 80·3.

78·7

80·3

Banded pyrrhotite-diopside skarn. Pyrrhotite (with minor chalcopyrite) up to 50%. Disharmonic folding.

82·8

Pale green diopside skarn with pyrrhotite blebs.

83·01

Dark grey, pyrrhotite-rich skarn. Silicate matrix varies from white to green - v.fine grained. Foliation is lenticular or disharmonically folded (wrigglite). 0·5mm wide pyrrhotite-filled fractures at 45° to core axis are common. Fine magnetite from 86·8-87·7. Fractures // core cont. fine grained magnetite-hulsite-arsenopyrite from 89·7 to 90·3.

91·9

White, fine-grained marble.

92·07

Ludwigite-mineralised fractures 0-10°

Banded pyrrhotite skarn with irregular magnetite masses. Borates from 93·24 to 93·45.

94·7

Grey mag.-fluoborite. Ptygmatic pyrrhotite bands at centre of interval.

95·17

Pale green diopside skarn. 3mm fluorite masses and pyrrhotite blebs. Some deep green amphibole masses to 15mm long. Veins at 98·04.

98·44

Dark grey, slightly brecciated chert. P.S.cleavage developed from 99·9 to 100·45 at 36°. 1mm quartz veins at 13° and 0° to core axis.

101·3

Very brecciated chert. Fractures at 0 to 15° common, some bearing pyrite. Chloritic sections.

102·5

White quartz - upper contact with chert at 75°. Has tiny fractures at all angles from 0 to 60°.

104·0

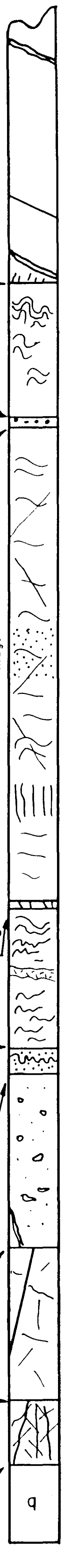

SAMPLES *MINERALOGY*

Metres	
78·2-78·4	
81·25-81·31	
82·17-82·23	Clinohumite in fluorite, mostly banded pyrrhotite in fluoborite
82·87-82·93	Fractured Px skarn: actinolite-fluorite-phlogopite-chlorite rep.
84·03-84·11	Relict chondrodite or clinohumite in magnetite and serpentine with fluoborite. Bands of fluoborite & pyrrhotite
86·78-86·82	Brecciated wrigglite. Brucite-phlogopite-magnetite. Zoned cassiterite.
89·82-89·93	Relict clinohumite & diopside. Veins have fluoborite selvedges that replaces the silicates & contains some pyrrhotite. Centres are fluorite & magnetite with phengite rim & serpentine core.
92·00-92·06	Calcite with veins of ludwigite. Contact with hülsite-phlogopite / magnetite-fluoborite wrigglite.
92·84-92·92	V. little remnant ? clinohumite, skeletal pyrrhotite, in 50% fluoborite
93·24-93·30	Wrigglite: c/humite-mag.-ludwigite-f/bor.-hüls.
93·60-93·66	
94·70-95·17	Banded magnetite-diopside skarn with fluoborite replacement
94·89-94·96	Coarse clinohumite relicts with magnetite & diops. Heavy f/borite rep.
95·63-95·72	Diopside replaced by fluoborite. A few scheelite crystals. Veins of fluorite & phlogopite cut the f/borite. Later brucite veins.
97·44-97·51	Coarse (to 5mm) Px with actin. & szaibelyite rep. Bands of hydrochlorborite
98·04-98·12	Px skarn with 2mm wide fluorite-hydrochlorborite vein at 32° to core.
99·53-99·70	
103·68-	

ASSAY, Sn (Newmont)

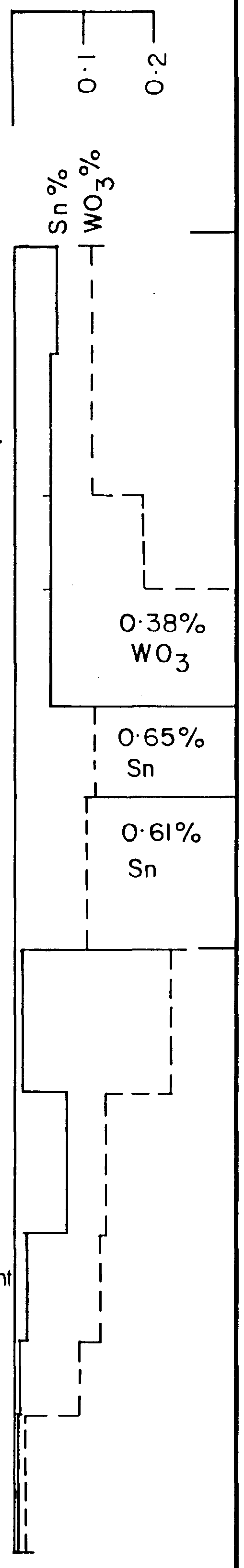

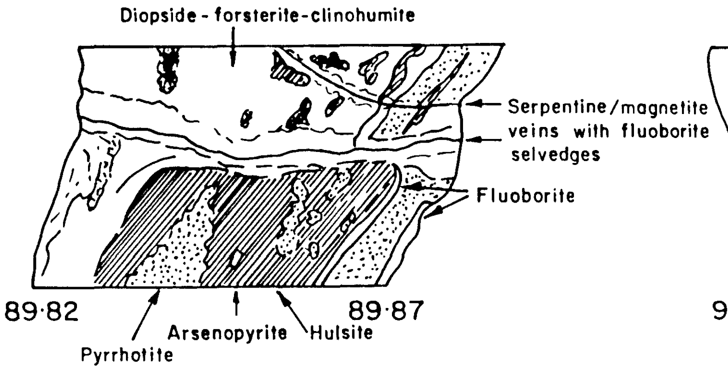

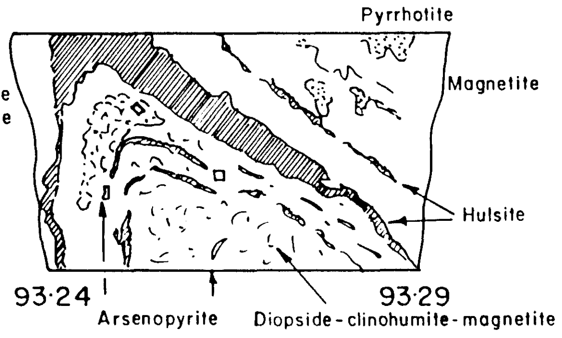

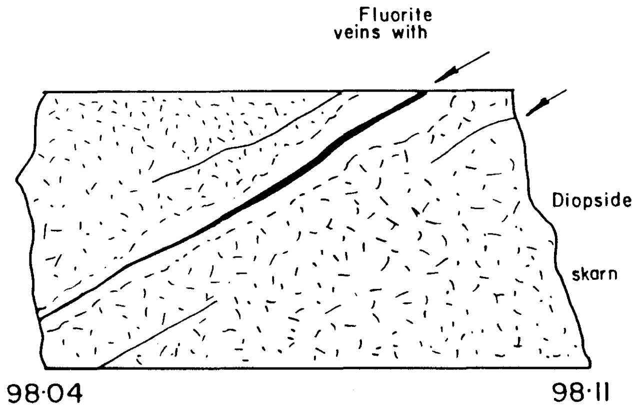

Dip -60°, Az 006°, Collar R.L. 1660·4

MINDY DDH 81-2

Appendix B·6

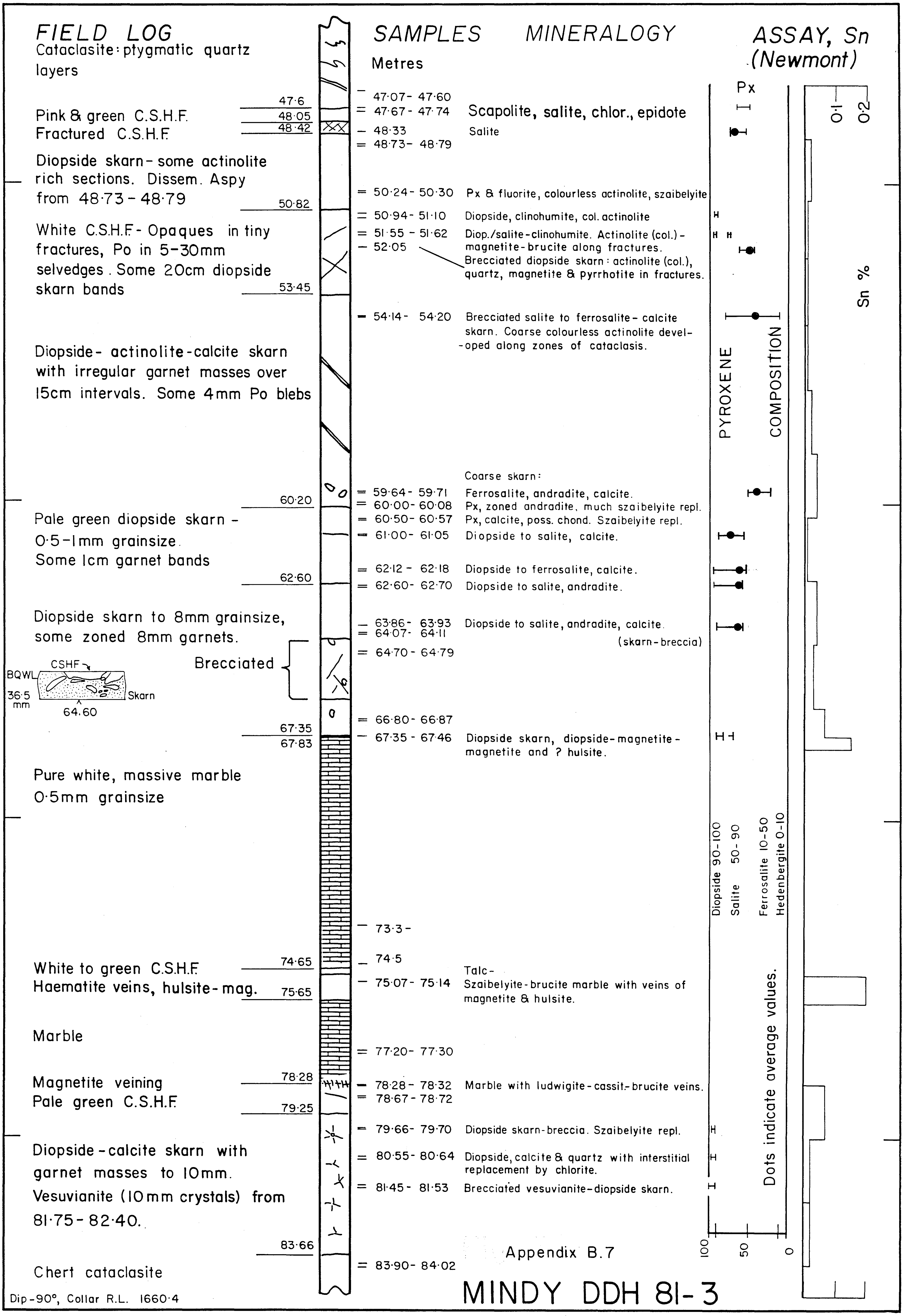

FIELD LOG

Cataclasite: ptygmatic quartz layers
47·6
Pink & green C.S.H.F.
48·05
Fractured C.S.H.F
48·42
Diopside skarn - some actinolite rich sections. Dissem. Aspy from 48·73 - 48·79
50·82
White C.S.H.F- Opaques in tiny fractures, Po in 5–30mm selvedges. Some 20cm diopside skarn bands
53·45
Diopside- actinolite-calcite skarn with irregular garnet masses over 15cm intervals. Some 4mm Po blebs
60·20
Pale green diopside skarn - 0·5-1mm grainsize. Some 1cm garnet bands
62·60
Diopside skarn to 8mm grainsize, some zoned 8mm garnets.
Brecciated
67·35
67·83
Pure white, massive marble 0·5mm grainsize
74·65
White to green C.S.H.F
Haematite veins, hulsite-mag.
75·65
Marble
Magnetite veining
78·28
Pale green C.S.H.F
79·25
Diopside-calcite skarn with garnet masses to 10mm. Vesuvianite (10mm crystals) from 81·75 - 82·40.
83·66
Chert cataclasite

SAMPLES Metres	MINERALOGY
47·07 - 47·60	
47·67 - 47·74	Scapolite, salite, chlor., epidote
48·33	Salite
48·73 - 48·79	
50·24 - 50·30	Px & fluorite, colourless actinolite, szaibelyite
50·94 - 51·10	Diopside, clinohumite, col. actinolite
51·55 - 51·62	Diop./salite-clinohumite. Actinolite (col.) - magnetite-brucite along fractures.
52·05	Brecciated diopside skarn: actinolite (col.), quartz, magnetite & pyrrhotite in fractures.
54·14 - 54·20	Brecciated salite to ferrosalite - calcite skarn. Coarse colourless actinolite developed along zones of cataclasis.
59·64 - 59·71	Coarse skarn: Ferrosalite, andradite, calcite.
60·00 - 60·08	Px, zoned andradite, much szaibelyite repl.
60·50 - 60·57	Px, calcite, poss. chond. Szaibelyite repl.
61·00 - 61·05	Diopside to salite, calcite.
62·12 - 62·18	Diopside to ferrosalite, calcite.
62·60 - 62·70	Diopside to salite, andradite.
63·86 - 63·93	Diopside to salite, andradite, calcite. (skarn-breccia)
64·07 - 64·11	
64·70 - 64·79	
66·80 - 66·87	
67·35 - 67·46	Diopside skarn, diopside-magnetite - magnetite and ? hulsite.
73·3 -	
74·5	Talc-
75·07 - 75·14	Szaibelyite-brucite marble with veins of magnetite & hulsite.
77·20 - 77·30	
78·28 - 78·32	Marble with ludwigite-cassit.-brucite veins.
78·67 - 78·72	
79·66 - 79·70	Diopside skarn-breccia. Szaibelyite repl.
80·55 - 80·64	Diopside, calcite & quartz with interstitial replacement by chlorite.
81·45 - 81·53	Brecciated vesuvianite-diopside skarn.
83·90 - 84·02	

Appendix B.7

MINDY DDH 81-3

Dip -90°, Collar R.L. 1660·4

FIELD LOG *SAMPLES* *MINERALOGY* *ASSAY, Sn (Newmont)*

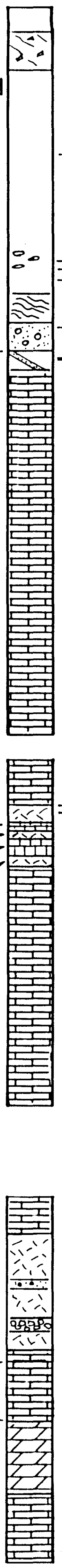

63·4
Chert cataclasite
63·9
Arkosic quartzite : 10% feldspar as 2–6 mm angular grains. Brecciated
64·7

Chert cataclasite with pelitic mylonite sections. Cordierite (2-3mm grains) developed from 68·44-68·50 and 68·57 to 68·85.

— 64·20–64·34

— 68·61 – 68·79
— 68·98 – 69·20

69·35
Pelitic mylonite cont. 1% pyrrhotite
69·90
Magnetite-andradite skarn. A 1cm sphalerite vein (55°) at 70·2
70·50
White marble with a 12mm magnetite andradite vein at 70·60.
70·90

— 69·92–69·96 Andradite-magnetite (& hulsite ?)- Px. Fractures at 70°.

— 70·68–70·74 Carbonate with andradite, a little diopside, a few laths of szaibelyite in the marble.

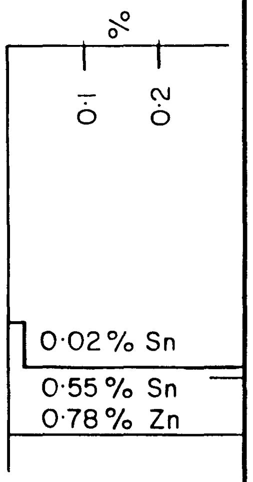

70·90–78·49: Massive white marble grainsize 1 to 3 mm.

78·49

78·49 – 99·52 : Drill core not preserved — Newmont logs indicate marble throughout.

99·52
Massive white marble: 0·5mm.
100·50
Wollastonite skarn: upper contact 90°, P.S.45°
100·82
White marble
Wollastonite following 45° fractures
Marble with irregular fractures 20–45°
101·75
Wollastonite: 8mm crystals. Contacts at 60°

— 100·47–100·61

Marble with frequent grey fractures and irregular banding.

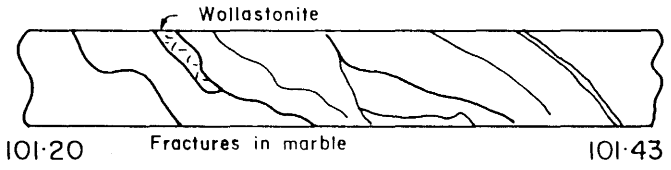

106·68

106·68 – 113·9 : Drill core not preserved — Newmont logs indicate marble and wollastonite skarn.

113·9
Massive white marble, 0·5mm.
114·68
Wollastonite-calcite skarn: 30% calcite.
115·60
Andradite-vesuvianite skarn
Wollastonite-calcite skarn
116·40
Massive andradite garnet zoned brown to green
Wollastonite-calcite skarn.

Marble-calcite. Brecciated 117·32 to 118·57.
Dolomitic from 118·57 to 120·09

Calcite from 120·09 to 121·5.

121·5

Stained with alizarin/ferricyanide solution during logging.

121·5 – 135·9: Drill core not preserved. Newmont logs indicate marble with patches of wollastonite-garnet-quartz skarn from 124·2 – 124·9 and from 131·6 to 135·9. From 128·3 to 128·6 vesuvianite-garnet skarn is indicated.

Dip -50°, Az 316° T, Collar R.L. 1657·6

MINDY DDH 81-4

FIELD LOG SAMPLES MINERALOGY ASSAY, Sn (Newmont)

135·9
Skarn-grading from massive diopside to a central calcite-diopside-actinolite-zone containing epidote masses, then calcite-brucite.
137·18
White marble, 1mm grainsize. Very brecciated-fractures every cm or so at all angles.
140·95
Grey dolomitic marble, banding at 55°.
141·10
White marble 1·5-2mm g/s, few fractures.
141·88
Grey dolomitic marble-irregularly mottled.
143·23
Pure white, massive marble. Grainsize up to 1mm. A few 0·5mm wide magnetite veins cut the interval 147·8-148·2. Angles from 30 to 38°.
148·20
Skarn-finely banded magnetite to 148·95, pyrrhotite predominant by 149·0. Fractured. Actinolite occurs with the sulphide. Massive magnetite 149·25-149·60.
150·27
Pink chert cataclasite.
151·03
Light grey chert cataclasite.
Dark grey pelite alternating with 5mm siliceous layers. P.S. at 60 to 73°.
151·76
Brown biotite-bearing siliceous mylonite with 3-5mm wide quartz bands.
152·84
Dark grey pelitic mylonite. Some 1 by 15mm quartz clasts visible. P.S. 55° at 154·5.
155·02
Sheared quartzite. P.S. seams are from 3 to 8mm apart. Clasts 5x15mm.
155·78
Dark grey pelite.
157·0

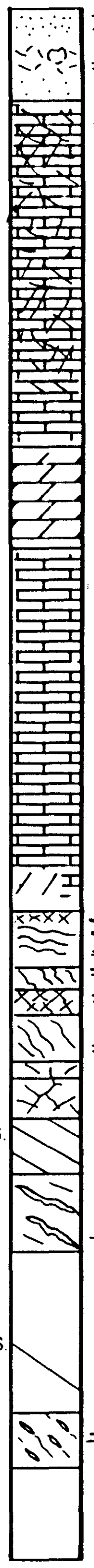

136·01-136·25
136·64-136·74
137·47-137·56 Carbonates and brucite.
148·30-148·36
148·50-148·56 Magnetite-fluoborite wrigglite with fluorite & some sphalerite
148·73-148·79 Ferrophengite & bandylite in one layer.
149·00-149·09
149·35-149·42 See below
150·00-150·07
152·65-152·72
155·31-155·40

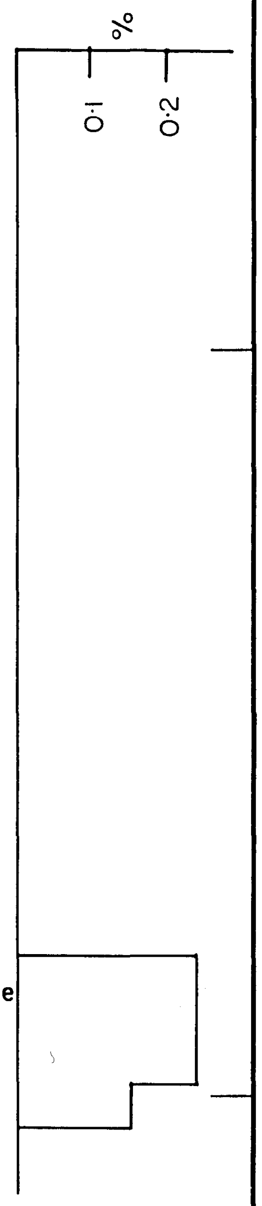

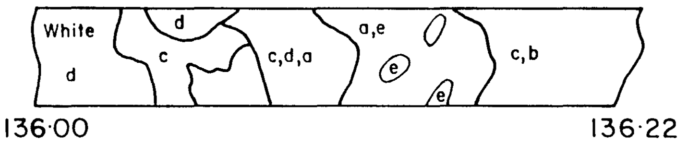

a= actinolite, b= brucite, c= calcite, d=diopside, e= epidote

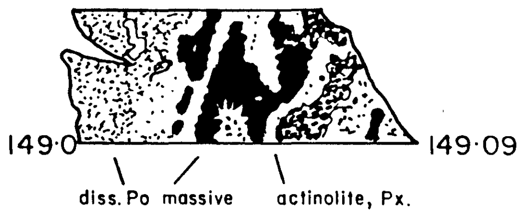

148·30= Coarse vesuvianite (4 mm laths) cut by magnetite-fluorite-phlogopite wrigglite. Massive opaques may include hulsite.

148·73= Garnet and magnetite replaced along fractures by actinolite and fluorite.

149·00= Remnant diopside and garnet replaced by actinolite - 50% of rock is pyrrhotite & fluorite. Tiny phengite veins.

149·35= A little ragged diopside in actinolite - coarse magnetite-fluorite

152·65= Biotite-quartz pelite with actinolite-calcite layers.
Quartz-scheelite veins at 60-75° to core.

Appendix B·8b

Dip -50°, Az 316°T, Collar R.L. 1657·6

MINDY DDH 81-4 (Cont.)

FIELD LOG *SAMPLES* *MINERALOGY* *ASSAY, Sn (Newmont)*

BQ Core
36·5 mm ø

61·66
Protomylonite: 5 to 25 mm quartz layers with disjointed fold hinges. Pelite from 61·6 - 62·1, 62·4 - 63·6, 63·64 - 66·53 with arkose clasts (1-2 mm feldspar grains, 20% of volume) in intervening intervals. Cordierite developed at 64·15, 65·0 and 65·70.

PS 60°

66·53
Brown garnet to 10mm in calcite. Coarse calcite 66·84 - 66·89

67·20
Banding 80°
White marble - 0·2 - 1mm grainsize

68·87
Diopside skarn (∠0·5 mm g/s), calcite veining.

69·20
Calcite marble: mostly 0·5 mm grainsize. Some coarser sections.

72·10
Diopside marble. Lower contact is faulted. (Marble breccia, calcite veining).

72·50
Massive calcite marble. Grainsize 0·5 to 2mm.

81·03
Brecciated diopside marble. Calcite veins at 22°.

81·78
Calcite marble: grainsize to 2mm.

89·99
Calc-silicate marble: 0·1m of andradite (30mm crystals), 0·5m of quartz-diopside-feldspar breccia skarn, 0·05m garnet and feldspar-diopside.

91·50
Calcite marble. Grainsize up to 2mm. Shows some irregular anastomosing dolomite layers to 10 mm thick.

98·30
White, massive marble: grainsize up to 1 mm.

102·98
Euhedral dark green andradite (15mm zoned crystals) in fine-grained lighter garnet, containing masses of fine grained yellow-green garnet.

103·90
Massive white marble.

104·30
Pale green garnet & buff-coloured garnet. → 104·45

Massive magnetite, pyrrhotite diss., hulsite →

105·15
Deep green, fine-grained garnet. Magnetite present after 106·35.

106·48
Fine grained magnetite skarn. 50% mag. with green silicates & 2-3mm pyrrhotite.

107·35
Deep green garnet with 4cm magnetite masses.

108·40
Deep green, fine-grained skarn. Contains up to 30% pyrrhotite. Cut by 5mm light yellow garnet veins every 5cm or so. (45° to core).

111·90
Black massive chert with quartz veins 1-3mm wide every 20-50mm at 70-80°. Rare veins at 55°.

113·00
Newmont log indicates some fluorite, pyrrhotite and arsenopyrite in quartz veins to the end of hole at 118m (core not preserved).

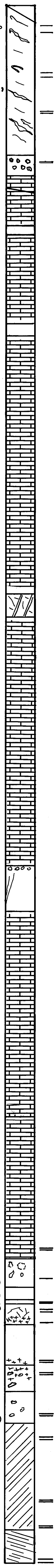

62·26 - 62·48	
63·79 - 63·95	
65·07 - 65·14	Quartz layers & clasts in biotite/muscovite rich pelite. A few cordierite patches to 5mm.
66·72 - 66·79	Yellow-green zoned birefringent garnet & coarse Px with interstitial concentric zones of magnetite in carbonate with cassiterite & szaibelyite.
102·63 - 102·70	Andradite - yellow
103·65 - 103·69	
104·40 - 104·45	
104·68 - 104·75	Carbonate with diopside. 18mm magnetite-sphal.-serp. band.
105·08 - 105·12	Garnet, fractured & replaced by f'actinolite which is serpentinised. Sheared contact with coarse actinolite-fluorite sk.
106·35 - 106·41	
106·75 - 106·83	Magnetite-fluorite-ferrophengite-fluoborite wrigglite with cassiterite.
108·10 - 108·18	Green Px altered along fractures & cleavages to f'actinolite with coarse anhedral garnet & much fluorite. Cassit. in veins.
108·87 - 108·94	70% euhedral magnetite & ludwigite alternating with phengite, fluorite & fluoborite containing cassiterite.
110·93 - 111·00	50% subhedral magnetite with Px, fluorite. Bands of vesuvianite-Px-magnetite-fluorite 4mm wide.
111·79 - 111·84	
112·88 - 113·00	

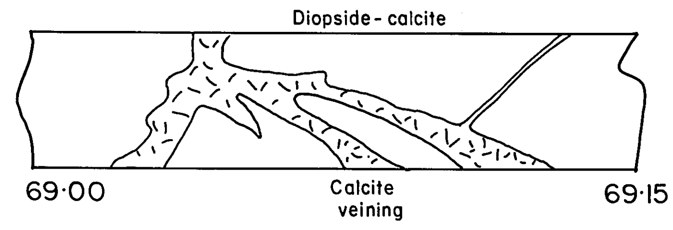

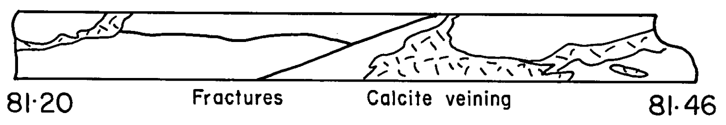

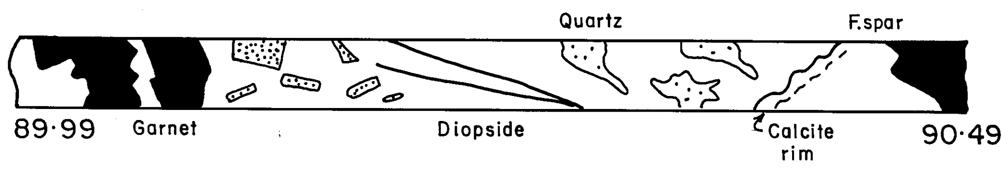

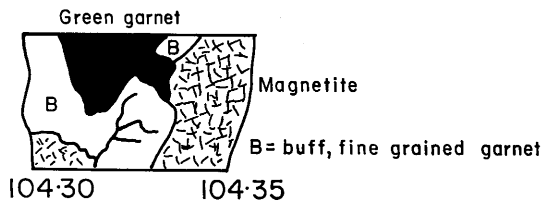

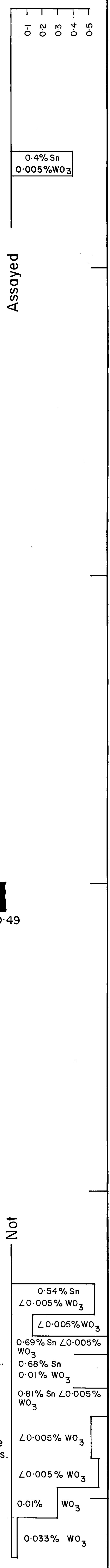

Dip -60°, Az 271°, Collar R.L. 1657·6

MINDY DDH 81-5B

App. B.9

FIELD LOG

SAMPLES

ASSAY, Sn, WO_3 % (Newmont)

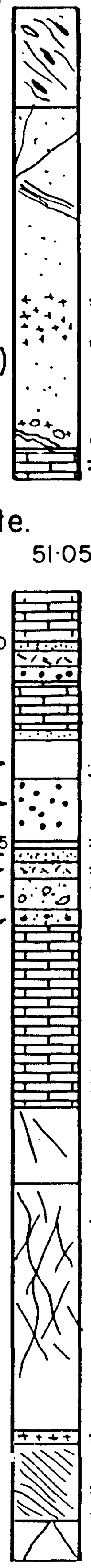

44·00 Protomylonite: lenticular quartz clasts to 30mm long in a dark grey pelitic matrix.

45·50 Deep green skarn.
Fine grained amphibole obvious to 47·8, where frequent pyrrhotite veins show dark alteration zones up to 4mm wide. (Veins at 15–60°).
Finely banded pyrrhotite cut by irregular arsenopyrite masses (to 8mm) from 46·3-46·6. By 48·4 magnetite with fluoborite is predominant.

50·60
49·0-49·07: hulsite & pyrrhotite

51·05
50·5: mag./garnet with 15mm sphalerite.
Contact with marble (50·60) at 90°.

- 45·80-45·85 White tremolite (confirmed by XRD) fluorite/fluoborite vein
- 46·31-46·36 Quartz, fluorite, fluoborite, pyrrhotite & pyrite
- 46·95-47·01
- 48·38-48·43
- 49·00-49·06 Massive pyrrhotite-hulsite replacement of wollastonite marble
- 50·47-50·51
- 50·81-50·90

51·05-80·62: Core not preserved. Newmont log indicates marble with magnetite-andradite skarn bands from 0·3 to 1·8m thick (6 bands in the interval). at 57·30 = coarse, deep green andradite (microprobe analysis obtained) with fine-grained yellow andradite (XRD powder data obtained).

80·62
White marble, ∠ 0·5mm grainsize.
81·38/·50 Hard white marble - probably cont. diopside.
81·75 Diopside marble with 20mm wollastonite vein.
81·98 Green garnet, calcite veins, arseno, vesuvian.
82·70 Marble with fractures at low angle to core
82·85 V. fine grained diopside.
83·44 Zoned andradite, calcite, diopside.
Yellow-brown garnet, arsenopyrite.
84·35/·45 Andradite-siderite masses veined by calcite
84·67 Diopside-siderite skarn.
84·90 Pale green actinolite-diopside skarn.
85·37 Brown/green/white mottled quartz-siderite-diopside skarn.
85·60 Green garnet-feldspar-brown garnet skarn.

White marble. Actinolite-brucite vein (40mm) at 87·78.

- 83·36 Andradite (deep green), some included Px, arsenopyrite.
- 84·35-84·45
- 84·77-84·83
- 85·04-85·17
- 87·78-87·95 Large biotite-quartz pelite clast in marble. Px-fluorite-vesuvianite-actin.
- 87·95-88·09 bimetasomatic skarn rim around clast.

88·3
White marble, 0·5-1mm grainsize. Fracturing at 12-40° common, 0·2-1mm wide with ludwigite filling.

89·45
White marble with many anastomosing fractures, subparallel to core and mineralised with ludwigite. Wider veins (5mm) have pyrrhotite cores.

- 90·02 Carbonates with zoned veins at 0°-30° to core = finely banded magnetite-ludwigite with a core of phengite, fluorite & brucite. Possibly a little fine-grained fluoborite. Szaibelyite replaces the carbonate up to 2mm out from the veins.

Grey and green, v. fine grained skarn.
93·13 Magnetite-hulsite with phengite veins.
93·35 Finely banded magnetite-pyrrhotite skarn.
Grey, finely banded pyrrhotite-diopside skarn.

94·50

95·10
Dark grey, massive chert. Shows a few quartz veins up to 2mm thick at all angles from 30-75°.

- 93·21-93·30
- 94·00-94·09 Brecciated skarn: Px in 2mm crystals & finer grains heavily rep. by actin. (0·2) coarser actin. rep. by fluorite & fluoborite
- 94·40-94·47 V. finely banded magnetite-fluorite, quartz, minor phengite in layers. Some remnant Px. (Wrigglite).

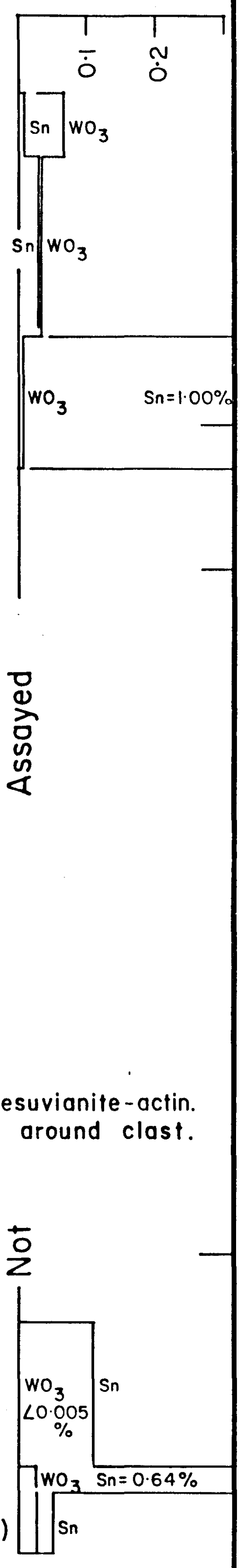

BQ core = 36·5 mm diameter.

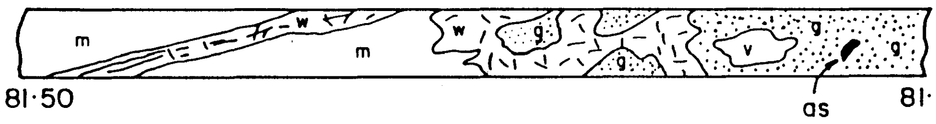

m= calcite marble, w = wollastonite, g=garnet, v= vesuvianite, as=arsenopyrite.

Dip -90°, Collar R.L. 1649·7

MINDY DDH 81-8

Appendix B·10

APPENDIX 'A' ANALYTICAL TECHNIQUES

Both X-ray Fluorescence (XRF) spectrometry and Inductively-coupled plasma optical emission spectrometry (ICP) were employed for analysis of major and trace element contents of rocks and minerals. Water and volatile contents were determined as loss on ignition (LOI) for rocks or absorbed and combined water (H_2O^- & H_2O^+) by gravimetry using the Penfield tube technique (micas).

Fe^{2+} in micas was determined as FeO using the Wilson method, as follows: digestion of a 0.25 g sample (depending upon material available) was performed in cold HF with excess accurately known ammonium metavanadate (0.05 to 0.15 g, depending upon the iron content of the specimen indicated by the ICP analysis) to oxidise all Fe^{2+} to Fe^{3+}. Remaining oxidant was determined by titration with standardised ferrous ammonium sulphate solution using sodium diphenylamine sulphate in phosphoric acid as a redox indicator. Amount of oxidant used was equated to the equivalent FeO. F in micas and rocks was determined by the colourimetric method of Hall and Walsh (1969), following fusion of a 0.2 g specimen in 1.5 g with Na_2CO_3.

A fusion similar to the preceding method was used for determination of Cl. After leaching the cooled fusion cake with water and filtration the solution was neutralised and brought to a pH of ≈ 5.5 with nitric acid. Dilution to 100 ml and determination of Cl by ion-selective electrode, using standards prepared form blank carbonate fusions with known amounts of NaCl added in solution. The same preparations were then acidified further (2 ml of concentrated HNO_3 added to a volumetric flask and made up to 100 ml with the solution) and Rb was determined using the Philips 9000 atomic absorption spectrophotometer. The micas for which isotope dilution Rb determinations were available were used as reference material. High Rb specimens were further diluted by a factor of 10 and made up to the same acidity to keep within operating range of the instrument.

XRF TECHNIQUES: major elements were determined on a 0.7 g sample that was fused to a glass with precisely six times its weight of lithium metaborate flux (Johnson Matthey Spectroflux 105 ™ , containing La_2O_3). Philips 1400 and 1480 automated X-ray fluorescent spectrometers were used for analysis. Trace elements were determined for 7 g samples of finely ground rock pressed into pellets using polyvinyl alcohol ('Mowiol') as a binder and boric acid as a mounting medium.

ICP TECHNIQUES: major elements were determined on 0.5 g specimens that were fused with 1.5g of lithium metaborate to which 1% Ga_2O_3 was added as an internal standard. The glass was dissolved in nitric acid, 20 ml of 250 ppm Cd solution (as $Cd(NO_3)_2$) added as a further internal standard for drift correction, and the solution made up to 0.5 l. Standard preparations were made from laboratory standard rocks and international reference material. For trace element analysis a 0.10g specimen was dissolved in a 1:2 HF-$HClO_4$ mixture, the resulting SiF_4 was volatilised and the residue re-dissolved in HCl and made up to 10.2 g liquid weight. Again, laboratory and international standards were prepared.

Analyses were made using a Philips PV8060 inductively-coupled plasma atomic emission spectrophotometer that was programmed to read the spectra emitted from Si, Al, Fe, Mg, Ca, Na, K, Ti, P, Mn, Ba, Cr, Ni, Sr, V, Y and Zr for the 'majors' programme and Al, Fe, Mg, Ca, Na, K, Ti, P, Mn, Ba, Co, Cr, Cu, Li, Mo, Nb, Ni, Sc, Sr, V, Y, Zn, Zr, La, Ce, Nd, Sm, Eu, Dy and Yb for the 'traces' programme.

RADIOGENIC ISOTOPE MASS SPECTROMETRY:

Chemical preparation was performed in Teflon beakers that were rigourously cleaned by successive leaching in hot HNO_3, boiling de-ionised water and washing in UHQ water. *0.1g specimens were dissolved in an HF-sub-boil HNO_3 mixture. After standing overnight SiF_4 was volatilised under heated air flow hoods, 2ml sub-boil HNO_3 added and the solution evaporated again, then converted to chloride in 6M HCl. After evaporation the solution for ion-exchange was prepared using 5ml of 2.5M HCl. Separation of Sr and Rb was achieved by ion-exchange columns (BIORAD Analytical Grade cation Exchange Resin AG 50W-X8 in 200-400 mesh hydrogen form) after centrifuging the solution to extract any possible solid contaminants. The chlorides collected were evaporated onto Ta filament assemblies that had been de-gassed at ≈1200°C in a vacuum of $<2x10^{-5}$ mbar. Isotopic ratios were determined using a VG 354 motorised multicollector thermal ionisation mass spectrometer. Isochrons were calculated using least-squares fitting after the method of York (1968).

APPENDIX B.12

Chemical parameters for selected unmineralised and Sn-mineralised granites.

UNMINERALISED: (a) Massif Centrale, France.

LITHOLOGY	L	Sr_i	K/Na	SiO_2	CaO	MgO	TiO_2	P_2O_5
Guéret Pluton:								
AS 54	12.84	0.7101	1.420	70.01	1.42	1.33	0.419	0.232
AS 2	13.82	0.7120	1.529	71.72	1.01	0.83	0.278	0.264
AS 19	13.56	0.7119	1.550	71.43	1.22	0.86	0.228	0.267
AS 24	12.13	0.7103	1.489	68.65	1.98	1.52	0.474	0.215
AS 63	11.79	0.7108	1.575	67.65	2.23	1.79	0.561	0.238
AS 68	9.50	0.7089	1.627	63.5	3.31	2.85	0.735	0.256
Margeride Pluton:								
MG 7	13.59	0.7109	1.759	71.49	1.25	1.29	0.353	0.209
MG 5	13.57	0.7111	1.480	72.56	1.08	1.17	0.328	0.200
MG 18	13.27	0.7110	1.832	70.84	1.62	1.17	0.319	0.182
MG 36	11.69	0.7111	1.724	68.30	2.07	2.19	0.577	0.266
MG 28	10.68	0.7113	1.665	65.65	2.41	2.60	0.667	0.282
MG 24	10.82	0.7111	1.649	66.52	2.55	2.39	0.635	0.263
Millevaches Pluton:								
MI 16	12.41	0.7073	1.923	65.61	1.83	1.28	0.370	0.236
MI 9	14.00	0.7109	2.026	70.11	1.48	1.07	0.437	0.184
MI 11	13.54	0.7064	1.624	71.26	1.69	1.04	0.290	0.218
MI 4	10.79	0.7100	1.199	67.03	2.55	1.93	0.530	0.308

L is the Larsen Index: L= ($^1/_3$ Si+K) - (Mg+Ca)

Data from Shaw, unpublished.

MAJOR ELEMENT CHARACTERISTICS OF SOME MASSIF CENTRALE GRANITES

LITHOLOGY	Rb	Sr	Ba	K/Rb	Ba/Rb	Ba/Sr
Guéret Pluton:						
AS 54	216	268	609	173.5	2.818	2.277
AS 2	211	159	484	183.6	2.298	3.040
AS 19	203	180	521	188.0	2.564	2.898
AS 24	202.8	274	737	185.8	3.636	2.693
AS 63	191	513	926	205.7	4.853	1.804
AS 68	184	419	979	201.0	5.328	2.338
Margeride Pluton:						
MG 7	294	168	316	140.2	1.073	1.884
MG 5	247	144	378	151.3	1.529	2.620
MG 18	234	192	649	174.9	2.775	3.377
MG 36	214	283	847	180.3	3.966	2.993
MG 28	208	286	842	180.0	4.051	2.947
MG 24	198	282	875	187.8	4.420	3.106
Millevaches Pluton:						
MI 16	233	275	927	183.2	3.983	3.378
MI 9	214	277	698	223.2	3.259	2.525
MI 11	191	494	801	223.6	4.197	1.621
M1 4	179	320	733	186.1	4.097	2.287

TRACE ELEMENT CHARACTERISTICS OF SOME MASSIF CENTRALE GRANITES (data from Shaw, unpublished).
Arranged in order of increasing Rb content.

UNMINERALISED: (b) Lachlan Fold Belt, N.S.W. & Victoria.

LITHOLOGY	L	Sr_i	K/Na	SiO_2	CaO	MgO	TiO_2	P_2O_5
Musc. Gr. KP 15	15.16	-	2.423	73.12	1.17	0.45	0.25	0.12
Cord. gar. WV115	14.07	-	1.995	73.65	1.20	0.61	0.36	0.17
Bt. Cord. KB 32 (Strathbogie)	10.58	-	2.098	67.68	2.26	2.22	0.64	0.15
Biot. G'dior. Beridale BB 34	13.24	-	0.925	74.87	1.47	0.05	0.26	0.05
Hb. KB 7	8.31	-	0.941	67.15	4.35	1.71	0.39	0.12
Hb. G'dior. Brogo AB 82	8.76	-	0.813	67.18	3.82	1.96	0.47	0.16

L is the Larsen Index: L= $(^1/_3\ \mathrm{Si+K}) - (\mathrm{Mg+Ca})$

MAJOR ELEMENT CHARACTERISTICS OF SOME L.F.B. GRANITES

LITHOLOGY	Rb	Sr	Ba	K/Rb	Ba/Rb	Ba/Sr
Musc. Gr. KP 15	526	61	196	798.6	0.373	3.213
Cord. gar. WV115	244	79	755	156.5	3.094	9.557
Cord. KB 2 (Strathbogie)	183	139	475	163.3	2.596	3.417
Biot. G'dior. Beridale BB 34	124	184	665	214.2	5.363	3.614
Hb. KB 7	106	206	395	187.1	3.726	1.917
Hb. Bt. G'dior. Brogo AB 82	92	406	495	239.9	5.380	1.219

TRACE ELEMENT CHARACTERISTICS OF LACHLAN FOLD BELT GRANITES Arranged in order of increasing Rb content (data from White, 1990).

MINERALISED: (a) S. Sardinia

LITHOLOGY	L	K/Na	SiO_2	CaO	MgO	TiO_2	P_2O_5
Granodiorite	>10	0.98	65.5	4.24	1.00	0.54	0.32
Monzogranite	10-12.5	1.40	67.0	2.47	0.99	0.44	0.18
Leucogranite	12.5-15.5	1.53	74.1	0.62	0.16	0.08	0.08
Biot.-musc. granite	>15.5	1.95	74.5	0.45	0.15	0.04	0.05

L is the Larsen Index: L= $(^1/_3\ \mathrm{Si+K}) - (\mathrm{Mg+Ca})$

MAJOR ELEMENT CHARACTERISTICS OF S. SARDINIAN GRANITES

LITHOLOGY	F	Rb	Li	Sr	Ba	K/Rb	Ba/Rb	Ba/Sr	Rank
Biot.-musc. granite	170	493	21	23	267	96	0.54	11.6	M, 5
Biot.-musc. granite	990	379	58	20	361	107	0.95	18.00	M, 8
Leucogranite	270	356	38	11	223	153	0.76	7.82	M, 7
Leucogranite	479	312	38	27	243	127	0.78	9.00	M, 4
Biot.-musc. granite	276	288	62	28	219	153	0.76	7.82	M, 6
Leucogranite	395	258	17	33	341	160	1.32	10.3	X, 2
Leucogranite	333	258	15	39	330	162	1.28	8.46	X, 1
Leucogranite	213	253	39	51	390	162	1.54	7.65	X, 3

TRACE ELEMENT CHARACTERISTICS OF S. SARDINIAN GRANITES

X= Barren, M= Sn/W mineralised, Rank= 'Degree of specialisation' according to Biste. Arranged in order of increasing Rb content (after Biste, 1982).

Sn-MINERALISED: (b) Mole granite, Torington, N.S.W.

LITHOLOGY	L	K/Na	SiO_2	CaO	MgO	TiO_2	P_2O_5
Micro	15.70	1.47	75.75	0.08	0.10	0.07	-
Micro	15.40	1.68	76.61	0.58	0.17	0.19	-
Seriate	15.08	1.44	77.26	0.43	0.43	0.10	-
Press.-Q	15.70	1.96	77.05	0.15	0.13	0.13	-
Press.-Q	15.42	1.60	77.38	0.34	0.15	0.13	-
Seriate	15.61	1.51	76.35	0.29	0.14	0.14	-
Press.-Q	15.64	1.43	76.82	0.55	0.02	0.14	-
Micro	16.36	1.69	77.31	0.30	0.00	0.09	-
Seriate	15.37	1.45	78.09	0.56	0.05	0.22	-

L is the Larsen Index: $L = (^{1}/_{3}\,Si+K) - (Mg+Ca)$

Press.-Q= Pressure-quench variety; Seriate= Seriate-textured variety &Micro= Microgranite

Data from Plimer and Kleeman (1985). No F determinations are available.

MAJOR ELEMENT CHARACTERISTICS OF THE MOLE GRANITE, N.S.W.

LITHOLOGY	Rb	Li	Sr	Ba	K/Rb	Ba/Rb	Ba/Sr
Micro	817	180	15	61	49.16	0.075	4.067
Micro	712	81	5	8	55.83	0.011	1.600
Seriate	641	154	11	36	56.32	0.056	3.273
Press.-Q	547	81	16	65	70.85	0.119	4.063
Press.-Q	543	99	19	64	68.01	0.118	3.368
Seriate	532	134	20	91	75.19	0.171	4.550
Press.-Q	431	56	40	142	94.54	0.329	3.550
Micro	384	10	12	49	117.78	0.128	4.083
Seriate	379	65	34	136	95.91	0.359	4.000

Data from Plimer and Kleeman (1985).

TRACE ELEMENT CHARACTERISTICS OF THE MOLE GRANITE, N.S.W.

MINERALISED: (c) Cornubian batholith.

LITHOLOGY	L	K/Na	SiO_2	CaO	MgO	TiO_2	P_2O_5
MG: 27	13.68	1.596	72.80	1.28	0.05	0.04	0.48
E: 5	14.62	1.452	71.10	0.59	0.09	0.06	0.50
D: 13	15.43	1.754	73.01	0.44	0.14	0.14	0.33
GP: 34	17.34	71.43	72.80	0.28	0.26	0.20	0.26
C: 43	15.01	1.866	73.70	0.56	0.05	0.06	0.32
D: 35	15.02	1.753	72.73	0.41	0.33	0.13	0.15
F: 15	14.45	1.284	74.20	1.31	0.08	0.07	0.46
B: 39	14.17	2.028	71.20	1.12	0.60	0.35	0.24
B: 9	14.07	1.569	72.63	1.12	0.48	0.28	0.18
C: 21	15.88	2.340	74.08	0.44	0.18	0.07	0.25
B: 18	14.62	1.821	72.43	0.84	0.44	0.21	0.25

L is the Larsen Index: $L = (^{1}/_{3}\ Si + K) - (Mg + Ca)$

MAJOR ELEMENT CHARACTERISTICS OF CORNUBIAN GRANITES

LITHOLOGY	F	Rb	Li	Sr	Ba	K/Rb	Ba/Rb	Ba/Sr	
MG: 27	6500	2293	4400	47	197	14.30	0.086	4.191	
E: 5	5660	1218	1250	61	204	32.98	0.167	3.344	
D: 13	3800	982	835	41	83	45.30	0.085	2.024	Meta
GP: 34	-	814	139	34	699	78.09	0.859	20.56	
C: 43	-	760	325	22	15	52.09	0.020	0.682	
D: 35	3800	695	510	175	150	60.06	0.216	0.857	Meta
F: 15	6300	615	46	64	43	62.88	0.070	0.672	Meta
B: 39	-	480	370	95	230	88.35	0.479	2.421	
B: 9	-	462	325	92	397	78.32	0.859	4.315	
C: 21	-	444	185	43	102	107.1	0.230	2.372	
B: 18	-	419	280	94	196	100.2	0.468	2.085	

Meta= metasomatic (Stone). Letters A to D refer to granite type and numbers to localities as in Stone (1985). GP= granite porphyry and MG= microgranite. F values have been recalculated from percentages and rounded.
TRACE ELEMENT CHARACTERISTICS OF THE CORNUBIAN GRANITES
Arranged in order of increasing Rb content (data from Stone, 1985).

MINERALISED: (d) Seagull-Thirtymile suite.

LITHOLOGY	L	K/Na	SiO_2	CaO	MgO	TiO_2	P_2O_5
Li-mica	15.07	0.923	75.61	0.12	0.01	0.01	0.01
STQ	15.29	1.553	76.48	0.43	0.14	0.06	0.02
Seagull	15.65	1.750	76.50	0.56	0.08	0.12	0.03
Even-Gr.	15.53	1.561	76.97	0.60	0.07	0.12	0.03
Hake	15.41	1.783	76.04	0.71	0.23	0.20	0.05
Megacrystic	14.98	1.496	75.19	0.86	0.23	0.23	0.06
Porphyry	14.70	1.723	72.70	1.17	0.41	0.40	0.10

L is the Larsen Index: $L= (^{1}/_{3}\ \mathrm{Si+K}) - (\mathrm{Mg+Ca})$

MAJOR ELEMENT CHARACTERISTICS OF THE SEAGULL/THIRTYMILE SUITE

LITHOLOGY	n	Rb	Li	Sr	Ba	K/Rb	Ba/Rb	Ba/Sr	Rank
Li-mica	5	2087	626	0.9	15	17.1	0.008	22.1	M, 6
STQ	3	886	-	13	35	42.4	0.040	3.6	M, 5
Seagull	10	515	-	16	94	93.9	0.361	7.5	M, 4
Even-Gr.	11	497	147	23	96	86.7	0.159	3.7	X, 3
Hake	10	424	-	46	192	105.7	0.484	4.3	X, 3
Mega.	9	419	88	60	222	105.3	0.774	4.4	X, 2
Porphyry	5	304	79	123	782	160.2	2.755	6.4	X, 1

No F determinations are available.
Li values are from very few specimens: Li= 3; Mega= 2; E.G.= 4 & Por= 3.
n= number of analyses used for means of the other elements.
STQ is alaskite stock material and dykes (3 specimens) from the STQ tin stockwork (east side of the Seagull batholith).
X= Barren, M= Sn/W mineralised, Rank= 'Degree of specialisation'.

TRACE ELEMENT CHARACTERISTICS OF THE THIRTYMILE/HAKE/SEAGULL GRANITES

APPENDIX C.1 TABLE OF ROCK ANALYSES

Field No.	78/23-1	78/23-1	78/23-2	98/5-1	ORK	ORK
Crush/Grind	Roll/WC	Same prep.	WC	WC	WC	Same prep
Pluton/facies	Ork/ Li		Ork/ Li	Ork/ Li	Ork/ Li	
Lab. No.	TIM01	TIM 01	78232	TIM37	TIM39	TIM39
WTr: CaO	0.14			0.13	0.17	
WTr: TiO2	0.013			0.008	0.008	
Majors.	XRF		XRF	XRF	XRF	
SiO2	77.57	76.78	75.15	73.42	72.96	
Al2O3	13.52	13.31	14.57	16.04	15.93	
Fe2O3	0.65	0.68	0.51	0.85	0.35	
MgO			0.06		0.01	
CaO	0.18	0.18	0.13	0.18	0.23	
Na2O	5.20	5.05	5.28	5.51	7.07	
K2O	3.63	3.54	4.35	3.66	3.99	
TiO2	0.01	0.02		0.01	0.02	
MnO	0.04	0.04	0.05	0.04	0.05	
P2O5	0.01	0.01	0.02	0.02	0.03	
Total	100.81	99.59	100.12	99.71	100.63	
LOI	0.31	0.31		0.53	0.53	
Ni	4.1	4.5		3.9	3.8	4.2
Cr	9.1	8.8		1.2	1.3	1.4
V	2.2	1.7		2.0	1.9	1.4
Sc	6.8	6.5		4.7	5.1	5.8
Cu						
Zn	12.9	13.1		15.9	11.9	11.4
Cl				30		
Ga	44.9	44.9		58.2	56.3	56.3
Pb	41.4	41.1		29.8	42.4	42.4
Sr	1.6	1.6		1.0	0.2	0.2
Rb	1392.0	1392.1		2153.0	1884.5	1884.5
Ba	14.6	23.1		12.2	16.1	18.2
Zr	78.1	78.1		18.2	52.1	52.1
Nb	79.6	79.6		66.9	93.5	93.5
Th	21.5	21.5		14.9	22.5	22.5
Y	18.7	18.7		5.8	19.2	19.2
La	17.9	16.8		6.2	10.8	10.0
Ce	51.0	50.9		22.8	39.1	40.9
Nd	14.7	14.2		6.0	12.6	12.7

CIPW Norms are shown below:

Field No.	78/23-1	78/23-2	98/5-1	ORK
Qtz	32.60	27.20	26.50	16.10
Or	21.50	25.72	21.70	23.60
Ab	44.10	44.62	46.70	59.70
An	0.82	0.51	0.76	
Leu				
Nep				
Cor	0.72	0.97	2.74	
Acm				0.05
C/Woll				0.41
C/En				0.03
C/Fer				0.43
O/En		0.15		0.01
O/Fer	0.98	0.73	1.27	0.15
Fo				
Fa				
Mt	0.09	0.06	0.11	0.02
Ilm	0.03		0.03	0.03
Ap	0.03	0.05	0.04	0.06
Fe ratio used	0.1	0.1	0.1	0.1
"D"	98.20	97.54	94.90	99.40

Field No.	97/26-3	97/28-2	97/28-4	88/14-7 S	97/17-1 A	97/26-5
Crush/Grind	WC		WC	Roll/WC	WC	WC
Pluton/facies	TM/ Li	TM/ Li	TM/ Li	Mega	Mega	Mega
Lab. No.	TIM19		TIM33	TIM06	TIM09	TIM20
WTr: CaO				0.78	0.73	1.08
WTr: TiO2	0.011		0.008	0.222	0.173	0.301
Majors.	XRF		XRF	XRF	XRF	XRF
SiO2	77.54	74.12	75.02	75.70	75.98	74.59
Al2O3	12.94	15.79	14.43	12.60	12.97	13.27
Fe2O3	0.80	0.33	0.26	1.87	1.62	1.94
MgO			0.09	0.22	0.09	0.34
CaO	0.04	0.03	0.01	0.80	0.71	1.06
Na2O	4.62	6.09	4.33	3.42	4.03	3.55
K2O	3.88	3.62	5.03	4.88	4.48	4.89
TiO2	0.01		0.02	0.23	0.16	0.31
MnO	0.05	0.05	0.06	0.04	0.04	0.03
P2O5	0.02	0.02	0.02	0.06	0.04	0.09
Total	99.88	100.03	99.26	99.81	100.14	100.06
LOI	0.34	0.36	0.46	0.24	0.48	0.60
Ni	3.5		5.2	4.1	4.7	4.3
Cr	1.8		1.8	11.0	1.8	2.7
V	1.4		2.0	13.0	10.1	23.0
Sc	6.6		2.2	2.7	4.0	5.7
Cu				1.1	0.3	0.6
Zn	11.6		25.9	27.7	22.5	15.5
Cl	13		64	159	212	89
Ga	43.1		58.8	21.3	23.8	22.3
Pb	38.0		33.0	19.4	175.7	35.6
Sr	0.2		1.6	53.5	44.2	101.7
Rb	1517.6		3424.3	350.0	482.7	407.4
Ba	10.3		22.1	226.7	192.5	470.6
Zr	87.7		12.0	177.0	133.1	188.9
Nb	115.0		33.9	62.9	72.4	57.0
Th	24.2		4.1	60.0	55.5	44.5
Y	8.9		3.6	49.1	64.8	49.0
La	26.5		4.1	52.7	36.7	50.6
Ce	71.6		9.1	104.9	78.9	98.5
Nd	15.3		1.5	34.6	29.7	35.5

CIPW Norms are shown below:

Field No.	97/26-3	97/28-2	97/28-4	88/14-7 S	97/17-1 A	97/26-5
Qtz	35.30	24.60	30.30	34.20	32.90	31.70
Or	23.00	21.40	29.70	28.90	26.50	28.90
Ab	39.10	51.60	36.60	29.00	34.20	30.10
An	0.08	0.02		3.63	3.29	4.71
Leu						
Nep						
Cor	1.10	1.84	1.90	0.37	0.29	0.42
Acm						
C/Woll						
C/En						
C/Fer						
O/En			0.21	0.54	0.23	0.85
O/Fer	1.22	0.55	0.46	2.37	2.13	2.32
Fo						
Fa						
Mt	0.11	0.04	0.04	0.25	0.21	0.26
Ilm	0.02	0.01	0.03	0.44	0.31	0.59
Ap	0.04	0.04	0.39	0.13	0.09	0.20
Fe ratio used	0.1	0.1	0.1	0.1	0.1	0.1
"D"	97.40	97.60	96.60	92.10	93.60	90.70

Field No.	97/26-5	97/27-2	97/27-5	97/27-5	97/27-6	97/28-5
Crush/Grind	Repeat prep.	WC	WC	Same prep	Roll/WC	
Pluton/facies	Mega	Mega	Mega	Mega	Mega	Mega
Lab. No.		TIM22	TIM28	TIM 28	TIM29	TIM94
WTr: CaO		1.25	0.62		1.17	1
WTr: TiO2		0.358	0.120		0.320	0.227
Majors.	XRF	XRF	XRF		XRF	XRF
SiO2	74.52	72.96	76.99	76.90	73.64	74.57
Al2O3	13.28	13.63	12.36	12.42	13.41	13.32
Fe2O3	1.89	2.68	1.29	1.28	2.34	1.55
MgO	0.34	0.42	0.04	0.08	0.40	0.20
CaO	1.08	1.22	0.66	0.68	1.21	0.94
Na2O	3.65	3.40	3.64	4.04	3.66	3.67
K2O	4.89	5.11	4.76	4.79	4.86	5.34
TiO2	0.31	0.35	0.11	0.12	0.34	0.22
MnO	0.04	0.06	0.03	0.03	0.05	0.04
P2O5	0.09	0.11	0.03	0.03	0.09	0.06
Total	100.08	99.94	99.90	100.36	99.98	99.90
LOI	0.50	0.51	0.23	0.51	0.26	0.33
Ni		5.1	2.9	3.3	4.2	3.1
Cr		4.6	2.5	2.0	2.9	1.8
V		26.7	4.9	4.6	23.0	15.1
Sc		4.7	1.4	0.8	5.1	4.8
Cu		1.4	0.2	0.2	1.1	0.5
Zn		29.2	14.3	14.4	30.0	18.6
Cl		308	65	65	267	127
Ga		21.5	20.6	20.6	21.5	21.6
Pb		25.9	26.1	26.1	26.1	26.7
Sr		110.2	26.0	26.0	106.6	73.2
Rb		370.4	428.0	428.1	286.5	482.6
Ba		520.2	84.2	92.8	516.9	353.2
Zr		214.8	123.3	123.2	195.2	131.6
Nb		58.8	59.2	59.2	58.2	53.2
Th		40.6	57.2	57.2	34.0	49.7
Y		48.7	43.5	43.5	43.7	33.7
La		58.8	34.2	33.4	55.5	31.8
Ce		110.2	70.2	70.1	97.0	59.9
Nd		40.6	25.6	25.5	34.8	21.9

CIPW Norms are shown below:

Field No.		97/27-2	97/27-5		97/27-6	97/28-5
Qtz		29.20	35.50		29.60	29.90
Or		30.30	28.20		28.80	31.60
Ab		28.90	30.80		31.00	31.10
An		5.37	3.06		5.44	4.10
Leu						
Nep						
Cor		0.54	0.11		0.15	
Acm						
C/Woll						0.07
C/En						0.02
C/Fer						0.06
O/En		1.04	0.09		1.00	0.49
O/Fer		3.37	1.71		2.88	1.88
Fo						
Fa						
Mt		0.35	0.17		0.31	0.21
Ilm		0.67	0.22		0.65	0.41
Ap		0.25	0.07		0.20	0.14
Fe ratio used		0.1	0.1		0.1	
"D"		88.40	94.50		89.40	92.60

Field No.	97/28-5	TOR	TOR	97/28-5	97/28-5	97/28-5
Crush/Grind	Same prep	WC	Same prep	1/4 split WC	1/4 split WC	1/4 split WC
Pluton/facies	Mega	Mega	Mega	Mega	Mega	Mega
Lab. No.	TIM94	TIM38	TIM38	MG 1	MG 2	MG 3
WTr: CaO		0.79		0.85	0.87	0.86
WTr: TiO2		0.162		0.208	0.224	0.216
Majors.		XRF		XRF	XRF	XRF
SiO2	74.75	77.27				
Al2O3	13.39	12.46				
Fe2O3	1.67	0.96				
MgO	0.18	0.16				
CaO	0.94	0.77				
Na2O	3.63	4.08				
K2O	5.33	4.80				
TiO2	0.22	0.16				
MnO	0.04	0.02				
P2O5	0.05	0.05				
Total	100.18	100.74				
LOI	0.33	0.30				
Ni	3.7	3.9	3.3	3.9	3.8	4.1
Cr	2.7	1.7	2.2	2.5	1.8	1.9
V	15.6	7.7	8.3	13.6	13.2	13.3
Sc	4.5	2.1	2.5	4.0	3.2	3.9
Cu		0.2		0.7	0.3	0.8
Zn	18.2	14.5	14.4	19.5	21.0	21.1
Cl	127	157	157	133	146	128
Ga	21.6	20.6	20.6	22.0	21.9	21.9
Pb	26.7	16.7	16.8	20.3	20.4	21.1
Sr	73.2	52.3	52.3	67.7	65.0	63.7
Rb	482.6	324.0	324.0	451.6	441.9	448.2
Ba	356.0	176.9	184.3	310.7	286.8	271.9
Zr	131.6	141.6	141.6	160.4	161.9	160.8
Nb	53.2	51.4	51.4	57.0	58.7	58.0
Th	49.7	68.7	68.8	58.1	58.5	58.3
Y	33.7	47.4	47.4	41.8	41.0	40.6
La	31.8	47.9	47.4	48.6	47.6	47.7
Ce	60.0	97.2	96.7	92.7	91.2	89.6
Nd	22.0	34.2	34.9	31.5	32.0	31.1

Replicates for traces only
1-4= 1/4 of split 3, 1st. half: WC
(MG 1-4)

CIPW Norms are shown below:

Field No.	TOR
Qtz	33.30
Or	28.40
Ab	34.60
An	1.48
Leu	
Nep	
Cor	
Acm	
C/Woll	0.85
C/En	0.24
C/Fer	0.65
O/En	0.18
O/Fer	0.50
Fo	
Fa	
Mt	0.13
Ilm	0.30
Ap	0.11
Fe ratio used	0.1
"D"	96.30

Field No.	97/28-5	97/28-5	97/28-5	97/28-5	97/28-5	97/28-5
Crush/Grind	1/4 split WC	Grab/WC	1/4 split WC	1/4 split WC	1/4 split WC	1/4 split WC
Pluton/facies	Mega	Mega	Mega	Mega	Mega	Mega
Lab. No.	MG 4	MG 5	MG6/T 42	MG7/T 43	MG8/T 44	MG9/T 45
WTr: CaO	0.91	0.88	0.95	0.94	0.94	0.94
WTr: TiO2	0.224	0.216	0.214	0.219	0.219	0.211
Majors.	XRF	XRF	XRF	XRF	XRF	XRF
SiO2			74.56	Replicates for traces		
Al2O3			13.31	1/4 of split 3, 2nd. half: Roll/WC		
Fe2O3			1.55	(MG 6-9)		
MgO			0.20			
CaO			0.94			
Na2O			3.67			
K2O			5.34			
TiO2			0.22			
MnO			0.04			
P2O5			0.06			
Total			99.98			
LOI			0.33			
Ni	4.2	4.0	3.7	3.9	4.5	4.3
Cr	2.5	2.1	11.1	11.1	11.2	10.4
V	14.1	13.8	14.1	14.4	14.2	14.3
Sc	4.2	3.8	3.3	3.2	3.9	1.6
Cu	1.5	1.0	1.7	0.9	0.8	1.3
Zn	21.7	21.7	19.3	20.8	20.0	19.4
Cl	134	121	157	141	118	126
Ga	21.8	22.6	22.0	21.1	22.2	22.1
Pb	20.2	20.5	26.6	27.7	26.1	31.6
Sr	64.4	65.8	72.2	71.7	71.8	71.9
Rb	434.1	449.7	475.1	473.5	476.9	473.6
Ba	273.8	299.3	358.8	358.4	357.0	363.4
Zr	170.4	157.1	157.3	154.1	156.6	149.5
Nb	59.6	59.0	53.4	53.8	55.8	53.7
Th	57.0	59.4	51.9	53.2	52.0	52.0
Y	42.8	42.1	34.1	35.1	33.9	34.8
La	47.5	50.2	44.0	44.6	45.4	44.6
Ce	87.4	95.2	84.4	83.0	85.9	83.3
Nd	31.1	33.0	30.3	29.2	30.0	30.1

CIPW Norms are shown below:

Field No.	
Qtz	
Or	
Ab	
An	
Leu	
Nep	
Cor	
Acm	
C/Woll	
C/En	
C/Fer	
O/En	
O/Fer	
Fo	
Fa	
Mt	
Ilm	
Ap	
Fe ratio used	
"D"	

Field No.	88/8-8	88/8-8	88/15-2	88/15-2	97/23-3	97/23-5
Crush/Grind	Roll/WC	Repeat prep.			WC	Ag
Pluton/facies	Even	Even	Even	Even	Even	Even
Lab. No.	TIM02	TIM03			TIM10	TIM12
WTr: CaO	0.37	0.38			0.53	0.7
WTr: TiO2	0.104	0.104			0.101	0.171
Majors.	XRF	XRF			XRF	XRF
SiO2	77.97		72.90	72.86	77.28	76.83
Al2O3	12.27		13.34	13.29	12.44	12.48
Fe2O3	0.98		3.19	3.18	1.14	1.29
MgO	0.02		0.53	0.39	0.03	0.13
CaO	0.41		0.98	0.99	0.54	0.65
Na2O	2.98		3.07	3.01	3.67	3.26
K2O	5.52		5.48	5.45	4.87	5.26
TiO2	0.11		0.42	0.42	0.11	0.17
MnO	0.01		0.04	0.05	0.03	0.03
P2O5	0.03		0.10	0.09	0.02	0.05
Total	100.28		100.05	99.72	100.12	100.15
LOI	0.50	0.50	0.49	0.49	0.31	0.60
Ni	3.3	3.8			3.1	3.3
Cr	6.7	7.0			1.8	1.9
V	4.9	4.2			3.0	8.8
Sc	1.5	1.5			0.5	2.5
Cu	9.8	7.2			0.3	0.6
Zn	13.3	13.5			12.2	15.8
Cl	13	21			126	181
Ga	20.5	19.8			20.7	19.7
Pb	26.9	27.6			35.0	20.1
Sr	15.2	15.6			16.1	43.9
Rb	439.4	440.8			483.7	379.6
Ba	56.1	57.4			50.3	179.5
Zr	133.1	132.8			123.5	131.5
Nb	69.4	69.3			62.5	53.3
Th	74.9	74.6			64.7	68.7
Y	25.8	25.9			41.0	40.1
La	24.5	23.3			36.5	46.6
Ce	54.8	54.1			74.1	87.4
Nd	18.3	17.7			27.0	31.1

CIPW Norms are shown below:

Field No.	88/8-8	88/15-2	97/23-3	97/23-5
Qtz	38.20	29.70	35.50	35.60
Or	32.70	32.50	28.80	31.10
Ab	25.20	26.00	31.00	27.60
An	1.85	4.26	2.57	2.95
Leu				
Nep				
Cor	0.73	0.81	0.20	0.34
Acm				
C/Woll				
C/En				
C/Fer				
O/En	0.04	1.32	0.08	0.32
O/Fer	1.24	3.94	1.50	1.62
Fo				
Fa				
Mt	0.13	0.42	0.15	0.17
Ilm	0.20	0.81	0.20	0.31
Ap	0.06	0.22	0.04	0.10
Fe ratio used	0.1	0.1	0.1	0.1
"D"	96.10	88.20	95.30	94.30

Field No.	97/23-5	97/24-5	97/25-1B	97/25-1B	97/26-6	97/27-4
Crush/Grind	WC	WC			Roll/WC	Prep. 1
Pluton/facies	Even	Even	Even	Even	Even	Even
Lab. No.	TIM13	TIM16	TIM17	TIM18	TIM21	TIM23
WTr: CaO	0.64	0.8	0.63	0.64	0.62	0.61
WTr: TiO2	0.176	0.201	0.086	0.091	0.112	0.095
Majors.	XRF	XRF	XRF	XRF	XRF	ICP
SiO2	76.83	76.50	76.68		76.01	77.51
Al2O3		12.59	12.53		12.81	12.37
Fe2O3		1.70	1.23		2.06	1.21
MgO		0.19	0.05		0.06	0.23
CaO		0.78	0.64		0.61	0.62
Na2O		3.68	3.93		4.39	4.10
K2O		4.81	4.45		4.39	4.66
TiO2		0.19	0.09		0.11	0.10
MnO		0.04	0.03		0.04	0.02
P2O5		0.05	0.02		0.03	0.02
Total		100.51	99.64		100.49	100.85
LOI		0.44	0.44		0.14	0.43
Ni	2.9	4.1	3.5	3.9	3.2	3.0
Cr	0.9	2.4	1.4	2.5	4.0	0.4
V	8.1	12.4	2.9	2.7	6.0	3.3
Sc	2.7	2.6	1.4	0.9	3.5	2.2
Cu			0.4	0.1		0.8
Zn	17.3	16.1	12.2	11.9	17.9	10.7
Cl	208	151	4	16	136	
Ga	19.3	22.3	23.3	23.3	25.2	20.3
Pb	19.9	26.4	32.7	32.9	40.6	56.8
Sr	43.1	43.1	14.1	14.1	20.5	15.8
Rb	382.0	497.3	636.2	633.7	701.2	307.3
Ba	180.2	178.8	42.3	44.8	83.5	62.2
Zr	154.4	172.0	113.0	115.6	119.6	112.3
Nb	62.8	85.7	81.2	82.0	78.8	68.7
Th	71.1	63.3	60.4	62.6	57.9	56.6
Y	44.4	59.5	75.3	80.1	54.3	47.8
La	47.5	49.8	37.7	38.0	40.4	34.1
Ce	88.6	101.8	78.2	76.7	83.5	71.7
Nd	31.8	36.0	31.7	32.3	29.7	26.3

CIPW Norms are shown below:

Field No.	97/24-5	97/25-1 B	97/26-6	97/27-4
Qtz	34.00	34.60	31.30	33.80
Or	28.50	26.60	26.00	27.60
Ab	31.20	33.30	37.20	34.70
An	3.56	3.01	2.28	1.60
Leu				
Nep				
Cor	0.04	0.17		1.90
Acm				
C/Woll			0.25	0.55
C/En			0.01	0.15
C/Fer			0.27	0.43
O/En	0.47	0.41		0.42
O/Fer	2.18	1.67	2.58	1.17
Fo				
Fa				
Mt	0.23	0.16	0.27	0.16
Ilm	0.37	0.19	0.20	0.19
Ap	0.11	0.06	0.06	0.06
Fe ratio used	0.1	0.1	0.1	0.1
"D"	93.70	94.50	94.50	96.10

Field No.	97/27-4	97/27-4	97/27-4	97/27-4	97/27-7	97/27-7
Crush/Grind	Rep. pellet	Prep. 2	Prep. 3	Prep. 4	Ag	WC
Pluton/facies	Even	Even	Even	Even	Even	Even
Lab. No.	TIM24	TIM25	TIM26	TIM27	TIM30	TIM31
WTr: CaO	0.59	0.6	0.6	0.61	0.59	0.54
WTr: TiO2	0.094	0.094	0.093	0.095	0.129	0.126
Majors.	ICP	ICP	ICP	ICP	XRF	XRF
SiO2		77.55			77.05	
Al2O3		12.34			12.43	
Fe2O3		1.22			1.09	
MgO		0.09			0.10	
CaO		0.62			0.59	
Na2O		3.93			3.57	
K2O		4.59			5.05	
TiO2		0.10			0.12	
MnO		0.03			0.03	
P2O5		0.03			0.04	
Total		100.47			100.05	
LOI		0.43			0.26	
Ni	3.6	3.3	3.6	2.3	3.2	4.1
Cr	2.1	3.0	2.4	1.3	1.6	2.7
V	3.0	3.2	3.3	3.0	5.3	5.8
Sc	1.8	1.1		1.0	0.8	1.5
Cu	0.3	1.1	0.9		0.7	0.5
Zn	11.2	11.4	10.8	10.5	13.9	14.9
Cl	32	35	36	10	119	125
Ga	20.7	20.7	20.9	19.4	21.4	21.9
Pb	58.3	53.7	52.2	56.4	52.4	31.2
Sr	15.8	14.8	15.3	15.4	27.9	27.1
Rb	300.5	300.9	302.0	306.9	457.6	455.9
Ba	65.0	65.0	63.8	65.0	104.6	107.6
Zr	115.4	113.6	110.6	114.0	145.5	143.1
Nb	73.2	70.9	70.4	69.0	78.6	78.5
Th	57.2	57.0	56.8	56.2	68.2	66.8
Y	51.4	49.4	49.0	48.3	28.4	27.1
La	34.8	36.7	33.8	34.2	31.8	39.0
Ce	74.8	74.5	71.6	70.9	65.3	79.6
Nd	27.9	27.4	27.4	26.7	22.8	25.7

CIPW Norms are shown below:

Field No.	
Qtz	
Or	
Ab	
An	
Leu	
Nep	
Cor	
Acm	
C/Woll	
C/En	
C/Fer	
O/En	
O/Fer	
Fo	
Fa	
Mt	
Ilm	
Ap	
Fe ratio used	
"D"	

Field No.	97/27-7	97/29-1	98/1-1 A	98/1-1 B	98/1-1 B	88/12-1
Crush/Grind	WC Repeat	WC	WC	WC	WC	Roll/WC
Pluton/facies	Even	Even	Even	Even	Even	Porphyry
Lab. No.	TIM32	TIM34	TIM35	TIM36	TIM36K	TIM05
WTr: CaO	0.67	0.73	0.53	0.32	0.32	0.87
WTr: TiO2	0.122	0.132	0.109	0.074	0.074	0.249
Majors.	XRF	XRF	XRF	XRF	XRF	XRF
SiO2		76.27	76.93	77.77		75.67
Al2O3		12.74	12.53	12.37		12.91
Fe2O3		1.42	1.21	1.04		1.96
MgO		0.05	0.05	0.01		0.23
CaO		0.69	0.54	0.35		0.88
Na2O		4.43	3.54	3.84		3.70
K2O		4.75	5.00	4.59		4.94
TiO2		0.12	0.11	0.07		0.25
MnO		0.02	0.04	0.04		0.05
P2O5		0.02	0.03	0.01		0.06
Total		100.50	99.97	100.09		100.65
LOI		0.51	0.30	0.34		0.19
Ni	3.6	3.3	3.9	2.9	2.8	4.4
Cr	2.2	3.2	1.9	1.3	1.4	10.7
V	4.8	6.3	4.4	2.2	2.2	14.0
Sc	3.5	3.0	1.2	2.6	1.4	3.5
Cu			1.0	0.1		1.7
Zn	14.4	12.6	14.3	13.6	14.0	24.3
Cl	40	91	136	85	52	222
Ga	19.6	22.9	20.6	20.5	20.8	20.2
Pb	25.9	58.5	24.8	27.2	27.3	17.2
Sr	26.9	24.5	24.2	7.7	7.7	73.9
Rb	429.3	592.8	443.0	512.2	514.1	393.8
Ba	85.2	98.7	88.2	27.1	26.3	346.2
Zr	112.1	136.3	116.9	110.3	109.0	196.9
Nb	59.6	77.1	57.6	78.7	78.6	60.2
Th	55.3	60.3	58.8	54.7	54.9	56.8
Y	53.2	75.1	32.8	34.1	33.9	42.3
La	26.3	43.4	40.8	22.3	22.3	55.3
Ce	58.0	87.4	98.1	54.5	55.6	105.6
Nd	24.0	32.2	35.7	19.6	20.0	34.0

CIPW Norms are shown below:

Field No.	97/27-7	97/29-1	98/1-1 A	98/1-1 B		88/12-1
Qtz	35.10	30.60	35.30	36.50		32.10
Or	29.80	28.10	29.60	27.10		29.20
Ab	30.20	37.50	30.00	32.50		31.30
An	2.71	0.87	2.52	1.67		3.98
Leu						
Nep						
Cor	0.11		0.37	0.47		0.03
Acm						
C/Woll		1.00				
C/En		0.07				
C/Fer		1.04				
O/En	0.24	0.06	0.12	0.03		0.59
O/Fer	1.41	0.83	1.62	1.44		2.48
Fo						
Fa						
Mt	0.14	0.19	0.16	0.14		0.26
Ilm	0.23	0.23	0.21	0.14		0.48
Ap	0.08	0.05	0.06	0.02		0.14
Fe ratio used	0.1	0.1	0.1	0.1		0.1
"D"	95.10	96.20	94.90	96.10		92.60

Field No.	88/12-1	88/15-2	97/12-1 E	97/23-4 A	97/24-3	97/24-3
Crush/Grind	Same prep	Roll/WC	WC	WC	Ag	WC
Pluton/facies		Porphyry	Porphyry	Porphyry	Porphyry	Porphyry
Lab. No.	TIM05	TIM07	TIM08	TIM11	TIM14	TIM15
WTr: CaO		0.98	0.98	1.49	1.27	1.2
WTr: TiO2		0.403	0.359	0.514	0.391	0.338
Majors.		XRF	XRF	XRF	XRF	XRF
SiO2		72.90	73.38	70.04	73.65	
Al2O3		13.34	13.53	14.56	13.40	
Fe2O3		3.19	2.18	3.32	2.46	
MgO		0.53	0.31	0.62	0.41	
CaO		0.98	0.95	1.46	1.13	
Na2O		3.07	3.23	3.88	3.48	
K2O		5.48	5.66	5.55	5.02	
TiO2		0.42	0.37	0.52	0.36	
MnO		0.04	0.04	0.08	0.05	
P2O5		0.10	0.08	0.14	0.10	
Total		100.05	99.73	100.15	100.07	
LOI		0.49	0.38	0.59	0.40	
Ni	3.7	5.1	3.9	5.1	4.2	4.7
Cr	9.9	15.2	2.7	2.9	4.5	3.9
V	13.0	27.8	24.3	36.1	30.6	27.1
Sc	3.1	4.2	3.6	5.1	5.5	5.0
Cu	0.8	7.0	1.9	3.1	1.4	2.1
Zn	25.4	34.5	29.1	49.7	32.9	31.9
Cl	222	247	308	461	194	234
Ga	20.2	18.9	18.6	20.3	20.3	21.0
Pb	17.3	17.6	30.3	44.3	37.2	36.6
Sr	73.9	127.3	122.3	149.9	117.7	118.3
Rb	393.8	276.4	279.9	318.7	363.8	363.0
Ba	350.7	909.1	915.9	894.7	707.3	716.2
Zr	196.8	327.9	289.2	347.7	166.7	200.3
Nb	60.2	54.0	47.8	58.8	56.3	57.5
Th	56.9	49.7	49.8	38.9	44.0	46.3
Y	42.3	35.5	31.9	41.6	45.2	47.0
La	54.6	88.8	75.1	69.0	53.5	52.7
Ce	104.3	148.2	139.0	126.3	98.8	101.2
Nd	35.1	48.0	42.3	46.1	36.3	36.6

CIPW Norms are shown below:

Field No.	97/12-1 E	97/23-4 A	97/24-3
Qtz	29.50	20.90	30.10
Or	33.50	32.90	29.70
Ab	27.40	32.90	29.50
An	4.24	5.96	4.97
Leu			
Nep			
Cor	0.53		0.42
Acm			
C/Woll		0.15	
C/En		0.04	
C/Fer		0.11	
O/En	0.76	1.51	1.03
O/Fer	2.59	3.92	3.01
Fo			
Fa			
Mt	0.29	0.44	0.32
Ilm	0.70	0.99	0.69
Ap	0.18	0.33	0.23
Fe ratio used	0.1	0.1	0.1
"D"	90.40	86.70	89.30

Field No.	HPG	HPG	HPG	HPG	POR	POR
Crush/Grind	Ag	WC	Repeat fusions		WC	Rep. fusion
Pluton/facies	Porphyry	Porphyry	Porphyry	Porphyry	Porphyry	
Lab. No.	TIM40	TIM41			TIM95	
WTr: CaO	1.44	1.34			1.52	
WTr: TiO2	0.390	0.392			0.448	
Majors.	XRF	XRF			XRF	XRF
SiO2	72.99	72.69	72.66	72.92	70.38	70.91
Al2O3	13.64	13.60	13.59	13.63	14.33	14.44
Fe2O3	2.32	2.41	2.47	2.42	2.87	2.82
MgO	0.45	0.45	0.43	0.45	0.46	0.46
CaO	1.30	1.31	1.30	1.31	1.45	1.44
Na2O	3.55	3.53	3.56	3.41	3.59	3.75
K2O	5.24	5.30	5.31	5.25	5.64	5.69
TiO2	0.39	0.38	0.37	0.38	0.47	0.47
MnO	0.05	0.05	0.05	0.05	0.06	0.06
P2O5	0.10	0.09	0.10	0.09	0.11	0.11
Total	100.02	99.81	99.83	99.90	99.36	100.14
LOI	0.49	0.46	0.45	0.34	0.40	0.40
Ni	3.4	4.4			3.9	3.8
Cr	6.3	2.6			0.8	0.8
V	25.2	23.5			26.5	26.5
Sc	4.6	4.8			4.4	4.4
Cu	1.6	1.6			2.8	2.7
Zn	32.6	36.4			39.8	39.7
Cl	345	345			351	350
Ga	19.0	19.6			18.9	18.8
Pb	63.2	55.2			50.7	50.5
Sr	125.7	122.0			147.4	146.8
Rb	233.9	233.2			260.8	259.7
Ba	656.7	682.8			1114.7	1115.0
Zr	252.3	285.9			346.0	344.6
Nb	51.5	54.8			48.9	48.7
Th	45.1	47.3			36.0	35.9
Y	39.1	40.1			36.0	35.8
La	51.4	62.5			55.0	55.0
Ce	94.1	118.3			101.1	101.1
Nd	33.3	39.9			36.8	36.8

CIPW Norms are shown below:

Field No.	HPG	POR
Qtz	27.50	23.00
Or	31.40	33.40
Ab	29.90	30.40
An	5.64	6.38
Leu		
Nep		
Cor		
Acm		
C/Woll	0.11	0.06
C/En	0.03	0.02
C/Fer	0.08	0.05
O/En	1.09	1.14
O/Fer	2.83	3.40
Fo		
Fa		
Mt	0.32	0.38
Ilm	0.73	0.90
Ap	0.22	0.25
Fe ratio used	0.1	0.1
"D"	88.80	86.80

Field No.	POR	PM 1	PM 1A	PM 2	PM 3	PM 4
Crush/Grind	Rep. fusion		Replicates of trace pellets			
Pluton/facies						
Lab. No.		PM 1	PM 1A	PM 2	PM 3	PM 4
WTr: CaO						
WTr: TiO2						
Majors.	XRF					
SiO2	70.47					
Al2O3	14.31					
Fe2O3	2.97					
MgO	0.45					
CaO	1.44					
Na2O	3.71					
K2O	5.62					
TiO2	0.47					
MnO	0.06					
P2O5	0.12					
Total	99.62					
LOI	0.45					
Ni		4.1	3.3	4.1	4.2	4.3
Cr		0.7	1.5	1.8	3.0	2.9
V		26.8	26.6	27.6	27.0	26.4
Sc		4.9	5.5	4.6	5.0	5.3
Cu		2.8	3.5	2.6	3.0	1.9
Zn		40.0	40.1	39.3	40.4	41.0
Cl		342	365	438	344	364
Ga		19.4	18.8	19.0	18.5	18.9
Pb		47.4	46.8	31.3	56.2	53.7
Sr		144.5	146.0	145.2	144.4	145.4
Rb		257.4	258.0	258.3	257.9	258.0
Ba		1123.5	1121.9	1125.3	1123.3	1121.8
Zr		358.1	363.0	366.5	352.9	358.2
Nb		47.0	49.0	49.5	48.5	49.3
Th		37.0	36.6	35.9	37.5	37.7
Y		34.4	35.7	35.9	35.3	35.6
La		60.9	60.5	56.2	60.2	64.4
Ce		111.1	112.0	104.3	112.3	118.2
Nd		38.4	39.4	37.3	38.9	41.0

CIPW Norms are shown below:

Field No.	
Qtz	
Or	
Ab	
An	
Leu	
Nep	
Cor	
Acm	
C/Woll	
C/En	
C/Fer	
O/En	
O/Fer	
Fo	
Fa	
Mt	
Ilm	
Ap	
Fe ratio used	
"D"	

Field No.	PM 5	88/11-3	08/17-1	08/17-2	08/21-14	08/17-3
Crush/Grind			WC	WC	WC	WC
Pluton/facies		Lampro.	Hake Mar.	Hake Mar.	Hake Mar.	Hake
Lab. No.	PM 5		TIM64	TIM65	TIM84	TIM66
WTr: CaO			1.04	1.22	0.6	0.72
WTr: TiO2			0.250	0.344	0.207	0.255
Majors.		XRF	ICP	ICP	ICP	ICP
SiO2		53.93	75.57	74.54	73.85	76.51
Al2O3		15.37	12.97	13.11	13.03	12.74
Fe2O3		9.22	2.07	2.43	1.83	1.96
MgO		6.55	0.28	0.41	0.25	0.28
CaO		8.16	0.94	1.06	0.54	0.67
Na2O		2.85	3.50	3.27	3.18	3.10
K2O		2.81	4.97	5.21	5.76	5.28
TiO2		0.69	0.25	0.34	0.19	0.24
MnO		0.22	0.03	0.04	0.03	0.03
P2O5		0.35	0.06	0.10	0.04	0.06
Total		100.14	100.64	100.51	98.70	100.87
LOI		0.82	0.40	0.41	0.47	0.54
Ni	3.9		3.6	4.4	4.3	4.4
Cr	2.1		3.4	2.9	3.3	3.1
V	26.8		12.1	17.9	7.3	10.8
Sc	2.8		2.8	4.1	2.8	3.6
Cu	3.0		0.7	2.4	3.9	0.8
Zn	39.2		21.6	36.9	36.7	20.7
Cl	403		125	411	604	181
Ga	19.1		19.5	18.3	20.6	19.4
Pb	37.3		19.7	22.8	34.8	22.5
Sr	146.5		75.1	92.8	39.6	60.0
Rb	258.8		393.6	336.9	480.7	414.7
Ba	1133.3		268.9	353.0	202.5	251.8
Zr	360.2		162.3	196.4	163.5	175.2
Nb	49.0		45.8	48.8	63.7	48.1
Th	37.7		66.0	69.7	77.5	71.8
Y	35.5		44.5	33.8	47.9	40.1
La	62.6		54.8	63.4	59.0	60.3
Ce	112.0		104.1	116.2	115.7	114.6
Nd	40.1		36.4	37.9	37.0	37.0

CIPW Norms are shown below:

Field No.	08/17-1	08/17-2	08/21-14	08/17-3
Qtz	32.81	31.69	30.76	35.38
Or	29.42	30.86	34.10	31.26
Ab	29.67	27.73	26.95	26.28
An	4.28	4.62	2.42	2.94
Leu				
Nep				
Cor	0.27	0.41	0.68	0.85
Acm				
C/Woll				
C/En				
C/Fer				
O/En	0.70	1.02	0.62	0.70
O/Fer	2.60	2.99	2.62	2.80
Fo				
Fa				
Mt	0.27	0.32	0.24	0.26
Ilm	0.48	0.65		
Ap	0.14	0.23	0.09	0.14
Fe ratio used	0.1	0.1	0.1	0.1
"D"	91.90	90.30	91.80	92.90

Field No.	08/17-4	08/17-5	08/17-6	08/17-7	08/21-3	08/21-11
Crush/Grind	WC	WC	WC	WC	WC	WC
Pluton/facies	Hake	Hake	Hake	Hake	Hake	Hake
Lab. No.	TIM67	TIM68	TIM69	TIM70	TIM81	TIM82
WTr: CaO	0.86	0.56	0.68	0.94	0.67	0.86
WTr: TiO2	0.269	0.152	0.071	0.246	0.103	0.228
Majors.	ICP	ICP	ICP	ICP	ICP	ICP
SiO2	73.63	77.87	78.29	74.69	77.80	77.01
Al2O3	12.54	11.75	12.13	13.37	11.76	12.41
Fe2O3	2.10	1.54	0.76	1.85	1.79	1.88
MgO	0.24	0.15	0.08	0.28	0.22	0.24
CaO	0.71	0.48	0.60	0.84	0.76	0.75
Na2O	3.33	3.08	3.49	3.28	3.08	3.19
K2O	5.23	4.86	4.72	5.57	4.87	4.99
TiO2	0.24	0.14	0.07	0.24	0.20	0.22
MnO	0.03	0.03	0.02	0.03	0.03	0.03
P2O5	0.06	0.03	0.02	0.07	0.03	0.07
Total	98.11	99.93	100.18	100.22	100.54	100.79
LOI	0.40	0.40	0.70	0.42	0.20	0.32
Ni	2.9	2.7	3.7	4.1	4.4	3.6
Cr	1.7	2.1	1.8	3.1	1.2	2.6
V	10.0	4.8	2.6	13.3	0.2	8.7
Sc	4.8	2.7	0.5	2.6	4.3	3.2
Cu		0.9	2.7		4.4	1.6
Zn	32.0	31.7	25.8	21.9	33.0	32.6
Cl	200	338	47	109	215	341
Ga	19.5	20.5	22.5	19.7	27.4	19.9
Pb	38.4	40.7	28.5	20.8	28.9	29.7
Sr	62.9	24.5	12.2	78.6	4.2	47.1
Rb	344.0	460.8	441.1	447.1	576.1	396.8
Ba	292.2	115.4	43.2	322.9	28.9	202.2
Zr	175.3	151.4	95.9	154.1	185.8	178.0
Nb	37.5	58.5	118.5	45.5	91.3	48.2
Th	65.7	72.6	47.4	63.2	89.9	76.5
Y	38.9	43.8	83.6	37.7	157.5	44.0
La	60.3	58.9	16.1	48.0	90.8	63.3
Ce	125.5	114.0	42.5	93.8	180.3	120.8
Nd	38.0	36.7	20.2	32.3	69.7	38.8

CIPW Norms are shown below:

Field No.	08/17-4	08/17-5	08/17-6	08/17-7	08/21-3	08/21-11
Qtz	31.23	39.24	38.11	31.13	38.28	36.43
Or	30.97	28.76	27.91	32.97	28.83	29.54
Ab	28.23	26.10	29.55	27.80	26.10	27.04
An	3.14	2.19	2.85	3.72	3.58	3.27
Leu						
Nep						
Cor	0.25	0.62	0.24	0.59	0.11	0.57
Acm						
C/Woll						
C/En						
C/Fer						
O/En	0.60	0.37	0.20	0.70	0.55	0.60
O/Fer	3.00	2.20	1.09	2.64	2.56	2.69
Fo						
Fa						
Mt	0.28	0.20	0.10	0.24	0.24	0.25
Ilm						
Ap	0.14	0.07	0.16	0.16	0.07	0.16
Fe ratio used	0.1	0.1	0.1	0.1	0.1	0.1
"D"	90.40	94.10	95.60	91.90	93.20	93.00

Field No.	08/21-12	07/30-1	07/30-3	07/30-4	8/1/01	8/2/01
Crush/Grind	WC	WC	WC	WC	WC	WC
Pluton/facies	Hake	Sea NW	Sea NW	Sea NW	Sea NW	Sea NW
Lab. No.	TIM83	TIM57	TIM58	TIM59	TIM60	TIM61
WTr: CaO	0.51	0.69	0.66	0.4	0.57	0.82
WTr: TiO2	0.087	0.093	0.150	0.094	0.170	0.212
Majors.	ICP	ICP	ICP	ICP	ICP	ICP
SiO2	76.66	76.11	76.69	78.48	77.49	75.60
Al2O3	12.51	12.62	12.13	11.91	12.29	12.89
Fe2O3	1.20	1.73	1.47	1.34	1.49	1.89
MgO	0.09	0.04	0.08	0.05	0.12	0.20
CaO	0.44	0.59	0.60	0.33	0.54	0.75
Na2O	2.77	3.53	3.14	3.18	2.97	3.20
K2O	5.92	4.92	5.26	5.02	5.40	5.44
TiO2	0.09	0.09	0.14	0.09	0.16	0.21
MnO	0.02	0.01	0.02	0.01	0.02	0.02
P2O5	0.02	0.01	0.03	0.02	0.03	0.04
Total	99.72	99.65	99.56	100.43	100.51	100.24
LOI	0.48	0.63	0.58	0.43	0.07	0.47
Ni	3.6	4.2	3.7	4.0	3.3	4.1
Cr	1.6	2.0	2.4	2.7	1.2	2.4
V	1.6	0.5	3.1	1.7	4.5	7.8
Sc	0.6	4.3	4.5	4.4	3.2	3.9
Cu	6.4			0.4	2.1	1.1
Zn	16.7	30.7	55.3	34.1	45.1	38.8
Cl	196	79	133	163	270	315
Ga	20.9	27.3	23.2	24.5	20.8	21.9
Pb	53.8	33.9	38.2	31.2	34.8	32.2
Sr	12.2	1.4	12.0	6.7	32.6	43.0
Rb	371.9	625.5	448.4	470.1	241.0	350.6
Ba	32.6	19.2	91.4	49.3	260.9	332.5
Zr	125.3	194.5	279.2	135.9	164.4	200.5
Nb	85.8	92.6	81.7	62.0	37.7	44.5
Th	77.1	97.1	52.8	59.0	44.6	51.0
Y	70.7	175.0	114.4	94.3	33.3	53.8
La	31.9	79.4	70.4	70.9	80.4	61.6
Ce	66.8	159.0	146.5	138.6	161.7	125.2
Nd	23.6	70.7	60.1	53.6	55.8	47.9

CIPW Norms are shown below:

Field No.	08/21-12	07/30-1	07/30-3	07/30-4	8/1/01	8/2/01
Qtz	36.13	34.38	36.07	39.22	37.38	33.21
Or	35.02	29.12	31.13	29.70	31.95	32.20
Ab	23.46	29.92	26.61	26.94	25.17	27.12
An	2.05	2.87	2.78	1.51	2.49	3.47
Leu						
Nep						
Cor	0.79	0.44	0.25	0.69	0.65	0.47
Acm						
C/Woll						
C/En						
C/Fer						
O/En	0.22	0.10	0.20	0.13	0.30	0.50
O/Fer	1.71	2.47	2.10	1.92	2.13	2.70
Fo						
Fa						
Mt	0.16	0.23	0.19	0.18	0.20	0.25
Ilm						
Ap	0.05	0.02	0.07	0.05	0.07	0.09
Fe ratio used	0.1	0.1	0.1	0.1	0.1	0.1
"D"	94.60	93.40	93.80	95.90	94.50	92.50

Field No.	08/02-1 A	07/21-1	07/21-2	08/21-1	08/21-2	08/21-03
Crush/Grind	WC	WC	WC	WC	WC	WC
Pluton/facies	Sea NW	Sea E	Sea E	Sea E	Sea E	Sea E
Lab. No.	TIM62	TIM52	TIM53	TIM79	TIM80	No traces
WTr: CaO	0.86	0.68	0.67	0.51	0.62	
WTr: TiO2	0.216	0.116	0.103	0.097	0.091	
Majors.	ICP	ICP	ICP	ICP	ICP	ICP
SiO2	75.60	76.53	76.23	76.20	76.63	75.00
Al2O3	12.89	12.65	12.45	12.60	12.65	12.33
Fe2O3		1.64	1.55	1.44	1.39	1.39
MgO		0.08	0.05	0.06	0.05	0.09
CaO	0.75	0.57	0.60	0.45	0.54	0.58
Na2O		3.40	3.50	3.55	3.63	3.38
K2O		4.91	5.21	5.13	5.19	5.31
TiO2		0.12	0.10	0.09	0.09	0.10
MnO		0.02	0.01	0.01	0.01	0.02
P2O5		0.04	0.02	0.03	0.02	0.01
Total		99.96	99.72	99.56	100.20	98.21
LOI		0.44	0.47	0.24	0.59	0.29
Ni	3.1	3.6	4.4	3.9	4.0	N.D.
Cr	2.1	1.8	1.5	1.6	1.9	
V	8.4	2.6	0.1	1.3	0.6	
Sc	4.6	4.3	4.3	2.5	4.7	
Cu	3.4	2.4	4.3	3.4		
Zn	42.0	59.3	24.5	23.8	22.8	
Cl	315	72	58	99	24	
Ga	22.1	26.5	28.1	27.7	28.1	
Pb	30.1	28.3	32.3	27.5	32.2	
Sr	45.4	12.6	2.6	4.6	2.2	
Rb	351.2	588.3	630.7	617.9	662.0	
Ba	382.1	38.9	14.5	26.0	16.0	
Zr	196.7	168.7	201.1	175.4	192.6	
Nb	45.3	80.7	91.5	81.6	80.9	
Th	51.4	67.8	100.4	79.4	86.4	
Y	60.5	126.6	163.9	122.1	163.8	
La	62.0	69.2	98.3	70.6	71.9	
Ce	125.8	146.7	201.0	147.0	151.9	
Nd	48.0	56.0	74.2	57.7	61.8	

CIPW Norms are shown below:

Field No.		07/21-1	07/21-2	08/21-1	08/21-2	08/21-03
Qtz		35.72	33.67	34.06	33.62	32.81
Or		29.06	30.83	30.35	30.71	31.42
Ab		28.81	29.66	30.08	30.76	28.64
An		2.57	2.85	2.04	2.55	2.79
Leu						
Nep						
Cor		0.80	0.01	0.46	0.13	
Acm						
C/Woll						0.01
C/En						
C/Fer						0.01
O/En		0.20	0.13	0.15	0.13	0.22
O/Fer		2.34	2.22	2.06	1.99	1.98
Fo						
Fa						
Mt		0.22	0.21	0.19	0.18	0.18
Ilm						
Ap		0.09	0.05	0.07	0.05	0.02
Fe ratio used		0.1	0.1	0.1	0.1	0.1
"D"		93.60	94.20	94.50	95.10	92.90

Field No.	STQ	07/24-1	07/24-2	98/16-2	98/16-1	98/16-3
Crush/Grind	WC	WC	WC	WC	WC	WC
Pluton/facies	STQ Core	STQ Dykes	STQ Dykes	NWTM Dk.	NW TM	NW TM
Lab. No.	TIM86	TIM55	TIM56	TIM47	TIM46	TIM48
WTr: CaO	0.57	0.31	0.58	7.57	4.69	5.74
WTr: TiO2	0.058	0.059	0.062	0.862	0.519	0.701
Majors.	ICP	ICP	ICP	ICP	ICP	ICP
SiO2	77.16	76.08	76.19	53.64	63.20	60.17
Al2O3	12.52	13.54	12.99	14.56	15.25	15.75
Fe2O3	1.39	1.04	0.98	8.91	5.55	7.31
MgO	0.14	0.12	0.15	7.35	2.01	2.75
CaO	0.50	0.27	0.51	6.92	4.59	5.54
Na2O	3.22	3.51	3.39	1.84	3.67	3.71
K2O	4.34	4.75	4.83	4.34	3.82	3.59
TiO2	0.06	0.06	0.06	0.78	0.54	0.70
MnO	0.01	0.01	0.01	0.17	0.12	0.15
P2O5	0.02	0.02	0.01	0.45	0.27	0.33
Total	99.36	99.40	99.12	98.96	99.02	100.00
LOI	0.59	1.33	1.04	8.02	0.20	1.18
Ni	4.4	4.4	3.9	146.1	9.4	12.3
Cr	1.4	1.7	0.8	409.0	15.7	22.3
V	0.7	1.0		257.3	138.7	189.7
Sc	1.9	3.1	2.5	27.5	14.9	19.8
Cu	2.0	48.5	52.1	149.7	7.3	11.7
Zn	45.1	56.7	28.4	81.6	68.6	79.9
Cl	139			15	107	262
Ga	36.1	39.3	35.4	16.1	18.5	19.3
Pb	23.2	25.7	35.5	26.3	21.4	26.3
Sr	22.4	7.1	10.0	641.1	846.6	1026.4
Rb	843.8	908.3	904.7	170.9	97.8	82.9
Ba	28.3	42.6	34.6	2252.2	1823.2	2237.6
Zr	122.0	138.4	136.3	131.7	85.5	100.4
Nb	111.4	114.5	117.2	10.9	8.7	9.7
Th	87.8	56.5	70.8	7.5	7.0	5.8
Y	156.8	108.9	166.8	20.3	16.0	20.9
La	70.6	53.0	100.6	17.1	16.1	19.3
Ce	165.4	98.1	188.5	38.8	31.9	41.4
Nd	56.3	37.0	74.2	16.8	13.6	19.0

CIPW Norms are shown below:

Field No.	STQ	07/24-1	07/24-2	98/16-2	98/16-1	98/16-3
Qtz	39.75	36.14	36.10		13.75	7.95
Or	25.68	28.10	28.57	25.84	22.68	21.34
Ab	27.28	29.73	28.71	15.69	31.20	31.58
An	2.35	1.21	2.47	18.79	13.92	15.82
Leu						
Nep						
Cor	1.67	2.18	1.28			
Acm						
C/Woll				5.36	3.00	4.04
C/En				3.21	1.29	1.77
C/Fer				1.87	1.71	2.26
O/En	0.35	0.30	0.37	14.55	3.74	5.12
O/Fer	1.99	1.49	1.40	8.48	4.96	6.54
Fo				0.48		
Fa				0.31		
Mt	0.18	0.14	0.13	2.39	1.49	1.96
Ilm						
Ap	0.05	0.05	0.02	1.05	0.63	0.77
Fe ratio used	0.1	0.1	0.1	0.2	0.2	0.2
"D"	92.70	94.00	93.40	41.50	67.60	60.90

Field No.	98/16-5	98/17-1	98/17-2	8/4/01	08/18-1	08/18-2
Crush/Grind	WC	WC	WC	WC	WC	WC
Pluton/facies	NW TM	NW TM	NW TM	NW TM	SW TM	SW TM
Lab. No.	TIM49	TIM50	TIM51	TIM63	TIM71	TIM72
WTr: CaO	4.92	4.61	5.54	5.19	6.1	6.47
WTr: TiO2	0.641	0.521	0.484	0.653	0.387	0.747
Majors.	ICP	ICP		ICP	ICP	ICP
SiO2	60.96	64.14		61.67	60.58	59.64
Al2O3	15.57	15.37		15.58	15.93	16.44
Fe2O3	6.84	5.73		6.73	5.16	7.18
MgO	2.60	2.04		2.60	4.37	2.83
CaO	4.67	4.36		4.91	5.98	6.35
Na2O	3.70	3.69		3.58	3.45	3.67
K2O	3.94	3.82		3.59	2.69	2.67
TiO2	0.67	0.55		0.66	0.36	0.74
MnO	0.15	0.13		0.16	0.10	0.13
P2O5	0.33	0.27		0.34	0.23	0.28
Total	99.43	100.10		99.82	98.85	99.93
LOI	0.95	0.84		1.01	0.92	0.71
Ni	11.1	9.8	13.2	11.0	77.5	13.8
Cr	19.0	14.2	14.1	18.9	203.2	22.8
V	175.3	140.6	134.1	173.3	108.2	179.5
Sc	18.6	15.2	15.0	18.1	14.3	20.3
Cu	18.9	8.2	43.0	10.0	38.6	7.5
Zn	83.1	65.0	71.5	83.0	56.0	73.6
Cl	190	157	72	240	55	110
Ga	19.7	19.1	18.5	19.2	14.9	19.3
Pb	27.9	31.3	31.9	52.0	23.0	27.9
Sr	831.7	838.4	1069.7	865.9	690.3	658.6
Rb	99.3	102.4	68.3	80.0	67.6	64.0
Ba	2188.5	1909.6	2154.0	2126.2	1322.9	1272.5
Zr	102.4	92.5	101.2	100.2	75.6	108.7
Nb	9.7	9.5	4.7	9.8	4.0	7.1
Th	6.7	7.4	4.7	8.1	2.9	4.1
Y	19.5	17.5	17.2	20.1	12.3	25.0
La	18.9	15.0	12.6	17.6	7.0	11.8
Ce	38.3	31.8	32.4	40.1	17.8	25.5
Nd	16.8	13.4	14.2	17.7	8.1	13.9

CIPW Norms are shown below:

Field No.	98/16-5	98/17-1		8/4/01	08/18-1	08/18-2
Qtz	9.20	14.63		11.36	10.53	9.16
Or	23.42	22.68		21.33	15.96	15.87
Ab	31.49	31.37		30.46	29.32	31.24
An	14.32	14.16		15.93	20.12	20.62
Leu						
Nep						
Cor						
Acm						
C/Woll	2.84	2.42		2.77	3.41	3.85
C/En	1.25	1.03		1.23	2.06	1.73
C/Fer	1.58	1.39		1.53	1.17	2.11
O/En	5.26	4.07		5.28	8.87	5.36
O/Fer	6.65	5.50		6.57	5.04	6.54
Fo						
Fa						
Mt	1.83	1.53		1.80	1.38	1.92
Ilm						
Ap	0.77	0.63		0.79	0.54	0.65
Fe ratio used	0.2	0.2		0.2	0.2	0.2
"D"	64.10	68.70		63.20	55.80	56.30

Field No.	08/18-3	08/20-2	08/20-6	08/20-3	08/20-4	07/23-1
Crush/Grind	WC	WC	WC	WC	WC	WC
Pluton/facies	SW TM	SW TM	SW TM	SW TM Gr	SW TM Gr	Cresc. L.
Lab. No.	TIM73	TIM75	TIM78	TIM76	TIM77	TIM54
WTr: CaO	5.95	7.75	9.59	4.64	5.02	5.22
WTr: TiO2	0.639	0.806	0.995	0.472	0.477	0.716
Majors.	ICP	ICP	ICP	ICP	ICP	ICP
SiO2	60.61	54.22	50.93	61.95	59.39	60.96
Al2O3	16.22	14.07	13.18	16.21	16.36	16.68
Fe2O3	6.66	9.46	11.40	5.25	6.38	6.57
MgO	2.90	5.93	7.83	2.31	2.70	2.45
CaO	5.90	7.96	9.78	4.44	4.86	5.40
Na2O	3.59	3.10	2.59	4.53	4.34	3.39
K2O	2.83	3.89	2.77	4.17	4.40	3.07
TiO2	0.64	0.75	0.88	0.49	0.48	0.73
MnO	0.10	0.15	0.18	0.11	0.11	0.11
P2O5	0.26	0.40	0.48	0.23	0.29	0.27
Total	99.71	99.93	100.02	99.69	99.31	99.63
LOI	1.15	0.85	2.20	0.62	0.69	1.69
Ni	17.0	65.0	82.4	19.9	24.8	6.8
Cr	41.2	168.3	243.0	40.4	51.1	5.4
V	179.0	245.0	323.9	136.1	141.3	130.6
Sc	18.3	25.8	34.6	12.5	15.0	12.9
Cu	8.2	81.5	130.8	14.7	23.2	12.6
Zn	56.0	87.8	100.9	68.2	64.6	63.1
Cl	165	607	265	345	369	170
Ga	19.0	17.4	16.1	19.0	18.6	19.3
Pb	14.0	12.4	19.5	35.5	12.1	30.4
Sr	597.5	626.8	615.9	960.7	960.7	438.4
Rb	55.2	79.5	69.5	94.3	102.1	115.4
Ba	1642.5	1066.4	1145.5	1190.8	1499.0	1511.0
Zr	91.0	43.5	30.5	94.6	86.9	141.4
Nb	6.3	3.7	3.2	7.9	5.5	11.7
Th	3.5	0.6	1.1	4.6	3.7	15.2
Y	20.3	20.7	20.9	18.6	18.0	20.6
La	10.1	9.5	7.2	10.6	10.3	27.8
Ce	23.3	23.8	22.8	24.3	22.0	56.2
Nd	11.4	11.4	12.3	11.5	10.3	21.9

CIPW Norms are shown below:

Field No.	08/18-3	08/20-2	08/20-6	08/20-3	08/20-4	07/23-1
Qtz	10.78			6.43	2.39	12.34
Or	16.82	23.17	16.52	24.75	26.14	18.24
Ab	30.55	26.44	21.85	38.50	36.92	28.84
An	19.90	13.09	16.31	11.63	12.23	21.35
Leu						
Nep			0.15			
Cor						
Acm						
C/Woll	3.27	10.05	12.32	3.75	4.22	1.59
C/En	1.54	5.49	6.95	1.77	1.96	0.70
C/Fer	1.70	4.21	4.86	1.93	2.22	0.90
O/En	5.73	2.03		4.01	4.80	5.44
O/Fer	6.32	1.56		4.38	5.46	7.01
Fo		5.16	8.93			
Fa		4.36	6.89			
Mt	1.78	2.54	3.06	1.40	1.71	1.76
Ilm						
Ap	0.61	0.93	1.12	0.54	0.68	0.63
Fe ratio used	0.2	0.2	0.2	0.2	0.2	0.2
"D"	58.20	49.60	38.40	69.70	65.50	59.40

Field No.	REED (U)	REED (R)	207/144.7	208/92.25	ORK
Crush/Grind	WC	WC	WC	WC	Fused &
Pluton/facies	Cassiar	Cassiar	Hundere dykes		re-ground
Lab. No.	TIM89	TIM90	TIM87	TIM88	TIM96
WTr: CaO	1.53	1.26	6.23	1.57	0.16
WTr: TiO2	0.244	0.193	0.011	0.010	0.008
Majors.	ICP	ICP	Approx.	ICP	ICP
SiO2	74.76	74.13		71.93	73.76
Al2O3	13.63	13.63		15.14	15.21
Fe2O3	1.74	1.49		0.19	0.38
MgO	0.51	0.40		0.07	0.01
CaO	1.42	1.16		1.32	0.20
Na2O	3.35	3.39		0.53	6.18
K2O	4.71	4.97		10.79	3.57
TiO2	0.25	0.19		0.01	0.01
MnO	0.07	0.07		0.01	0.05
P2O5	0.09	0.06		0.02	0.01
Total	100.53	99.49		100.01	99.38
LOI	0.31	0.09		1.89	0.82
Ni	4.5	3.6	7.9	5.6	Cont.
Cr	2.8	2.2	1.8	0.3	2.2
V	18.4	11.0	7.0	14.7	1.4
Sc	7.0	5.5	11.4	8.6	6.2
Cu	1.3	1.4	0.9	3.6	
Zn	30.2	34.0	7.8	3.8	12.1
Cl					N.D.
Ga	18.1	17.8	66.6	43.2	N.D.
Pb	27.9	27.2	40.4	25.5	N.D.
Sr	270.2	223.0	162.0	175.1	N.D
Rb	304.8	294.6	1790.2	2080.2	N.D.
Ba	526.5	708.3	859.9	2225.4	36.8
Zr	129.4	126.3	46.1	47.0	N.D.
Nb	44.3	45.2	107.6	96.4	N.D.
Th	25.4	25.5	21.1	18.8	N.D.
Y	27.0	30.5	2.9	1.6	N.D.
La	31.6	33.4	0.9		13.8
Ce	62.7	67.1	9.6	7.4	50.9
Nd	24.8	27.5	1.6	0.6	14.7

CIPW Norms are shown below:

Field No.	REED (U)	REED (R)	208/92.25
Qtz	32.62	31.55	24.56
Or	27.88	29.41	63.77
Ab	28.39	28.72	4.49
An	6.47	5.37	6.42
Leu			
Nep			
Cor	0.66	0.71	0.24
Acm			
C/Woll			
C/En			
C/Fer			
O/En	1.27	1.00	0.17
O/Fer	2.49	2.13	0.27
Fo			
Fa			
Mt	0.23	0.20	0.03
Ilm			
Ap	0.21	0.14	0.05
Fe ratio used	0.1	0.1	0.1
"D"	88.90	89.70	92.80

Field No.	97/25-1 B	97/26-3	97/28-4	97/29-1	
Crush/Grind	Fused on graphite-covered nickel, reground				Repeat
Pluton/facies	to check Rb values				of XRF
Lab. No.	TIM97	TIM98	TIM99	TIM100	POR
WTr: CaO	0.62			0.65	1.52
WTr: TiO2	0.086	0.012	0.007	0.120	0.450
Majors.		ICP			XRF
SiO2		77.54			70.36
Al2O3		12.94			14.28
Fe2O3		0.80			2.97
MgO					0.44
CaO		0.04			1.45
Na2O		4.62			3.67
K2O		3.88			5.61
TiO2		0.01			0.47
MnO		0.05			0.06
P2O5		0.02			0.11
Total		99.88			99.43
LOI		0.34			0.45
Ni	Cont.	Cont.	Cont.	Cont.	3.9
Cr	2.7	1.8	2.6	2.9	1.8
V	3.2	1.8	2.0	5.7	26.5
Sc	1.4	8.5	3.8	1.3	6.4
Cu	2.6	2.5	5.5	3.5	3.7
Zn	13.7	14.4	28.6	13.4	40.0
Cl					N.D.
Ga	23.6	42.8	62.1	23.5	N.D.
Pb	32.0	35.8	34.3	29.7	N.D.
Sr	13.6	0.3	1.7	23.9	N.D.
Rb	597.3	1474.5	3469.2	578.2	N.D.
Ba	52.3	12.0	24.8	104.6	1106.1
Zr	125.9	87.8	12.7	146.4	N.D.
Nb	80.7	116.4	37.6	75.1	N.D.
Th	60.3	24.0	3.9	59.4	N.D.
Y	75.0	7.4	0.8	73.6	N.D.
La	41.4	26.3	2.8	48.0	55.2
Ce	84.8	76.3	9.4	98.0	100.3
Nd	34.0	15.6	1.5	35.9	36.3

Field No.	
Qtz	
Or	
Ab	
An	
Leu	
Nep	
Cor	
Acm	
C/Woll	
C/En	
C/Fer	
O/En	
O/Fer	
Fo	
Fa	
Mt	
Ilm	
Ap	
Fe ratio used	
"D"	

APPENDIX C.2 TABLE OF MICA ANALYSES

SPECIMEN PLUTON SIZE PROGRAM	08/17-1 Hake Margin 250–500μ Majors: Pt	08/21-3 Hake Margin 250–500μ Majors: Pt	08/21-14 Hake Margin 250–500μ Majors: Pt	08/17-2 Hake 250–500μ Majors: Pt	08/17-3 Hake 250–500μ Majors: Pt
SiO_2	36.03	34.27	34.02	35.07	35.21
Al_2O_3	12.70	13.32	13.78	12.21	14.42
Fe_2O_3*	31.08	32.31	33.46	31.17	30.55
MgO	4.69	4.43	3.72	5.70	4.66
CaO	0.99	1.01	0.67	0.84	0.68
Na_2O	0.41	0.26	0.21	0.31	0.34
K_2O	7.65	7.41	7.48	8.30	7.56
TiO_2	3.47	3.64	3.37	3.81	3.51
P_2O_5	0.34	0.27	0.29	0.35	0.26
MnO	0.42	0.45	0.35	0.43	0.34
Li_2O	0.20	0.32	0.26	0.18	0.26
Rb_2O				0.16	
Ba	250	205	198	407	340
Co					
Cr	32	22	29	31	26
Cu					
Nb					
Ni	9	28	33	23	39
Sc					
Sr	9	8	8	8	9
V	179	119	162	193	152
Y	181	174	183	70	141
Zn					
Zr *	339	488	750	314	540
La					
Ce					
Nd					
Sm					
Eu					
Dy					
Yb					
H_2O -				0.12	
H_2O+ Pyr				1.18	
H_2O+ Silica					
F				0.65	
Cl				0.41	
TOTAL	97.98	97.69	97.61	100.88	97.79
OH=F,Cl				0.37	
TOTAL	97.98	97.69	97.61	100.52	97.79

"Size" indicates grainsize of mica concentrate.

"Majors: Pt" indicates lithium metaborate fusion in a platinum crucible, "Majors: C" in a graphite crucible; "Trace" preparation by dissolution in HF-perchloric acid mixture.

SPECIMEN	08/17-4	08/17-5	08/17-7	08/21-11	08/21-12
PLUTON	Hake	Hake	Hake	Hake	Hake
SIZE	250-500µ	250-500µ	250-500µ	250-500µ	250-500µ
PROGRAM	Majors: Pt	Majors: Pt	Majors: Pt	Majors: Pt	Majors: Pt
SiO2	34.49	34.44	34.71	35.64	36.49
Al2O3	12.95	13.53	12.71	14.06	16.97
Fe2O3*	32.58	34.55	32.66	30.44	30.43
MgO	4.68	2.69	4.64	4.13	2.13
CaO	0.74	0.41	0.63	0.76	0.31
Na2O	0.16	0.29	0.27	0.30	0.26
K2O	7.72	7.87	8.27	8.44	7.62
TiO2	3.54	3.13	3.54	3.31	2.54
P2O5	0.24	0.12	0.25	0.28	0.06
MnO	0.46	0.44	0.46	0.41	0.45
Li2O	0.25	0.33	0.24	0.31	0.36
Rb2O		0.26		0.22	
Ba	215	130	325	245	72
Co					
Cr	24	16	34	26	17
Cu					
Nb					
Ni	28	17	17	28	12
Sc					
Sr	11	7	6	7	9
V	140	109	207	136	40
Y	129	101	86	189	162
Zn					
Zr *	178	365	159	611	141
La					
Ce					
Nd					
Sm					
Eu					
Dy					
Yb					
H2O -		0.06			
H2O+ Pyr	2.82	1.74	1.83		
H2O+ Silica					
F		1.26		2.03	
Cl		0.63		0.41	
TOTAL	100.63	101.75	100.21	100.74	97.62
OH=F,Cl		0.67		0.95	
TOTAL	100.63	101.08	100.21	99.79	97.62

"Size" indicates grainsize of mica concentrate.
"Majors: Pt" indicates lithium metaborate fusion in a platinum crucible, "Majors: C" in a graphite crucible; "Trace" preparation by dissolution in HF-perchloric acid mixture.

SPECIMEN	08/17-1	08/21-3	08/21-14	08/17-2	08/17-3
PLUTON	Hake Margin	Hake Margin	Hake Margin	Hake	Hake
SIZE	250-500μ	250-500μ	250-500μ	250-500μ	250-500μ
PROGRAM	Trace	Trace	Trace	Trace	Trace
SiO2					
Al2O3	12.70	13.01	13.35	11.81	13.60
Fe2O3*	32.25	33.45	34.81	30.86	30.53
MgO	4.67	4.29	3.63	5.46	4.40
CaO	0.88	0.93	0.60	0.87	0.78
Na2O	0.35	0.15	0.11	0.14	0.18
K2O	7.41	7.06	6.85	4.98	7.26
TiO2	3.49	3.56	3.17	3.61	3.41
P2O5	0.35	0.29	0.29	0.37	0.37
MnO	0.44	0.44	0.34	0.42	0.33
Li2O					
Rb2O				0.16	
Ba	269	215	204	384	376
Co	41	41	33	44	38
Cr	20	11	17	21	19
Cu	9	11	22	8	9
Nb	391	439	486	318	399
Ni	30	32	30	31	30
Sc	45	42	45	45	52
Sr	7	6	5	9	8
V	189	123	169	193	156
Y	160	183	164	93	174
Zn	259	337	281	311	188
Zr *	184	355	451	197	477
La	155	145	207	157	229
Ce	272	270	399	265	423
Nd	92	90	113	77	129
Sm	21	22	27	15	29
Eu	1	0	1	0	1
Dy	19	21	22	11	21
Yb	16	16	16	8	16
H2O -				0.12	
H2O+ Pyr				1.18	
H2O+ Silica					
F					
Cl					
TOTAL					
OH=F,Cl					
TOTAL					

"Size" indicates grainsize of mica concentrate.
"Majors: Pt" indicates lithium metaborate fusion in a platinum crucible, "Majors: C" in a graphite crucible; "Trace" preparation by dissolution in HF-perchloric acid mixture.

SPECIMEN	08/17-4	08/17-5	08/17-6	08/17-7	08/21-11
PLUTON	Hake	Hake	Hake	Hake	Hake
SIZE	250-500μ	250-500μ	250-500μ	250-500μ	250-500μ
PROGRAM	Trace	Trace	Trace	Trace	Trace
SiO_2					
Al_2O_3	12.52	12.83	16.71	11.89	13.58
Fe_2O_3*	33.33	34.56	39.88	33.04	31.15
MgO	4.57	2.53	2.44	4.31	3.97
CaO	0.64	0.42	0.57	0.65	0.73
Na_2O	0.07	0.15	0.17	0.06	0.22
K_2O	7.61	7.68	0.94	7.64	7.95
TiO_2	3.47	2.98	2.91	3.45	3.25
P_2O_5	0.23	0.16	0.06	0.30	0.32
MnO	0.45	0.44	0.62	0.42	0.41
Li_2O					
Rb_2O		0.26			0.22
Ba	223	111	46	339	251
Co	42	34	34	41	36
Cr	11	9	6	19	17
Cu	10	13	40	6	11
Nb	405	557	1303	400	434
Ni	29	24	31	33	28
Sc	60	46	44	38	40
Sr	8	5	8	4	5
V	148	119	132	205	144
Y	121	103	385	103	202
Zn	397	337	523	251	281
Zr *	84	322	305	117	399
La	39	245	38	27	155
Ce	75	476	78	63	298
Nd	34	136	38	20	94
Sm	12	26	26	11	24
Eu	0	0	0	0	0
Dy	14	15	58	12	24
Yb	9	11	67	10	18
H_2O -	0.24	0.06		0.30	
H_2O+ Pyr	2.82	1.74		1.83	
H_2O+ Silica					
F		1.26			
Cl					
TOTAL					
OH=F,Cl					
TOTAL					

"Size" indicates grainsize of mica concentrate.
"Majors: Pt" indicates lithium metaborate fusion in a platinum crucible, "Majors: C" in a graphite crucible; "Trace" preparation by dissolution in HF-perchloric acid mixture.

SPECIMEN	08/21-12	07/30-3	07/30-4	8/1/01	08/02-1
PLUTON	Hake	Seagull (W)	Seagull (W)	Seagull (W)	Seagull (W)
SIZE	250-500μ	250-500μ	250-500μ	250-500μ	250-500μ
PROGRAM	Trace	Majors: Pt	Majors: Pt	Majors: Pt	Majors: Pt
SiO_2		38.46	35.81	37.12	34.89
Al_2O_3	16.32	17.20	18.34	12.35	15.30
Fe_2O_3*	31.90	28.93	30.31	34.36	31.70
MgO	2.07	1.36	0.90	2.30	2.67
CaO	0.25	0.29	0.22	0.60	0.62
Na_2O	0.15	0.44	0.38	0.49	0.38
K_2O	7.41	8.23	8.43	6.96	7.39
TiO_2	2.43	2.55	2.19	3.18	3.34
P_2O_5	0.06	0.10	0.03	0.09	0.27
MnO	0.43	0.25	0.27	0.33	0.27
Li_2O		0.44	0.66	0.11	0.31
Rb_2O		0.30			0.17
Ba	71	54	29	130	193
Co	29				
Cr	4	22	16	24	29
Cu	54				
Nb	641				
Ni	27	48	Neg	25	23
Sc	76				
Sr	7	3	5	8	8
V	45		56	102	129
Y	108		46	88	307
Zn	280				
Zr *	96		172	447	1116
La	162				
Ce	333				
Nd	88				
Sm	20				
Eu	0				
Dy	17				
Yb	13				
H_2O-					0.14
H_2O+ Pyr		1.23			1.55
H_2O+ Silica					
F		1.98			1.76
Cl		0.41			0.70
TOTAL			97.54	97.89	101.46
OH=F,Cl		0.93			0.90
TOTAL		-0.93	97.54	97.89	100.56

"Size" indicates grainsize of mica concentrate.

"Majors: Pt" indicates lithium metaborate fusion in a platinum crucible, "Majors: C" in a graphite crucible; "Trace" preparation by dissolution in HF-perchloric acid mixture.

SPECIMEN	07/21-1	07/21-2	08/21-1	08/21-2	08/21-03
PLUTON	Seagull	Seagull	Seagull	Seagull	Seagull
SIZE	250-500µ	250-500µ	250-500µ	250-500µ	250-500µ
PROGRAM	Majors: Pt	Majors: Pt	Majors: Pt	Majors: Pt	Majors: Pt
SiO2	34.85	35.83	36.33	36.69	36.26
Al2O3	19.28	18.99	18.62	19.19	18.54
Fe2O3*	29.68	29.68	29.43	29.02	29.94
MgO	1.13	0.59	0.67	0.56	0.69
CaO	0.46	0.37	0.24	0.24	0.25
Na2O	0.35	0.33	0.36	0.33	0.35
K2O	6.76	7.62	8.24	8.90	8.75
TiO2	1.98	1.96	2.03	1.93	2.03
P2O5	0.22	0.02	0.04	0.03	0.02
MnO	0.20	0.18	0.23	0.27	0.22
Li2O	0.53	0.65	0.69	0.88	0.72
Rb2O					
Ba	69	29	38	16	20
Co					
Cr	19	16	8	12	17
Cu					
Nb					
Ni	17	36	12	15	12
Sc					
Sr	15	6	6	5	6
V	63	45	44	45	47
Y	618	192	186	47	58
Zn					
Zr *	1479	171	824	498	231
La					
Ce					
Nd					
Sm					
Eu					
Dy					
Yb					
H2O -					
H2O+ Pyr					
H2O+ Silica					
F					
Cl					
TOTAL	95.44	96.22	96.88	98.04	97.77
OH=F,Cl					
TOTAL	95.44	96.22	96.88	98.04	97.77

"Size" indicates grainsize of mica concentrate.
"Majors: Pt" indicates lithium metaborate fusion in a platinum crucible, "Majors: C" in a graphite crucible; "Trace" preparation by dissolution in HF-perchloric acid mixture.

SPECIMEN PLUTON SIZE PROGRAM	08/21-03 Seagull 250-500µ Repeat	07/30-1 Seagull (W) 250-500µ Trace	07/30-3 Seagull (W) 250-500µ Trace	07/30-4 Seagull (W) 250-500µ Trace	08/01-1 Seagull (W) 250-500µ Trace
SiO2	36.11				
Al2O3	18.47	19.25	16.91	18.00	11.78
Fe2O3*		29.62	31.34	32.16	34.99
MgO	0.68	0.46	1.39	0.86	2.15
CaO		0.28	0.23	0.16	0.63
Na2O	0.32	0.23	0.14	0.16	0.27
K2O	8.78	8.50	8.31	8.85	6.64
TiO2	2.04	1.80	2.63	2.25	3.44
P2O5	0.03	0.04	0.07	0.04	0.14
MnO	0.22	0.25	0.27	0.29	0.34
Li2O	0.72				
Rb2O					
Ba	18	30	55	24	132
Co		17	23	20	33
Cr	12	3	Neg	3	11
Cu		10	6	6	12
Nb		909	670	749	539
Ni	9	20	23	21	28
Sc		59	96	85	61
Sr	5	3	3	2	5
V	47	45	94	63	122
Y	54	130	59	34	121
Zn		339	474	437	592
Zr *	241	263	173	85	77
La		81	199	79	223
Ce		160	420	158	398
Nd		53	141	45	150
Sm		15	30	10	29
Eu		0	0		0
Dy		16	11	5	18
Yb		13	5	3	10
H2O -					
H2O+ Pyr					
H2O+ Silica					
F		2.33			
Cl					
TOTAL	67.37				
OH=F,Cl					
TOTAL	67.37				

"Size" indicates grainsize of mica concentrate.
"Majors: Pt" indicates lithium metaborate fusion in a platinum crucible, "Majors: C" in a graphite crucible; "Trace" preparation by dissolution in HF-perchloric acid mixture.

SPECIMEN PLUTON SIZE PROGRAM	08/02-1 Seagull (W) 250-500µ Trace	07/21-1 Seagull 250-500µ Trace	07/21-2 Seagull 250-500µ Trace	08/21-1 Seagull 250-500µ Trace	08/21-2 Seagull 250-500µ Trace
SiO2					
Al2O3	14.58	18.66	18.09	18.17	18.44
Fe2O3*	32.46	30.96	30.72	30.66	30.24
MgO	2.55	1.10	0.55	0.65	0.52
CaO	0.61	0.38	0.28	0.27	0.18
Na2O	0.17	0.18	0.13	0.40	0.16
K2O	5.85	6.91	7.66	7.87	8.41
TiO2	3.20	1.71	1.90	1.90	1.90
P2O5	0.28	0.20	0.04	0.04	0.03
MnO	0.27	0.22	0.19	0.22	0.26
Li2O					
Rb2O	0.17				
Ba	195	66	25	35	9
Co	31	19	18	18	18
Cr	20	11	2	10	2
Cu	19	41	32	32	6
Nb	555	901	837	944	917
Ni	28	23	23	20	23
Sc	69	72	76	75	85
Sr	5	11	3	3	2
V	134	68	51	55	51
Y	198	248	208	224	46
Zn	460	738	309	353	395
Zr *	622	1384	161	754	406
La	361	675	152	169	46
Ce	747	1395	309	352	99
Nd	248	460	96	110	18
Sm	54	106	24	30	6
Eu	1	1	0	1	0
Dy	31	50	24	29	7
Yb	17	20	16	24	5
H2O -					
H2O+ Pyr					
H2O+ Silica					
F					
Cl					
TOTAL					
OH=F,Cl					
TOTAL					

"Size" indicates grainsize of mica concentrate.
"Majors: Pt" indicates lithium metaborate fusion in a platinum crucible, "Majors: C" in a graphite crucible; "Trace" preparation by dissolution in HF-perchloric acid mixture.

SPECIMEN	08/21-03	REED	REED	78/23-1	88/10-4
PLUTON	Seagull	Haskin	Haskin	Li-mica	Li-mica
SIZE	250-500μ	250-500μ	250-500μ	250-500μ	250-500μ
PROGRAM	Trace	Majors: Pt	Trace	Majors: Pt	Majors: C
SiO_2		37.96		44.57	42.69
Al_2O_3	17.61	14.10	13.86	21.31	21.36
Fe_2O_3*	31.46	21.10	21.34	14.73	19.73
MgO	0.63	10.01	9.78	0.07	0.05
CaO	0.21	0.67	0.56	0.14	0.02
Na_2O	0.17	0.45	0.37	0.57	0.27
K_2O	8.03	8.37	8.69	8.86	9.43
TiO_2	1.97	3.22	3.14	0.11	0.22
P_2O_5	0.03	0.21	0.21	0.03	0.02
MnO	0.22	1.49	1.39	0.99	0.75
Li_2O		0.29		2.85	1.82
Rb_2O		0.13			
Ba	14	1467	1607	13	12
Co	19		38		
Cr	2	34	25	12	Neg.
Cu	11		5		
Nb	881		248		
Ni	23	28	29	70	33
Sc	80		172		
Sr	2	16	15	5	7
V	54	115	118		12
Y	60	56	57		21
Zn	398		599		
Zr *	222	250	51		63
La	63		178		
Ce	126		322		
Nd	25		100		
Sm	9		17		
Eu	0		1		
Dy	8		11		
Yb	5		5		
H_2O -		0.22			
H_2O+ Pyr		0.94		0.49	
H_2O+ Silica					
F		2.50		6.16	
Cl		0.02			
TOTAL		101.68		100.88	96.36
OH=F,Cl		1.06		2.59	
TOTAL		100.63		98.29	96.36

"Size" indicates grainsize of mica concentrate.

"Majors: Pt" indicates lithium metaborate fusion in a platinum crucible, "Majors: C" in a graphite crucible; "Trace" preparation by dissolution in HF-perchloric acid mixture.

SPECIMEN	97/26-3	97/28-4	97/28-4	98/5-1	ORK
PLUTON	Li-mica	Li-mica	Li-mica	Li-mica	Li-mica
SIZE	250-500μ	250-500μ	250-500μ	250-500μ	250-500μ
PROGRAM	Majors: C	Majors: Pt	Majors: C	Majors: Pt	Majors: Pt
SiO2	44.97	52.54	53.61	45.57	46.48
Al2O3	21.42	19.12	19.38	21.19	20.47
Fe2O3*	16.08	6.44	6.21	14.24	12.35
MgO	0.04	0.01	0.03	0.02	0.02
CaO	0.42			0.08	
Na2O	0.78	0.88	0.84	0.72	0.62
K2O	8.75	9.21	8.78	8.62	9.53
TiO2	0.14	0.04	0.04	0.03	0.08
P2O5	0.01	0.02	0.01	0.03	0.02
MnO	0.74	1.64	1.64	0.63	1.36
Li2O	2.43	4.67	4.67	2.90	3.75
Rb2O		1.69	1.69		1.44
Ba	65	10	11	2	7
Co					
Cr	Neg.	1		8	3
Cu					
Nb					
Ni	28	9	12	8	6
Sc					
Sr	34	11	10	5	10
V	48				8
Y	8		1		10
Zn					
Zr *	103	25	29		154
La					
Ce					
Nd					
Sm					
Eu					
Dy					
Yb					
H2O -		0.08		0.04	0.06
H2O+ Pyr		0.68		0.77	0.33
H2O+ Silica					0.33
F		7.55			7.03
Cl		0.02	0.02		
TOTAL	95.78	104.59	96.92	94.84	103.54
OH=F,Cl		3.18	0.00		2.96
TOTAL	95.78	101.41	96.92	94.84	100.58

"Size" indicates grainsize of mica concentrate.
"Majors: Pt" indicates lithium metaborate fusion in a platinum crucible, "Majors: C" in a graphite crucible; "Trace" preparation by dissolution in HF-perchloric acid mixture.

SPECIMEN	ORK	88/12-1	97/12-1 E	97/24-3	HPG
PLUTON	Li-mica	Porphyry	Porphyry	Porphyry	Porphyry
SIZE	250-500μ	250-500μ	250-500μ	250-500μ	250-500μ
PROGRAM	Majors: C	Majors: C	Majors: Pt	Majors: C	Majors: Pt
SiO_2	44.97	36.71		35.76	35.66
Al_2O_3	21.30	12.94		13.24	11.79
Fe_2O_3*	15.40	31.00		29.19	30.45
MgO	0.07	3.96		5.60	5.71
CaO	0.07	0.87		2.18	2.24
Na_2O	0.56	0.30		0.34	0.48
K_2O	9.09	8.15		5.78	7.42
TiO_2	0.12	3.54		4.07	3.64
P_2O_5	0.01	0.26		0.37	0.39
MnO	1.05	0.65		0.50	0.45
Li_2O	3.75	0.19	0.12	0.18	0.19
Rb_2O				0.13	0.11
Ba	19	428		458	734
Co					
Cr	2	21		38	47
Cu					
Nb					
Ni	31	39		82	71
Sc					
Sr	8	24		18	19
V	9	207		297	250
Y	9	149		219	166
Zn					
Zr *	133	497		569	448
La					
Ce					
Nd					
Sm					
Eu					
Dy					
Yb					
H_2O -				0.41	0.16
H_2O+ Pyr				2.30	1.05
H_2O+ Silica					
F				0.94	0.96
Cl				0.26	0.40
TOTAL	96.39	98.57		101.25	101.11
OH=F,Cl				0.45	0.49
TOTAL	96.39	98.57		100.80	100.61

"Size" indicates grainsize of mica concentrate.
"Majors: Pt" indicates lithium metaborate fusion in a platinum crucible, "Majors: C" in a graphite crucible; "Trace" preparation by dissolution in HF-perchloric acid mixture.

SPECIMEN	88/14-1	88/14-8	97/23-3	97/23-5	97/23-5
PLUTON	Even grained	Even grained	Even grained	Even grained	Even grained
SIZE	250-500μ	250-500μ	250-500μ	250-500μ	250-500μ
PROGRAM	Majors: C	Majors: C	Majors: Pt	Majors: Pt	Majors: C
SiO2	35.13	48.06	35.71	35.44	
Al2O3	12.21	17.98	13.85	12.43	
Fe2O3*	31.74	10.10	32.01	32.97	
MgO	5.21	7.75	2.13	3.86	
CaO	1.15	11.46	0.50	0.63	
Na2O	0.14	2.54	0.36	0.26	
K2O	8.07	0.25	7.33	8.29	
TiO2	3.66	0.85	2.73	3.66	
P2O5	0.38	0.13	0.11	0.20	
MnO	0.48	0.13	0.53	0.49	
Li2O	0.13	0.20	0.23	0.23	0.23
Rb2O					
Ba	496	153	237	283	
Co					
Cr	24	360	22	42	
Cu					
Nb					
Ni	41	223	38	59	
Sc					
Sr	14	346	8	16	
V	214	221		196	
Y	173	13		195	
Zn					
Zr *	508	34		678	
La					
Ce					
Nd					
Sm					
Eu					
Dy					
Yb					
H2O -					
H2O+ Pyr					
H2O+ Silica					
F					
Cl					
TOTAL	98.30	99.45	95.49	98.46	
OH=F,Cl					
TOTAL	98.30	99.45	95.49	98.46	

"Size" indicates grainsize of mica concentrate.
"Majors: Pt" indicates lithium metaborate fusion in a platinum crucible, "Majors: C" in a graphite crucible; "Trace" preparation by dissolution in HF-perchloric acid mixture.

SPECIMEN	97/24-5	97/24-5	97/25-1 B	97/26-6	97/27-7
PLUTON	Even grained	Even grained	Even grained	Even grained	Even grained
SIZE	250-500μ	250-500μ	250-500μ	250-500μ	250-500μ
PROGRAM	Majors: Pt	Majors: C	Majors: C	Majors: C	Majors: Pt
SiO_2	35.76	36.40	38.88	38.98	37.37
Al_2O_3	14.43	14.56	21.14	19.46	13.83
Fe_2O_3*	30.72	30.06	25.52	24.85	30.93
MgO	3.70	3.66	1.61	1.71	2.94
CaO	0.64	0.71	0.40	0.22	0.37
Na_2O	0.27	0.22	0.65	0.23	0.42
K_2O	8.18	7.90	6.04	8.71	8.70
TiO_2	3.07	3.13	1.86	2.04	3.20
P_2O_5	0.23	0.22	0.10	0.11	0.15
MnO	0.51	0.52	0.61	0.66	0.63
Li_2O	0.45	0.45	0.73	1.04	0.45
Rb_2O					0.28
Ba	266	262	93	185	183
Co					
Cr	48	22	7	13	40
Cu					
Nb					
Ni	71	60	25	39	47
Sc					
Sr	17	20	11	11	8
V	219	215	52	108	160
Y	242	318	205	118	120
Zn					
Zr *	557	555	384	494	578
La					
Ce					
Nd					
Sm					
Eu					
Dy					
Yb					
H_2O -				0.21	
H_2O+ Pyr				1.52	
H_2O+ Silica					
F					1.76
Cl					0.42
TOTAL	97.96	97.83	97.54	99.75	101.45
OH=F,Cl					0.84
TOTAL	97.96	97.83	97.54	99.75	100.61

"Size" indicates grainsize of mica concentrate.
"Majors: Pt" indicates lithium metaborate fusion in a platinum crucible, "Majors: C" in a graphite crucible; "Trace" preparation by dissolution in HF-perchloric acid mixture.

SPECIMEN	97/29-1	98/1-1 B	88/14-7 S	97/17-1 A	97/26-5
PLUTON	Even grained	Even grained	Megacrystic	Megacrystic	Megacrystic
SIZE	250-500μ	250-500μ	250-500μ	250-500μ	250-500μ
PROGRAM	Majors: Pt	Majors: Pt	Majors: Pt	Majors: C	Majors: C
SiO2	34.45	38.41	35.91	36.90	32.45
Al2O3	17.34	16.40	13.01	15.45	14.64
Fe2O3*	31.16	30.79	29.06	29.90	29.52
MgO	1.97	1.07	5.10	3.09	6.20
CaO	0.72	0.23	0.77	0.61	2.48
Na2O	0.41	0.48	0.28	0.25	0.27
K2O	4.71	7.79	7.82	7.86	4.46
TiO2	2.08	2.24	3.28	2.86	4.99
P2O5	0.13	0.06	0.26	0.23	0.39
MnO	0.39	0.63	0.54	0.49	0.48
Li2O	0.66	0.41	0.32	0.43	0.34
Rb2O	0.15		0.11		
Ba	144	111	272	224	368
Co					
Cr	8	4	28	22	40
Cu					
Nb					
Ni	20	33	33	39	71
Sc					
Sr	8	6	8	13	30
V	119	43		173	368
Y	415	201		255	376
Zn					
Zr *	928	568		625	552
La					
Ce					
Nd					
Sm					
Eu					
Dy					
Yb					
H2O -	0.28	0.21	0.24		0.33
H2O+ Pyr	3.30	2.87	1.24		4.21
H2O+ Silica					
F	1.14		1.65		
Cl	0.17		0.34		
TOTAL	99.05	101.59	99.92	98.07	100.75
OH=F,Cl	0.52		0.77		
TOTAL	98.53	101.59	99.15	98.07	100.75

"Size" indicates grainsize of mica concentrate.
"Majors: Pt" indicates lithium metaborate fusion in a platinum crucible, "Majors: C" in a graphite crucible; "Trace" preparation by dissolution in HF-perchloric acid mixture.

SPECIMEN	97/27-2	97/27-5	97/27-5	97/27-5	97/28-5
PLUTON	Megacrystic	Megacrystic	Megacrystic	Megacrystic	Megacrystic
SIZE	250-500μ	250-500μ	250-500μ	250-500μ	250-500μ
PROGRAM	Majors: Pt	Majors: Pt	Majors: Pt	Repeat	Majors: Pt
SiO2	33.83	35.46	35.35	35.96	35.92
Al2O3	12.84	14.33	14.35	14.69	13.62
Fe2O3*	31.84	31.52	31.47	32.49	30.63
MgO	5.29	2.53	2.52	2.77	4.29
CaO	1.69	0.24	0.26	0.39	0.81
Na2O	0.27	0.25	0.24	0.41	0.30
K2O	7.13	7.78	7.81	7.63	8.45
TiO2	3.32	2.70	2.70	2.70	3.33
P2O5	0.36	0.11	0.12	0.11	0.35
MnO	0.49	0.79	0.79	0.77	0.54
Li2O	0.17	0.41	0.41	0.41	0.44
Rb2O					0.22
Ba	473	131	133	138	363
Co					
Cr	67	2	1	30	48
Cu					
Nb					
Ni	89		11	83	41
Sc					
Sr	13	9	9	11	13
V	308	80	82	94	224
Y	158	163	164	154	201
Zn					
Zr *	527	306	293	200	646
La					
Ce					
Nd					
Sm					
Eu					
Dy					
Yb					
H2O -	0.19				
H2O+ Pyr	3.06				1.25
H2O+ Silica					
F					1.84
Cl					0.25
TOTAL	100.48	96.12	96.02	98.33	102.24
OH=F,Cl					0.83
TOTAL	100.48	96.12	96.02	98.33	101.41

"Size" indicates grainsize of mica concentrate.
"Majors: Pt" indicates lithium metaborate fusion in a platinum crucible, "Majors: C" in a graphite crucible; "Trace" preparation by dissolution in HF-perchloric acid mixture.

SPECIMEN	TOR	78/23-1	88/10-4	97/26-3	97/28-2
PLUTON	Megacrystic	Li-mica	Li-mica	Li-mica	Li-mica
SIZE	250-500µ	250-500µ	250-500µ	250-500µ	250-500µ
PROGRAM	Majors: Pt	Trace	Trace	Trace	Trace
SiO_2	36.48				
Al_2O_3	12.52	18.89	17.48	19.01	18.71
Fe_2O_3*	29.88	16.08	19.10	16.90	10.12
MgO	4.48	0.05	0.03	0.01	0.14
CaO	0.90	0.12	0.04	0.04	0.03
Na_2O	0.41	0.50	0.25	0.70	1.24
K_2O	7.59	9.22	8.24	8.69	9.01
TiO_2	3.85	0.13	0.20	0.13	0.08
P_2O_5	0.23	0.02	0.02	0.02	0.04
MnO	0.48	1.02	0.69	0.73	0.95
Li_2O					
Rb_2O					
Ba	265	14	8	6	21
Co		5	6	5	4
Cr	35	6	3	3	5
Cu		4	5	4	4
Nb		349	399	332	294
Ni	38	11	15	12	11
Sc		126	96	120	78
Sr	20	5	3	5	10
V		18	20	16	14
Y		6	14	7	9
Zn		273	230	193	260
Zr *		72	34	60	92
La		15	2	28	25
Ce		51	11	82	118
Nd		4		6	21
Sm		2	2	3	6
Eu		0	0		0
Dy		3	4	3	5
Yb		6	6	5	17
H_2O -		0.21			
H_2O+ Pyr		0.49			
H_2O+ Silica					
F		6.16			
Cl					
TOTAL					
OH=F,Cl					
TOTAL					

"Size" indicates grainsize of mica concentrate.
"Majors: Pt" indicates lithium metaborate fusion in a platinum crucible, "Majors: C" in a graphite crucible; "Trace" preparation by dissolution in HF-perchloric acid mixture.

SPECIMEN	97/28-4	98/5-1	88/12-1	97/24-3	88/15-2
PLUTON	Li-mica	Li-mica	Porphyry	Porphyry	Porphyry
SIZE	250-500μ	250-500μ	250-500μ	250-500μ	250-500μ
PROGRAM	Trace	Trace	Trace	Trace	Trace
SiO2					
Al2O3	18.59	19.39	11.53	12.60	11.21
Fe2O3*	6.62	14.62	30.39	29.51	29.61
MgO	0.01	0.02	3.56	5.37	5.30
CaO	0.02	0.07	0.91	2.12	1.22
Na2O	0.78	0.84	0.33	0.37	0.19
K2O	9.90	8.81	7.05	5.33	6.59
TiO2	0.05	0.04	3.32	3.80	3.38
P2O5	0.01	0.02	0.34	0.39	0.41
MnO	1.63	0.62	0.60	0.47	0.40
Li2O					
Rb2O					
Ba	7	7	453	448	668
Co	3	5	36	44	41
Cr	7	4	12	29	17
Cu	2	3	11	9	26
Nb	71	207	397	421	269
Ni	7	12	26	33	32
Sc	102	80	38	55	28
Sr	7	6	16	16	12
V	7	14	194	298	258
Y		2	153	189	109
Zn	648	204	282	223	274
Zr *	8	13	295	234	222
La	1	4	175	114	113
Ce	2	21	313	211	205
Nd			90	66	65
Sm		0	23	22	18
Eu			1	1	1
Dy	1	1	19	25	15
Yb	1	2	14	18	9
H2O -					
H2O+ Pyr					
H2O+ Silica					
F					0.70
Cl					
TOTAL					
OH=F,Cl					
TOTAL					

"Size" indicates grainsize of mica concentrate.

"Majors: Pt" indicates lithium metaborate fusion in a platinum crucible, "Majors: C" in a graphite crucible; "Trace" preparation by dissolution in HF-perchloric acid mixture.

SPECIMEN PLUTON SIZE PROGRAM	97/12-1 E Porphyry 250-500μ Trace	97/24-3 Porphyry 250-500μ Trace	HPG Porphyry 250-500μ Trace	88/8-8 Red alt. even 250-500μ Trace	88/14-1 Even grained 250-500μ Trace
SiO2					
Al2O3	11.41	12.60	11.84	13.75	11.74
Fe2O3*	30.39	29.51	30.42	32.01	32.57
MgO	5.11	5.37	5.65	2.28	5.09
CaO	0.97	2.12	2.11	0.54	1.07
Na2O	0.21	0.37	0.41	0.11	0.15
K2O	6.81	5.33	6.76	7.18	7.53
TiO2	3.33	3.80	3.34	3.75	3.54
P2O5	0.19	0.39	0.35	0.19	0.40
MnO	0.44	0.47	0.41	0.46	0.47
Li2O					
Rb2O					
Ba	608	448	672	263	491
Co	40	44	43	34	41
Cr	17	29	15	9	15
Cu	8	9	7	147	9
Nb	277	421	306	1030	443
Ni	31	33	27	23	31
Sc	36	55	36	54	34
Sr	21	16	18	5	12
V	264	298	246	136	225
Y	68	189	158	115	176
Zn	282	223	281	268	298
Zr *	213	234	162	322	219
La	56	114	66	58	39
Ce	93	211	152	133	76
Nd	30	66	75	40	41
Sm	11	22	21	14	18
Eu	1	1	1	0	1
Dy	10	25	21	15	21
Yb	6	18	13	17	16
H2O -					
H2O+ Pyr					
H2O+ Silica					
F					
Cl					
TOTAL					
OH=F,Cl					
TOTAL					

"Size" indicates grainsize of mica concentrate.
"Majors: Pt" indicates lithium metaborate fusion in a platinum crucible, "Majors: C" in a graphite crucible; "Trace" preparation by dissolution in HF-perchloric acid mixture.

SPECIMEN PLUTON SIZE PROGRAM	88/14-8 Even grained 250-500μ Trace	97/23-3 Even grained 250-500μ Trace	97/23-5 Even grained 250-500μ Trace	97/24-5 Even grained 250-500μ Trace	97/25-1 B Even grained 250-500μ Trace
SiO_2					
Al_2O_3	13.84	12.96	12.43	14.07	16.91
Fe_2O_3*	36.61	33.86	34.04	31.32	25.57
MgO	2.46	2.00	3.86	3.62	1.45
CaO	0.73	0.47	0.61	0.67	0.37
Na_2O	0.17	0.24	0.20	0.23	0.35
K_2O	6.05	6.72	7.70	7.57	6.28
TiO_2	2.85	2.66	3.89	3.07	1.65
P_2O_5	0.13	0.11	0.18	0.23	0.09
MnO	0.68	0.51	0.49	0.50	0.58
Li_2O					
Rb_2O					
Ba	261	254	263	251	85
Co	30	28	38	32	19
Cr	3	6	13	17	6
Cu	12	15	13	9	10
Nb	508	696	517	701	632
Ni	27	27	27	28	20
Sc	52	37	49	54	36
Sr	13	8	12	14	7
V	94	113	200	219	58
Y	181	184	168	176	180
Zn	280	242	252	191	220
Zr *	211	901	347	281	294
La	151	235	130	145	276
Ce	302	440	230	284	570
Nd	90	115	75	89	167
Sm	24	27	21	25	40
Eu	1	1	1	1	1
Dy	23	24	19	23	37
Yb	20	27	14	19	26
H_2O -					
H_2O+ Pyr					
H_2O+ Silica					
F					
Cl					
TOTAL					
OH=F,Cl					
TOTAL					

"Size" indicates grainsize of mica concentrate.
"Majors: Pt" indicates lithium metaborate fusion in a platinum crucible, "Majors: C" in a graphite crucible; "Trace" preparation by dissolution in HF-perchloric acid mixture.

SPECIMEN	97/26-6	97/27-7	97/29-1	98/1-1 A	98/1-1 B
PLUTON	Even grained	Even grained	Even grained	Even grained	Even grained
SIZE	250-500μ	250-500μ	250-500μ	250-500μ	250-500μ
PROGRAM	Trace	Trace	Trace	Trace	Trace
SiO_2					
Al_2O_3	18.92	13.63	18.20	13.52	15.98
Fe_2O_3*	27.17	32.08	34.88	35.62	32.93
MgO	1.63	2.89	2.29	2.23	1.25
CaO	0.22	0.43	0.90	0.50	0.28
Na_2O	0.28	0.30	0.37	0.19	0.26
K_2O	9.20	8.24	4.68	5.70	6.48
TiO_2	2.02	3.25	1.96	2.73	2.08
P_2O_5	0.12	0.15	0.13	0.13	0.05
MnO	0.67	0.61	0.40	0.63	0.59
Li_2O					
Rb_2O					
Ba	162	174	156	236	139
Co	21	33	29	29	22
Cr	11	12	15	10	2
Cu	9	9	9	27	14
Nb	671	734	681	771	874
Ni	23	26	26	26	22
Sc	53	61	45	44	46
Sr	3	4	7	10	5
V	112	162	144	138	60
Y	91	116	316	259	281
Zn	233	251	204	275	266
Zr *	282	334	439	444	409
La	352	118	176	253	165
Ce	757	228	351	490	308
Nd	222	57	106	162	122
Sm	50	18	35	39	34
Eu	1	0	1	1	1
Dy	26	16	44	31	32
Yb	14	15	36	34	37
H_2O -					
H_2O+ Pyr					
H_2O+ Silica					
F					
Cl					
TOTAL					
OH=F,Cl					
TOTAL					

"Size" indicates grainsize of mica concentrate.
"Majors: Pt" indicates lithium metaborate fusion in a platinum crucible, "Majors: C" in a graphite crucible; "Trace" preparation by dissolution in HF-perchloric acid mixture.

SPECIMEN	98/1-1 B	88/14-7 S	88/14-7 S	97/17-1 A	97/26-S
PLUTON	Even grained	Megacrystic	Megacrystic	Megacrystic	Megacrystic
SIZE	250-500μ	250-500μ	250-500μ	250-500μ	250-500μ
PROGRAM	Trace	Trace	Trace	Trace	Trace
SiO2					
Al2O3	15.46	12.32	11.62	14.90	14.10
Fe2O3*	31.82	30.02	29.51	31.38	29.82
MgO	1.22	4.66	4.57	3.00	6.05
CaO	0.27	0.93	0.77	0.56	2.23
Na2O	0.39	0.32	0.16	0.23	0.30
K2O	6.77	7.47	7.13	7.66	4.34
TiO2	2.19	3.31	3.18	2.69	4.67
P2O5	0.07	0.37	0.32	0.22	0.38
MnO	0.60	0.53	0.51	0.48	0.45
Li2O					
Rb2O					
Ba	111	312	273	214	352
Co	23	38	38	29	44
Cr	2	12	11	15	29
Cu	18	10	8	10	11
Nb	820	530	437	720	532
Ni	20	31	28	26	32
Sc	46	55	53	62	70
Sr	5	12	9	9	13
V	56	157	152	186	341
Y	208	301	217	168	200
Zn	248	346	341	275	154
Zr *	353	382	258	262	262
La	195	246	57	127	63
Ce	393	469	128	265	128
Nd	132	139	48	82	54
Sm	33	35	20	26	22
Eu	1	1	0	0	1
Dy	27	37	25	24	28
Yb	28	28	20	21	21
H2O -					
H2O+ Pyr					
H2O+ Silica					
F			1.65		
Cl					
TOTAL					
OH=F,Cl					
TOTAL					

"Size" indicates grainsize of mica concentrate.
"Majors: Pt" indicates lithium metaborate fusion in a platinum crucible, "Majors: C" in a graphite crucible; "Trace" preparation by dissolution in HF-perchloric acid mixture.

SPECIMEN	97/26-5	97/27-2	97/27-5	97/28-5	97/29-1
PLUTON	Megacrystic	Megacrystic	Megacrystic	Megacrystic	Even-Grained
SIZE	250-500μ	250-500μ	250-500μ	250-500μ	250-500μ
PROGRAM	Trace	Trace	Trace	Trace	Trace
SiO2					
Al2O3	13.42	13.44	14.58	13.87	17.09
Fe2O3*	28.26	33.68	33.84	32.10	32.96
MgO	5.87	5.54	2.70	4.37	2.21
CaO	2.64	1.66	0.52	0.83	0.54
Na2O	0.29	0.18	0.35	0.22	0.14
K2O	4.83	6.98	7.06	8.07	5.79
TiO2	4.37	3.51	2.67	3.53	2.20
P2O5	0.55	0.36	0.12	0.37	0.12
MnO	0.41	0.50	0.73	0.55	0.44
Li2O					
Rb2O					
Ba	426	470	126	367	222
Co	43	40	29	38	30
Cr	27	26	7	17	15
Cu	9	8	12	8	7
Nb	507	399	523	544	616
Ni	32	35	26	28	27
Sc	75	56	49	62	45
Sr	13	9	8	10	4
V	336	308	96	228	153
Y	253	162	150	199	191
Zn	151	255	278	279	190
Zr *	382	203	155	353	281
La	84	45	165	212	122
Ce	173	81	330	402	241
Nd	78	36	88	122	79
Sm	28	17	23	31	22
Eu	1	1	1	1	0
Dy	35	21	20	27	24
Yb	26	15	17	18	20
H2O -					
H2O+ Pyr					
H2O+ Silica					
F					
Cl					
TOTAL					
OH=F,Cl					
TOTAL					

"Size" indicates grainsize of mica concentrate.
"Majors: Pt" indicates lithium metaborate fusion in a platinum crucible, "Majors: C" in a graphite crucible; "Trace" preparation by dissolution in HF-perchloric acid mixture.

SPECIMEN PLUTON SIZE PROGRAM	ORK Li-mica 250-500μ Trace	08/17-1 Hake Margin >500μ Majors: Pt	08/21-3 Hake Margin <250μ Majors: Pt	08/17-5 Hake >500μ Majors: Pt	08/17-1 Hake Margin >500μ Majors: Pt
SiO2		34.63	34.18	34.58	
Al2O3	20.12	12.60	13.48	13.37	12.08
Fe2O3*	12.73	32.55	32.55	34.33	32.93
MgO	0.02	4.82	4.42	2.68	4.66
CaO	0.09	0.82	0.84	0.50	0.75
Na2O	0.55	0.19	0.23	0.30	0.08
K2O	9.78	8.23	7.29	7.83	6.41
TiO2	0.08	3.68	3.86	3.11	3.58
P2O5	0.02	0.32	0.15	0.17	0.35
MnO	1.42	0.46	0.48	0.43	0.44
Li2O					
Rb2O					
Ba	4	324	211	131	339
Co	6				42
Cr	7	31	24	18	20
Cu	7				8
Nb	554				371
Ni	12	23	28	20	31
Sc	109				46
Sr	6	6	9	7	4
V	20	175	119	106	183
Y	9	119	182	124	127
Zn	315				257
Zr *	121	280	225	521	125
La	36				34
Ce	124				64
Nd	20				35
Sm	4				12
Eu					0
Dy	1				13
Yb	9				12
H2O -					
H2O+ Pyr					
H2O+ Silica					
F					
Cl					
TOTAL		98.30	97.48	97.30	
OH=F,Cl					
TOTAL		98.30	97.48	97.30	

"Size" indicates grainsize of mica concentrate.

"Majors: Pt" indicates lithium metaborate fusion in a platinum crucible, "Majors: C" in a graphite crucible; "Trace" preparation by dissolution in HF-perchloric acid mixture.

SPECIMEN PLUTON SIZE PROGRAM	08/21-3 Hake Margin <250µ Trace	08/21-14 Hake Margin >500µ Trace	08/17-2 Hake >500µ Trace	08/17-5 Hake >500µ Trace	08/17-7 Hake >500µ Trace
SiO2					
Al2O3	12.94	12.88	11.75	13.03	12.36
Fe2O3*	33.49	34.04	31.56	35.91	34.04
MgO	4.23	3.56	5.53	2.63	4.50
CaO	0.82	0.56	0.76	0.48	0.69
Na2O	0.15	0.10	0.10	0.11	0.08
K2O	6.69	6.67	8.40	5.51	7.97
TiO2	3.87	3.11	3.74	3.11	3.57
P2O5	0.16	0.26	0.36	0.18	0.32
MnO	0.48	0.33	0.43	0.43	0.43
Li2O					
Rb2O					
Ba	215	209	426	137	360
Co	43	33	46	35	42
Cr	12	14	21	8	20
Cu	12	18	6	14	7
Nb	488	430	293	562	413
Ni	33	29	36	27	34
Sc	44	43	41	45	40
Sr	7	4	5	5	3
V	127	155	195	118	212
Y	211	333	74	123	110
Zn	343	282	313	342	259
Zr *	202	429	133	344	134
La	867	138	23	211	26
Ce	1536	291	50	423	61
Nd	383	103	27	116	23
Sm	59	35	9	28	12
Eu	1	1	0	1	0
Dy	29	43	9	19	13
Yb	20	30	6	13	11
H2O -					
H2O+ Pyr					
H2O+ Silica					
F					
Cl					
TOTAL					
O=F,Cl					
TOTAL					

"Size" indicates grainsize of mica concentrate.

"Majors: Pt" indicates lithium metaborate fusion in a platinum crucible, "Majors: C" in a graphite crucible; "Trace" preparation by dissolution in HF-perchloric acid mixture.

SPECIMEN	08/21-12	08/21-03	08/21-03	97/29-1	97/29-1
PLUTON	Hake	Seagull	Seagull	Even gr./Li	Even gr./Li
SIZE	<250μ	>500μ	>500μ	>500μ	>500μ
PROGRAM	Trace	Majors: Pt	Trace	Majors: Pt	Trace
SiO2		35.54		40.64	
Al2O3	16.76	18.11	17.03	16.22	15.82
Fe2O3*	32.73	31.05	31.94	25.90	26.54
MgO	2.05	0.67	0.62	1.91	1.87
CaO	0.28	0.24	0.16	1.27	1.10
Na2O	0.12	0.31	0.16	0.67	0.55
K2O	6.94	8.75	8.08	5.47	5.67
TiO2	2.73	2.34	2.28	2.41	2.26
P2O5	0.04	0.02	0.03	0.25	0.25
MnO	0.44	0.23	0.22	0.35	0.37
Li2O					
Rb2O					
Ba	71	18	12	180	195
Co	33		19		27
Cr	4	15	2	23	17
Cu	76		9		7
Nb	600		804		855
Ni	24	7	18	9	24
Sc	76		85		42
Sr	7	5	2	11	9
V	47	51	54	123	137
Y	116	25	22	472	328
Zn	295		403		157
Zr *	54	110	75	1134	508
La	83		30		409
Ce	174		65		814
Nd	45		7		251
Sm	13		5		58
Eu	0		0		1
Dy	17		4		47
Yb	15		2		37
H2O -				0.28	
H2O+ Pyr				3.30	
H2O+ Silica					
F				1.14	
Cl				0.17	
TOTAL		97.26		99.97	
OH=F,Cl				0.52	
TOTAL		97.26		99.45	

"Size" indicates grainsize of mica concentrate.
"Majors: Pt" indicates lithium metaborate fusion in a platinum crucible, "Majors: C" in a graphite crucible; "Trace" preparation by dissolution in HF-perchloric acid mixture.

APPENDIX C.3 TABLE OF ELECTRON MICROPROBE MINERAL ANALYSES

DRILL HOLE	81-1 69.06	81-1 69.06	81-1 69.06	81-1 69.06	81-1 69.06
MINERALOGY	PYROXENE	PYROXENE	PYROXENE	PYROXENE	PYROXENE
FILE NO.	LIV1223	LIV1225	LIV1227	LIV1231	LIV1236
SiO2	54.45	54.61	52.25	54.82	55.38
CaO	25.75	26.09	24.46	26.42	25.74
MgO	17.37	17.40	11.38	16.09	17.17
FeO	2.99	2.60	10.91	3.60	2.30
MnO			1.96		0.15
Al2O3					
TiO2/others					
K2O					
Na2O					
TOTAL	100.56	100.70	100.96	100.93	100.75

DRILL HOLE	81-3 50.94	81-3 50.94	81-3 50.94	81-3 50.94	81-3 50.94
MINERALOGY	PYROXENE	PYROXENE	PYROXENE	ACTINOLITE	ACTINOLITE
FILE NO.	LIV759	LIV761	LIV764	LIV768	LIV769
SiO2	54.96	55.10	55.33	56.48	56.14
CaO	25.59	25.57	25.61	12.58	13.29
MgO	15.86	15.75	15.63	15.68	14.69
FeO	2.21	2.24	2.46	10.81	11.97
MnO	15.86	0.15	0.29	0.63	0.58
Al2O3	0.12	0.19	0.13	0.41	0.70
TiO2/others					
K2O					
Na2O					
TOTAL	98.99	99.00	99.45	96.59	97.37

DRILL HOLE	81-3 61.00 PB	81-3 61.00 PB	81-3 62.12TS	81-3 62.12	81-3 62.12
MINERALOGY	PYROXENE	CALCITE	PYROXENE	PYROXENE	PYROXENE
FILE NO.	LIV1340	LIV1342	LIV247	LIV248	LIV267
SiO2	52.89	1.18	53.82	53.32	53.34
CaO	25.13	50.41	26.06	25.59	25.69
MgO	13.70	0.79	12.35	10.87	11.06
FeO	8.33	0.69	7.46	9.50	8.74
MnO	1.03	2.73	1.23	1.76	1.57
Al2O3			*0.47	*0.33	0.00
TiO2/others					
K2O					
Na2O					
TOTAL	101.08	55.80	101.37	101.35	100.40

DRILL HOLE	81-3 75.07PB	81-3 78.67	81-3 78.67	81-3 79.65PB	81-3 79.65PB
MINERALOGY	CALCITE	FRDK	FRDK	CALCITE	PYROXENE
FILE NO.	LIV1241	LIV1587	LIV1602	LIV1386	LIV1391
SiO2	*0.163	47.66	34.55	1.15	55.73
CaO	46.09	18.30	10.50	53.19	26.66
MgO	2.60	15.39	12.43	0.72	17.26
FeO	*0.487	0.92	0.41	*.009	1.59
MnO				0.78	*.10
Al2O3					
TiO2/others					
K2O					
Na2O					
TOTAL	49.34	82.27	57.89	55.86	101.33

DRILL HOLE		81-1 76.54	81-1 76.54	81-1 76.54	81-1 76.54
MINERALOGY	PYROXENE	PYROXENE	PYROXENE	PYROXENE	PYROXENE
FILE NO.	LIV1237	LIV468	LIV469	LIV470	LIV477
SiO2	54.54	55.01	55.12	55.36	55.23
CaO	26.79	26.79	26.34	26.19	26.56
MgO	16.99	15.61	15.85	16.10	15.83
FeO	3.86	1.77	1.42	1.53	1.37
MnO		0.47	0.17	0.35	0.44
Al2O3		0.00	0.38	0.28	0.44
TiO2/others		0.15	0.00	0.01	0.00
K2O					
Na2O					
TOTAL	102.19	99.79	99.27	99.82	99.86

DRILL HOLE	81-3 50.94	81-3 50.94	81-3 50.94	81-3 50.94	81-3 50.94
MINERALOGY	ACTINOLITE	ACTINOLITE	ACTINOLITE	ACTINOLITE	ACTINOLITE
FILE NO.	LIV770	LIV771	LIV774	LIV775	LIV777
SiO2	56.19	55.57	56.17	54.61	54.81
CaO	12.71	12.84	12.69	12.54	12.13
MgO	14.66	15.03	15.44	13.42	13.00
FeO	12.33	11.62	11.37	13.88	13.09
MnO	0.51	0.58	0.46	0.66	0.70
Al2O3	0.72	0.55	0.57	0.81	1.34
TiO2/others					
K2O					
Na2O					
TOTAL	97.13	96.19	96.69	95.92	95.06

DRILL HOLE	81-3 62.12	81-3 62.12	81-3 62.12	81-3 62.12	81-3 62.12
MINERALOGY	PYROXENE	PYROXENE	PYROXENE	PYROXENE	PYROXENE
FILE NO.	LIV268	LIV269	LIV270	LIV271	LIV272
SiO2	55.03	55.18	55.85	55.78	54.69
CaO	26.57	26.11	26.75	26.70	26.19
MgO	15.75	15.18	15.74	15.72	12.56
FeO	2.02	3.35	1.91	1.91	6.58
MnO	0.45	0.60	*0.28	0.28	0.76
Al2O3	0.00	0.01	*0.16	0.18	0.69
TiO2/others					
K2O					
Na2O					
TOTAL	99.83	100.42	100.69	100.56	101.46

DRILL HOLE	81-3 79.65PB	81-3 79.65PB	81-3 79.65PB	81-3 79.65PB	81-3 79.65PB
MINERALOGY	PYROXENE	PYROXENE	PYROXENE	PYROXENE	PYROXENE
FILE NO.	LIV1392	LIV1394	LIV1395	LIV1397	LIV1398
SiO2	55.75	55.18	53.74	54.90	55.31
CaO	25.67	25.78	25.41	26.53	25.47
MgO	17.42	16.00	18.44	17.98	17.84
FeO	1.77	3.08	1.28	1.82	1.47
MnO			*.21		
Al2O3					
TiO2/others					
K2O					
Na2O					
TOTAL	100.61	100.03	99.07	101.23	100.08

DRILL HOLE	81-1 77.92PB	81-1 77.92PB	81-1 77.92PB	81-1 77.92PB	81-1 77.92PB
MINERALOGY	CHON/HUM	CHON/HUM	CHON/HUM	CHON/HUM	CHON/HUM
FILE NO.	LIV1287	LIV1288	LIV1291	LIV1292	LIV1295
SiO2	34.83	54.00	48.66	49.33	36.89
CaO	16.35	*0.229	0.31	*0.111	0.76
MgO	23.50	28.54	29.92	31.01	29.15
FeO	6.44	3.98	6.17	7.12	8.76
MnO					
Al2O3	5.72	2.18	6.23	6.55	11.36
TiO2/others					
K2O					
Na2O					
TOTAL	86.83	88.93	91.29	94.11	86.91

DRILL HOLE	81-3 50.94	81-3 50.94	81-3 50.94	81-3 50.94	81-3 50.94
MINERALOGY	ACTINOLITE	ACTINOLITE	ACTINOLITE	ACTINOLITE	ACTINOLITE
FILE NO.	LIV781	LIV783	LIV786	LIV787	LIV788
SiO2	55.44	54.94	54.86	54.34	55.76
CaO	12.58	12.12	12.06	12.53	12.23
MgO	13.34	13.47	13.28	13.46	13.84
FeO	14.51	13.50	14.80	13.91	13.77
MnO	0.68	0.77	0.63	0.69	0.52
Al2O3	1.10	0.55	0.85	1.08	0.97
TiO2/others				Zn= 0.01	
K2O			0.19	0.19	0.22
Na2O					
TOTAL	97.64	95.34	96.66	96.21	97.29

DRILL HOLE	81-3 62.12	81-3 62.12	81-3 62.12	81-3 62.12	81-3 62.12
MINERALOGY	PYROXENE	PYROXENE	PYROXENE	PYROXENE	PYROXENE
FILE NO.	LIV276	LIV277	LIV282	LIV283	LIV286
SiO2	54.12	55.67	53.88	54.49	54.14
CaO	25.75	27.01	25.86	26.14	26.26
MgO	11.22	15.57	11.64	13.33	12.99
FeO	8.65	1.70	8.04	5.50	5.20
MnO	1.24	0.28	1.49	0.87	0.87
Al2O3	0.00	0.00	*0.31		0.46
TiO2/others					
K2O					
Na2O					
TOTAL	100.98	100.23	101.21	100.34	99.90

DRILL HOLE	81-3 79.65PB	81-3 79.65PB	81-3 79.65PB	81-3 79.65PB	81-3 79.65PB
MINERALOGY	PYROXENE	PYROXENE	PYROXENE	PYROXENE	PYROXENE
FILE NO.	LIV1399	LIV1400	LIV1402	LIV1405	LIV1407
SiO2	54.14	55.34	55.87	54.42	54.07
CaO	25.73	26.16	24.94	26.05	25.67
MgO	18.70	17.80	17.45	17.73	17.58
FeO	1.80	2.14	2.49	1.65	1.98
MnO				0.77	0.61
Al2O3					
TiO2/others					
K2O					
Na2O					
TOTAL	100.37	101.44	100.76	100.63	99.91

DRILL HOLE MINERALOGY FILE NO.	81-1 77.92PB CHON/HUM LIV1296	81-1 81.32 PYROXENE LIV1154	81-1 81.32 PYROXENE LIV1157	81-1 81.32 PYROXENE LIV1160	81-1 81.32 PYROXENE LIV1161
SiO2	56.17	54.75	54.88	54.74	54.15
CaO	*0.149	25.87	26.21	26.53	26.22
MgO	29.67	18.39	18.15	17.66	16.39
FeO	4.29	0.87	0.91	1.62	2.07
MnO		0.28	0.32		0.15
Al2O3	1.29				
TiO2/others					
K2O					
Na2O					
TOTAL	91.56	100.15	100.48	100.55	98.98

DRILL HOLE MINERALOGY FILE NO.	81-3 51.55 PYROXENE LIV332	81-3 51.55 PYROXENE LIV334	81-3 51.55 PYROXENE LIV335	81-3 51.55 PYROXENE LIV338	81-3 51.55 ACTINOLITE LIV342
SiO2	55.90	56.12	55.47	54.65	56.48
CaO	26.70	26.06	26.81	25.86	13.57
MgO	16.62	15.88	15.96	12.27	13.45
FeO	0.81	1.54	1.21	6.68	14.36
MnO	0.21	0.42	0.29	0.63	0.81
Al2O3	0.11	0.14	0.00	0.23	0.52
TiO2/others					0.02
K2O					
Na2O					
TOTAL	100.35	100.15	99.74	100.31	99.22

DRILL HOLE MINERALOGY FILE NO.	81-3 62.12TS PYROXENE LIV288	81-3 62.12TS PYROXENE LIV1640	81-3 62.12TS PYROXENE LIV1642	81-3 62.12PB PYROXENE LIV1347	81-3 62.12PB PYROXENE LIV1348
SiO2	53.03	54.38	52.75	52.75	54.17
CaO	25.31	26.37	25.83	24.98	25.30
MgO	9.49	16.79	11.99	13.11	17.13
FeO	11.36	1.29	9.28	7.53	3.06
MnO	1.51			1.35	0.95
Al2O3	0.18				
TiO2/others					
K2O					
Na2O					
TOTAL	100.87	98.83	99.85	99.72	100.62

DRILL HOLE MINERALOGY FILE NO.	81-3 79.65PB PYROXENE LIV1408	81-3 79.65PB PYROXENE LIV1411	81-3 79.65PB PYROXENE LIV1416	81-3 79.65PB PYROXENE LIV1420	81-3 79.65PB PYROXENE LIV1423
SiO2	54.40	54.72	56.60	54.45	54.48
CaO	26.07	25.95	26.09	25.41	25.44
MgO	17.38	16.30	16.73	18.06	17.14
FeO	2.18	2.52	2.12	1.42	1.96
MnO					
Al2O3					
TiO2/others					
K2O					
Na2O					
TOTAL	100.03	99.50	101.53	99.34	99.02

DRILL HOLE MINERALOGY FILE NO.	81-1 81.32 PYROXENE LIV1163	81-1 81.32 PYROXENE LIV1164	81-1 81.32 PYROXENE LIV1167	81-1 81.32 PYROXENE LIV1171	81-1 81.32 PYROXENE LIV1175
SiO2	53.94	54.66	54.90	55.19	54.26
CaO	26.28	26.48	26.64	26.73	26.90
MgO	18.02	18.76	17.69	16.59	17.86
FeO	0.54	0.39	1.50	2.26	2.03
MnO	0.41				
Al2O3					
TiO2/others					
K2O					
Na2O					
TOTAL	98.77	100.29	100.72	100.77	101.04

DRILL HOLE MINERALOGY FILE NO.	81-3 51.55 ACTINOLITE LIV343	81-3 51.55 ACTINOLITE LIV344	81-3 51.55 ACTINOLITE LIV349	81-3 51.55 ACTINOLITE LIV352	81-3 51.55 ACTINOLITE LIV353
SiO2	56.85	56.69	54.55	57.03	57.03
CaO	12.94	11.99	12.00	13.21	13.21
MgO	14.77	13.79	13.86	14.32	14.32
FeO	15.20	15.47	17.12	15.13	15.13
MnO	0.64	1.15	0.48	0.86	0.86
Al2O3	0.62	0.54	0.57	0.47	0.47
TiO2/others		0.04	0.19	0.01	0.01
K2O					
Na2O					
TOTAL	101.02	99.65	98.78	101.03	101.03

DRILL HOLE MINERALOGY FILE NO.	81-3 62.12PB PYROXENE LIV1354	81-3 62.12PB PYROXENE LIV1357	81-3 62.12PB PYROXENE LIV1358	81-3 62.12PB PYROXENE LIV1359	81-3 62.12PB PYROXENE LIV1362
SiO2	55.62	53.24	53.93	53.27	53.83
CaO	24.89	25.21	24.75	24.99	25.80
MgO	17.30	13.90	11.63	14.30	16.21
FeO	2.60	6.61	8.72	6.88	2.76
MnO		0.81	1.16	0.72	0.86
Al2O3					
TiO2/others					
K2O					
Na2O					
TOTAL	100.40	99.77	100.19	100.15	99.45

DRILL HOLE MINERALOGY FILE NO.	81-3 79.65PB Mean 1391-1423	81-3 79.65PB σ 16 Analyses	81-3 80.55 PYROXENE LIV560	81-3 80.55 PYROXENE LIV566	81-3 80.55 CARBONATE LIV568
SiO2	54.95	0.78	54.95	55.92	0.32
CaO	25.81	0.45	26.33	26.37	53.81
MgO	17.49	0.71	15.93	16.11	0.24
FeO	1.95	0.47	1.93	1.47	0.05
MnO	0.11	0.24	0.35	0.61	1.43
Al2O3			0.44	0.39	0.62
TiO2/others					
K2O					
Na2O					
TOTAL	100.31		99.92	100.87	56.49

DRILL HOLE	81-1 81.32	81-1 81.32	81-1 81.32	81-1 81.32	81-1 81.32
MINERALOGY	PYROXENE	PYROXENE	PYROXENE	PYROXENE	PYROXENE
FILE NO.	LIV1178	LIV1181	LIV1182	LIV1183	LIV1189
SiO2	54.82	54.54	54.52	54.62	54.68
CaO	25.89	25.87	26.40	26.18	26.20
MgO	17.13	17.10	18.34	16.43	18.54
FeO	2.78	2.45	1.35	1.81	
MnO					
Al2O3					
TiO2/others					
K2O					
Na2O					
TOTAL	100.61	99.97	100.61	99.04	99.42

DRILL HOLE	81-3 51.55	81-3 51.55	81-3 51.55	81-3 51.55	81-3 52.05
MINERALOGY	ACTINOLITE	ACTINOLITE	ACTINOLITE	ACTINOLITE	PYROXENE
FILE NO.	LIV354	LIV360	LIV363	LIV364	LIV856
SiO2	56.59	55.63	56.94	56.59	52.67
CaO	13.00	12.28	13.56	13.05	24.85
MgO	14.47	12.55	13.93	12.36	6.84
FeO	14.08	16.88	14.57	17.74	15.51
MnO	0.60	0.83	0.80	0.93	1.90
Al2O3	0.88	0.83	0.51	0.24	
TiO2/others	0.00		0.00	0.00	
K2O					
Na2O		0.69			
TOTAL	99.63	99.69	100.32	100.90	101.77

DRILL HOLE	81-3 62.12PB	81-3 62.12PB	81-3 62.12PB	81-3 62.12PB	81-3 62.12PB
MINERALOGY	PYROXENE	PYROXENE	PYROXENE	PYROXENE	CHOND.?
FILE NO.	LIV1363	LIV1364	LIV1365	LIV1370	LIV1371
SiO2	52.93	53.73	53.08	54.43	47.51
CaO	24.25	25.34	24.90	26.05	4.19
MgO	13.34	16.56	11.90	17.48	16.00
FeO	7.50	3.09	9.88	1.69	13.16
MnO	1.32	0.32	1.32	0.51	0.81
Al2O3					
TiO2/others					
K2O					
Na2O					
TOTAL	99.32	99.03	101.08	100.15	81.67

DRILL HOLE	81-3 80.55	81-3 80.55	81-3 80.55	81-3 80.55	81-3 80.55
MINERALOGY	PYROXENE	PYROXENE	PYROXENE	PYROXENE	PYROXENE
FILE NO.	LIV573	LIV574	LIV575	LIV578	LIV579
SiO2	54.87	55.43	55.48	55.64	55.22
CaO	26.47	26.67	26.27	26.86	26.35
MgO	15.18	15.58	15.71	16.21	15.01
FeO	2.70	1.55	1.62	1.05	2.84
MnO	0.43	0.28	0.27	0.59	0.47
Al2O3	0.38	0.23	0.00	0.10	
TiO2/others					
K2O					
Na2O					
TOTAL	100.03	99.74	99.36	100.44	99.89

DRILL HOLE	81-1 81.32	81-1 81.32	81-1 81.32	81-1 81.32	81-1 81.32
MINERALOGY	PYROXENE	PYROXENE	PYROXENE	PYROXENE	PYROXENE
FILE NO.	LIV1190	LIV1193	LIV1196	LIV1199	LIV1200
SiO2	55.31	55.12	54.15	54.88	53.91
CaO	26.02	26.29	26.23	26.53	25.94
MgO	18.11	17.93	19.01	17.72	17.28
FeO	1.08	0.40	1.19	1.29	2.19
MnO					
Al2O3					
TiO2/others					
K2O					
Na2O					
TOTAL	100.52	99.74	100.58	100.43	99.32

DRILL HOLE	81-3 52.05	81-3 54.14	81-3 54.14	81-3 54.14	81-3 54.14
MINERALOGY	PYROXENE	CALCITE	PYROXENE	PYROXENE	PYROXENE
FILE NO.	LIV857	LIV482	LIV489	LIV490	LIV492
SiO2	51.95	0.40	53.48	54.19	53.31
CaO	22.67	51.78	25.42	26.06	25.06
MgO	9.06	0.00	10.59	13.17	9.69
FeO	14.98	0.24	9.63	5.55	11.12
MnO	1.11	3.30	1.32	0.84	1.47
Al2O3		0.37	0.35	0.38	0.35
TiO2/others		0.00	0.03	0.00	0.00
K2O					
Na2O					
TOTAL	99.78	56.09	100.82	100.18	100.98

DRILL HOLE	81-3 62.12PB	81-3 62.12PB	81-3 62.12PB	81-3 62.12PB	81-3 62.60PB
MINERALOGY	PYROXENE	PYROXENE	PYROXENE	PYROXENE	PYROXENE
FILE NO.	LIV1374	LIV1375	LIV1376	LIV1379	LIV1506
SiO2	51.78	52.81	50.78	52.53	56.94
CaO	25.02	25.03	24.13	25.29	20.91
MgO	9.97	15.23	9.18	13.82	20.76
FeO	10.15	6.66	13.18	6.33	1.65
MnO	2.43	0.76	1.89	1.04	0.41
Al2O3					
TiO2/others					
K2O					
Na2O					
TOTAL	99.35	100.48	99.16	99.01	100.66

DRILL HOLE	81-3 80.55	81-3 80.55	81-3 80.55	81-3 80.55	81-3 80.55
MINERALOGY	PYROXENE	PYROXENE	PYROXENE	PYROXENE	PYROXENE
FILE NO.	LIV581	LIV583	LIV584	LIV586	LIV587
SiO2	55.72	55.98	55.15	55.14	55.55
CaO	25.91	26.89	25.29	26.40	26.75
MgO	15.29	15.70	15.63	15.00	15.90
FeO	2.80	1.30	2.41	2.79	1.31
MnO	0.50	0.32	0.35	0.41	0.56
Al2O3	0.05	0.10	0.26	0.02	0.03
TiO2/others					
K2O					
Na2O					
TOTAL	100.25	100.29	99.09	99.75	100.09

DRILL HOLE MINERALOGY FILE NO.	81-1 81.32 PYROXENE LIV1203	81-1 81.32 PYROXENE LIV1204	81-1 81.32 QUARTZ LIV1206	81-1 81.32 PYROXENE LIV1211	81-1 81.32 PYROXENE LIV1213
SiO2	54.11	54.60	99.66	54.15	54.72
CaO	25.99	26.60	0.00	26.43	25.76
MgO	17.56	16.47	*.201	16.40	16.75
FeO	1.60	2.67	*.131	2.63	3.23
MnO					
Al2O3					
TiO2/others					
K2O					
Na2O					
TOTAL	99.26	100.34	99.99	99.61	100.46

DRILL HOLE MINERALOGY FILE NO.	81-3 54.14 F/ACTIN. LIV501	81-3 54.14 PYROXENE LIV511	81-3 54.14 PYROXENE LIV520	81-3 59.64 GARNET LIV649	81-3 59.64 PYROXENE LIV842
SiO2	52.44	49.61	50.01	38.13	51.02
CaO	3.66	23.33	23.75	35.36	24.47
MgO	3.80	1.74	3.31	0.02	6.07
FeO	36.27	23.35	20.32	17.07	16.92
MnO	5.53	3.76	3.09	1.38	2.18
Al2O3			0.21	9.28	
TiO2/others					
K2O					
Na2O					
TOTAL	101.70	101.79	100.69	101.24	100.65

DRILL HOLE MINERALOGY FILE NO.	81-3 62.60PB PYROXENE LIV1507	81-3 62.60PB PYROXENE LIV1508	81-3 62.60PB PYROXENE LIV1509	81-3 62.60PB PYROXENE LIV1510	81-3 62.60PB PYROXENE LIV1512
SiO2	55.17	54.50	53.80	53.05	54.17
CaO	23.53	24.02	22.86	25.95	21.41
MgO	18.77	17.85	17.83	14.85	16.52
FeO	1.83	2.06	1.99	4.63	5.32
MnO		*0.05	*0.29		
Al2O3					
TiO2/others					
K2O					
Na2O					
TOTAL	99.31	98.48	96.77	98.48	97.42

DRILL HOLE MINERALOGY FILE NO.	81-3 80.55 PYROXENE LIV594	81-3 81.45 PYROXENE LIV871	81-3 81.45 PYROXENE LIV872	81-3 81.45 PYROXENE LIV874	81-3 81.45 PYROXENE LIV875
SiO2	56.37	56.15	56.30	56.55	56.70
CaO	26.68	26.51	26.78	26.80	27.18
MgO	16.17	15.75	15.81	16.67	16.30
FeO	1.24	1.25	0.79	0.88	
MnO	0.17	0.27	0.33		
Al2O3	0.31	0.31	0.00		
TiO2/others		0.03	0.00		
K2O					
Na2O					
TOTAL	100.95	100.27	100.01	100.90	100.17

DRILL HOLE MINERALOGY FILE NO.	81-1 81.32 PYROXENE LIV1215	81-1 81.32 PYROXENE LIV1218	81-1 81.32 PYROXENE LIV1219	81-1 81.32 PYROXENE LIV1220	81-1 81.32 PYROXENE LIV1223
SiO2	54.50	54.18	55.30	54.38	54.45
CaO	26.71	26.22	26.69	26.66	25.75
MgO	17.16	18.13	16.91	18.11	17.37
FeO	2.05	1.45	1.60	1.29	2.99
MnO					
Al2O3					
TiO2/others					
K2O					
Na2O					
TOTAL	100.42	99.96	100.50	100.43	100.56

DRILL HOLE MINERALOGY FILE NO.	LIV843	81-3 59.64 PYROXENE LIV845	81-3 59.64 GARNET LIV656	81-3 60.00 GARNET LIV162	81-3 60.00 GARNET LIV164
SiO2	52.38	52.08	38.09	37.01	37.22
CaO	25.26	24.30	35.12	34.81	35.03
MgO	8.28	6.52		0.00	0.00
FeO	13.54	15.54	17.16	22.23	21.53
MnO	1.67	2.53	1.24	1.19	0.88
Al2O3		0.05	9.10	5.15	5.83
TiO2/others					
K2O					
Na2O					
TOTAL	101.13	101.00	100.70	100.38	100.48

DRILL HOLE MINERALOGY FILE NO.	81-3 62.60PB AMPHIBOLE LIV1514	81-3 62.60PB PYROXENE LIV1515	81-3 62.60PB PYROXENE LIV1516	81-3 62.60PB AMPHIBOLE LIV1518	81-3 62.60PB PYROXENE LIV1521
SiO2	56.82	52.47	54.38	57.63	50.98
CaO	14.05	26.10	26.69	13.95	24.50
MgO	21.47	15.40	17.28	22.61	9.86
FeO	3.94	2.41	1.54	2.60	12.12
MnO			0.61	0.33	2.03
Al2O3					
TiO2/others					
K2O					
Na2O					
TOTAL	96.28	96.37	100.51	97.11	99.49

DRILL HOLE MINERALOGY FILE NO.	81-3 81.45 PYROXENE LIV877	81-3 81.45 PYROXENE LIV878	81-3 81.45 VESUVIANITE LIV882	81-3 81.45 VESUVIANITE LIV883	81-3 81.45 VESUVIANITE LIV884
SiO2	56.01	55.29	38.66	37.78	38.10
CaO	26.38	26.91	36.43	36.36	37.37
MgO	16.33	16.30	1.94	2.77	1.88
FeO	0.77	1.10	3.34	4.22	3.47
MnO	0.23	0.24	0.26	0.49	0.16
Al2O3			17.24	13.31	16.35
TiO2/others			1.26	3.76	1.13
K2O					
Na2O			Cl=0.64	Cl=0.70	Cl=0.65
TOTAL	99.71	99.84	99.77	99.38	99.10

DRILL HOLE	81-1 81.32	81-1 81.32	81-3 47.67	81-3 47.67	81-3 47.67
MINERALOGY	Mean of:	σ	PYROXENE	PYROXENE	AUGITE (?)
FILE NO.	1154-1223	27 Analyses	LIV296	LIV297	LIV300
SiO2	54.59	0.40	51.53	52.19	48.24
CaO	26.31	0.32	24.08	25.37	24.44
MgO	17.59	0.76	6.61	7.51	6.04
FeO	1.65	0.83	17.05	14.10	6.30
MnO	0.05	0.11	1.19	1.61	0.89
Al2O3			0.00	0.32	8.46
TiO2/others					
K2O					
Na2O					
TOTAL	100.18		100.46	101.10	99.58

DRILL HOLE	81-3 60.00	81-3 60.00	81-3 60.00	81-3 60.00	81-3 60.00
MINERALOGY	GARNET	GARNET	GARNET	GARNET	GARNET
FILE NO.	LIV166	LIV171	LIV175	LIV176	LIV177
SiO2	37.11	37.96	37.55	37.37	37.32
CaO	34.15	34.72	34.97	34.85	34.22
MgO	0.00	0.00	0.00	0.06	0.00
FeO	17.74	21.66	20.17	21.22	20.94
MnO	1.60	1.33	1.34	0.77	1.03
Al2O3	8.88	5.54	6.87	6.14	5.76
TiO2/others					
K2O					
Na2O					
TOTAL	99.48	101.21	100.90	100.41	99.28

DRILL HOLE	81-3 62.60PB	81-3 62.60PB	81-3 62.60TS	81-3 62.60TS	81-3 62.60TS
MINERALOGY	PYROXENE	PYROXENE	PYROXENE	PYROXENE	PYROXENE
FILE NO.	LIV1523	LIV1524	LIV1565	LIV1567	LIV1568
SiO2	51.45	52.73	52.01	51.72	50.96
CaO	25.61	25.31	24.91	25.00	24.86
MgO	10.75	11.01	10.91	10.08	10.83
FeO	9.63	9.45	9.54	11.26	9.99
MnO	2.57	2.29	2.47	2.68	3.20
Al2O3					
TiO2/others					
K2O					
Na2O					
TOTAL	100.00	100.79	99.83	100.74	99.84

DRILL HOLE	81-3 81.45	81-3 81.45	81-3 81.45	81-3 81.45	81-3 81.45
MINERALOGY	VESUVIANITE	PYROXENE	PYROXENE	VESUVIANITE	VESUVIANITE
FILE NO.	LIV885	LIV889	LIV890	LIV891	LIV892
SiO2	38.59	55.91	55.55	37.55	37.95
CaO	37.03	26.72	27.57	36.49	36.89
MgO	1.44	15.87	15.91	1.85	1.90
FeO	4.29	1.34	1.75	3.18	3.33
MnO	0.04				0.42
Al2O3	16.53	0.04		16.63	17.00
TiO2/others	1.44			1.33	1.17
K2O		0.08			
Na2O	Cl=0.71			Cl=0.76	Cl=0.74
TOTAL	100.09	99.95	100.77	98.12	99.40

DRILL HOLE MINERALOGY FILE NO.	81-3 47.67 SCAPOLITE LIV302	81-3 47.67 SCAPOLITE LIV305	81-3 47.67 SCAPOLITE LIV316	81-3 47.67 SCAPOLITE LIV317	81-3 47.67 PYROXENE LIV319
SiO2	44.97	44.70	44.88	44.33	52.75
CaO	20.02	19.61	19.07	20.22	25.63
MgO	0.00	0.06		0.00	9.81
FeO	0.15	1.68		0.45	11.14
MnO	0.00	0.10		0.28	1.35
Al2O3	35.00	34.40	34.61	33.11	
TiO2/others	0.21	0.00		0.27	
K2O					
Na2O			1.41		
TOTAL	100.35	100.56	99.98	98.67	100.66

DRILL HOLE MINERALOGY FILE NO.	81-3 60.00 GARNET LIV178	81-3 60.00 GARNET LIV190	81-3 60.00 GARNET LIV192	81-3 60.00 CALCITE LIV199	81-3 60.00 GARNET LIV202
SiO2	37.39	37.03	37.20	0.98	37.48
CaO	33.65	34.67	34.85	53.91	34.73
MgO	0.00	0.00	0.00	0.13	0.00
FeO	20.09	22.65	22.72	0.65	20.32
MnO	1.65	0.76	0.77	1.65	1.15
Al2O3	7.63	4.54	4.55	0.52	6.66
TiO2/others					
K2O					
Na2O					
TOTAL	100.45	99.64	100.09	57.84	100.33

DRILL HOLE MINERALOGY FILE NO.	81-3 62.60TS PYROXENE LIV1569	81-3 62.60TS PYROXENE LIV1572	81-3 62.60TS PYROXENE LIV1574	81-3 63.86 PYROXENE LIV597	81-3 63.86 PYROXENE LIV598
SiO2	51.51	52.54	51.86	53.40	53.66
CaO	25.21	26.03	25.58	25.14	25.90
MgO	10.18	12.45	9.96	12.05	11.65
FeO	11.07	7.51	10.46	7.50	6.66
MnO	2.84	0.71	2.63	1.76	2.40
Al2O3				0.00	0.00
TiO2/others					
K2O					
Na2O					
TOTAL	100.80	99.25	100.49	99.84	100.27

DRILL HOLE MINERALOGY FILE NO.	81-3 81.45 VESUVIANITE LIV895	81-3 81.45 PYROXENE LIV898	81-3 81.45 PYROXENE LIV899	81-3 81.45 PYROXENE LIV901	81-3 81.45 PYROXENE LIV902
SiO2	38.76	56.63	56.59	56.42	56.61
CaO	36.89	27.03	26.84	26.77	26.74
MgO	1.72	16.05	16.31	16.71	16.51
FeO	3.73	1.05	0.98	1.20	0.80
MnO	0.39				0.40
Al2O3	16.81				
TiO2/others	1.36				
K2O					
Na2O	Cl=0.72				
TOTAL	100.38	100.75	100.73	101.09	101.06

DRILL HOLE	81-3 47.67	81-3 47.67	81-3 47.67	81-3 47.67	81-3 47.67
MINERALOGY	SCAPOLITE	SCAPOLITE	SCAPOLITE	SCAPOLITE	AMPHIBOLE
FILE NO.	LIV321	LIV323	LIV324	LIV327	LIV328
SiO2	44.30	44.96	43.95	44.40	51.67
CaO	20.58	20.34	20.70	20.14	24.29
MgO	0.00	0.00	0.09	0.00	8.75
FeO	0.19	0.00	0.49	0.38	9.67
MnO	0.04	0.09	0.00	*0.068	0.93
Al2O3	35.39	35.17	33.50	34.76	3.82
TiO2/others	0.06	0.00	0.94	0.00	*0.11
K2O					
Na2O					
TOTAL	100.54	100.56	99.68	99.75	99.24

DRILL HOLE	81-3 60.00	81-3 60.50	81-3 60.50	81-3 60.50	81-3 60.50
MINERALOGY	CALCITE				
FILE NO.	LIV204	LIV1301	LIV1302	LIV1303	LIV1304
SiO2	0.37	44.46	40.62	41.15	41.40
CaO	52.36	16.47	14.22	14.43	14.99
MgO	0.08	11.25	9.83	11.79	7.47
FeO	0.52	4.39	3.96	3.69	7.08
MnO	1.76	0.82	0.87	0.45	1.06
Al2O3	0.45				
TiO2/others					
K2O					
Na2O					
TOTAL	55.51	77.39	69.49	71.53	72.00

DRILL HOLE	81-3 63.86	81-3 63.86	81-3 63.86	81-3 63.86	81-3 63.86
MINERALOGY	PYROXENE	PYROXENE	PYROXENE	PYROXENE	PYROXENE
FILE NO.	LIV599	LIV604	LIV606	LIV618	LIV619
SiO2	54.00	54.04	54.04	53.86	54.61
CaO	25.27	25.46	25.98	25.89	25.23
MgO	12.05	12.14	12.21	12.02	11.84
FeO	6.45	7.14	7.51	7.71	7.19
MnO	2.03	1.47	0.96	1.44	1.94
Al2O3	0.00	0.12	0.18	0.00	0.00
TiO2/others					
K2O					
Na2O					
TOTAL	99.80	100.37	100.89	100.92	100.81

DRILL HOLE	81-3 81.45	81-3 81.45	81-3 81.45	81-3 81.45	81-3 81.45
MINERALOGY	PYROXENE	PYROXENE	PYROXENE	GARNET	PYROXENE
FILE NO.	LIV907	LIV909	LIV911	LIV914	LIV916
SiO2	56.42	56.26	55.58	37.75	56.17
CaO	27.22	26.94	26.19	36.66	26.71
MgO	15.95	15.85	15.93	2.55	15.09
FeO	1.10	1.17	1.94	4.94	2.53
MnO	0.26	0.24	0.19	0.22	0.26
Al2O3				14.39	
TiO2/others				2.50	
K2O				0.05	
Na2O				Cl=0.60	
TOTAL	100.95	100.46	99.83	99.66	100.78

DRILL HOLE MINERALOGY FILE NO.	81-3 47.67 SCAPOLITE LIV801	81-3 47.67 SCAPOLITE LIV802	 PYROXENE LIV807	81-3 47.67 SCAPOLITE LIV809	81-3 47.67 PYROXENE LIV812
SiO2	44.74	44.99	53.70	46.45	52.80
CaO	19.65	18.90	25.20	19.45	24.74
MgO	0.00	0.00	9.43	1.07	10.22
FeO	0.00	0.03	11.53	1.87	9.77
MnO	0.32	0.03	1.58	0.21	0.99
Al2O3	35.12	34.76	0.00	29.63	0.32
TiO2/others				0.16	0.00
K2O	0.02	0.08	0.00	0.08	0.00
Na2O	0.99	0.89	0.16	0.16	0.00
TOTAL	100.83	99.68	101.60	100.08	98.83

DRILL HOLE MINERALOGY FILE NO.	81-3 60.50 LIV1307	81-3 60.50 LIV1309	81-3 60.50 LIV1310	81-3 60.50 LIV1311	81-3 60.50 LIV1312
SiO2	43.62	39.53	40.14	39.74	43.63
CaO	17.21	14.09	13.61	14.61	16.09
MgO	7.68	6.82	12.14	8.91	6.96
FeO	9.21	5.57	2.44	5.02	8.62
MnO	1.74	0.99	0.59	0.81	1.94
Al2O3					
TiO2/others					
K2O					
Na2O					
TOTAL	79.46	67.00	68.91	69.09	77.23

DRILL HOLE MINERALOGY FILE NO.	81-3 63.86 PYROXENE LIV622	81-3 63.86 GARNET LIV625	81-3 63.86 PYROXENE LIV631	81-3 63.86 PYROXENE LIV634	81-3 66.80 LIV1536
SiO2	54.65	37.00	54.60	54.93	
CaO	25.72	34.07	25.67	27.08	
MgO	12.75	0.00	12.08	14.82	
FeO	6.49	25.93	7.46	2.60	
MnO	1.43	0.71	1.43	0.44	
Al2O3		2.42		0.52	
TiO2/others					
K2O			0.03		
Na2O					
TOTAL	101.04	100.13	101.26	100.39	

DRILL HOLE MINERALOGY FILE NO.	81-5B 106.75 PHENGITE LIV1251	81-5B 106.75 PHENGITE LIV1253	81-5B 106.75 PHENGITE LIV1255	81-5B 106.75 PHENGITE LIV1256	81-5B 106.75 PHENGITE LIV1257
SiO2	38.76	40.98	35.81	39.03	35.11
CaO	0.27	0.02	0.13	0.11	0.14
MgO					
FeO	27.66	24.69	31.97	27.23	31.63
MnO	1.39	0.98	1.84	2.46	2.81
Al2O3	18.98	20.36	17.60	19.12	16.45
TiO2/others					
K2O	9.18	9.63	9.03	9.08	8.70
Na2O	0.00	0.00	0.41	0.10	0.69
TOTAL	96.23	96.66	96.79	97.13	95.52

DRILL HOLE	81-3 47.67	81-3 47.67	81-3 47.67	81-3 47.67	81-3 48.33
MINERALOGY	PYROXENE	SCAPOLITE	SCAPOLITE	SCAPOLITE	ACTINOLITE
FILE NO.	LIV820	LIV827	LIV829	LIV831	LIV1120
SiO2	52.28	47.61	45.01	44.91	54.80
CaO	13.12	19.41	19.64	20.03	13.02
MgO	0.02	2.56	0.00	0.00	11.67
FeO	0.12	3.03	0.51	0.10	18.59
MnO	0.10	0.25	0.09	0.06	0.65
Al2O3	30.73	27.15	33.83	35.18	1.25
TiO2/others	0.15	0.00	0.00	0.00	
K2O	0.97	0.13	0.05	0.00	
Na2O	4.07	0.55	0.27	0.58	
TOTAL	101.55	100.68	99.40	100.86	99.98

DRILL HOLE	81-3 60.50	81-3 60.50	81-3 60.50	81-3 60.50	81-3 60.50
MINERALOGY	CALCITE				
FILE NO.	LIV1315	LIV1316	LIV1317	LIV1322	LIV1323
SiO2	12.24	39.66	40.97	46.06	42.64
CaO	27.78	13.76	15.10	18.32	15.98
MgO	2.38	9.23	10.68	9.92	7.36
FeO	2.38	5.17	4.93	7.52	8.39
MnO	1.66	0.72	0.94	1.05	1.51
Al2O3					
TiO2/others					
K2O					
Na2O					
TOTAL	46.44	68.54	72.62	82.87	75.89

DRILL HOLE	81-3 66.80	81-3 66.80	81-3 66.80	81-3 66.80	81-3 66.80
MINERALOGY					
FILE NO.	LIV1543	LIV1549	LIV1580	LIV1606	LIV1614
SiO2	25.10	23.46		23.50	23.43
CaO	5.98	6.98		5.44	6.05
MgO	9.90	8.45		8.88	9.73
FeO					
MnO					
Al2O3					
TiO2/others					
K2O					
Na2O					
TOTAL	40.98	38.90		37.82	39.21

DRILL HOLE	81-5B 106.75	81-5B 106.75	81-5B 106.75	81-8 188	81-8 188
MINERALOGY	PHENGITE	PHENGITE	PHENGITE	ANDRADITE	ANDRADITE
FILE NO.	LIV1259	LIV1260	LIV1261	LIV749	LIV750
SiO2	36.07	36.04	35.87	36.65	37.20
CaO	0.21	0.16	0.01	33.86	34.04
MgO				0.00	0.00
FeO	30.44	30.25	31.09	27.55	28.10
MnO	2.63	2.71	2.58	0.63	0.72
Al2O3	17.63	18.67	18.26	0.28	0.41
TiO2/others				0.00	0.02
K2O	8.91	9.12	8.78		
Na2O	0.78	0.31	0.00		
TOTAL	96.67	97.26	96.58	98.96	100.50

DRILL HOLE	81-3 48.33	81-3 48.33	81-3 48.33	81-3 48.33	81-3 48.33
MINERALOGY	PYROXENE	ACTINOLITE	PYROXENE	PYROXENE	PYROXENE
FILE NO.	LIV1125	LIV1126	LIV1128	LIV1131	LIV1134
SiO2	54.25	55.41	53.72	54.69	53.30
CaO	25.56	12.79	25.11	26.19	25.68
MgO	11.01	11.06	10.82	12.47	10.08
FeO	9.18	19.03	9.72	7.39	10.29
MnO	1.04	0.60	1.06	0.64	0.94
Al2O3	0.12	0.54	0.08	0.26	0.17
TiO2/others		Cl=0.11			Cl=0.05
K2O					
Na2O					
TOTAL	101.17	99.55	100.51	101.64	100.51

DRILL HOLE	81-3 60.50	81-3 61.00 TS	81-3 61.00 TS	81-3 61.00	81-3 61.00
MINERALOGY		PYROXENE	PYROXENE	PYROXENE	PYROXENE
FILE NO.	LIV1324	LIV213	LIV221	LIV228	LIV237
SiO2	41.01	52.43	55.72	54.34	54.27
CaO	15.09	25.40	25.77	26.14	25.79
MgO	4.46	9.08	14.63	11.54	11.01
FeO	7.87	12.61	4.22	8.20	8.95
MnO	1.93	1.35	0.57	0.92	1.22
Al2O3		0.16	0.11	0.00	0.24
TiO2/others					
K2O					
Na2O					
TOTAL	70.35	101.02	101.01	101.15	101.49

DRILL HOLE	81-3 66.80	81-3 67.35	81-3 67.35	81-3 67.35	81-3 67.35
MINERALOGY			MAGNETITE	PYROXENE	MAGNETITE
FILE NO.	LIV1615	LIV528	LIV534	LIV543	LIV547
SiO2	25.42	56.07	0.50	55.55	0.28
CaO	6.00	27.27	0.07	26.68	0.04
MgO	9.56	15.60	0.84	16.02	0.26
FeO		2.17	95.40	2.15	96.27
MnO		0.45	1.03	0.28	0.68
Al2O3		0.39	1.55	0.17	1.50
TiO2/others					
K2O					
Na2O					
TOTAL	40.98	101.95	99.38	100.85	99.04

DRILL HOLE	81-8 188	81-8 188	81-8 188	81-8 188	81-8 273'6"
MINERALOGY	ANDRADITE	ANDRADITE	ANDRADITE	ANDRADITE	ANDRADITE
FILE NO.	LIV752	LIV753	LIV754	TEST 2	LIV708
SiO2	36.96	36.33	36.61	36.91	37.44
CaO	33.86	33.92	33.90	34.10	34.25
MgO	0.07	0.23	0.30	0.23	0.00
FeO	27.71	27.72	28.23	28.14	27.34
MnO	0.46	0.70	0.23	0.44	0.43
Al2O3	0.25	0.34	0.21	0.11	0.48
TiO2/others	0.00	0.00	0.06	0.00	0.25
K2O					
Na2O					
TOTAL	99.30	99.28	99.54	99.92	100.19

DRILL HOLE MINERALOGY FILE NO.	81-3 48.33 PYROXENE LIV1136	81-3 48.33 PYROXENE LIV1137	81-3 48.33 ACTINOLITE LIV1141	81-3 48.33 PYROXENE LIV1143	81-3 48.33 PYROXENE LIV1144
SiO2	53.24	53.99	54.72	54.57	53.91
CaO	25.02	25.02	13.08	25.66	26.22
MgO	11.44	11.10	11.21	12.30	11.37
FeO	8.80	8.92	18.79	7.74	8.51
MnO	0.68	0.85	0.61	0.86	0.99
Al2O3	0.07	0.12	1.29	0.40	0.00
TiO2/others	Cl=0.03	Cl=0.01	Cl=0.05		
K2O					
Na2O					
TOTAL	99.28	100.00	99.74	101.56	101.00

DRILL HOLE MINERALOGY FILE NO.	81-3 61.00 TS PYROXENE LIV241	81-3 61.00 PYROXENE LIV243	81-3 61.00 PB PYROXENE LIV1328	81-3 61.00 PB PYROXENE LIV1332	81-3 61.00 PB PYROXENE LIV1333
SiO2	55.02	55.93	53.18	54.99	53.02
CaO	26.05	26.48	25.37	25.70	25.10
MgO	15.31	15.81	12.86	17.42	13.14
FeO	3.21	2.46	8.08	2.79	10.24
MnO	0.46	0.33	1.32	0.18	
Al2O3	0.30	0.13			
TiO2/others					
K2O					
Na2O					
TOTAL	100.35	101.13	100.81	101.08	101.49

DRILL HOLE MINERALOGY FILE NO.	81-3 67.35 PYROXENE LIV552	81-3 67.35 PYROXENE LIV554	81-3 67.35 PYROXENE LIV555	81-3 70.63TS LIV1623	81-3 70.63TS LIV1624
SiO2	55.91	55.37	54.62	33.64	33.68
CaO	26.33	26.42	26.73	9.84	9.63
MgO	15.66	15.82	15.42	*0.194	
FeO	1.82	1.80	2.78	22.13	22.92
MnO	0.46	0.30	0.59	1.61	0.74
Al2O3	0.18	0.19	0.05		
TiO2/others				*0.30	
K2O				1.71	1.47
Na2O				Cl=0.45	Cl=0.35
TOTAL	100.37	99.89	100.19	69.88	68.77

DRILL HOLE MINERALOGY FILE NO.	81-8 273'6" ANDRADITE LIV709	81-8 273'6" ANDRADITE LIV711	81-8 273'6" ANDRADITE LIV713	81-8 273'6" ANDRADITE LIV716	81-8 273'6" ANDRADITE LIV727
SiO2	36.98	37.39	36.30	36.46	37.26
CaO	34.51	34.20	34.40	34.09	34.21
MgO	0.36	0.00	0.10	0.09	0.05
FeO	27.90	28.36	27.84	27.63	27.24
MnO	0.48	0.33	0.45	0.82	0.52
Al2O3	0.46	0.69	0.51	0.43	0.80
TiO2/others	0.00	0.32	0.00	0.00	0.00
K2O					
Na2O					
TOTAL	100.70	101.29	99.58	99.51	100.07

DRILL HOLE	81-3 48.33	81-3 50.94
MINERALOGY	PYROXENE	PYROXENE
FILE NO.	LIV1149	LIV756
SiO2	51.85	55.41
CaO	24.42	26.30
MgO	8.91	16.53
FeO	13.79	1.79
MnO	1.11	0.48
Al2O3	0.49	0.15
TiO2/others		0.00
K2O		
Na2O		
TOTAL	100.57	100.65

DRILL HOLE	81-3 61.00 PB	81-3 61.00 PB
MINERALOGY	PYROXENE	PYROXENE
FILE NO.	LIV1338	LIV1339
SiO2	51.78	55.56
CaO	23.86	26.28
MgO	9.75	17.37
FeO	12.68	2.35
MnO	1.91	0.75
Al2O3		
TiO2/others		
K2O		
Na2O		
TOTAL	99.98	102.30

DRILL HOLE	81-3 70.63TS	81-3 70.63TS
MINERALOGY		
FILE NO.	LIV1625	LIV1626
SiO2	33.10	33.79
CaO	10.01	9.51
MgO		
FeO	21.52	23.48
MnO	0.78	1.07
Al2O3		
TiO2/others		
K2O	1.70	1.36
Na2O	Cl=0.52	Cl=0.33
TOTAL	67.64	70.26

DRILL HOLE	81-8 273'6"
MINERALOGY	ANDRADITE
FILE NO.	LIV728
SiO2	37.49
CaO	34.14
MgO	
FeO	27.90
MnO	0.70
Al2O3	
TiO2/others	0.00
K2O	
Na2O	
TOTAL	100.23

SPECIMEN	Facies/Pluton	K-FELDSPAR	PLAGIOCLASE	QUARTZ	BIOTITE	HORNBLENDE	MONAZITE	SPHENE	APATITE	ALLANITE	ZIRCON	OPAQUES	FLUORITE	TOTAL	TRAV. SPACE	NOTES
78/23-5	Ork/Li-mica	2358/ 36.0%	1931/ 29.5%	2258/ 34.5%	7/ 0.11%	0	0.00			0.00	0.00			6550	1/3 mm	
88/6-3	Megacrystic	3225/ 43.9%	1409/ 19.2%	2328/ 31.7%	383/ 5.2%	0	2/ 0.03%			0.00	0.00			7347	1/5 mm	
88/7-3	Even grained	3500/ 44.0%	1823/ 22.9%	2158/ 27.1%	476/ 6.0%	0	0.00			1/ 0.01%	3/ 0.04%			7961	1/5 mm	
88/8-9	Even grained	2302/ 30.6%	1680/ 22.3%	3121/ 41.4%	426/5.7%	0	0.00			0.00	4/ 0.05%			7533	1/5 mm	
88/9-8	Megacrystic	2761/ 38.0%	2191/ 30.2%	1746/ 24.0%	566/ 7.8%	0	0.00			0.00	3/ 0.04%			7267	1/5 mm	
88/9-9	Even grained	3520/ 47.2%	1426/ 19.1%	2233/ 30.0%	273/ 3.7%	0	0.00			0.00	1/ 0.01%			7453	1/5 mm	
88/11-1	Megacrystic	1780/ 46.4%	508/ 13.2%	1198/ 31.2%	330/ 8.6%	0	5/ 0.13%			15/0.39%				3836	1/5 mm	
88/12-1	Porphyry	2792/ 37.8%	1462/ 19.8%	2683/ 36.3%	435/ 5.9%	0	0.00			4/ 0.05%	0.00		11/ 0.15%	7387	1/3 mm	
88/12-7		3388/ 51.1%	958/ 14.4%	1837/ 27.7%	409/ 6.2%	34/ 0.51%	0.00			8/ 0.12%	0.00			6634	1/3 mm	
88/14-5	Even-grained	3096/ 43.9%	794/ 11.3%	2780/ 39.4%	357/ 5.1%	11/ 0.16%	0.00			1/ 0.01%	17/ 0.24%			7056	1/5 mm	
88/14-7N	Megacrystic	3670/ 46.5%	981/ 12.4%	2822/ 35.7%	383/ 4.9%	30/ 0.38%	7/ 0.09%			0.00	3/ 0.04%			7896	1/5 mm	
88/14-7S	Megacrystic	3755/ 47.6%	1315/ 16.7%	2563/ 32.5%	240/ 3.0%	0	0.00			22/ 0.28%	2/ 0.03%			7897	1/5 mm	
88/14-8	Even-grained	2196/ 36.0%	1434/ 23.5%	2388/ 39.1%	85/ 1.4%	0	0.00			0.00	0.00			6103	1/5 mm	
88/15-2	Porphyry	7954/ 51.3%	2344/ 15.1%	4051/ 26.1%	1001/ 6.5%	120/ 0.77%	26/ 0.2%			11/ 0.07%	3/ 0.02%			15510	1/10 mm	
88/15-3	Porphyry	4466/ 57.4%	1091/ 14.0%	1709/ 22.0%	451/ 5.8%	32/ 0.41%	29/ 0.37%				0.00		0	7778	1/3 mm	
88/15-6	Megacrystic	3373/ 43.7%	1485/ 19.2%	2407/ 31.2%	451/ 5.8%	0	0.00			0.00	10/ 0.13%			7726	1/3 mm	
88/17-2	Megacrystic	2225/ 37.4%	1377/ 23.1%	2063/ 34.6%	287/ 4.8%	0	0.00			3/ 0.05%	0.00			5955	1/3 mm	
97/28-5 L1	Megacrystic	3905/44.8%	1780/20.4%	2564/29.4%	426/4.8%	0	0.00	0.00	2.00	0.00	3/0.03%	32/0.37%	0	8712	1.2x0.05 mm	* Repeats
97/28-5 L2	Megacrystic	2163/28.3%	2584/33.8%	2407/31.5%	465/6.0%	0	0.00	0.00	5/0.07%	2/0.03%	0.00	11/0.14%	0	7638	0.6x0.1 mm	* cut
97/28-5 E1	Megacrystic	2482/31.06%	2414/30.21%	2507/31.37%	576/7.21%	0	0.00	0.00	2/0.03%	0.00	3/0.04%	2/0.03%	6/0.08%	7992	0.6x0.1 mm	* from
97/28-5 E2	Megacrystic	2297/39.66%	1585/27.37%	1610/27.80%	295/5.09%	0	0.00	0.00	2/0.03%	1/0.02%	2/0.03%	0.00	0	5793	0.6x0.1 mm	* same
97/28-5 W1	Megacrystic	2974/33.99%	2891/33.04%	2559/29.25%	302/3.45%	0	0.00	0.00	2/0.02%	0.00	2/0.02%	8/0.09%	11/0.13%	8749	0.6x0.1 mm	* block
97/28-5 W2	Megacrystic	2455/33.05%	1830/24.64%	2839/38.22%	287/3.86%	0	0.00	0.00	0.00	0.00	2/0.03%	4/0.05%	0	7428	0.6x0.1 mm	*
98/16-1	NWTM	2164/24.06%	3509/39.01%	1972/21.92%	0	1233/13.71%	0.00	50/0.56%	9/0.10%	0.00	5/0.06%	53/0.59%	0	8995	0.6x0.05 mm	
98/16-3	NWTM	1362/18.28%	2779/37.30%	1246/16.72%	47/0.63%	1792/24.05%	0.00	48/0.64%	55/0.74%	0.00	1/0.01%	82/1.10%	38/0.51%	7450	0.6x0.05 mm	
98/16-5	NWTM	1191/14.67%	3550/43.72%	1119/13.78%	0	2008/24.73%	0.00	41/0.50%	29/0.36%	0.00	0.00	162/2.00%	19/0.23%	8119	0.6x0.05 mm	
98/17-1	NWTM	1653/22.91%	2622/36.34%	1204/16.69%	0	1607/22.27%	0.00	40/0.55%	20/0.28%	0.00	0.00	66/0.91%	3/0.04%	7215	0.6x0.05 mm	
08/18-2	SWTM	118/1.31%	4744/52.78%	1704/18.96%	388/4.32%	1841/20.48%	0.00	35/0.39%	29/0.32%	0.00	0.00	127/1.41%	0	8988	1.2x0.05mm	Qtz may include KFS
08/18-3	SWTM	1382/13.87%	4436/44.52%	1575/15.81%	559/5.61%	1947/19.54%	0.00	4/0.04%	22/0.22%	0.00	1/0.01%	38/0.38%	0	9965	1.2x0.05mm	More reliable FS props.

Appendix C.4

Modal analyses of specimens from the Thirtymile, NW Thirtymile and SW Thirtymile stocks. Count per mineral phase, total for the section and percentages are shown. Note that the six sections of megacrystic granite 97/28-5 were sawn from the same block (one from each face of a rectangular parallelepiped). These demonstrate the variation resulting when a coarse-grained facies is counted. For this reason no counting was attempted from the Hake batholith megacrystic specimens, which are even coarser-grained.

d	81-3/ 60.50	6.55	6.51	4.496	3.262	3.028	3.003	2.975	2.905	2.579	2.536	2.324	2.1705	2.1435	2.1165	2.0527	2.0165	1.9685	1.8493	1.7638	1.6276	1.5847	1.5594	1.5586
ntensity	Fink Index	8	11	7	100	25	80	68	19	16	43	10	31	15	6	8	5 <1		5	36	24	24	9	9
illeyite	24-184			4.2	3.27		3.005	2.972			2.532	2.328			2.115					1.764 xxx	xxx	xxx		
illeyite	25-159			4.391	3.324	3.046	3.005	2.972		2.558	2.534	2.327			2.116		2.016	1.9719	1.8473 xxx	xxx	xxx	xxx	xxx	
hondrodite	14- 10			4.854	3.39		3.007		2.91		2.512			2.149			2.025			1.737			1.561	
linohumite	14- 9				3.224				2.919		2.538				2.188					1.79			1.541	
linohumite	31- 809				3.262		2.99			2.582	2.553			2.158			2.091		xxx	xxx	xxx	xxx		
lumite	12- 755				3.312				2.885	2.572			2.189			2.057				1.794				1.5575
	Diffractogram: Quartz used as internal standard																							

d	81-8/ 45.80	8.33	4.79	4.51	4.215	3.878	3.336	3.122	2.93	2.81	2.709	2.6	2.529	2.365	2.2675	2.166	2.045	2.017	1.9665	1.927	1.892	1.8645	1.801 Several	1.4428
ntensity	Fink Index s	w	w	w	w	vs	vs	w	vvw	s	w	m	m	w	m	m	m	vw	vw	vw	vvw	m		
remolite	13- 437	8.38	4.76	4.51	4.2	3.87	3.376	3.121	2.938	2.805	2.705	2.592	2.529	2.335	2.273	2.163	2.042	2.015	1.963	1.929	1.892	1.864	xxx	
remolite	31- 1285	8.44	4.76	4.51		3.87	3.38	3.13	2.944	2.805	2.706	2.59	2.527	2.331	2.269	2.162	2.047	2.018	1.961	1.932 xxx	xxx	xxx	xxx	
	Gandolfi camera																							

d	81-8/ 106.7	10.080	4.592				3.676		3.350		3.150	2.940	2.640	2.444	2.392			2.254		2.181	2.058	2.005	1.929	1.893	1.716	1.678	1.646	1.549	1.363	1.338	1.313	1.258
hlog. 2M1	10- 493	10.1	5.056	4.612	4.515	4.079	3.814	3.54	3.362	3.283	3.156	3.04	2.946	2.818	2.651	2.624																
hlogopite 3T	10- 492	10.1	5.022	4.596	4.558	3.941	3.663	3.408	3.354		3.148		2.917	2.71	2.643	2.618	2.511					2.009										
	Gandolfi camera																															

UNKNOWN	Fink Index	8.78	8.45 ±0.04	4.90	4.57	3.87	3.39	3.26	3.13	3.019	2.938	2.720 ±0.001	2.590	2.540	2.487	2.328	2.276	2.166	2.089	2.042	2.016	1.909 ±0.0008	1.870	1.6234	1.6006	1.4375	1.4188	1.3366	1.2948
Intensity		vvw	s	vw	vw	w	m	w	m	s	w	s	vw	w	s	vw	s	w	s	vvw	w	s	s	w	m	m	w	w	w
Calciborite	27-67					3.81	3.44					2.730	2.630		2.470	2.310	2.270	2.141	2.098		2.007		1.870	1.6150	1.6000			1.3990	
Johachidolite	29-280					3.99	3.30				2.931				2.434	2.361	2.230		2.075	2.049	2.001		1.887	1.6290				1.3340	1.2950
Sibirskite	15-282				4.65	3.74	3.29			3.000	2.930		2.580			2.330		2.130		2.050			1.878	1.6110			1.4180		1.3010
Kurchatovite	19-648				4.05	3.91	3.52			3.040	2.890	2.780	2.580	2.530	2.460	2.320	2.260	2.170	2.080		2.010		1.878	1.6330		1.4420	1.4100		1.2930
Gaudefroyite	17-154	9.10		4.89	4.54	3.88	3.58			3.020	2.950	2.770	2.620	2.520	2.460	2.390	2.310	2.120	2.090			1.910	1.880	1.6400		1.4300		1.3300	1.2800
Harkerite	10-465			4.45		3.84	3.39			3.010	2.950		2.610	2.530	2.460	2.330	2.250	2.160			2.000	1.920	1.840	1.6500	xxx	xxx	xxx	xxx	xxx
Ammonioborite	12-637	8.98		4.82	4.37		3.37			3.090		2.763	2.578		2.468	2.324	2.262	2.176				1.920	1.888	xxx	xxx	xxx	xxx	xxx	xxx
Gowerite	12-528	9.20	8.20	4.89		3.84	3.34	3.23	3.14	3.050	2.960	2.730	2.650	2.530	2.458	2.334		2.165	2.079	2.060	2.015	1.942	1.895	xxx	xxx	xxx	xxx	xxx	xxx
Volkovskite	18-1460		8.10	4.94	4.41	3.87	3.33	3.28	3.15	2.980	2.860	2.690	2.630		2.490	2.360	2.310	2.150		2.040				1.6390		1.4280		1.3410	xxx
Ginorite	8-116			4.92		3.90	3.42	3.28	3.12	2.980	2.880	2.730	2.580	2.530	2.470	2.360	2.280	2.160	2.090	2.030	1.960	1.920	1.821	xxx	xxx	xxx	xxx	xxx	xxx
Chelkarite	27-72	10.40		4.96	4.19	3.53	3.34	3.23		3.020	2.930	2.751	2.579			2.335				2.029			1.868		1.6040		1.4170		
McAllisterite	18-767	8.72			4.36	3.76	3.35	3.26		3.033	2.964				2.462		2.265	2.178	2.090	2.040	1.985	1.926	1.870		1.6000	1.4370		1.3380	
Admontite	34-1438			4.92	4.57	3.93				3.090	2.960	2.680	2.580	2.520	2.450	2.360	2.240	2.160	2.110	2.050	2.000	1.964	1.854					1.3660	
Aksaite	15-654			4.98	4.48	3.86	3.34	3.28	3.11	3.050	2.920	2.740	2.690	2.520	2.480	2.310	2.270	2.180	2.093	xxx	xxx	xxx	xxx	xxx	xxx	xxx	xxx	xxx	xxx
Halurgite	15-180			4.81	4.41	3.87		3.29			2.973	2.726	2.640	2.529	2.480			2.116	2.077		2.016	1.920		xxx	xxx	xxx	xxx	xxx	xxx
Veatchite	12-712				4.51	3.81	3.37	3.22		3.000	2.936		2.600	2.564	2.495			2.155	2.079	2.045			1.876	xxx	xxx	xxx	xxx	xxx	xxx
Hambergite	17-475			4.88	4.52	3.81	3.36		3.13	3.050	2.987		2.594	2.562	2.444	2.400	2.271	2.167	2.092	2.041	1.994	1.910			1.6110	1.4390		1.3350	1.2850
Vimsite	21-134							3.26	3.15	3.040		2.710	2.610	2.550	2.460	2.305			2.060	2.037	2.016	1.906			1.6060	1.4350		1.3390	1.2940
Fedorovskite	29-347				4.50	3.92		3.25		3.020	2.960	2.720	2.590		2.430	2.390	2.280	2.163	2.067		2.004	1.909						1.3330	
Hydrochlorborite	**29-312**		**8.48**	**4.93**	**4.47**	**3.89**	**3.39**	**3.29**	**3.14**	**3.000**	**2.959**	**2.720**	**2.594**		**2.494**	**2.332**	**2.275**	**2.162**	**2.091**	**2.040**		**1.912**	**xxx**	**xxx**	**xxx**	**xxx**	**xxx**	**xxx**	**xxx**
Ekaterinite	33-270			5.02	4.77	3.84	3.50	3.24	3.15	3.020	2.880	2.770	2.580	2.560	2.510	2.310	2.240	2.160	2.090	2.047	2.025	1.916		1.6270				1.3310	1.2900
Taleuchite	33-864									3.020		2.730	2.600	2.526	2.458	2.356	2.238		2.075	2.035	2.007								
Okanoganite	35-483	9.01			4.57	3.82	3.39		3.11	3.010	2.939	2.734	2.598	2.554		2.338	2.285	2.154	2.101	2.030		1.978	1.866		1.5900	1.4320		1.3250	
Tinzenite	6-444	8.83		4.94	4.55	3.87	3.42	3.28	3.14	3.060	2.975	2.734	2.620	2.553	2.474	2.323	2.254	2.152	2.060	2.033	2.008	xxx	xxx	xxx	xxx	xxx	xxx	xxx	xxx
Leucosphenite	25-784		8.45	4.87	4.22	3.94	3.37	3.25	3.19	2.982	2.930	2.732	2.577		2.460	2.327	2.280	2.169	2.105	2.045	2.018	1.899	1.847	1.6280	1.5940	xxx	xxx	xxx	xxx

vvw= very, very weak   w= weak   m= medium   s= strong   : xxx= published data does not cover this range

81-8/ 57.30	Green andradite	2d	4.23		3.03		2.67		2.55			2.421	2.349		2.187			1.945	1.898			1.7315		1.6632		1.5842	1.5016	1.3434	1.3068	1.2806		1.2142 Diffractometer
81-8/ 57.30	Green andradite	2d	4.29		3.02		2.70				2.469			2.208			1.959						1.676		1.6135 Debye-Scherrer							
		Rel Int.	7		2		1				4			8			5						6		3							
81-8/ 59.44	Yellow andradite	2d		3.26	3.00	2.97	2.70	2.60	2.58	2.534	2.467			2.207		2.145	1.96			1.796	1.743		1.675								1.255	
		Rel int.		10	2	11	1	9	7	5	4			15		12	8			13	14		6								3	
Fink 10-288	Syn. Andradite	2d			3.015		2.696				2.462			2.202			1.956				1.741		1.673									
81-4/ 115.55		2d	3.26	3.01	2.976	2.904	2.577	2.535	2.172	2.141	2.016	1.629																				
		Rel int.	1	2	3	9	8	5	4	6	7	10																				
Fink 29-372	Wollastonite	2d	3.228	3.002	2.976	2.892	2.572		2.179		2.017																					